PROCEEDINGS OF THE INTERNATIONAL SYMPOSIUM

TC 211 IS-GI Brussels 2012

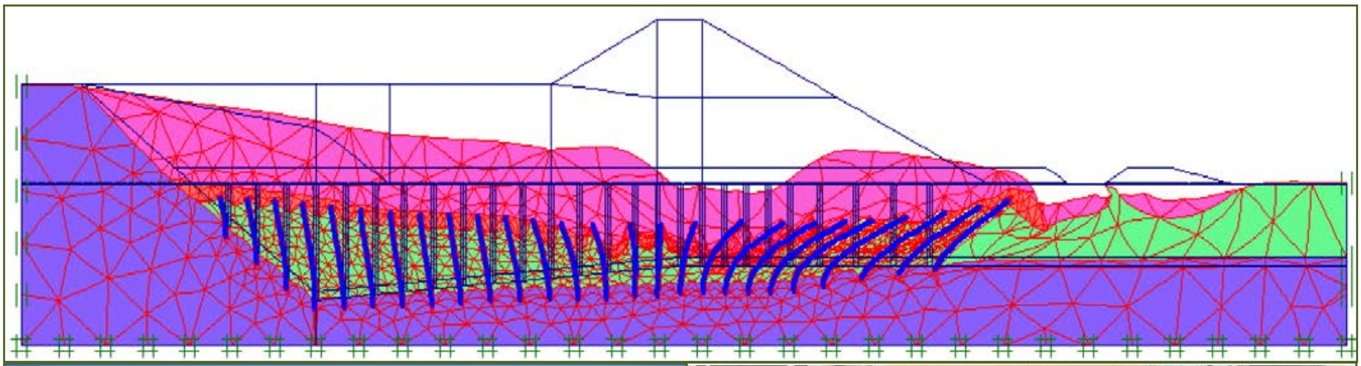

Recent Research, Advances & Execution Aspects of
GROUND IMPROVEMENT WORKS
31 May – 1 June 2012, Brussels, BELGIUM

VOLUME I

Organised by:

ISSMGE Technical Committee TC 211 Ground Improvement

Belgische Groepering voor Grondmechanica en Geotechniek
Groupement Belge de Mécanique des Sols et de la Géotechnique

Comité Français de Mécanique des Sols

Edited by:

Nicolas Denies & Noël Huybrechts

SIMSG ISSMGE

GBMS BGGG

CFMS

Recent Research, Advances & Execution Aspects of Ground Improvement Works

Edited by

Dr. Ir. Nicolas Denies
Belgian Building Research Institute (BBRI-CSTC-WTCB), Belgium

Ir. Noël Huybrechts
Belgian Building Research Institute (BBRI-CSTC-WTCB), Belgium

Introductory address

Dear TC 211 members, organising committee members, execution committee members, TOC members and delegates,
The internet site www.bbri.be/go/tc17 summarised the activity of the various meetings and seminars conducted all around the world by the undersigned, also culminating in an active participation in the state of the art report of ICSMGE 2009.
The same team was reconducted in 2009 for a four year term under the guidance of the T.O.C.
Soon, it was realised that to organise exchanges between newly nominated country members, imposing present guidelines would lead to a dilution of interest and a common focus had to be decided upon.
The idea of a symposium to strongly unify all efforts and exchanges in a common event has to be credited to the Belgian arm of the TC soon to be endorsed by it is French counterpart.
Indeed the capacity of the BBRI to organise such an event was recognised by the respective Belgian and French societies.
Today it is our greatest pleasure to submit the proceedings materialising from the contributions of the various authors from 35 different countries on 5 different continents.
We would like to stress the point that due to the involvement of the undersigned in National research programmes being the “ASIRI”, national project in France; and the “ Soil Mix”, national project in Belgium, the theme of ‘RECENT RESEARCH, ADVANCES AND EXECUTION ASPECTS OF GROUND IMPROVEMENT WORKS’ was selected as the chosen subject presenting a global picture of all efforts by academicians, consultants and practitioners throughout the industry associating the impact of specialised equipment.
The aspect of knowledge sharing has been enhanced by the nomination of general reporters from various continents and their commitment to report on research and development.
State of the art reports have been left to the regional and international conferences however short courses have been included in the symposium program for information transfer to non ground improvement specialists.

The main credit is to the authors and the general reporters who have offered all their efforts to make the symposium, a milestone in the ground improvement knowledge, this being the essence of a T.C.

Over 140 articles are presented and seven general reports that include the major research programmes presently ongoing on the planet.
Credit must be given to the equipment manufactures, as techniques which were only ideas could now become reality.
Also to our sponsors, for without their continued support and financial backing, this symposium may never have taken place in affordable conditions.

Special mention would have to go to our president, Jean-Louis Briaud, who has continually supported the idea of introducing a “Louis Menard Lecture” and actively contributes through his special lecture.

Also many thanks should be expressed to:

- the BBRI for the practical organisation of the symposium and the short courses, with special thanks to Carine Godard and Nicolas Denies;

- to IWT for their financial support to the practical organisation through the TIS-SFT program;

- to ABEF, BGGG/GBMS and CFMS.

Serge Varaksin and Jan Maertens
TC 211 Chairmen

Noël Huybrechts
TC 211 Secretary

Editorial address

Ground Improvement is a large and important domain in soil mechanics and geotechnical engineering and consists in a wide variety of techniques and methods adapted to a broad range of problems. The amount of contributions to the proceedings of this symposium is certainly a proof of that.

It cannot be denied that during the last decades the importance of the ground improvement market has enormously increased. New methods, tools and procedures have been developed and applied in practice.
In order to support this evolution in a scientific way, research programs have been and are being carried out worldwide, leading to more and better insights and delivering the basis for the establishment of design methods, quality control procedures and standards.

Due to the increasing interest of the construction sector for Ground Improvement techniques, the Belgian Building Research Institute (BBRI) has got more and more involved in projects addressing ground improvement during the last decade, most of them in a fruitful partnership with the Belgian Association of Foundation Contractors (ABEF).
In line with this evolution, the Geotechnical Division of the BBRI supports since 2005 the activities of the ISSMGE TC 211 Ground Improvement, which results today in the organization of an international symposium with more than 1600 pages of publications spread out over 4 Volumes:

- *Volume 1* of the proceedings contains the contributions of the 7 General Reporters, the Louis Ménard lecture held by *Patrick Mengé*, and the specialty lecture of the ISSMGE president *Jean-Louis Briaud*.
- *Volumes 2 to 4* contain more than 140 papers, subdivided in 7 Sessions, each of them dealing with a particular domain of Ground Improvement.

It can be noted that 40% of the papers deal with soil stabilisation and deep mixing, proving the huge interest in these techniques. This is not surprising, as they are outstanding and competitive sustainable construction methods.

We believe that the content of the present proceedings gives a very good overview of recent and on-going research actions and practices with regard to Ground Improvement. Moreover, we are convinced that they will contribute significantly to the further development of quality control procedures and standards.

Finally we would like to thank the Belgian Federal Public Service Economy, the NBN (Belgian standardization organization) and the Flemish Governmental Agency for Innovation by Science and Technology (IWT) for their financial support of the BBRI research programs addressing Ground Improvement techniques.

The Editors,

Nicolas Denies & Noël Huybrechts
Geotechnical Division, Belgian Building Research Institute, Brussels, Belgium

Welcome address

The mission of International Society for Soil Mechanics and Geotechnical Engineering, ISSMGE, technical committees is to provide a forum for active participation by the individual members of ISSMGE, and discussing, developing and applying specialist geotechnical knowledge related to the behavior of geo-materials, geo-engineering and engineering for society. Wherever possibly, it should seek to synthesize this knowledge into a form that is of use to the geotechnical profession and to disseminate it worldwide. There should be a balance between the advancement of academic research and the translation of appropriate research findings into practice. This international seminar and the associated short courses, under the framework of ISSMGE technical committee TC 211 "Ground improvement", fulfill these objectives balancing recent research, advances and execution aspects of ground improvement works. The material compile in this book is valuable for the different players in geotechnical and environmental engineering and shows the continuous development of this technology, mainly regarding its applicability. Furthermore, some papers deals also with the mechanisms and chemical reactions involved in the mixing of binders into soil, which should be of more future development with the integration of nanotechnologies in the mixtures. Therefore, on behalf of the ISSMGE, we would like to thank Serge Varaksin and Jan Maertens for their active TC 211 chairmanship.

S. Lacasse
Chair of ISSMGE Technical Oversight Committee (TOC)

A. Gomes Correia
TOC liaison of ISSMGE TC 211

Foreword

Ground improvement techniques are the toolbox for the geotechnical engineer who doesn't accept the ground as it is. To the contrary, their goal is to solve the particular problem by modifying the ground characteristics and behavior - together or not with complementary materials – in order to fulfill our demands. These demands are not new, and the history proves that the improvement of ground is an ancient concept. For many years, say centuries, the improvement has been focusing on the geomechanical characteristics: strength, deformability, homogeneity, long term stability and weight. Also the hydraulic conductivity has been a ground mass parameter to be tuned by the engineer, either to be increased (e.g. by drainage or soil fracturing) or to be decreased (e.g. by grouting or soil mixing).

The strategy of modifying to the best the ground composition, parameters and behavior is quite complex and calls for a large field of knowledge but also a high creative capacity, from the designer as well as from the industry (specialized contractors, material suppliers, equipment manufacturers, …). The analysis first starts from a good knowledge and understanding of the ground characteristics, its weaknesses and limitations but also its potential for upgrading. Second, the engineer has to deal with the process of pre-selection and evaluation of the possible techniques within the large panoply of available execution methods. And third, the treatment must be designed, including a reliable prediction of the expected "improved ground" parameters, of the "ground-reinforcement" installation and of the final behavior of the composed ground mass.

Within the field of ground improvement techniques, beside the ongoing acquisition of values of experience, a number of remarkable evolutions may be noticed:

1. the relevance of environmental demands, that has extended the field of application (e.g. stabilization of contaminated soil) as well as influenced the chosen method (e.g. soil mix retaining walls instead of bored pile walls)
2. the extended research programs to identify and quantify the material (ground, with or without binder) characteristics
3. the better understanding of the interactive soil-inclusion composite and the development of analytical design tools
4. the infiltration of remedial solutions from other sciences such as biochemistry.

The combination of our regional geology with the multiple impulses from scientists and contractors has resulted – in France as in Belgium – in a very extensive knowledge, application and export of ground improvement techniques. On behalf of the Belgian and French society for soil mechanics and geotechnical engineering, we therefore warmly thank and congratulate the Technical Committee TC211 and both its chairmen for their great efforts to organize and run this International Symposium and their ongoing actions within the TC211. We are convinced that all participants will largely benefit from the contributions and input from recent research work and advances in design and execution.

Flor De Cock
Chairman BGGG/GBMS

Philippe Mestat
Chairman CFMS

Organization

The International Symposium on Recent Research, Advances & Execution Aspects of Ground Improvement Works was organized by the ISSMGE-TC211 "Ground Improvement" under the auspices of the Belgische Groepering voor Grondmechanica en Geotechniek (BGGG)/Groupement Belge de Mécanique des Sols et de la Géotechnique (GBMS) and the Comité Français de Mécanique des Sols (CFMS).

Technical Committee 211

Serge Varaksin (France) & Jan Maertens (Belgium)	Chairmen
Noël Huybrechts, Belgium	Secretary

Executive Committee

D.T. Bergado, Thailand
J. Chu, USA-Singapore
T. Durgunoglu, Turkey
R. Essler, United Kingdom
M. Nozu, Japan
J. Sankey, United States
J. Wehr, Germany

Members of TC 211

Nidhal Al-Alusi, New Zealand
Abir Al-Tabbaa, United Kingdom
Gustavo Armijo, Spain
T.N. Baytasov, Kazakhstan
A.Boominathan, India
Zsolt Borocky, Hungary
Sylvie Bretelle, France
Gye Chun Cho, Korea
Nilo C. Consoli, Brazil
Marcio de Souza Soares de Almeida, Brazil
J.W. Dijkstra, Netherlands
Alessandro Flora, Italy
Massimo Grisolia, Italy
Babak Hamidi, Australia
Göran Holm, Sweden
Buddhima Indraratna, Australia
Yeon-Soo Jang, Korea
Ian Jefferson, United Kingdom
Johannes Kirstein, Germany
Masaki Kitazume, Japan
Leena Korkiala-Tanttu, Finland
Stefan Larsson, Sweden
Alain Le Kouby, France
Hanlong Liu, China
Ionnis Markou, Greece
Yoshihisa Miyata, Japan
Ta Ooi, SEAGS
Alexandre Pinto, Portugal
Isabel Pinto, Portugal
Athanassios Platis, Greece
Anand Puppala, USA
Andrea Richwien, Germany
Mohamed A. Sakr, Egypt
Jianyong Shi, China
Pedro Sola, Spain

Janos Szendefy, Hungary
Peter Thompson, Hong Kong
L.M. Timofeeva, Russia
M. Topolnicki, Poland
Almer E.C. van der Stoel, Netherlands
Alejandro Velasco, Ecuador
D. Verastegui, Belgium
J.-C. Verbrugge, Belgium
Kenny Yee, SEAGS
Jian-Hua Yin, Hong Kong

Local organizing committee

Chairmen: S. Varaksin & J. Maertens
Secretary: N. Huybrechts
Treasurer: G. Simon

Members

M. Bottiau, ABEF & Franki Foundations Belgium, Belgium
S. Bretelle, GDH, France-Australia
F. De Cock, chairman BGGG & GEO.BE, Belgium
R. Frank, ENPC-CERMES, France
A. Holeyman, UCL-Université Catholique de Louvain, Belgium
C. Jacquard, Fondasol, France
A. Le Kouby, IFSTTAR/LCPC, France
Ph. Liausu, Ménard, France
W. Maekelberg, TUC RAIL, Belgium
Ph. Mestat, chairman CFMS & IFSTTAR/LCPC, France
M. Roovers, ABEF & FONDEDILE, Belgium
M. Van Den Broeck, DEME, Belgium
R.D. Verastegui, Ghent University, Belgium
J.C. Verbrugge, ULB-Université Libre de Bruxelles, Belgium

ISSMGE-TOC Liaison member

A. Gomes Correia, University of Minho, Portugal

Table of contents

VOLUME I

VOLUME II

Session 1 - VIBRO and IMPACT COMPACTION

Session 2 – VERTICAL DRAINS, VACUUM CONSOLIDATION and PRELOADING

VOLUME III

Session 4 – SOIL MIXING 2 - DEEP MIXING

Session 5 - RIGID INCLUSIONS and STONE COLUMNS

VOLUME IV

Session 6 – SOIL REINFORCEMENT IN FILL AND IN CUT

OTHER

GENERAL REPORTS

SESSION 1 - VIBRO AND IMPACT COMPACTION

General Report
SESSION 1 - VIBRO AND IMPACT COMPACTION

Johannes F. Kirstein, BVT DYNIV GmbH, Germany, jkirstein@dyniv.com

ABSTRACT

Session 1 starts with SHRP 2 R02: Geotechnical Solutions for Transportation Infrastructure - A Web-based Toolkit concerning all soil improvement techniques.
The rest of the general report concentrates on vibro and impact compaction and takes all articles of the session into account. Below the topic "Basics of Vibro and Impact Compaction" there is a short summarize, which are the special common characteristics of the techniques finished with a look to a second web system about earth quake engineering.
With the focus on innovations, interesting new developments and case histories the traditional vibro and dynamic compaction take the largest part of the articles in session 1.
Techniques which go deep with low vibration are younger developments with a good future. Finally youngest case histories of cheap newer techniques close to surface give an overview, how deep they can reach in good conditions. Newer vibration free techniques are mentioned together with their success in cases of earthquakes.

1. INTRODUCTION

The intention of this general report in not complete state of the art of Vibro and Impact Compaction but like the focus of the conference a spotlight view to new developments and further possibilities of research and development.

Below the topic "Basics of Vibro and Impact Compaction" there is a short summarize, which are the special common characteristics of the techniques.

Each common technique gets a special topic. First the interesting articles (complete printed with abstracts in the volume) are fully named with their authors extracts are highlighted with a clear focus to the innovations with an opportunity of further research and industrial use.
Directly below follow the personal view und words of the author. His personal experience is added and as well other developments outside the range of the special articles are mentioned.

In order to find different soil improvement techniques a god new Web-based Toolkit is described in the following article "Geotechnical Solutions for Transportation Infrastructure - A Web-based Toolkit". It is placed in the first session of this conference, because this Web-based Toolkit gives an overview also about the techniques in the other sessions.

In the internet you find different links concerning SHRP 2 R02: Geotechnical Solutions for Transportation Infrastructure - A Web-based Toolkit. But the website is NOT open to the public as this time. The author Vernon R. Schaefer, Iowa State University explains, that they currently undergoing Beta testing of the website with a planned public opening later this summer 2012. The test account, which was given to the author, and the Geotechnical Solutions for Transportation Infrastructure web-based Toolkit is already working very well. A short demonstration is given in the session and we look forward for the date it is published to the public.

1.1. SHRP 2 R02: Geotechnical Solutions for Transportation Infrastructure - A Web-based Toolkit (Schaefer et al. 2012 [21])

The second Strategic Highway Research Program (SHRP 2) was created by the U.S. Congress to address challenges of moving people and goods efficiently and safely on the nation's highways. Geotechnical transportation issues are addressed under the SHRP 2 Renewal Focus Area, in which the goal is to develop a consistent, systematic approach to the conduct of highway renewal that is (1) rapid, (2) causes minimal disruption, and (3) produces long-lived facilities. The R02 project is aimed at identifying geotechnical solutions for three elements: (1) construction of new embankments and roadways over unstable soils; (2) widening and expansion of existing roadways and embankments; and (3) stabilization of working platforms. The project includes evaluation of the effectiveness of mitigation measures; a catalog of materials and systems for rapid renewal projects; guidance for design and QC/QA procedures; methods for estimating costs; and sample specifications for the identified geotechnical materials, systems and technologies. This has all been integrated into a web-based, interactive information and guidance system to provide the data necessary for determining the applicability of 46 specific ground improvement and geoconstruction technologies to specific projects.

2. BASICS OF VIBRO AND IMPACT COMPACTION

2.1. History and common technique - soil improvement in granular soil

The vibro compaction is the oldest soil improvement technique. The almost granular soil is compacted by different kind of vibration and shear force. Compared with other newer soil improvement techniques no other additives are used. The soil itself is improved by a reduction of pore volume so that it gets a higher relative density.

Photo 1 history: pictures of starting technique with first Keller vibroflots[19]

The first deep vibrators were developed in the 1930th by the Keller company. Actually worldwide there are more than five producers of electrical or hydraulic vibrators with different amplitudes from 10 mm to 48 mm.

According to Keller website [19] the record of depth 1939 was in Berlin with 35 m later 1993 is mentioned with 45 m. By the time other companies followed and a 65 m deep vibroflotation is explained in this article.

By the time the following well known alternative techniques which are cheaper but end in higher elevations were developed:

1960 Invention of the MENARD Pressuremeter and
1965 based on Pressuremeter the development of DYNAMIC COMPACTION for frictional fills through Ménard actually working normally to 15 m deep (exceptions with huge energy or free fall even deeper)

1990th the rapid impaction up to 5 m in some cases 7 m deep followed as well as impact rollers with almost effective depth of 1.5 maximum depth of 2.5 m.

All described soil improvement techniques are not able to compact directly at the surface, where normally rollers are used to compact the upper 0.5 m.

2.2. Soil parameters

Confirming [25] soils in this study are mostly sands and gravels. The efficiency of vibrocompaction techniques is optimum if the fine content (passing through the n°200 sieve or grain size smaller than 75 µm) doesn't exceed 10 to 15% of the total weight of the soil sample (Mitchell and al. 2002) and less than 2% of clay (grain size smaller than 2 µm). Figure 2 shows validity domain for each technique versus grain size. Some authors suggest using CPT results to judge the suitability of the vibrocompaction method (Massarsch, 1991).

Table 1 Soil particle size main condition for ground densification techniques as dynamic compaction or vibrocompaction [25].

	Soil types	
Size range	**Sands**	**Gravels to cobbles**
ASTM	> 0.074 mm < 4.75 mm	> 4.75 mm < 350 mm
British/European Standard	> 0.06 mm < 2.0 mm	> 2.0 mm < 200 mm
Ground improvement without admixtures in non-cohesive soils or fill materials	Dynamic compaction Vibrocompaction	

Compared with vibrocompaction the Dynamic compaction can treat a wider range of soil not only larger gravel but also material with more than 10-15 % fines.

For all technique referred in this article it is easier to compact lose material than already medium dens material. According to [11] it is more difficult to compact a already dense soil from Ie = 60% to Ie = 80 % than to compact a lose soil from a relative density of Ie = 38 % to Ie = 80 %.

Sometimes it is especially difficult to compact fine sands with only a very small range of grain size. In fine soil it is necessary to have the right water content for the compaction and afterwards enough time to wait for the results. The articles of this session show good and interesting results, but mostly do not mention the water content of the soil and the time to wait for this results. This was the reason to take water and time to the separate next topic and to add some experience in this direction.

2.3. Influence of water and time to the messuared compation values

The water content and water table is very important in all kind of compaction works, for example
- with vibroflotation huge amounts of additional water are necessary in thick layers of dry soil above ground water level,
- with dynamic compaction the working platform should be 1.5 m above ground water level und enough time (normally less than 24 h) for the pore pressure decrease and the next phase of compaction is necessary
- and in soils with higher fine contents the right Proctor water content is necessary.

According to [18] a remarkable doubling of the stiffness modulus in the grid centred between the stone columns was made possible by the optimum Proctor water content of the mixed-grain dump (fine particle fraction> 20% ... 25%), and also by the powerful V23 (23 mm amplitude) vibrator. With wn = 10% ... 14%, the calculated current water content under the influence of dewatering was in the normal range of natural humidity. Laboratory tests showed a proctor density about ρPr = 1.846 g/cm3, and a proctor humidity ratio about wPr = 9.9% and thus good compaction and compression was achieved. Even in the middle of the grid more than dumbled cone penetration (CPT) were measured. Absolute values of the stiffness modulus in cohesive soils can be measured only with help of additional calibrations like the executed pressuremeter and oedometer tests on undisturbed soil samples. A transfer of these high values to other constructions projects without these optimal conditions is not possible and it is highly recommended to use a project-specific calibration with test fields for example the Ménard pressuremeter. Not only in consolidation theory but also in the soil improvement with compaction we have to consider the time effects.

Not everything can be explained by the pore pressure according to consolidation.

Treating fine sand follows the time experience:

- directly after compaction (approximately within on day) the cone penetration (CPT) is less than the values before the compaction,
- within one week CPT values reach and brake the original level
- and sometimes it takes one month or longer to show significant improvement.

An impressive example is given by topic 3.6 Measurement of depth and time influence with up to 65 m deep vibroflot.

2.4. Applications

The mail tasks of the soil improvement techniques are necessary stability and acceptable settlements of buildings and infrastructure projects.
A big part of the applications special in granular soil is the liquefaction risks:
Knew damages in brown coals dumps show that other initials like increasing water tables and other dynamic inputs like wind in the trees or windmills can cause large size landslides even when the surface is nearly flat before the damage.
Earth quakes are the traditional and well known source of large damages, where the granular soil is not compacted well enough. The scientific field of earthquakes in only shortly mentioned with the following task “Networks and databases for Earthquake engineering” as well with the interesting Japanese article “Sand Compaction Pile Technology and its Performance in both Sandy and Clayey Grounds” with geotechnical examples of the describe technique and their behaviour during of the terrible Japanese earthquakes in this session 1 Vibro and Impact Compaction.

2.5. Networks and databases for Earthquake engineering

Actually in march 2012 the joint conference 9th International Conference on Urban Earthquke Engineering (9CUEE) an d4th Asia Conference on earthquake Engineering (4ACEE) proceedered at the Center for Urban Earthquake Engineering, Tokyo Institue of Technology, Japan.

Julio A. Ramirez explains in his article [1]: The George E. Brown, Jr. Network for Earthquake Engineering Simulation (NEES) is a network of 14 experimental sites (https://nees.org/sites-mainpage/laboratories) connected by a cyberinfrastructure that fosters collaboration in research and education. The current experimental reach of the laboratories ranges from the marine to the geotechnical to the structural environments and can address almost any technical question related to the safety of the built-environment in earthquakes.

The eathquake resistand foundations are exacly one large field of our execution works and that gives the reason to join the network called NEES Hub (*https://nees.org/sites-mainpage/laboratories*).

Only 25 $ pear year costs the online acess to the website http://nisee.berkeley.edu/elibrary/about.html where is acually written the following information: “The Earthquake Engineering Online Archive is a database of significant, publicly-funded research and development literature, photographs, data and software in earthquake, structural, and geotechnical engineering.
The archive is updated daily. The UCB-EERC reports, PEER Center reports, selected UCB-SEMM reports, selected UCB-GEOTECH reports, other university research reports, and selected papers and

reports from the NISEE Online Library are included in the archive with earthquake damage images, experimental data and movies, and research software.
Any findings, conclusions and opinions expressed in materials available within The Earthquake Engineering Online Archive are those of the author(s) and do not necessarily reflect the views of either the University of California, Berkeley (UCB) or the Earthquake Engineering Research Center (EERC). Neither UCB nor EERC assume any liabilities with respect to the use of, or damage resulting from the use of, any information disclosed in The Earthquake Engineering Online Archive."

2.6. Innovations – interesting articles and other techical knowledge

The focus of the international conference is on innovations and the general report tries to follow. The call for papers was worldwide and every session got good feedback. In the session of compaction we have the oldest soil improvement technique with good experience. So there is less space for innovations than with younger technique.

So we treat a new depth of 63 m vibroflotation like in innovation, because the last record was published with 40 m in 1993, but for sure deeper elevations were reached in between. Compaction technology has been checked again, that the limits of fines in the soil keep the same.
With new earth quake standards and soil investigation methods we have to think about soil dynamic response after ground improvement.

The dynamic compaction possibly can be optimized with new tamper shapes and grids. The testing perion of MARS shows a big success with higher energies and equivalent deeper influence.

The compaction technique with low vibration is almost new in the public.

By the articles in session 1 the limits of new techniques close to surface get clear.

The general report keeps close to the articles and the common techniques in the session. At some places the personal experience of the author is added.

Information about other not so common used technique like MRC compaction machines, explosive compaction and electric pulse compaction can be found in the "Construction Processes, State of the Art Report" [1].

3. VIBRO TECHNIQUE AND PERFORMANCE

3.1. General

"Vibro" methods (with or without addition of stone) have been commonly employed in practice for densification of granular soils since the 1930´s (Slocombe et al., 2000). The principal piece of equipment used to carry out vibro ground improvement techniques is the vibroflot (also referred to as a vibrating poker or depth vibrator), which is either suspended from a crawler crane or mounted on a leader attached to a base machine, dependent upon the specific application. The principles of vibro techniques in granular soils is based upon particles of coarse grained soil being rearranged into a denser state by means of dominantly horizontal vibration from the vibroflot (vibrating opoker). The densification of the soil optimizes void ratio and corresponding increased angle of shearing and so increases stiffness and strength in the function of lesser settlement. So the stability increasing technique reduces liquefaction risk and ground deformations during seismic events.

The major problem with this method is, that, inspite of the fact that the method performs well, everyone thinks, there is nothing new in the technique.

Mainly the execution depth developed the last years according to 3.6. Nowadays The Deep vibration compaction (vibroflotation) is a method of ground improvement up to depths of 70 m.

The Ph.D Thesis of Dr. Fellin [11] written at the University Innsbruck Austria and proved by Pro. Dimitrios KOLYMBAS gives a good overview about quantities influencing the compaction:

- like different machines (vibrators)
- soil (which has to be compacted) and grain size distribution of the added material
- spacing of the compaction points

- compation pattern

In the Ph.D Thesis of Dr. Fellin [11] it is shown, what information from the movement of the vibrator can be used as additional quality control and indicator for the compaction. Such information can be analysed directly during compaction, and offers thereby the possibility of an "on line compaction control".

The wave propagation in inelastic soil is treated as a plastodynamic problem. The soil is described by means of a hypoplastic constitutive law. The inelastic wave equation is solved using a numerical method for conservation laws.

From the analyses of the wave propagation an estimation of the density increase and compaction range is given.

3.2. Vibro Ground Improvement Techniques – A UK Perspective (Serridge, 2012 [22])

Mr. Serridge gives a good overview of vibro techniques in the UK from the beginning since 1950´s till up to now. Whilst the basic components of the equipment have changed very little over the years, there have been significant developments in the reliability (with extended lifespans and reduced maintenance) and power ratings of the equipment with the objective of achieving greater efficiency in densification and stone column production.

He explains well the worldwide similar experience that in situ vibro compaction is appropriate for granular soils with a total fines (particles finer than 0.06 mm) content of up to 15% of which the clay and fine silt content (particles maller than 5 µm) should be less than 2% (Slocombe et al., 2000).

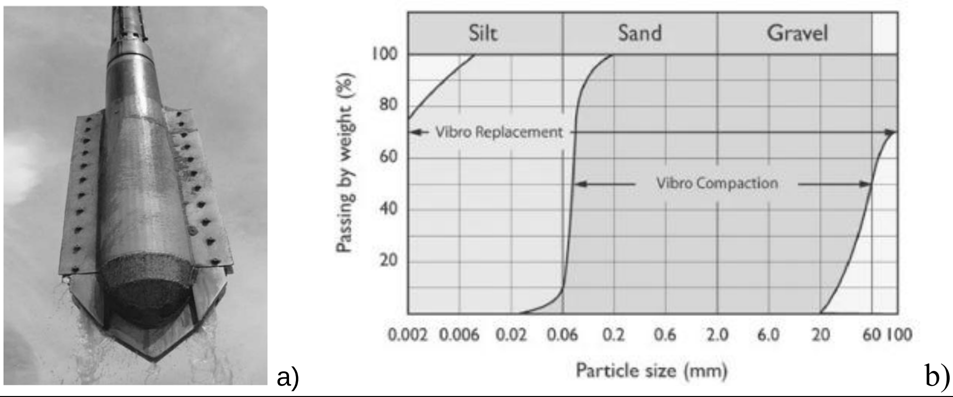

Figure 1 a) Top-feed Vibroflot b) Range of soils treatable by vibrocompaction and vibro stone columns

The rest of the article is about vibro column technique with stone and concrete fitting well in the chapter of rigid inclusions.

3.3. Article "Effects of Fines on Vibro-compaction" and article "Stone Column and Vibro-compaction of Soil Improvement for liquefaction (Wong et al., 2012 [23])

The both article "Effects of Fines on Vibro-compaction" and "Stone Column and Vibro-compaction of soil Improvement for liquefaction" deal with the same Port Said Container Terminal, Phase 2 extension work along the Suez Canal in Egypt.

The article confirms the knowledge that at fines content less than 15% (in contrast to a recommended value of 10% in practice), the soil improvement resulted from the vibro-compaction process can impose significant improvement. No improvement can generally be made for soils where fines content are high, say over 20-25%.

Figure 2 shows a homogenous quality of vibroflotation from 0,5 m to 4.5 m elevation in the clean sands (less than 5% fines).

On Figure 3 (only one CPT) the Chinese colleagues start the theory, that fines migration from the upper soils occurred and increased the fines content of the soil below.

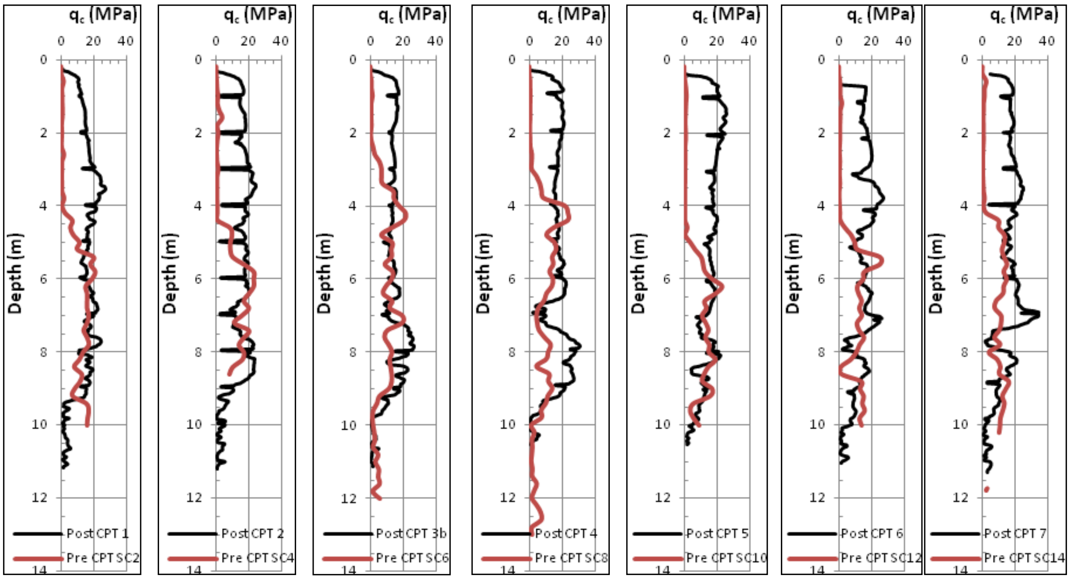

Figure 2: Pre-CPT and Post-CPT results near N750 and N550 before and after improvement implemented

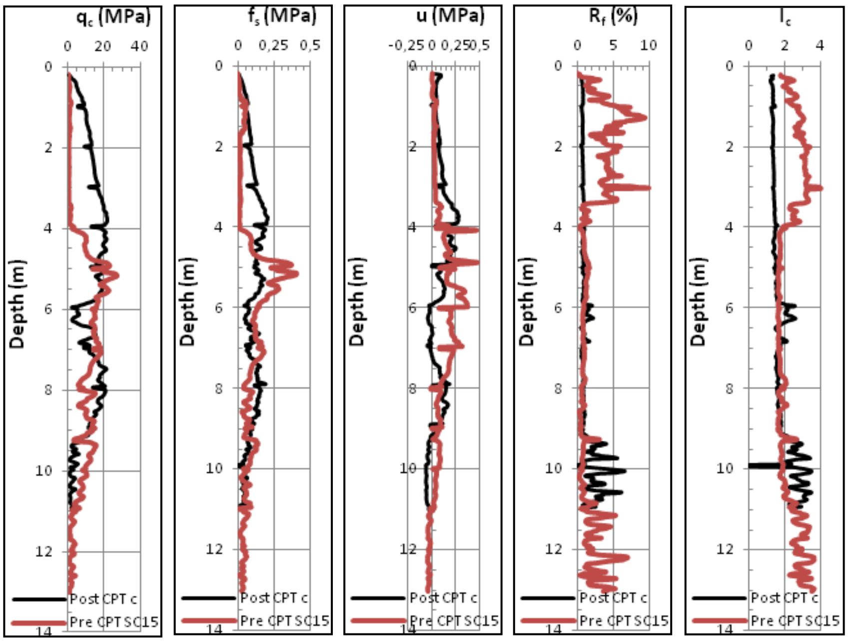

Figure 3: CPT results qc, fs, u and Rf of PRE-SC15 and POST-CPT

Normally the fines wash out with the vibroflotation at the surface (it can be seen on Photo 2) and do not sink down so this theory should be validated with more CPT Tests.

It can be seen in Figure 4 that the top 5m of the soils are stiff fine grained sand to clayey sand. The underlying soils are mixed layers of silty sand, clayey silts and silty clay extending to over 15m below ground level.
So in large parts of the projects with fines higher than 15 % stone columns were executed.

Photo 2: Execution of the vibroflot

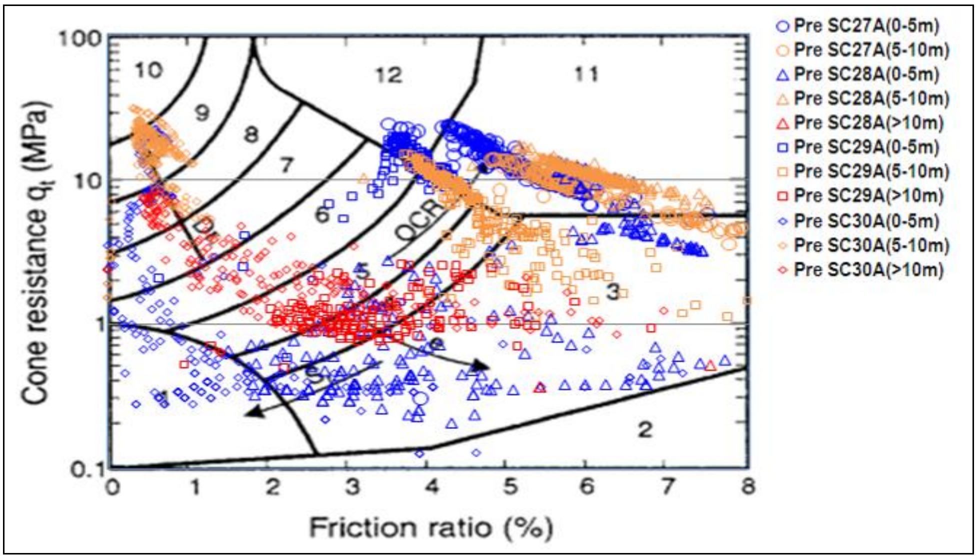

Soil Behavior Type (Robertson et al.,1986; Robertson & Campanella, 1988)

1 – Sensitive fine grained	**5 – Clayey silt to silty clay**	**9 – sand**
2 – Organic material	**6 – Sandy silt to silty sand**	**10 – Gravelly sand to sand**
3 – Clay	**7 – Silty sand to sandy silt**	**11 – Very stiff fine grained***
4 – Silty clay to clay	**8 – Sand to silty sand**	**12 – Sand to clayey sand***
	**** Overconsolidated or cemented***	

Figure 4: Classification Plot by CPT, based on qt and FR (Robertson et al., 1986)

3.4. A comparison of soil improvement achieved using different vibro methods (Jimenez et al., 2012 [24])

In this paper, the spanish coleguases report the results of a recent experience of application of vibro-methods in a hhydraulic fill made of marine sands (with a varying but generally small amount of silt) that were dredged from nearby locations. Three vibro-methods for soil improvement are compared: *(i)* stone columns executed by the water-flushing technique ("wet method") with stone added from the surface ("top-feed"); *(ii)* stone columns ("wet method") with bottom-feed delivery of stone; and *(iii)* vibro-compaction (with addition of the same sand to increase efficiency and to maintain site level). Three field tests were developed (one for each treatment type indicated above) and a series of in-situ tests were employed to compare the conditions before and after treatment. (In-situ tests included dynamic penetration using DPSH penetration tests; seismic cone penetration tests or SCPTU; and seismic wave velocity analyses.)

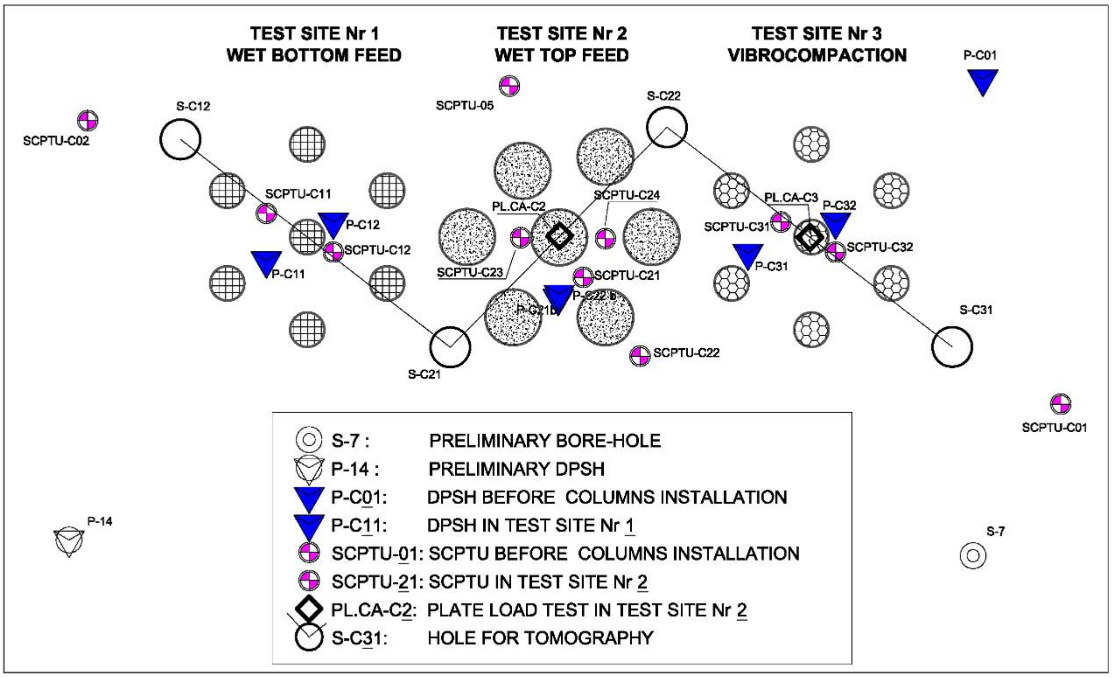

Figure 5: Location of treatments and of control tests at test sites

Figure 6 presents a comparison between DPSH N20 dynamic penetration values measured before and after treatment for each of the test sites. (There were two DPSH available before treatment ---one at the lower-left corner and one at the upper-right corner---; since their results are very similar, they have been considered as representative of "before treatment" conditions in all test sites.) It can be observed that the vibro-treatments produce a significant increase in the compacity (as measured by penetration resistance) of the fill. The highest values of very dense conditions are reached with vibroflotation. The comparison of SCPTU tip resistance fits well but the comparison of wave velocities (vs) measured with SCPT brought highest values with the whet bottom feed method.

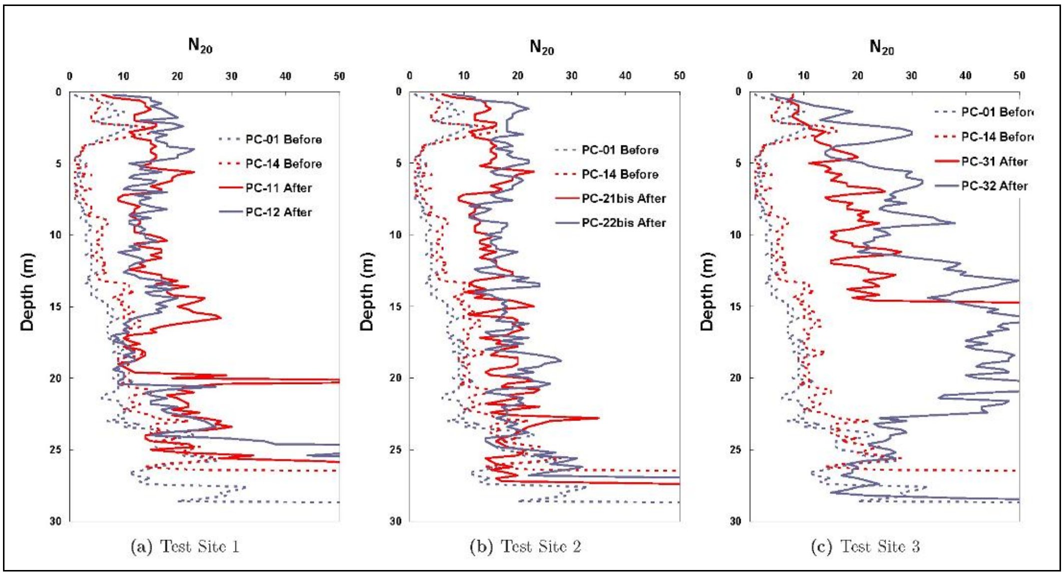

Figure 6: Comparison of DPSH values

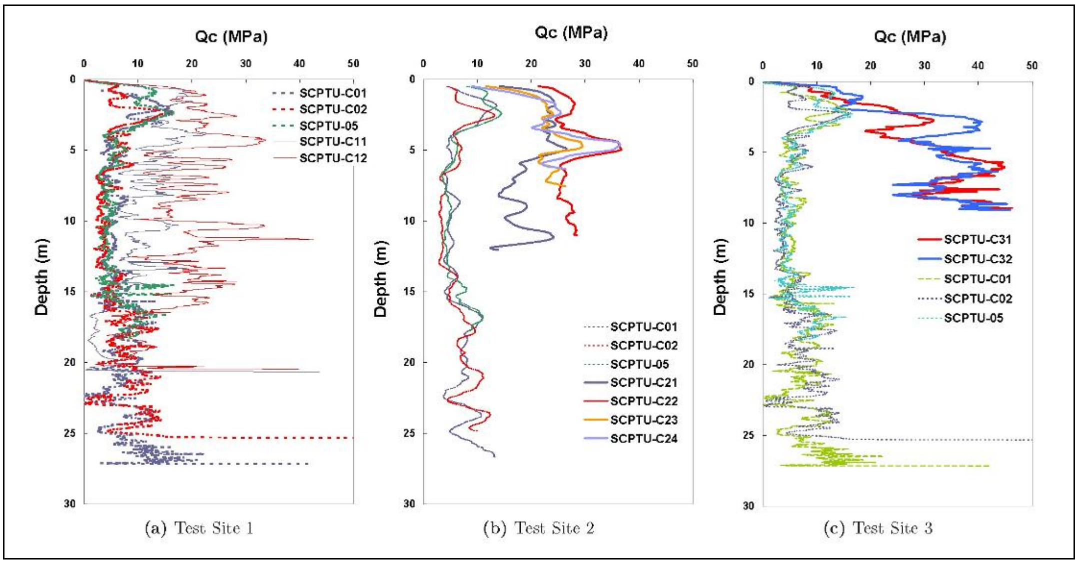

Figure 7: Comparison of SCPTU tip resistance

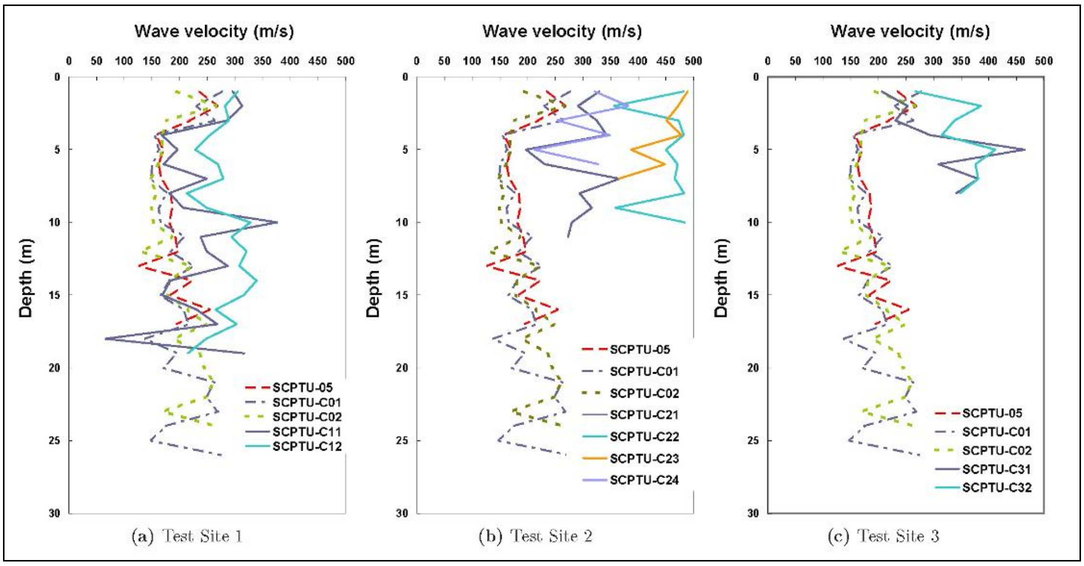

Figure 8: Comparison of wave velocities (vs) measured with SCPTU

Figure 9 shows the result of a seismic tomography (using the cross-hole method) that has been developed employing the boreholes indicated in Figure 5. It can be noted that, in all cases, a "loosened" zone remains at locations close to the surface. (In this case, and to fulfil the required design specifications, the surface had to be excavated and replaced by a granular and compacted material.) . It is also observed that areas treated with stone columns tend to produce higher seismic velocities than those observed in the area treated with vibro-densification (with sand addition). Similarly, and although differences are not very high, results suggest that the bottom-feed method employed at Test Site 1 provides higher (and more uniform) seismic velocities. (Note the "gaps" observed at the location of the bottom feed treatment at Test Site 2.) This is probably due to the higher diameter control achieved with the bottom-feed method (in agreement with previous observations of Slocombe et al. (2000), our experience suggests that a more controlled and uniform shape is obtained), although more research is probably needed on this topic to verify this observation.

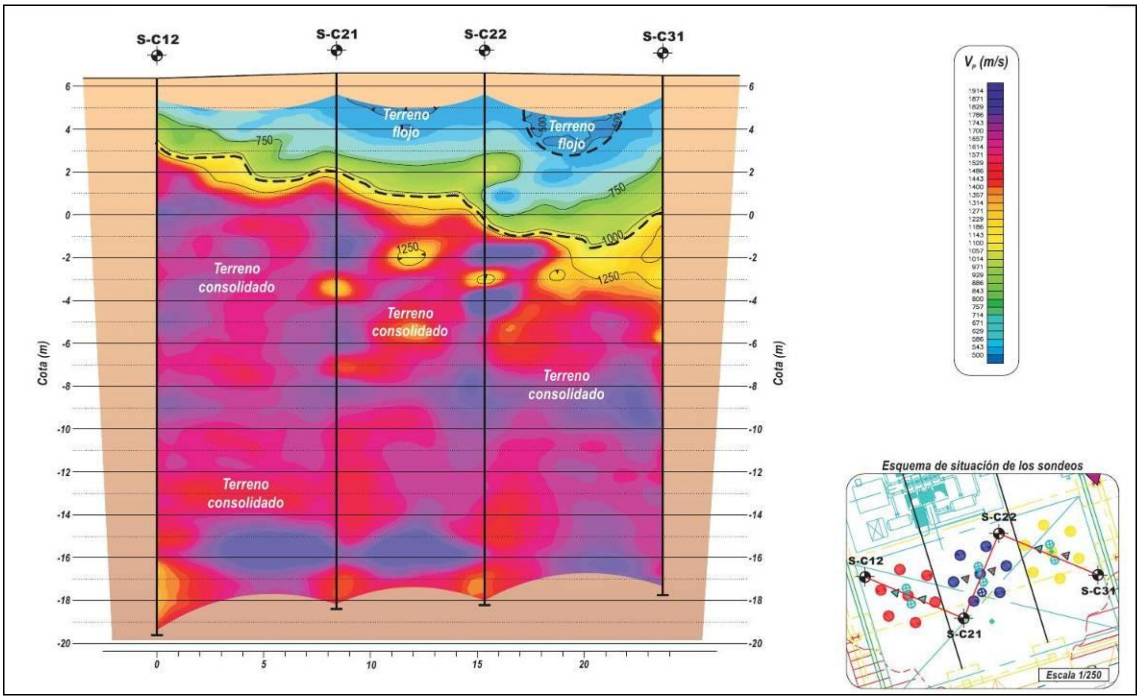

Figure 9: Profiles of seismic velocities (vp) across test sites (GEOCISA-ICT, 2010)

Finally is not clear, if it was really necessary to execute this project with stone columns and soil substitution at the surface. More soil investigation methods should have been done to prove why the high dynamic penetration and cone penetration values do not correspond with the values of wave velocity and seismic velocities.

3.5. Soil dynamic response after ground improvement by heavy dynamic compaction or vibrocompaction (Brûlé and Javelaud, 2012 [25])

Soil improvement work by dynamic compaction or vibrocompaction improves the granular soils' mechanical characteristics obtained by in situ investigations. The shear wave velocity parameter Vs could increase as well but in a much smaller proportion than those measured by mean of the cone penetration test or the pressurmeter test. Parameters tested within the elastic range of deformation, as Vs for instance, could increase enough and lead to a soil classification change. First experiences feedback points out the geotechnical conditions which are able to induce an Eurocode 8 ground type change after dynamic compaction or vibrocompaction works.

It is well known that ground densification increases the mechanical characteristics of soils tested with cone penetration test (CPT) or pressurmeter test (PMT). To rule on the relevance of an effective change of class of ground, the classical site investigation is not sufficient. In fact, it is necessary to prefer shear wave velocity measurement (V_s) more adapted to the soil small strain parameters inferred by seismic waves ($\varepsilon <<10^{-4}$). Most of the worksites in Western Europe are concerned with a small strain seismicity (Semblat and al. 2009).

Geotechnical investigation CPT, SPT test ($\varepsilon>10^{-4}$) or geophysical methods ($\varepsilon<<10^{-4}$) based on V_s measures can be used for Eurocode 8 ground type. Results from both methods are depicted in this article.

The geophysical method is Multichannel Analysis of Surface Wave method (Bitri and al. 1998). Soil classes are defined with the harmonic mean, formula (1), calculated for thirty meter of soil below the ground surface. Ground densification works are often concerned with A, D, E, S_1 and S_2 ground type (table 1).

$$V_{s,30} = \frac{30}{\sum_{i=1}^{n} \frac{h_i}{V_{si}}} \tag{1}$$

Table 2: Eurocode 8 ground types

Ground type and description of stratigraphic profil
A : Rock or other rock-like geological formation, including at most 5 m of weaker material at the surface. **$V_{s,30}$> 800 m/s.**
D : Deep deposits of dense or medium dense sand, gravel or stiff clay with thickness from several tens to many hundreds of metres. **$V_{s,30}$< 180 m/s.**
E : A soil profile consisting of a surface alluvium layer with V_s values of type C or D and thickness varying between about 5 m and 20 m, underlain by stiffer material with V_s > 800 m/s.
S_1, S_2 : Soils potentially concerned with liquefaction (see EN 1998).

Table 3 Results of site investigations done before and after densification

Project	**Site investigation**				**$V_{s,30}$ (m/s)**	
	CPT	SPT	MASW	PMT	Before	After
Givors	x		x	x	244	252
Dakar	x	x			-	-
Peribonka Dam	x		x		Non calculated	

Project	**N_{SPT}**		**CPT q_c (MPa)**		**PMT p_{l*} (MPa)**	
	Before	After	Before	After	Before	After
Givors	-	-	3.7	7.3	0.5	2.4
Dakar	< 15	> 50	< 8	> 15	-	-
Peribonka Dam	-	-	< 10	> 10	-	-

The site investigation results show that the mechanical parameters obtained from in situ tests can increase by a factor of two after soil improvement works. The shear wave velocity Vs increases also but in a smaller proportion. At Givors were dynamic compaction work was performed from the surface, the shear wave velocity over the first five meters increased by about 20%. Calculated according to (1), the Vs,30 increases by about 3%. Regarding the Péribonka Dam, we note that the shear wave velocity increase can be greater than 15% over the whole improved layer. The vibrocompaction technique's effect on the Vs,30 can therefore be important even if the soil is not improved down to 30 m depth.
Basing the classification on in situ parameters, a modification of the ground type is possible. Modifying the ground type is however more difficult when the proxy used is the shear wave velocity, although it may be possible if the soil compaction is carried out for that purpose.

This article has the same problem like the Spanish case history before, that the wave velocities (Vs) measured with SCPTU does not fit to the significant improved density measured with cone penetration and pressuremeter. It seems that the investigation methods of wave velocity and seismic velocities have to be proved because they get more and more important in our seismic calculations.

3.6. Measurement of depth and time influence with up to 65 m deep vibroflot

One of the largest German onshore windmill with rated power of 7.500 kW has a hub heigth of 135 m and a rotor diameter of 127 m, wich means it reaches a maximum heith of about 200 m.
It was a special task to find the right foundation to install this special windmill on an old brown coal dump with up to 63 m of loose partitionally silty fine sands and small clay layers before the natural soil starts 60 – 63 m meter below the surface. Photo 3 shows what are the technical reasons for having lose and inhomogenius material of such a thickness.

Photo 3: Development of a dump in the actual brown coal industry [18]

The water level is about 30 m deep and piles would help nothing because the neagtive skin friction of the lose inhomogen fill takes nearly complete the pile resistance.
A design according to [13] with a large grid of vibroflots 40 to 63 m deep was chosen to minimize liquifaction risks over the complete depth of the dump. In order to reach strict differential settlement criteria in the foundation level around 20 m deep stone columns in a 1.5 m grid were chosen in the second step of soilimprovement, finalized with 4 m of gravel in the load transition layer.

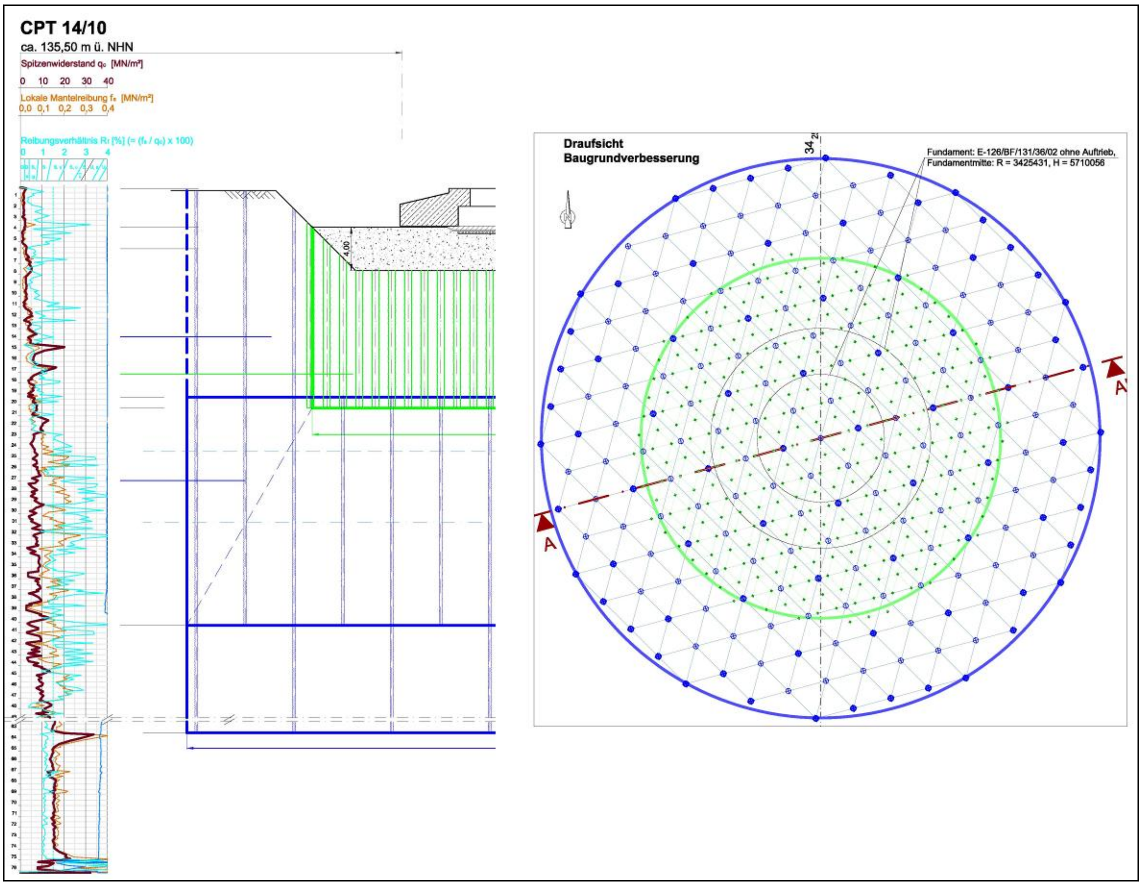

Figure 10: CDM Smith foundation design with 40 and 63 m deep vibroflots (blue), 20 m deep stone columns (green) and a 4 m thick gravel layer (gray)

The CDM Smith article at the university of Darmstadt [13] described the big sucess of the vibloflotation quality this way, that around 55 % of the original planned stone columns in the upper layer could be saved due to very dense conditions after vibroflotation.

The impressive 63 m deep compaction (around 65 m are the depest vibroflots) values illustrated by the following CPT tests can be explained as followed:

- The soils changes in fast layers of sand and silt very. Due to the right percentage of fines in the sand, the hole of the vibro stood open 63 m (there was nealy no crater on the top and the author proved that with a weigth and 70 m long cable) and was as well comactable material.
- A lot of crushed material (several trucks per point) were allways brouth in the elevation of the vibrator and secured a god contact to the surronding soil. This was later seen with around 1.2 m diameter stone columns in the center of the vibroflot points.
- The dump was almost dry and through the right amount of water (a lot of water) good compation sucess was possible with the right proctor density.

Recording the CPT's in Figure 11 it has to be mentioned that zero (0m) is in the bottom of the 4 m thick crushed stone layer deeper than the original ground level and execution platform of the vibroflotation. So everywhere around 6 m on top have to be added. The green line of CPT in october 2010 let understand, why stone coulums where chosen above the vibroflotation.

Photo 4 550 t crane with the 68 m long and 40 t heavy vibrator

The yellow CPT were performed end of may 2011 around 2 to 3 weeks after finishing the vibroflotaion in this area of the CPT. The red CPT were performed in the middle of July around 8 to 9 weeks after vibroflotation at the same position, all by the same CPT machine of Geotechnik Heiligenstadt. A strong time relevant increase from somthing like 8 MN/m² CPT values to over 20 MN/m² somtimes up to 50 MN/m² took place in the sand. The lightblue may 2011 and darkblue july 2011 kurves show the friction release und high values fit good together with lower cone penetration. These layers with more fine particle have had end of may a surprising high cone penetration values and did increase not so much during time. If such layers bring also increased values by longer consolidation times than 2 month could not be tested, because the foundation of the mill was started.

The results show, that we have to give enouth time even in sand to achieve good CPT values. This time has to be considered during our modern and fast building processes.

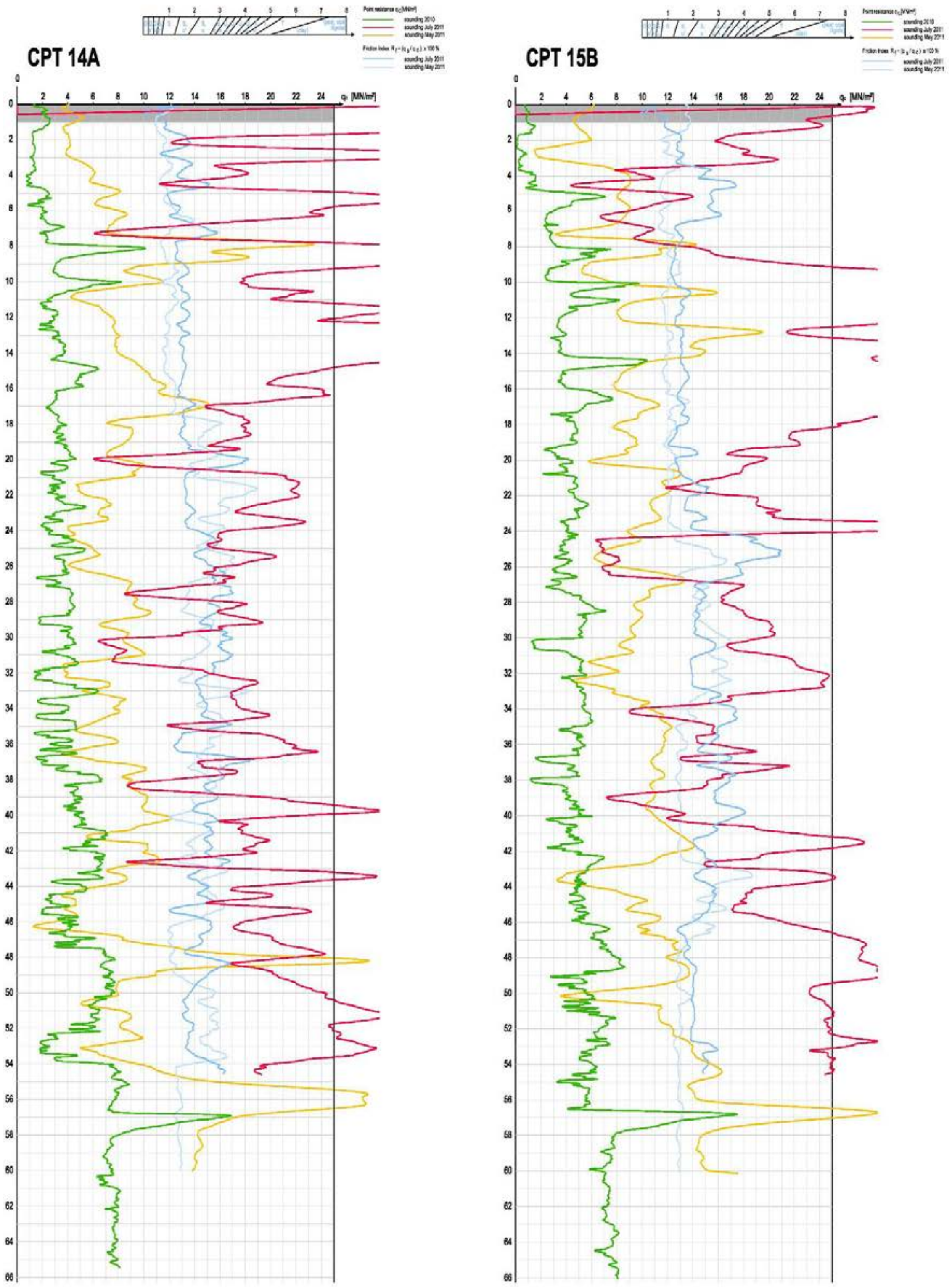

Figure 11: CPT tests 6 m below surface elevation with cone penetration in MN/m² October 2010 (green), end of may 2011 (yellow) and July 2011 (red) as well as friction relation in blue

4. DYNAMIC COMPACTION (CONSOLIDATION)

4.1. The Process of Dynamic Compaction

Dynamic compaction developed by Ménard in the 1960´s is a ground improvement technique that involves dropping a tamper several times from a predetermined height in a coordinated grid pattern over the treatment area and mainly used to densify loose granular soil deposits from a working platform above the water table by systematically dropping flat bottomed tampers of 5 -20 tons from heights of 10 -40 m on a selected impact grid to compact the underlying soil layers. The improvement in soil behaviour due to the compaction process depends upon factors such as the grid pattern and spacing, the tamper shape and weight, the number of passes and the number of drops used at each grid point.

The innovative MARS (Ménard Accelerated Release System) technology was developed and patented to drop pounder in actual free fall. A 35 ton pounder is used with the largest standard cranes in order to improve security and the possible energy range significant.

4.2. Assessment of Grid Spacing for Dynamic Compaction (Moyle and Turner, 2012 [26])

The grid pattern adopted for the dynamic compaction process is usually formed by undertaking multiple passes, commencing with a wide primary spacing (pass 1) which is in-filled by secondary (pass 2) and tertiary passes (pass 3). An illustration of a typical grid pattern used in dynamic compaction is presented in Figure 1.

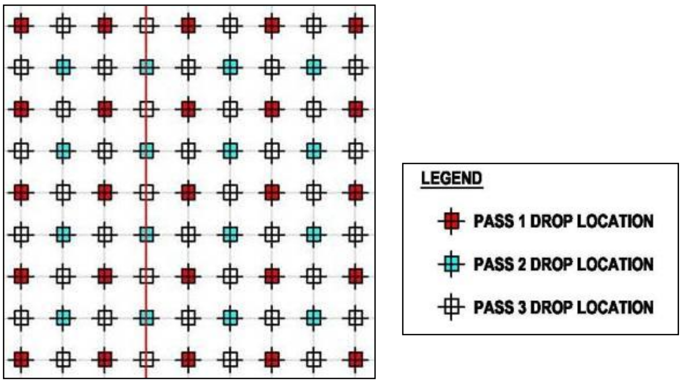

Figure 12: Example of Grid Pattern for Dynamic Compaction

The orthogonal distance between adjacent points on the grid pattern after pass 3, referred to as the grid spacing, has a significant effect on the ground improvement achieved by dynamic compaction (Lukas, 1992); and also the rate at which dynamic compaction can be applied over a given area. As such, the grid spacing becomes an important design parameter when assessing dynamic compaction.

The influence of grid spacing in dynamic compaction has been the subject of numerous numerical studies.

Chow, Yong, Yong and Lee (1994) also investigated the effect of print spacing (distance between drop locations) on ground improvement using dynamic compaction. They presented a different approach to Poran and Rodriguez (1992) that estimated the lateral extent of the ground improvement based on assessment of the increase in friction angle in cohesionless materials.

The depth of influence (or the *b* parameter noted above) of dynamic compaction has been the focus of studies by Menard (1977), Luongo (1992), Lukas (1992) and others. Lukas (1992) presented the depth of influence of the dynamic compaction process to be as follows:

$$D = n\,(W \times H)^{1/2} \qquad (2)$$

where n = empirical coefficient
W = weight of the pounder (tonnes)
H = drop height (metres)

The studies by Menard (1977), Luongo (1992) and Lukas (1992) relate the depth of influence to the pounder weight and drop height but do not consider the effect of the grid spacing.

Dynamic compaction was undertaken to compact the fill using a 20-tonne tamper dropped from 23m height over a square grid pattern with grid spacings that ranged from 4.2m to 6.0m, as shown on Figure 1.

The purpose of this investigation was to assess the influence of grid spacing on the degree of compaction of the material between the drop points (termed here "interaction"). The compaction requirements for the project were set to achieve a density of at least $2t/m^3$ over the upper 6m of fill.

The assessment of the "interaction" between drop points was based on a series of key monitoring indicators namely:

- Heave/Penetration Tests;
- Subsurface settlement monitoring (extensometers); and,
- Downhole Gamma Density testing.

These indicators are described in the following section.

4.2.1. Heave / Penetration Tests

Heave/penetration testing was typically carried out at the commencement of each pass within each area of different grid spacing. A heave/penetration test involves dropping the pounder on a single location up to 40 times and the measurement of the volume generated by a) the penetration of the pounder and b) the soil heave above original soil level prior to, during and after the test adjacent to the pound location.

This was measured through the establishment of 12 survey stations around a drop location along three equally spaced axes where the change in level was monitored. Four stations were established on the pounder to monitor the depth of penetration. This configuration is shown on Figure 3.

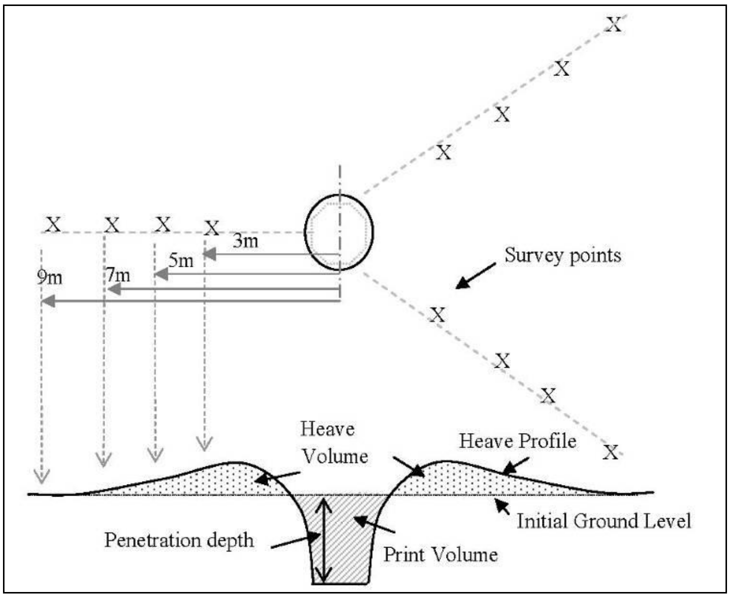

Figure 13: Typical Configuration of Heave / Penetration Test

The survey stations were monitored prior to the commencement of the heave/penetration test and then generally after every 4 blows, up to a maximum of 40 blows. In addition, the diameter of the resultant crater was monitored.

The results of the monitoring and testing of dynamic compaction being carried out using a drop weight of 20 tonne and a drop height of 23m, can be summarised as follows:

- The results of the heave / penetration testing show a decreasing interaction between drop locations as the grid spacing is increased from 4.2m to 6.0m;
- The extensometer results also show a decreasing interaction between drop locations as the grid spacing increases from 4.2m to 6.0m;
- The extensometer results showed a decrease in the depth of influence of the dynamic compaction process with increasing grid spacing; and,

- The density test results show a higher density recorded for a grid spacing of 4.5m, which decreases slightly with an increasing grid spacing.

Based on the results of the trial, and the monitoring it was concluded that a grid spacing of 4.5m had sufficient interaction between drop locations and the required density criterion was achieved.

Using the formulae presented by Poran and Rodriguez (1992) and the results of the dynamic compaction trial, relationships have been established between parameters *j* and *k*; and between parameters *l* and *m*; which are as follows:

$$j = 3.410k - 1.25 \tag{3}$$

$$l = 3.410m - 5.55 \tag{4}$$

The relationships presented above are different to those postulated by Poran and Rodriguez (1992). The main difference identified is that the dataset supporting the work done by Poran and Rodriguez (1992) was predominantly derived from work on cohesionless fill. The data set could be correlated with data of similar soil types in order to refine the work carried out thus far.

Based on the results of the extensometer monitoring assessing the depth of influence of the dynamic compaction process, should be a function of the grid spacing, as well as the drop height and pounder weight. Based on the result presented herein, the following is recommended as a revised equation for assessing the depth of influence of dynamic compaction:

$$D = 0.58(WH)^{1/2} - 1.3(S - 4.5) \tag{5}$$

where D = Depth of Influence (m)
W = Pounder Weight (tonnes)
H = Drop Height (metres)
S = Grid Spacing (m)

The experience in the auto route projects A71 and A72 in Germany [17] show that mainly large starting grid spacing is necessary to reach larger depth of compaction. In order to reach a homogeneous block of compacted soil the number of phases has also to the size of starting and finishing grid. Test at the A72 project in silty soil shows that 3 phases reach up to 8 m deep, 4 phases 10-12 m deep and 5 phases like in the figure below reach around 15 m deep. The final grid after 5 phases of compaction was only 3.5 m.

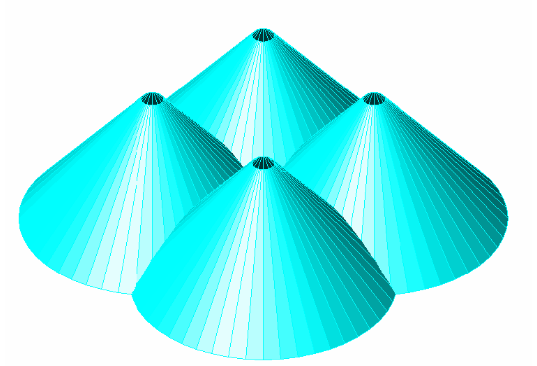	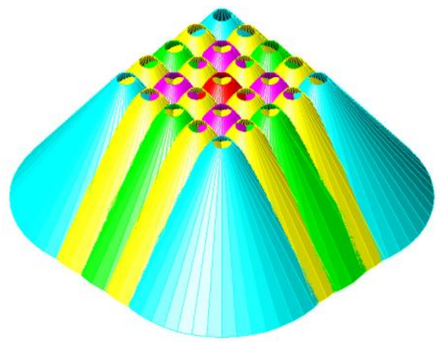
1. phase: DYNIV grid : 14 · 14 m energy: 1050 t·m	5. phase: DYNIV grid: 3.5 x 3.5 m energy: 500 bis 700 t·m

Figure 14: First and fifth phase of dynamic compaction idealized shaded in A71 project[17]

4.3. The Effect of Different Tamper Geometries on the Dynamic Compaction of Sandy Soils (Nazhat and Airey, 2012 [27])

This paper reports the results of a series of 2-D dynamic compaction experiments that have investigated the effect of the tamper shape on the response of the underlying granular soils using high-speed photography.

Flat, conical, shell and convex shaped tampers have been used. Each tamper shape has been dropped on two soil types, uniform sand and a sand-silt mixture. The photographic data are used to evaluate the effect of the shape of the tampers on the compaction efficiency, depth of improvement and the internal densification mechanism. The results indicate the different tamper shapes lead to significant differences in the magnitude of densification and depth of improvement, and reveal unique patterns of propagating shock waves.

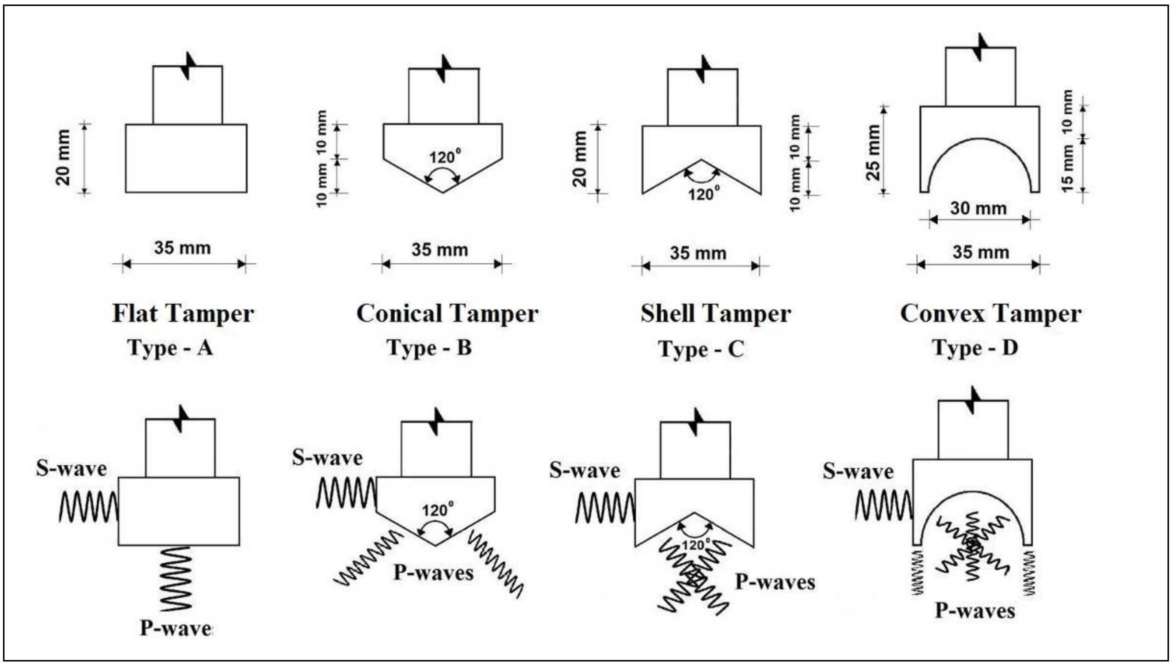

Figure 15: Geometries of studied tampers and directions of their anticipated body waves

High speed photography and DIC have been used to characterise the response of two types of soil to dynamic compaction using four different tamper profiles. As a quantitative tool, digital high speed photography has allowed the propagation of localised deformation and strain fields to be identified and has suggested that compaction shock bands control the kinematics of dynamic compaction. The results have revealed distinctive internal densification mechanisms that depend on the tamper geometry and the type of target soil.

The direct applicability of the results may be limited by the small scale and low stress levels in the model tests, however, they indicate that the response of soil to dynamic compaction is likely to be strongly influenced by the soil type and tamper geometry. The results show that there are significant differences in the extent and magnitude of the compacted zone at depth, and suggest that there may be significant benefits from considering different tamper shapes in future field studies. It was found that no single tamper shape performed well across both soil types investigated.

This paper reports the results of a series of 2-D dynamic compaction experiments that have investigated the effect of the tamper shape on the response of the underlying granular soils using high-speed photography.

Flat, conical, shell and convex shaped tampers have been used. Each tamper shape has been dropped on two soil types, uniform sand and a sand-silt mixture. The photographic data are used to evaluate the effect of the shape of the tampers on the compaction efficiency, depth of improvement and the internal densification mechanism. The results indicate the different tamper shapes lead to significant differences in the magnitude of densification and depth of improvement, and reveal unique patterns of propagating shock waves.

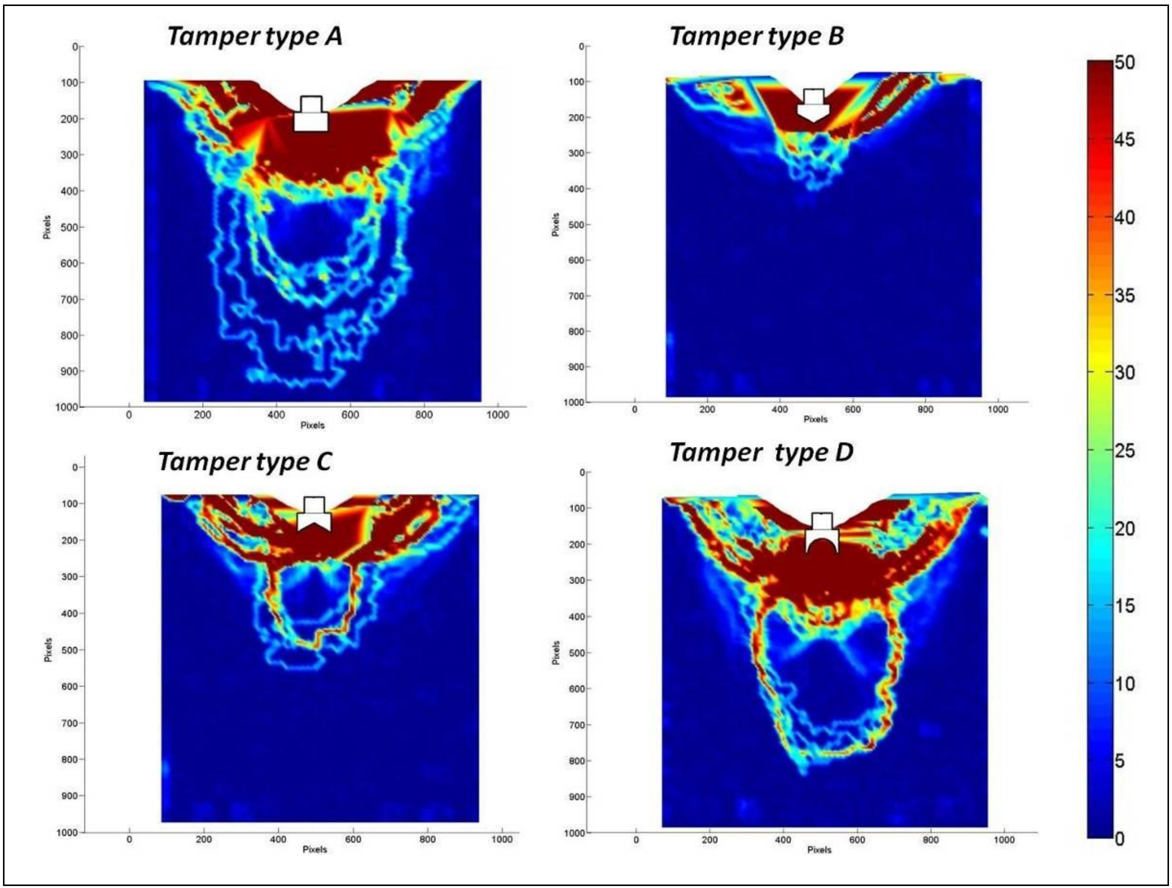

Figure 16: Total Shear Strain at end of 6 impacts on dry sand models using four types of tampers

The high speed photography fits well to the coloured models. Finally the interesting results have to be validated in large scale tests. Furthermore the high speed photography could be calibrated with field test where we have other and better knowledge. The knowledge about tamper shapes before these article was for instance, that we have the best experience with round tamper shapes at the bottom, because we can get them easier out of cohesive soils.

4.4. Lessons Learned from Millions of Square Metres of Ground Improvement (Hamidi and Varaksin, 2012 [28])

Ground improvement can be applicable to projects of any size; however there are certain delicacies that necessitate special attention when ground treatment is implemented in large size projects.
Regardless of the project size and all other conditions, constraints and parameters the intended ground improvement method should suit the problem. Any one ground improvement technique is not suitable and applicable to all ground conditions.
The adoption of suitable acceptance criteria is probably almost as important as selecting the appropriate ground improvement technique itself, and unsuitable criteria can erroneously fail or pass a treatment programme.

Acceptance criteria can be envisaged to be in three main forms based on quality of work, minimum test values or directly on design criteria (Hamidi et al, 2011a).

The authors name several large scale projects, here shortly repeated one using the MARS technology:

Al Quoa'a is a remote and isolated desert township on the border of the United Arab Emirates and Oman (Hamidi et al, 2010d). The second phase of Al Quoa'a, consisting of 450 two floor villas and associated infrastructure has been constructed on a site with an area of more than 3.8 million m^2. As shown in Figure 17, the dune hills were cut and dumped into the lower level areas to provide a level platform. The maximum depth of the fill was 28 m.
CPT results indicated that the ground in the cut areas was satisfactory enough to support the structures and infrastructures, but the dumped dune sands in the fill areas were in a loose state and except for the

upper 2 m, cone resistance, q_c, was in the range of 2 to 4 MPa. PMTs that were later carried out as part of the post ground improvement programme indicated that limit pressure, P_l, was in the range of 0.1 to 0.5 MPa. Sieve analyses of the dune sand showed that the soil was poorly graded fine clean sand, and groundwater was not observed down to the maximum testing termination depth of about 30 m.

Figure 17: Backfilling and construction of the working platform by dumping

It was understood by the project's designers that in addition to settlements originating from structural loads, the very young fill could have also been subject to settlements under its own weight, or to subsidence due to vibration or washing and densification of material.

Ground improvement was deemed as a possible solution for the treatment of the very loose fill, and consequently a design and construct project was awarded to a specialist geotechnical contractor who had proposed dynamic compaction. Although original acceptance criteria were based on minimum q_c values, alternative acceptance criteria based on design bearing capacity, acceptable settlements and elimination of self weight creep were proposed and approved.

As bearing capacity, load induced and creep settlements can all be calculated using PMT (Menard, 1975), this testing method was chosen for verification of results. P_l is also a suitable characteristic for evaluating soil creep. Thus, acceptance criteria as shown in Tables 1 and 2 were approved. It is the author's opinion that acceptance criteria could have been further optimised if acceptance was only agreed and approved to be based on design criteria.

Table 4: Acceptance criteria for villa areas

Criteria for Villa Areas	Safe bearing	Self bearing
Thickness where parameters prevail	-0.75 to-5.50 m RL	From -5.50 m RL
PMT limit pressure	750 kPa	600 kPa
Menard Modulus	4.8 MPa	4 MPa

Table 5: Acceptance criteria for non-villa areas

Criteria for Non-Villa Areas	Safe bearing	Self bearing
Thickness where parameters prevail	From ±0.00 m RL	From ±0.00 m RL
PMT limit pressure	600 kPa	600 kPa
Menard Modulus	4 MPa	4 MPa

A total of 6 rigs were used for this10 month long project. Utilizing heavy duty cranes could have provided sufficient lift capacity to treat about one half of the project; however the remaining areas were deeper than what could have been treated by such equipment and specialised rigs including the specially designed Menard 700 t.m rig were mobilised to perform deeper treatment by dropping 25 ton pounders. These rigs were able to treat up to about 90% of the site. The innovative MARS (Menard Accelerated Release System) technology was developed and patented to drop a 35 ton pounder in actual free fall (Figure 18).
Dynamic compaction energy was optimised based on the treatment thickness and acceptance criteria. MARS and special rigs were used for the first phase treatment of the deep fill areas. Heavy duty cranes were used for the treatment of subsequent phases of those areas and the remaining zones.

250 PMT were carried out at the site. For comparison purposes, 50 tests were carried out before dynamic compaction, and the remaining 200 tests were performed after the works. Depth of testing was based on the fill thickness and depth of dense in-situ soil. Figure 19 shows P_l values before and after dynamic compaction in four locations.

Figure 18: MARS automated drop and grab system

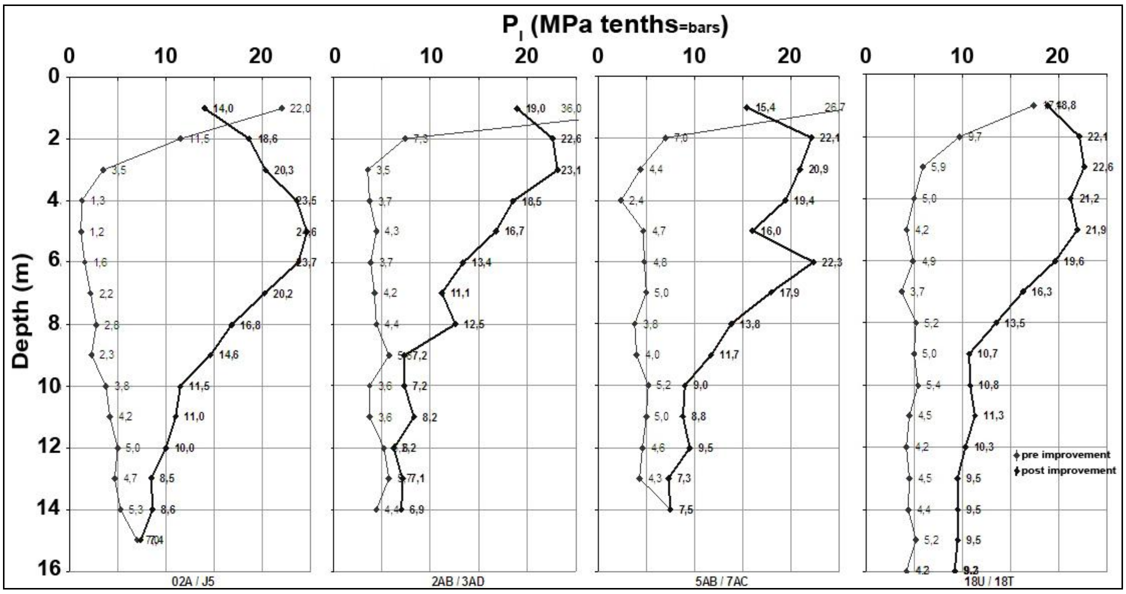

Figure 19: PMT limit pressure before and after dynamic compaction at 4 locations

To the knowledge of the authors Hamidi and Varaksin, the 5.6 million m^2 King Abdulla University of Science and Technology (KAUST) project, located in Rabigh on the coast of the Red Sea, is the world record for the number of dynamic compaction/dynamic replacement rigs working at the same time on a single project. Ground improvement was carried out basically over a period of 8 months using a total of 13 rigs working two shifts per day. A review of the treatment rates shows that at its peak, about 600,000 m^2 of ground was treated in one month.

The investigation and further testing during the works indicated that more than 2,600,000 m^2 of the construction area was to be built on soil consisting of up to 9 m of loose silty sand or soft sandy silt (locally called sabkah).

As groundwater level was less than 1 m below in-situ ground level it was decided to raise the ground by about 3 m to be safely above high tide. Approximately 1 to 1.5 m of this granular fill was placed before ground improvement.

Only a well worked out schedule that incorporated design and construction could have met the project's deadline. However, the problematic soil posed as a serious obstacle to this programme as it was not possible to design the foundations without finalisation of the buildings' locations and architectural drawings.

The design and construct ground improvement proposal that met the project manager's technical requirements, schedule and budget was based on the below design criteria:

- Footing location: Any place within the treatment area
- Maximum footing load: 1,500 kN
- Allowable bearing capacity: 200 kPa
- Maximum total settlement: 25 mm
- Maximum differential settlement between two adjacent footings: 1/500
- Liquefaction mitigation for an earthquake with PGA= 0.07g
- Level: 0.8 m below final ground level, but in any case at least 2 m above sabkah level

The construction method was a combination of dynamic compaction and dynamic replacement.

Dynamic compaction energy was optimised based on the treatment thickness and acceptance criteria. MARS and special rigs were used for the first phase treatment of the deep fill areas. Heavy duty cranes were used for the treatment of subsequent phases of those areas and the remaining zones.

250 PMT were carried out at the site. For comparison purposes, 50 tests were carried out before dynamic compaction, and the remaining 200 tests were performed after the works. Depth of testing was based on the fill thickness and depth of dense in-situ soil. Figure 19 shows P_l values before and after dynamic compaction in four locations.

4.5. MARS experience and advantages in Europe

The new German express highways A71 and A72 described in [17] cross special risky areas with collapse sinkholes. The reason at the A71 is the natural geology with karst cavities explained by the following figure.

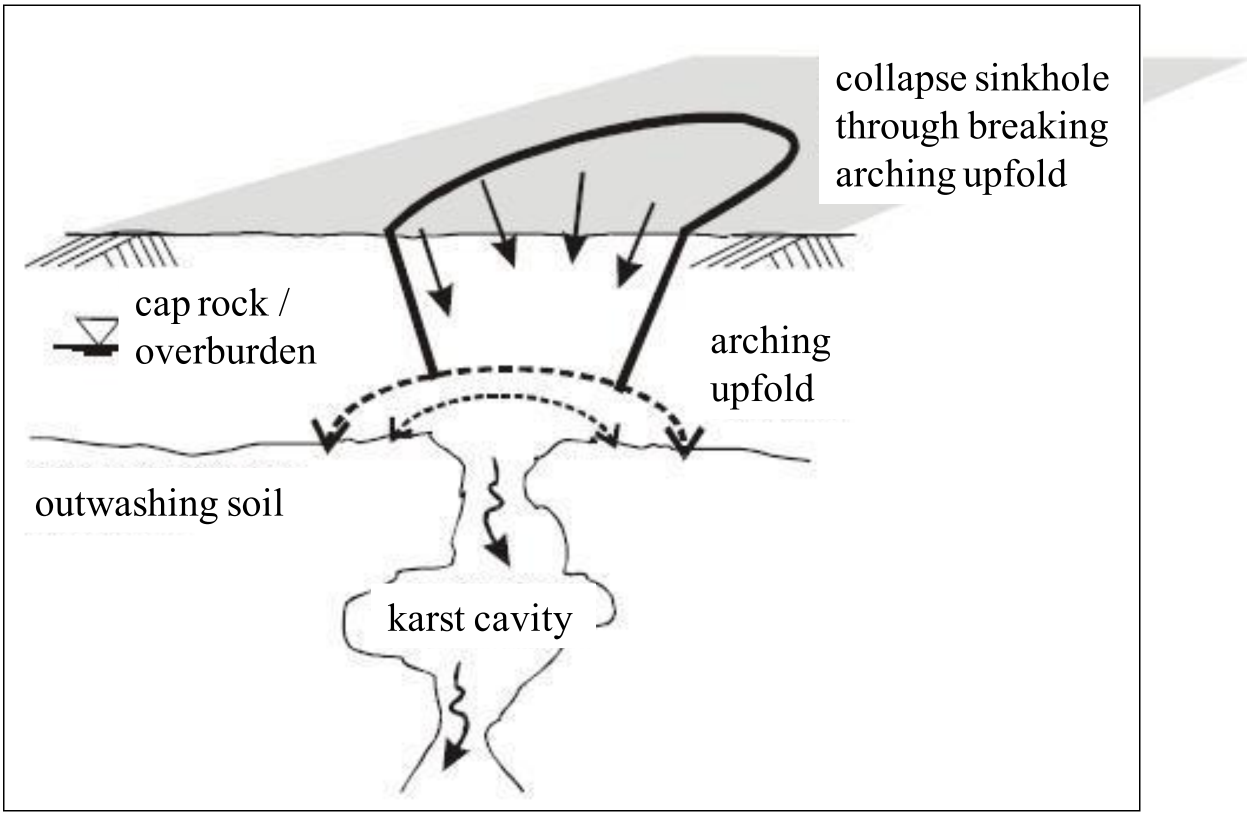

Figure 20: Collapse sinkhole through breaking arching upfold above karst cavities

Photo 5: The karst cavity with more than 5 m diameter was found during earth works at A71 project[17]

In express highway A72 collapse sinkholes find their reason in former subsurface mining. The sinkholes shown in the following photos at A72 are almost smaller than the natural sinkholes.

Photo 6: Collapse sinkholes with 2-3 m diameter and depth due to former subsurface mining at A72 [17]

In these two cases of German express highways the innovative MARS (Menard Accelerated Release System) technology was used the first time in Europe. It was a question security:

- The MARS system was installed outside the dangerous areas on a Liebherr 895 HD crawler. Due to security reasons of the crane the first compaction phase was only by one 1050 tm free fall blow beside the other 14 m ahead from the crane.
- The security of the highway is given by the special high MARS energy taking more than the future dynamic live loads ahead.

The following picture sequence illustrates a 35t pounder falling free from 30 m height.

Photo 7: MARS automated drop and grab system working at A71 site with 35t from 30 m height [17]

The innovative MARS (Menard Accelerated Release System) technology was developed in the desert to reach maximum depth by higher energy.
Large visitor groups followed the energy test at the A72 project: Two crawler cranes (one traditional dynamic compaction crane in the back and the MARS technology in the front of the following photo) were brought in position and it was measured and visible for all visitors: The MARS fall was much faster. The back calculations of the field tests demonstrate that between 30 % to 40 % more energy it activated by the MARS technology compared with dynamic compaction on the same crawler crane.

Photo 8: Field tests at A72 demonstrate between 30 % to 40 % more energy with the MARS [17]

5. RELATIVE NEW COMPACTION METHODS WITH LOW VIBRATION

Vibroflotation and dynamic compaction work with strong dynamic shear waves. The vibrations can be measured and the measurement defines the necessary distance to existing structure. In most cases the necessary distance varies between 10 and 50 m and depends mostly from buildings (to be protected), energy and frequency used for compaction and water level.

Going clothe to existing structure requests sometimes vibration free technique and in the field of compaction there are not many techniques, what go deep with low vibrations. The Japanese article is the only one, who considers such a method beside the traditional sand piles and the earthquake experience. This was the reason to put this article together with compaction grouting under this theme of compaction methods with low vibration.
Both methods use the displacement technique for compaction. It is important to know, that displacement in such kind of granular soils is difficult without vibration. Furthermore displacement with low vibration (only low, because the machines produce vibrations due to their tracks) also produces shear forces (but less than the dynamic methods), which are necessary for compaction.

The Japanese technology has the advantage of using drainage material. This is important in earthquake regions and here the theme of vibration free technique is extended towards the theme of earthquakes.

5.1. Compaction Grouting

The Ménard Compaction Grouting [20] is a pressure grouting technique, with the primary objective to densify the surrounding soils. Compaction Grouting is per formed by pumping a cement mortar under pressure through the tip of a drilling tool to displace laterally and densify the surrounding soil over apredetermined volume, resulting in a global compaction of the soil. The Compaction Grouting Columns are vertical cylinders of a viscous low-slump grout. By sequencing the grouting work during the controlled continuous extraction of the tool, a grout column is formed with -in the densified surrounding soils.

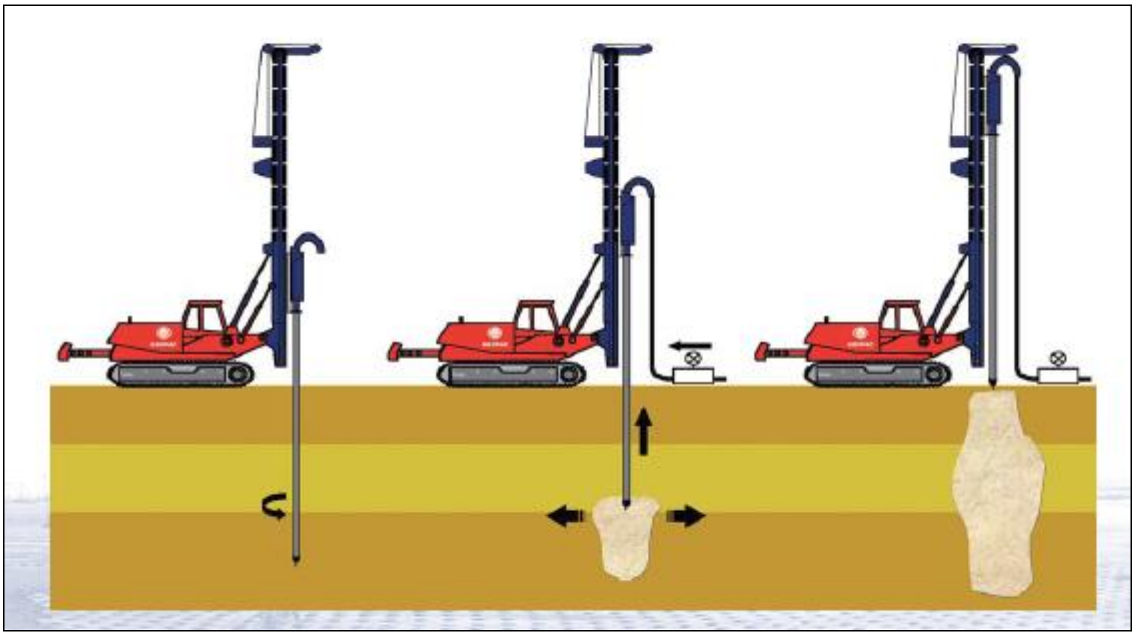

Figure 21: Ménard Compaction Grouting [20]

A global improvement of a volume of compressible soils requires sequencing the grouting work into a series of primary, secondary and even tertiary grid locations.

Implementation and methods Drilling using a displacement auger produces an initial lateral displacement of the soil over the volume of the auger (typically smaller than 280 mm). During the extraction phase, a secondary compression is achieved by pressure injection of a highly viscous low slump cement mortar, combined with a time controlled extraction of the injection tool.
Compaction grouting columns are generally performed on a square grid pattern to allow for multiple grouting phases which would be more complex with triangular grids. With the first phase grouting

locations, the surrounding soil is first stabilized. Subsequent phases (installation of the compaction grouting columns installed in the following sequence: A, C, D, B – see following sketch) result in a more homogeneous densification effect.
The speed of withdrawal of the tool is controlled to avoid soil fracturing (formation of large cracks in the soil, enlarged by the pressure grouting). The final diameter of the column and the densification improvement are dependent on the initial compressibility of the soils. For Compaction Grouting, a highly viscous cement mortar mix with very high friction angle is recommended. The grout mix is made of sand, cement and cementitious fines (slag, fly ashes,…), water and chemical admixtures (retarders, plasticizers,…). The mix is rich in sand and cementitious fines to get a well graded grain size distribution.

Impressive Compaction Grouting Pilot test reports can be found [20] Fos Cavaou - Gas Terminal (FRANCE).
A pilot test area is recommended at the beginning of each Compaction Grouting project to select/validate the following parameters:
- Optimal grout mix depending on locally available aggregates;
- Define maximum pressure and injection parameters;
- Select the replacement ratio required to obtain the design improvement;
- Optimize the method of performance of the treatment: grid of installation for each phase, volume of grout per column and grouting parameters (speed, pressure...);

Ground improvement can be assessed by in situ testing as CPT with measurement of the pore pressure (piezocones or CPTU). The requirements for the mix properties are:
- The grout shall be pumpable under high pressure;
- Injection shall not induce soil fracturing;
- The grout shall not prematurely lose its free water which would prevent an efficient expansion of the injected volume.

The required replacement ratio and densification are controlled by carefully monitoring the volume of grout incorporated in the soil with depth. Data recording of the drilling and grouting parameters provides an efficient quality control tool. Compaction Grouting is classically used to densify loose sands for liquefaction mitigation for the following reasons:
- Compaction Grouting increases the relative density of sandy soils;
- Compaction Grouting increases the horizontal coefficient of earth pressure at rest K0;
- Compaction Grouting induces aging of the soil by low amplitude shear deformation.

Compaction Grouting is used to stabilize and improve compressible soils, including for liquefaction mitigation. It is not necessary to improve the whole length of the columns. A selective treatment limited to compressible layers can be achieved. The technique is vibration free, creates no apparent damage to surface layers and can thus be performed in close vicinity of sensitive structures. Compaction grout columns can also be used as vertical reinforcement elements similar to Rigid Inclusions.

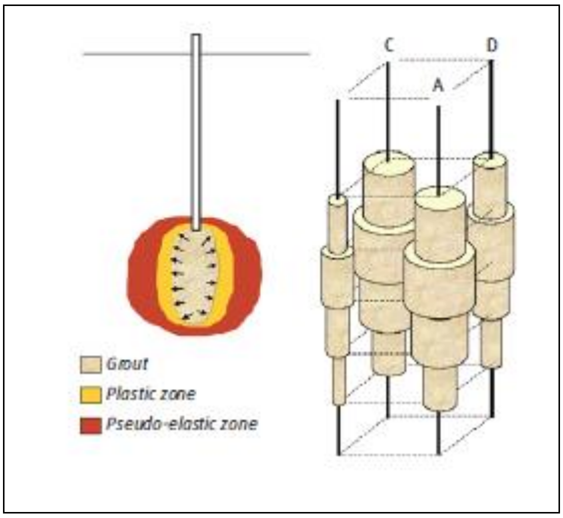

Figure 22: with compaction grouting it is not necessary to improve the whole length of the columns

5.2. Sand Compaction Pile Technology and its Performance in both Sandy and Clayey Grounds (Kinoshita et al., 2012 [29])

Sand Compaction Pile (SCP) technology has been developed in Japan since the 1950s and has been widely applied to various structures on both clayey and sandy grounds (as liquefaction mitigation). The SCP method has both vibratory system with vibro-hammer and non-vibratory system with forced lifting/driving device. In both cases, the necessary reaction force for the forced lifting/driving device comes from the total equipment weight, and the sprocket or pinion gear is rotated by a hydraulic motor. The operating procedure for the non-vibratory SCP method, shown in Figure 23, is discussed below and is identical to that adopted in the conventional SCP method. A 400~500 mm diameter casing pipe is used to create well compacted sand piles of 700 mm diameter and as a result, the surrounding ground is densified.

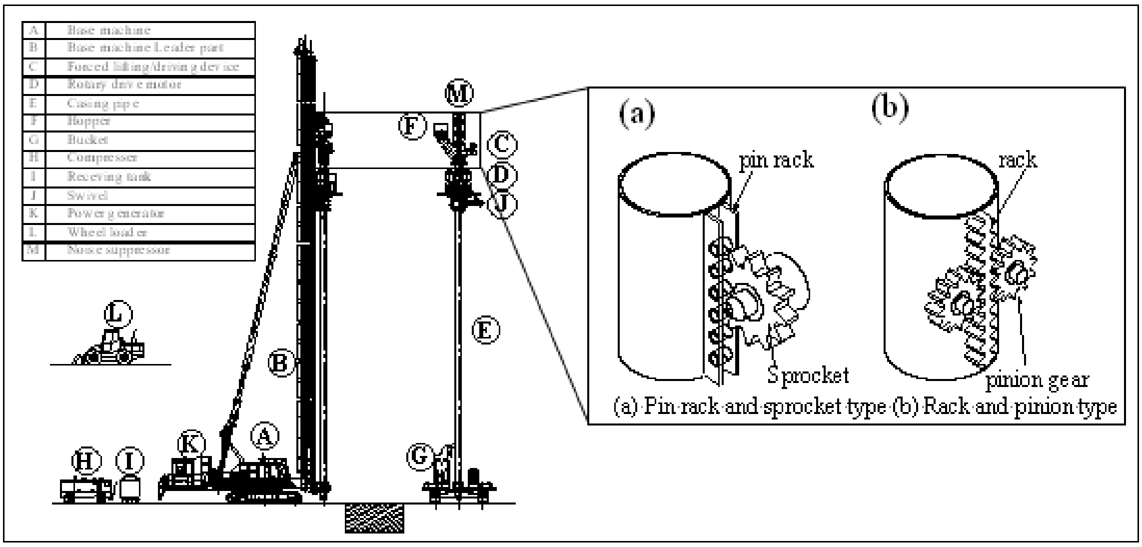

Figure 23: Non-vibratory SCP equipment and main components of forced lifting/driving device

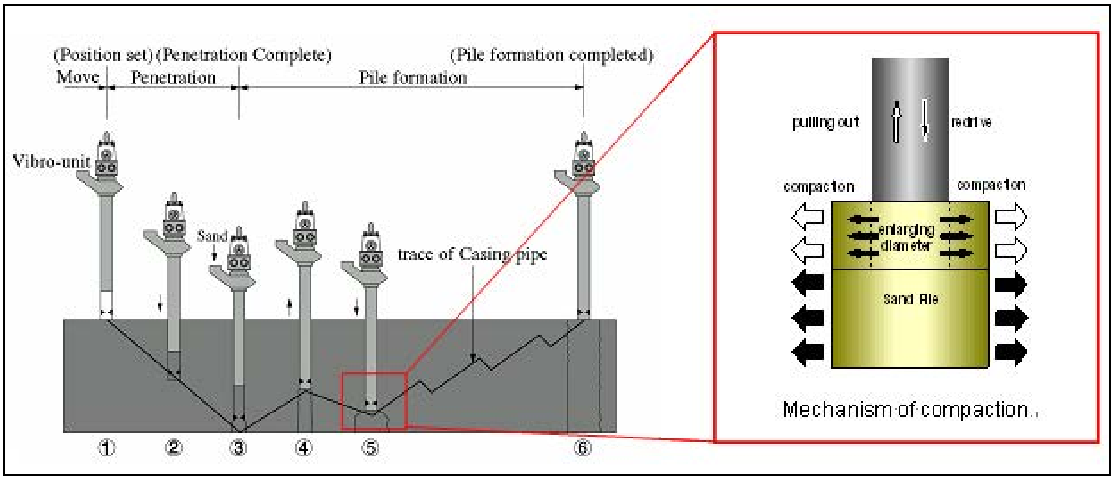

Figure 24: Operating procedure of non-vibratory SCP method

To summarize, the features of the SCP method are as follows:

(1) Strong sand pile with consistent diameter is possible to be installed even with using top vibrator and vertical vibration sequence.
(2) SL-gauge system which has been developed in Japan is able to secure uniform diameter sand pile installation.
(3) Top vibrator system has lot of advantages, such as sand and other material can be used, and addition of water is not necessary during installation.
(4) SCP method has also a non-vibratory system using forced lifting/driving device.

Moreover, results of cases where various instruments (e.g., pressuremeters and dilatometers) were used to measure the lateral stresses before and after implementation of both vibratory and non-vibratory SCP methods are presented in Figure 8. In the figure, the relation between the lateral stress ratio, K_C, and replacement ratio, a_s, are plotted 1 month and 2 years after the SCP operation. Note that the data points corresponding to improvement ratio a_s=0 refer to the condition prior to the implementation of SCP method. It can be observed that substantial increase in K_C–values(also in sandy ground) is observed 2 years after implementation, with larger increase in K_C values occurring at higher a_s.

CASES WHERE IMPROVEMENT EFFECT OF SCP METHOD HAS BEEN VERIFIED IN INTENSE EARTHQUAKES

Figure 25 shows the epicenter locations and characteristics of the 1974 Miyagiken-oki earthquake and seven other large-scale earthquakes which occurred later, including the 2011 Tohoku Pacific earthquake, and gives information on the performance of SCP-improved ground as a result of these earthquakes. As the figure shows, there has been no report of major disruption to structures erected on SCP-compacted ground, thus confirming in a qualitative sense the validity of compaction-type ground improvement. The following are some representative cases of ground improvement performance related to important structures.

Figure 26 shows a standard section of the Kushiro West Port that was affected by the 1993 Kushiro-oki Earthquake (Yamada et al. 1990). At this location, countermeasures to resist earthquakes, mostly compaction by the vibratory SCP method, were implemented in the ground behind the quay walls. In areas adjacent to steel structures, gravel drain method was adopted to avoid any negative effects of vibration or displacement from the improvement work. SPT N-values in areas between sand piles in the compaction-improved areas were around 20~30. The maximum horizontal acceleration recorded at the Kushiro Port Construction Office, located about 1.5 km from the quay walls, was 470 gal but no damage due to the earthquake was observed, and port activities resumed the day following the earthquke. However, in unimproved grounds within the same wharf area, large cracks appeared in quay walls (approx. 10 cm wide, 20 cm vertical offset) and the quays could not be used.

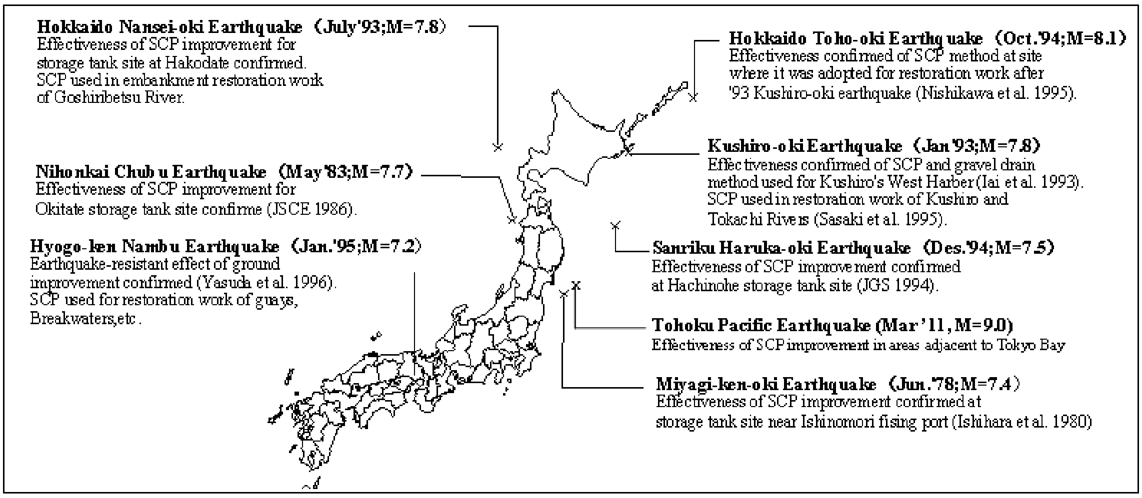

Figure 25: Recent intense earthquakes and information gained on ground improvement performance

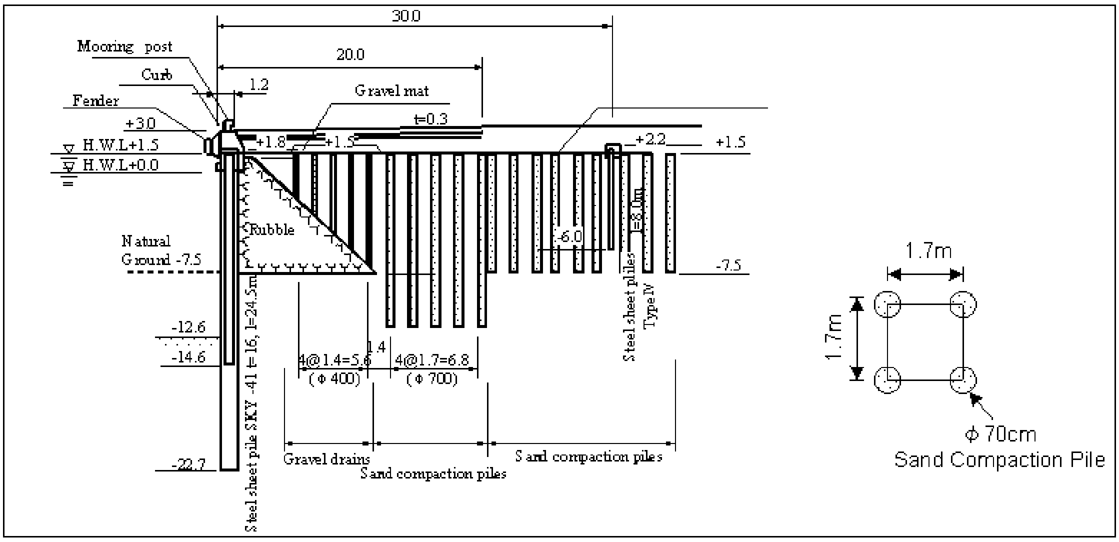

Figure 26: Standard section of revetment

Large scale liquefaction occurred in the two man-made islands, Port Island and Rokko Island, in the Kobe Port area as a result of the 1995 Kobe Earthquake. For structures in both islands, various types of ground improvement were undertaken as measures to accelerate consoliation settlement in the alluvial clay layer due to excess weight, and to increase the bearing capacity of the landfill soil layer. In the improved sections, there was little damage caused by settlement etc. as compared wit h the damage in unimproved areas. Figure 13 shows the measured post-earthquake settlements of the buildings with pile foundations in the areas of improved grounds. In both islands, 40-50 cm settlement occurred in the unimproved areas, but in the areas improved by compaction methods, including SCP, the settlement was negligible (Yasuda et al. 1996).

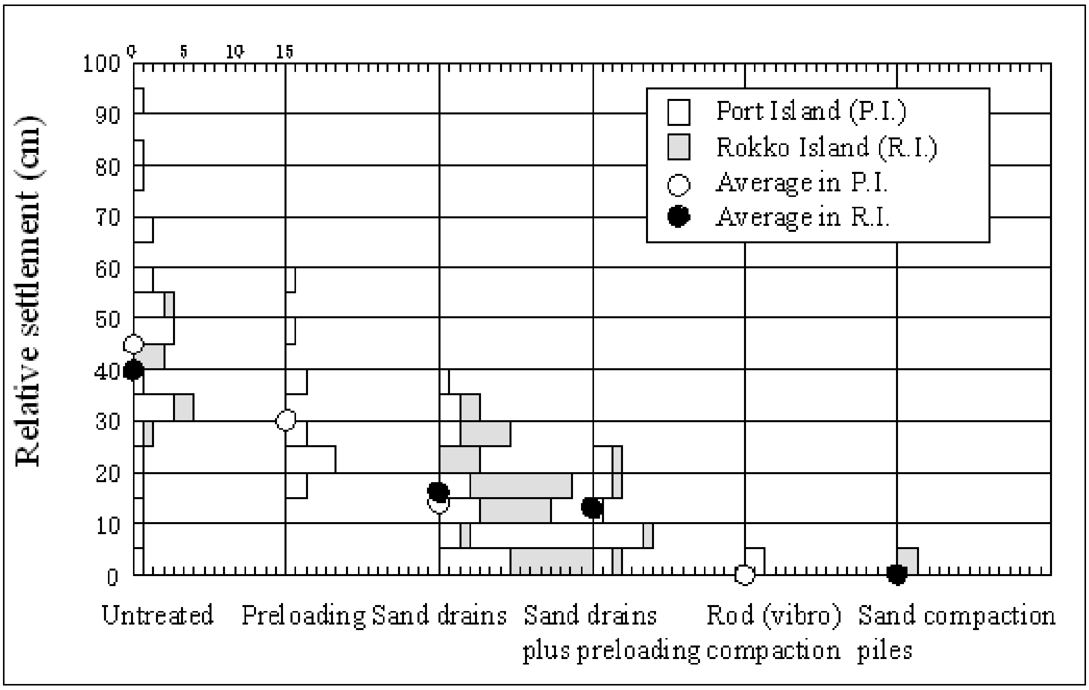

Figure 27: Relative settlement and methods of ground improvement Buildings with pile foundation)

Following the 11 March 2011 Tohoku Pacific Earthquake (M_w 9.0), liquefaction was observed in many areas adjacent to Tokyo Bay, about 390 km from the epicentre, as shown in Figure 15. Manholes were uplifted, grounds settled, and buildings and bridges were damaged as a result of liquefaction.

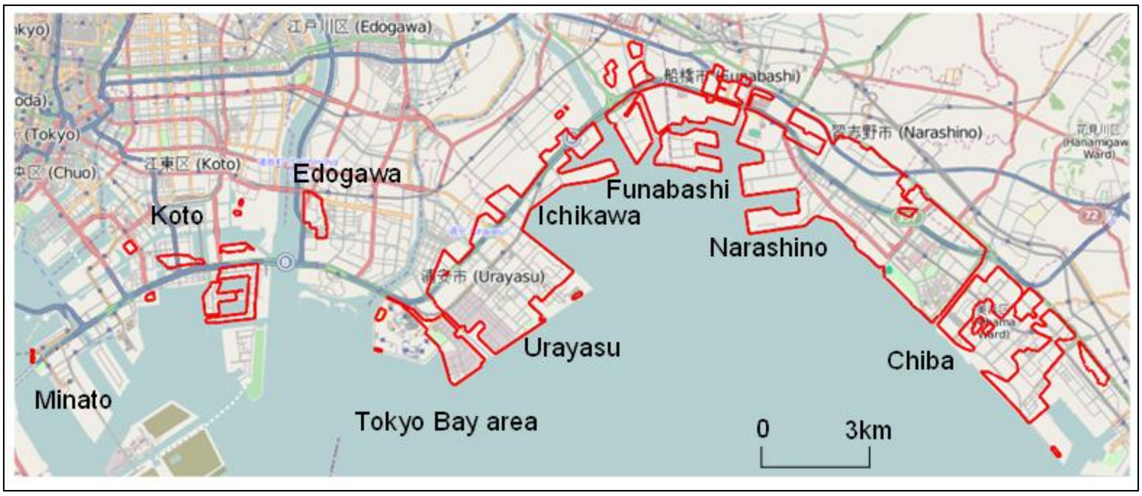

Figure 28: Liquefied zones along Tokyo Bay (Ishikawa et al, 2011)

A medical center building is located in reclaimed land along the Tokyo Bay as shown in Photo 9. The building is 5 stories high and supported by piles. After the liquefaction assessment, it was judged that there is a high potential for liquefaction and consequently, non-vibratory SCP was adopted at this site as a countermeasure against liquefaction. The improvement specification is square arrangement with pitch of 1.5m (a_s=16.7%) and the length of the pile is 12m. In the surrounding area of the improved site, gravel instead of sand was used to dissipate the excess water pressure from liquefied area. The effectiveness of this method was verified for a building in Rokko Island during the 1995 Hyogo-ken Nambu Earthquake. As shown in Photo 1, although liquefaction-induced damage was observed outside the improved area, no damage was observed within the improved area.

There was no damage on the improved area during the 2011 Tohoku Pacific Earthquake. This showed that the improved ground by SCP method is effective not only against intense earthquakes such as the 1995 Hyogo-ken Nambu Earthquake but also against earthquakes having long duration time. A qualitative understanding of these factors and analyses should be undertaken in future studies.

Photo 9: Successful ground improvement in Tatsumi area

6. IMPACT COMPACTION CLOSER TO SURFACE

6.1. Rapid Impact Compaction

Photo 10: Typical machine of rapid impact compaction [20]

Due to [20] Rapid Impact Compaction was originally developed in the early 1990' s in the United Kingdom and is a safe controlled compaction technique where dynamic energy is imparted by a falling dropweight dropping from a controlled height onto a circular foot assembly.
Energy is transferred to the ground safely and efficiently as the foot remains incontact with the ground at all times and eliminates the risk of flying debris. Its base carrier is a track-mounted excavator, which provides the dual benefit of allowing improved mobility and site accessibility and it gives the versatility to move about in narrow and limited height spaces, such as within existing warehouses.

Compared to regular Dynamic Compaction, high frequency compaction provides for better efficiency at lower vibration levels, allowing for work in close vicinity with existing structures. At 30m the peak particle velocities have been measured to vary from 1.2 to 5mm/sec. Vibrations will vary with material type, and will increase as the degree of compaction achieved increases. Site results indicate that without site specific testing, a safe working distance to structures can be on the order of 5 to 6m. At that distance, noise levels are lower than 90 dBA. The Rapid Impact Compactor employs an on-board computer to control impact set termination criteria, and to record critical data. Acquired data at each impact point include: total energy input, total penetration, and penetration of final set.

6.2. Ground improvement tank terminal Amsterdam - The Netherlands (Dijkstra and Nooy van der Kolff, 2012 [30])

The site investigation revealed that underneath a single tank the thickness of the compressible layers could differ up to 3 meters. The initial ground improvement design proposed by the client consisted of the application of dynamic replacement (DR). The accompanying design made by the client consisted of dropping a 12.5 ton weight 4 times from a height of 6m in a grid of 3.5m by 3.5m. A trial showed that the traditional DR method as well as the CDC (Cofra Dynamic Compaction) technique with a hammer of 9 – 16 t with drop height of 1.2 m did not achieve sufficient improvement.

First the soil conditions (found only after the test?) were really difficult for DR and absolutely impossible for CDC.

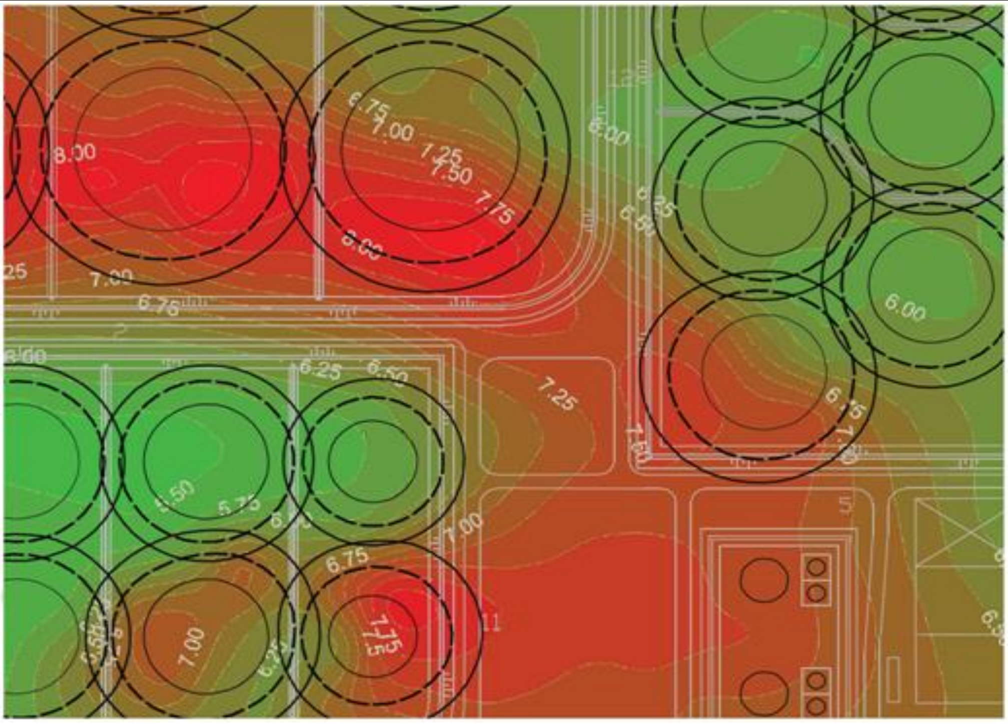

Figure 29: Interpolated bottom of the compressible peat and clay layer from the CPT information

The explained reasons for the fault are the following: The water was quite close to the surface in the upper sand layer and the Interpolated bottom of the compressible peat and clay layer in Figure 1 goes up to 7.75 m deep. The article decribes well the limits of fines and water contend, which are relevant to this technique.

A specialist in DR would add that

- higher energies above 20 t x 15 m = 300 tm
- with much more blows (up to 40 per print),
- additional vertical drains
- in combination with a distance of around 1.5 to to the water table

are necessary to reach and improve the soft soils. The following Photo 11 [17] is a 7 m deep print of the dynamic replacement DR.

Photo 11: DR print 7 m deep, diameter more than 2 m at the A72 [17] motorway

With a new design in the Amsterdam project the water was lowered not to perform real DR but in order to excavate of compressible layers underneath the sand layer up to 8 m deep. The soft soil was replaced with dredged North Sea sand. Of course this sand, with a fines content of about 0%, compacted much better than the local sand with fines content above 10% using similar compaction energy. With settlements of 0.3 to 0.5 m the CDC shows in one CPT dense conditions in the clean North between 1 and 7 m below the initial surface. These values on substituted sand would also have been reached with a simple and light DC (Dynamic compaction).

It has to be said, that 7 m compaction depth with CDC is the limit depth of this method is only possible in clean sands.
With the right investigation and soil improvement technique in the beginning of the project the large and expensive excavations up to a depth of 8 meters below the surface, removing more than 1,000,000m3 of material could have been avoided.

There are other companies on the market, who say that their technique is suitable in lose (that means granular) materials in order to bring them in medium dense conditions.

The limits in depth are the following:

1. Stones and sand:	limit 5 to 7 m deep
2. Sand with fines (maximum 10 to 15 %):	limit 3 to 5 m deep
3. Mixed soils 5% < fines smaller than 0,063mm < 40%:	limit 3 to 5 m deep

Our experience gives a border of compactions with this method at 15 % fines – not higher.

6.3. Quantifying the Zone of Influence of the Impact Roller (Jaksa et al., 2012 [31])

Rolling dynamic compaction (RDC) involves traversing the ground by means of a non-circular module consisting of 3, 4 or 5 sides. Significant and quantifiable improvement with the roller is approximately 2.1 m below the ground surface and this corresponded to soil stress readings of between 150 and 200 kPa. Positive pressure readings due to RDC were also measured by the EPCs buried up to 3.85 m below the ground surface, indicating that the actual zone of influence (for which there is improvement) extends beyond this depth.

The sentence "modern RDC speed of 12 km/h is fast compared with 4 km/h using traditional rollers (Pinard 1999) and the technique reaches deeper far deeper than conventional static or vibratory rolling (Clegg & Berrangé 1971, Clifford 1976, 1978), which is generally limited to depths of less than 0.5 m." can be updated by [1] other modern surface compaction machines.

The in situ testing included dynamic cone penetration testing in the form of the Perth penetrometer, sand replacement field density tests and the spectral analysis of surface waves (SASW) geophysical technique. In order to classify the soil and quantify its compaction characteristics, laboratory testing was undertaken which involved standard and modified Procter compaction tests, particle size distribution and Atterberg limits tests. In addition, earth pressure cells (EPCs) were installed at different depths to measure dynamic pressures induced by RDC.

The Atterberg limits tests and the particle size distributions suggest that the soil is a well-graded sand (SW) with some clay fines of low plasticity.

Extrapolating the trend line obtained from the data shown in this figure, it can be estimated that the effective depth for 8 passes is approximately 1.3 m (i.e. 8 passes of the impact roller will achieve a dry density ratio of 95%, provided that the layer thickness does not exceed 1.3 metres).

Photo 12: Rolling dynamic compaction modules: (a) 4-sided (Broons), (b) 3-sided (Landpac), (c) 5-sided (Infratech)

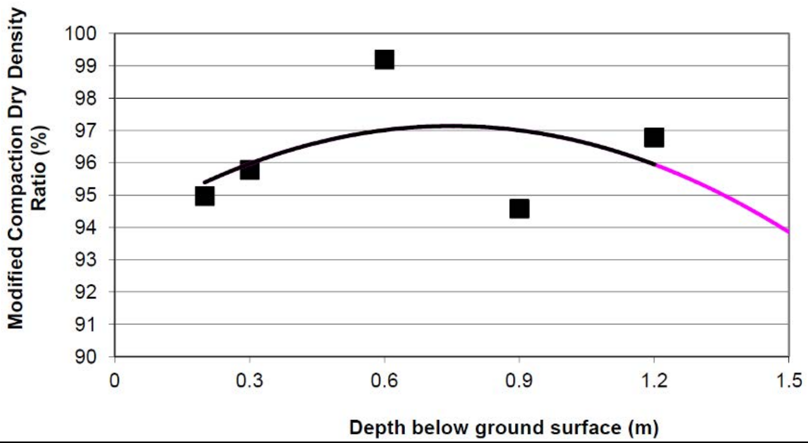

Figure 30: Modified dry density ratio versus test depth (8 passes of the impact roller).

Figure 32 shows a summary contour plot of peak pressure imparted by the impact roller with depth after 16 passes of the impact roller. It can be observed that the highest pressure readings recorded (> 200 kPa) are located in the upper 2 m; supporting other test data that suggests most of the quantifiable ground improvement occurs within this zone.

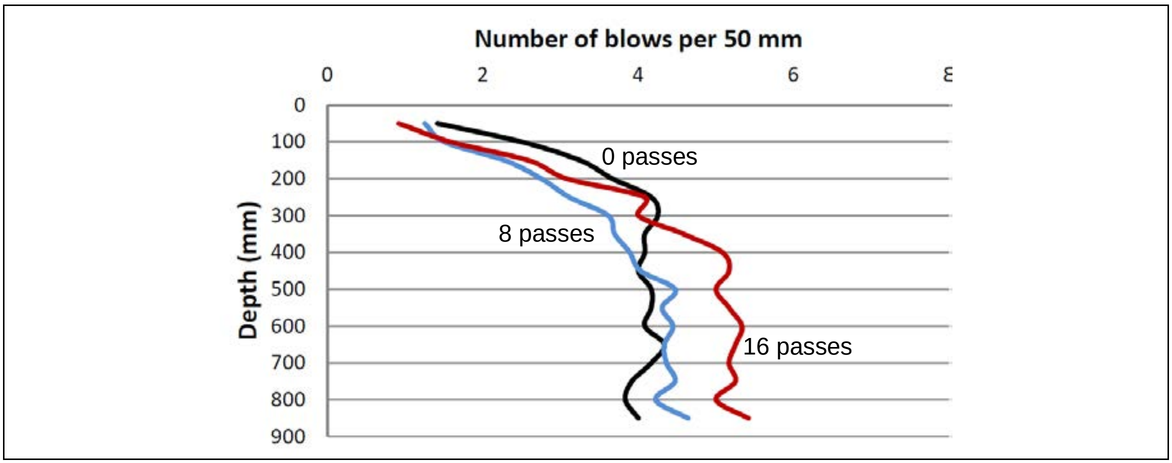

Figure 31: Results of dynamic cone penetrometer tests

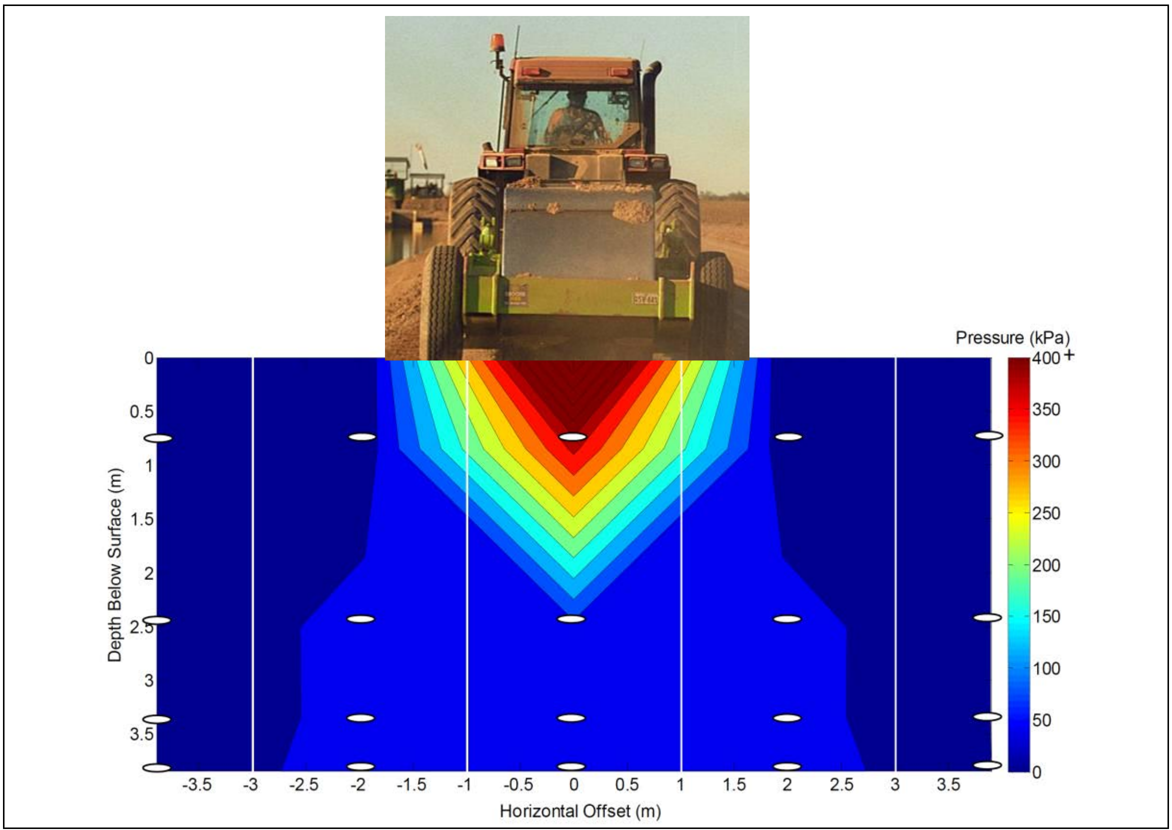

Figure 32: Pressure contours with depth after 16 passes in plane perpendicular to direction of travel

With the test results there is a large difference in the compaction success between 8 and 16 phases with a 4-sided impact roller. It is interesting to know, if the roller starts each phase exactly at the same position and if the starting position plays an important rule with the results especially with a low number of phases.

The plot of pressure shows, that if we want to reach deeper than 1-1.5 m it is necessary to drive up to 16 times in lines of around 1 m distance. The efficiency in m² per 8 h shift would be interesting maybe compared with traditional rollers. The question how to compact the upper 30 cm keeps open till the last article. The main reason for such condition is likely that the confining pressure acting on sands at shallow depths is small so that ground vibration generated by compaction tends to loosen up the previously compacted sands.

6.4. Laboratory study of disc rotation for densification of loose sands (Feng, 2012 [32])

Thin layer of loose sands near the ground surface is likely unavoidable as a result of vibratory or impact compaction. In developing a method for densification of such loose sands, the disc rotation method was examined in the laboratory with a test tank of 600-mm in diameter and two discs of 150-mm and 200-mm in diameter.
Rotation of the disc induces shear stress on sand particles and causes them to rearrange so that a denser state may be achieved. Significant factors involved in the disc rotation operation include static vertical pressure on the disc, amplitude of disc roration, and accumulated angle of disc rotation.
Experiences show that, after ground improvement by vibratory compaction method, dynamic compaction method, and sand compaction pile method of dynamic nature, loose sands are commonly found near ground surface.

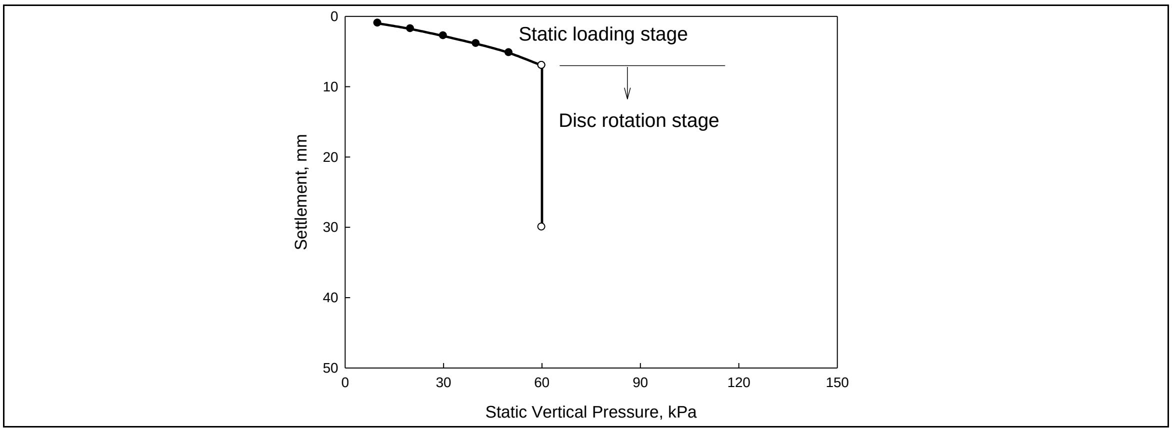

Figure 33: Illustration of static vertical pressure-settlement relationship from the disc rotation test

The tests with to diffferent sands are only 150 mm deep. Before disc rotation operation, the specimen was prepared to have an initial relative density of 50%. The obtained test results show that, under only 50 ~ 70 kPa of static pressure, the disc rotation method can increase the relative density of loose sands to about 70 ~ 85%.
Interisting can be the messurement of settlements only due to the influence of vibartion in the test box. Futhermore interesting are test with deeper sample (up to 30 cm) as well outside of te lab with large practical machines.

7. SUMMARY AND CONCLUSIONS

In the future independent web based toolkits will help the planning engineers with a good overview and selection of the right technique. Even with this support personal experience with the different soils and technique are necessary. A simple vibro compaction can bring difficulties in the evaluation of the results when the tests are done to early afterward the work. In the fast modern building process enough time for investigations and successful compaction has to be planned. In the content of nearly vibration free technique the borders of well compacted areas are obviously by cruel earthquake in Japan. The dramatic damages visualize the big tasks of the technique even compacting vibration free close to structure.
The general report starts with the oldest vibroflot, nowadays going up to 63 m deep in one example. The dynamic compaction possibly can be optimized with new tamper shapes and grids. The testing of MARS shows a big success bringing security with higher energies and equivalent deeper influence. Compaction techniques with low vibration are described. Clother to surface Rapid Impact Compaction as well as impact rollers reach with the right grain size and number of compaction phases interesting compaction depth.

8. ACKNOWLEDGMENTS

This general report is based on the interesting articles send to the international symposium, well collected and prepared for download in the intranet by volunteers in the organizing committee. As well we have to thank the authors of the articles for their work.
The general reporter would like to acknowledge the efforts of CDM Smith and Ménard Group upon which the articles are added.

REFERENCES

[1] *Chu, J., Varaksin, S., Ulrich, K. and Mengé, P. (2009),"Construction Processes, State of the Art Report", 17th International Conference on Soil Mechanics and Geotechnical Engineering, TC17 meeting ground improvement, Alexandria,Egypt.*

[2] *Eurocode 8 (2005) Design of structures for earthquake resitance – Part 1 : General rules, seismic actions and rules for buildings. The European Standard EN 1998-1.*

[3] *Menard, L., Broise, Y., 1975, "Theoretical and Practical Aspects of Dynamic Compaction", Geotechnique 25, No 1, March pp 3 – 18.*

[4] *Moyle, R., Redman, P G., 2009, "Optimization of Dynamic Compaction Processes – A Case Study", Ground Improvement Technologies and Case Histories, December 2009, Singapore, pages 739 – 746.*

[5] *Poran, C. J., Rodriguez, J. A., 1991, "Design of Dynamic Compaction. Canadian Geotechnical Journal", Vol 29, pages 796 – 802.*

[6] *Clegg, B., Berrangé, A. R., 1971," The development and testing of an impact roller", The Civil Engineer in South Africa, 13(3), 65–73.*

[7] *Clifford, J. M., 1976, "Impact rolling and construction techniques", Proc. ARRB Conf., Vol. 8, 21–29.*

[8] *Clifford, J. M., 1978, The impact roller – problems solved, The Civil Engineer in South Africa, 20(12), 321–324.*

[9] *Slocombe, B.C., Bell, A.L. and Baez, J.I. (2000) The densification of granular soils using vibro methods. Geotechnique, 50(6), pp 715-725.*

[10] *Robertson. P.K., Campanella, R.G., Gillespie, D., and Greig, J., (1986). "Use of Piezometer Cone data", In-Situ'86 Use of In-situ testing in Geotechnical Engineering, GSP 6 , ASCE, Reston, VA, Specialty Publication, pp 1263-1280.*

[11] *Fellin, W., 2000, "Rütteldruckverdichtung als plastodynamisches Problem", A.A. Balkema*

[12] *Julio A. Ramirez, 2012, "THE GEORGE E. BROWN, JR., NETWORK FOR EARTHQUAKE ENGINEERING SIMULATION (NEES): REDUCING THE IMPACT OF EARTHQUAKES AND TSUNAMIS ON SOCIETY, 9th International Conference on Urban Earthquke Engineering (9CUEE) an d4th Asia Conference on earthquake Engineering (4ACEE) proceedered at the Center for Urban Earthquake Engineering, Tokyo Institue of Technology, Japan*

[13] *Meyer, F., Breitsprecher,G., Dennhardt M., Glaesener U,2012 „Gründung einer 7,5 MW Windenergieanlage auf der Kippe eines ehemaligen Tagebaus",Vorträge zum 19. Darmstädter Geotechnik-Kolloquium Symposium Baugrundverbesserung in der Geotechnik, Heft Nr. 92 page 31-42*

[14] *Professor, Structural Engineering, School of Civil Engineering, Purdue U., NEES Chief Officer and NEEScomm Center* [*Directorramirez@purdue.edu*](mailto:Directorramirez@purdue.edu)

[15] *Chaumeny, J.L.; Hecht, T.; Kirstein, J.F.; Krings,M.; Lutz, B., 2008, Dynamische Intensivverdichtung (DYNIV®) für die Kreuzung eines aktiven Erdfallgebietes im Zuge der Bundesautobahn BAB A 71. VERÖFFENTLICHUNGEN des Grundbauinstitutes der Technischen Universität Berlin, Heft 42, Berlin*

[16] *ISO/FDIS 22476-4:2009, 2009, Geotechical investigation and testing – Field testig – Part 4: Ménard pressuremeter*

[17] *Kirstein, J.F., Krings, M., Prangen, A., Siemund, P., 2010, „Dynamische Intensivverdichtung (DYNIV®) für die Überbauung in Streckenabschnitten mit schwierigen Baugrundverhältnissen im Zuge der Bundesautobahnen BAB A71 und A72“, Symposium Baugrundverbesserung in der Geotechnik, Veröffentlichung des Institutes für Geotechnik der Universität Siegen Eigenverlag D. Adam, R. Herrmann Siegen*

[18] *Kirstein, J.F., Ahner, C., Uhlemann,S, Uhlich, P. 2012, "Ground improvement methods for establishment of the federal road B 176 on a new elevated dumb in the brown coal area of MIBRAG ", ISSMGE - TC 211 International Symposium on Ground Improvement IS-GI Brussels*

[19] *http://www.kellergrundbau.de/de/Ingenieure-und-Architekten/Ueber-Keller/Geschichte-und-Tradition__26/*

[20] *http://www.geopac.ca/*

[21] *Schaefer, V., Berg, R, Douglas, S.C, .2012, "SHRP 2 R02 : Geotechnical Solutions for Transportation Infrastructure - A Web-based Toolkit", ISSMGE - TC 211 International Symposium on Ground Improvement IS-GI Brussels*

[22] *Colin J. Serridge, 2012, Vibro Ground Improvement Techniques – A UK Perspective, ISSMGE - TC 211 International Symposium on Ground Improvement IS-GI Brussels*

[23] *C. H. Wong, C.H., Yeo, K.C., Yung, S.H., Liu, S.J., 2012, "Effects of Fines on Vibro-compaction" and article "Stone Column and Vibro-compaction of Soil Improvement for liquefaction", ISSMGE - TC 211 International Symposium on Ground Improvement IS-GI Brussels*

[24] *Jimenez, R.; Roman, F, Garcia-Gutierrez, J.M., 2012, 3.4., "A comparison of soil improvement achieved using different vibro methods", ISSMGE - TC 211 International Symposium on Ground Improvement IS-GI Brussels*

[25] *Brûlé , S., Javelaud , E., 2012, "Soil dynamic response after ground improvement by heavy dynamic compaction or vibrocompaction", ISSMGE - TC 211 International Symposium on Ground Improvement IS-GI Brussels*

[26] *Moyle, R-, Turner, R., 2012, "Assessment of Grid Spacing for Dynamic Compaction", ISSMGE - TC 211 International Symposium on Ground Improvement IS-GI Brussels*

[27] *Nazhat, Y., Airey, D., 2012, "The Effect of Different Tamper Geometries on the Dynamic Compaction of Sandy Soils", ISSMGE - TC 211 International Symposium on Ground Improvement IS-GI Brussels*

[28] *Hamidi, B., Varksin, S., 2012, "Lessons Learned from Millions of Square Metres of Ground Improvement", ISSMGE - TC 211 International Symposium on Ground Improvement IS-GI Brussels*

[29] *Kinoshita, H., Harada, K., Nozu, M., Ohbayashi, J., 2012, "Sand Compaction Pile Technology and its Performance in both Sandy and Clayey Grounds", ISSMGE - TC 211 International Symposium on Ground Improvement IS-GI Brussels*

[30] *Dijkstra, J.W., Nooy van der Kolff, A.H., 2012, "Ground improvement tank terminal Amsterdam - The Netherlands", ISSMGE - TC 211 International Symposium on Ground Improvement IS-GI Brussels*

[31] *Jaksa, M.B., Scott, B.T., Mentha, N.L., Symons, A.T., Pointon, S.M., Wrightson, P.T., Syamsuddin, E., 2012, "Quantifying the Zone of Influence of the Impact Roller ",ISSMGE - TC 211 International Symposium on Ground Improvement IS-GI Brussels*

[32] *Tao-Wei, F., 2012, "Laboratory study of disc rotation for densification of loose sands ",ISSMGE - TC 211 International Symposium on Ground Improvement IS-GI Brussels*

SESSION 2 - VERTICAL DRAINS, VACUUM CONSOLIDATION & PRELOADING

General Report
SESSION 2 – VERTICAL DRAINS, VACUUM CONSOLIDATION & PRELOADING

Buddhima Indraratna
Centre for Geomechanics and Railway Engineering,
Faculty of Engineering,
University of Wollongong, NSW, Australia, indra@uow.edu.au

1. INTRODUCTION

Due to the rapid increase in population, and the subsequent industrial and construction boom, especially in the urban and coastal regions, many countries have intensified the inevitable need for developing infrastructure on problematic soils, including soft compressible clays and deposits with low bearing capacities. Moreover, good quality geological materials for construction are also becoming scarce, a problem exacerbated by the numerous environmental constraints imposed in various countries. Because of these reasons, and environmental restrictions on certain public works, ground improvement has now become an integrated and essential component of infrastructure development. Consequently, civil engineers are forced to utilise even the softest and weakest of natural deposits for foundations, and therefore, the application of ground improvement techniques, including preloading and consolidation, vacuum consolidation, among other methods, have now become common practice in heavy construction.

There are 8 papers allocated to this Technical Session, composed of 25 Authors and co-authors from 5 countries.

This General Report attempts to offer a review of the majority of papers that have made significant contributions, but due to its imposed brevity, not all the papers could be reviewed and commented on in detail. Nevertheless, brief comments on all papers have been provided, as warranted, to provide a balanced overview of the entire Technical Session. Most papers elucidate already established technologies, but provide greater insight into the processes, supplemented with well compiled field and laboratory data. While a few papers have drawn on modified theoretical concepts, most papers presented field studies, including comparisons between predictions and observations, as warranted.

The following part of the Report describes the contributions to this session in relation to vertical drains and vacuum consolidation.

2. SOFT CLAY CONSOLIDATION WITH VERTICAL DRAINS

There are 8 articles in this section. This category of papers describes the consolidation process with time, with very useful information on field data, laboratory testing, analytical formulations and numerical modelling, including some reference to the comparison of observed data with consolidation predictions.

Indraratna et al. (2012) analysed case histories from Australia using schemes that combined PVD and vacuum preloading. The theory of equivalent 2D consolidation gives almost the same settlement-time curves as the true 3-D analysis, as shown in Fig. 1 (source Fig. 9). It also shows that a relative high vacuum pressure of up to -70 kPa can significantly decrease the required fill height and achieve a desirable degree of consolidation exceeding 95%. They also show that for these normally consolidated soft clays, the modified Cam-clay parameters are sufficient to predict the settlement, pore pressures and lateral displacements with acceptable accuracy.

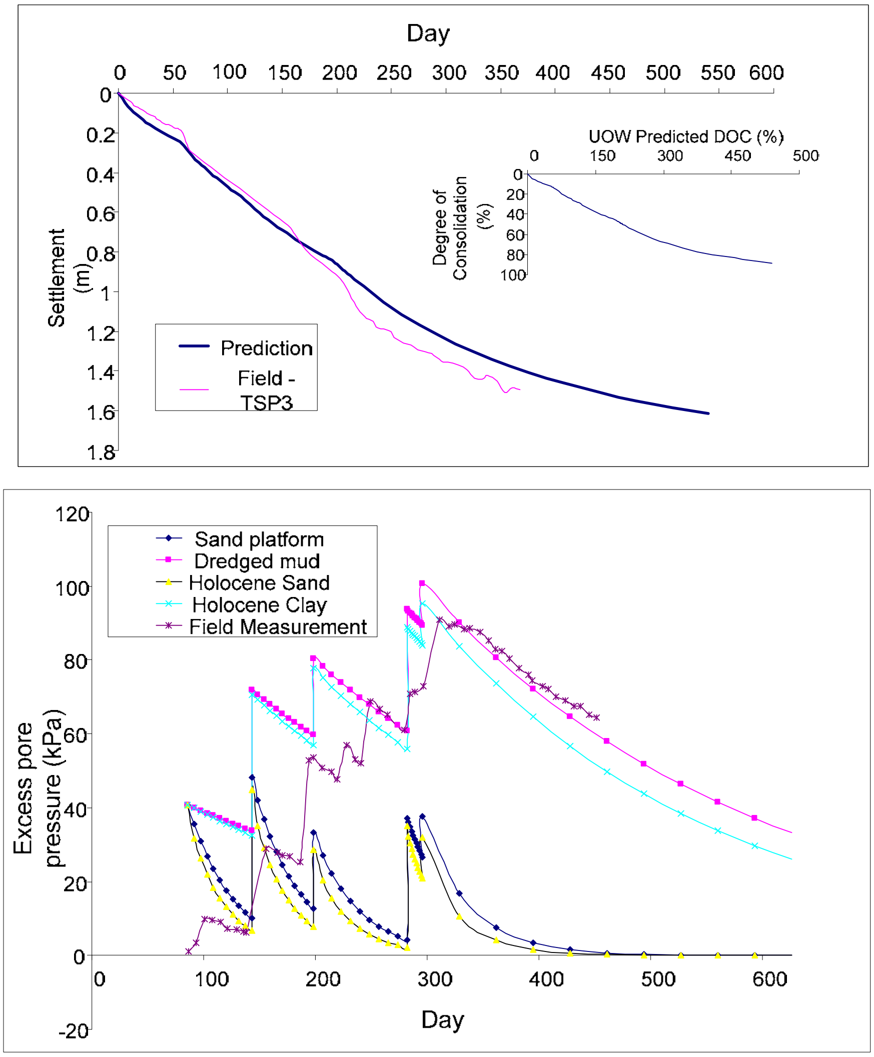

Figure 1: (a) Settlement; and (b) excess pore water pressure predictions and field data for a typical settlement plate location. (Source: Fig. 9, Indraratna et al. 2012)

Rujikiatkamjom and Indraratna (2012) proposed a radial consolidation model using a piecewise technique to investigate the smear effect in layered soil. The effects of permeability of the penetrating upper layer of soil on the underlying layer are discussed in terms of the degree of consolidation. The intrusion of the upper layer into the underlying layer creates an additional zone where the remoulded permeability of this zone can be increased or decreased depending on the initial permeability of the upper layer. In the intrusion zone located in the lower layer, the change in permeability can be divided into 3 distinct zones, including (a) a smear zone due to the upper layer of soil being dragged down, (b) a smear zone due to the underlying soil being remoulded, and (c) an undisturbed lower layer of soil (Fig 2, source Fig 3). The piecewise-linear technique has been considered to be an appropriate approach to determine the effect of soil dragdown on overall consolidation. An array of design procedures with an example already worked out illustrates the role of down-dragged soil.

Kirstein and Wittorf (2012) analysed a case history in Germany where a stone column was used. In order to deal with dump soil, a very comprehensive site investigation was carried out. A technical and economic optimisation was achieved by an additional investigation of the soil using a Ménard pressure meter, and then adjusting the ground improvement methods to the respective sections. The high quality of construction with stone columns, and dynamic replacement and CMC-columns was documented not only in the foundation with the usual manufacturing protocols, but also tested regularly during construction phase with a Ménard pressure meter. The stone columns were 10 to 15 m deep. The improved soil characteristics were determined in relation to the stresses, according to Figure 3 (Source Fig. 6): by the load below the maximum height of the dam, where there was a big improvement in the characteristic values than on the parts with lower stresses, and where a less optimal angle of friction by installed gravel was taken into account. Large shear tests were used to check the friction angle of the gravel.

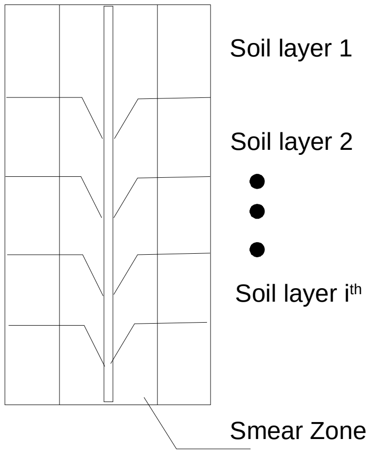

Figure 2: Down drag effects due to mandrel installation in layered soil (Source: Fig. 3, Rujikiatkamjorn and Indraratna 2012)

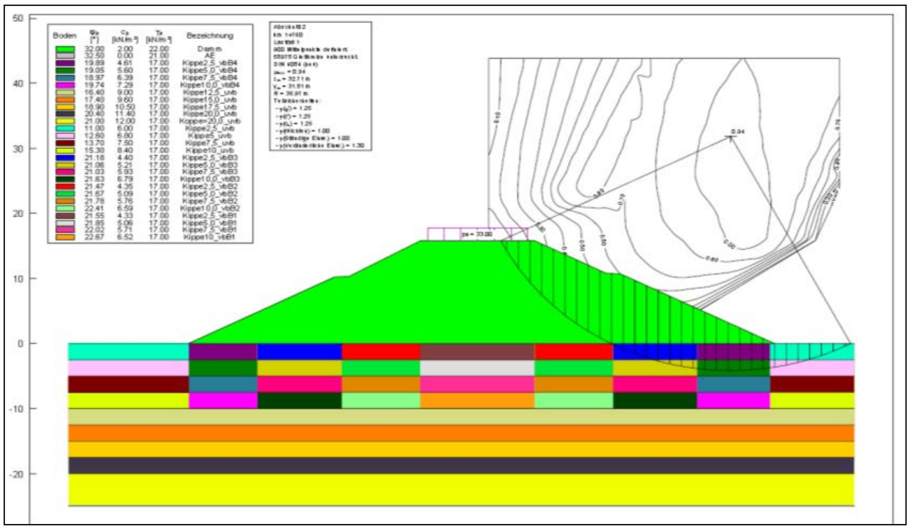

Figure 3: Stability analysis taking stress-dependent soil parameters into account (Source: Fig. 3, Kirstein and Wittorf 2012)

Kirstein et al. (2012) investigated the effect of wick drain consolidation as a soil improvement method in very soft clay and fat northern German clay (Figure 4, Source: Fig. 1). The example from Germany consisted of a new road crossing with 1.5 to 7.0 m high dams alongside the Danish border, where very soft clays were found 13 to 20 m below sea level (Figure 5, Source: Fig. 2). The undrained shear strength of the clay varied between 7 and 20 kN/m², the water content was almost 100 % and the organic matter below 6 %. A consolidation coefficient $C_v < 0.3$ m²/year revealed a significant fat clay which required long settlement time or a small grid of vertical drains for consolidation. From the stability calculations, the smallest grid of vertical drains were placed 0.5 m apart in part of the highest dam, which was built in three load steps, each of which required from 60 to 80 % consolidation before the next step could be loaded. The first 1.29 m of total settlements were calculated in the area west of the bridge with the following timeline of primary and secondary consolidation according to Figure 6 (Source: Fig. 5). Even using 600 kN/m geogrids totaling around 150 cm vertical settlements, around 20 cm horizontal deformation in each direction were measured throughout one year of monitoring. The stability calculations were based on C_u and required three steps of loading with beams and waiting twice for a sufficient degree of consolidation. The control results of the final stability analysis based on phi´, C´ and pore water pressure showed that the calculations based on undrained shear strength Cu were on the safe side. The settlement calculation had to be repeated according to the stability analysis with a fitting consolidation process in each of the three load steps. The measured settlements during consolidation in Figure 7 (Source: Fig. 7) fit the predictions given in Figure 8 (Source: Fig. 8). With a detailed planning of the steps in the workflow, the correct predictions, and a monitoring system fitted, economic soil improvement techniques can be combined with deep foundations in one project, and even very soft soil can be treated successfully.

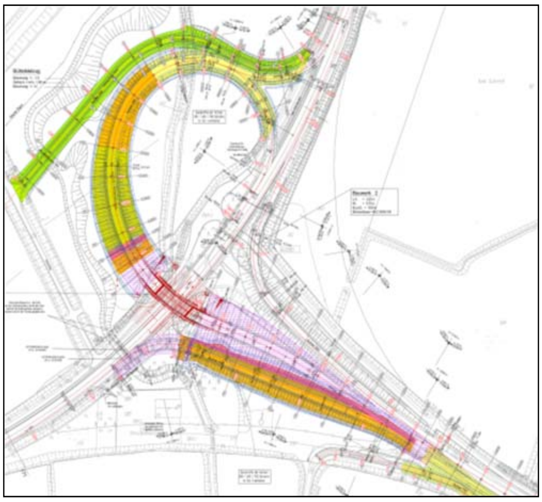

Figure 4: project overview: crossing highways B5 and B202 (CMC close to bridge and coloured areas with vertical drains and preloading) (Source: Fig. 1, Kirstein et al. 2012)

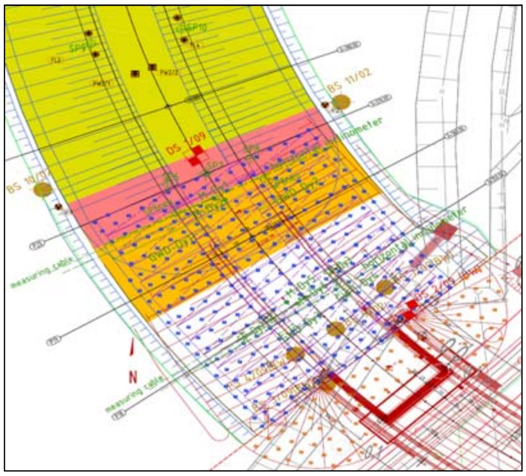

Figure 5: detail of the highest dam west with the bridge abutment over the highway B5 (CMC close to bridge and coloured areas with vertical drains and preloading) (Source: Fig. 2, Kirstein et al. 2012)

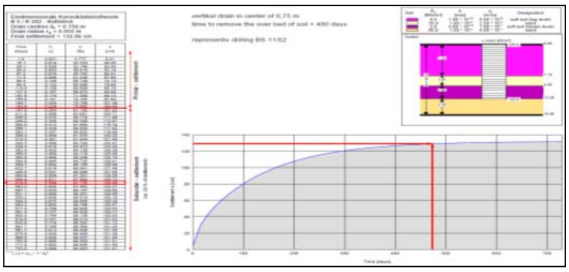

Figure 6: ½ year of primary consolidation even with vertical drains in a grid of 0.75 m (Source: Fig. 5, Kirstein et al. 2012)

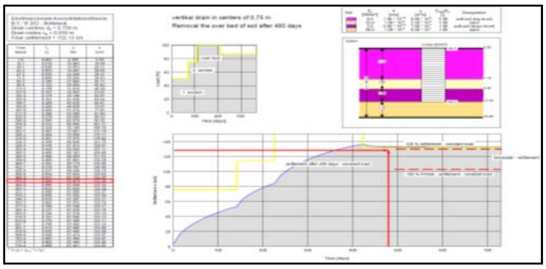

Figure 7:settlement calculation with consolidation time and degree of the three loading steps (Source: Fig. 7, Kirstein et al. 2012)

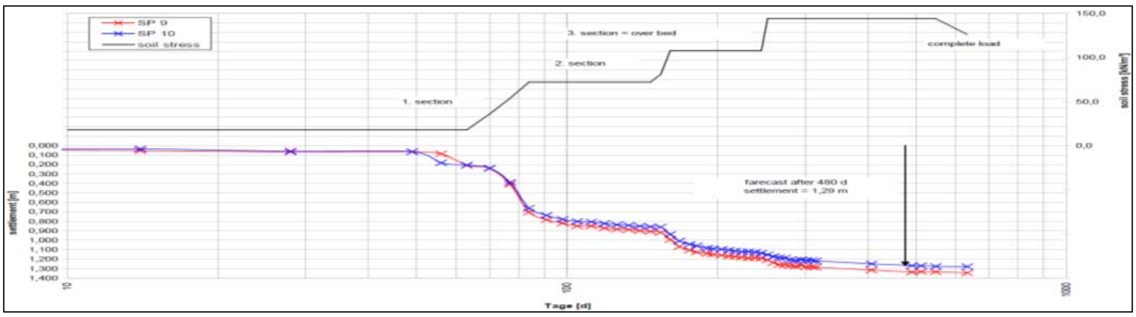

Figure 8: Measurement at the settlement plates SP 9 und SP10. (Source: Fig. 8, Kirstein et al. 2012)

Witasse et al. (2012) using the finite element package PLAXIS 2D, analyzed a vertical drain combined with vacuum pressure under conditions of unsaturated soil. The paper presented the set-up and results of a finite element analysis performed for a reclamation project in Vietnam. This FE analysis was carried out in the framework of a fully coupled flow-stress analysis with unsaturated soil. For this purpose, a new drain element was implemented on which negative pore pressure (vacuum induced suction) can be applied as a flow boundary condition. Advanced constitutive modelling for the non-linear behavior of the constitutive soft soil layers was also considered. As we are assuming plane-strain modelling, real in-situ vertical soil permeability values need to be modified to account for the fact that the drainage path is different than in reality, as presented in Figure 9 (Source Fig 3).

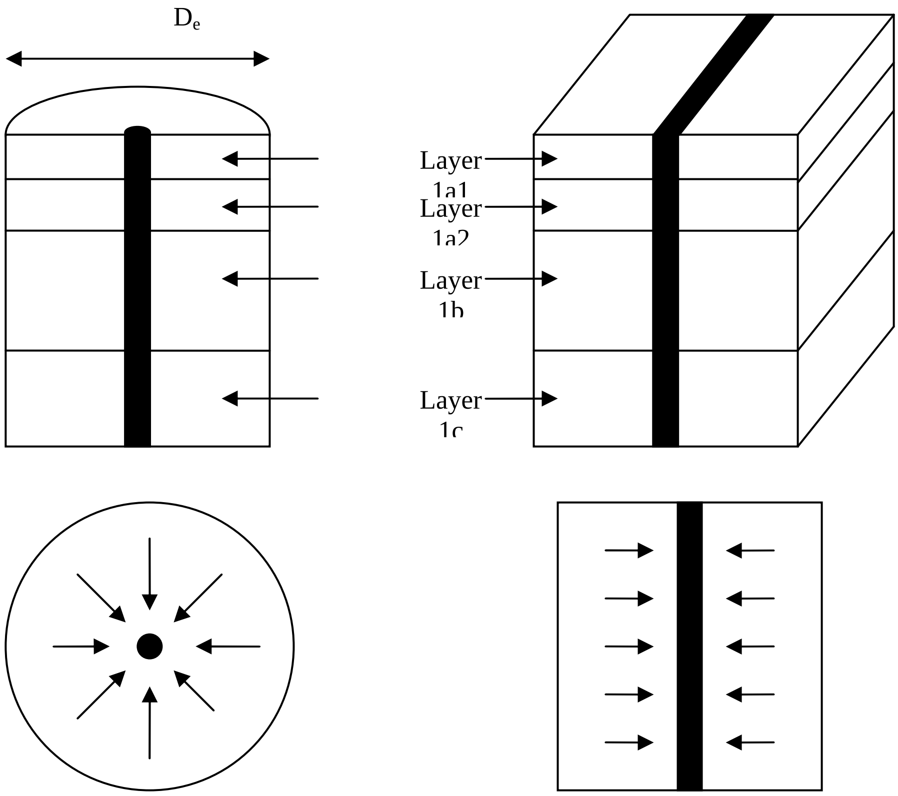

(a) Axisymmetric radial flow (b) Plane strain flow

Figure 9: Comparison of axisymmetric unit cell radial flow into plane strain flow (Source: Fig. 3, Witasse et al. 2012)

Eight Gauss points K, L, M, N, O, R, P and Q located respectively at the centre of layers 1a1, 1a2, 1b and 1c were chosen to follow the main parameters in this analysis: total vertical stress, effective vertical stress and active pore pressures (see Figures 10 and 11, (Source Figs 6 and 7)). Figure 12 (Source Fig 1) summarises the evolution of the lateral displacement induced by the vacuum pressure. These figures show the ability of the vacuum consolidation process to generate lateral displacement inwards to the treated area, as expected for a porous medium subjected to an isotropic depression. Figure 13 (Source Fig 12) presents the typical slope failure mechanism obtained using a phi-c reduction analysis (at 290 days for the situation presented where the vacuum treatment is active). More particularly, it was found that the developed FE model could show: (a) a higher rate of effective stress increase as the applied vacuum pressure increased, (b) the vacuum pressure induced inward lateral displacement, and (c) there was an increase in the safety factor when the vacuum consolidation was active.

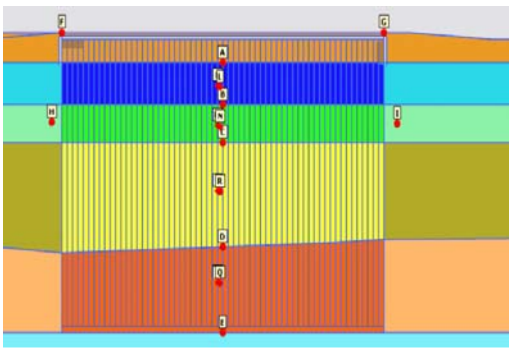

Figure 10: Location of Gauss points and nodes for results post-processing (Source: Fig. 6, Witasse et al. 2012)

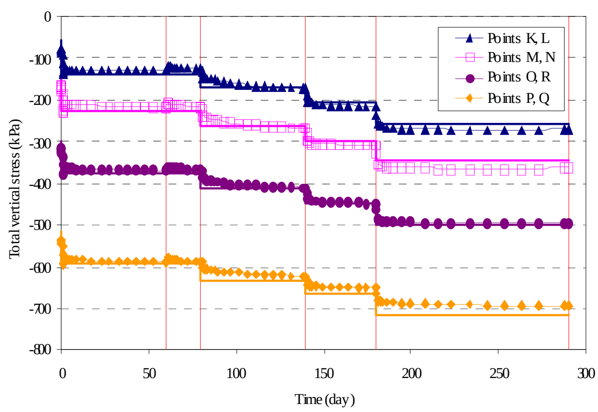

Figure 11: Total vertical stresses variation with time (Source: Fig. 7, Witasse et al. 2012)

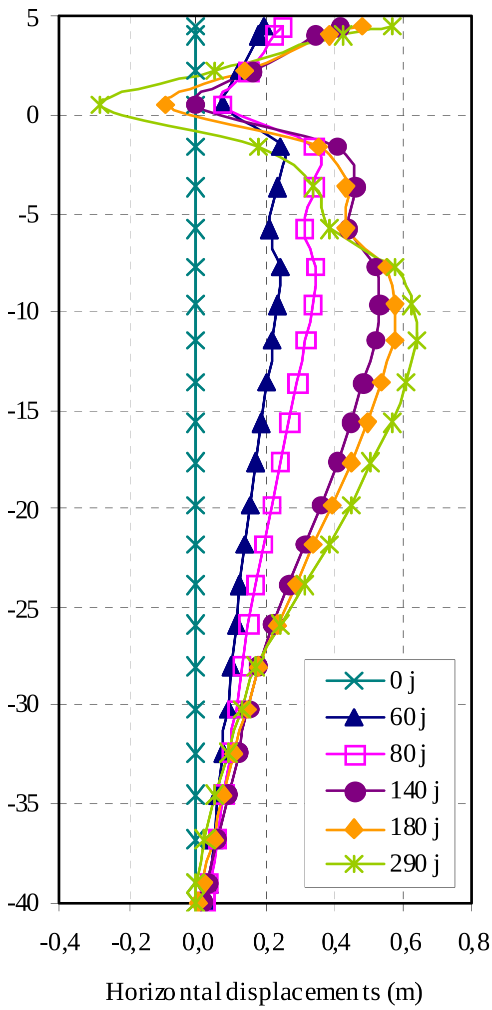

Figure 12: Horizontal displacements at the edge of vacuum consolidation area. (Source: Fig. 11, Witasse et al. 2012)

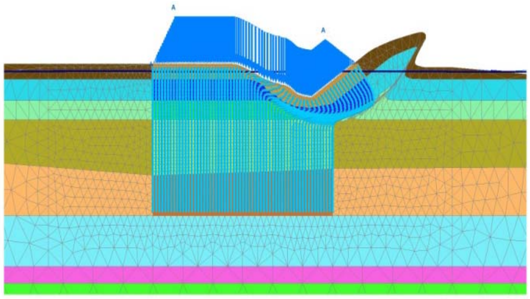

Figure 13: Failure mechanism after 6.7m fill construction (Source: Fig. 12, Witasse et al. 2012)

Mateos (2012) shows some results by using a back analysis of a trial embankment settlement based on CPTu and odeometric tests in order to accurately predict the settlement under a long embankment being built for a new "High speed rail track" in southeast Spain. The new rail track was designed along earth fills 4 to 8 m high. Due to the enormous deformability of the marsh sediments underneath, important settlements were forecast along the embankment, but to check this approach, a trial embankment was built over a section treated with 20m deep vertical distributed in a triangular mesh whose side is 1.66 m long. Data from this embankment was recorded for more than 15 months. The soil profile in the area of the study comprised 32 metres of sedimentary marsh overlaying alluvial fan sediments. The horizontal consolidation coefficient was estimated from the dissipation tests in CPTu. A total of 41 tests were performed and the results of CPTu tests conducted close to the trial embankment, showed there are many granular levels in the profile (Figure 13b. Source: Fig. 4). A trial embankment was built after this treatment by vertical drains to better understand how marsh soils consolidated. The trial embankment was 4 m high, 25.45 m wide and 64 m long. Data obtained since the beginning of the construction to September 2011 showed that most of the settlement developed during construction (Figure 14, Source: Fig. 6 and in the next two months (Figure 15, Source: Fig. 7). Since then, the rate of settlement decreased continually, and is now less than 0.5 cm per month. Data were analysed by the Asaoka method in order to predict the magnitude of final settlement. From this analysis a magnitude close to 30 cm was obtained (Figure 16, Source: Fig. 9).

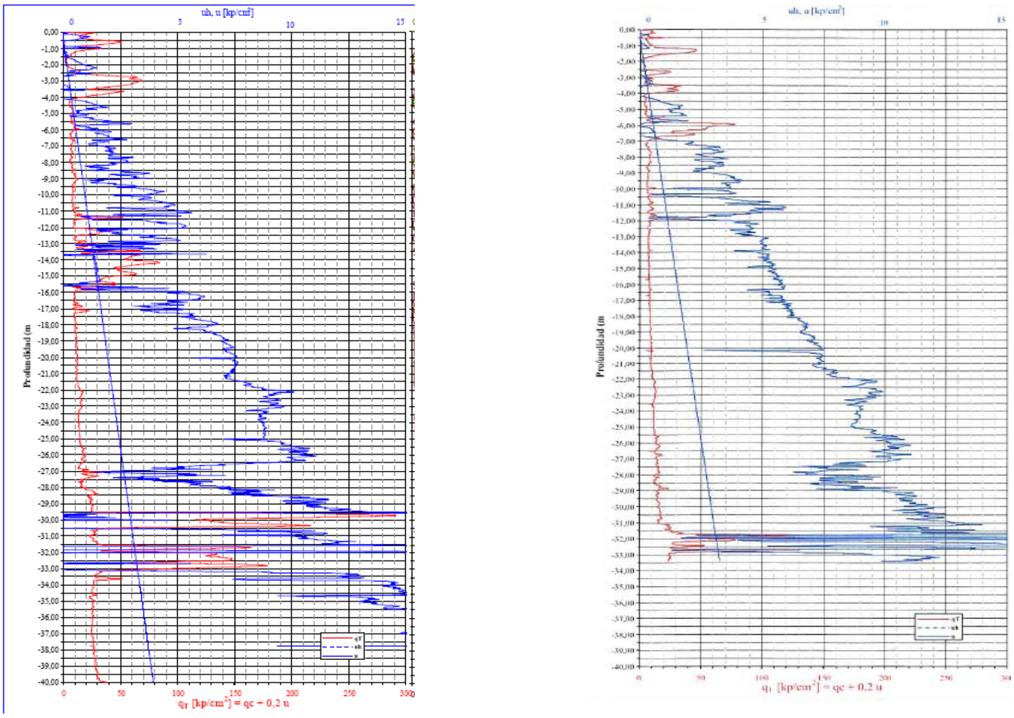

Figure 13b: Excess pore pressure registered by CPTu tests close to the trial embankment (Source: Fig. 4, Mateos 2012)

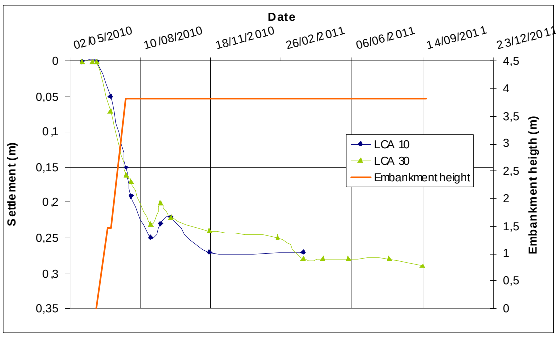

Figure 14: Settlement data from horizontal inclinometers (LCA) along embankment axis. (Source: Fig. 6, Mateos 2012)

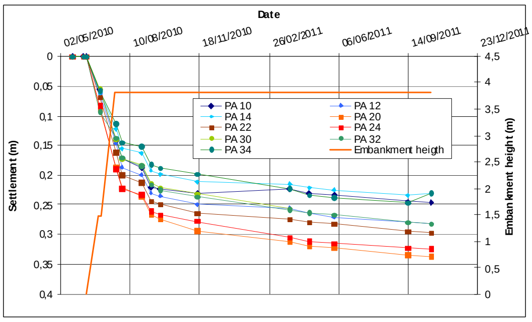

Figure 15: Settlement data obtained from settlement plates. PA 12, PA 22 and PA 32 are located over the embankment axis. (Source: Fig. 7, Mateos 2012)

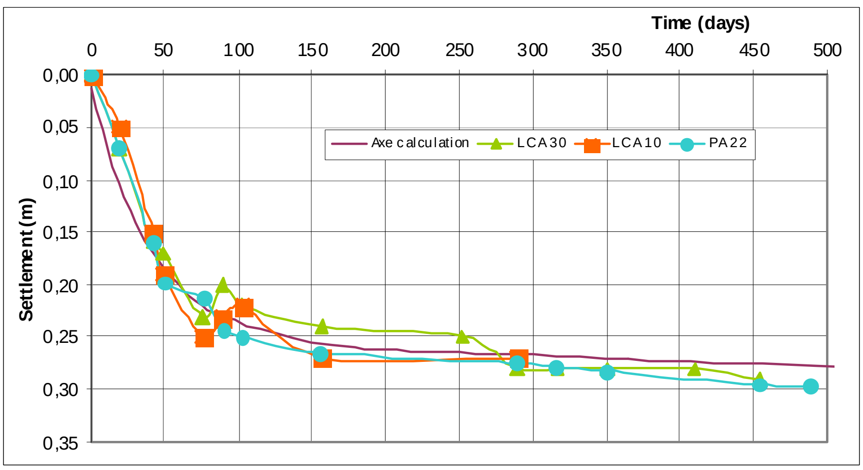

Figure 16: Comparison between instrumentation data and calculation results. (Source: Fig. 9, Mateos 2012)

Belén and Schmidt (2012) presented a numerical 3D comparison between real PVD and equivalent permeability during consolidation: one simulating soil with a real PVD installed, and the other one simulating soil with equivalent permeability (k_{ve}) (Figure 17 Source: Fig. 9). For the 3D simulation of the unit cell, a hexagonal cross-section of three different zones: unit cell, smear zone and equivalent PVD was considered. The simulation with real PVD and a smear effect presented a discharge of approximately of 20 % through the upper face and 80 % through the PVD, as can be seen in Fig. 17 (Source: Fig. 9), showing that the PVD worked well. Both the unit cell with real PVD and the unit cell with k_{ve} gave similar final settlement results, but the consolidation rate and predicted excess pore pressure were somewhat different (Figure 18 and 19, Source: Figs. 6 and 7). The unit cell with a real PVD simulation resulted in a faster consolidation rate and lower predicted excess pore pressure.

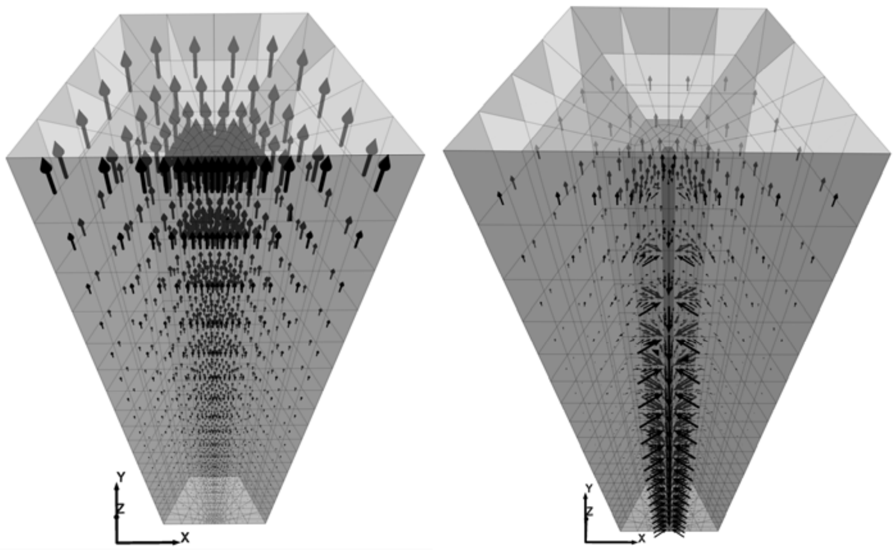

k_{ve} simulation

real PVD simulation

Figure 17: Discharge vectors (models with smear effect) (Source: Fig. 9, Belén and Schmidt 2012)

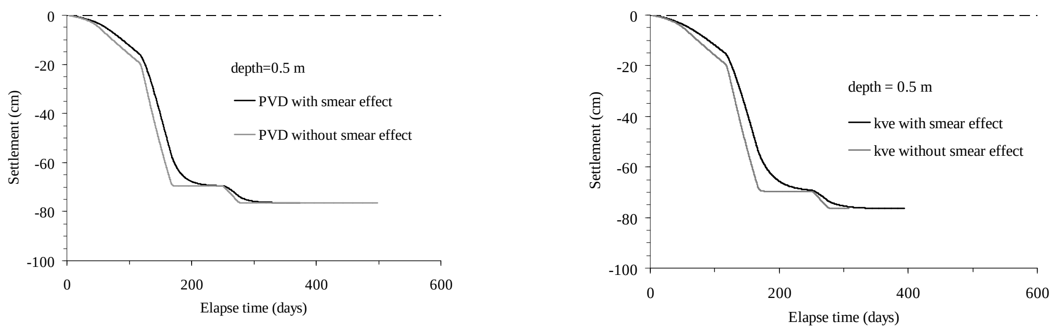

Figure 18: Settlement at depth of 0.5 m for the simulations with and without smear effect (Source: Fig. 6, Belén and Schmidt 2012)

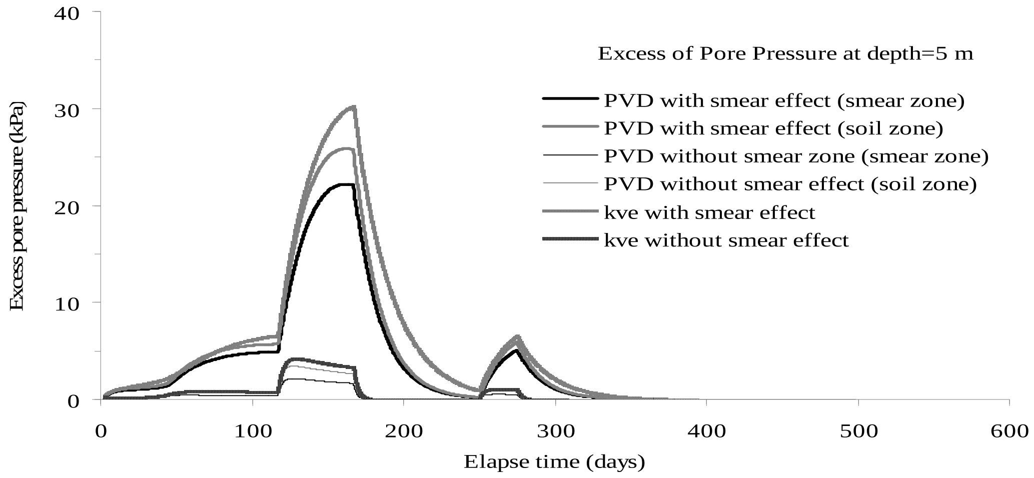

Figure 19: Comparison of excess pore pressure unit cell with and without smear (Source: Fig. 7, Belén and Schmidt 2012)

Román et al. (2012) presented the preloading progress of a hydraulic fill for the foundation of LNG tanks currently being constructed in El Musel Prot (Gijon, Northern Spain Figure 20, Source: Fig. 1). The hydraulic fill is mainly composed of marine sands dredged from nearby locations (Figures 21 and 22, Source: Figs. 3 and 16), which was placed on site using rainbow and pipeline discharge and the bottom dump method. Among several alternatives, preloading was selected as the ground improvement method to reduce the settlement of the LNG tanks. The preloading magnitude had to be equivalent to the load transmitted to the foundation during the hydraulic proof (285 kPa). Since during the earthworks it could be verified that the apparent density was over 20 kN/m^3, the height could be limited to 16 m. The preloading fill was a conical frustum shape, with a 130 m diameter base and a 80 m diameter top. Figure 23 (Source: Fig. 17) shows the load (expressed as preloading height) vs. settlement curve observed during preloading construction and unloading. Note that during unloading the recovered deformation (upwards movement) during preloading removal was 8.6 times smaller than the settlement during first loading. Figure 24 (Source: Figs. 18 and 19) shows the results of the inclinometer with the highest deformation, as well as the variation of maximum measured displacements with time and fill height. Figure 25 (Source: Fig. 21) shows the settlement as the exterior "ring" concrete structure was being constructed. The maximum load, once the ring is constructed, will be of 230 kPa acting over a width of approximately 5-6 meters. The observed settlement was smaller than predicted. Therefore, preloading has been shown to in this case to be an efficient alternative for improving the tank foundations, albeit with limited settlement during unloading-reloading that is below the accepted thresholds.

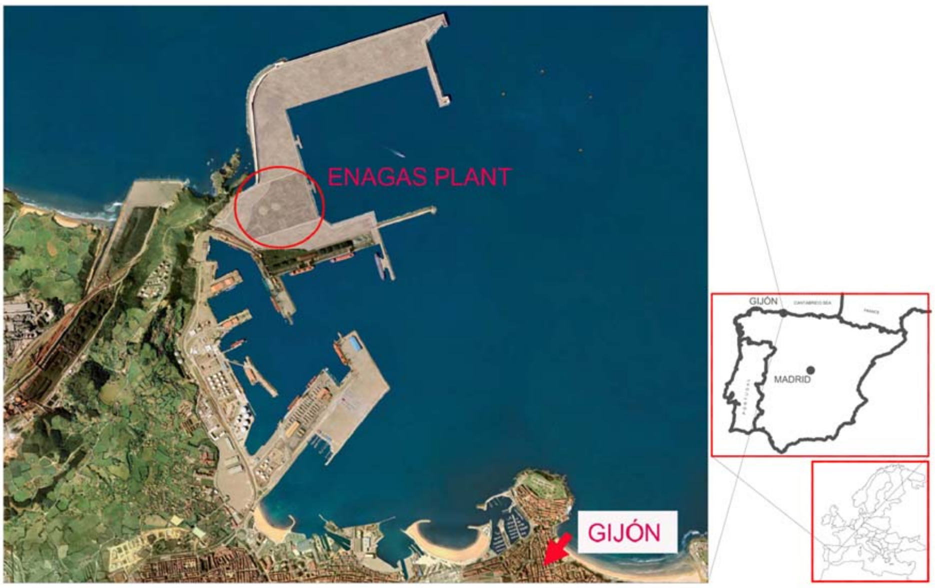

Figure 20: Location of Enagás Plant (Source: Fig. 1, Román et al. 2012)

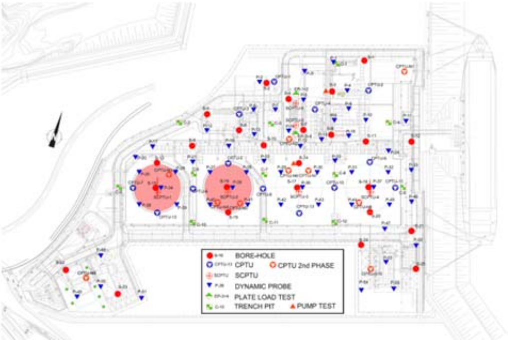

Figure 21: Lay out of the site characterization program (Source: Fig. 3, Román et al. 2012)

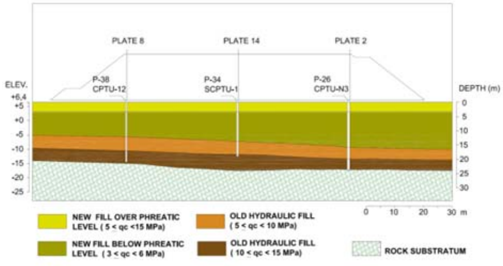

Figure 22: Representative cross-section under Tank 1 (Source: Fig. 16, Román et al. 2012)

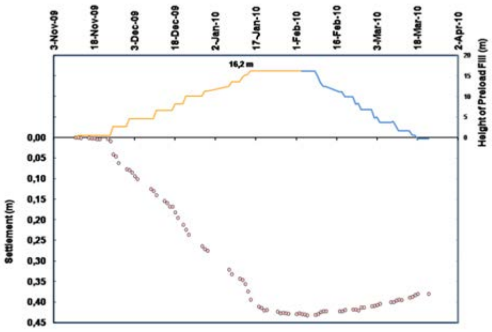

Figure 23: Preload height and settlement vs. time (Source: Fig. 17, Román et al. 2012)

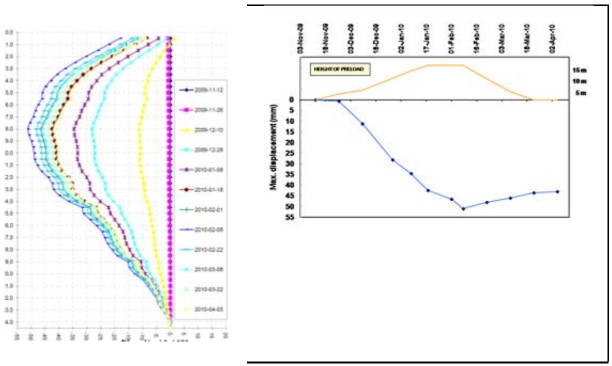

Figures 24: Results of Inclinometer Nr 1 and evolution of maximum displacement versus time and height of preload. (Source: Fig. 18 and 19, Román et al. 2012)

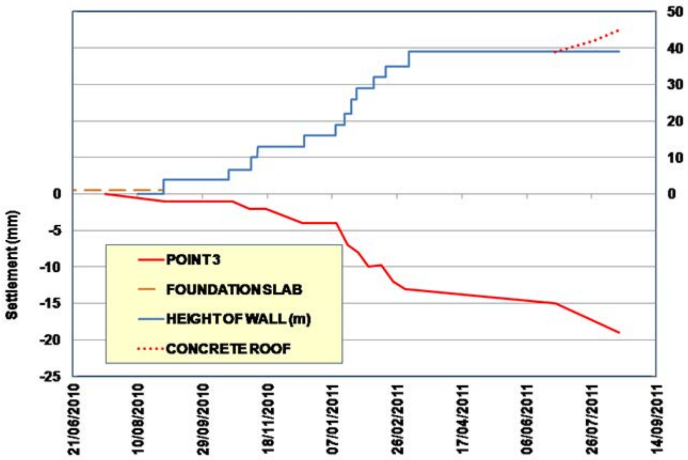

Figure 25: Settlement during the concrete ring construction (Source: Fig. 21, Román et al. 2012)

3. RECENT ADVACEMENT IN SOFT CLAY CONSOLIDATION WITH VACUUM APPLICATION

3.1. Vacuum preloading system

This section elucidates a technological advancement that contributes to our understanding of the intricate mechanics of the different PVD-vacuum systems (membrane system and membraneless system) (Figure 26), to minimise consolidation, excessive post-construction settlement and lateral ground movement, as well as operational costs. Therefore, the specific aims must address both fundamental and applied components that not only assist in an analytical assessment of the most appropriate vacuum system for a given combination of soil-drain characteristics, but also to quantify the role of soil-drain interaction mechanics on soft soil stabilisation to support the anticipated infrastructure load (Geng et al. 2012).

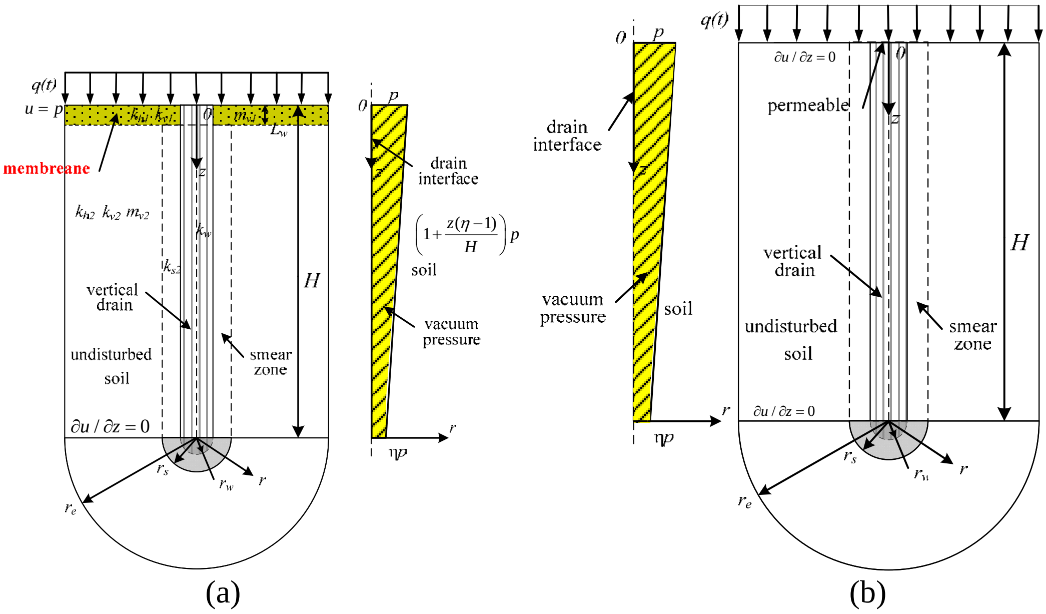

Figure 26: Analysis schemes of unit cell with vertical drain: (a) membrane system; and (b) membrane system. (Geng et al. 2012)

Figure 27 illustrates the effect of the permeability of a sand blanket in a membrane system and membraneless system. As expected, when permeability decreases consolidation takes longer. When the PVD's are short, say around 10 metres long (Fig. 2a), the permeability of the sand blanket should not be less than 0.01 times the permeability of the PVD and 10^4 times the permeability of the clay to maintain consolidation and achieve a 90% degree of consolidation. With longer drains (Fig. 2b), the ratios between the permeability of the sand blanket and the PVD, and between the permeability of the sand blanket and the clay layer should be more than 0.1 and 10^5, respectively.

3.2. Partially penetrating drain

Analytical solutions for partially penetrating PVDs are derived by considering the vacuum pressure (suction), time-dependent embankment surcharge, well resistance, and smear zone. Three-dimensional seepage with a virtual vertical drain is assumed to reflect real seepage into the soil beneath the tip of a PVD. Analytical solutions were then used to examine the length of the vertical drain and vacuum pressure on soft clay to determine the consolidation time and degree of consolidation, associated settlement, and distribution of suction along the drain.

Regardless of PVD spacing, with 20m thick clay, a penetration ratio of 0.9 can provide a normalised settlement of 0.9 within an increased consolidation time ($T_{h\,req}$) of less than 20% of $T_{h\,i}$. For a 10m thick layer of clay with 1.0m drain spacing, the applied surcharge pressure should be more than 40% of the total applied pressure (vacuum plus surcharge), in order to obtain a normalised settlement of 0.9 within 1.25 $T_{h\,i}$. However, for a 10m thick layer of clay with 1.5m drain spacing, the surcharge pressure must be more than 50% of the total applied pressure to achieve 90% normalised settlement within 1.25 $T_{h\,i}$. This analysis shows that to overcome the loss of vacuum caused by the bottom pervious layer, a combination of vacuum with surcharge pressure is most beneficial when the length of the PVD is less than 90% of the total thickness of clay. Generally, the vertical drain penetration ratio can be reduced by up to 20% of the total thickness of clay without significantly affecting the settlement time for surcharge loading alone. In contrast, for a surcharge load combined with vacuum pressure, the length of the vertical drain can be reduced by 10% of the total thickness of soft clay with an appropriate combination of vacuum and surcharge (see Table 1).

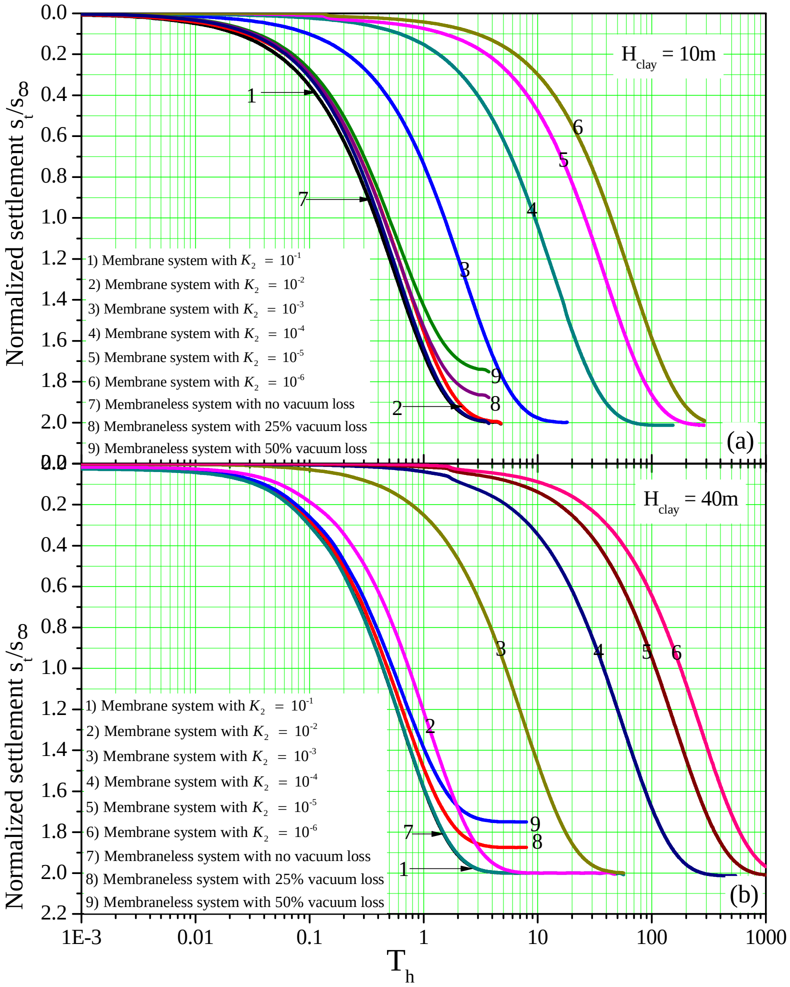

Figure 27: Normalized settlement-time factor curves for varying K_2 (for membrane system) and η (for membraneless system): (a) the thickness of the clay is 10 m; (b) the thickness of the clay is 40 m (Geng et al. 2012).

Table 1: Vertical drain penetration ratio (ρ) for different conditions to achieve 90% normalised settlement

	$d_e = 1.0$ **m**			$d_e = 1.5$ **m**		
	ρ			ρ		
	SP (80kPa)	VP (-80kPa)	VP&SP	SP (80kPa)	VP (-80kPa)	VP&SP
H = 10 m	0.8	cannot achieve 90% nomalised settlement	0.9 and SP>50% Total applies pressure	0.8	cannot achieve 90% nomalised settlement	0.9 SP>50% Total applies pressure
	ρ			ρ		
	SP (80kPa)	VP (-80kPa)	VP&SP	SP (80kPa)	VP (-80kPa)	VP&SP
H = 20 m	0.85	0.9	0.9 SP>40% Total applies pressure	0.8	cannot achieve 90% nomalised settlement	0.9 SP>40% Total applies pressure

Note: SP = Surcharge preloading, VP= Vacuum Preloading, VP&SP= vacuum combined surcharge loading

When a vacuum is applied to a layer of clay sandwiched between the top and bottom drainage layers, the PVDs must be shorter than the thickness of the clay to prevent the vacuum from leaking through the bottom drainage layer. When PVDs only partially penetrate the layer of clay, the soft clay beneath the tip of the PVD does not consolidate the same as the overlying stratum. Due to the complexity of the problem, soil consolidation with partially penetrated vertical drains has already been analysed by numerical methods.

4. CONCLUSION

This category of eight papers describes the consolidation process with time, with very useful information on field data, laboratory testing, analytical formulations and numerical modelling, including reference to the comparison of observed data with predictions. The overall findings are as follows:

- A relative high vacuum pressure of up to -70 kPa can significantly decrease the required fill height and achieve a desirable degree of consolidation exceeding 95%.
- 2D finite element analysis for vacuum consolidation showed: (a) a higher rate of effective stress increase as the applied vacuum pressure was increased, hence the increase in shear strength, and (b) the vacuum pressure application has the favourable effect of inducing inward lateral displacement.
- Vacuum consolidation performance depends on the actual distribution of vacuum along the drain length and permeability and the thickness of the sand blanket.
- During PVD installation, the intrusion of the upper layer into the underlying layer creates an additional zone where the remoulded permeability of this zone can retard the consolidation process
- Economic soil improvement techniques such as PVD can be combined with rigid inclusions to accelerate consolidation process and to enhance the shear strength.
- Coefficient of consolidation determined from oedometer tests and CPTu profiling provide an accurate description of soil consolidation behaviour and estimations for settlement development.
- The simulation of three dimensional unit cell with a PVD resulted in a faster consolidation rate and a lower predicted excess pore pressure.
- Vertical drain length can be reduced by up to 20% of the total thickness of clay without significantly affecting the settlement time for surcharge loading alone.

5. ACKNOWLEDGEMENT

The assistance of Dr Geng Xueyu, and Dr Cholachat Rujikiatkamjorn of the School of Civil, Mining & Environmental Engineering and Centre for Geotechnical Engineering, University of Wollongong is gratefully appreciated.

REFERENCES

Bacas, B.M. and Schmidt, F. (2012). Numerical 3D comparison between real PVD and equivalent permeability in consolidation process. ISSMGE - TC 211 International Symposium on Ground Improvement IS-GI Brussels.

Geng, X. Y., Indraratna, B. and Rujikiatkamjorn, C. (2012). Analytical solutions for a single vertical drain with vacuum and time-dependent surcharge preloading in membrane and membraneless systems. International Journal of Geomechanics, ASCE, 12(1), 27-42.

Indraratna, B., Rujikiatkamjorn, C. and Xueyu, G. (2012). Performance and prediction of surcharge and vacuum consolidation via prefabricated vertical drains with special reference to highways, railways and ports. ISSMGE - TC 211 International Symposium on Ground Improvement IS-GI Brussels.

Kirstein, J. and Wittorf, N. (2012). Rigid inclusions in combination with fast wick drain consolidation as soil improvement method in very soft and fat northern German clay. ISSMGE - TC 211 International Symposium on Ground Improvement IS-GI Brussels.

Kirstein, J. F., Ahner, C., Uhlemann, A. and Uhlich, P. (2012). Ground improvement methods for establishment of the federal road B 176 on a new elevated dumb in the brown coal area of MIBRAG. ISSMGE - TC 211 International Symposium on Ground Improvement IS-GI Brussels.

Mateos, t.. (2012). Back analysis of a trial embankment settlement based on CPTu and oedometric test results. ISSMGE - TC 211 International Symposium on Ground Improvement IS-GI Brussels.

Román, F., Jimenez, R., Suarez, J. C. G., Coz, A. (2012). Preloading of a hydraullic fill for foundation of LNG tanks. ISSMGE - TC 211 International Symposium on Ground Improvement IS-GI Brussels.

Rujikiatkamjorn, C. and Indraratna, B.. (2012). Radial Consolidation Modelling Incorporating Downdrag Effect for a Multi-Layer Soil. ISSMGE - TC 211 International Symposium on Ground Improvement IS-GI Brussels.

Witasse, R., Racinais, J., Maucotel, F., Galavi, V., Brinkgreve, R., and Plomteux, C. (2012). Finite Element Modeling of Vacuum Consolidation using Drain Elements and Unsaturated Soil Conditions. ISSMGE - TC 211 International Symposium on Ground Improvement IS-GI Brussels.

SESSION 3 - SOIL MIXING 1 – SOIL STABILISATION:
SURFACE MIXING AND LABORATORY MIXTURES

General Report
SESSION 3 – SOIL MIXING 1 – SOIL STABILISATION: SURFACE MIXING AND LABORATORY MIXTURES

Abir Al-Tabbaa, University of Cambridge, United Kingdom, aa22@cam.ac.uk

ABSTRACT

This session on Soil stabilisation: surface mixing and laboratory mixtures contains 31 papers with authors from 15 countries from all six continents. Those papers generally divide into three topic areas: (i) Soil stabilisation with cement, with 12 papers (ii) Soil stabilisation with lime, ash, slag and other binders and additives, with 11 papers and (iii) Procedures, design, modelling and construction with 8 papers. The session papers are summarised under those headings with selected figures included. The papers demonstrate the diversity of research work currently being undertaken in this field. The author concludes with a brief overview of recent research activities in her group including work on novel binders and on the stabilisation of contaminated soils as well as on correlation between laboratory and field results.

1. INTORDUCTION

Soil stabilisation continues to be an active area of research fuelled by a number of different factors. On one level, a number of changes have recently taken place which have affected cement-based grouts and binders which include: (i) they are being used in an increasing variety of contexts, both geotechnical and geoenvironmental; (ii) they are increasingly being used in more aggressive environments e.g. contaminated land; (iii) there is an increased incorporation of industrial by-products, which are continually changing in composition because of cleaner production processes; (iv) there is a need to increase the lifespan of materials because of the drives towards sustainability and (v) there is continued developments of more environmentally acceptable and sustainable cements and binders to reduce the environmental impacts from the production of Portland cement. Extensive research efforts are required to assess the impact of those changes on the performance of current and future grouts and binders. A different set of factors are related to the introduction of legislations such the EU Landfill Directive which requires pre-treatment of most wastes and which has resulted in significant increase in the use of stabilisation as a methodology for such a pre-treatment. Again with the publication of the waste acceptance criteria, different binders can be assessed for their applicability as pre-treatments for waste and contaminated soils destined to landfill. Another set of factors is related to the development of a range of new equipment for soil stabilisation, including surface treatments and mass stabilisation, where the effectiveness of the mixing and optimum binder dosages require investigation particularly in field trials and field applications.

This session on Soil stabilisation: surface mixing and laboratory mixtures contains 31 papers with authors from 15 countries and from all six continents. Those papers have been divided into three main topic areas: (i) Soil stabilisation with cement (covering 12 papers), (ii) Soil stabilisation with lime, ash, slag and other binders and additives (covering 11 papers) and (iii) Procedures, design, modelling and applications (covering 8 papers). The following three sections present an overview of the content of the papers within each topic. The report concludes with a fourth section which contains an overview of some of the author's recent work in this area.

2. SOIL STABILISATION WITH CEMENT

There are 11 papers in this area with topic ranging from investigations of the strength, durability, stiffness, rheology, time related behaviour, effect of chemicals and the incorporation of materials such tyre chips, polypropylene and carpet fibres and the testing of a wide range of soils from sand to clay to peat.

The paper by Guimond-Barrett et al (2012a) invstigated the effect of time, up to 90 days, and cement content (up to 400kg/m^3) on the increase in strength of sandy soils treated in the laboratory with cement using unconfined compressive strength and ultrasonic pulse wave velocity measurements and developed an empirical correlation for such a relationship. The developed correlation, which linearly relates the unconfined compressive strength at a given time, as a ratio to that at 7 days, to the natural log of time, as shown in Figure 1, was not found valid for when bentonite is added or in the presence of sulfates which were found to alter the strength development with time and hence the correlation will require modifications.

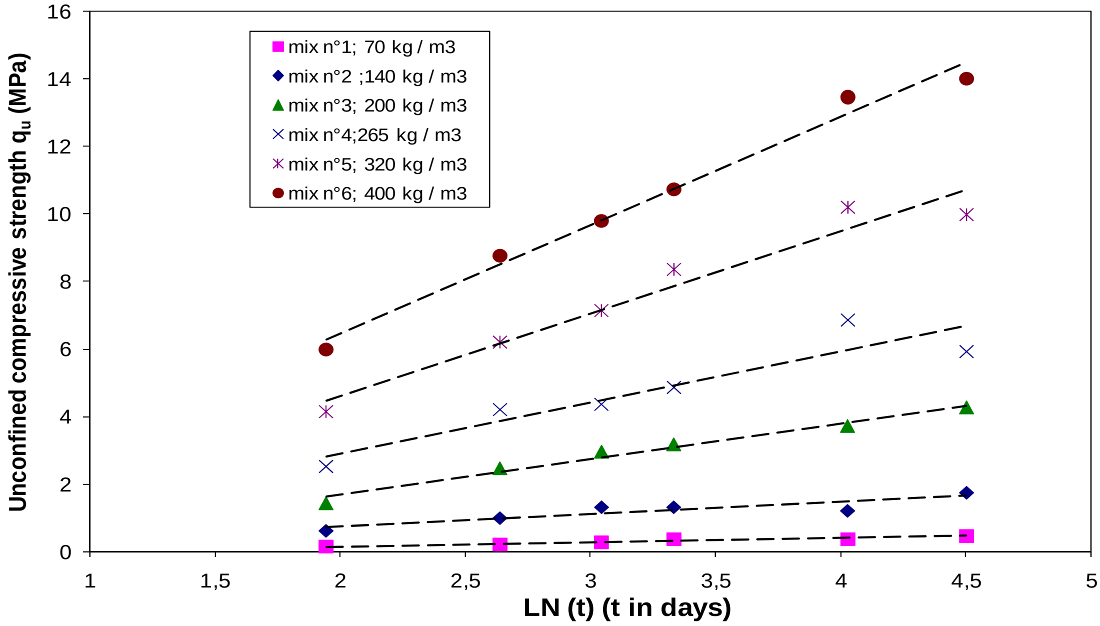

Figure 1: Unconfined compressive strength of Fontainebleau sand – cement mixes versus the logarithm of time Ln(t) (Guimond-Barrett et al, 2012a)

Saussaye et al (2012) investigated the effect of the presence of potentially deleterious anions such as chlorides (in NaCl) and sulfates (in $CaSO_4.2H_2O$), of up to 10g/kg dry soil, on the swelling and strength performance of three soils, silts and sand & gravel soils, generally similar geotechnically, treated with 1% quicklime and 6% cement CEM II. The paper shows that the soils performance improved by the presence of NaCl. The performance in the presence of the sulfate depended on the soil type, as shown in Figure 2, where swelling and reduction in strength were observed.

Piriyakul and Pochalard (2012) used bender elements and UCS to determine the stiffness and strength respectively of Bangkok clay (natural water content of 66.3% and LL of 88%) stabilised with Portland cement (20% w/w) and fly ash (up to 30% w/w content) over time (up to 90 days). Their results showed that 15-20% fly ash content provided the optimum results at 90 days; similar UCS to and higher stiffness than 0% fly ash content. Their work also showed linear relationships between UCS and log time, similar to the findings of Guimond-Barrett et al (2012a) and a good correlation between the strength and stiffness results as shown in Figure 3.

Moretti et al (2012) investigated the strength development over time of Brazilian alluvial clay stabilised with different dosages of cement (up to 600kg/m^3). The paper reports a successful homogenisation process. The results, presented in Fig. 4, are consistent with the findings of Piriyakul and Pochalard (2012) and Guimond-Barrett et al (2012a) and show a linear relationship between UCS and log time and close to linear relationship with cement dosage.

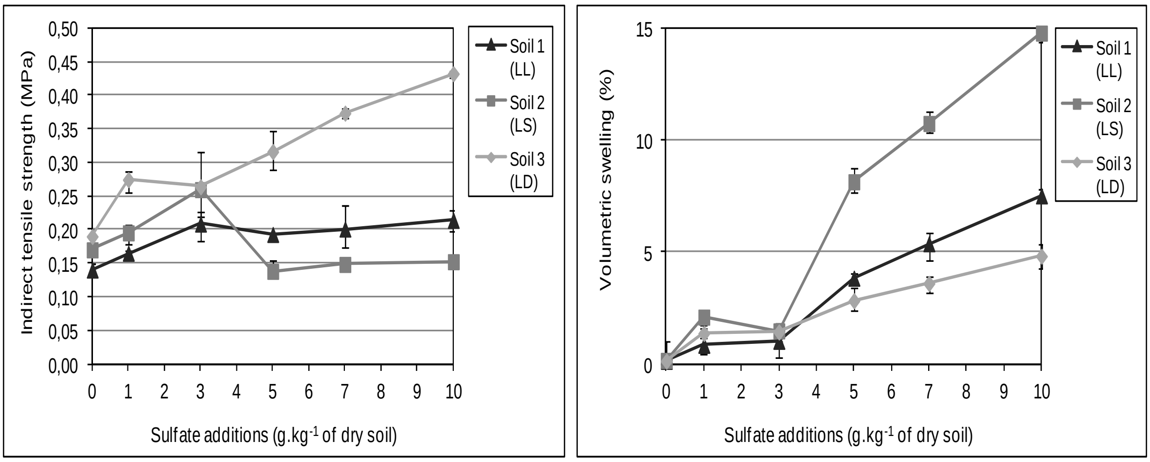

(a) *(b)*

Figure 2: Influence of sulfate (in $CaSO_4.2H_2O$ form) on treated soils in terms of (a) indirect tensile strength and (b) volumetric swelling (Saussaye et al, 2012)

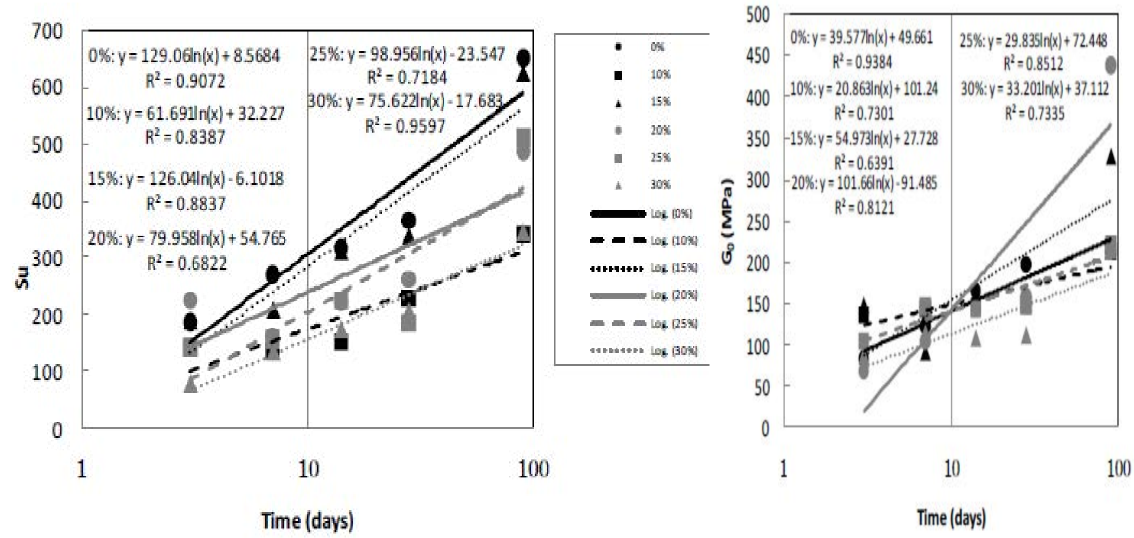

(a) *(b)*

Figure 3: Performance of cement stabilised Bangkok clay with time in terms of (a) undrained shear strength and (b) initial shear modulus (Piriyakul et al, 2012).

Timoney et al (2012) presented results on the performance of a range of Irish peats in terms of strength, stiffness, compressibility and creep. The water to binder ratio was used as a means of combining the influence of water and binder quantity on the stabilised strength, as shown in Figure 5a, for different peats and binder types. While peats are generally difficult to stabilise, the figure shows that some high strength values of stabilised peats can be achieved. The correlation between the E_{50} and UCS are shown in Figure 5b with an average ratio of 150. Embodied energy calculations performed as part of the study showed that the contribution of binder production is much more significant that its transportation.

A second paper by Guimond-Barrett et al (2012b) investigated the effect of the addition of cement on the rheological charactertics of kaolin clay by measuring the flow properties at various moisture contents using a rheometer with two different geometries: parallel plates and ball measuring system. They found good agreement between the stresses measured and both rheometers validating the use of the shear geometry and proposed that observations made in the field on the relation between blade rotation speed and strength and homogeneity of treated soils can be explained by the shear-thinning of clays. The effect of the cement and water contents can be clearly seen in Figure 6.

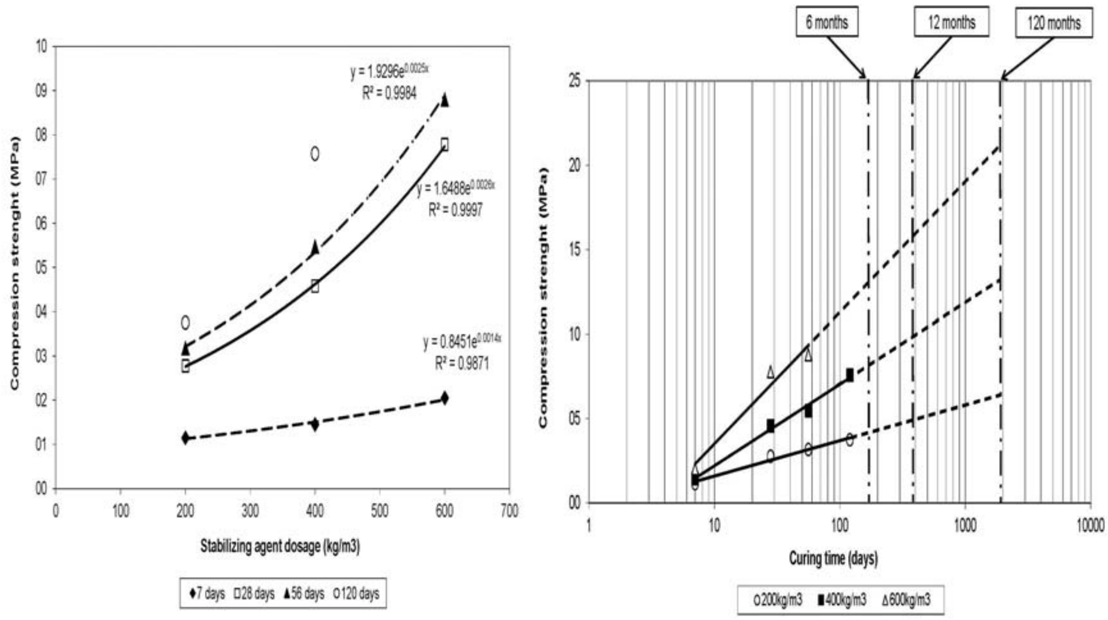

(a) *(b)*

Figure 4: The compressive strength of Brazilian soil alluvial clay vs (a) cement dosage and (b) time (Moretti et al, 2012).

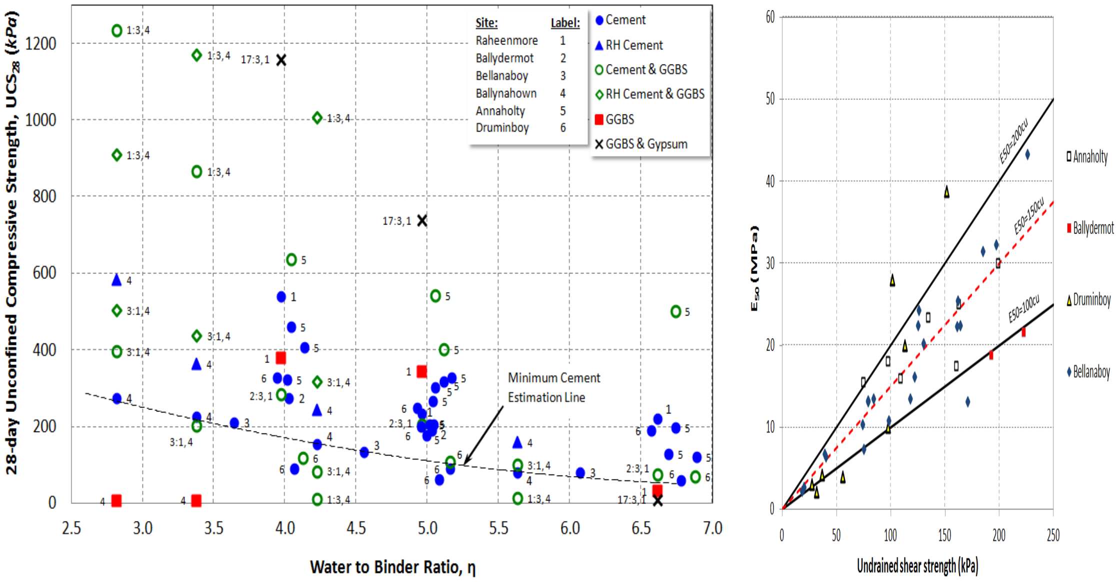

(a) *(b)*

Figure 5: The performance of different Irish peats in terms of (a) UCS vs water:binder ratio and (b) E_{50} vs UCS (Timoney et al, 2012).

The effect of tyre chips (D_{50} of 2mm added at up to 20%w/w) on the mechanical and hydraulic performance of 10% cement-treated clayey sand was investigated in the paper by Grisolia et al (2012) together with the use of x-ray computed tomography scanning. The results showed that while the expected decrease in strength and stiffness and increase in failure strain and permeability were observed, it was found that the presence of the tyres prevented the development of large cracks and hence as the tyre content increased the permeability decreased as shown in Figure 7.

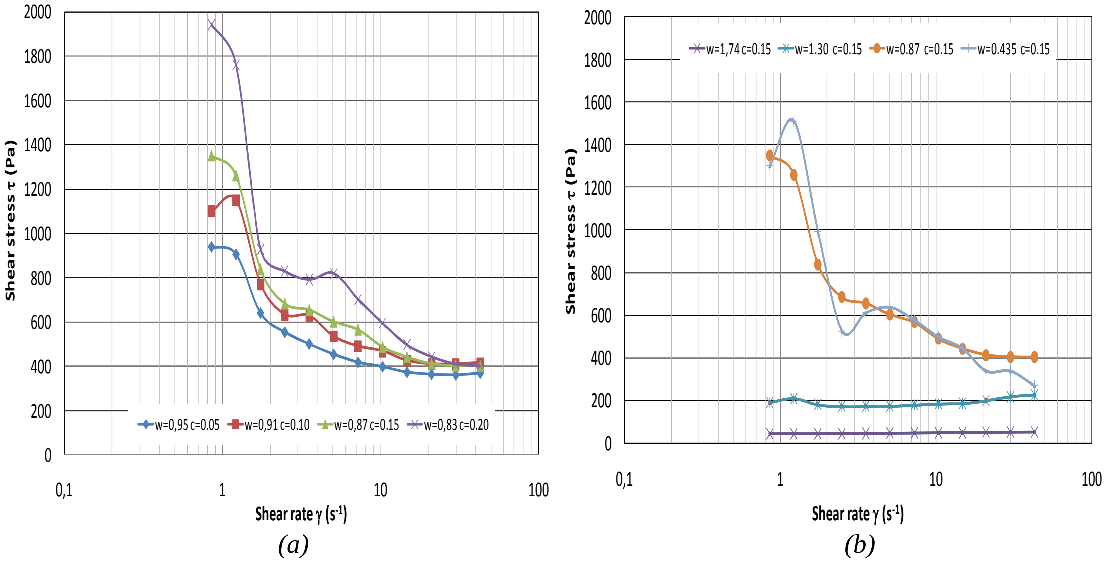

Figure 6: Flow curves for kaolin-cement mixes using the Ball measuring system (a) for constant water: clay ratio and different cement contents and (b) constant cement content and different water: dry solids ratios (Guimond-Barrett et al, 2012b).

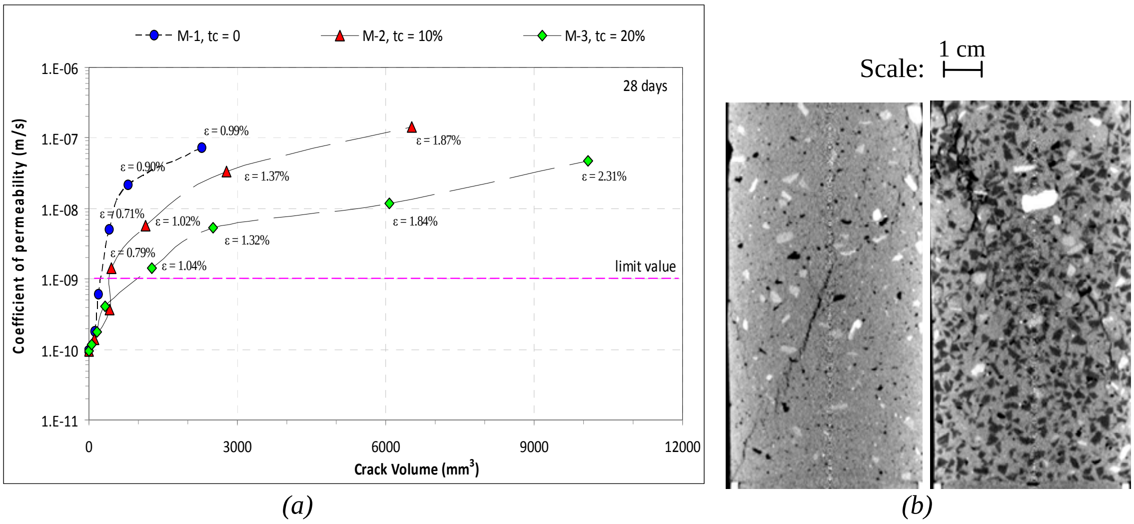

Figure 7: The performance of cement-treated clayey sand with the addition of tire chips (a) permeability vs crack volume and (b) a section of 0% (left) and 20% (right) tire content showing cracks profile (Grisolia et al, 2012).

The application of polyprolylene and carpet fibres on the mechanical properties of cement treated clay was investigated by Fatahi et al (2012) by varying the cement and fibre contents and showed that the introduction of both fibres had a positive effect on the strength and of the former only on stiffness of the treated clay and hence that polypropylene fibres could be a more environmentally friendly alternative to increasing the cement content.

Consoli and Viana de Fonseca (2012) showed that an index, they named as porosity-cement ratio, expressed as the porosity of a sample divided by the volumetric cement content as a percentage of the total volume, η/C_{iv}, not only controls the UCS, but also the splitting tensile strength of a soil-cement mixture, Figure 8a, as well as the initial shear modulus, Figure 8b, leading to a linear correlation between G_o/q_u vs η/C_{iv}.

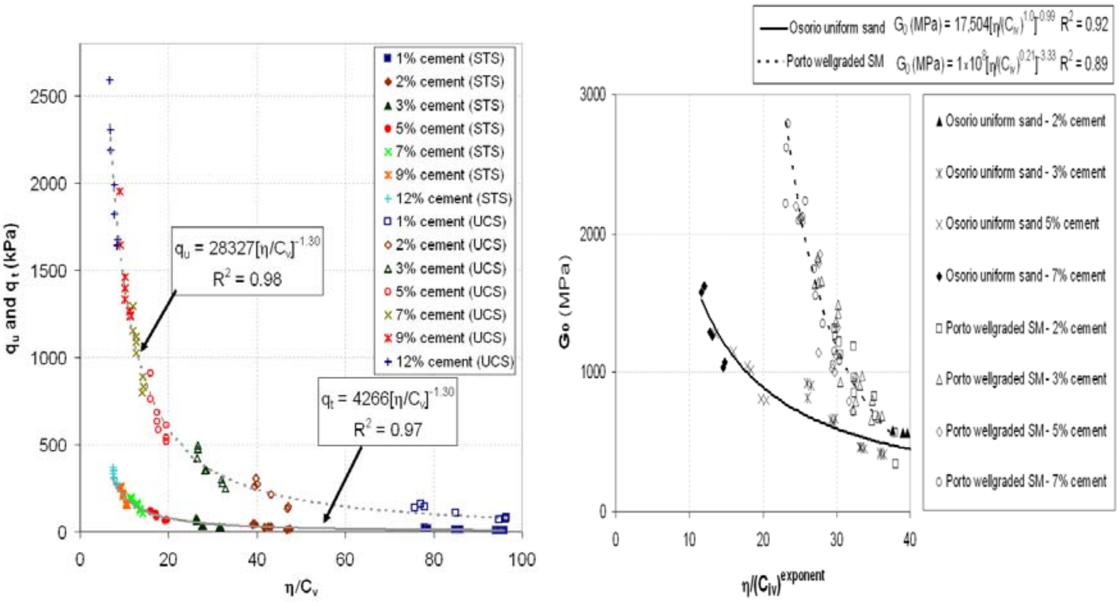

(a) *(b)*

Figure 8: The mechanical properties of cement treated soils in terms of the porosity-cement ratio for (a) UCS and splitting tensile strength and (b)initial shear modules (Consoli and Viana de Fonseca, 2012).

The groutability of alluvial soils from Iran treated with cement for underground construction application was investigated by Gharouni et al (2012) looking at pressure, water:cement ratio, aggregation and compaction. The authors found that the groutability was directly proportional to pressure, increased with water:cement ratio and the samples with the lower percentage compaction achieved better grouting. A relationship between those variables was proposed which also took into account the soil and grout particle sizes.

The stabilisation of marine delta clays from the southern region of Vietnam and from Louisiana, USA with cement was performed by Nozu et al (2012). The authors report that given the inclusion of montmorillonite and its high electric conductivity, there were serious condensation problems when cement was mixed with the clay and hence binders should be tested to mitigate condensation and increase liquidity to achieve the desired mixing quality and a sufficient UCS value.

Szymkiewics et al (2012) imvestigated the impact of Portland blastfurnace cement content on the workability (associated with the Liquid Limit) of five soils, ranging from low plastic silts to very high plastic clays to assess the self-compaction quality of treated soils in their fresh state. The soils were dried and mixed with the cement before water was added. The different performances achieved by the different soils and cement contents can be clearly seen in Figure 9 in terms of liquid limit and water sensetivity. One of the authors conclusions is that cement cannot be considered as simply a fine soil fraction at a very young age.

3. SOIL STABILISATION WITH LIME, ASH, SLAG AND OTHER BINDERS AND ADDITIVES

This section includes summaries of the eleven papers which cover all other binders including lime, ash, natural pozzolan, slag, gypsum and their blends as well as other additives such recycled bassanite, sulfonated limonene and potassium silicates on a wide range of soils and properties.

Beetham et al (2012) investigated whether finely ground limestone may have similar potential benefit as nucleation centres within the lime stabilisation process, as observed in cement hydration by accelerating the formation of hydration products and enhancing the uniformity of the microstructure. From CBR results, the paper concluded that greater pozzolanic development did take place due to the addition of the finely ground limestone, although triaxial test results did no support such findings.

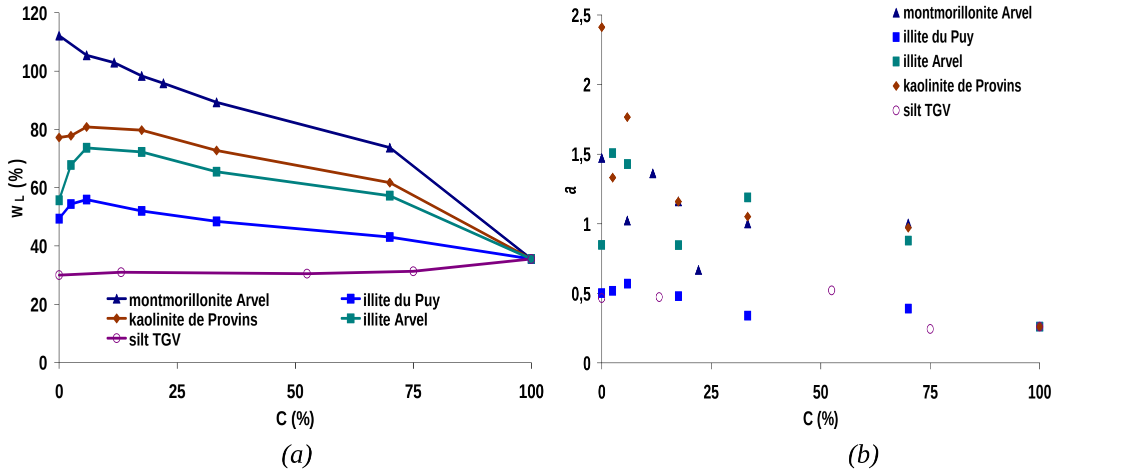

Figure 9: The performance of five silts and clays stabilised with cement in their fresh state in terms of (a) liquid limit and (b) water sensetivity (Szymkiewics et al, 2012).

Hashemi et al (2012) investigated whether the addition of a small quantity of bentonite with lime when treated granular soils could significantly enhance the properties of sand by lime treatment. They presented results for 30-60% bentonite addition which showed reduction in UCS as bentonite content increases. They suggested that a 10% bentonite content, which gave the optimum density in proctor compaction could be the optimum value to use.

Lutenegger (2012) tested eight different high plasticity clays in terms of the alternation to their grain size distribtuion due to the immediate modification by quicklime by plotting % change in clay content against activity, initial clay content and specific surface are as shown in Figure 10. The results confirmed the immediate modification to the grain size with different alternation degrees observed in different clays which appear to be strongly related to the specific surface area.

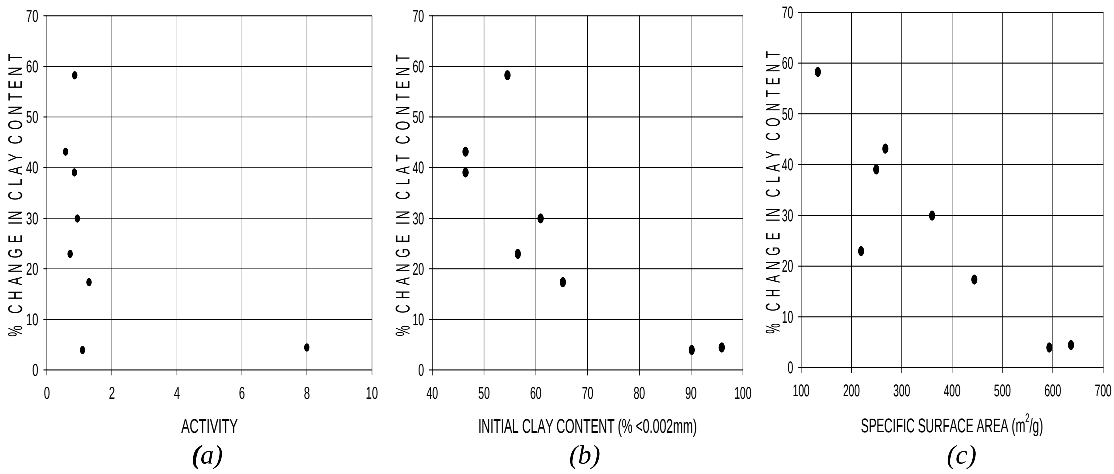

Figure 10: Percentage reduction in clay content due to 4% quicklime addition of eight different clays compared in terms of (a) activity, (b) initial clay content and (c) specific surface area (Lutenegger, 2012)

Mohd Yunus et al (2012) investigated the effect of humic acid content (0.5-3%) on the strength of organic clay stabilised with hydrated lime (5-15%). The results showed that the 5% lime addition produced the highest strength results with higher lime content producing lower strength and the strength reduced with time for add mixes (Figure 11). The microstructure of the treated high humic acid content showed significant number of cracks. The strength of the 5% lime treated clay with 1.5% humic acid was enhanced with the addition of 0.5% of chloride salts (NaCl and $CaCl_2$).

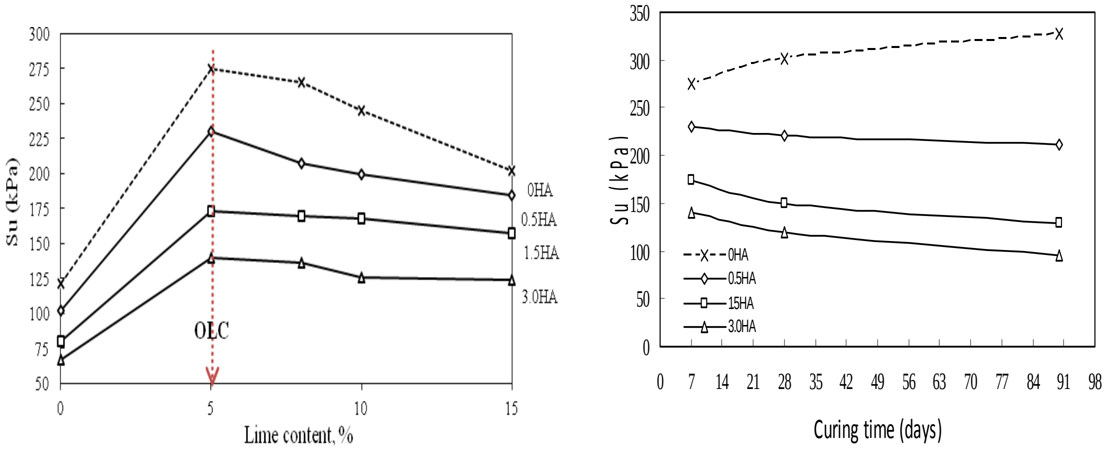

(a) *(b)*

Figure 11: The UCS of organic clay with Humic acid (HA) at 0, 0.5, 1 and 3% content against (a) lime content and (b) with time at 5% lime addition (Mohd Yunus et al, 2012).

Ramadas et al (2012) presented a study of the strength and swelling characteristics of three expansive soils from India treated with fly ash. The results showed that the Atterberg limits, optimum water content, swelling pressure and swell potential all decreased and the strength increased. The optimum fly ash content was found to be 25% for strength and CBR performance.

Abbasi et al (2012) investigated the improvement of silty sand desert soil from Iran using natural pozzolan from a cement factory (up to 15%) and lime (up to 7%). Their results showed that the addition or either or both additives increased the optimum water content and decreased the maximum dry density and that adding both the natural pozzolan and lime together resulted in a significant strength increase. The optimum binder for the stabilisation of this silty sand was found to be a combination of 15% natural pozzolan and 3% lime.

The work by Kamei et al (2012) investigation the stabilisation effect of recycled bassanite, a product from gypsum waste, with coal ash for a soft clay. The bassanite-coal ash is treated with a small quantity of cement to prevent the solubility of the bassanite. The paper shows that the strength increased with the increase in admixture content and curing time as well as the increase in the relative bassanite content in the mix. Through microstructural images, Figure 12, the authors deduced that the strength improvement was mainly due to the formation of ettringite, binding the soil particles, and the quantity and size of the formed ettringite was found to increase with the increase in the bassanite content. The bassanite also absorbed water from the soils and the Ca ions caused its flocculation. The pozzolanic nature of the coal ash also contributed to the strength development.

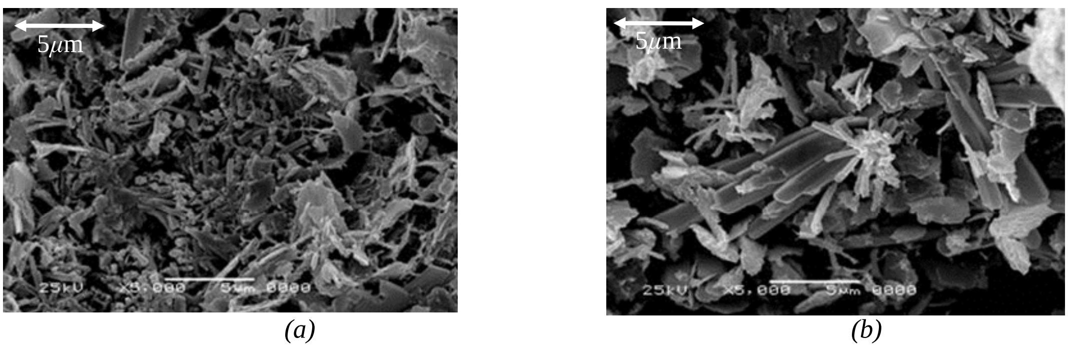

(a) *(b)*

Figure 12: SEM images of soil stabilised with different contents of bassanite and coal ash (a) 20% bassanite and no coal ash and (b) 20% bassanite and 10% coal ash (Kamei et al, 2012).

The paper by Sargent et al (2012) investigated the use of industrial by-products, namely ground granulated blast furnace slag (GGBS), fly ash and red gypsum, activated by an alkali (mix of sodium hydroxide and sodium silicate) in the stabilisation of an artificial silty sandy clay at 10% binder dosage. Figure 13 of the UCS values and percentage volume change in freeze-thaw cyclic testing clearly shows the superior performance of the alkali activated GGBS where very high UCS values were obtained and minimal volume change during freeze-thaw cycling. Investigation of the pH showed that the alkali activation applied did raise the pH to values about the minimum required 10.5 for pozzolanic reactions. Further work in enhancing the stabilisation potential of red gypsum and fly ash is required.

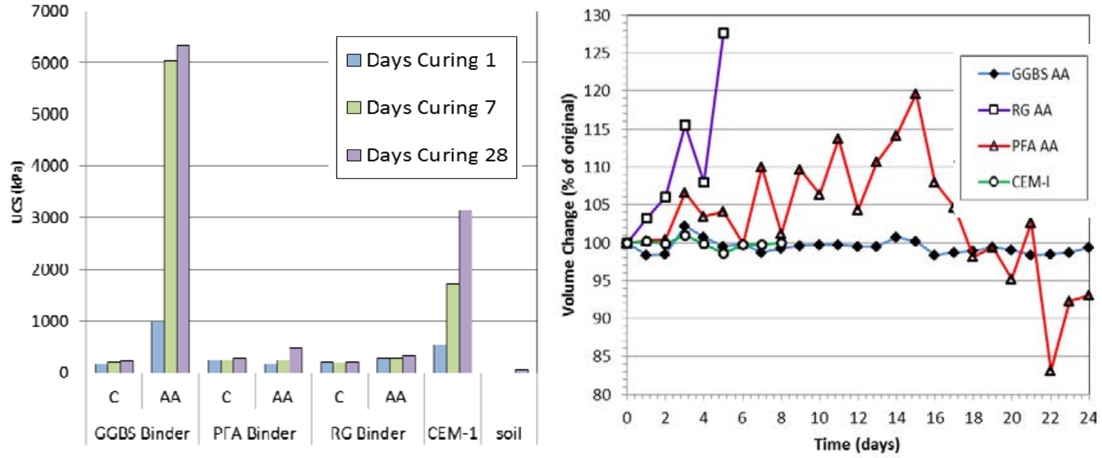

(a) *(b)*

Figure 13: The performance of the alkali activated industryal by-products in the stabilisation of a silty sandy clay in terms of (a) UCS and (b) volume change during freeze-thaw cycling (Sargent et al, 2012).

Mirzaeifar and Abdi (2012) concentrated on the investigation of the use of basic oxygen steel slag (BOS) and lime for the stabilisation of kaolin clay. They added lime (1-5%) and BOS (10-20%) separately and together and tested for UCS and freeze-thaw cycles. The results shows significantly enhanced strength (Figure 14a) and resistance to freeze-thaw cycles (Figure 14b) with the addition of both lime and BOS due to the combined modification and pozzolanic reactions between the lime, BOS and clay soil. The highest lime content together with all the BOS ratios tested performed the best.
Blanck et al (2012) investigated the effect of the use of an acid containing sulfonated limonene, a by-product from the citrus industry, on the compaction behaviour of three silts. The results showed a highly dependent behaviour on the nature of the soil, with a reduction in optimum water content observed for one soil leading to improved UCS and for two for the silts there was improved compaction particularly on the dry side of optimum.

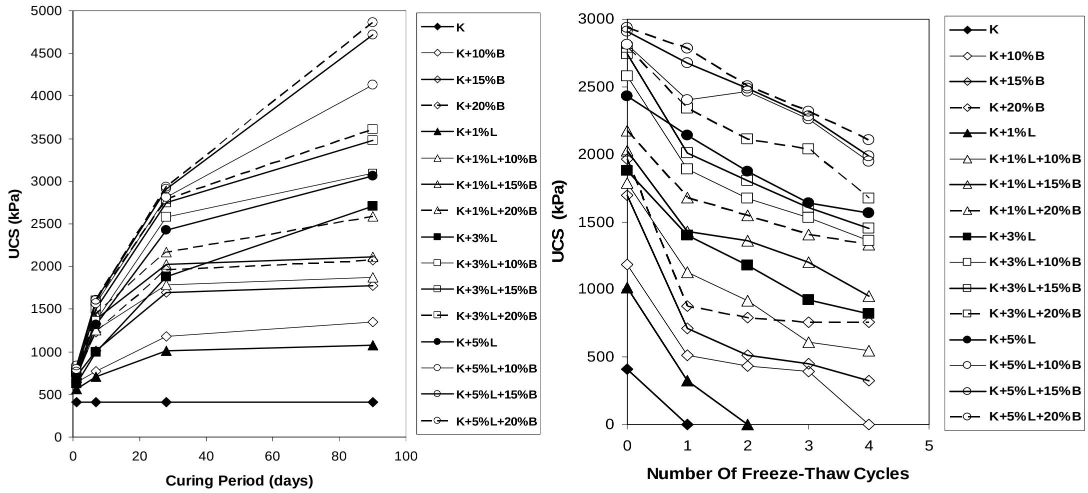

(a) *(b)*

Figure 14: The performance of kaolin clay stabilised with BOS and lime in terms of (a) UCS and (b) UCS after freeze-thaw cycles Mirzaeifar and Abdi (2012).

The paper by Ajdari and Bahmyari (2012) investigated the potential for potassium silicate as a stabiliser (up to 12% content) for sand-bentonite mixes, with bentonite content of 15 & 25%. The results showed that the addition of the potassium silicate that wetting induced swelling of the stabilised soil was less than that of the unstabilised soil and the drying induced shrinkage was negligible.

4. PROCEDURES, DESIGN, MODELLING AND CONSTRUCTION

This section includes all the eight papers that address aspects other than the binder type nad this includes laboratory moulding procedures, integrated treatments, numerical modelling, investigation of field failure mechanisms, proposal of revised guidelines and novel field stabilisation processes.

The two related papers by Grisolia et al (2012) and Kitazume (2012) addressed the influence of four different moulding procedures, namely dynamic compaction (D.C.), tapping (TA.), rodding (RO.) and no compaction (N.C.), on the performance of cement-stabilised soils. Figure 15 for cement-treated Kawasaki marine clay (Grisolia et al, 2012), clearly shows the different achieved UCS values for different intitial strength soils (Figure 15a) and the wide variation of the wet density with UCS (Figure 15b). The paper concludes that TA. and RO. techniques are most suitable for the very soft clays and D.C. or the stiffer clays. Similarly, for cement-treated Kaolin clay (Kitazume, 2012) compared the first three methods as well as static compaction (S.C.) and confirmed the significant effect that the moulding technique has on the strength and density of the resulting stabilised clay. This work also confirmed that TA. And RO. were far more suitable for very soft clays than D.C. and S.C.

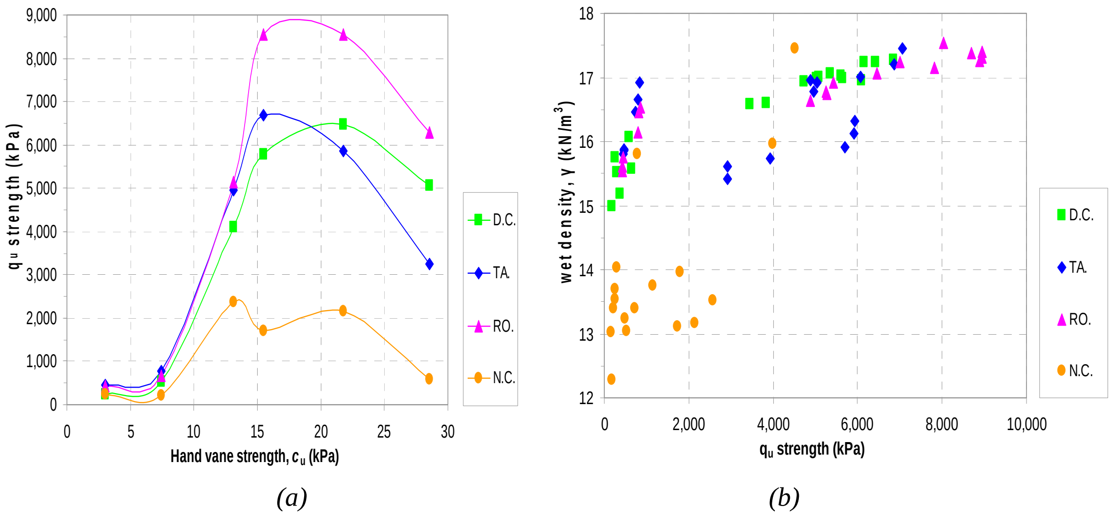

Figure 15: Effect of four different moulding procedures in terms of (a) UCS vs initial soil strength and (b) wet density vs UCS of all the cement-treated Kawasaki samples (Grisolia et al, 2012).

Vanni and Preda (2012) present an integrated process for the management of dredged lagoon sediments which involve granulometric separation of the coarse and fine fractions by means of vibrosieving, cycloning and centrifuging, in-line stabilisation of the fluidised mud by continuous injection of cement into the centrifuge, which ensure homogenous mixing, and treatment of contamination with wet oxidation. Figure 16 shows the process plant used and thickened silt and clay emerging from the centrifuge following continuous cement treatment.

Mukabi (2012) presented a number of recent case studies to illustrate the use of the Optimum Mechanical and Chemical Stabilisation (OPMC) technique in enhancing the geotechical properties of ground and geomaterials. These include the design and construction of a runway pavement for an International Airport, a road pavement structure, a pad foundation and a retaining wall along a steep slope.

Sonon et al (2012) presented an integrated framework for the computational generation and homogenisation of large sets of soil representative volume elements (RVE) combined with extended finite element method (XFEM) for the assessment of the effect of fabric on the mechanical performance of binder-treated soils. They modelled lime treated clay-sand mix with different contents of clay/lime (active phase), sand (inert phase) and macro-voids in terms of effect on the elastic properties of the mix and confirmed that the developed methodology was able to identify morphological effects. Figure 17 shows the vertical strain distribtuion under vertical compression computed with XFEM for two different RVEs.

(a) *(b)*

Figure 16: Parts of the integrated management treatment proposed by Vannie and Preda (2012) for dredged lagoon mud in Italy (a) the process plant used and (b) thickened silt and clay fractions coming out of the centrifge (Vannie and Preda, 2012).

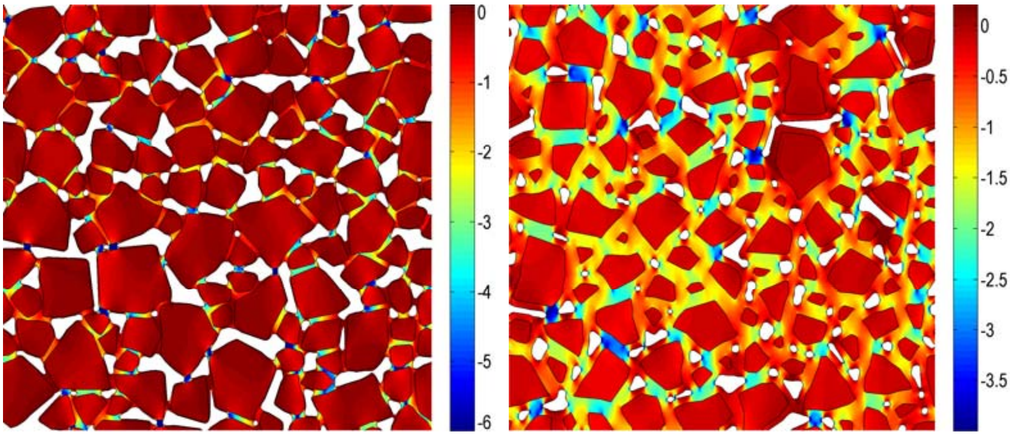

(a) *(b)*

Figure 17: Vertical strain distributions modelled with XFEM for two different RVEs with average volume fractions of sand/clay/macro-voids of (a) 0.70/0.14/0.16 and (b) 0.41/0.50/0.089 (Sonon et al, 2012).

Ghorbanbeigi et al (2012) performed finite element analyses, Figure 18a, of the behaviour of sand treated with different binders and observed that depending on the amount of binders, the treated sand exhibited a moderate material softening behaviour and showed that the Mohr-Coulomb is an effective model for the identification of the soil strength parameters because of its simplicity, accuracy and efficiency. However, for larger binder contents, it may be necessary to use a more complex constitutive model to reproduce the softening observed for large strain and that this behaviour was better simulated using the Modsol model, because of its ability to reproduce the hardening and softening behaviour of the mixed soil, Figure 18b.

Recent research at the University of Texas at Arlington explored the causes of poor stabilisation problems experienced in the field for subgrade soil treatment; one being the lack of understanding of the chemical interaction between the binder and soil minerals and the second being durability issues with montmorillonite dominent clay and Chittoori and Puppala (2012) presented results of laboratory studies that provided insight into these aspects and proposed the revisions shown in Figure 19 to current guidelines.

Gomez and Anderson (2012) presented details of the design, field-laboratory procedure and performance related to the surface treatment by cement-soil stabilisation of an active two-lane US State Highway in Virginia. The stabilisation consisted of pulverising the existing asphalt and mixing it with existing base materials which were then combined with 4% cement; Proctor compaction was used to optimise the compaction behaviour.

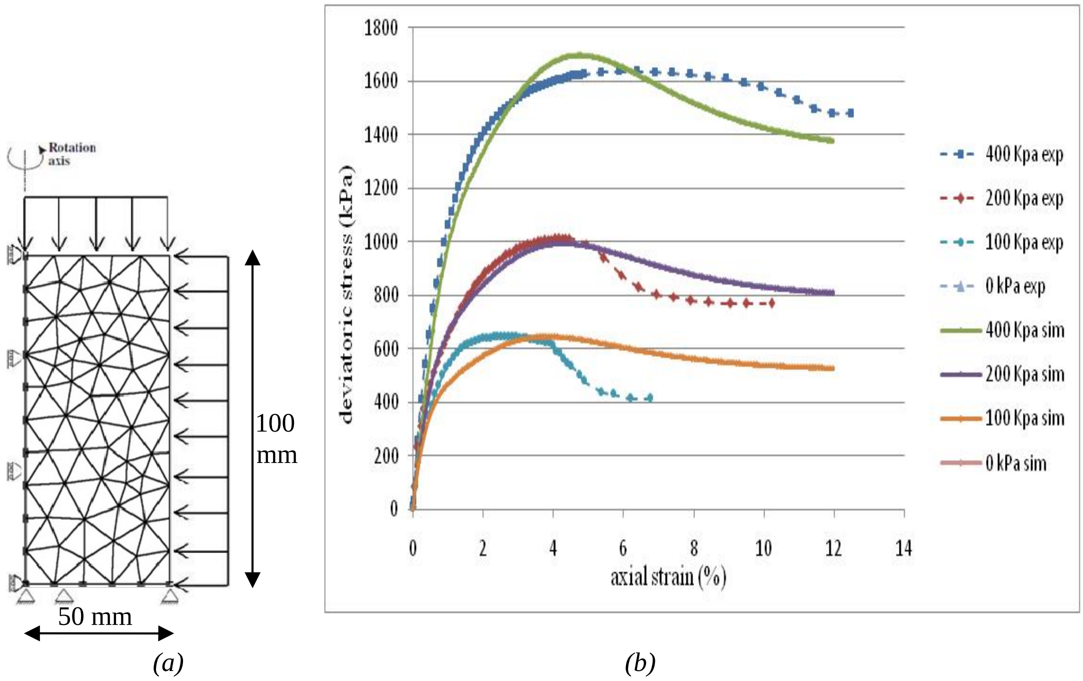

Figure 18: Finite element modelling and results of sand treated with a range of binders (a) the finite element mesh and (b) modelling results from Modsol and the corresponding laboratory triaxial results (Ghorbanbeigi et al (2012).

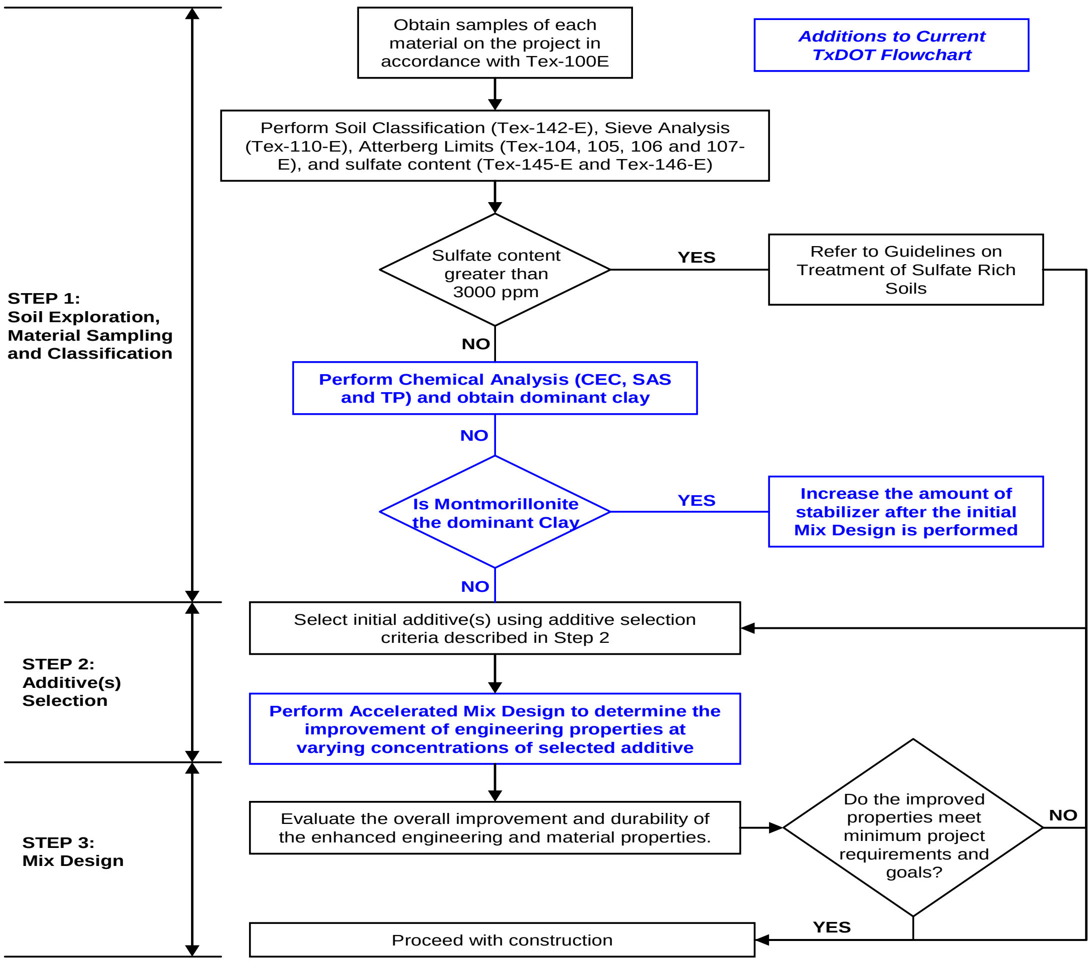

Figure 19: The current flow chart for subgrade soil treatment from TxDOT guidelines together with the proposed revision (in blue) by Chittoori and Puppala (2012).

5. AREAS OF RECENT RELEVANT RESEARCH BY THE AUTHOR

The author has been involved in extensive research work on soil stabilisation for many years. The most recent work has concentrated on the development of novel binders which either have sustainability benefits or enhance the mechanical performance/durability or both. Work on enhancing the durability of cement-stabilised soils involved the incorporation of zeolites, which are widely used in China as a cement blending material. Zeolites blended with PC have been shown to offer enhanced strength as well as durability over PC alone in concrete applications (Feng et al., 1992; Janotka et al., 2003, Perraki et al., 2003) based on the following: (a) the highly porous structure of zeolite provides large reaction surfaces for the interaction with portlandite hence consuming it; (b) zeolite in a cement matrix produces a hydration phase which contains less portlandite and less Ca-rich C–S–H reducing leachability; (c) zeolite produces a finer pore matrix in cement paste, reducing the permeability; and (d) zeolite has a higher pozzolanic activity than commonly used pozzolans, such as ashes and slag, offering much improved durability. The expected significant enhancement in technical performance will lead to a significantly increased lifespan of construction products. Details of this work have been reported by Osman and Al-Tabbaa; 2006; 2009 and Jegandan et al, 2010. Typical observations are shown in Figures 20 and 21 which show the strength, permeability and durability enhancements that were achieved in laboratory testing.

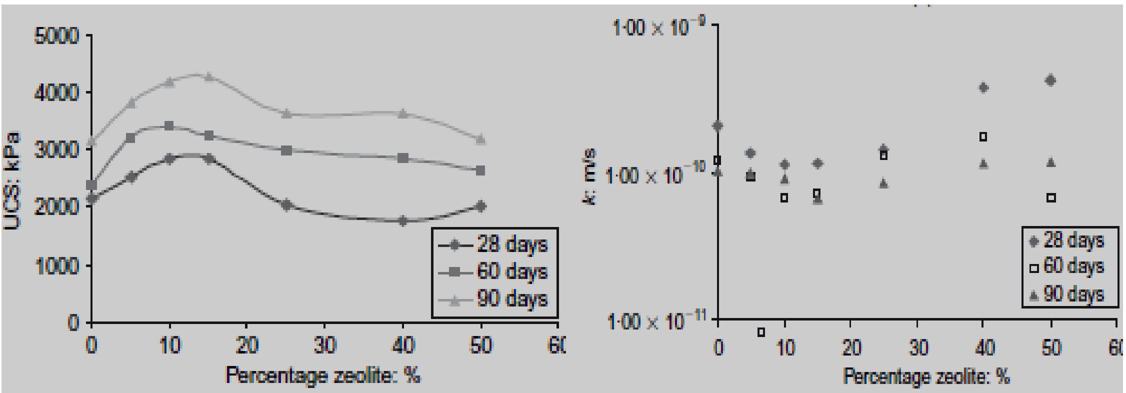

(a) *(b)*

Figure 20: The effect of zeolite on the performance of cement-bentonite treated clays in terms of (a) UCS and (b) permeability (Jegandan et al, 2010).

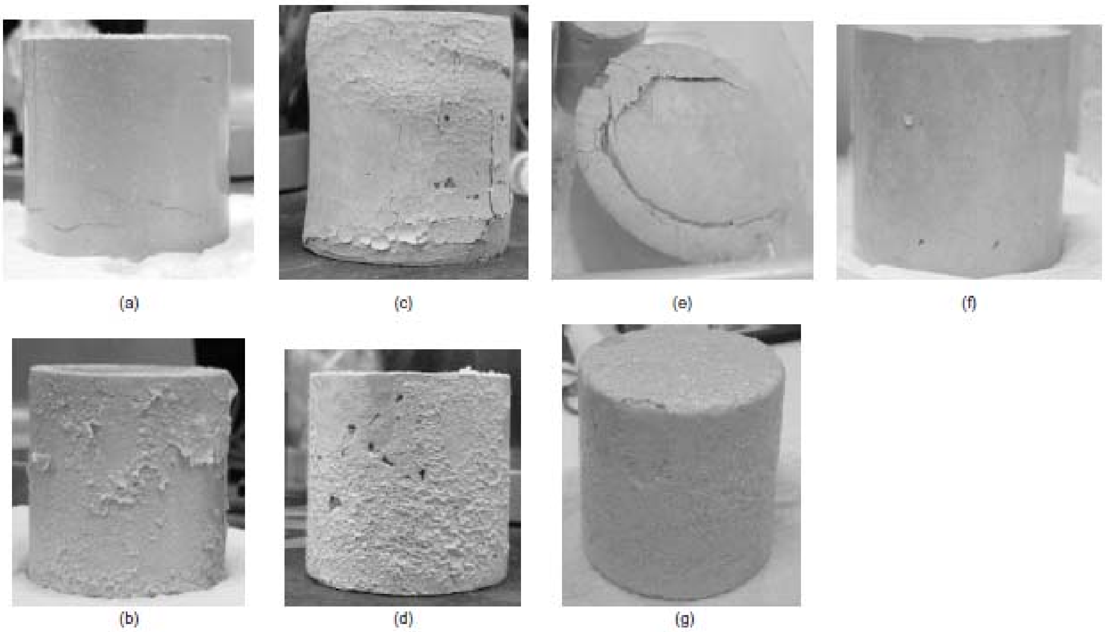

Figure 21: Physical damage caused to stabilised clay: (a) with CEM I in sulfate solution for 18 days; (b) with CEM I in acid solution for 36 dats; (c) with CEM I-bentonite in sulfate solution for 4 days; (d) with CEM I-bentonite in acid solution for 4 days; (e) with CEM 1-PFA in sulfate solution for 12 days; (f) with CEM I-zeolite in sulfate solution for 1.5 years and (g) with CEM 1-zeolite in acid solution for 200 day (Jegandan et al, 2010).

The other binder that has been extensively studied by the author's research team over the past eight years is reactive magnesia for a range of applications including concrete, porous blocks, ground improvement, waste immobilisation and land remediation, extreme environment applications such as oilwell cements and for geothermal applications as well as geological sequestration (Al-Tabbaa, 2013). Reactive magnesia cements, which are blends of reactive magnesia and PC, have been developed by the Australian scientist John Harrison (Harrison, 2008) as a sustainable alternative to PC. Reactive magnesia is mainly produced from the calcination of magnesite (magnesium carbonate) at temperatures of ~700-850^{o}C, this being much lower than the temperature used to produce Portland cement, as well as from seawater and/or brine (Shand, 2006). One of the main advantages of reactive MgO is the fact that it hydrates to form magnesium hydroxide, which is far less soluble and far less reactive than Portlandite. Another advantage is that in the presence of CO_2, MgO will carbonate to form a number of different hydrated magnesium carbonates, which are significantly stronger than calcium carbonate. Both sets of reactions are expansive contributing to a dense microstructure. For ground improvement applications, the author's team have been investigating the use of MgO in two ways: (i) alone as a soil stabilisation additive, where MgO is carbonated and its performance is compared to the use of PC alone, (ii) in blends with GGBS and performance compared to blends of GGBS and lime and (iii) in blends with PC or PC and fly ash and compared to mixes with no MgO content. Details of this work can be found elsewhere (Jegandan et al, 2010; Al-Tabbaa et al, 2011; Yi et al 2012a; 2012b).

The results of laboratory experiments in triaxial set-up of the permeation of CO_2 under various pressure conditions, through MgO-stabilised soils are shown in Figure 22 (Yi et al, 2012b). The figures clearly show the significantly enhanced strength achieved by carbonation of the MgO compared to ambient curing where the strength values achieved are equivalent to those of corresponding PC stabilised sand and silt. Microstructural analyses of those samples as well as samples cured in CO_2 incubators at 20% CO_2 content, Figure 23, clearly show the presence of nesquehonite, hydromagnesite and dypingite, which are the main hydrated magnesium carbonates formed and confirm their strength enhancing properties.

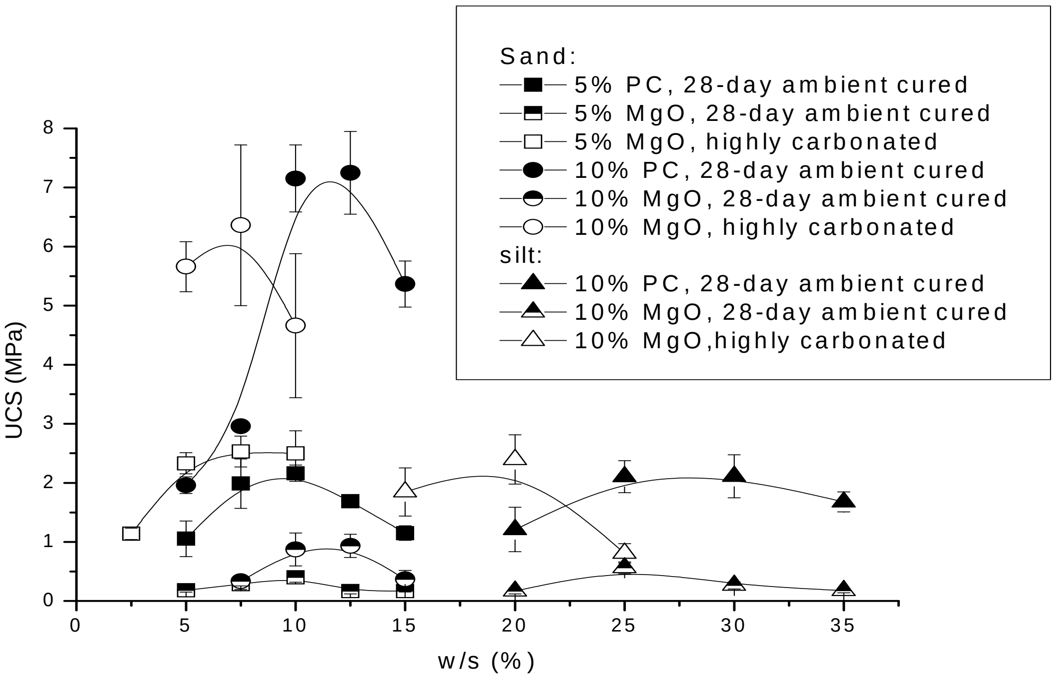

Figure 22: The UCS of 28-day ambient cured MgO- and PC-stabilised soils and the highly carbonated MgO-stabilised soils (Yi et al, 2012b).

A range of GGBS and MgO blends were tested and compared with blends of GGBS and lime and some results are presented in Figure 24 (Yi et al, 2012c), which clearly show an optimum MgO content of 10-20% and superior performance of the MgO blends even in comparison with corresponding PC stabilised soils. The significant strength enhancement correlates well with significant reduction in permeability (Figure 24b) for the optimum MgO content range confirming the formation of a denser microstructure caused by the expansive hydration products.

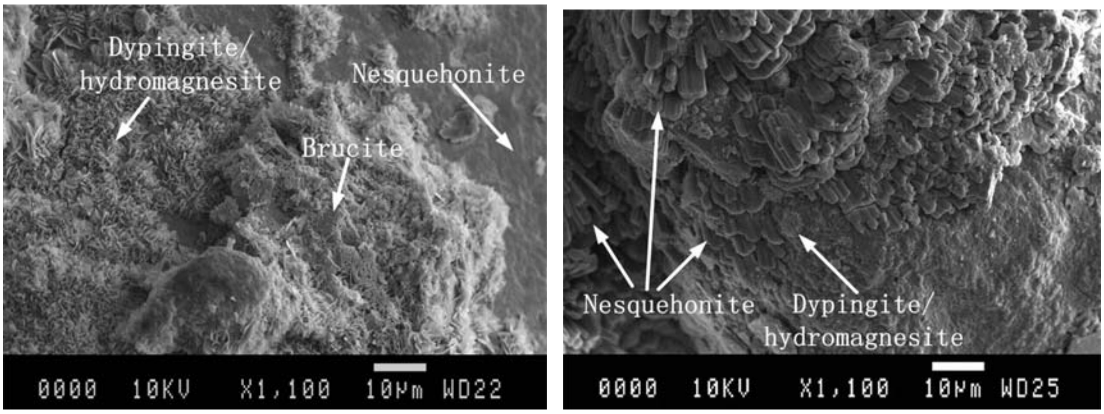

(a) *(b)*

Figure 23: Scanning electron micrographs of the stabilised sand with 5% MgO content at 7.5% soil water content (a) carbonated in the triaxial cell set-up with 200kPa CO_2 pressure for 0.5 hours and (b) carbonated in a CO_2 incubator for 7 days (Yi et al, 2012b).

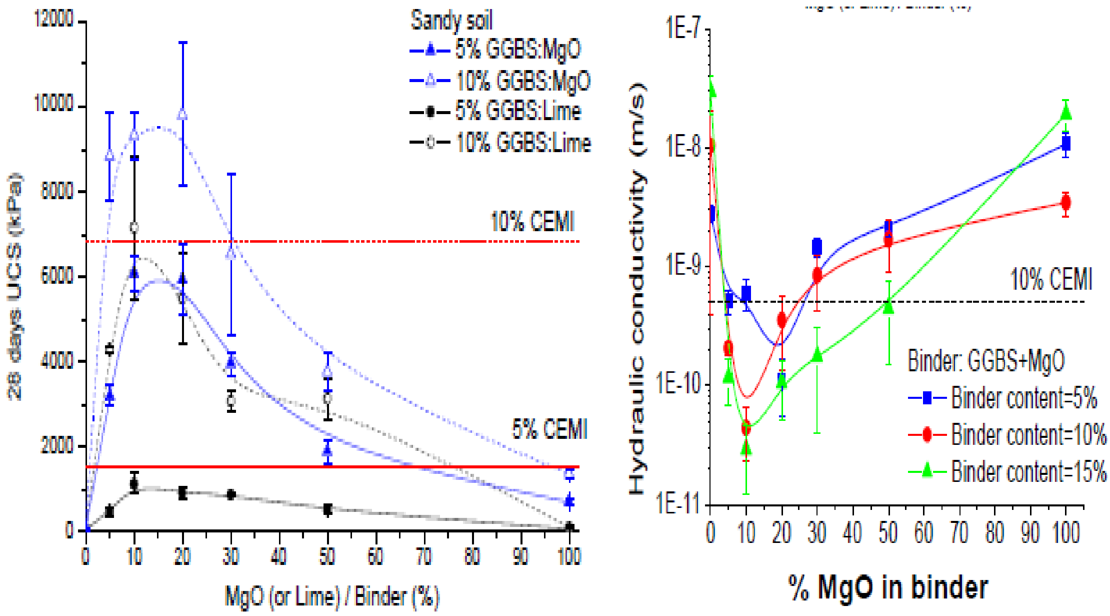

(a) *(b)*

Figure 24: The performance of GGBS-MgO blends in the stabilisation of a sand in terms of (a) UCS and (b) permeability (Yi et al, 2012c).

Given the differences commonly observed between laboratory treatability study results and field performance, the author's group has also been performing laboratory soil stabilisation work using a laboratory-scale auger set-up, shown in Figure 25a and 26a-b, as previous work has shown good correlation between the laboratory-scale auger results and full scale results (Al-Tabbaa and Evans, 1999). Recent studies have looked at the stabilisation performance in peats and clays (Figure 25, Hernandez-Martinez et al, 2007) as well as of carbonated MgO (Figure 26, Yi et al 2012d).

(a) *(b)*

Figure 25: The laboratory scale auger system (a) the laboratory scale set up and auger and (b) examples of resulting columns in clay, organic clay and peat (from left to right) (Hernandez-Martinez et al, 2007).

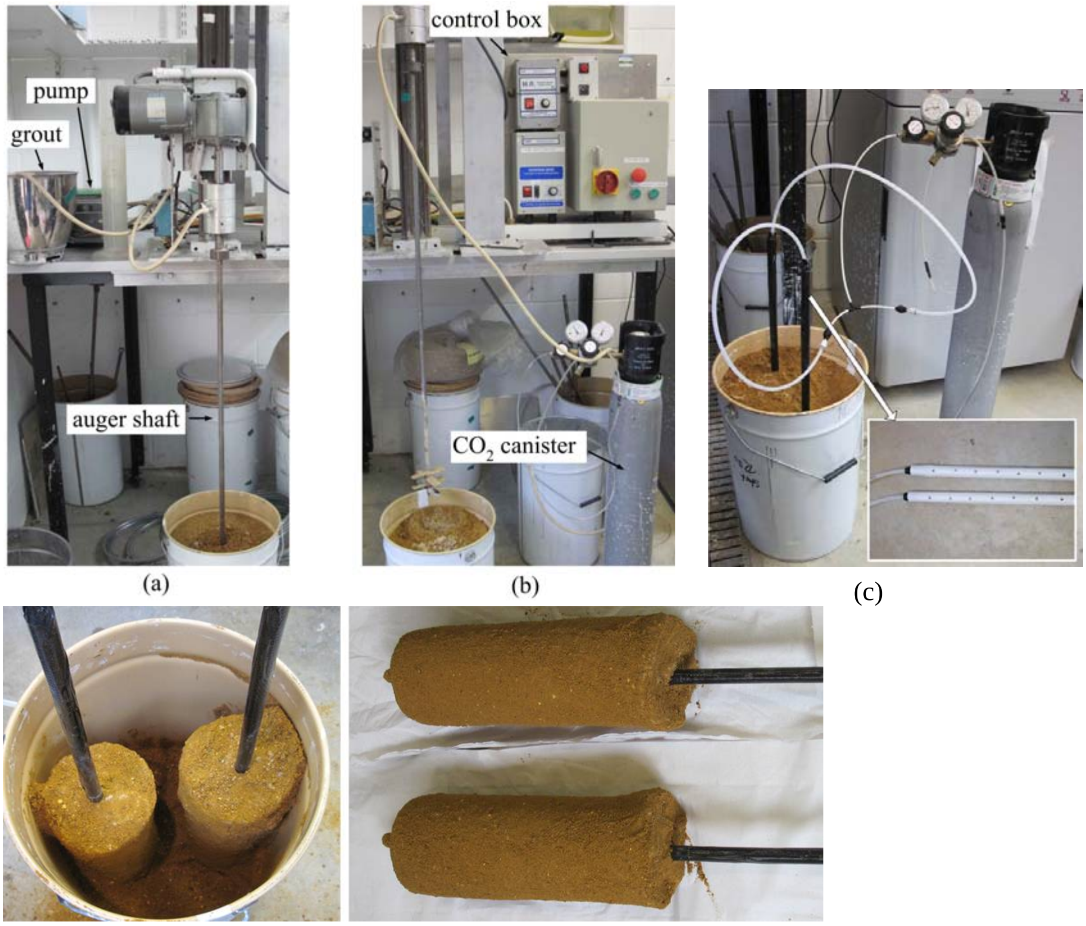

(d)

Figure 26: The laboratory scale set up for the installation of carbonation MgO (a-b) pumping CO_2 through the auger, (c) pumping the CO_2 through a separate pipe system and (d) examples of extrdued columns following carbonation (Yi et al, 2012d).

A wide range of binders, including blends of PC, GGBS, PFA, zeolite, MgO, cement kiln dust (CKD), bentonite, were recently tested in full scale field using auger systems (single and triple) as well as mass stabilisation systems to develop further correlation between field trials and laboratory performance. Those field trials were part of an extensive industry-academia collaboration in the UK, (project SMiRT, Al-Tabbaa et al 2009a, 2009b, 2011, 2012a, 2012b) which aimed to advance the use of deep soil mix technology for both ground improvement as well as land remediation. The binders were hence investigated for their ability to immobilise contaminants (organics and heavy metals). Tables 1a and b below summarise some of the results, compared under four different binder groups and comparisons were also made between wet mixing and dry mixing, model soils and site soils in the laboratory, laboratory results and field results as well as different field results (surface samples and window samples).

Table 1: Preliminary results from Project SMiRT comparing binders as well as laboratory and field results in terms of (a) UCS and (b) leachability of both total organics and metals (Al-Tabbaa, 2012b)

			Dry binder (%)	Group 1 (CEM I) (kPa)	Group 2 (CEM I:PFA) (kPa)	Group 3 (CEM I:GGBS) (kPa)	Group 4 (MgO + (CKD (lab only)) (kPa)
S/S Wet mixing	Treatability study (50x100)	Model Sand (w/b=0.5)	6.7 13.3 20	560-2050 4000-8500 6000-14600	470-690 230-4500 400-6950	420-930 970-5200 140-6670	220-1000 800-5400 1100-7300
		Model Silt (w/b=0.5)	13.3	520-5500	1420-3170	470-6100	200-4600
		Site soil (w/b=1)	10	260-2700	160-1230	110-2150	100-1870
	Field trials (55x110-85x170)	Surface samples (w/b=1)+OC/IOC	7.5-15	160-1900	120-160	100-770	140-600
		Window samples (w/b=1)+OC/ IOC		240-1500	160-600	100-3600	120-3250
GI Dry Mixing	Field trials (55x110-85x170)	Surface samples (w/b=1)	2.5-10	20-220	80-100	110-430	100-420
		Window samples (w/b=1)		270-2940	20-250	100-2270	160-1200
	Treatability study (50x100)	Model sand	2.5 5 10	500-800 1800-2200 6800-8400	200-800 500-1900 1200-5100	500-2000 2000-3200 6400-9000	200-2100 450-2500 950-6000
		Model silt	2.5 5-10	50-200 250-900	50-160 500-2600	50-190 500-1300	50-200 350-1460

(a)

			Binder (%)	Group 1 (CEM I) (mg/L)	Group 2 (CEM I:PFA) (mg/L)	Group 3 (CEM I:GGBS) (mg/L)	Group 4 (MgO + (CKD lab only)) (mg/L)	All Groups total metals (mg/L)
S/S Wet Mixing	Treatability study	Model Sand (w/c=0.5)	6.7 13.3 20	15-60 4-25 3-23	30-190 15-95 5-30	55-145 35-75 10-35	85-260 60-235 20-240	0.02-1.1
		Model Silt (w/c=0.5)	13.3	1-5	5-20	5-10	1-5	0.1-1.2
		Site soil (w/c=1)	10	15-350	10-180	15-370	10-205	0-0.2
	Field trials	Surface samples (w/c=1)	7.5-15	35-195	25-200	40-195	20-175	0-2.3
		Window samples (w/c=1)		1-200	2-135	6-130	3-115	0-0.2

(b)

6. CONCLUSIONS

Recent advances in soil stabilisation research is shaped by recent changes including increased context applications, applications in aggressive environments, incorporation of industrial by-products and wastes, emphasis on sustainability as well as recent legislations. The 31 session papers presented a wide range of studies on various aspects of soil stabilisation covering materials, procedures, design, modelling and construction. A wide range of binders and additives and different performance aspects assessed.

A number of papers developed linear correlations between the unconfined compressive strength of stabilised soils and the logarithm of curing time. In terms of additives, the use of tyre chips was observed to prevent the development of large cracks, the addition of polypropylene fibres enhanced the strength and stiffness of stabilised clay. A proposal was made that the relation between field blade rotation speed and strength and homogeneity of treated soils can be explained by the shear-thinning of clays. A porosity-cement ratio index, expressed as the porosity of a sample divided by the volumetric cement content as a percentage of the total volume, was correlated with compressive strength, tensile splitting strength and initial shear modulus of stabilised soil. The groutability of alluvial soils was found to increase with pressure, water:cement ratio and lower percentage compaction. Investigationo of PC on the workability/liquid Limit showed that cement cannot be considered as simply a fine soil fraction at a very young age.

Greater pozzolanic development was seen to have taken place due to the addition of finely ground limestone, to lime stabilisation, presenting evidence of the formatio of nucleation centres. The addition of bentonite to lime stabilisation of sand, to enhance pozzolanic activities, was reported to be beneficial at 10% addition. The immediate modification to grain size of quickime stabilised clay was confirmed. The addition of 5% lime was found to produce optimum results for 0.5-3% humic acid content organic clays and the strength was enhanced with the addition of chloride salts. The use of fly ash, at optimum value of 25%, was found to decrease the Atterberg limits, optimum water content, swelling pressure and swell potential and increase the strength. A significant increase in strength was observed with the addition of a natural pozzolan (up to 15%) and lime (up to 7%) to Iranian silty sands. The use of industrial by-products from gypsum waste (recycled bassanite) and fly ash showed strength increase attributed to the formation of ettringite, binding the soil particles. The use of GGBS, fly ash and red gypsul activated by an alkali to stabilised silty sandy clay showed superior performance by the GGBS in terms of higher strength and lower volume change in freeze-thae cycling. The addition of both lime (1-5%) and Basic oxygen slag (10-20%) showed enhanced strength and resistance to freeze-thaw due to the combined modification and pozzolanic reactions between the lime, BOS and clay soil. The use of an acid containing sulfonated limonene, a by-product from the citrus industry, on the compaction behaviour of three silts, showed a highly dependent behaviour on the nature of the soil. The addition of potassium silicate to sand-bentonite mixes showed that wetting induced swelling was less than that of the unstabilised soil and the drying induced shrinkage was negligible.

Two related papers confirmed the significant effect of the moulding procedure and that tamping and rodding were far more suitable for very soft clays than static and dynamic compaction. A proposed process of continuous injection of the stabilising grout through a centrifuge containing dredged lagoon sediments was shown to produce homogeneous mixing.

An integrated framework for the computational generation and homogenisation of large sets of soil representative volume elements combined with extended finite element method for the assessment of the effect of fabric on the mechanical performance of binder-treated soils was presented. Finite element modelling of treated sand showed that for large binder contents, it may be necessary to use a more complex constitutive model, than Mohr-Coulomb such as Modsol, in order to reproduce the softening observed for large strain.

Revision to current guidelines for subgrade soil treatment was proposed based on the development of understanding of the chemical interaction between the binder and soil minerals. Details of the design, field-laboratory procedure and performance related to the surface treatment by cement-soil stabilisation of an active US Highway were presented which consisted of pulverising the existing asphalt and mixing it with existing base materials and 4% cement.

Finally, the authors most recent work in soil stabilisation has concentrated on the use of novel binders and additives such as zeolites and reactive magnesia for enhanced sustainability and durability as well as detailed investigation of the performance of a wide range of binders in contaminant immobilisation. In addition correlations between laboratory and field results are being investigated and developed.

REFERENCES

Abbasi, N., Mahdieh, M. and Davoudi, M.H. (2012). Improvement of geotechnical properties of silty sand soils using natural pozzolan and lime. ISSMGE-TC211 International Symposium on Ground Improvement IS-GI, Brussels.

Ajdari, M. And Bahmyari, H. (2012). Oedometric Response of a Sand-Bentonite Mixture Improved by Potassium Silicate. ISSMGE-TC211 International Symposium on Ground Improvement IS-GI, Brussels.

Al-Tabbaa, A. and Evans, C.W. (1999). Laboratory-scale soil mixing of a contaminated site. Ground Improvement, 3: 119-134.

Al-Tabbaa, A., Liska, M., Jegandan, S. and Barker, P. (2009a). Overview of project SmiRT for integrated remediation and ground improvement. Proc International Symposium on Deep Mixing and Admixture Stabilisation, Okinawa, May.

Al-Tabbaa, A., Barker, P. And Evans, C.W. (2009b). Innovation in soil mix technology for remediation of contaminated land. Proc International Symposium on Deep Mixing and Admixture Stabilisation, Okinawa, May.

Al-Tabbaa, A., Barker, P and Evans, C.W. (2011). Soil mix technology for land remediation: recent innovations. ICE Ground Improvement, 164(3): 127-137.

Al-Tabbaa, A, Liska, M, McGall, R and Critchlow, C (2012a). Soil mix technology for integrated remediation and ground improvement: Field trials. Invited Lecture, International Symposoium and Short Courses on Recent Research, Advances and Execution Aspects of Ground Improvement Works, IS-GI 2012, Brussels, May.

Al-Tabbaa, A., Liska, M., McGall, R., Critchlow, C. And Sweeney, R. (2012b). Soil mix technology for integrated remediation and ground improvement: Design and field performance. International Conference on Ground Improvement and Ground Control (ICGI 2012), Oct., Wollongong.

Al-Tabbaa, A. (2013). Reactive Magnesia cements, Chapter 18 in Eco-Efficient Concrete (Torgal and Jalali, ed), Woodhouse Publishers (in press).

Beetham, P., Dijkstra, T. And Dixon, N. (2012). Nucleation centres in lime stabilised soils. ISSMGE-TC211 International Symposium on Ground Improvement IS-GI, Brussels.

Blanck, G., Cuisinier, O. And Masrouri, F. (2012). A non-traditional treatment for the compaction of fine-grained soils. ISSMGE-TC211 International Symposium on Ground Improvement IS-GI, Brussels.

Chittoori, B. And Puppala, A. (2012). Chemical stabilization for pavement subgrades. ISSMGE-TC211 International Symposium on Ground Improvement IS-GI, Brussels.

Consoli, N. C. And Viana da Fonseca, A. (2012). Rational criteria for the assessment of the target mechanical strength and stiffness of artificially soil-cement mixtures. ISSMGE-TC211 International Symposium on Ground Improvement IS-GI, Brussels.

Fatahi, B., Khabbaz, H. And Fatahi, B. (2012). Application of polypropylene and carpet fibres to improve strength and stiffness properties of cement treated clay using deep soil mixing. ISSMGE-TC211 International Symposium on Ground Improvement IS-GI, Brussels.

Feng, N.Q., Ma, C.C. and Ji, X.H. (1992). Natural zeolite for preventing expansion due to alkali–aggregate reaction. Cement, Concrete and Aggregates, ASTM 14(2): 93–96.

Gharouni, N., Esmaelli, M. And Hosseinpour, H. (2012). Laboratory investigations on groutability of type C alluvial used in ground improvement for construction metro tunnels. ISSMGE-TC211 International Symposium on Ground Improvement IS-GI, Brussels.

Ghorbanbeigi, H., Mroueh, H., Lancelot, L. And Shao, J.F. (2012). Numerical analysis of the behavior of cement treated sand. ISSMGE-TC211 International Symposium on Ground Improvement IS-GI, Brussels.

Gomez, J. And Anderso, D.M. (2012). Soil cement stabilization - mix design, control and results during construction. ISSMGE-TC211 International Symposium on Ground Improvement IS-GI, Brussels.

Grisolia, M., Leder, E. Marzano, I.P., Mizutani, T. and Morikawa, Y. (2012). Influence of tire chips on the mechanical properties of cement treated soil. ISSMGE-TC211 International Symposium on Ground Improvement IS-GI, Brussels.

Guimond-Barrett, A., Szymkiewics, F., Reiffsteck, P., Pantet, A., Le Kouby, A. and Guedon, S. (2012). On the strength and durability of cement-stabilised sands. ISSMGE-TC211 International Symposium on Ground Improvement IS-GI, Brussels.

Guimond-Barrett, A., Touati, A., Pantet, A., Reiffsteck, P and Le Kouby, A. (2012). Rheological properties of cement-stabilised kaolin clay. ISSMGE-TC211 International Symposium on Ground Improvement IS-GI, Brussels.

Harrison, A.J.W. (2008), Reactive magnesium oxide cements. United States Patent 7347896.

Hashemi, M.A., Kadiri, H., Massart, T., Verbrugge, J.-C. And Francois, B. (2012). Influence of the clay content of a lime-treated soil on its compression strength. ISSMGE-TC211 International Symposium on Ground Improvement IS-GI, Brussels.

Hernandez-Martinez, F. G., Osman, A. and Al-Tabbaa, A. (2007). Wet soil mix improvement of soft clays and organic soils: Laboratory investigation. Proceedings of the XIV European Conference on Soil Mechanics and Geotechnical Engineering, Madrid, September, Vol. 3, pp1329-1334.

Janotka, I., Krajci, L. and Dzivak, M. (2003). Properties and utilisation of zeolite-blended portland cements. Clays and Clay Minerals 51(6): 616–624.

Jegandan, S., Liska, M. Osman, A. A-M. and Al-Tabbaa, A. (2010). Sustainable binders for soil stabilisation. ICE Journal of Ground Improvement, 163(1), pp 53-61.

Kamei, T., Ahmed, A. and Shibi, T. (2012). Recycled bassanite in conjunction with coal ash for stabilization of soft clay soil. ISSMGE-TC211 International Symposium on Ground Improvement IS-GI, Brussels.

Kitazume, M. (2012). Influence of specimen preparation on unconfined compression strength of cement-stabilized Kaolin clay. ISSMGE-TC211 International Symposium on Ground Improvement IS-GI, Brussels.

Lutenegger, J.A. (2012). Immediate modification of clays with quicklime: alteration of grain-size distribution. ISSMGE-TC211 International Symposium on Ground Improvement IS-GI, Brussels.

Grisolia, M., Kitazume, M., Leder, E., Marzano, I.P. and Morikawa, Y. (2012). Laboratory study on the applicability of molding procedures for the preparation of cement stabilised specimens. ISSMGE-TC211 International Symposium on Ground Improvement IS-GI, Brussels.

Mirzaeifar, H and Abdi, M.R. (2012). Stabilizing clays using basic oxygen steel slag (BOS). ISSMGE-TC211 International Symposium on Ground Improvement IS-GI, Brussels.

Mohd Yunus, N.Z., Wanatowski, D. and Stace, L.R. (2012). Effectiveness of lime stabilisation in organic clay. ISSMGE-TC211 International Symposium on Ground Improvement IS-GI, Brussels.

Moretti, G., Viana da Fonseca, A., Paschoalin Filho, J. A. and de Carvalho, D. (2012). Strength increase over time of an alluvial clay, typical of the coast of Brazil´s Northeastern, mixed with different dosages of cement. ISSMGE-TC211 International Symposium on Ground Improvement IS-GI, Brussels.

Mukabi, J.N. (2012). Case study analysis of OPMC improved foundation ground, pavement and other geo-structures employing the GECPRO model. ISSMGE-TC211 International Symposium on Ground Improvement IS-GI, Brussels.

Nozu, M., Anh, N.T., Shinkawa, N. and Matsushita, K. (2012). Remedy of deep soil mixing quality for montmorillonite clay deposited in the Mekong and Mississippi deltas. ISSMGE-TC211 International Symposium on Ground Improvement IS-GI, Brussels.

Osman, A. A-M. and Al-Tabbaa, A (2006). Effect of zeolite and bentonite on the mechanical properties of cement-stabilised soft clay. Proceedings of Fourth International Conference on Soft Soil Engineering, Vancouver, October, pp 681-690.

Osman, A A-M. and Al-Tabbaa, A. (2009). Effect of cement-zeolite grouts on the durability of stabilised clays. XVII International Conference on Soil Mechanics and Geotechnical Engineering, Alexandria, October, pp 3-6.

Perraki, T., Kakali, G. and Kontoleon, F. (2003). The effect of natural zeolites on the early hydration of Portland cement. Microporous and Mesoporous Materials 61(1): 205–212.

Piriyakul, K. and Pochalard, S. (2012). Stiffness of soil-cement-fly ash by means of shear wave velocity. ISSMGE-TC211 International Symposium on Ground Improvement IS-GI, Brussels.

Ramadas, T.L., Darga Kumar, N and Yesuratnam, G. (2012). A study on strength and swelling characteristics of three expanisve soils treated with fly ash. ISSMGE-TC211 International Symposium on Ground Improvement IS-GI, Brussels.

Sargent, P., Rouainia, M., Hughes, P.N. and Glendinning, S. (2012). Alkali activation of industrial by-products for use in soil stabilisation. ISSMGE-TC211 International Symposium on Ground Improvement IS-GI, Brussels.

Saussaye, L., Boutouil, M., Baraud, F. And Leleyter, L. (2012). Soils treatment with hydraulic binders: physicochemical and geotechnical investigations of a chemical disturbance. ISSMGE-TC211 International Symposium on Ground Improvement IS-GI, Brussels.

Shand, MA (2006), The Chemistry and Technology of Magnesia. Wiley, New York, 2006.

Sonon, B., Hashemi, M.A., Verbrugge, J.-C., Francois, B. and Massart, T.J. (2012). Effect of fabric on elastic properties of lime treated clayey sand. ISSMGE-TC211 International Symposium on Ground Improvement IS-GI, Brussels.

Szymkiewics, F., Tamga, F.-S., Le Kouby, A., Reiffsteck, P and Tacita, J.-L. (2012). Laboratory study of the workability of the deep soil-mixing material and in situ applications. ISSMGE-TC211 International Symposium on Ground Improvement IS-GI, Brussels.

Timoney, M., Quigley, P. And McCabe, B.A. (2012). Some laboratory soil mixing trials of Irish peats. ISSMGE-TC211 International Symposium on Ground Improvement IS-GI, Brussels.

Vanni, D. And Preda, G. (2012). Consolidation of dredged mud in the Venice Lagoon. ISSMGE-TC211 International Symposium on Ground Improvement IS-GI, Brussels.

Yi, Y, Liska, M and Al-Tabbaa, A (2012a). Initial investigation into the use of GGBS-MgO in soil stabilisation. Proc 4th Int. Conf. Grouting and Deep Mixing, New Orleans, Feb.

Yi, Y, Liska, M, Unluer, C. and Al-Tabbaa, A (2012b). Carbonating magnesia for soil stabilisation. Submitted to Geotechnique Symposium in print on Bio and Chemo-mechanical processes in geotechnical engineering in 2013 (submitted).

Yi, Y, Liska, M and Al-Tabbaa, A (2012c). Performance of GGBS-MgO stabilised soil. In preparation for submission to the ICE Journl of Ground Improvement.

Yi, Y, Liska, M, Akinyugha, A., Unluer, C. and Al-Tabbaa, A (2012d). Preliminary laboratory-scale model auger installation and testing of carbonated soil-MgO columns. Submitted to ICE Journal of Geotechnical Engineering.

SESSION 4 – SOIL MIXING 2 – DEEP MIXING

General Report
SESSION 4 – SOIL MIXING 2 – DEEP MIXING

Nicolas Denies
Belgian Building Research Institute, Geotechnical division, Belgium, nde@bbri.be

Gust Van Lysebetten
KU Leuven, Belgium, gust.vanlysebetten@bwk.kuleuven.be

ABSTRACT

The present General Report highlights the significant contributions of the papers of Session 4 of the IS-GI Brussels 2012 dedicated to Deep Mixing. As not all papers are reviewed in detail, references are given in order to provide a balanced overview of the entire Technical Session.
This General Report discusses the latest developments and current researches in the deep soil mix (DSM) technique. Different ***execution processes*** *are summarized or classified and their mechanisms are outlined. The* ***DSM material*** *is discussed in detail and various* ***applications*** *of the process are illustrated with the help of case histories. Indeed, during several decades, the DSM technique has been used for ground improvement (GI) applications, but in recent years, DSM was also dedicated to various structural and environmental functions: earth/water retaining structures, foundations, soil reinforcement, land levees and slope stabilization, in situ remediation and barriers against liquefaction. In the present report, the temporary and permanent characters of the DSM structures are also mentioned with regard to the durability aspects of the soil mix material. Current* ***Quality Assurance/Quality Control activities*** *for DSM projects are highlighted.* ***Design*** *of in-situ soil mixing in geotechnical practice is reappraised considering the nature of the DSM material. Many references on the topics discussed are also given in the report.*

1. INTRODUCTION

The DSM process was introduced in the 70's in Japan and in the Scandinavian countries. Since several decennia, DSM has been known as a Ground Improvement (GI) technique, as reported in Porbaha et al. (1998 and 2000). Porbaha has notably proposed a terminology for the DSM technology, as presented in Table 1. According to the classification of GI methods adopted by the ISSMGE TC 211 Ground Improvement, formerly TC 17, DSM can be classified as ground improvement with grouting type admixtures, as illustrated in Table 2 (Chu et al. 2009). A lot of reviews describing various Deep Mixing Methods (DMM) are available in Terashi (2003), Topolnicki (2004), Larsson (2005), Essler and Kitazume (2008) and Arulrajah et al. (2009). In parallel, the results of national and European research programs have been published in multiple interesting reports (such as Eurosoilstab, 2002), while also the European standard for the execution of deep mixing "Execution of special geotechnical works – Deep Mixing" (EN 14679) was published in 2005. Most of these research projects focused on the global stabilization of soft cohesive soils such as peat, clay, gyttja and silt.

Table 1: Terminology of the deep mixing family, after Porbaha (1998)

CCP: chemical churning pile	DeMIC: deep mixing improvement by cement stabilizer
CDM: cement deep mixing	*In situ* soil mixing
CMC: clay mixing consolidation method	JACSMAN: jet and churning system management
DCCM: deep cement continuous method	Lime-cement columns
DCM: deep chemical mixing	Mixed-in-place piles
DJM: dry jet mixing	RM: rectangular mixing method
DLM: deep lime mixing	Soil-cement columns
DMM: deep mixing method	SMW : soil mix wall
DSM : deep soil mixing	SWING: spreadable WING method

Table 2: Classification of GI methods adopted by TC211, formerly TC 17 (after Chu et al., 2009)

D. Ground improvement with grouting type admixtures	D1. Particulate grouting	Grout granular soil or cavities or fissures in soil or rock by injecting cement or other particulate grouts to either increase the strength or reduce the permeability of soil or ground.
	D2. Chemical grouting	Solutions of two or more chemicals react in soil pores to form a gel or a solid precipitate to either increase the strength or reduce the permeability of soil or ground.
	D3. Mixing methods (including premixing or deep mixing)	**Treat the weak soil by mixing it with cement, lime, or other binders in-situ using a mixing machine or before placement.**
	D4. Jet grouting	High speed jets at depth erode the soil and inject grout to form columns or panels.
	D5. Compaction grouting	Very stiff, mortar-like grout is injected into discrete soil zones and remains in a homogeneous mass so as to densify loose soil or lift settled ground.
	D6. Compensation grouting	Medium to high viscosity particulate suspension is injected into the ground between a subsurface excavation and a structure in order to negate or reduce settlement of the structure due to ongoing excavation.

2. CONSTRUCTION PRINCIPLES AND EQUIPMENT

In the DSM process, the ground is in situ mechanically (and possibly hydraulically or pneumatically) mixed while a binder, based on cement or lime, is injected with the help of a specially made machine. DMM can be classified according to its execution process. Two types of installation methods are generally considered with regard to the way the binder is injected into the ground (with or without water addition): the wet and the dry mixing methods. In the wet mixing method, which is more frequently applied, a mixture of a binder and water with possibly sand or additives is injected and mixed with the soil. Depending on the type of soil and binder, a mortar-like mixture is created which hardens during the hydration process (Essler and Kitazume, 2008). In the dry soil mixing process, the binder is directly mixed with the soil. The binding agents directly react with the prevailing soil and the contained water and form a soil mortar. In the present proceedings, Quasthoff (2012) provides a State of the Art in dry soil mixing and reviews its construction principles, its equipment and its field of applications.
Depending on the applications, different improvement patterns can be designed with the wet and dry mixing methods with the help of soil-cement columns, rectangular soil mix panels, continuous barriers or global mass stabilization. In the present symposium, different types of DSM systems are presented, as reported hereunder.

2.1. Soil-cement column systems

2.1.1. CVR C-mix® system

The CVR C-mix® is performed with an adapted bored pile rig and a specific designed shaft and mixing tool. This tool rotates around a vertical axis at about 100 rpm and cuts the soil mechanically. Simultaneously, the water/binder mixture (w/b weight ratio between 0.6 and 0.8), is injected at low pressure (< 5 bar). The injected quantity of binder amounts mostly to 350 and 450 kg binder/m³, depending on the soil conditions and specifications. The binder partly (between 0% and 30%) returns to the surface, as 'spoil return'. The resulting DSM elements are cylindrical columns with diameter corresponding to the mixing tool diameter, varying between 0.43 and 1.03 m. As a wide range of tools has seen the light of day in the field of DSM technology, recent developments have mainly taken place in the optimization of tools for mass production in particular with the design and construction of triple (or more) auger systems. In this way, a CVR Twinmix® and a CVR Triple C-MIX® have been designed to increase the production rate. Figure 1 illustrates the CVR C-mix® machine and its Triple version.

2.1.2. SMET Tubular Soil Mix (TSM®) system

As represented in Fig. 2, the TSM® technique uses a mechanical and a hydraulic way of mixing. Apart from the rotating (around the vertical axis) mixing tool, the soil is cut by the high pressure injection (till 500 bars) of the water/binder mixture. The resulting DSM elements are cylindrical columns with a diameter between 0.38 and 0.73 m. Again, a twin and a triple version exist (Denies et al., 2012a).

a) b)

Figure 1: a) The CVR C-mix® machine (single auger system) and b) its Triple version, after Denies et al. (2012a)

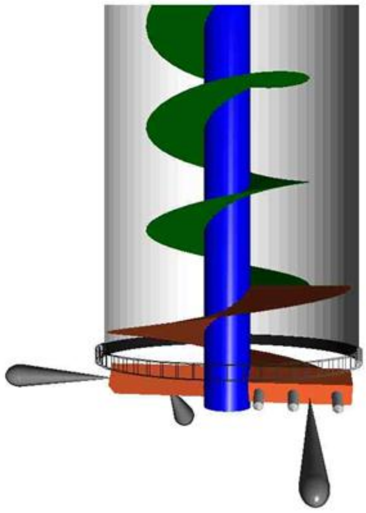

Figure 2: Scheme of the TSM® system (Smet-F&C), after Denies et al. (2012a)

2.1.3. Keller Foundations FLAPWINGS® system

Within the framework of the European Research project INNOTRACK which is presented in paragraph 4.2, SNCF, Keller Foundations and IFSTTAR tested the feasibility of an alternative soil reinforcement technique the FLAPWINGS, based on vertical soil-cement mixed columns with variable diameter (Lambert et al., 2012). Keller Foundations has designed the FLAPWINGS soil mix tool with the purpose of executing soil-cement columns in a railway environment. This is a wet soil mixing system. As illustrated in Fig. 3, it consists of a 150 mm core retractable tool able to open up in order to perform the soil mixing phase on a 600 mm diameter column. The opening and closing of the retrieval blades are ensured with the help of a two way hydraulic jack located in the mixing tool.

2.1.4. Soletanche Bachy SPRINGSOL® system

Within the framework of the Rufex project (reinforcement and re-use of railway tracks and existing foundations, see paragraph 4.2 for a presentation of the project), soil-cement columns were installed with the help of the Soletanche Bachy 'Springsol' wet soil mixing tool (Guimond-Barrett et al, 2012a). As illustrated in Fig. 4, this tool is equipped with two mixing blades that spread out under the action of springs. In its folded configuration, the tool diameter is 160 mm enabling its insertion into a temporary casing. By increasing the length of the mixing blades, the column diameter can be adapted (e.g. 400 and 600 mm as illustrated in Fig. 4). The binder is delivered through outlet holes in the drag bit located at the bottom end of the tool. The main interest of the Springsol tool is the possibility to reinforce the ground under an existing railway track.

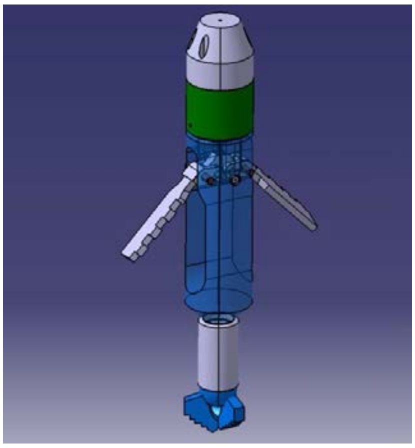

Figure 3: FLAPWINGS® system (Keller Foundations), after Lambert et al. (2012)

Figure 4: Soletanche Bachy Springsol® systems with 400 mm (left) and 600 mm (right) diameters, after Guimond-Barrett et al. (2012a)

2.1.5. *Other developments*

Figure 5 illustrates the two single auger systems used in the framework of the SMiRT research project (Al-Tabbaa et al., 2012). The first one consists of standard single auger which can be directly mounted on the end of a continuous flight auger (CFA) pile shaft (see Fig. 5a). The second one is the double rotary head auger system developed by Eco Foundations (see Fig. 5b).

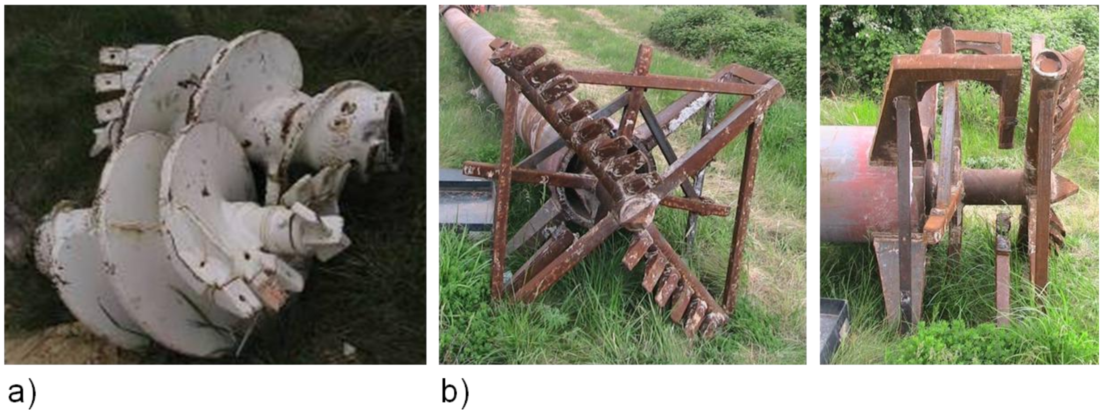

Figure 5: Single auger systems: (a) standard single auger system (b) double rotary head auger, after Al-Tabbaa et al. (2012)

Within the framework of a land levee project in New Orleans (the LPV111 project), two different technologies were applied to treat over 1.3 million cubic meters of foundation soil: the Trevi Turbo Mix (TTM), in single and double versions, and the Contrivance Innovation Cement Mixing Columns (CI-CMC), as reported in Leoni and Bertero (2012). These innovative and distinct wet soil mix systems are able to produce large (1.6 m diameter), uniform, and continuous improved columns.

2.2. CSM panels

The execution of soil mix rectangular panels can easily be performed with the help of the Cutter Soil Mixing (CSM) system, recently developed by Bauer Maschinen GmbH. As reported in Gerressen and Vohs (2012), the CSM is based on the principle of the trench cutter technique. It is mainly used for the construction of cut-off walls, earth retaining structures and ground improvement. As it is derived from BAUER Cutter technology, the system extends the applicability of soil mixing to much harder strata. While a self-hardening water/binder (w/b) mixture is being introduced, soil formations are easily penetrated, broken down, and mixed with the w/b mixture, using the cutter wheels as cutting and mixing tool. As illustrated in Fig. 6, the two cutting wheels rotate independently about a horizontal axis and cut the soil. At the same time, the water/binder mixture is injected at low pressure (commonly < 5 bar) with w/b ratio chosen in function of the design strength and permeability. The injected quantity of binder amounts mostly to 200 and 400 kg binder/m³. Again, spoil return usually ranges between 0% and 30%. The CSM system is in operation since 2003 and it is commercially available.

Figure 6: The cutting wheels of the CSM machine

2.3. Trenchmix method

The Trenchmix method produces a soil mix barrier, up to a depth of 10 m, in a single continuous pass which is an advantage particularly in case of water retaining function (no joints). The Trenchmix uses cutting tools as shown in Fig. 7 to mix trenches. It has a dry and a wet method. Figure 7 shows the dry method.

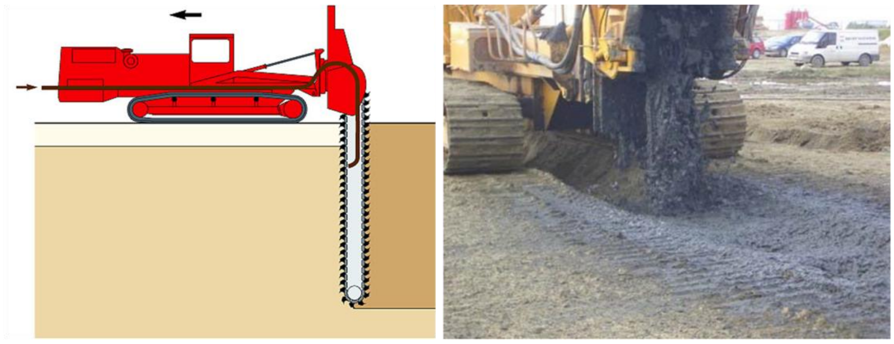

Figure 7: Trenchmix method (after Borel, 2007)

2.4. ALLU® mass stabilization

The ALLU® mass stabilization system is developed for mass stabilization of soil. It has a dry and a wet method. It was in particular used within the framework of the SMiRT project for land remediation (Al-Tabbaa et al., 2012). Figure 8 illustrates this system, which consists of a power mix mounted on the dipper arm of an excavator with a pair of mixing drums at the end and a pressure feeder mounted on a powered crawler chassis which delivers dry binder into the ground with the aid of compressed air (ALLU, 2010).

Figure 8: The ALLU® system used in the ground improvement treatment sections (Al-Tabbaa, 2012)

In general, the various DSM equipments presented in this paragraph allow the execution in a large range of soils with the following advantages:
- the use of the existing soil as a construction material,
- the independence with regard to the supply of fresh concrete (delay due to traffic jams),
- the limited spoil return (in comparison with jet grouting),
- a control of the geometry of the DSM element with depth,
- and the absence of important vibrations during the execution process.

3. DEEP SOIL MIX MATERIAL

3.1. Governing parameters

Several parameters have an influence on the produced DSM material. Terashi (1997) highlights the factors affecting the strength of the DSM material, as illustrated in Table 3. The DSM material quality depends on the cement type and content, on the in situ soil and on the execution process. The hardening agent is usually a mixture of cement and/or lime, water (for wet mixing), and in several cases bentonite. Sometimes ashes and gypsum are used as additive.

Table 3: Factors affecting the strength of the DSM material, after Terashi (1997)

I. Characteristics of hardening agent	1. Type of hardening agent 2. Quality 3. Mixing water and additives
II. Characteristics and conditions of soil	1. Physical chemical and mineralogical properties of soil 2. Organic content 3. pH of pore water 4. Water content
III. Mixing conditions	1. Degree of mixing (Mixing energy) 2. Timing of mixing/re–mixing 3. Quantity of hardening agent
IV. Curing conditions	1. Temperature 2. Curing time 3. Humidity 4. Wetting and drying/freezing and thawing, etc.

The water/binder weight ratio also plays a major role in the mechanical/durability characteristics of the material. Moreover, the nature of the ground has a huge impact on the strength and uniformity of the material. For example, stiff cohesive soils do not allow an effective mix of the components, which can lead to the presence of unmixed material in the DSM element. Finally, the final product will be the result of a given DSM system available on the local market. There are a lot of differences between the various systems – especially with regard to the drilling/mixing tools – and the execution process influences the quality of the DSM material in terms of strength, uniformity and continuity.

3.2. Hydro-mechanical characterization of DSM material

In the context of the European standardization and for the purpose of investigating these questions, in 2009, the Belgian Building Research Institute (BBRI) initiated the "Soil Mix" project in collaboration with KU Leuven and the Belgian Association of Foundation Contractors (ABEF). In the framework of this research, numerous tests on in situ DSM material have been performed. A good insight has been acquired with regard to strength and stiffness characteristics that can be obtained with the C-mix®, the TSM® and the CSM systems in several Belgian soils. All the results and the developments related to the BBRI "Soil Mix" project are detailed in four papers of the present symposium:
- Denies et al. 2012a. *SOIL MIX WALLS as retaining structures – Belgian practice,*
- Denies et al. 2012b. *SOIL MIX WALLS as retaining structures – Mechanical characterization,*
- Denies et al. 2012c. *Mechanical characterization of DEEP SOIL MIX material – procedure description,*
- Vervoort et al. 2012. *Mechanical characterization of large scale soil mix samples and the analysis of the influence of soil inclusions.*

Main results of the BBRI "Soil Mix" project are presented in the present paragraph.

Bellato et al. (2012) present the results of a laboratory study carried out on DSM samples from more than 50000 m^2 CSM panels performed for the construction of the new railway station in Bologna (Italy). The subsoil is constituted mostly by overconsolidated clays. Hydraulic and mechanical laboratory tests were conducted at different curing time, from 14 days to more than 2 years, to study the influence of curing time on the properties of the mixture.

In a first step, the BBRI "Soil Mix" project focused on the mechanical characterization of the DSM material with regard to the sampling of cores from soil mix walls (SMW), its unconfined compressive strength UCS (1073 tests, up to now), its modulus of elasticity E (152 tests) and its tensile splitting strength (95 tests). Moreover, the influence of unmixed soft soil inclusions in the soil mix on the material characteristics was also analyzed. In parallel, numerous tests dealing with ultrasonic pulse velocity, porosity, permeability and adherence with steel reinforcement have been launched (Denies et al., 2012b).
In the framework of the research program, long term behavior is currently investigated with the help of creep tests and considering the effect of time on the UCS. Indeed, while SMW were previously used only for temporary excavation support, permanent retaining and foundation applications with soil mix are increasingly applied. Hence, durability aspects of DSM material have to be considered not only with regard to its mechanical properties but also from a chemical point of view.
In the second period of the research program, the DSM material shall be investigated in terms of its alkalinity properties, with the help of pH long term measurements, in order to evaluate its level of corrosion protection. The viability of the process in presence of polluted soils shall also be considered.

Finally, a design method for the soil mix structures, accounting for the presence of heterogeneities and soil inclusions, the scale effects and the time effects shall be developed.

During the first part of the experimental campaign, cores of DSM material have been drilled at 38 Belgian construction sites, with different soil conditions and for various DSM systems. Details of the tests are given in Denies et al. (2012b). Figure 9 illustrates the correlation between the modulus of elasticity and the UCS of the tested DSM material, without distinction of the soil type.

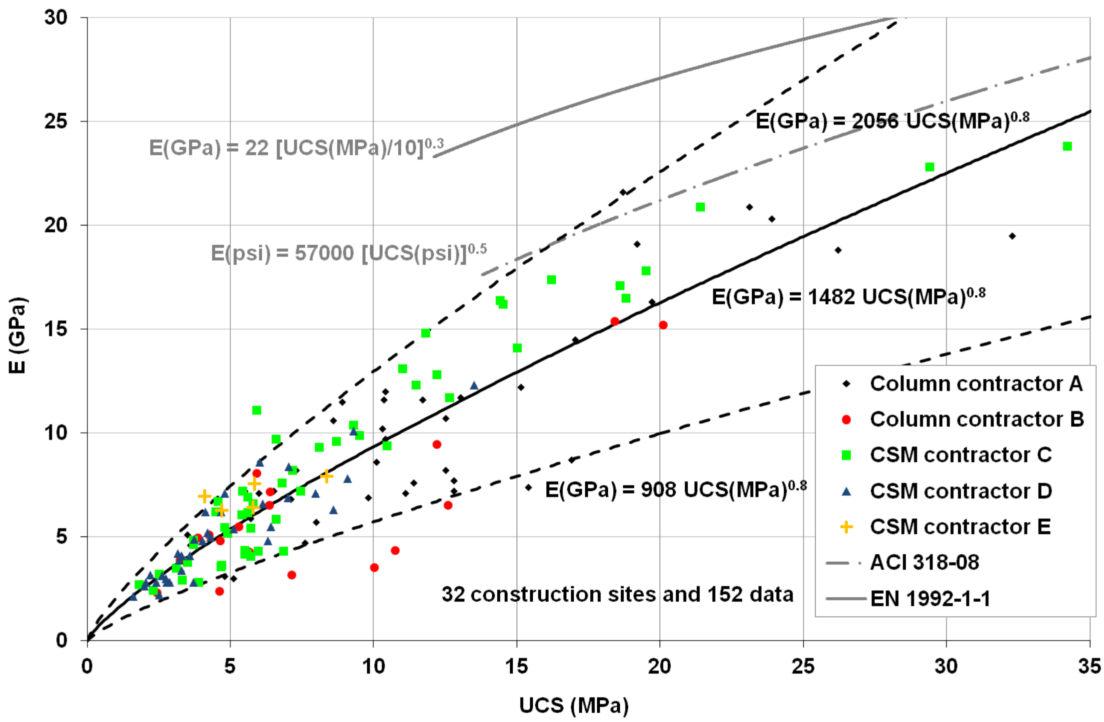

Figure 9: Relationship between the modulus of elasticity and the UCS of DSM material, after Denies et al. (2012b)

The samples were tested after a period ranging between 30 and 200 days. Since the aim is to determine the correlation between the modulus of elasticity and the UCS, the test results are not corrected for the age of the samples.
The best fit corresponds to:

$$E = 1482\, UCS^{0.8} \tag{1}$$

with a coefficient of determination close to 0.80 (-). Lower and higher 5% quantile estimations of E respectively correspond with:

$$E = 908\, UCS^{0.8} \tag{2}$$

and

$$E = 2056\, UCS^{0.8} \tag{3}$$

These estimations are valid for the range 1.5 MPa < UCS < 35 MPa.
In Fig. 9, relationships for normal concrete, from ACI 318-08 and EN 1992-1-1, are given for comparison. According to ACI 318-08**,** the modulus of elasticity for normalweight concrete can be defined with regard to the UCS with the help of the following equation:

$$E(psi) = 57000\sqrt{UCS\,(psi)} \tag{4}$$

where E is defined as the secant modulus of elasticity between 0 and 45% ($\sigma_{40\%UCS}$) of the UCS. Based on previous research of Pauw (1960), equation (4) is valid for UCS values larger than 2000 psi (or 13.8MPa).
Eurocode 2 (EN 1992-1-1) provides the following relationship for concrete:

$$E(GPa) = 22[UCS(MPa)/10]^{0.3} \tag{5}$$

where E is the secant modulus of elasticity between 0 and 40% ($\sigma_{40\%UCS}$) of the UCS. Equation (5) is only valid for concrete samples containing quartzite aggregates and for a range of UCS varying between 12 and 90 MPa.

Figure 10 gives the relationship between the tensile splitting strength (T) and the UCS, without distinction of the soil type. The samples were tested after a period varying between 32 and 200 days. Test results are not corrected for the age of the sample. In Fig. 10, experimental results for DSM cores are compared with well-established empirical relationships for concrete.

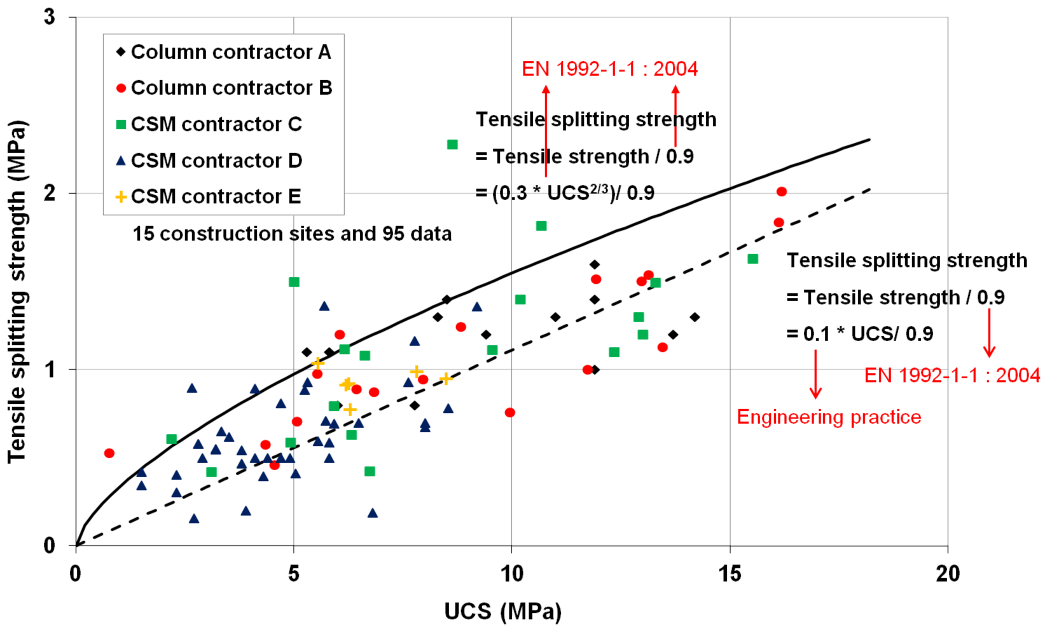

Figure 10: Relationship between the tensile splitting strength and the UCS of DSM material, after Denies et al. (2012b)

According to Eurocode 2 (EN 1992-1-1), when the tensile strength is determined as the splitting tensile strength, an approximate value of the axial tensile strength, T_a, may be determined as:

$$T_a = 0.9T \tag{6}$$

Eurocode 2 also provides a correlation with the UCS:

$$\mathrm{T_a} = 0.30\ \mathrm{UCS}^{2/3} \tag{7}$$

which is only valid for concrete with UCS values less than the UCS of the C50/60 concrete type.
In the engineering practice, the axial tensile strength of concrete is often related to the UCS by the following relationship:

$$T_a = 0.1UCS \tag{8}$$

It is interesting to note that Bellato et al. (2012) obtained a similar range of values for the modulus of elasticity and the tensile splitting strength of DSM material performed with CSM technology applied in overconsolidated clays.

In Denies et al. (2012b), the coefficient of hydraulic conductivity varies between 10^{-8} and 10^{-12} m/s, regardless of the soil conditions. In overconsolidated clays, Bellato et al. (2012) measured coefficients of permeability around 10^{-11} m/s.

In both studies, results of petrographic analysis are also presented in order to obtain a microscopic view of the DSM material.

In Denies et al. (2012b), porosity values were measured and vary between 25 and 65% for all soil types.

Due to the specific DSM procedure, unmixed soil inclusions are inevitable. Within the framework of the BBRI ‘Soil Mix’ research, all inclusions in DSM material are considered as unmixed soft soil inclusions. A methodology taking into account these inclusions was developed and illustrated with case studies of DSM material executed in several Belgian soils. This methodology is summarized in Denies et al. (2012c) and detailed in Ganne et al. (2011 and 2012). Figure 11 gives an overview of the results for 27 Belgian construction sites.

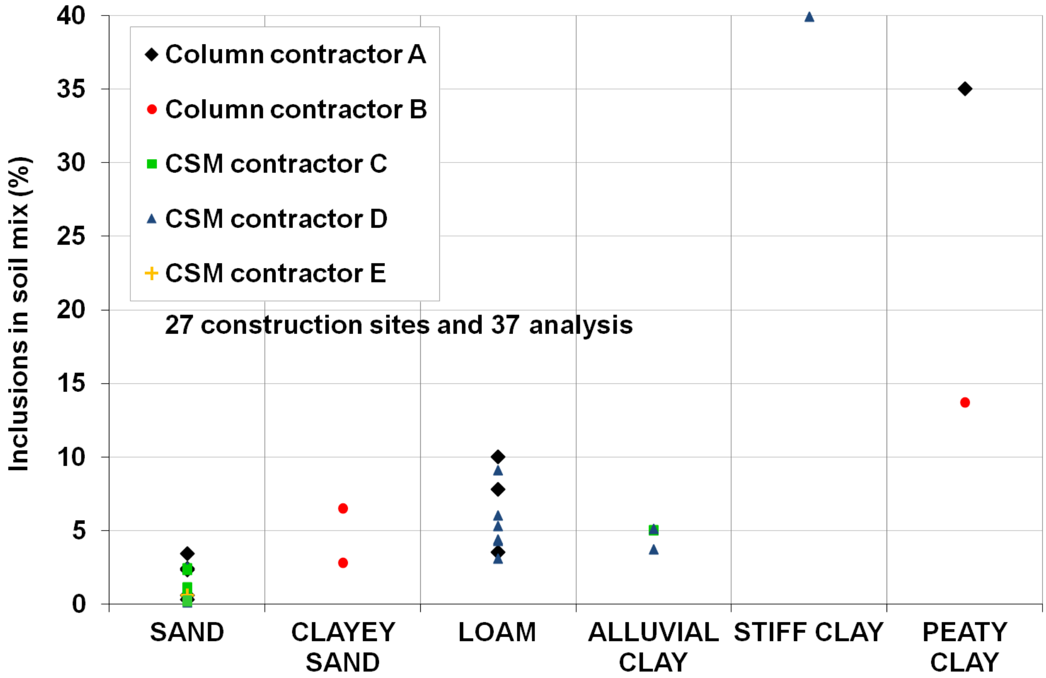

Figure 11: Percentage of soil inclusions in DSM material, after Denies et al. (2012b)

The amount of soil inclusions in DSM material mainly depends on the nature of the soil:

- in quaternary or tertiary sands, it is less than 3.5%,
- in silty (or loamy) soils and alluvial clays, it ranges between 3 and 10%,
- in clayey soils with high organic content (such as peat) or in tertiary (overconsolidated) stiff clays, it can amount up to 35% and higher.

One major issue concerns the representativeness of the core samples with regard to the in situ executed DSM material. On the one hand, there is the question of the scale effect and on the other hand, the question of the influence of soil inclusions. Both have an influence on the UCS test results. To investigate these topics, an experimental, as well as a numerical simulation research program has been initiated at KU Leuven (Vervoort et al., 2012).

As the design and the Quality Control (QC) of the execution process are generally based on laboratory tests performed on cored material, each sample is characterized by its own history influencing the test results and its interpretation. Beyond the question of the representativeness of the core samples with regard to the in situ executed material, Denies et al. (2012c) concentrate on the sampling, the transport, the storage, the handling and the preparation of the DSM test specimens and propose test procedures in the continuity of the content of the European standard EN 14679 (2005) for deep mixing.

Due to the DSM procedure, it is partly to be expected that the mixed material is not perfectly homogeneous. In other words, inclusions of poorly mixed or even unmixed (i.e. soil) material are present. The amount of such inclusions can be less than 1% of the total volume at some sites, but 10% or more is also observed (as illustrated in Fig. 11). Some of these inclusions are very small, while in other cases they can have dimensions of several centimeters. It is generally assumed that below a certain volume percentage and/or for small dimensions of the individual inclusions, these inclusions have no negative impact on the behavior and on the strength of the SMW. To quantify the maximum acceptable limits of volume percentages, an experimental as well as a numerical simulation research program has been initiated (Vervoort et al., 2012). This research aims also to better understand the behavior of this material and the failure of it.

The experimental part of the research focuses on laboratory experiments. The behavior in laboratory is certainly affected by the scale and the dimensions of the test samples. Apart from traditional cores (e.g. with a diameter of about 10 cm), large scale tests are being conducted on rectangular blocks with approximately a square section, with a width corresponding to the width of the in situ wall (about half a meter) and with a height approximately two times the width (see Fig. 12.a). The influence of the scale effect was found to be limited for the Young's modulus. The UCS values of the large samples show a reduction of 30 to 50% in comparison to these of the 10 cm diameter cores.

By conducting numerical simulations (2D), one tries to better understand the effect of unmixed soft soil inclusions, i.e. the effect of their size, total surface percentage, the number of inclusions, the relative position, etc. Three approaches with increasing complexity are conducted:

- elastic models, whereby the focus is on the material stiffness,
- elasto-plastic models, whereby apart from the stiffness, the strength is analyzed,
- and a discontinuous approach, whereby individual fracture initiation and growth can be modeled, apart from the stiffness and strength (see Fig. 12 b and c).

The most prominent conclusion is that even a small percentage of inclusions has a significant effect on the DSM strength. For a mere 1% of unmixed material, the strength is reduced by 20%, while for 10% of unmixed material about half of the strength disappears. The effect on the stiffness is more limited. Another consistent result is that other characteristics than the total surface percentage of unmixed material can have a significant effect, e.g. large sharp-ended individual inclusions have a negative effect on the strength and stiffness.

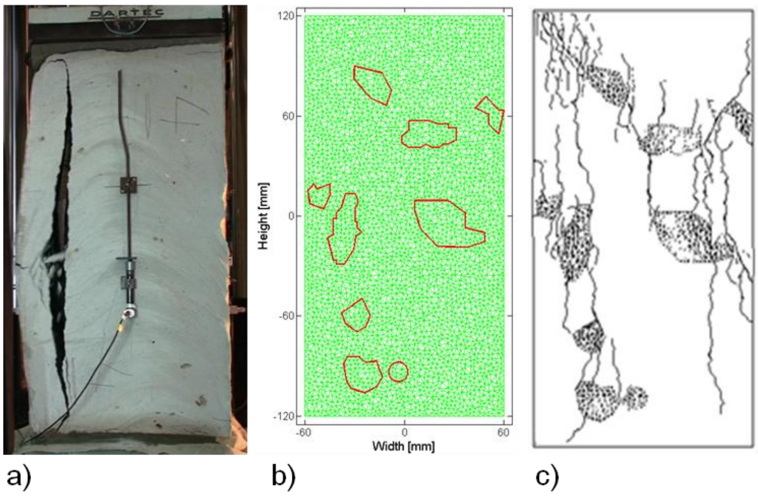

Figure 12: a) Large scale test on DSM material (block of dimensions 61 × 53 × 124 cm), b) Mesh generated for the discontinuous simulations of a sample with dimensions 120×240 mm (red lines indicate the soil inclusions) and c) Simulated fracture pattern of the model, after Vervoort et al. (2012)

3.3. Mixing and curing conditions

3.3.1. Mixing degree and homogeneity of the DSM material

At the present time, a wide variety of different machines and tools are available on the market for in situ deep mixing. As reported in Topolnicki and Pandrea (2012), the mixing technology has to ensure that the soil is mixed sufficiently with the binder to achieve a homogeneous product with a low coefficient of variation for its strength. The quality control of mixing can be performed with regard to the "*Blade rotation number*", as introduced in the CDIT (2002):

$$BRN = \sum M \, x \left(\frac{N_d}{V_d} + \frac{N_u}{V_u} \right) \tag{9}$$

where BRN is the Blade Rotation Number (1/m), ΣM the total number of mixing blades, N_d the rotation speed of the blades during penetration (rpm), V_d the mixing blade penetration velocity (m/min), N_u the rotational speed of the blades during withdrawal (rpm) and V_u the mixing blade withdrawal velocity (m/min). The BRN evaluates the mixing degree. It gives the total number of mixing blades passes during 1 m of shaft movement (CDIT, 2002). A high value of BRN decreases the coefficient of variation of the DSM strength. According to Topolnicki and Pandrea (2012), the minimum required BRN depends on the soil type. For cohesive and fine grained soils (loose sands and clays) about 400 (1/m) should be achieved

to keep the coefficient of variation for the strength within acceptable limits. In non-cohesive and coarse soils slightly lower values can be sufficient.
As the BRN was introduced for soil-cement column technique, Bellato et al. (2012) propose an equivalent factor for the evaluation of the mixing degree for DSM material performed with CSM technology: the "*Mixing quality parameter*", μ, which represents an estimate of the homogeneity achieved in the CSM panel and takes into account the effect of the real soil conditions. According to Bellato et al. (2012), μ (1/m) can be defined as:

$$\mu = \left[\left(\varphi_d R_{d,i} T_{d,i}\right) + \left(R_{u,i} T_{u,i}\right)\right] \frac{N_c M}{100 V_c} \tag{10}$$

where $R_{d,i}$ and $R_{u,i}$ are the average rotational speed of the mixing wheels during the penetration and the withdrawal phase, respectively. $T_{d,i}$ and $T_{u,i}$ are the total time taken to blend the soil during the downstroke and the upstroke, respectively. N_c is the number of mixing wheels (2 for the CSM machine). M is the number of mixing element per wheel and V_c the volume occupied by the cutter. All quantities with the subscript "i" are referred to a single i^{th} layer of predefined thickness. φ_d is called phase factor and takes into account the different role played by the executive procedure adopted for the realization of the panel, i.e. one phase ($\varphi_d = 1$) or two phases system ($\varphi_d = 0.5$).
Indeed, as explained in Gerressen and Vohs (2012), deep mixing with CSM can be performed in one phase mixing procedure (for applications less than 15m deep in relatively soft ground) or with a two phase system (when mixing deeper panels or penetrating difficult – slow – to mix soils or rocks). In the one phase procedure, the final mixture product consists of cement and water (and possibly bentonite), which is injected on both the down stroke and the upstroke of the machine. In the two phase procedure, just bentonite is used on the down stroke. Once the final depth is achieved, the water/binder mixture is introduced and mixed on the upstroke. This method prevents the mixing tool from being trapped in the panel if the panel construction time exceeds the initial set time of the water/binder mixture.

3.3.2. Influence of the cement content

As the degree of mixing is the governing factor of the homogeneity of the DSM material, its strength is mainly related to the amount of cement (or binder) introduced during the mixing process. According to Maswoswe (2001), the critical factor in the execution of DSM structures is to maintain the auger withdrawal rate consistent with the grout flow rate. One way to evaluate the success of the procedure and its efficiency is to estimate the cement factor or cement content (the cement mass per cubic meter of DSM material) at different locations. On the one hand, the cement factor can be estimated considering the grout flow rate, the auger withdrawal rate and the assumed percentage of grout loss during the process. On the other hand, the cement content is directly related to the water/cement factor, w/c, (or water/binder factor, w/b) of the injected mixture.
Bellato et al. (2012) propose a procedure for the estimation of the UCS at 28 days of curing with regard to the amount of injected cement. Their approach takes into account the fine content (FC), the mixing quality parameter (μ) and if necessary the effects of the *pH* on the UCS of the DSM material.

3.3.3. Influence of curing conditions

According to Bellato et al. (2012), several relationships are developed in the past to take into account the effect of the curing time on the strength development of concrete, such as those based on linear and double hyperbolic equations, exponential and logarithmic functions. Bellato et al. (2012) tried to fit their experimental data of CSM treated overconsolidated clays to these empirical relationships, but with unsatisfactory results except the case of the formula provided by EN 1992-1-1 (Ganne et al., 2010):

$$UCS(t) = \beta_{cc}(t)\, UCS_{28days} \tag{11}$$

where UCS(t) expresses the evolution of the strength with the time, t is the time and UCS_{28days} the UCS value at 28 days of curing time. β_{cc} is defined as:

$$\beta_{cc}(t) = \exp\left(s\left(1 - \sqrt{\frac{28}{t}}\right)\right) \tag{12}$$

where s is an empirical factor mainly depending on the type of cement.
According to Bellato et al. (2012), the most satisfactory fit for a curing time larger than 3 days was found with the equation:

$$\mathrm{UCS}(t) = \ln(t) - 1 \tag{13}$$

To better represent the increase of the UCS with the curing time observed in the Bologna specimens, Bellato et al. (2012) proposed a new empirical equation, based on a double hyperbolic function. This function is composed of two terms. The first one describes the increase of the UCS in the first 28 curing days, whereas the second one defines the development of the long-term strength. This relationship is given by:

$$\mathrm{UCS}(t) = \frac{\mathrm{UCS}_{28days} \cdot t}{t + K_1 \cdot \mathrm{UCS}_{28days}} + \frac{\Delta \mathrm{UCS}_{\infty} \cdot t}{t + K_2 \cdot \Delta \mathrm{UCS}_{\infty}} \tag{14}$$

in which UCS_{28days} can be corrected to take into account the amount of injected cement, the fine content, the mixing quality parameter and the *pH*. $\Delta\mathrm{UCS}_{\infty}$ is the strength increment due to long-term reaction products. K_1 and K_2 are two constants dependent on the type of clay and cement used in the treatment (in the case of the CSM treated Bologna overconsolidated clays K_1 =1 and K_2 =100).

4. FIELD OF APPLICATIONS AND CASE HISTORIES

Originally, DMM was developed for GI applications in soft clays and organic soils. More recently, it was dedicated to various structural and environmental applications: earth/water retaining structure, foundation and soil reinforcement, land levee and slope stabilization, in situ remediation and barrier against liquefaction. The following paragraphs illustrate these applications with the help of case histories presented by authors of the Deep Mixing session.

4.1. DSM technique as excavation support: earth/water retaining structure

In recent years, DSM has increasingly been used for the retaining of soil and water in the case of excavations. As a matter of fact, soil mix walls (SMW's) represent a more economical alternative to concrete secant pile walls and even in several cases for king post walls (i.e. soldier pile walls). Rutherford et al. (2005) proposed a historical background of excavation support using SMW. They also compared SMW with usual types of excavation support and with other GI techniques used for retaining wall construction.
The DSM cylindrical columns or rectangular panels can be placed next to each other, in a secant way. By overlapping the different DSM elements, a continuous SMW is realized. Steel H- or I-beams are inserted into the fresh DSM material to resist the shear forces and bending moments. The maximum installation depth of the SMW lies – so far – in the order of 25 m. The main structural difference between SMW and the more traditional secant pile walls is the constitutive soil mix material instead of traditional concrete.

In the present symposium, several papers report case histories related to permanent or temporary earth/water retaining structures. Table 4 summarizes these papers with regard to the DSM function (water and/or earth retaining structure), the temporary or permanent character of the construction, the type of soil, the localization of the project and their content.

Peixoto et al. (2012a) describe the construction of a retaining wall designed to allow the excavation of the underground floors of a new building block near existing buildings. The main challenge of this project consisted in the execution of an urban excavation with an average depth of 9 m under demanding ground and water table conditions. The design of the retaining wall had to guarantee minimum interference with the surrounding area, the security during and after the works (long term study) and the reduction of the water inflow into the excavation. In this context, a SMW was designed and performed with the help of CSM panels (see Fig. 13). The SMW was reinforced by vertical IPE 450 steel profiles and horizontally supported by two levels of horizontal struts in order to limit disturbance of the surrounding area and to use the SMW as foundation element of the internal structure. According to the surrounding conditions, horizontal displacements were limited to 5 mm at the top of the SMW and 20 mm along its height for design consideration. The analysis of the SMW was carried out using the Finite Element Method (FEM) program PLAXIS® with acceptable results.

The paper of Peixoto et al. (2012b) concerns the construction of a temporary SMW for the excavation of an underground parking lot. The solution consisted in a CSM retaining structure ensuring the stability of the nearby infrastructures and reducing the inflow of water into the excavation during the construction phase. The CSM panels were reinforced by vertical IPE 330 steel profiles and one level of ground anchors was performed in the top of the wall, as illustrated in Fig. 14.

Table 4: Summary of the papers concerning SMW with earth/water retaining functions

Papers	DSM function and duration	Type of soil	Contents
Peixoto et al. (2012a) *Permanent Excavation Support in Urban Area using Cutter Soil Mixing technology at Cannes, France*	Permanent excavation support, permanent foundation and water retaining applications with CSM	Stratified soil: clayey and silty fill, sandy clays and bedrock (sandstone)	Description of the design of the solution and numerical modeling with Finite Element Method FEM (Plaxis®) Execution details, QC aspects (UCS on wet grab samples) and monitoring plan (surveying targets, inclinometers and extensometers in the struts)
Peixoto et al. (2012b) *The application of Cutter Soil Mixing to an urban excavation at the riverside of Lagos, Portugal*	Temporary earth/water retaining wall for excavation with CSM	Sandy fill and calcarenite substratum	Description of the CSM technique, the design and the execution of the solution QC aspects (UCS, modulus of elasticity (E) and tensile splitting strength (T) tests on 36 wet grab samples) and monitoring plan (5 inclinometers, 5 load cells and 17 surveying targets)
Peixoto et al. (2012c) *Earth Retaining Structure using Cutter Soil Mixing technology for the "Villa Paradisio" Project at Cannes, France*	Temporary earth/ water retaining wall for excavation with CSM	Clayey fills and fractured dolomitic rock	General description of CSM technique Details of the design and execution of the solution and FEM of the retaining wall with Plaxis®
Peixoto et al. (2012d) *Solution of earth retaining structure using Cutter Soil Mixing technology: "Parking Saint Nicolas" Project at Cannes, France*	Temporary earth/water retaining wall with CSM	Sandy clay overlying substratum of marls	Details of the design and execution process and FEM of the retaining wall with Plaxis® QC aspects (UCS tests on wet grab samples) and monitoring plan (19 survey targets and 3 inclinometers)
Pinto et al. (2012) *Ground Improvement Solutions using CSM Technology*	Temporary circular shaft for excavation below ground water table at Ponte de Lima (Portugal)	Heterogeneous soil: heterogeneous landfills, sandy and gravel soils and weathered schist	General description of CSM technique Different case histories with CSM: design/execution criteria for foundation, slope stabilization and temporary or permanent earth retaining structures above and below ground water table QA/QC aspects (UCS and E tests on core samples) and monitoring plan
	Permanent earth retaining wall for excavation in Lisbon (Portugal) with geodrains for the control of the water table	Heterogeneous soil: heterogeneous landfills and Miocene medium dense to dense sands and sandstones	
	Permanent earth/water retaining wall and foundation solution in Lisbon (Portugal)	Heterogeneous soil (heterogeneous landfills and alluvial muddy soils, located over the Miocene very stiff clays) with the water table up to ground level	

Figure 13: View of the excavation after the execution of the second level of struts, after Peixoto et al. (2012a)

Figure 14: View of the excavation, after Peixoto et al. (2012b)

Peixoto et al. (2012c) present the design and execution aspects of a SMW performed for the construction of the underground floors of "Villa Paradisio", at Cannes, France. The building was located in a densely built-up area and bounded by streets, buildings and an old concrete pipeline. This urban excavation presented a maximum depth of 12 m. The ground water level was situated halfway up the excavation. The presence of dolomitic bedrock, under the clayey fills, constituted a good support for the bottom of the SMW, allowing the design of a safe solution with only one level of horizontal steel pipe struts, as illustrated in Fig. 15. The SMW consisted in a continuous CSM wall. The minimum length of the CSM panels was 15 m ensuring a minimum penetration of 3 m into the bedrock. The CSM wall was reinforced with the help of IPE 450 steel profiles. A concrete beam was executed at the top of the SMW to connect the vertical steel piles. According to the surrounding conditions, horizontal displacements were limited to 15 mm at the top of the SMW and 25 mm along its height. Once again, the analysis of the SMW was carried out using the FEM program PLAXIS® with acceptable results.

Figure 15: View of the SMW with the steel waler beams, the internal struts and the concrete wall, after Peixoto et al. (2012c)

Peixoto et al. (2012d) present the design and execution aspects of a retaining structure for the construction of an underground parking lot. The retaining wall for the construction of the four underground floors was executed with the help of CSM panels reinforced with vertical IPE steel profiles. The depth of the excavation rose up to 14 m. The SMW was horizontally supported by two levels of reinforced concrete slab bands rigidified and supported by temporary micropiles, as illustrated in Fig. 16. The excavation was once again located in an urban zone and bounded by streets and buildings. The performance of the retaining wall was evaluated using the FEM program PLAXIS®. All the execution phases were modeled. The analysis included the determination of the maximum values for the strength and displacements of the SMW.

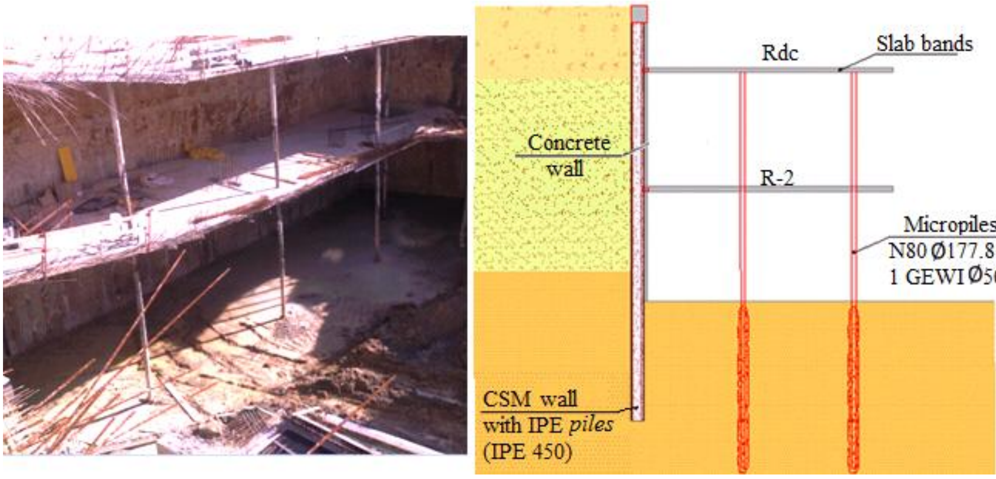

Figure 16: Partial view of the excavation (on the left) and cross-section of the retaining wall (on the right), after Peixoto et al. (2012d)

Pinto et al. (2012) first present an example of the CSM technique applied for the construction of two shafts with earth and water retaining function. Those shafts with about 18 m depth and 15 m diameter were built in order to allow the installation of a water supply pipe, under the river using micro tunneling technology. The CSM panels were built with an overall depth of 24 m and reinforced with vertical IPE300 steel profiles. The CSM panels were designed to transmit horizontally the earth and water pressures to the vertical profiles. The profiles were braced, at the top, by a reinforced concrete capping beam and by three lower levels of steel ring beams, as illustrated in Fig. 17. For the design, a 2D FEM axisymmetric model was adopted using Plaxis® software.

Figure 17: Inside view of the right bank shaft after excavation, after Pinto et al. (2012)

In the following, Pinto et al. (2012) concentrate on an earth retaining solution for the enlargement of a railway platform, in order to accommodate the new infrastructures of High Speed train in Lisbon. The maximum depth of the excavation was 13 m. CSM panels were executed with maximum depth of 18 m and reinforced with the help of IPE240 hot rolled steel profiles. The CSM panels were designed in order to be integrated with the final earth retaining solution and in such a way to limit the water inflow in the excavation. For the design, FEM analysis was carried out using Plaxis® software. Figure 18 respectively presents the excavation works and the designed solution.

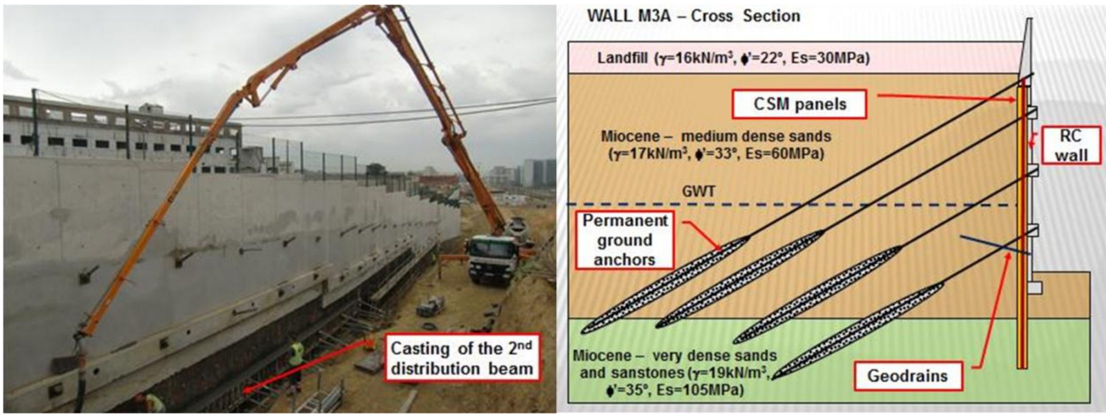

Figure 18: Excavation works (on the left) and cross section of the adopted solution with geological conditions (on the right), after Pinto et al. (2012)

Finally, Pinto et al. (2012) give the details of an earth/water retaining and foundation structure realized for the construction of a pumping station. The depth of the excavation was 12m. CSM panels with an overall depth of about 24 m were performed and reinforced with vertical IPE300 hot rolled steel profiles in order to resist to the structural loads, the earth and water pressures, and to limit the deformations. Buttress panels were also built in order to increase the earth retaining structure overall stiffness, as illustrated in Fig. 19. The CSM panels were designed in order to be integrated with the final foundation and earth retaining solution and to limit the water inflow into the excavation. For the design, 2D FEM analysis were carried out using Plaxis® software.

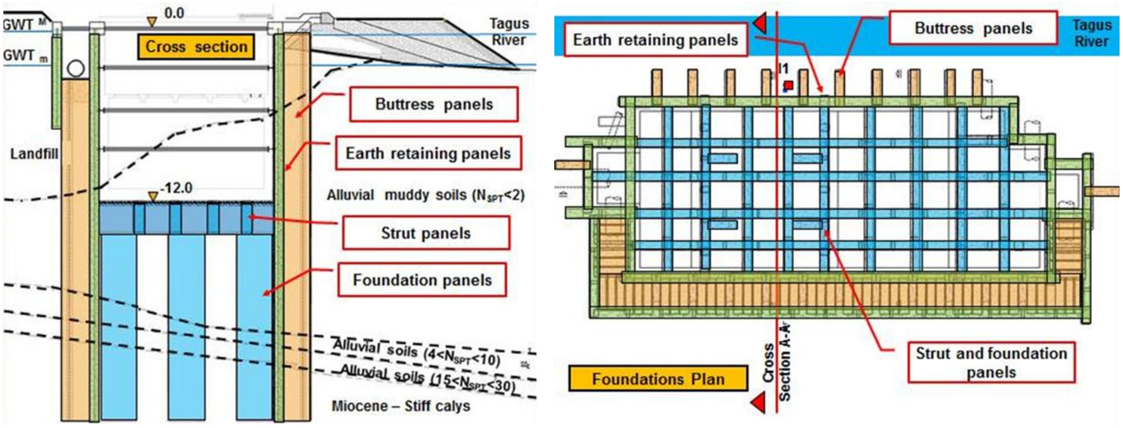

Figure 19: Cross section (on the left) and plan of the adopted solution (on the right), after Pinto et al. (2012)

4.2. DSM technique for foundation applications and soil reinforcement

Since several years, there is an increasing need of establishing new constructions on soils of poor quality and especially in alluvial area. That need resulted in the developments of new suitable and sustainable GI and foundation solutions with special attention with regard to the execution time and economic questions. In this respect, DMM constitutes an interesting alternative to the traditional foundation solutions, with some technical, economic and environmental advantages.

In the present symposium, several papers report case histories related to permanent use of DSM material for foundation applications. Table 5 summarizes these papers with regard to the DSM function, the type of soil, the localization of the project and their content.

Chapman et al. (2012) present GI works performed to found a liquefied natural gas (LNG) tank with 85 m diameter and 54 m high on tidal mangrove mud flats which have been reclaimed using dredged spoil. The traditional engineering solution for this type of site is to use deep foundation (piles). However, this solution was found to be excessively expensive. Hence, the solution consisted in a granular load transfer layer placed over the top of CSM panels. The design comprised 605 CSM panels with depths varying between 13 and 15 m below the bottom of the proposed load transfer layer. Figure 20 illustrates the soil layering below the tank and the CSM panel layout.

Table 5: Summary of the papers concerning DSM technique for foundation applications

Papers	DSM function	Type of soil	Contents
Chapman et al. (2012) *Ground Improvement works for an LNG storage tank foundation*	GI with CSM for permanent foundation of a liquefied natural gas (LNG) tank in Coast of North Queensland	Tidal mangrove mud flats (dredged spoil)	Details of the design of CSM foundation Description of laboratory UCS tests on wet grab samples and mention of plate load tests 2D plane strain and axisymmetric 2D analyses with Plaxis®
Mendes et al. (2012) *Assessing the feasibility of a foundation treatment solution based on CSM panels at a river dock in Lisbon*	CSM panels for permanent foundation of buildings	Landfill (soft soils)	Laboratory test campaign on mixture specimens (to determine the cement, organic matter and sulphates contents): water content, small strain stiffness (P wave velocity propagation tests), UCS, E, T and shear strength (CU TX) tests Effect of curing (14, 28, 54 and 91 days) Quality index for sample selection
Peixoto et al. (2012e) *Solutions for soil foundation improvement of an industrial building using Cutter Soil Mixing technology at Fréjus, France*	CSM for permanent GI application: foundation of an industrial building	1 m thick layer of predominantly gravelly fills, 2-6 m thick layer of colluvial soils with low strength and deformability over a marl-sandstone substrate	Description of the design and numerical modeling with FEM (Plaxis®) Details of the execution process and QA/QC aspects (UCS on wet grab samples)
Pinto et al. (2012) *Ground Improvement Solutions using CSM Technology*	Permanent foundation solution in Lisbon	Landfill with demolishing waste, alluvial soft soils and Miocene bed rock	Description of the design and execution criteria for foundation below ground water table QA/QC aspects (UCS and E tests on core samples) and monitoring of the building during and after construction
Lambert et al. (2012) *Soil-cement columns, an alternative soil improvement method*	Soil reinforcement for railway infrastructure with soil-cement columns performed with the help of the FLAPWINGS® tool (Keller Foundations)	Silty soil	Description of the European Research Project INNOTRACK (2006-2009) Details of the execution, the excavation, the field load tests on 2 columns and the laboratory tests on core samples Comparison with Jet grouting
Guimond-Barrett et al. (2012a) *Deep mixing for reinforcement of railway platforms with a spreadable tool*	Reinforcement and re-use of railway platforms and existing foundations with the help of soil-cement columns executed with the SPRINGSOL® tool (Soletanche-Bachy)	Stratified soil: fill, clay/silt and gravelly sand	Description of the Rufex project Details of the execution and QC aspects with the excavation of the columns and the laboratory tests on cores
Dhaybi et al. (2012) *Foundations reinforced by soil mixing: Physical and numerical approach*	Shallow foundations on DSM columns	Hostun sand	Reduced scale modeling and axisymmetric FEM of shallow foundations on soil-cement columns
Suganya et al. (2012) *Parametric study of embankments founded on soft organic clay using numerical simulations*	Embankments founded on soil-cement columns	Soft organic clay	Parametric study of embankments founded on soil-cement columns for the reinforcement of soft organic clay using FDM with FLAC 2D®: influence of the column properties, spacing, area, mass stabilized zone and pile material modeling

The optimization of the DSM material was conducted through laboratory and trial panel tests. 2D plane strain and axisymmetric 2D analyses were carried out using the FEM Plaxis 2D® program. The analyses were carried out to estimate the long term settlement as well as the variation of the normal stresses and the coefficients of subgrade reaction.

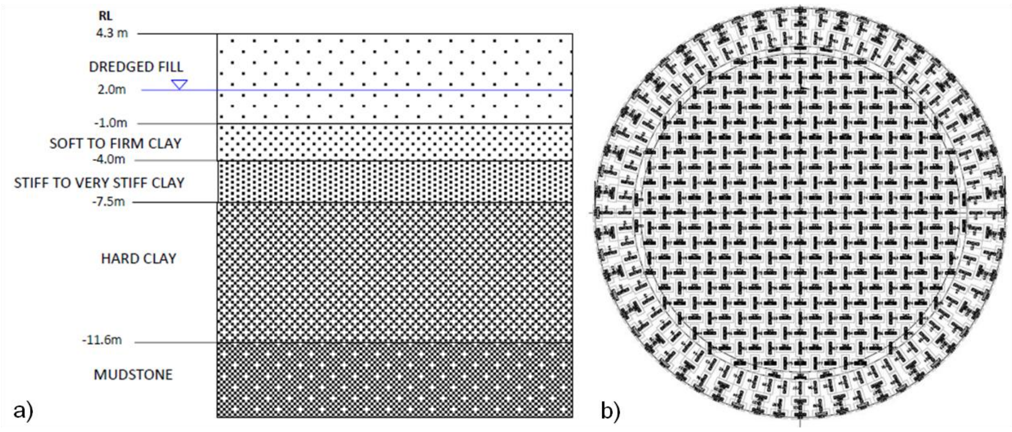

Figure 20: a) Soil layering below the LNG tank and b) CSM panel layout, after Chapman, et al. (2012)

Mendes et al. (2012) discuss the construction of an embankment on CSM panels within the framework of a project of soil reinforcement of a reclamation area in Lisbon (Portugal). The design consisted in a load transfer platform (geosynthetics and landfill) installed on the top of CSM panels. Despite the use of several cement contents, the UCS of wet grab and core samples remained below the minimum required UCS value. A method based on X-ray fluorescence was implemented to determine the real cement content of the CSM test panels. Figure 21a presents the measured cement content with regard to the nominal cement content injected in the panels. On the basis of these results, it can be concluded that the low UCS values were partly due to a deficient soil-cement mixture. That was confirmed by the visual quality of the core specimens (see Fig. 21b). Next, the increase of the UCS with time was studied. It must be noted that in the case of this project, organic and sulfate contents were observed in the field. The presence of organic matter in the mix restrains the cement hydration. If pozzolanic cement was used to reduce, yet not avoid, the sulfate attack, it is still expected that sulfates influence the mechanical behavior of soil-cement panels in the long term, as demonstrated in Guimond-Barrett et al. (2012b).

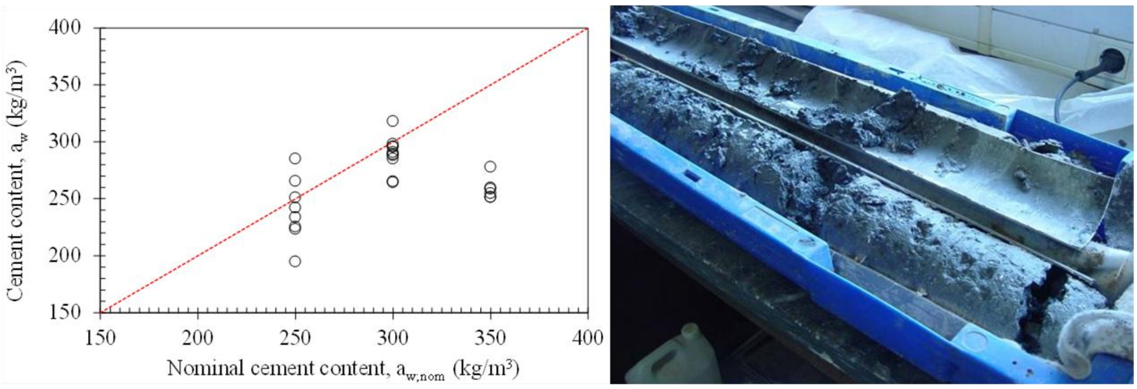

Figure 21: (a - Left) Measured cement content versus nominal cement content injected in the CSM panels. (b - Right) Core samples from the CSM test panels, after Mendes et al. (2012)

Peixoto et al. (2012e) describe the application of the CSM technology for the foundation of an industrial building at Fréjus, France. The main concern during the design was the minimization of the total and differential settlements of the building structure. The loads were transmitted to the marl-sandstone substrate, detected at a depth varying between 3 and 7 m. As illustrated in Fig. 22a, an enlargement of the top of the panels was also executed to ensure an efficient transfer of the load to the CSM panels. The panel caps were filled by the overflow mixture resulting from the execution of the CSM panels. Figure 22b presents the distribution of the CSM panels. A load transfer layer made of granular material and with a thickness of 0.60 m was finally performed, upon which the concrete bottom slab of the building was placed. The analysis of the solution in terms of long-term settlements was carried out using the FEM Plaxis® program.

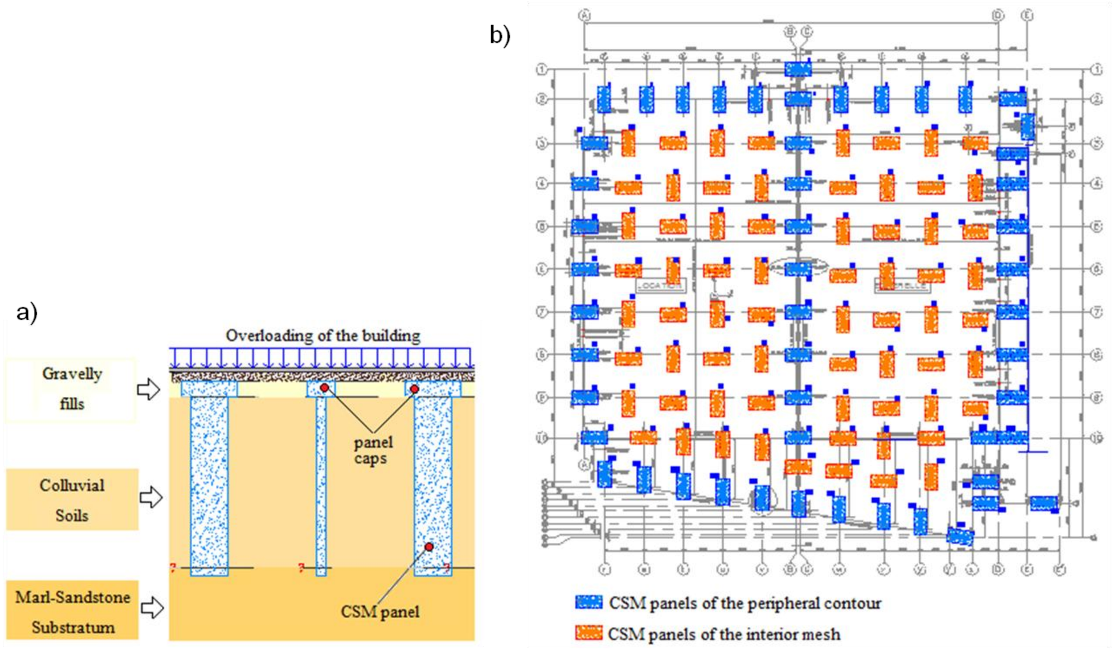

Figure 22: a) Cross section of the performed solution and b) plan view of the CSM panel distribution, after Peixoto et al. (2012e)

Pinto et al. (2012) present a foundation solution based on the CSM technique for the construction of the "Pedro Arrupe Scholl", in Lisbon (Portugal). CSM panels were executed with a maximum depth of about 25 m and reinforced with vertical HEB steel profiles. The profiles were capped by reinforced concrete caps, braced by a network of beams. As illustrated in Fig. 23, the CSM panels were designed in order to transmit the building loads to the Miocene bed rock and to resist to seismic loads.

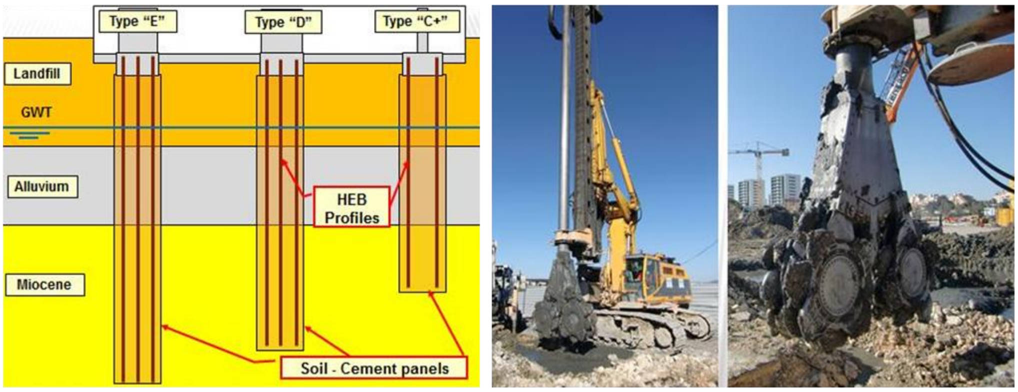

Figure 23: Cross section of the performed solutions (on the left) and execution of the CSM panels (on the right), after Pinto et al. (2012)

In order to reduce the life cycle cost of railway infrastructure, much research was performed on the track support structure. As reported in Lambert et al. (2012), development and implementation of several subgrade improvement methods allowing limited traffic interruption and privileging use of local material were the core activities of the European research project INNOTRACK (INNOvative TRACK system 2006-2009). The technique proposed by the SNCF/KELLER/IFSTTAR was ground reinforcement with vertical soil-cement columns. Lambert et al. (2012) discuss some experiments on soil-cement columns mixed by the FLAPWINGS® tool (see Fig. 3) within the framework of the INNOTRACK project. The FLAPWINGS® tool is presented in paragraph 2.1.3 of the present General Report. The device meets the execution requirements in a railway environment, but other applications are also possible. The technique only requires a small drilling machine and can thus be applied in difficult accessible field areas. Another advantage is that the drilling can be protected by steel tubes in order to avoid grout pollution of the top layers like ballast of railways. Lambert et al. (2012) discuss static load tests (SLT's) on two columns with 600 mm diameter and instrumented with the French removable extensometer (see Fig. 24a and b). The

influence of the water/cement, w/c, ratio and the effect of the cement density have been studied. It was shown that 70% of the load was taken by the shaft and 30% by the tip of the column.
Finally, it was observed that the mechanical behavior of the soil-cement column is comparable to jet grouting inclusions in terms of UCS resistance for similar soils and similar cement contents.

a) b)

Figure 24: a) View of an excavated column with diameter about 640 mm and b) view of the load test system, after Lambert et al. (2012)

Subsequently to the INNOTRACK project, the RUFEX project, which started in 2010, focuses on the reinforcement and re-use of existing railway tracks and on the DSM technique for foundation application. Its main objectives are to investigate the behavior of DSM structures with the study of the tools and binder compositions and to focus on the design aspects of wet soil mix. Guimond-Barrett et al. (2012a) present results of field tests carried out as part of the RUFEX project. They study the installation of soil-cement columns of 400 mm and 600 mm diameters constructed under existing railway lines without removing the tracks. Soil mixing is performed by the Springsol® mixing tool (see Fig. 4 and paragraph 2.1.4). In its folded configuration, the tool diameter is 160 mm enabling its insertion into a temporary casing to protect railway ballast from grout pollution (see Fig. 25). Once it reaches the end of the casing and penetrates the underlying soil, the blades spread out and the mixing operation begins. Two sets of columns were respectively installed under an existing and under a planned track. Two other sets were installed to be excavated and for SLT's. Penetration and rotation speed were varied for investigation purposes.

Figure 25: Installation procedure for soil-cement columns under existing tracks, after Guimond-Barrett et al. (2012a)

Dhaybi et al. (2012) discuss the behavior of shallow foundations reinforced by soil-cement columns and mechanisms of composite interface. This is done on the basis of physical and numerical models. For the physical model, an experimental setup is constructed in a tank with dimensions of 2×1×1 m³, as illustrated in Fig. 26. The soil-cement column is installed by sinking a steel tube in the sandy soil, emptying it and filling up with a laboratory mixture. A rigid steel plate is placed on the top of the column for the loading. Three tests are conducted: one without column and two with soil-cement column at 7 and 14 curing days. Apart from the physical model, an identical setup is simulated in ABAQUS by an axisymmetric FEM model calibrated with the experimental results. The numerical simulations show a good agreement with the physical modeling in cases of axial stresses, displacements and failure mode.

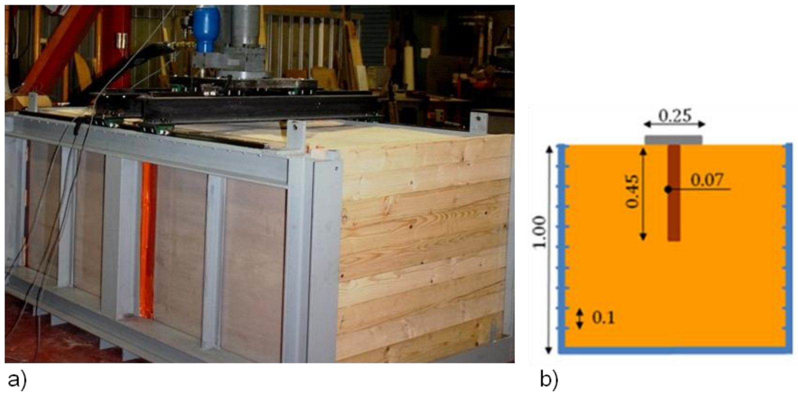

Figure 26: a) Experimental setup and b) schematic cross section of this setup, after Dhaybi et al. (2012)

Suganya and Sivapullaiah (2012) describe a similar study of soil-cement columns as Dhaybi et al. (2012). In this case, embankments are founded on soft organic clay ground which is reinforced with soil-cement columns to enhance bearing capacity and reduce settlements (see Fig. 27). The extent of improvement in stability and settlement characteristics of embankments mainly depends on the properties of the soil-cement columns, the column spacing and the column diameter. Suganya and Sivapullaiah (2012) investigate these factors through simulations based on the 2D finite difference method using FLAC 2D®. The simulations show clearly how the soil-cement columns reduce the settlements and horizontal displacements and how they increase the safety factor. A lower w/c ratio of the soil-cement columns (and thus higher shear strength) improves the stability and settlement characteristics of the embankment foundation. It is also observed that a sodium silicate (NaSi) additive considerably improves the column strength characteristics, but its effect on the safety factor and settlements is less significant. Finally, decreasing column spacing and increasing column area reduce settlements and horizontal displacements. Suganya and Sivapullaiah (2012) provide information on bearing capacity, settlements and global stability of embankments founded on soil-cement columns. In the same framework, the following paragraph concentrates on this application with the help of two history cases.

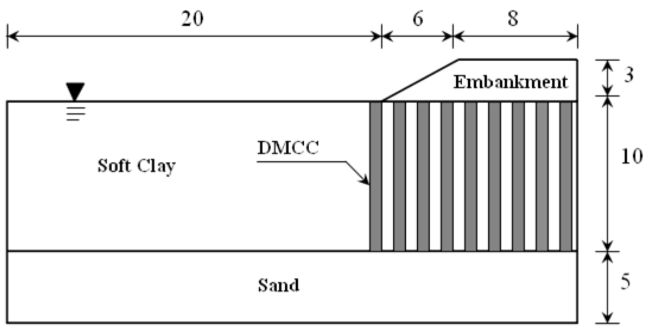

Figure 27: Embankment on soil-cement columns, after Suganya and Sivapullaiah (2012)

4.3. DSM technique for land levee

In the present symposium, two papers report case histories related to permanent use of DSM material for foundation of land levee projects, both in New Orleans. Indeed, the effects of Hurricane Katrina which passed southeast of New Orleans on August 29, 2005, have been long-lasting. The storm caused more than 50 breaches in drainage canal levees and also in navigational canal levees and precipitated one of the worst engineering disasters in the history of the United States of America. In response, construction and reconstruction of levee were planned; in several cases, with the help of the DSM technique. Table 6 summarizes these papers with regard to the DSM function, the type of soil and their content.

The LPV111 project (Leoni and Bertero, 2012) consisted in the raising of an existing 8.5 kilometer levee, which rests on a foundation of soft organic clay. LPV111 is part of the New Orleans East Back Levee, which is an essential component of the New Orleans Hurricane Protection System. DMM was selected to stabilize and support the burden of the new levee, as illustrated in Fig. 28. A preliminary laboratory program (Bench-Scale Test) and a field test program (Validation Tests) were conducted to estimate the appropriate binder type and dosage and equipment configuration capable to efficiently meet the technical requirements of the project.

Table 6: Summary of the papers concerning DSM technique for foundation and stabilization of land levee

Papers	**DSM function**	**Type of soil**	**Contents**
Leoni and Bertero (2012) *Soil mixing in highly organic materials: the experience of LPV111, New Orleans, Louisiana (USA)*	DMM applied for permanent foundation and stabilization of a land levee (LPV111 project) with the help of the TTM single, TTM double and CI-CMC double systems	Existing levee fill, soft clay, marsh/peat deposits, fat clay, and Pleistocene soils	General description of the project Preliminary laboratory program: Bench-scale test with the study of the effect of the w/c ratio, the type and the amount of cement on the UCS Field test program (Validation tests) QA/QC testing (5000 cores with UCS tests) and UCS design consideration
Mc Guire et al. (2012) *Stability Analyses of a Floodwall with Deep-Mixed Ground Improvement at Orleans Avenue Canal, New Orleans (USA)*	Dry Deep Mixing method for the permanent stabilization of a section of a land levee and floodwall	Clays and cohesionless soils	Numerical analysis of the stability of a section of a land levee and floodwall with the finite difference method and a limit equilibrium analysis (using Spencer's method) Study of the influence of vertical joints in the deep-mixed zone and study of the influence of a water-filled gap on the flood side of the cantilevered floodwall

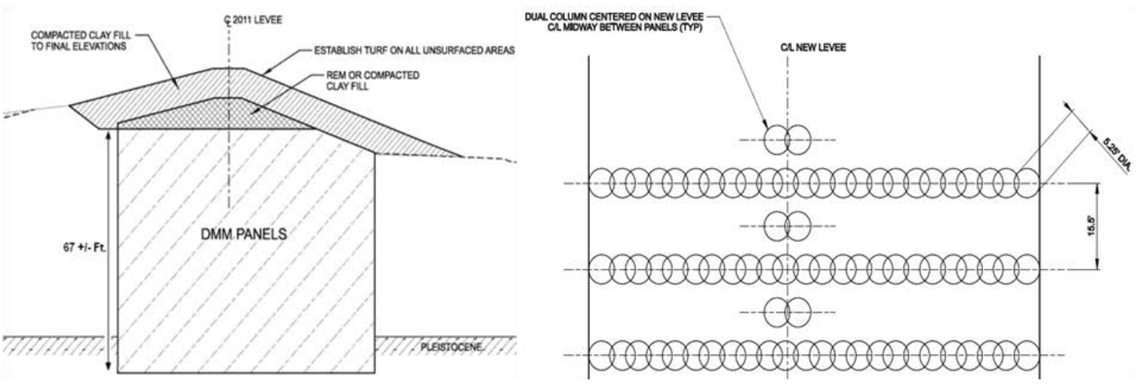

Figure 28: Typical design of DMM stabilization at LPV111 (cross section & plan view), after Leoni and Bertero (2012)

In New Orleans, dry deep mixing was used to improve the stability of a section of the land levee and floodwall along Orleans Avenue Canal. McGuire et al. (2012) studied the stability of this construction with the help of the finite difference method (using FLAC® program) and the limit equilibrium analysis (using the Spencer's method). The influence of the following parameters on the stability was taken into account in the analysis:

- the presence of vertical joints in the deep-mixed zone,
- the emergence of a water-filled gap on the flood side of the floodwall,
- and the potential water-filled tension cracks in the ground on the flood side of the floodwall.

The influence of joint efficiency was investigated by performing FLAC® analyses. It was shown to be very small with and without a water-filled gap. The influence of the water-filled gap on the safety factor was more significant than the influence of vertical joints. The shear strain contours at failure for both analyses (including or not a gap) are similar. They are shown in Fig. 29 and indicate a global failure mode.

Limit equilibrium analyses were also performed for the analysis of the cross section of the levee. The safety factors calculated using FLAC® and Spencer's method without a tension crack are within 5% for all comparable cases. As illustrated in Fig. 29, the primary mode of failure in the FLAC® analyses is global rotation and translation of the levee and I-Wall with shearing through the DMM zone. This mode of failure is also captured by the limit equilibrium analyses. The presence of a water-filled gap adjacent to the sheet piles produces a decrease of about 2 to 5% in the calculated factor of safety, depending on the analysis method.

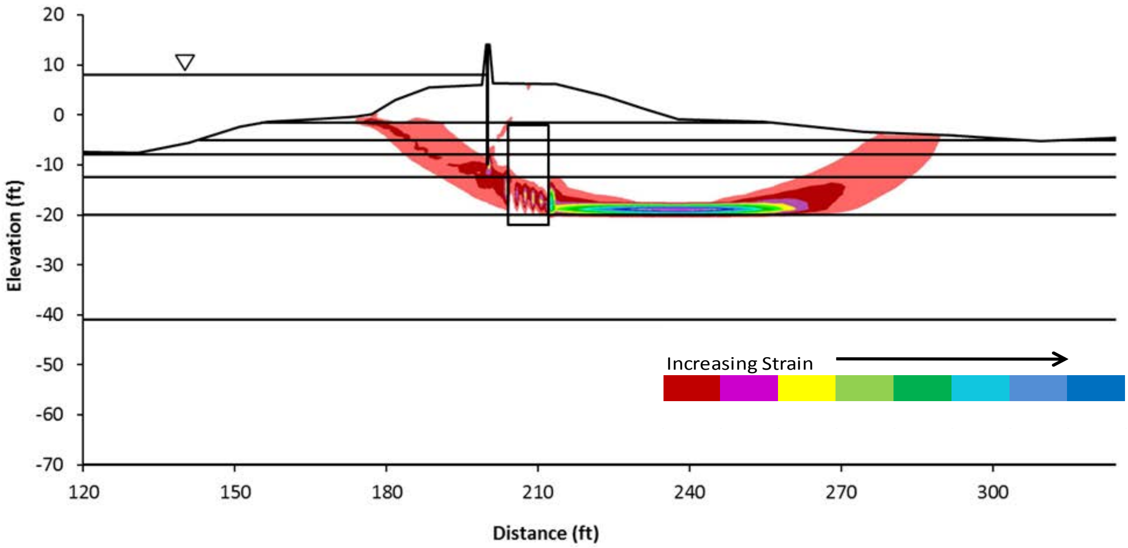

Figure 29: Example of shear strain contours for the numerical stability analyses performed without a water-filled gap and with 0% joint efficiency, after McGuire et al. (2012)

4.4. DSM technique for slope stabilization

Another application area of the DSM technique is slope stabilization. Pinto et al. (2012) and Gaib et al. (2012) both present a case history of this type of application. Table 7 summarizes these papers with regard to the DSM function, the type of soil and their content.

Table 7: Summary of the papers concerning DSM technique for slope stabilization

Papers	DSM function	Type of soil	Contents
Pinto et al. (2012) *Ground Improvement Solutions using CSM Technology*	Permanent slope stabilization and foundation in Amarante (Portugal)	Heterogeneous landfills located over weathered granite	Description of the design and construction 2D analyses using Slide® and Plaxis® softwares for the evaluation of the overall stability for static and seismic loads
Gaib et al. (2012) *Design, Construction and Monitoring of a Test Section for the stabilization of an Active Slide Area utilizing Soil Mixed Shear Keys installed using Cutter Soil Mixing*	CSM for permanent slope stabilization in British Colombia (Canada): DSM shear keys	Post glacial earthflow: poorly lithified tertiary sediments dominated by shale, mudstone, or clay	Stability analysis with the limit equilibrium slope stability program SLIDE 5.0 Description of the design solution General description of DSM and CSM technologies Design of field trial sections and strength selection Field implementation and QA/QC aspects with regard to the UCS tests on wet grab and core samples at different time and to the monitoring plan (during execution and after stabilization with the help of inclinometers, surveying targets and LIDAR – Light Detection And Ranging – measurements)

The case history described by Pinto et al. (2012) concerns the widening of an existing road platform (indicated by IP4 in Fig. 30) near the city of Amarante in Portugal. CSM panels were installed for slope stabilization of the heterogeneous landfills that were used for the construction of the existing road platform. A cross section of the geological conditions and the adopted solution with CSM panels is shown in Fig. 30. CSM panels also serve as foundation for the wall self-weight (maximum height is about 20 m) and the motorway traffic with the help of a load transfer platform (LTP). For the design, 2D analyses were carried out using Slide® and Plaxis® softwares in order to evaluate the overall stability for static and seismic loads.

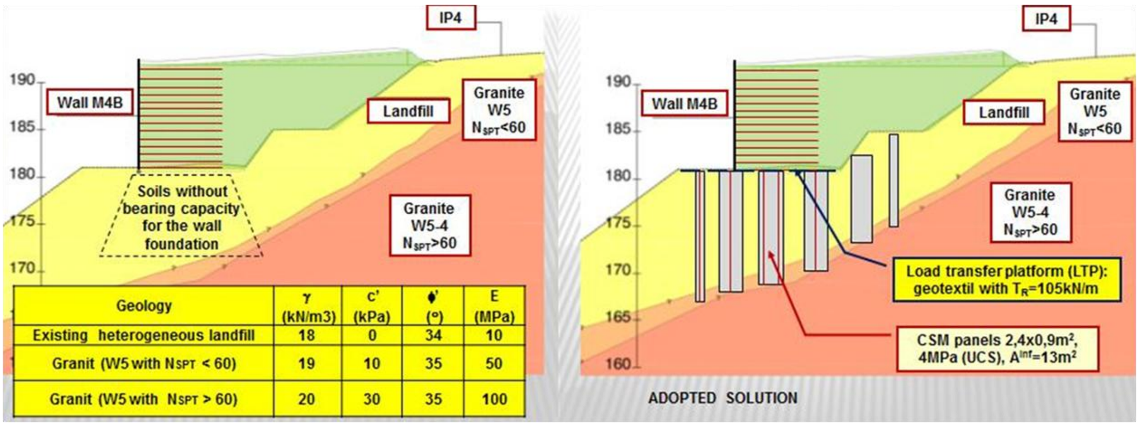

Figure 30: Cross section of the geological conditions and adopted solution, after Pinto et al. (2012)

Gaib et al. (2012) describe another example of the use of CSM panels for slope stabilization. The "Fountain Slide" has been active for decades and it is part of a massive postglacial earthflow known as the Tunnel Earthflow in British Colombia in Canada (see Fig. 31). The estimated landslide volume is 750 000 m³. Since 2009, movement rates have reached an average value of 5 mm/day, with observations up to 10 mm/day. As a result, significant ongoing maintenance of the highway has been required and investigation of stabilization options was need. Slide analysis was carried out using the limit equilibrium slope stability program Slide 5.0®. The chosen alternative was the use of the CSM technique to develop in-situ shear keys across the sliding area. In order to evaluate this approach, a trial section consisting of a number of subsurface shear walls, or barrettes, across the eastern end of the active slide area was proposed. A total of 20 barrettes, approximately 8 m long and each made up of 3 individual panels was constructed with an orientation perpendicular to the slide. Gaib et al. (2012) discuss the design approach, the monitoring and the problems encountered during the execution. Though monitoring and observation of the slope is still ongoing, the test section has already demonstrated that the installation of CSM shear keys through the failure horizon is technically feasible and allows the decrease of the slope movements.

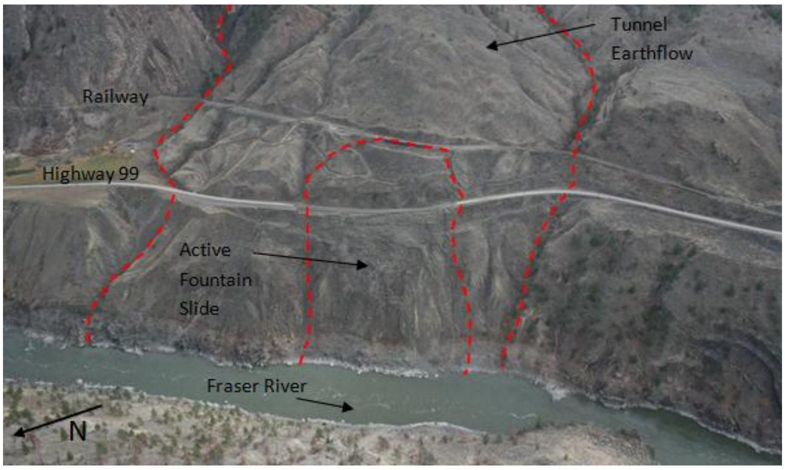

Figure 31: Aerial view of Tunnel Earthflow and Fountain Slide, after Gaib et al. (2012)

4.5. Soil Mix Remediation Technology

The in-situ remediation of contaminated land applying the DSM technique involves the use of mixing tools and additives to construct permeable reactive in-ground barriers (PRB) and low-permeability containment walls. As described in Al-Tabbaa et al. (2012), PRB walls are installed in the ground to intersect the flow of contaminated groundwater. Reactive material placed in the barrier removes the contaminants by one or more processes including sorption, precipitation, oxidation, biodegradation and encapsulation. In contrast with PRB walls, low permeability containment walls are cut-off low permeability walls designed to isolate a contaminated area from the surrounding area. Apart from these remediation techniques, the DSM technique can also be used for 'hot-spot' soil treatment by stabilization/solidification (S/S). This includes the physical encapsulation and chemical fixation of contaminants in place through a range of processes including sorption, precipitation, lattice incorporation, complexation and encapsulation (Al-Tabbaa et al., 2012).

Soil Mix Remediation is a cost-effective and versatile approach, with numerous technical and environmental advantages including the use of simple and well-established techniques, speedy implementation, applicability to sites of any size and to multiple contaminants, elimination of off-site disposal as well as low risk and low emissions. Water and soil contaminations consisting of heavy metals and/or organic contamination can be treated. This, combined with recent innovations in DSM equipment, treatments and materials, makes the DSM technology a promising and timely contender to lead the market place in offering a cost-effective, efficient and low risk solution to contaminated soil and groundwater remediation. All of this led in October 2008 to the start of the Soil Mix Remediation Technology (SMiRT) project in the UK (Al-Tabbaa et al., 2012).

Within the framework of this project, Al-Tabbaa et al. (2012) present the details of a large scale field trial application of DSM technology to the integrated remediation and ground improvement of a contaminated site with the use of a range of mixing tools. The influence of several parameters is studied, e.g. the type of binder as well as the installation variables including speed of rotation, speed of penetration and withdrawal and the number of mixing cycles. The setup of the field trials, the used DSM systems and some provisional results are summarized in Al-Tabbaa et al. (2012).

4.6. DSM barrier against liquefaction

The DSM technique can also be used to prevent soil liquefaction and post-liquefaction damage caused by soil flow along the substratum slope. An example of such application is described by Benhamou and Mathieu (2012). Martinique (France) is an area particularly exposed to seismic risks. For the construction of two buildings on very soft silty/sandy alluvia, a new type of permanent foundation based on a Geomix caisson arrangement (36 × 40 m) is presented as liquefaction remediation technique. This type of DSM treatment is already used in Japan, where for example foundation piles where surrounded by a grid-type structure made of SMW's. As illustrated in Fig. 32, the arrangement consists in a grid performed with the help of Geomix trenches. The Geomix technique is based on the hydrofraise technology combined with the CSM principle. Due to the strong inertia and the geometry of the caisson arrangement, the displacements of the Geomix panels are limited during earthquakes. Additional shear stress of the soil and horizontal forces from the structure are concentrated on Geomix bands and liquefaction of the encased ground is avoided. This treatment also resists to the external post-liquefaction soil flow. Finally, in a general way, the Geomix foundations also reduce settlements under the structure.

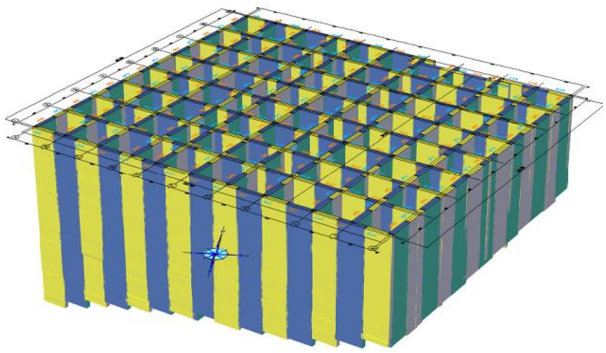

Figure 32: 3D view of the Geomix caisson structure, after Benhamou and Mathieu (2012)

5. INTERNATIONAL QA/QC PROCEDURES

5.1. QA/QC procedures and workflow of DMM project

In 2001, Maswoswe described the development and the implementation of Quality Assurance/Quality Control (QA/QC) procedures for the installation of 410 000 m³ of DSM material with the help of triple auger DSM rigs, in the framework of the Central Artery/Tunnel (CA/T) project, in Boston. At the beginning of the 90's, it was the largest land-based DSM installation in the USA, and perhaps in the world. Maswoswe (2001) related the **QC activities** to:
- the choice of the **suitable DSM equipment**,
- the determination of the **process parameters** ensuring acceptable performances: the grout mix composition, the auger rotation (or withdrawal) rate and the grout (and drilling water) flow rate,
- and the selection of **procedures** allowing auger penetration and verticality.

If the choice of the DSM equipment, the installation parameters and the procedure were left up to the contractors, specifications would require the DSM material to meet the following **acceptance criteria for QA** related to:

- the minimum and maximum values of **UCS** on samples, after a determined number of curing days,
- the verification of the **homogeneity and uniformity**,
- the minimum **unit weight** of core samples,
- the **vertical tolerance** with a limitation of the horizontal deviation with depth in any direction,
- the verification of the auger penetration and the **final depth**.

In 2011, Terashi and Kitazume have proposed a workflow for DSM projects. Their study was conducted in collaboration with experts of 45 organizations from seven countries and resulted nowadays in the relation of QA/QC activities to laboratory mix tests, field tests, monitoring and control of the execution parameters and control of the final products by measuring the mechanical characteristics of the DSM material by tests on core samples (usually UCS tests) or by sounding.

The DSM process design and the QC of DSM material, as described in Terashi and Kitazume (2011), constitutes a major schedule for the deep mixing contractors with the following steps:

- **laboratory mix test** for process design,
- **field trial installation** for confirming practicability,
- **process design** to determine final mix design and construction control values,
- **production with QC** by monitoring, control and recording the monitored data of the construction process.

In view of QA/QC development and in the context of European standardization, info sheets have been developed within the framework of the BBRI 'Soil Mix' project (Denies et al., 2012a). They consist in guidelines for execution phases and give some requirements with regard to the QC of the DSM material, the characteristic dimensions, the bearing capacity and the lateral SMW displacement. As BBRI info sheets support all QA/QC activities reported by Maswoswe (2001), they specify the QA/QC aspects in function of the DSM application (retaining wall, water barrier or foundation) and take the temporary or permanent character of the construction into account (Denies et al., 2012a).

5.2. DSM process design in practice

In the present proceedings, Leoni and Bertero (2012) describe the execution of DSM panels for land levee project LPV111 (see paragraph 4.3). The QA/QC activities related to this project follow the previous schedule with the realization of a Bench Scale Test program (BST), a Field Scale Program as Validation Test (VT) and a QC procedure during the production.

The main objective of the BST program was to investigate the impacts of the type and the amount of binder and the influence of the w/b ratio on the UCS of mixtures from the various types of soil that would be treated during production mixing.

According to Leoni and Bertero (2012), the field tests should follow a comprehensive but flexible approach, allowing adjustments and modifications to the parameters initially foreseen as the operations proceed and new or more detailed information is acquired. For that purpose, at the LPV111 project, the Field Scale Program or Validation Test (VT) was conceived to achieve the following objectives:

- verify and refine the type and content of binder, preliminarily determined through the BST, to attain the target mechanical characteristics of the treated soil,
- determine the most appropriate DMM operating parameters and equipment configuration,
- and develop QA/QC procedures for the DMM production stages.

In addition to laboratory mix test campaign, field trial installation is an essential step of the process design because the quality of the DSM material, in terms of strength, stiffness, continuity and uniformity mainly depends on the execution process. Moreover, the laboratory test results are influenced by the test procedure, especially by the method of preparation (mixing time/energy, time between mixing and molding, molding procedure) and by the curing of the specimens (temperature, humidity, potential application of surcharge). Hence, in addition to the laboratory mix test program, a field test program should systematically be performed prior to actual production mixing.

During the production stage, over 500 DSM samples were cored and tested for UCS assessment. All the results were tracked, analyzed, and combined with the other available data from the BST and VT programs on a day-by-day basis to fine tune the production parameters and the QA/QC procedures, and to determine whether corrective actions had to be taken.

All data obtained through the QA/QC program at LPV 111 allowed the optimization of both installation time and cement consumption. Generally, the adjustments were the result of observations carried out in the field and through QA/QC testing during the production stages. Nonetheless, all changes, especially if entailing a reduction of the cement dosage, were validated before they were implemented for the production elements, as prescribed by the project requirements. This iteration gave an opportunity for a better design of the BST and VT stages as the project progressed. The most significant consequence of this process was primarily related to the cement consumption. The dosage of the binder was, in fact, reduced without affecting the overall quality of the ground improvement. As a conclusion, the consideration of the BST, VT, and QA/QC programs allowed the optimization of the mixing parameters and equipment configuration to continuously improve economy and effectiveness as the project progressed.

5.3. Laboratory and field characterization of DSM material for QC

In practice, the quality of DSM material is often controlled with the help of UCS tests regardless of the DSM application. Nevertheless, various tests can be performed to determine characteristics of DSM material. Table 8 summarizes several case histories of the Deep Mixing session with regard to the application of the DSM structure and provides some information concerning the QC aspects of the project.

As illustrated in Table 8, the most common testing method for the mechanical characterization of the DSM material is related to the **realization of UCS tests on DSM samples**. Though, differences still exist between the various projects with regard to the type of test specimens. Indeed, UCS tests can be performed on water/binder mixture samples (Benhamou and Mathieu, 2012), on wet grab samples - from the surface (Lambert et al. (2012), Benhamou and Mathieu (2012), Chapman et al. (2012) and in the contributions of Peixoto et al. (2012)) or recovered at several depths (Gaib et al., 2012) - and finally on core samples (Guimond-Barrett et al. (2012a), Lambert et al. (2012), Benhamou and Mathieu (2012), Pinto et al. (2012) and Gaib et al. (2012)). For several authors and according to the experience acquired within the framework of the BBRI 'Soil Mix' project, cores can be considered more representative than wet grab samples. Nevertheless, coring also presents challenges as explained in Denies et al. (2012c) and illustrated by Gaib et al. (2012) with a case history. DSM samples from fresh material and cores should be collected, from test and final panels, in order to assess the strength and the homogeneity of the material, as well as to perform tests at different ages. In Gaib et al. (2012), UCS tests were conducted at 7, 14 and 28 curing days. The seven day tests were used to provide an indication of any suspect columns, the fourteen day tests to allow comparison to the specification values, and the 28 day tests to ensure that the target strength is met, if there was concern regarding a 14 day result.

In Gaib et al. (2012), **density measurements** of the water/cement mixture and review of the automated batch plant records were taken into account to verify the w/c ratio of the injected mixture. Similar measurements are reported in Guimond-Barrett et al. (2012a) who also determined the density of the spoil produced during mixing to control the blending of the water/binder mixture with the soil.

Several authors also refer to tests for the determination of the **modulus of elasticity** (Benhamou and Mathieu, 2012, Peixoto et al., 2012b and Pinto et al., 2012) and to **tensile splitting tests** (Peixoto et al. 2012b).

In parallel to laboratory mechanical characterization, several authors present results of field tests. Lambert et al. (2012) describe **static load tests** (SLT's) performed on two soil-cement columns, characterized by two different w/c ratios (paragraph 4.2). Their bearing capacity as well as the local response in terms of shaft friction and tip resistance have been analysed. **Plate load tests** are mentioned in Chapman et al. (2012). For the case history reported in Pinto et al. (2012) concerning the slope stabilization (paragraph 4.4), the execution control included **CPT tests**, inside and outside the CSM panels, in order to access the panel's resistance, as well as the confinement effect on the soil located between the panels.

Quasthoff (2012) refers to the **column penetration test** which is the most widely spread testing method for lime-cement columns in Sweden. According to EN 14679, column penetration test is carried out using a probe that is pressed down into the centre of the soil-cement column at a speed of about 20 mm/s and with continuous registration of the penetration resistance. As illustrated in Fig. 33, the probe is equipped with two opposite vanes. The method can normally be used on columns with a maximum length of 8 m and with UCS smaller than 300 kPa. The undrained shear strength of the DSM material can be deduced from the column penetration test.

Table 8: QC of DSM material for several case histories of the Deep Mixing session

***DSM functions* and QC information**
Peixoto et al. (2012a) *Permanent earth/water retaining and foundation structure*: monitoring and recording of the execution parameters, UCS tests on wet grab samples from test and production panels. Monitoring plan for the excavation: surveying targets, inclinometers and extensometers in the struts
Peixoto et al. (2012b) *Temporary earth/water retaining wall*: monitoring and recording of the execution parameters, UCS, E and T tests on 36 wet grab samples from test panels. Monitoring plan for the excavation: 5 inclinometers, 5 load cells for the anchors and 17 surveying targets
Peixoto et al. (2012c) *Temporary earth/ water retaining wall*: monitoring and recording of the execution parameters, UCS tests on wet grab samples from test and product panels
Peixoto et al. (2012d) *Temporary earth/water retaining wall*: monitoring and recording of the execution parameters, UCS tests on wet grab samples from test and product panels. Monitoring plan for the excavation: 19 survey targets, 3 inclinometers and load cells for temporary foundation elements
Chapman et al. (2012) *Permanent foundation of tank*: UCS tests on wet grab samples and plate load tests
Peixoto et al. (2012e) *Permanent foundation of an industrial building*: monitoring and recording of the execution parameters, UCS tests at 7 days on wet grab samples
Pinto et al. (2012) *Permanent foundation solution*: monitoring and recording of the execution parameters, UCS and E tests on core samples. Monitoring of building during and after construction *Temporary circular shaft*: monitoring and recording of the execution parameters, UCS and E tests on core samples. Monitoring plan for the excavation: inclinometers *Permanent earth retaining wall*: monitoring and recording of the execution parameters, UCS tests on core samples. Monitoring plan for the excavation: inclinometers and topographic marks *Permanent retaining wall and foundation solution*: monitoring and recording of the execution parameters, UCS tests on core samples. Monitoring plan for the excavation: inclinometers and topographic marks *Permanent slope stabilization and foundation*: monitoring and recording of the execution parameters, UCS and E tests on core samples, CPT's inside and outside the panels. Monitoring plan for the wall behavior: inclinometers and extensometers
Lambert et al. (2012) *Permanent reinforcement of railway platforms and existing foundations*: column excavation, SLT's on 2 columns and UCS tests on wet grab and core samples
Guimond-Barrett et al. (2012a) *Permanent reinforcement of railway platforms and foundations*: monitoring and recording of the execution parameters, grout and spoil density measurements, column excavation, UCS and density determination tests on core samples
Benhamou and Mathieu (2012) *Permanent Geomix caissons vs. liquefaction*: monitoring and recording of the execution parameters, UCS tests on water/binder mixture, wet grab and core samples, determination of the E-modulus and visual analysis of the product material after excavation of one cell of the Geomix caissons
Gaib et al. (2012) *Permanent slope stabilization*: monitoring and recording of the execution parameters, UCS tests on wet grab and core samples at 7, 14 and 28 curing days. Monitoring plan of the slope: inclinometers, surveying targets and LIDAR (LIght Detection And Ranging) measurements

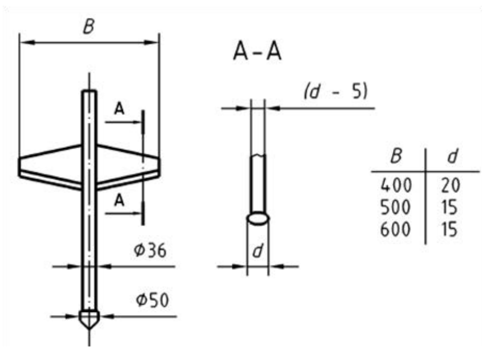

Figure 33: Vanes used in the conventional column penetration test, after EN 14679-2005

Quasthoff (2012) illustrates the use of this method with the help of a case history.

For the control of the **homogeneity and uniformity** of the product DSM material, several authors report the excavation of soil-cement columns or CSM panels. In Benhamou and Mathieu (2012), partial excavation of one cell of the Geomix caisson arrangement was performed after completion of works for the purpose of controlling the visual aspect of the product DSM material (see also paragraph 4.6). Figure 34 illustrates the excavated Geomix caisson. In Guimond-Barrett et al. (2012a), three columns were excavated to verify the column geometry and to examine the homogeneity of the DSM material (see Fig. 35 and paragraph 4.2). Similar work is reported in Lambert et al. (2012) also for soil-cement columns.

Figure 34: Excavated Geomix caisson, after Benhamou and Mathieu (2012)

Figure 35: Excavated soil-cement columns 1 month after construction, after Guimond-Barrett et al. (2012a)

As explained in Holm (2000), uniformity and homogeneity of DSM material can also be controlled computing the coefficient of variation of UCS test results on core samples or comparing field and laboratory UCS test results (calculation of q_{uf}/q_{ul}, where q_{uf} means UCS of core samples and q_{ul} UCS of laboratory mix samples). Nevertheless, in the framework of the BBRI 'Soil Mix' project, a methodology taking into account the amount of unmixed soil inclusions into the mix was developed and illustrated with case studies of DSM material executed in several Belgian soils (Denies et al., 2012b).

5.4. QC by execution monitoring

Beyond the mechanical characterization, the **execution tolerances** and possibly **the continuity and the overlapping of the DSM elements** (columns/panels) must be verified. Locations and verticality of the DSM elements should be controlled during execution. As emphasized by all authors presenting DSM case histories, **the best way to ensure QC during execution is by monitoring, adjusting, recording and reporting the execution parameters**. Current technology allows not only to record execution data but also to visualize the execution parameters during the production process, as illustrated in Fig. 36. For dry and wet mixing, EN 14679 (2005) puts the emphasis on the continuous monitoring (or at least at a depth interval of 0.5m) of the construction parameters as reported in Table 9.

Finally, it is important to note that the recorded execution data must be summarized in a **report for each DSM element for final control of the product**. For example, in Benhamou and Mathieu (2012), verticality data were post-processed to construct the as-built 3D Geomix caisson structure, as illustrated in Fig. 32, allowing the verification of the continuity at different depths.

5.5. QC of the DSM structure by monitoring plan

The implementation of a monitoring plan for an engineering solution allows the reduction of the risk for the neighbouring buildings and structures. If necessary preventive measures can be applied. As reported in Table 8, several authors report temporary or long-term monitoring plan for permanent and temporary DSM structures in the cases of earth/water retaining wall, foundation and slope stabilization applications.

For permanent and temporary earth/water retaining walls, Peixoto et al. (2012a, b and d) report that the control of vertical and horizontal displacements can be performed with the help of a monitoring plan including surveying targets and inclinometers. Extensometers can be placed in pipe struts (Peixoto et al., 2012a) and load cells can be used for monitoring anchors (Peixoto et al., 2012b) and temporary foundation elements (Peixoto, 2012d).

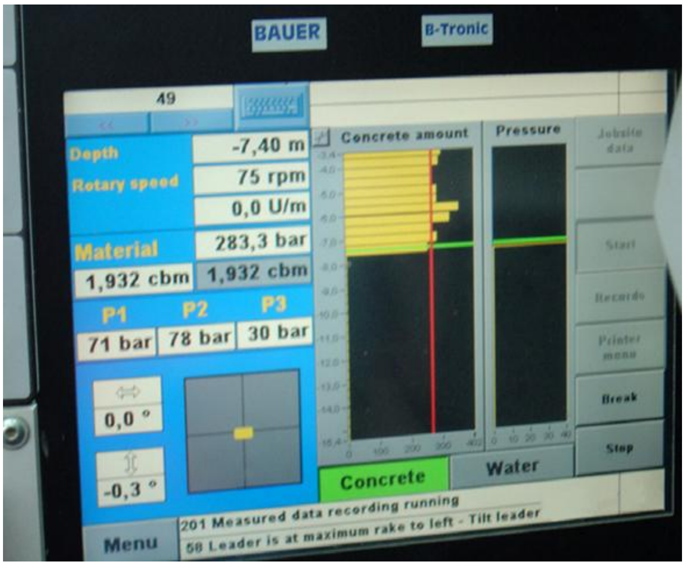

Figure 36: QC monitoring of grout flow rates, injection volume and pressure and penetration rate during execution of CSM walls (photo with courtesy of Malcolm Drilling Company)

Table 9: Construction parameters to be recorded according to EN 14679: 2005

Dry mixing	Wet mixing
Air tank pressure	Slurry pressure; air pressure (if any)
Penetration and retrieval rate	Penetration and retrieval rate
Rotation speed (revs/min. during penetration and retrieval)	Rotation speed (revs/min. during penetration and retrieval)
Quantity of binder per meter of depth during penetration and retrieval	Quantity of slurry per meter of depth during penetration and retrieval

In this way, the recorded values (displacements, deformations and loads) can be compared, on the one hand, with the expected values which can be computed with the help of FEM simulations as reported in Pinto et al. (2012) and, on the other hand, with the alert limits according to the surrounding conditions and the characteristics of the excavation.

For permanent slope stabilization, Pinto et al. (2012) present a monitoring plan including extensometers and inclinometers as represented in Fig. 37. The maximum measured displacements were very similar to the estimated horizontal displacements (5 mm) computed on the basis of the equilibrium limit method and with the help of a 2D FEM analysis (Pinto et al., 2012). The monitoring plan executed in the Fountain slide site (Gaib et al., 2012) includes surveying targets and inclinometers for long term measurements. In addition, aerial LIDAR (LIght Detection And Ranging) measurements have been completed bi-monthly since the completion of the works for the detection of localized slope movement.

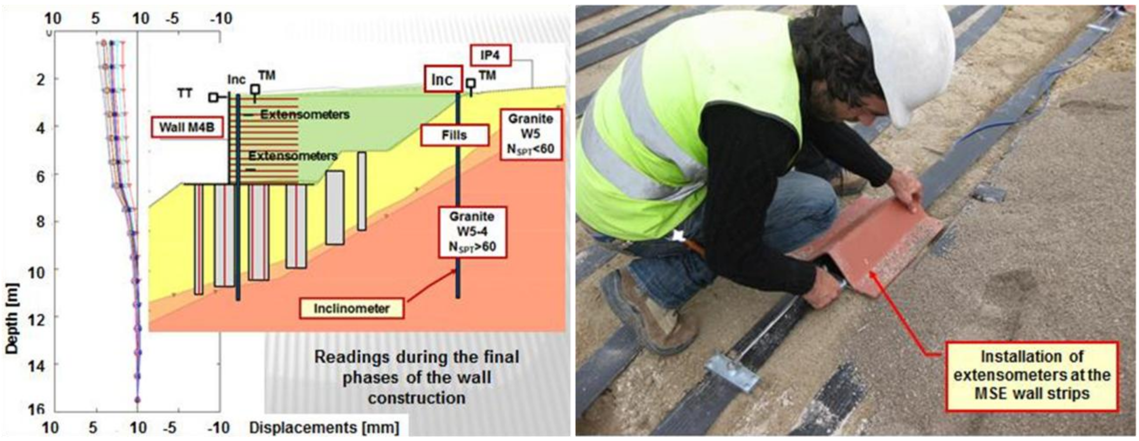

Figure 37: Measured horizontal displacements (on the left) and installation of the extensometers in the retaining wall (on the right), after Pinto et al. (2012)

6. DESIGN RULES

Currently, no universal accepted design approach exists for DSM material. Several methodologies have been presented, though it is still unclear in which way a design value should be calculated for DSM constructions. In this paragraph, an overview of some design methodologies is proposed with regard to the contributions of the Deep Mixing session.

6.1. Methodologies for the determination of the characteristic UCS value

Elements such as piles, diaphragm walls and others comprise only standardized and fully controllable components (Topolnicki and Pandrea, 2012). For these applications the characteristic strength can be defined by the category of concrete. The design procedure for the DSM material is very different since the existing soil is used as an essential component of the final product. Moreover, the characteristic strength depends not only on the soil type, but also on the DSM technique, the amount and type of the binder, etc. In the present proceedings, Denies et al. (2012b) and Topolnicki and Pandrea (2012) discuss the determination of the characteristic strength on the basis of a dataset of UCS values of DSM samples. The paper of Denies et al. (2012b) provides an analysis of several methodologies for the computation of the characteristic UCS value. Topolnicki and Pandrea (2012) present specific design approaches as applied in Japan and Germany.

The first methodology consists in the calculation of the characteristic strength as the X% lower limit on the basis of a distribution function. In both papers, the authors agree that often the wrong assumption is made that the dataset of UCS values is normally distributed (see Fig. 38a). The characteristic UCS value is then erroneously calculated as the X% lower quantile of the normal distribution with parameters corresponding to the dataset. Moreover, this often results into negative and thus useless characteristic UCS values. The correct solution would be to apply the best fitting standard distribution function, for example a lognormal distribution in case the distribution is skewed and/or does not contain subpopulations. The X% lower limit can then be calculated based on this theoretical distribution function, as illustrated in Denies et al. (2012b) for a lognormal distribution (see Fig. 38b). Possibly, a factor β has to be added to the values to obtain an optimal fit with a normal distribution after transformation. Both authors agree that this way of working is probably too complex to apply in practical applications. Denies et al. (2012b) suggest a second methodology to determine the X% lower limit. It is based on the cumulative curve of the original experimental dataset and thus independent of any theoretical distribution function. Note that to apply this method, enough data points have to be available (for the determination of the 5% lower limit, at least 20 samples are necessary) but any other method probably results also in a large uncertainty.

For this first category of approaches (based on the distribution function and based on the cumulative curve of the experimental dataset), Denies et al. (2012b) specify that a value for the X% lower limit has to be defined. In the case of UCS values of DSM material, a more detailed analysis of all the experimental test data is necessary in order to determine if a 5% lower limit, as often stated in Eurocode 7 design, is a representative characteristic strength value.

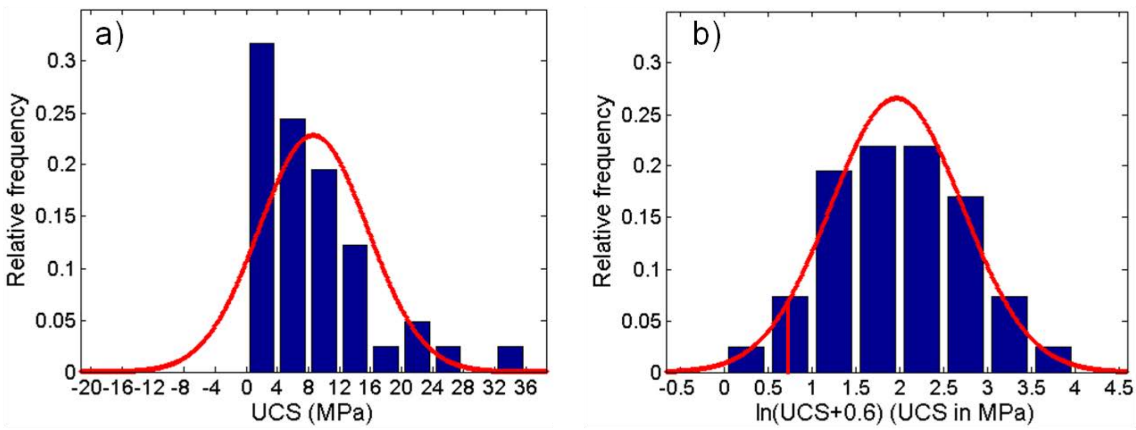

Figure 38: a) Distribution of the UCS values of 41 cores of DSM material from a site in Gent and the corresponding theoretical Gaussian curve. b) Distribution of the logarithm of the UCS values of the same site but increased with β = 0.6 and the corresponding Gaussian curve. The vertical red line indicates the 5% lower limit value, after Denies et al. (2012b)

Denies et al. (2012b) propose a second category of approach to determine the characteristic UCS value which uses the average value of the dataset in combination with a safety factor. This method is described in more detail by Topolnicki and Pandrea (2012) as it has been developed in Japan and Germany for formalized design approach. The characteristic value f_c is then calculated as:

$$f_c = \alpha \overline{q_{uf}} \tag{15}$$

where $\overline{q_{uf}}$ is the mean UCS value from field tests and α a factor representing a certain confidence and safety level (α < 1).

In Japan the value of α depends on:

- the coefficient of variation,
- the reliability of the overlap of columns,
- the untreated soil between the columns,
- the difference between field and laboratory data.

In Germany, the characteristic UCS value is defined as the minimum value of three parameters:

$$f_c = \min \begin{bmatrix} f_{m,min} \\ \alpha f_{m,mittel} \\ 12\,\text{MPa} \end{bmatrix} \tag{16}$$

where $f_{m,min}$ is the minimum value found for UCS and $f_{m,mittel}$ the mean UCS value from a series of at least 4 samples.

In order to obtain the design value, both German and Japanese approaches consider global or partial safety factors applied to the characteristic value:

$$f_{c,d} = \frac{f_c}{F_s} \tag{17}$$

where $f_{c,d}$ is the design value and F_s is a safety factor (global or partial).

A factor to consider long term load (for permanent loading) is considered in the German approach. Moreover, if independent and separate design calculations are performed for compressive and shear stresses (i.e. no 3D stress analysis), the maximum allowed compressive stress is 0.7 x $f_{c,d}$ and the maximum allowed shear stress is 0.2 x $f_{c,d}$ (Topolnicki and Pandrea, 2012).

The Japanese approach considers the design value, $f_{c,d}$ as a prediction to find an arrangement pattern for the columns. Hence, it has to be compared with the real results obtained from field. For that purpose, a statistical approach is used based on the number of test specimens and depending on the mixing method (see details in Topolnicki and Pandrea, 2012). In the Japanese approach, a more detailed design calculation including 3D stress analysis has no effect on the safety factors to be applied.

Concerning this third methodology, Denies et al. (2012b) make two important remarks. First, the definition of the mean that is most suitable (arithmetic mean, median, geometric mean, etc.) depends on the type of distribution of the set of UCS values. Second, it is mentioned that problems may arise when:

- the number of samples is limited,
- the population is skewed,
- and when a population is composed of different subpopulations.

Denies et al. (2012b) also note that the DSM samples with soft soil inclusions larger than 1/6 will have a considerable influence on the deduction of the engineering values.

6.2. Reliability-based design (RBD) approaches applied to DSM structures

Al-Naqshabandy and Larsson (2012) propose a partial factor design by using reliability-based design (RBD) approaches. This methodology takes the distribution of all random variables and their correlation into account in a rational way. However, these parameters are often poorly estimated or even unknown. This approach is applied on the geotechnical design of highway embankments, for which the ground properties are improved with lime-cement columns. Since a high degree of uncertainty exists on the ground properties, a deterministic approach, which represents the soil parameters by for example their mean values, is considered to be unsuitable. Instead of this, a partial factor design for safety and reliability assessment is considered. In this way, the authors believe that the uncertainties are treated in a more rational way than when a deterministic design method is used with the application of a global safety factor. This is illustrated by two RBD methods to find the target value of the undrained shear strength of the lime-cement columns. Both methods are applied on a trial embankment with a height of 6 meters (see Fig. 39) and compared with the deterministic results.

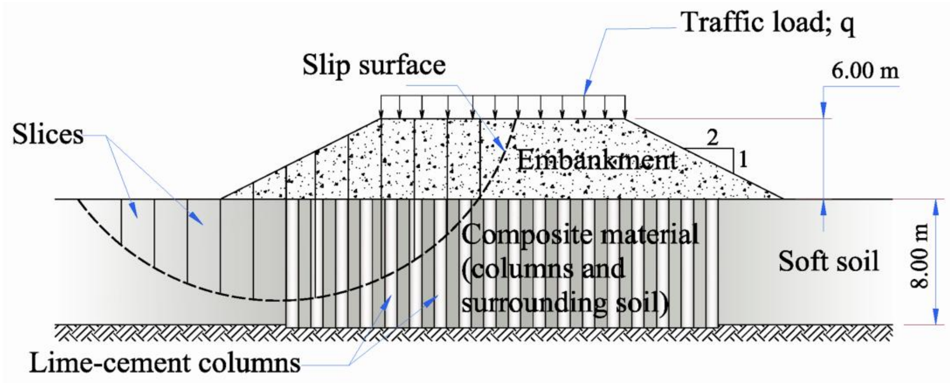

Figure 39: Cross-section of the trial embankment, after Al-Naqshabandy and Larsson (2012)

The first RBD method is known as the first order reliability method (FORM). It takes the uncertainties about the soil parameters into account by including the probability distribution function (PDF) of all random variables and the correlation among them into a performance function. The second RBD method is based on partial factor design and is a more simple form of RBD. Its basic principle is that it replaces the single (or global) factor of safety by a set of partial safety factors of the individual parameters. The partial factors can be evaluated in such a way that they consider different sources of uncertainty associated with the individual parameters.
The study shows that deterministic analysis fails to capture the effect of the total uncertainty on the design of the lime-cement columns. However, this can be avoided relatively easy by the partial factor method, instead of conducting a full probabilistic analysis by FORM.

6.3. Lateral displacements due to installation of soil-cement columns

Because injecting admixtures into the ground under pressure causes deformation of the surrounding subsoil, predicting the lateral displacements and ultimately verifying them are important design considerations. Chai and Carter (2012) present a method for predicting the lateral displacements of the ground induced by the installation of soil-cement columns. It is believed to be the only semi-theoretical method currently available for the analysis of multi-column installation.
In a first step, the prediction method is shortly summarized. It is based on the (cylindrical) cavity expansion theory. The parameters of the method are the diameter of the cavity, R_u, the injection pressure, the volume injected into the soil per unit length of column, the soil shear strength and the Young's modulus of the soil. So far, no theoretical expression for the determination of R_u in terms of all these factors exists. Hence, Chai and Carter (2012) propose empirical equations for the evaluation of R_u. The effect of the construction method is empirically taken into account. The results of the prediction method are finally compared with the results of field tests of two sites in Japan. In both sites, the soil consists of a sandy layer underlain by clays. Below these clays, sandy layers are present again. For these particular sites, it can be concluded that the prediction method generally underestimates the lateral displacement of the clayey layers but overestimates the values of the sandy layers.

7. CONCLUSIONS

The present General Report highlights the significant contributions of the papers of Session 4 of the IS-GI Brussels 2012 dedicated to the Deep Soil Mix (DSM) technique. It is organized with regard to the following aspects: the description of the execution processes and tools, the study of the DSM material, the review of the various applications, the Quality Assurance/Quality Control (QA/QC) requirements and the developments related to the design approaches.

In the DSM process, two types of installation methods are generally considered with regard to the way the binder (based on cement or lime) is injected into the ground: the wet and the dry mixing. Depending on the applications, different improvement patterns can be designed with the help of soil-cement columns, rectangular soil mix panels, continuous barriers or global mass stabilization. In the proceedings of the Deep Mixing session, the following DSM systems have been described in detail:

- the CVR C-mix®, the SMET Tubular Soil Mix TSM®, the Keller Foundations Flapwings® and the Soletanche Bachy Springsol® systems for soil-cement columns,
- the CSM® method for rectangular soil mix panels,
- and the ALLU® mass stabilization for global soil stabilization.

Several parameters have an influence on the produced DSM material: the characteristics of the water/binder mixture, the soil conditions, the mixing conditions (mixing energy and process) and the curing conditions. In the papers of the Deep Mixing session, numerous test results on in situ DSM material have been reported. On the basis of tests on core samples, the density, the UCS, the modulus of elasticity and the tensile strength have been determined, as well as the porosity, the permeability and the ultrasonic pulse velocity. Moreover, the adherence between steel and soil mix has been studied. As illustrated in Fig. 9 and 10, UCS, modulus of elasticity and tensile strength are correlated with the help of equations (1) to (3) and (6) to (8). The results of a methodology taking into account the presence of soft soil inclusions into the mix is then illustrated with case studies. With the help of large scale tests and numerical simulations, the representativeness of the core samples is analyzed with regard to the question of the scale effect and the influence of the unmixed soft soil inclusions.

The mixing technology has to make sure that the soil is mixed sufficiently with the binder to achieve a homogeneous product. For that purpose, the quality control of mixing can be performed with the help of the "*Blade rotation number*" (equation 9) for soil-cement columns or with the help of the "*Mixing quality parameter*" (equation 10) for CSM panels. A procedure is proposed for the estimation of the UCS at 28 curing days with regard to the amount of injected cement, the fine content (FC), the Mixing quality parameter (μ) and if necessary the effects of the *pH*. The effect of curing time on the development of the UCS can be considered with the help of equations (11) to (14).

In the Deep Mixing session, several papers are dedicated to case histories related to various structural and environmental applications of DSM technique: earth/water retaining structure (Table 4), foundation and soil reinforcement (Table 5), land levee (Table 6) and slope stabilization (Table 7), in situ remediation (paragraph 4.5) and barrier against liquefaction (paragraph 4.6). These papers describe the DSM structures with regard to their function, the surrounding soil and the temporary or permanent character of the construction.

Paragraph 5 of the present General Report describes the basics and the recent developments with regard to the Quality Assurance/Quality Control activities related to the DSM technique. The DSM process design can be described by the following steps: a laboratory mix test campaign, a field trial installation, the determination of the final process design (including the definition of the final mix design and construction control values) and the production with QC by monitoring. This DSM process design is illustrated with a case history. In addition, BBRI info sheets (Denies et al. 2012a) have been developed in the continuity of the European standard EN 14679 – 2005 for deep mixing. They provide for the owner/contractor/engineer practical criteria in terms of the execution sequence and tolerances and give some requirements with regard to the quality of the DSM material.

In practice, the DSM material quality is often controlled in laboratory with the help of UCS tests performed on water/binder mixture, wet grab and core samples at different ages. The determination of the density, the coefficient of permeability, the modulus of elasticity and the tensile strength can be required. In the present Deep Mixing session, results of field tests (SLT's, plate load tests, CPT's and column penetration tests) are also presented. For the control of the homogeneity and uniformity of the product DSM material, several authors refer to the excavation of DSM elements. The execution tolerances and possibly the continuity and the overlapping of the DSM elements must be verified. According to all authors of case histories, locations and verticality of the DSM elements should be controlled during execution by monitoring, adjusting, recording and reporting the execution parameters. In addition, the implementation of a monitoring plan for the post-control of the DSM structure can be required.

Finally, paragraph 6 gives an overview of some design methodologies for the determination of the characteristic UCS value for the DSM material. These methodologies can be divided into two categories. The first one uses the average value of the population combined with a safety factor, while the second category defines the characteristic value as a lower limit (e.g. 5% quantile). Moreover, two methodologies are presented to calculate this lower limit. The first methodology consists in the computation of the characteristic strength as the X% lower limit on the basis of a distribution function. The second

methodology is based on the cumulative curve of the original experimental dataset. For these two approaches the X% lower limit has to be defined for DSM material in particular with regard to the amount of soft soil inclusions in the mix.
The first category is discussed with regard to the Japanese and German formalized design approaches. In parallel, a partial factor design for safety and reliability assessment is considered on the basis of the reliability-based design (RBD) approaches. Finally, a semi-theoretical method for predicting the lateral displacements of the ground induced by the installation of soil-cement columns is presented.

REFERENCES

References in bold are part of the present proceedings.

ACI 318-08. 2008. American Concrete Institute. Building Code Requirements for Structural Concrete (ACI 318-08) and Commentary. An ACI Standard. Fourth printing January 2011.

ALLU. 2010. Mass Stabilisation Manual, ALLU Finland Oy.

***Al-Naqshabandy, M. S. and Larsson, S. 2012**. Partial Factor Design for a Highway Embankment Founded on Lime-cement Columns. International symposium of ISSMGE - TC211. Recent research, advances & execution aspects of ground improvement works. 31 May-1 June 2012, Brussels, Belgium.*

***Al-Tabbaa, A., Liska, M., McGall, R. and Critchlow, C. 2012**. Soil Mix Technology for Integrated Remediation and Ground Improvement: Field Trials. International symposium of ISSMGE - TC211. Recent research, advances & execution aspects of ground improvement works. 31 May-1 June 2012, Brussels, Belgium.*

Arulrajah, A., Abdullah, A, Bo, M.W. & Bouazza, A. 2009. Ground improvement techniques for railway embankments, Ground Improvement, Vol. 162, issue 1, pp. 3-14.

***Bellato, D., Dalle Coste, A., Gerressen, F.-W. and Simonini, P. 2012**. Long-term performance of CSM walls in slightly overconsolidated clays. International symposium of ISSMGE - TC211. Recent research, advances & execution aspects of ground improvement works. 31 May-1 June 2012, Brussels, Belgium.*

***Benhamou, L. and Mathieu, F. 2012**. Geomix Caissons against liquefaction. International symposium of ISSMGE - TC211. Recent research, advances & execution aspects of ground improvement works. 31 May-1 June 2012, Brussels, Belgium.*

Borel, S. 2007. Soil mixing innovations: Geomix, SpringSol and Trenchmix. Presentation at Joint BGA/CFMS meeting, London.

CDIT. Coastal Development Institute of Technology. 2002. The Deep Mixing Method – Principle, Design and Construction. Edited by CDIT, Japan. A. A. Balkema Publishers/Lisse/Abingdon/Exton (PA)/Tokyo.

***Chai, J. and Carter, J. 2012**. Lateral displacements due to installation of soil-cement columns. International symposium of ISSMGE - TC211. Recent research, advances & execution aspects of ground improvement works. 31 May-1 June 2012, Brussels, Belgium.*

***Chapman, G., Gniel, J., Greenough, M. and Bouazza, A. 2012**. Ground improvement works for an LNG storage tank foundation. International symposium of ISSMGE - TC211. Recent research, advances & execution aspects of ground improvement works. 31 May-1 June 2012, Brussels, Belgium.*

Chu, J., Varaskin, S., Klotz, U. and Mengé, P. 2009. Construction Processes, Proceedings of the 17th International Conference on Soil Mechanics and Geotechnical Engineering, 5-9 October 2009, Alexandria, Egypt, M. Hamza et al. (Eds.), IOS Press, Amsterdam, Vol. 4, pp. 3006-3135.

***Denies, N., Huybrechts, N., De Cock, F., Lameire, B., Maertens, J. and Vervoort, A. 2012a**. Soil Mix walls as retaining structures – Belgian practice. International symposium of ISSMGE - TC211. Recent research, advances & execution aspects of ground improvement works. 31 May-1 June 2012, Brussels, Belgium.*

Denies, N., Huybrechts, N., De Cock, F., Lameire, B., Vervoort, A., Van Lysebetten, G. and Maertens, J. 2012b. *Soil Mix walls as retaining structures – mechanical characterization. International symposium of ISSMGE - TC211. Recent research, advances & execution aspects of ground improvement works. 31 May-1 June 2012, Brussels, Belgium.*

Denies, N., Huybrechts, N., De Cock, F., Lameire, B., Vervoort, A. and Maertens, J. 2012c. *Mechanical characterization of deep soil mix material – procedure description. International symposium of ISSMGE - TC211. Recent research, advances & execution aspects of ground improvement works. 31 May-1 June 2012, Brussels, Belgium.*

Dhaybi, M., Grzyb, A, TRUNFIO, R. and Pellet, F. 2012. *Foundations reinforced by soil mixing: Physical and numerical approach. International symposium of ISSMGE - TC211. Recent research, advances & execution aspects of ground improvement works. 31 May-1 June 2012, Brussels, Belgium.*

EN 14679 – 2005. Execution of special geotechnical works - Deep mixing. European Standard.

EN 1992-1-1 – 2004. Eurocode 2: Design of concrete structures - Part 1-1: General rules and rules for buildings. European Standard.

Essler, R. and Kitazume, M. 2008. Application of Ground Improvement: Deep Mixing. TC17 website: www.bbri.be/go/tc17.

Eurosoilstab. 2002. Development of design and construction methods to stabilise soft organic soils. Design Guide Soft Soil Stabilisation. EC project BE 96-3177.

Gaib, S., Wilson, B. and Lapointe, E. 2012. *Design, Construction and Monitoring of a Test Section for the stabilization of an Active Slide Area utilizing Soil Mixed Shear Keys installed using Cutter Soil Mixing. International symposium of ISSMGE - TC211. Recent research, advances & execution aspects of ground improvement works. 31 May-1 June 2012, Brussels, Belgium.*

Ganne, P., Huybrechts, N., De Cock, F., Lameire, B. and Maertens, J. 2010. Soil mix walls as retaining structures – critical analysis of the material design parameters, International conference on geotechnical challenges in megacities, June 07-10, 2010, Moscow, Russia, pp. 991-998.

Ganne, P., Denies, N., Huybrechts, N., Vervoort, A., Tavallali, A., Maertens, J, Lameire, B. and De Cock, F. 2011. Soil mix: influence of soil inclusions on structural behavior. Proceedings of the XV European conference on soil mechanics and geotechnical engineering, Sept. 12-15, 2011, Athens, Greece, pp. 977-982.

Ganne, P., Denies, N., Huybrechts, N., Vervoort, A., Tavallali, A., Maertens, J, Lameire, B. and De Cock F. 2012. Deep Soil Mix technology in Belgium: Effect of inclusions on design properties. Proceedings of the 4th International conference on grouting and deep mixing, Feb. 15-18, 2012, New Orleans, Louisiana, USA.

Gerressen, F.-W. and Vohs, T. 2012. *CSM-Cutter Soil Mixing – Worldwide experiences of a young soil mixing method in challenging soil conditions. International symposium of ISSMGE - TC211. Recent research, advances & execution aspects of ground improvement works. 31 May-1 June 2012, Brussels, Belgium.*

Guimond-Barrett, A., Mosser, J.-F., Calon, N., Reiffsteck, P., Pantet, A. And Le Kouby, A. 2012a. *Deep mixing for reinforcement of railway platforms with a spreadable tool. International symposium of ISSMGE - TC211. Recent research, advances & execution aspects of ground improvement works. 31 May-1 June 2012, Brussels, Belgium.*

Guimond-Barrett, A., Szymkiewicz, F., Reiffsteck, P., Pantet, A., Le Kouby, A. and Guédon, S. 2012b. *On the strength and durability of cement-stabilised sands. International symposium of ISSMGE - TC211. Recent research, advances & execution aspects of ground improvement works. 31 May-1 June 2012, Brussels, Belgium.*

Holm, G. 2000. Deep Mixing. ASCE, Geotechnical special publication, N°112, pp. 105-122.

Lambert, S., Rocher-Lacoste, F. and Le Kouby, A. 2012. *Soil-cement columns, an alternative soil improvement method. International symposium of ISSMGE - TC211. Recent research, advances & execution aspects of ground improvement works. 31 May-1 June 2012, Brussels, Belgium.*

Larsson, S.M. 2005. State of practice report - Execution, monitoring and quality control, International Conference on Deep Mixing, pp. 732-785.

Leoni, F. M. and Bertero, A. 2012. *Soil mixing in highly organic materials: the experience of LPV111, New Orleans, Louisiana (USA). International symposium of ISSMGE - TC211. Recent research, advances & execution aspects of ground improvement works. 31 May-1 June 2012, Brussels, Belgium.*

Maswoswe, J. J. G. 2001. QA/QC for CA/T Deep Soil-Cement. ASCE, Geotechnical special publication, N°113, pp. 610-624.

McGuire, M., Templeton, E. and Filz, G. 2012. *Stability Analyses of a Floodwall with Deep-Mixed Ground Improvement at Orleans Avenue Canal, New Orleans. International symposium of ISSMGE - TC211. Recent research, advances & execution aspects of ground improvement works. 31 May-1 June 2012, Brussels, Belgium.*

Mendes, B., Maranha das Neves, E., Caldeira, L. and Bilé Serra, J. 2012. *Assessing the feasibility of a foundation treatment solution based on CSM panels at a river dock in Lisbon. International symposium of ISSMGE - TC211. Recent research, advances & execution aspects of ground improvement works. 31 May-1 June 2012, Brussels, Belgium.*

Pauw, A. 1960. Static modulus of elasticity of concrete as affected by density. Journal of the American Concrete Institute, Vol. 32, N°6, pp. 679-687.

Peixoto, A., Sousa, E. and Gomes, P. 2012a. *Permanent Excavation Support in Urban Area using Cutter Soil Mixing technology at Cannes, France. International symposium of ISSMGE - TC211. Recent research, advances & execution aspects of ground improvement works. 31 May-1 June 2012, Brussels, Belgium.*

Peixoto, A., Matos Fernandes, M., Sousa, E. and Gomes, P. 2012b. *The application of Cutter Soil Mixing to an urban excavation at the riverside of Lagos, Portugal. International symposium of ISSMGE - TC211. Recent research, advances & execution aspects of ground improvement works. 31 May-1 June 2012, Brussels, Belgium.*

Peixoto, A., Sousa, E. and Gomes, P. 2012c. *Earth Retaining Structure using Cutter Soil Mixing technology for the "Villa Paradisio" Project at Cannes, France. International symposium of ISSMGE - TC211. Recent research, advances & execution aspects of ground improvement works. 31 May-1 June 2012, Brussels, Belgium.*

Peixoto, A., Sousa, E. and Gomes, P. 2012d. *Solution of earth retaining structure using Cutter Soil Mixing technology: "Parking Saint Nicolas" Project at Cannes, France. International symposium of ISSMGE - TC211. Recent research, advances & execution aspects of ground improvement works. 31 May-1 June 2012, Brussels, Belgium.*

Peixoto, A., Sousa, E. and Gomes, P. 2012e. *Solutions for soil foundation improvement of an industrial building using Cutter Soil Mixing technology at Fréjus, France. International symposium of ISSMGE - TC211. Recent research, advances & execution aspects of ground improvement works. 31 May-1 June 2012, Brussels, Belgium.*

Pinto, A., Tomásio, R., Pita, X., Godinho, P. and Peixoto, A. 2012. *Ground Improvement Solutions using CSM Technology. International symposium of ISSMGE - TC211. Recent research, advances & execution aspects of ground improvement works. 31 May-1 June 2012, Brussels, Belgium.*

Porbaha, A. 1998. State of the art in deep mixing technology: part I. Basic concepts and overview. Ground Improvement, Vol. 2, pp. 81-92.

Porbaha, A., Tanaka H. and Kobayashi M. 1998. State of the art in deep mixing technology, part II. Applications. Ground Improvement Journal, Vol. 3, pp. 125-139.

Porbaha, A. Shibuya, S. and Kishida, T. 2000. State of the art in deep mixing technology. Part III: geomaterial characterization. Ground Improvement, Vol. 3, pp. 91-110.

Porbaha, A. 2000. State of the art in deep mixing technology. Part IV: design considerations. Ground improvement. Vol. 3, pp. 111-125.

***Quasthoff, P. 2012**. State of the art in "Dry Soil Mixing" – Basics and case study. International symposium of ISSMGE - TC211. Recent research, advances & execution aspects of ground improvement works. 31 May-1 June 2012, Brussels, Belgium.*

Rutherford, C., Biscontin, G. and Briaud, J.-L. 2005. Design manual for excavation support using deep mixing technology. Texas A&M University. March 31, 2005.

***Suganya, K. and Sivapullaiah, P. V. 2012**. Parametric study of embankments founded on soft organic clay using numerical simulations. International symposium of ISSMGE - TC211. Recent research, advances & execution aspects of ground improvement works. 31 May-1 June 2012, Brussels, Belgium.*

Terashi M. 1997. Theme lecture: Deep mixing method – Brief state of the art. Proceedings of the 14th International Conference of Soil Mechanics and Foundation Engineering, Hambourg, 6-12 September 1997. A. A. Balkema/Rotterdam/Brookfield/1999. Vol. 4, pp. 2475-2478.

Terashi, M. 2003. The State of Practice in Deep Mixing Methods. Grouting and Ground Treatment (GSP 120), 3rd International Specialty Conference on Grouting and Ground Treatment New Orleans, Louisiana, USA, pp. 25-49.

Terashi, M. and Kitazume, M. 2011. QA/QC for deep-mixing ground: current practice and future research needs. Ground improvement, Vol. 164, Issue GI3, pp. 161-177.

Topolnicki, M. 2004. In situ soil mixing. In M. P. Moseley & K. Kirsch (Eds.), Ground improvement, 2nd ed., Spon Press.

***Topolnicki, M. and Pandrea, P. 2012**. Design of in-situ soil mixing. International symposium of ISSMGE - TC211. Recent research, advances & execution aspects of ground improvement works. 31 May-1 June 2012, Brussels, Belgium.*

***Vervoort, A., Tavallali, A., Van Lysebetten, G., Maertens, J., Denies, N., Huybrechts, N., De Cock, F. and Lameire, B. 2012**. Mechanical characterization of large scale soil mix samples and the analysis of the influence of soil inclusions. International symposium of ISSMGE - TC211. Recent research, advances & execution aspects of ground improvement works. 31 May-1 June 2012, Brussels, Belgium.*

SESSION 5 – RIGID INCLUSIONS AND STONE COLUMNS

General report
SESSION 5 – RIGID INCLUSIONS AND STONE COLUMNS

Bruno SIMON, TERRASOL, Paris, France, b.simon@terrasol.com

ABSTRACT

This general report about ground improvement using stone columns or rigid inclusions is organised into four general parts, not including the introduction and conclusion. The first part reviews features that these techniques share in common, as well as some of their differences. The second and third parts review recent developments on each ground improvement technique that the reporter considers important for the design of these techniques or for further investigation. The fourth part contains a detailed review of the 26 papers that have been received for this Session.

1. INTRODUCTION

Both rigid inclusions (RIs) and stone columns (SCs) are classified by the TC17 State of the Art Report about Construction Processes (Chu et al., 2009) as ground improvement methods with admixtures or inclusions in the same category as dynamic replacement, sand compaction piles and geotextile confined columns. Rigid inclusions and stone columns can be installed using many different techniques, which the same report describes in detail along with the latest developments in these techniques. Stone columns and rigid inclusions can also be described as two different methods for improving soil behaviour through the use of columns that are often cylindrical in shape, mechanically continuous and typically vertical.

Both of these methods are very cost-effective ways to obtain adequate foundation conditions for a wide range of engineering works, and their use is growing around the world. The scarcity of land for new projects in urban areas and the increased attention being given to project cost optimisation explain the growing interest in these techniques.

The use of stone columns is older than that of rigid inclusions. Stone columns are the product of a technique called vibro compaction that dates back to the late 1930s (Sondermann and Wehr, 2004). The use of rigid inclusions for ground improvement is documented only since the early 1980s, mostly for road embankment construction in northern Europe (Briançon, 2002). However, the emergence of this technique could be viewed as the rebirth of an antique construction technique, whereby a group of closely spaced timber piles topped with a stone cover served as the foundation for bridge piers. Auvinet and Rodriguez (2006) have described a pre-Columbian example in an aqueduct in the Mexico City area.

2. GROUND IMPROVEMENT USING COLUMNS

2.1. General concept

Ground improvement is achieved by constructing a regular grid of vertical elements, or inclusions (either stone columns or rigid inclusions), across soil layers with low bearing capacity and/or high compressibility, extending down to a more resistant layer. Because these vertical elements are stiffer than the surrounding soil, they “attract” a portion of the loads applied at the ground surface. The load share taken by the soft soil can thus be reduced to an acceptable level in terms of the soil bearing capacity or the accepted settlement value.

Columns make a unique contribution to ground improvement in that the soil bears a portion of the structural loads in relative proportion to its own strength, while the bulk of the loads are transmitted by various mechanisms to the columns. This process applies to earthworks as well as civil structures and buildings.

In the latter case, it offers a great advantage over deep foundation solutions, where piles are designed to bear the total loads generated by the structure (assuming that the structure itself is designed to transfer all loads to the piles).

RI and SC ground improvements, with their regular reinforcement patterns, are well-suited to a wide variety of applications (embankments, tank rafts, concrete industrial slabs, etc.) that transmit mostly uniform vertical loading. Their use has also been extended to smaller-scale works and other loading distributions, such as those from embankment slopes (adding some basal reinforcement) and isolated pad foundations or strip footings (using small groups of columns). However, the edge effects cannot be neglected in these situations.

2.2. Differences between SCs and RIs

Ground improvement elements deserve the adjective “rigid” whenever the component material displays a strong permanent cohesion, thereby generating a level of stiffness significantly greater than that of the surrounding soil. Nonetheless, this stiffness may vary widely depending on the type of inclusion developed, which can range from a lime column to a metal section, but also includes the vibro concrete column, mortar column and concrete column (both with and without reinforcement). The rigid inclusion concept assumes that column stability is achieved without any lateral confinement of the surrounding soil (ASIRI, 2012). From that standpoint, RI ground improvement can also be viewed as a soil reinforcement technique using resistant elements inserted in the soil in a similar manner to soil nailing, where the soil is reinforced by installing an array of tensile resistant steel elements.
Unlike rigid inclusions, stone columns require lateral confinement from the surrounding soil. Stone columns must undergo lateral deformations in order to mobilise the lateral support and generate an interaction between the soil and the columns. The plasticity of the columns strongly controls their behaviour, which is also quite different from that of rigid inclusions that exhibit small and nearly elastic deformations. Stone column behaviour depends on the angle of shear resistance of the granular material, as well as on its angle of dilatancy. Both techniques depend on the granular material’s in situ density that can be achieved by the vibration and construction process. Because the stone column behaviour is controlled by confinement of the soil, it will depend on two main factors: first, the modifications to soil properties caused by the installation process (including the consequences of the lateral displacement imposed by inserting and moving the vibrator and densifying the granular material, the increase in horizontal stress in the ground and the remoulding) and second, the time factor reflecting progressive dissipation of excess pore pressures created by the installation process and by the loads imposed at the ground surface.

The RI diameter can be any value permitted by the installation technique (whether it is one specific RI technique or any other among the common piling techniques) with a generally accepted minimum value close to 25 cm; stone columns most often have a diameter of greater than 0.8 m. Yet this parameter does not make a key difference because the replacement ratio (or coverage area ratio), which is the ratio of the cross-sectional area at the column head over the treatment mesh area, is more relevant. Both techniques employ a wide range of replacement ratio values: 10 to 35% for stone columns, but only 2 to 10 % for rigid inclusions. It should be noted that RI ground improvement can achieve a better settlement reduction factor than SC ground improvement.

The choice of grid layout and mesh size (which determines the replacement ratio) is a major step in designing column reinforcement. This step influences how loads will be shared between columns and the ground and, consequently, the overall efficacy of the ground improvement.

Another difference between the techniques is that rigid inclusions are always associated with a load transfer layer (generally a granular layer, known as the load transfer platform or LTP, unless the base of the embankment fill itself acts as this transition layer). Shear mechanisms that develop within the transfer layer and around the inclusion shafts are essential for this technique and are activated by differential settlements that arise between the “rigid” inclusion with low compressibility and the surrounding soil (Figure 1). Differential settlements, and therefore the shear, extend to the layers above the inclusion heads, between the column centrelines and the mesh centreline, meaning that some load transfer already takes place at a distance above the inclusion heads. If one considers the average soil settlement over one mesh and the settlement at the column centreline at any given elevation, it appears that these values are equal only in some horizontal planes: the upper plane located in the LTP or the fill (and all planes above), the plane located along the column length and the plane located at a certain depth below the column tip (and all planes below). The existence of these “equal settlement planes” is characteristic of RI ground improvements.
This scenario differentiates RI ground improvement from SC ground improvement. A stone column design generally assumes that settlements are uniform in any horizontal plane such that all planes are “equal settlement planes”.

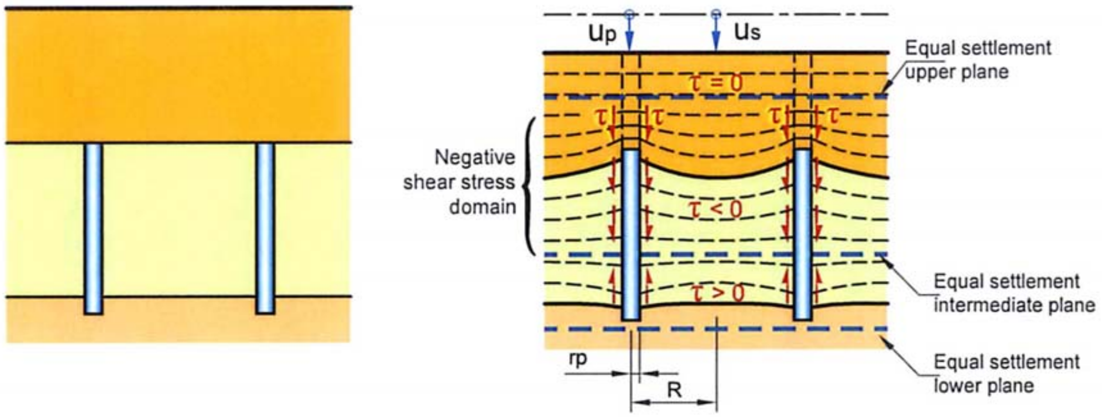

Figure 1: Equal settlement planes that develop in a ground improvement solution using rigid inclusions under an embankment.

2.3. Definitions

The following terms are used to describe grid layout and the amount of load transfer in ground improvement techniques:

- Coverage area ratio, area replacement ratio or simply area ratio, often denoted as α, is the ratio of column head cross-sectional area to the mesh area
- The stress concentration factor (SCF), denoted as m, is the ratio of the average vertical stress on the column head to the average vertical stress on the soil between inclusions at the same level
- The settlement reduction factor (SRF) is the ratio of the settlement with columns to the settlement without columns; this may also be expressed as the settlement efficacy, G = 1- SRF
- The inverse of SRF is the improvement factor n (the settlement of the untreated ground over the settlement of the column-reinforced ground)
- The load efficacy E is defined as the proportion of the load carried by the column heads (Hewlett and Randolph, 1988). It may be defined either globally (total load on the column/total load of the volume fill plus surcharge on the mesh tributary area) or incrementally for one loading step (increment of column load/increment of total load)
- The stress reduction ratio (SRR) is defined as the ratio of the average vertical stress applied on the soil at the column head elevation to the stress that would be applied without columns (Low, 1994). The stress reduction ratio is related to the load efficacy E by the equation $SRR = (1-E)/(1 - \alpha)$.

For a given coverage area ratio α, the higher the SCF, G and E values, the better the ground improvement. The SRR and SRF should be kept at low values.

Because serviceability requirements are of the utmost importance in judging ground improvement performance, the settlement reduction factor should normally be given a high level of importance in the design. Yet load efficacy and the stress reduction ratio are more often used as improvement descriptors than the SRF. They are indeed easily obtained at the design stage from the calculation of the reinforcement scheme or, later on, from the monitoring of the executed project. Assessing the settlement reduction factor requires two different calculations (with and without reinforcement) or, worse, the monitoring of two full-scale tests (one reinforced and the other un-reinforced to serve as a reference).

2.4. Common points among the column ground improvement techniques

2.4.1. Design models

Vertical load cases are usually calculated using a unit cell model, i.e., a column with its tributary soil volume. This model can simulate conditions prevailing in the central part of the column array under uniformly distributed vertical loading because there is no lateral displacement at the cell boundaries. This elementary cell model procedure leads to a less complex model than one covering the whole grid layout and is often further simplified by matching the tributary soil volume with a cylinder on the same axis as

the column and having the same cross-sectional area as the mesh, which leads to an axisymmetric model suitable for analytical or numerical methods (mostly finite element or finite difference methods).
Even with vertical loading, the unit cell model is invalid at the edges of the loaded area (the columns at the periphery of the group). It is also not applicable to a limited group of columns under a footing. 3D models can be used instead, but they remain a difficult task and are often out of the scope of a basic design project. Various simplified models are used as an alternative, such as plane strain models, in which column rows in the out-of-plane direction are transformed into equivalent “walls” with averaged geometrical and mechanical properties, or averaged models, in which the column-reinforced volume is transformed into a homogeneous equivalent material. However, equivalent plane strain models have many drawbacks, especially when used on RI ground improvements under concrete slabs or rafts (Simon and Schlosser, 2006).
Past studies have described many different averaging (or homogenisation) methods (Sudret and De Buhan, 2001, Hassen, 2006). Most of them can be implemented in a standard finite element package and appear to be powerful tools for numerical modelling within the serviceability state (Vogler and Karstunen, 2007). One advantage of these methods, aside from drastically reducing the computational demand over true 3D models, is that the improvement ratio can be varied without modifying the model’s geometry.

2.4.2. Full-scale tests and other physical models and their difficulties

Carefully monitored full-scale load tests and small-scale physical tests are prerequisites for the calibration of numerical methods and the structuring of new design guidelines. Such reference projects are heavy and often costly to implement.
Small-scale physical models are extensively used because they can be tested at a reduced cost. The behaviour of this “prototype” model at a reduced scale 1/N is representative of the behaviour of the full-scale structure only if similitude relations are fulfilled (Garnier et al, 2007): the model should be submitted to a gravitational field N times bigger than that of the prototype in order to reproduce stress and strain fields on a real-world scale. This requirement can be achieved only by geotechnical centrifuge modelling, so the lack of testing facilities, or of appropriate financial support, explains why many small-scale tests remain in 1-g and can give only a poor representation of stress level-dependent phenomena (such as skin friction along the inclusion shaft or the bond between the reinforcement and the adjacent soil). Duplicating the effects of installation in small-scale tests is also a challenge.
Full-scale loading tests may be performed on an isolated column or on a group of columns. The loading can be applied directly to the head of an isolated column to obtain a load-displacement curve that can be used to calibrate the values of relevant design parameters, such as skin friction and point resistance of a rigid inclusion. Loading can also be applied by a plate covering a column and some of the soil area around it. Though this technique cannot model the behaviour of a column in a periodic reinforcement grid, it may be used to check the validity of design parameters describing the soil, column and their interaction by introducing these values in a numerical model of the specific layout. In both cases, the column should be equipped with strain gauges or load cells to follow the load transfer between the column and the soil.
The loading of a group of columns, with appropriate instrumentation, is one unique way to collect data that are representative of the behaviour of one (or more) cell(s) in a reinforcement layout. The test area should cover at least 9 times the elementary mesh in order to simulate conditions under the central mesh that resemble those under an extended grid. Such full-scale tests are not frequently carried out, yet when funding is obtained and careful monitoring methods are set up, these tests prove to be the most valuable source of information to achieve a proper understanding of how the ground improvement works and to check the accuracy of design methods or numerical models. Representative examples are given in this Session by Çevik Özkeskin et al, Buschmeier et al and McGuire et al.
All tests, whether full- or small-scale, have more value if they consider the same foundation design on untreated soil so that a comparison can be made between the improved and unimproved cases on the same site.

2.4.3. General framework for design

Many countries have adopted, or are moving to adopt, limit state design based on load, material and resistance safety factors. In Europe this design method is described by the Eurocodes, with Eurocode 7-1 (2004) giving the technical rules for the geotechnical design of construction works that shall be implemented by 28 European countries. The general framework consists of limit state design based on partial safety factors. It requires verifying both the serviceability limit states (SLSs) and the ultimate limit states (ULSs) using design values for loads, resistances and material properties. These procedures are

detailed for spread foundations and pile foundations, but not for ground improvement. Transposing these general rules to the case of a raft, slab or footing lying on column-reinforced soil is left to the designer.
Writing detailed design rules for RI or SC ground improvement techniques to conform to these general rules is a challenging task. It first requires a proper understanding of all interactions between columns and the ground, followed by a rational decision on all sets of partial safety factors. Full-scale monitored projects are, again, an important step towards the elaboration of national guidelines complying with the limit state design general rules.
This work is being performed in many European countries and is illustrated in recent issues of the guidelines for rigid inclusion reinforcement design (BS 8006, 2010, EBGEO, 2010, CUR 226, 2010, ASIRI, 2012).

2.4.4. Quality Control

Because reinforcement grids are composed of a very large number of similar columns that can be fabricated at a high production rate, quality control during construction is of the utmost importance. Electronic monitoring of all installation phases has become the norm during these projects.

3. STONE COLUMNS

3.1. Installation effects

The installation of stone columns alters the soil around the column, causing effects that may be positive, negative or negligible. Installation effects are one of the major concerns in all stone column applications and require better understanding.
Magnan et al. (2005) presents empirical evidence suggesting that the column diameter depends on several factors, such as the strength of the soil, the type of construction (e.g., dry vs. wet methods), the energy transmitted to the soil by the vibrator and construction sequence, among others. Similarly, the quality of workmanship has a significant influence on the quality of the column and, in particular, on ensuring that the required column diameter is achieved (Slocombe et al., 2000). Alonso and Jimenez (2012) report an 8 – 10% variation in the diameters of more than 9000 stone columns built by a specialised contractor in a well-controlled environment.
The functions of such a column are to improve ground characteristics (i.e., increase bearing capacity and reduce settlement) and facilitate drainage by changing the preferred drainage path from vertical to horizontal.
During installation, as the soil is displaced laterally:

- excess pore pressure is generated and subsequently assumed to dissipate towards the permeable columns;
- horizontal stresses increase, leading to a post-construction coefficient of earth pressure K that exceeds the original rest coefficient K_0; and
- the surrounding soil is in part remoulded by the vibrator penetration.

Smear and plastic annuli that appear during installation can have a negative influence on both of the abovementioned functions of columns.
Lateral earth pressure clearly influences the improvement factor achieved with a stone column improvement because it provides lateral support for the column and influences its yielding. The K value is therefore an important parameter for stone column design and is generally assumed to be equal to 1 (Priebe, 1995).
Castro et al. (2012) also draw attention to the reduction of the undrained shear strength caused by the installation of vibro-displacement columns in sensitive soft soils.

3.2. Failure modes

Two failure mechanisms of stone columns are acknowledged under vertical loading (Figure 2). The failure results either from relatively low lateral support in the upper third of the column (“bulging failure”) or because the column toe is punched into the underlying soil, such as in “floating foundations” (Sondermann and Wehr, 2004). However, the failure is always preceded by such high rates of deformation that the column’s serviceability is generally no longer provided. Sondermann and Wehr observe that the equations used to calculate the deformations, or “serviceability state”, of the foundations in question are much more relevant than the outcome of the limit load assessment of stone columns. Columns belonging to a small group under a rigid footing, or columns placed close to the edges of a loaded area (embankment slopes), may fail by a combination of bulging and bending.

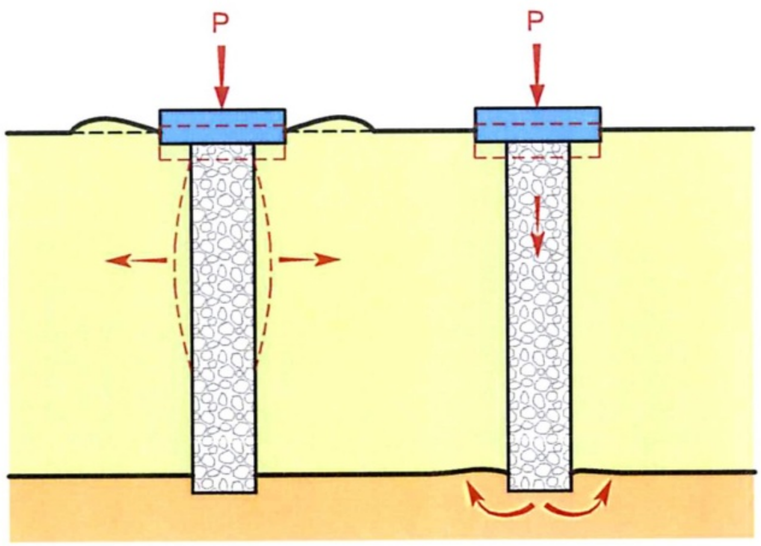

Figure 2: Failure mechanism in vibro-replacement stone columns under vertical loading (Brauns 1978 in Sondermann and Wehr, 2004)

3.3. Function

The stiffness of a stone column relative to that of the soil relies considerably on the lateral support provided by the surrounding soil when the columns have loads imposed on them. The lateral soil reaction σ_{hs} is limited by a value that depends on the undrained shear strength s_u of the soil at same depth. Different formulas are given to express the relationship between σ_{hs} and s_u, for example, $\sigma_{hs} = N_k\, s_u + \sigma_{vs}$, where N_k is a factor that can range between 6 and 8 and σ_{vs} is the stress on the soil in the final drained situation (Sagaseta, 2006, Castro, 2008).
The behaviour of the column is also affected by consolidation of the soil that commences when a load is applied. The stress on the column increases with time, whereas the stress on the soil decreases, and this also influences the consolidation process, impairing the use of classical solutions for radial consolidation (Castro and Sagaseta, 2009). The consolidation process controls the load share taken by the column through the difference in stiffness between the soil and the column and the gain in undrained shear strength, both of which can be achieved at any time during the column's life.

3.4. Design

Based on the considerations described above, the design of stone column ground improvements may therefore consider either the prevailing conditions when load is applied, which are governed by the initial undrained strength s_{u0} (possibly modified by column installation), or those attained later, when part or all of the excess pore pressure due to installation and loading has dissipated. If the load share taken by the soil is ignored, the column behaviour is treated as though it were that of an isolated foundation element in a soil retaining its initial undrained shear strength, a pessimistic assumption. However, this is implicitly assumed when a minimum undrained shear strength value, often s_u = 15 kPa, is given for SC ground improvement. Sonderman and Wehr (2004) show that this limit value is not adapted to the design of stone columns under spread loads, giving the example of columns being routinely installed in soils with shear strengths as low as 6 kPa in Malaysia to bear spread loads from embankments. The load share taken by the soil must be considered to produce an optimal design for SC grid patterns.
In Europe, Priebe's (1995) design method for vibro replacement stone columns has gained acceptance as a valid method (Figure 3). This method defines the improvement factor n as a function of the coverage area ratio and the angle of internal friction of the column material. Corrections are applied to cover the influence of column compressibility and overburdening. The improvement factor n falls within the range of 2 to 6, with values of 3 to 4 being more common (Mitchell, 1982). Because n should represent the ratio of the column and soil's constrained moduli in an equivalent linear elastic model of a unit cell, one assumes that plastic deformation of the columns is implicitly included in that experimental figure. A much higher stiffness ratio would be expected between gravel in a dense state and soil if the gravel behaved within the elastic range.

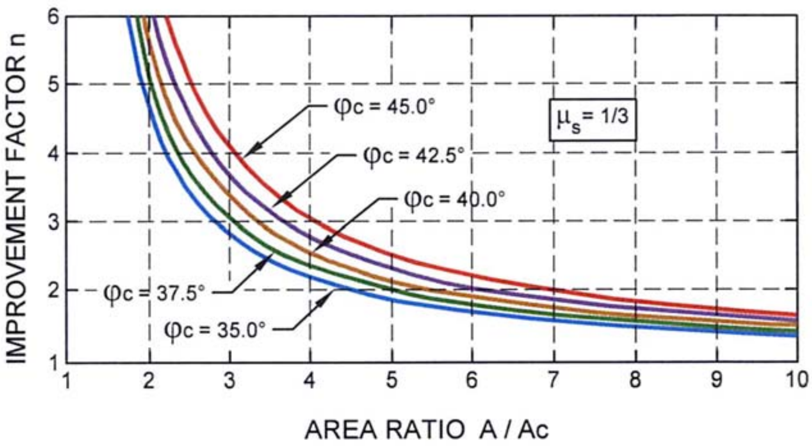

Figure 3: Design diagram for improving the ground conditions using vibro replacement stone columns (Priebe, 1995)

An interesting question is whether the improvement factor also depends on load intensity. Following Priebe's method, it would remain constant. Çevik Özkeskin et al. (2012) give an interesting example of full-scale group load tests where the improvement factor is found to increase with load intensity.

As already mentioned, a small group of columns does not match the assumptions of an infinite grid, and its design calls for more specific approaches. Priebe gives practical design charts that allow the settlement of a rigid foundation on a limited number of columns to be estimated as a proportion of the settlement of an infinite raft supported by an infinite grid of columns (as given in Figure 2). These charts are to be taken as approximations; Sondermann and Wehr (2004) recommend that it is best to install test columns with the achievable column diameters and load them to obtain results with an effective outcome before making final design decisions.

Numerical modelling can overcome some of the difficulties met when designing groups of columns and help determine their stress-deformation behaviour in the service load range. Numerical modelling has gained acceptance as a valuable tool in stone column ground improvement. Schweiger (2008) gives an overview of analytical and numerical methods for stone column design. Unless certain homogenisation methods are used, such models remain computationally demanding, particularly when they are 3D. The incorporation of installation effects in these models is still being researched.

Stone column design is concerned with the assessment of settlement (amount and rate) and safety against failure (bulging failure, punching failure or combined bending and bulging).

The verification of serviceability limit states is accomplished by calculating displacement with an adapted numerical model and characteristic values for the soil parameters.

The verification of ultimate limit states requires that an appropriate set of partial safety factors be set up so that safety against any failure mode can be calculated with appropriate design values for the soil parameters. Consensus on the most appropriate calculation models, together with the calibration of associated partial safety factor values, remains to be reached in many countries that lack national design guidelines that are in line with structural standards for SC ground improvement design.

3.5. Recent developments

Geotextile confined columns (GCCs) are made by driving or vibrating a 80-cm-diameter steel casing into the bearing soil, followed by the placement of a seamless cylindrical closed bottom geotextile "sock" with a tensile strength ranging from 200 to 400 kN/m (Chu et al, 2009). The sock is then filled with sand to form a sand column. The main advantage of this method over the SC technique is assumed to lie in its reduced installation effects (i.e., less alteration of the soil structure). GCCs were used for the construction of a dyke over a very soft surface mud layer of 3- to 12-m thickness in Hamburg. Accounting for the benefits of the geotextile confinement necessitated the use of refined numerical procedures (Raithel et al., 2005).

Granular pile anchors (GPAs) are another interesting development devised for mitigating the problems posed by swelling clay beds. In a granular pile anchor, the footing is anchored to an anchor plate at the bottom of the granular pile. This makes the granular pile tension-resistant and enables it to absorb the tensile force imposed on the foundation by the swelling clay (Rao A. S. et al., 2007). Aljorany (2012) presents a numerical study of this technique in this session.

3.6. Points requiring further research

Two main questions on the application of stone columns require further research.
First, the behaviour of stone columns under repeated loading may apply to columns installed under railway embankments or highway abutments. The same question is raised regarding the use of stone column ground improvements under wind turbines.
Second, it is not fully understood how stone columns can modify a soil's susceptibility to liquefaction. Changes in drainage paths around stone columns are known to allow rapid dissipation of the pore pressure induced by an earthquake (Seed and Booker, 1976). This behaviour is demonstrated by cases of sites treated with vibro replacement stone columns, and the buildings founded on them, incurring no damage despite evidence of liquefaction and minor structural damage nearby. This was the case in the 1991 Loma Prieta earthquake (Mitchell and Wentz, 1991) and the 2001 Nisqualli earthquake (Hausler and Koelling, 2004).
The sustainability of a SC's drainage capacity with time remains an acute question for the designer: Is there any risk of progressive clogging of the gravel material by fine particles from the soil, and how can this drainage capacity be monitored during the project's lifespan?
Improvement of the ground through vibro installation of stone columns is a factor that may also affect the ground's cyclic resistance to liquefaction (CRR). This can be controlled simply by comparing CPT results before and after installation of the columns. The mesh size and diameter of the columns can then be chosen based on the results of preliminary trials using different mesh sizes and column diameters, which would identify those measurements giving the required post-construction cone point resistance, q_c, to reach the target safety factor against liquefaction susceptibility (Youd et al., 2001).
Another point currently being debated is whether stone columns can decrease the cyclic stress ratio (CSR) (τ/σ'_{v0}) generated by earthquake movement. Priebe (1998) gives an adapted diagram chart to account for short-term seismic events. It gives a reduction factor (involving the remaining stress on the soil between columns over the total overburden pressure without soil improvement) that Priebe proposes for application to the CSR in order to evaluate the remaining liquefaction potential. Mitchell and Wentz (1991) express an opposite viewpoint, stating that improvement has little effect on the ground surface response.

4. RIGID INCLUSIONS

4.1. Description

This technique, which is seeing increased use in many countries, has many different names: piled-embankment, column-supported embankment, geosynthetic reinforced pile supported (GRPS) embankment, pile-supported earth platform or soil column reinforcement.
Rigid inclusions are also called columns, pile-like inclusions or non-contact settlement–reducing piles in a generic sense; deep mixed columns, lime columns, or jet grouting columns in reference to some of the installation techniques commonly used; and Controlled Modulus Columns (CMCs) or Vibro Concrete Columns (VCCs) in reference to proprietary names.
The general concept of the technique is the combination of an array of vertical rigid columns and a granular mattress (load transfer layer) so that loading from an embankment or slab is transferred to a deep bearing stratum (Figure 4). The columns may have enlarged heads or caps.
The presence of a transition layer with a load transfer function on top of the column heads is a primary attribute of RI ground improvement techniques. The fact that there is no connection between piles and the superstructure clearly distinguishes RI ground improvements from piled raft foundations.
The load transfer platform should ideally be made of high grade granular material, most often a gravel layer. The designer should carefully consider shear resistance and compactness in the design. Under an embankment, this layer may simply comprise the bottom fill layer if it is of good enough quality.
The load transfer layer may be reinforced by one or more high-strength geotextile or geogrid reinforcements or even welded wire mesh.
Hydraulically stabilised soils are sometimes used to build the transition layer when mineral resources are scarce or costly. Soil treatment with hydraulic binders leads to an enhanced tensile strength and improved shear resistance over the untreated soil, but care should be taken to ensure that treated soil retains its ductile behaviour. Brittle behaviour would put the shear mechanisms that operate the load transfer at risk.
The presence of a concrete slab or raft on top of the LTP causes other differences:

- Without a slab (piled embankments), the load transfer above the column head is operated only through a shear mechanism in the LTP and any fill layer on top of it. The applicable stress boundary conditions are found in a calculable surcharge at top of the model.

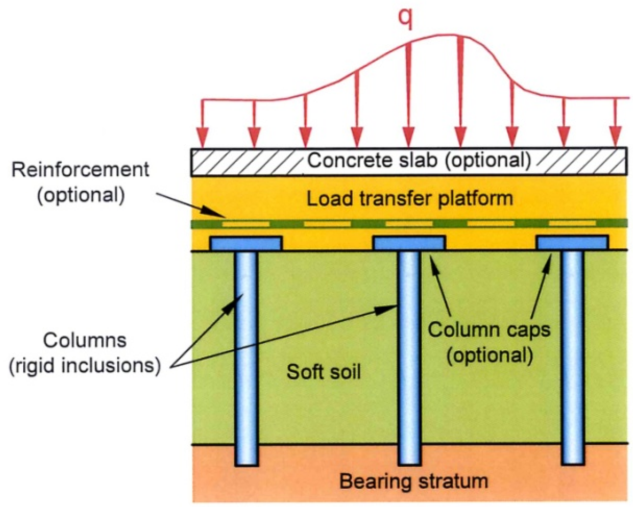

Figure 4: Constituents of the rigid inclusion ground improvement concept.

- With a slab or a raft, the structural element also contributes to the transferring of the load onto columns. Specific boundary conditions are obtained by assuming the settlement is uniform under the structural element base, which is justified by the fact that its own deformations are negligible when compared to the soil deformations. This assumption leads to a non-uniform vertical stress distribution on top of the LTP.

4.2. Development

The first applications of RIs date from the late 1970s, mainly in road embankments in Scandinavian countries (Rathmeyer, 1975). A renewed interest in this technique stemmed from a study about negative side friction by Combarieu during that time period (1974, 1988).

The technique has since been extended to a range of other construction types with wide spread loading, such as storage tanks, water treatment basins and slabs-on-grade for industrial or commercial facilities (Simon and Schlosser, 2006). In the latter case, concentrated loads from columns or bearing walls are often also supported by a compound foundation comprised of a concrete spread footing, a granular cover, and a limited number of inclusions below.

RI ground improvement is now a very cost-effective foundation solution for common construction projects. Several landmark applications punctuate its development and illustrate that this basic concept can be applied equally effectively to complex construction projects.

The four circular 90-m-diameter gravity caissons in the Rion-Antirion Bridge, engineered to withstand large static and seismic loadings, were founded on the seabed using the RI concept (Pecker, 2004). The site of the bridge is one of the most seismic areas in Europe, with a design peak ground acceleration of 0.48 g at seabed level. The reinforcement was composed of driven steel tubes that were 2 m in diameter and 25 to 30 m long and spaced at 7 m x 7 m. The 2-m-thick load transfer layer was designed to act as a fuse under seismic loading, limiting the maximum shear force at the interface, dissipating energy through sliding and forcing the foundation to “fail” according to a mode compatible with an acceptable behaviour of the structure (i.e., a horizontal translation).

The mobile barriers that are currently being built to safeguard Venice from flooding (MOSE project) are each composed of 7 to 9 concrete caissons with lengths of 40 to 60 m and widths of 30 to 50 m. The integrity of the joints between caissons imposes severe conditions of maximum differential settlements between adjacent caissons. The foundation’s final design incorporates an RI ground improvement concept: 0.5-m-diameter, 19-m-long spun concrete piles will be driven into the subsoil under each caisson footprint (Jamiolkowski et al, 2009). The pile heads will be covered by 1 m of compacted granular fill and 0.3 m of self-levelling mortar to obtain an evenly distributed contact surface under the concrete slab of each caisson.

It is noteworthy that centrifuge physical modelling was used in the design stage in addition to numerical modelling for both of these projects (Garnier and Pecker, 1999, Fioravante, 2011).

4.3. Present situation

As occurs in many fields, construction practice has developed ahead of the design methods adapted for this new foundation concept. Partial reference to pile foundation standards could be made during the design process, although designers recognise that these are not quite adapted to the columns most often used as settlement reducing elements instead of load-bearing elements.
Current practice varies between countries in which the applications of rigid inclusions pertain to piled embankments and those in which their use has been extended to occur under structural elements such as rafts, slabs or even spread footings. Briançon (2002) identified some of these differences: higher values for the coverage area ratio (10 to 35%) and a thicker transition layer (minimum thickness being taken as $H_{min} = 0.8(s - a)$, the clear span between inclusion heads along the mesh diagonal) are generally used in piled-embankment design, and geogrid reinforcement of the LTP is often the norm. Lower area ratio values (2 to 10%) apply under concrete slabs or rafts, while the thickness of the load transfer layer is commonly reduced to between 0.4 m and 0.8 m. The LTP is seldom reinforced under concrete slabs. The soil reaction between inclusion heads may be neglected (BS 8006, 2010) assuming that all loads are transferred to the inclusions by shear (arching) and membrane effects. The soil reaction may also be accounted for simply through the use of a subgrade reaction coefficient (EBGEO, 2010, CUR 226, 2010). The interaction between the soil and column is often treated as a secondary factor in load transfer design models, which focus on what happens above the inclusion heads.
Following different research programs on this theme (NO RECESS, AMGISS, ASIRI), several European countries have issued recommendations for the design, construction and control of rigid inclusions since 1990. In 2010, three of those countries (Germany, Britain and the Netherlands) published new or revised guidelines for the design of piled embankments (EBGEO 2010, BS8006, 2010 and CUR 226, 2010). France followed in 2012 with recommendations on rigid inclusion ground improvements that cover both embankments and slab or raft foundations (ASIRI, 2012).
With more widespread acceptance in the marketplace, many engineers are choosing RI ground improvement techniques to provide suitable foundation subgrades at sites that would have traditionally required deep foundations. Care should be taken that rigid inclusions are not seen simply as low-quality pile foundations with more lenient design rules.

4.4. A wide range of installation techniques

Ground improvement elements are installed through a variety of techniques. Some of these techniques include the usual pile installation techniques (driven piles, bored with or without casings, under slurry, continuous flight auger, etc.), but others have been more specifically developed for ground improvement applications, such as the patented Controlled Modulus Columns (CMCs), Vibro Concrete Columns (VCCs), and Deep Mixed Columns (DMCs). Other recent developments are described in TC17, Review of Construction Processes (Chu et al., 2009).
Installation techniques may also be classified as either displacement methods (in which the soil is laterally displaced and generates virtually no spoils) or non-displacement methods (in which the soil is replaced by column material). Non-displacement techniques are well suited to the redevelopment of brownfield sites.
A minimum diameter requirement must be established, which can be as high as 25 cm in the ASIRI recommendations for inclusions other than micro-piles but as low as 12 to 15 cm in the German Recommendation DGGT 2002 (Wehr et al., 2012). Imperfection risks increase with smaller diameters. Meanwhile, vertical loading acting on any out-of plumb inclusion gives rise to second-order bending moments that may become excessive with respect to the material design resistance. Integrity testing of small-diameter inclusions is also more difficult.
While typically not reinforced (especially in the presence of vertical loads), inclusions may sometimes contain rebar in order to resist the eventual shear forces and bending moments resulting from nonvertical or dissymmetric loading (as under an embankment slope). The quality and thickness of the Load Transfer Platform strongly influence the intensity of forces and bending moments in the inclusions, and hence the foundation behaviour, under seismic loading.
Most specialised equipment contains in-built functions for electronic monitoring and recording of installation parameters for quality control. The parameters related to the column diameter, the column continuity and embedment of each column in the bearing layer are most useful for quality control.

4.5. Advantages and drawbacks

The following advantages explain why RI ground improvement has drawn so much interest.
- Loading can be partly carried by the soil.
- A wide range of techniques may be used to install inclusions.

- There is no spoil to dispose of if a pile displacement technique is used, and the technique can be applied in brownfields or old landfills.
- More columns of smaller diameter and lesser embedment in the bearing stratum are generally faster and cheaper to build than an equivalent pile foundation for the same total load; this is a result of the steady capacity development of installation equipment by specialised contractors.
- There is no connection between columns and the structure above them, which generally simplifies structural design.
- The construction time period is significantly shorter than for other solutions, such as preloading with vertical drains.
- The technique provides good seismic performance when properly designed, as illustrated by the Rion-Antirion project (Pecker, 2004).

The following drawbacks, however, should not be ignored.

- The qualifications required to perform RI designs include knowledge of composite foundation systems, necessitating a comprehensive approach encompassing the design and execution phases.
- Execution constraints are more severe (e.g., interfacing between distinct contractors installing the inclusions, the load transfer platform and any slab on it).
- Newly completed inclusions are sensitive to asymmetric loadings that may have negative and potentially destructive effects.
- Horizontal forces and wide load differentials generate bending moments and shear forces in the inclusions that must remain within the capacity of the material's structural resistance.

4.6. Load transfer mechanisms

4.6.1. Above inclusion heads

Whether it is under an embankment or a concrete slab, shear develops in the load transfer platform as an outcome of differential settlements, generated by loading, between the column with low compressibility ("rigid") and the surrounding soil. All 3D numerical modelling led by the ASIRI project (2012) confirmed what is summarised in Figure 5. In a piled embankment (Figure 5, left), soil settlements at the column head elevation reveal a significant gradient close to the pile shaft that levels out further away. Significant shear can develop along the vertical cylindrical surfaces, causing directions of principal stresses to rotate, as seen on the right. When a 90° rotation is attained, the major principal stress has become horizontal: the stress field reveals an analogy with that of an arch extending in the granular fill and bearing on the pile heads. Arching is the basis of the load transfer models by Hewlett and Randolph (1988) and Zaeske and Kempfert (2002). Following these models, it is understood that surface settlements become uniform ("equal settlement plane") when the height of the embankment over the column heads exceeds some given ratio of the column's clear span along the diagonal mesh, which is called the critical embankment height (Mc Guire et al, 2012).

Under a concrete slab (Figure 5, right), the plane of equal settlement is "forced" to coincide with the slab's lower face. In that case, the flexural strength of the slab has to withstand non-uniform fill reactions. Due to the LTP's limited thickness, the stress rotation is limited, and the stress field within the granular fill shows no arching pattern, contrary to what is observed under a piled embankment. The arch design approach is thus ineffective for slab-on-grade applications.

Other numerical modelling using discrete elements (Chevalier et al, 2011) has shown that when the load transfer platform has no concrete slab on it, the zone within the LTP that reveals slight particle displacements takes the shape of an inverted pyramid lying on every inclusion head (Figure 6, left). This shape is similar to the load transfer model proposed by Carlsson (Nordic Handbook, 2005), though the angle θ defining the pyramidal shape is close to the peak friction angle by Chevallier et al (2011), while Carlsson's model assumes $\theta = 15°$. When the load transfer platform has a concrete slab on it, the zone with very slight displacement is primarily restricted to the cylindrical LTP volume between the column head and the concrete slab (Figure 6, centre). Most of the load is transferred onto the inclusion head through the bending of the concrete slab and compression of this volume. The total deformation in this volume controls slab settlement.

As seen also in Figure 6 right, a concrete slab on a LTP has an enhanced efficacy over that without a slab for the same LTP thickness. This difference between efficacy values obtained with or without a slab disappears when the LTP thickness increases.

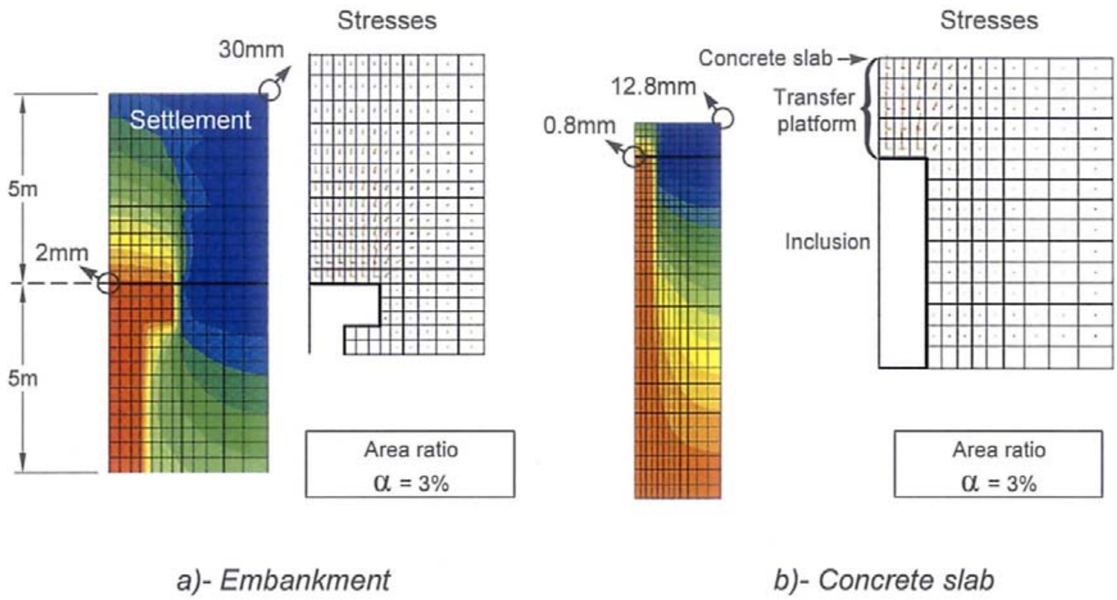

Figure 5: Comparison of load transfer mechanisms underneath a) an embankment and b) a concrete slab over rigid-inclusion-improved ground, including settlement field and principal stresses (Flac 3D models) (ASIRI, 2012)

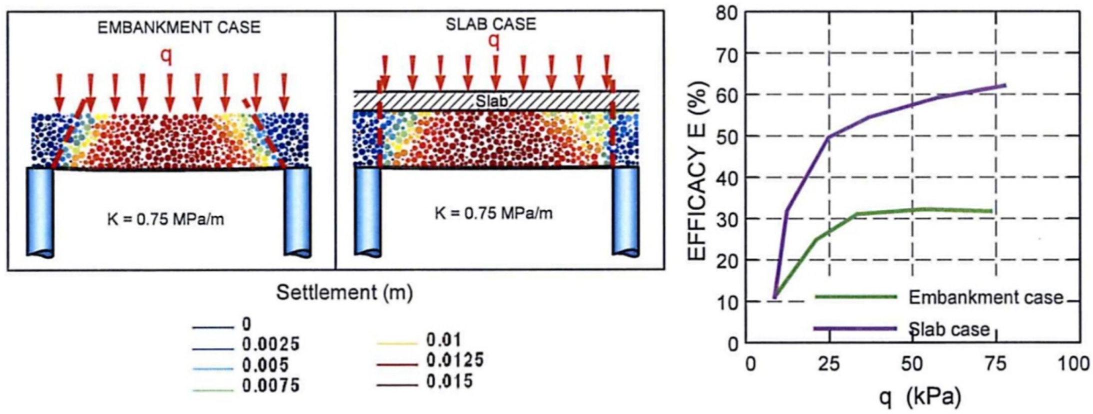

Figure 6: Comparison of the domains in LTP showing slight particle displacement and the efficacy obtained, with or without a slab (LTP with thickness of 0.5 m). (Chevalier et al, 2011)

Centrifuge physical modelling of the settlement at the base of the LTP was simulated by displacing a mobile tray with respect to model inclusions. This modelling has provided interesting information about the efficacy and its variation relative to soil-column displacement (Okyay et al., 2012). The tests demonstrated that the efficacy reaches an ultimate value after some amount of displacement, and for any given LTP thickness, this value depends on the shear strength of the LTP material and on whether the boundary conditions at the top of the LTP imitate those of a uniformly distributed load ("embankment case") or of a rigid plate load ("slab case"). In the slab case, the measured ultimate values of efficacy agree with the vertical stress values given by the Prandtl failure mechanism shown in Figure 7(right): $q_p^+ = N_q\ q_s^+$, where q_p^+ and q_s^+ are the average vertical stresses on the inclusion head and the soil, respectively, and N_q is calculated for the critical state friction angle. The ultimate efficacy value is therefore $E = \alpha\ N_q/[1 + \alpha(N_q\text{-}1)]$.

If no slab is laid on top of the LTP, both the Prandtl failure mode and the inverted pyramid mode may be critical. The ultimate efficacy value is given by the minimum value yielded by either of the models (ASIRI, 2012).

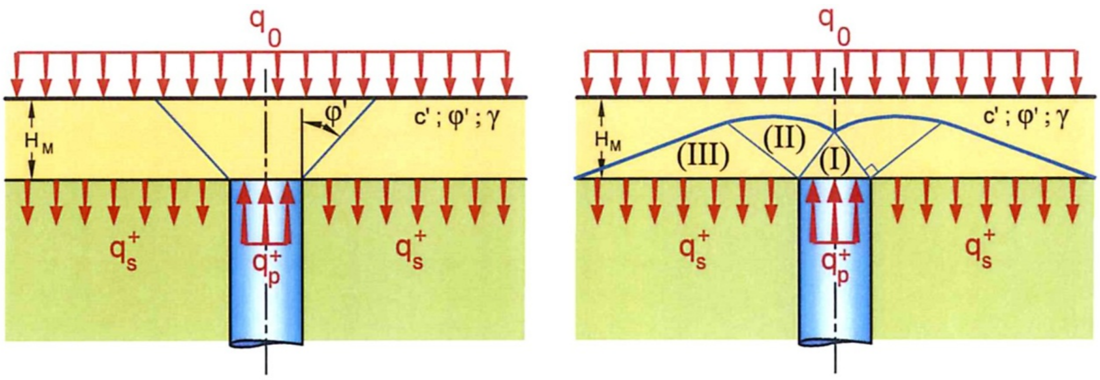

Figure 7: Two different failure modes in Load Transfer Platform. (ASIRI, 2012)

4.6.2. Along the inclusion shaft

Inclusions "attract" load as a result of the negative skin friction that develops wherever soft soil settles more than the inclusion. Unlike deep foundations, this negative skin friction is beneficial because it helps transfer load to the column. Because inclusions are much stiffer than the surrounding soil, the relative settlement becomes negative at some depth along the inclusion. Below that depth, the inclusion settles more than the soil, and the skin friction becomes positive.

At equilibrium, the axial load in the inclusions is as follows (Figure 8).

- A value Q(0) at the head, which represents the load share transmitted by the LTP onto the inclusion head.
- The load increases in proportion to the negative skin friction between the head and the neutral point (the intersection with the "equal settlement" intermediate plane).
- A maximum value Q_{max} is found at the neutral point (at a depth Z_c below the inclusion head).
- The load decreases in proportion to the positive skin friction between the neutral point and the bottom of the inclusion, known as the "tip".
- The load has a value Q(L) at the tip.

The elevation of the equal settlement intermediate plane may vary with the intensity of the loading.

Conventionally, the efficacy is evaluated at the head of the inclusion by considering the ratio $Q(0)/Q_{total}(0)$. In fact, the efficacy value could be more meaningful if it was evaluated at the elevation of the equal settlement intermediate plane by considering the ratio $Q_{max}/Q_{total}(Z_c)$.

Safety against bearing capacity failure depends on the comparison of the maximum axial load in the inclusion, Q_{max}, with the design bearing resistance of the lower part of the inclusion between the neutral point and inclusion's tip.

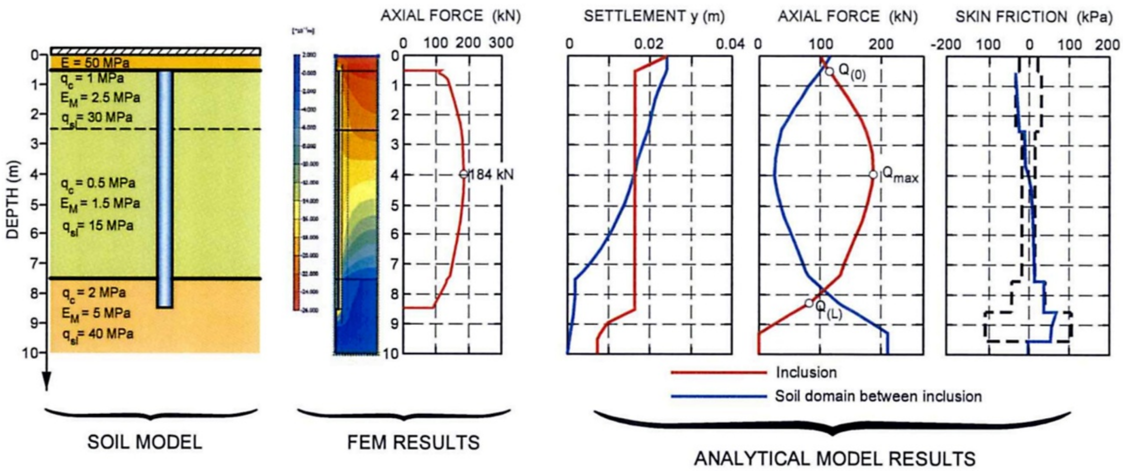

Figure 8: Simulation of a full-scale load test of a slab over an RI ground improvement with a 2D FE axisymmetric model and an analytical model (Full scale experimental test section 3 – load stage 1). (ASIRI, 2012)

4.7. Design considerations

4.7.1. General framework for design

The application of the EC7 design approach to foundations over RI-improved ground is by no means straightforward. These foundations cannot be considered in the category of either shallow foundations or deep foundations. Section 7 of the EC7 code, which focuses on deep foundations, stipulates that the set of provisions it describes should not be applied directly to the design of piles that are intended as settlement reducers, which is the main function of rigid inclusions in many ground improvement projects.

Considerable effort was made by the ASIRI cooperative research program to settle these issues (ASIRI, 2012). The design guidelines that have been issued are the outcome of an array of full-scale testing and both physical and numerical modelling. In order to comply with all EC7 general rules, the following distinction is made among inclusion-reinforced foundation projects:

- Projects where inclusions must be taken into account to demonstrate that safety against soil bearing failure has been verified at the ultimate limit states (ULSs) require that all prescriptions given by the national standard for the design of pile foundations are to be followed for checking Ultimate Limit States (soil failure and material failure) and Serviceability Limit States (SLSs). This means, for example, that the level of safety against bearing capacity failure is the same as that for deep foundations. The inclusion material design resistance is also considered the same as for piles, meaning that no tensile stresses are allowed in unreinforced concrete columns.
- Projects where safety against soil-bearing failure at the ULSs can be demonstrated without taking into account the inclusions (meaning that inclusions can be used simply as settlement reducers) require that a reduced set of verifications be imposed for design, all of which are related to the SLSs only. The calculation model used for SLSs must comply with the conditions arising, for example, from the limit values of the positive skin friction or the negative friction ratio that apply to the same installation technique and same category of soil.

4.7.2. Lessons from full-scale load tests

Well-instrumented full-scale tests provide a wealth of information about the behaviour of RI-improved ground. A few examples drawn from the ASIRI project are given here, while others will be discussed in the review of papers in Session 5 of this Symposium.

ASIRI full-scale load tests were set up on two different sites with 3 test sections in the embankment (Briançon and Simon, 2012) and 3 test sections in the slab over the RI-improved ground (Briançon and Simon, 2010). On each site, a fourth section without inclusions served as a reference. All test sections were instrumented with load cells, settlement transducers, extensometers and inclinometers.

Load efficacy / Settlement efficacy

There is no linear relationship between load efficacy (or stress reduction ratio, SRR) and settlement efficacy, which is illustrated in Figure 9, showing the results of the embankment test sections with 3 different reinforcement layouts (sections 2R, 3R and 4R). The load-settlement curves monitored at ground level between the columns show, in reference to the unreinforced reference section (1R), that a stress reduction ratio as low as approximately 10% (2R) led to a settlement reduction factor of 40% (settlement efficacy of 60%) and that a stress reduction of approximately 50% (3R or 4R) led to a settlement reduction factor of approximately 20% (settlement efficacy of 80%). The nonlinear stress-strain behaviour of the soil explains why a small gain in SRR can lead to a much higher gain in SRF. The development of negative and positive friction along the column shaft also contributes to this amplifying effect.

It is worth mentioning that there was no high-quality transfer layer and no geosynthetic reinforcement at the base of section 2R, yet settlement was still reduced by a factor of 2.5 with respect to untreated soil. A high-quality transfer layer with reinforcement in section 3R (one bi-directional reinforced geotextile) and 4R (two bi-directional geogrids) further reduced settlements to a final reduction factor between 4 and 5.

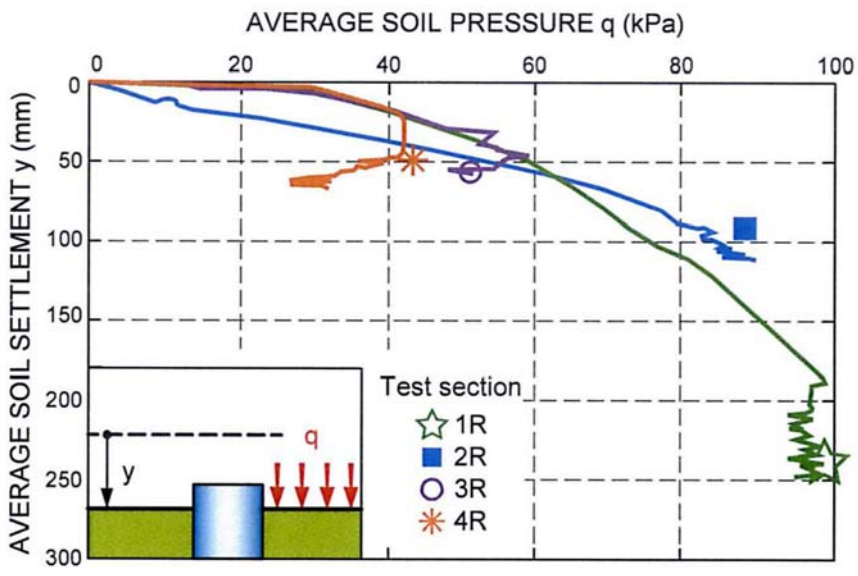

Figure 9: Non-proportionality between the soil settlement and the average vertical stress on the soil between inclusions in the horizontal plane at column head elevation (ASIRI piled embankment full-scale experiment) (Briançon and Simon, 2012).

Importance of the inclusion tip's behaviour

On both test sites, axial test loading was carried out on isolated inclusions located outside the grid layout to determine the load-displacement curves for each type of inclusion (solid lines are shown in Figure 10, with the slab test site on the left and the embankment test site on the right). Because removable extensometers were used, these tests also provided the load-displacement curves at the pile tip (dashed lines on the same figure). The stress and settlement measurements at the head of one inclusion, in the central part of the reinforcement network, are plotted as coloured markers (values were obtained after stabilisation). It is quite interesting to note that in the slab case, the relationship between stress and settlement at the top of one inclusion from the central part of the grid duplicates the load-displacement curve at the tip of an isolated and axially loaded inclusion. The same observation holds for the embankment case. This result demonstrates that the behaviour of an inclusion underneath the structure (slab or embankment) is the same as that of the tip of a single rigid inclusion subjected to axial loading.

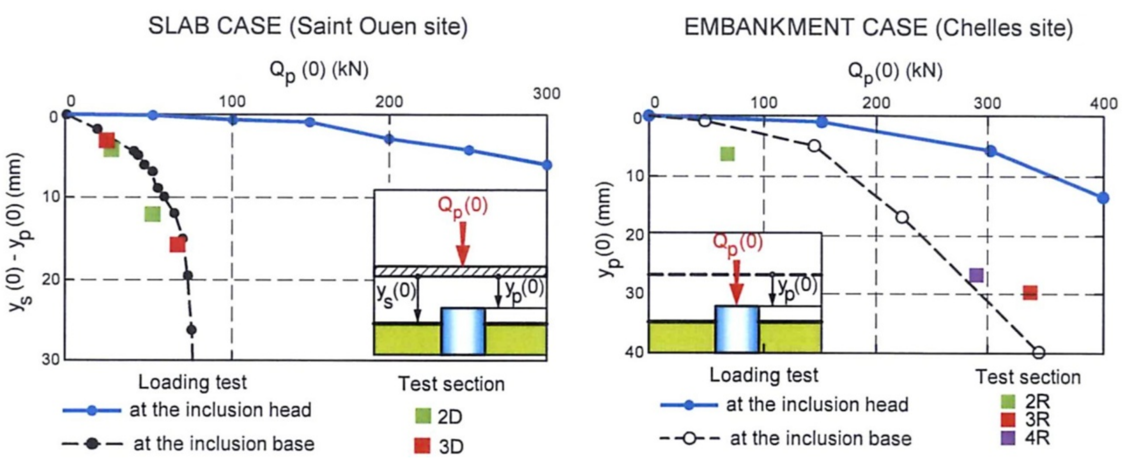

Figure 10: Comparison of the load-displacement curves at the head and base of an axially loaded isolated inclusion with the monitoring data at the head of one inclusion from the central part of the grid within the full-scale testing. Left: Slab case. Right: Embankment case (ASIRI, 2012).

These results have an important implication for design. If reliable results at the top of the inclusion are really expected, the capability of the numerical model to give a realistic simulation of the behaviour of soil under loading exerted at the tip of inclusions should be checked. It is highly recommended in the design of any RI ground improvement solution that the choice of constitutive model, element type and

size and soil parameter values that have been selected be validated by simulating the axial loading of an isolated inclusion and comparing the calculated load-displacement curve to that of an identical inclusion in similar soil conditions.
Setting up a database of load-displacement curves obtained by axial load tests on isolated inclusions that are installed using the same technique and in a variety of soil types will benefit all designers. The data accumulated thus far have demonstrated that the response of single columns subjected to axial loading is strongly dependent on the modification induced by the installation procedure and the surrounding soil properties. This point is also illustrated by papers in this Session (Modoni et al., Reeb et al.).
An alternate way of calibrating a numerical model is to compare the calculated load-displacement curve to a curve obtained through a semi-empirical approach combining shaft and point transfer laws with ultimate values of shaft friction and point resistance for the same type of inclusion and soil category.

4.7.3. Models for design – Unit cell models

The best design is based on models that enable the study of load transfer both above and below the inclusion heads.
Unit cell models are well adapted to the design of columns in the central part of the grid and under uniform vertical loading. Solutions for this scenario can be obtained by using finite element or finite difference methods.
Analytical solutions are also available (Chen et al, 2008, Cuira and Simon, 2009) and consist of simplified forms of a multiphase model (Hassen and De Buhan, 2005).
Data gathered by the French ASIRI national research project have demonstrated that simple analytical models are reliable and easy to use, provided that some basic requirements are fulfilled (ASIRI, 2012).

4.8. Points requiring further research

Because load transfer operates through shear within the load transfer platform and along the inclusion shaft, the stability of these mechanisms under repeated loading is a matter of concern to the designer. Eekelen et al. (2009) provide valuable information about the behaviour of a Kyoto road under the influence of traffic loads (including heavy trucks during the workweek). Monitoring data confirm that the load on the geogrid reinforcement decreases after daily traffic ends. However, the geogrid has an opportunity to restore itself again during traffic-free periods.
Okyay et al. (2012) report on their centrifuge physical testing using both a mobile tray simulating the ground settlement and a system to apply cyclic loading at the surface of the transfer layer, when required. They obtain similar results: the maximum forces on the inclusion heads are reduced by a series of loading-unloading cycles but tend to approach an asymptotic limit value. Despite this reduction in the measured forces at the end of each cycle, the initial load distribution (before cyclic loading) is restored by a small displacement of the mobile tray (settlement less than 4% of the inclusion diameter).
Another study by Heitz (cited by Eekelen et al., 2009) concludes that dynamic loading has more influence on arching when the relative thickness of the embankment (H/s or H/(s-a)) is smaller, or when the dynamic load is larger in comparison to the total load (static+dynamic). The influence of dynamic loading on RI ground improvement projects requires further investigation, specifically consideration of its potential implications for RI ground improvement projects under highway or railway embankments and wind turbines.
The performance of rigid inclusions during seismic loading is well-illustrated by the landmark Rion-Antirion Bridge project; however, the use of rigid inclusions in ordinary projects is still a matter of discussion, and design guidelines for such projects under seismic loading are needed to move forward.

5. REVIEW OF SESSION PAPERS

5.1. General overview

5.1.1. Stone columns

Six papers about stone columns describe small-scale physical models, but only one complies with all similitude requirements and describes testing in a geotechnical centrifuge.
Three papers detail the behaviour of full-scale projects, including one on the construction of a 15-m embankment over a large dump in Germany, one related to the qualification of SC soil improvement to mitigate liquefaction risks behind a quay wall in Egypt and one describing the full-scale load testing of groups of stone columns under rigid 3 m x 3 m footings in Turkey. One other paper describes the use of stone columns in the extension of a railway embankment in Belgium.

Four papers describe numerical models.
The behaviour of soil reinforced with stone columns is compared to that of untreated ground in only four cases, and two papers give a comparison between data from small-scale tests and calculations.
The most frequent subject of these papers is the behaviour of a limited group of columns under vertical loading, including, notably, two full-scale field projects.
Stone columns are most often installed in a soft clay layer. Only three cases describe installation in soils other than soft or very soft clay, which includes two of the three real-world cases.
Nearly all of the papers discuss settlement obtained from stone columns. Load failure is treated by only four papers. The installation techniques covered by these papers primarily involve the vibro replacement method (full-scale or replicated in the laboratory), with only one paper dealing with the more special case of rammed stone columns.
Geotextile confined stone columns are the subject of another paper.

5.1.2. Rigid inclusions

Nine papers about rigid inclusions, a majority of those submitted, describe field projects, whereas only three present small-scale tests (and none of these describe testing in a geotechnical centrifuge). Two papers compare the results of small-scale and full-scale tests.
Numerical modelling is employed in nearly half of the papers, but only two compare numerical results and field measurements.
None of the papers compare the behaviour of improved soil with that of untreated soil.
The cases described are evenly distributed between vertical loading and lateral loading (resulting either from loads applied on the inclusion heads or by lateral ground movement). Only one paper examines the influence of repeated loading.
A wide range of installation techniques is discussed, from in-place concrete displacement columns to non-displacement columns and even drilled shafts and jet grouting columns.
The load transfer platform is reinforced in one-third of the projects described. A non-treated granular transfer layer appears to be the norm in these studies.

5.2. Papers about stone columns

5.2.1. Installation effects

Castro et al present the results of a numerical study of installation effects on stone columns in natural soft clay, attempting to account for the influence of the clay's structure (bonding), anisotropy and viscosity. These features are most often ignored by the constitutive models used in common practice design. The installation of one end-bearing column is simulated as an undrained expansion of a free-draining cylindrical cavity using the finite element PLAXIS code and large displacement calculation mode. The study considers Bothkennar clay, the complexity of which is simulated using three advanced, recently developed constitutive formulations able to account for anisotropy, destructuration and viscosity.
Interesting results are obtained regarding the peak pore pressures developed during vibrator penetration and the change of the lateral earth pressure coefficient K. All models predict that the increase in pore pressure vanishes at a distance of nearly 12 times the column radius and that the maximum value at the cavity wall is close to 5 $c_{u.}$(Figure 11).These excess pore pressures quickly dissipate with time around the column, leading to an increase in the effective horizontal stresses as shown in Figure 12. A nearly constant value for the lateral earth pressure coefficient is found to lie between 4 and 8 column radii from the column axis. While this value is close to 1, as assumed by Priebe, in models that do not consider destructuration, it decreases to a much lower value when this factor is taken into account. These results lead the authors to question the applicability of Priebe's method for structured natural clays. The numerical results give additional insight into the amount of bonding degradation with regard to distance from the column axis. Some agreement is found with experimental data in Saint Alban clay, another sensitive clay type. Because the main interest lies in the average undrained strength between stone columns, a reduction of 15-20% of the initial c_u value is proposed by the authors for practical purposes.

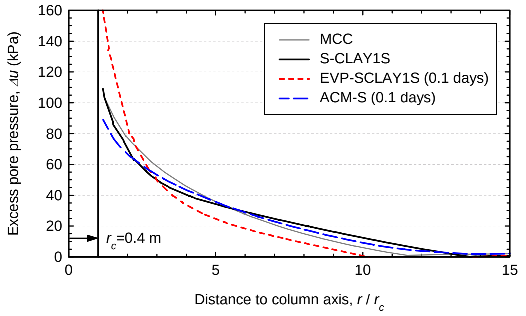

Figure 11: Excess pore pressure after undrained expansion (Source: Fig. 3, Castro et al.)

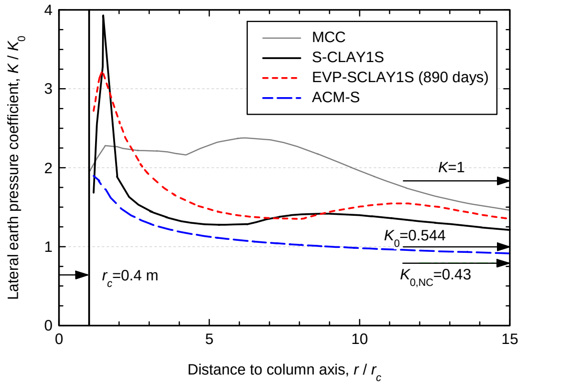

Figure 12: Change in lateral earth pressure for different soil models (Source: Fig. 4, Castro et al.)

Gautray et al. present an innovative experimental study of the development of smear and plastic annuli around stone columns during installation based on small-scale tests in a centrifuge. A stone column is installed on-flight in a soft reconstituted clay using a method that duplicates a dry bottom feed installation process, but without vibration. Some columns were loaded and others left unloaded. Samples taken at different depths and distances from the column axis are tested using the mercury intrusion porosimetry technique. Clay samples taken from close proximity to an unloaded column reveal the difference between soil cylinders located between R and 2R from the column axis that have a reduced porosity and soil cylinders located between 2R and 4R that maintain a higher porosity. This porosity distribution is also compared to that observed around a loaded column to show the influence of bulging near the top of the column. This experimental work is on-going with additional scheduled centrifuge tests as part of a research program about the effects occurring around stone columns during installation and loading.

5.2.2. Behaviour of a single isolated stone column

Kelly and Black utilise a transparent synthetic soil and a non-intrusive measurement of internal soil displacement and strain using laser-aided imaging and particle image post-processing. They apply this new methodology to evaluate the deformation and failure behaviour of stone column foundations in small-scale 1-g physical models. Tests are conducted on 18-mm-diameter isolated columns with L/d ratios between 4 and 8. They are installed in a synthetic soil with an undrained shear strength of s_u = 15 kPa using a process similar to the dry bottom feed and vibration method.
Loading is applied using a circular plate with a diameter of 33 mm. The visualisation of real-time internal displacement during loading indicates that an isolated stone column fails through a combination of compression, bulging and end bearing failure, each occurring at various levels of foundation displacement (Figure 13). Increasing the column length to produce a ratio of greater than L/d = 4 at a constant replacement ratio results in a negligible increase in load capacity, and the predominant failure mode observed is bulging failure. While some base penetration is observed in the shorter column (L/d=4) at smaller foundation displacements, the effect of this punching diminishes with an increasing foundation displacement of up to 20 mm. Longer columns exhibit virtually no end penetration, and the internal column compression extends to a depth of approximately L/d=6 (for the investigated soil undrained strength). Though one must agree with the authors that a great deal of pioneering work emerged from similar tests performed by Hughes et al, one wonders if such small-scale 1-g physical tests, which do not comply with similitude laws, offer increased interest and benefit over numerical models.
The authors note that further testing of a group of columns under both pad and strip footings is planned because the final goal of their research is directed towards making predictions of group performance less problematic.

Cañizal et al. use small-scale tests in the laboratory (scale 1/10) to study the deformation and radial consolidation around end-bearing stone columns under distributed loads. In fact, the analysis involves one horizontal slice of a unit cell representative of a column and the surrounding soil. They compare the results of these small-scale tests with theoretical analyses, and special emphasis is given to the analytical solution developed by Castro and Sagaseta (2009) that considers load transfer onto the columns, the plastic strains in the column and the consolidation process of the surrounding soil. Tests are run using kaolin clay, for which all geotechnical parameters have been carefully established.

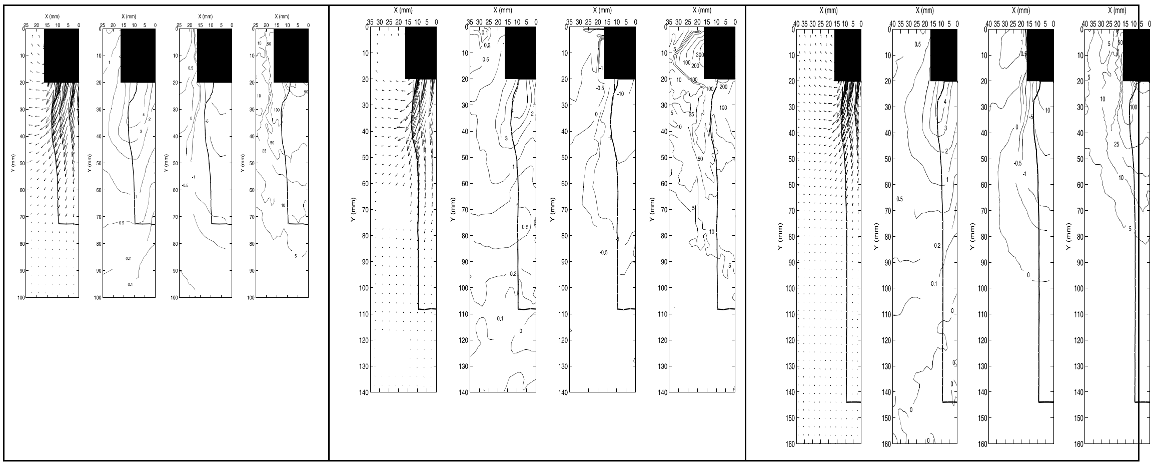

Figure 13: Velocity vector fields, displacement contours in the x and y directions (mm) and total shear strains (%) at 20-mm footing displacements for columns with L/d ratios of 4, 6 and 8 (Source: Fig. 5, 6 and 7, Kelly and Black).

As shown in Figure 14, the analytical solutions that assume elastic and confined (oedometric) behaviour for the column predict a stress concentration factor (*SCF)* equal to the ratio of the oedometric modulus, which is much higher (10-40) than the SCF values measured in the field and the laboratory (3-10). The final values for the SCF and final settlement reduction are adequately predicted only by the solutions that allow for plastic strain in the columns, such as those developed by Castro and Sagaseta (2009). The authors also note that the column stiffness, which is usually unknown, has a small influence on the results of these solutions. Conservative values for the column stiffness are often chosen when solutions neglecting column yielding are used.

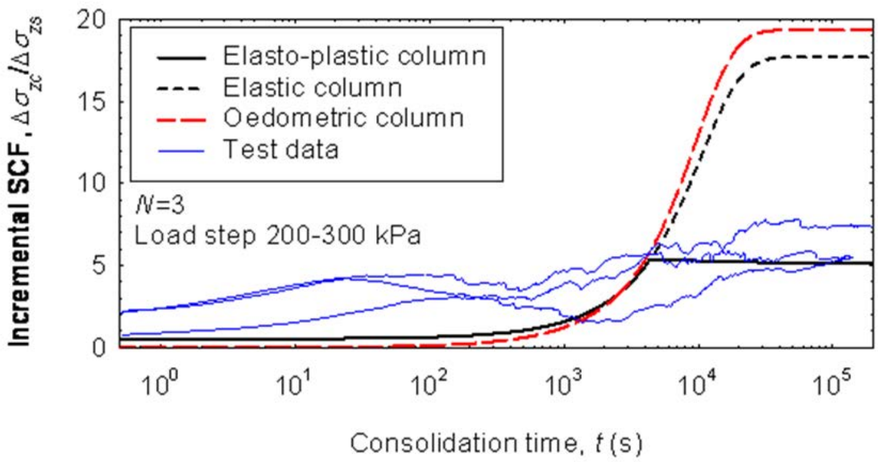

Figure 14: Incremental stress concentration factor (SCF) over time (Source: Fig. 4, Cañizal et al.).

5.2.3. Behaviour of a group of stone columns

Çevik Özkeskin et al present a full-scale field study of a group of floating stone columns in soft clay. Their work displays all the relevant features of a successful experiment because it allows comparison with the untreated case. As such, this paper should be used as a reference for anyone interested in calibrating numerical models in a well-documented field experiment.

Three large plate load test stations are prepared, and a rigid steel footing with plan dimensions of 3.0 m by 3.5 m is used for loading. The first test comprises the stage loading of the untreated soil up to failure, with monitoring of the settlements at ground level and at depth. The other two tests are carried out on ground improved by seven rammed stone columns, each with a diameter of 65 cm. The coverage area ratio α was 0.25. Floating columns, each 3 m long, were used in one station, and end-bearing columns, each 8 m long, were used in the other station. The field instrumentations included surface and deep settlement gauges and a load cell placed on a stone column to determine the distribution of the applied vertical load between the column and the ground.

As expected, the settlement reduction factor β is smaller in end-bearing columns than in floating columns (Figure 15), yet the settlement reduction observed in floating columns is also significant. The settlement ratio is not constant but decreases with increasing applied stress: the higher the load, the better the improvement efficacy.
One other very interesting result is the fact that the settlements measured in the soft soil below the floating column group are consistently smaller than the corresponding untreated soil settlements. This finding is illustrated in Figure 16, where the blue squares mark the settlement reduction ratio β_{Lz}, which represents the ratio between the settlements measured at the base of the floating columns and those measured at the same elevation in the untreated soil. It can be seen that this β_{Lz} ratio is much smaller than that representing the treated/untreated settlement ratio at the column head (β).

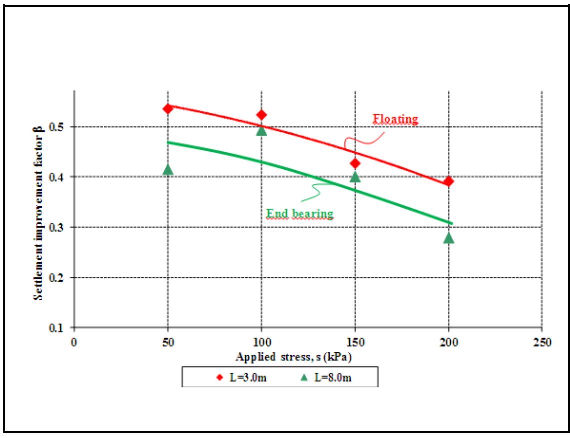

Figure 15: Variation of the β ratio with applied pressure (Source: Fig. 4, Cevik Özkeskin et al.)

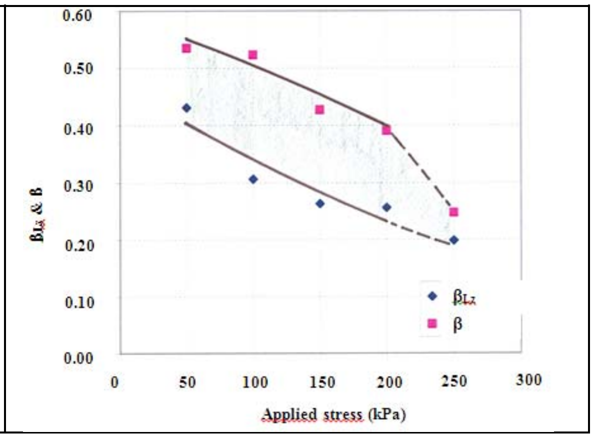

Figure 16: Variation of the β_{Lz} ratio with applied pressure on the floating column group (Source: Fig. 6, Cevik Özkeskin et al.)

A significant spreading of applied load towards the surrounding untreated soil may certainly account for such a reduction in the settlement below the group, one that acts rather like a monolithic pile embedded in the untreated soil. The authors propose that the increased stiffness of the treated upper zone may also be another factor. This factor could be demonstrated by the numerical modelling of the column group that this experiment deserves for completeness. It is nevertheless regrettable that not all the clay properties are given in this paper, such as natural moisture content, drained and undrained strength parameters, compressibility index and the overconsolidation state of the natural soil.
The stress concentration factor n, which ranges from 2.1 to 5.6, is comparable to previously reported values. It decreases with load, regardless of whether the columns are floating or end-bearing. The fact that both the settlement ratio β and the stress concentration ratio n decrease with applied load is of interest. According to any elementary cell model, these two ratios should vary in the opposite manner: if n decreases, β should increase. This discrepancy from the simple cell model also deserves further investigation, possibly with numerical modelling, as this research could lead to a better comprehension of the interaction of the reinforced soil volume with the untreated soil.

Tekin and Ergun report a small-scale model study of the factors affecting the settlement behaviour of stone columns. Tests were carried out in a tank with a diameter of 410 mm using reconstituted clay with an undrained shear strength of 25 kPa. Different group layouts, including from 7 to 85 columns, have been studied. The L/d ratios were chosen to obtain either floating or end-bearing scenarios. Each group of columns was loaded with plates of different diameter B, and specially devised deep settlement gauges were used to establish the vertical strain profile along the columns and below the floating columns.
Loading of the untreated soil enabled the settlement reduction factor SRF to be assessed in each case. One interesting point arises from the comparison of the SRF values obtained with groups of end-bearing columns of diameter 10 cm, 20 cm or 41 cm (the latter possibly approached as a nearly 1-D configuration and was thus studied using the unit cell model). Figure 17 makes clear that the SRF under a footing with diameter B < 41 cm is considerably lower than those measured in 1D conditions (B = 41 cm). The small-diameter groups develop friction on their outer boundaries with the unreinforced soil, enhancing load diffusion. The group of columns therefore behaves similarly to a block punching into the unreinforced soil, demonstrating that a group of floating columns can provide significant settlement improvement

under footings. Figure 17 also shows that the settlement estimates obtained with the methods used by different authors all overestimate the experimental SRF value of the 1-D case. Future studies should nevertheless consider if any tank side effects may have caused a bias of the measured settlements in this limiting case.

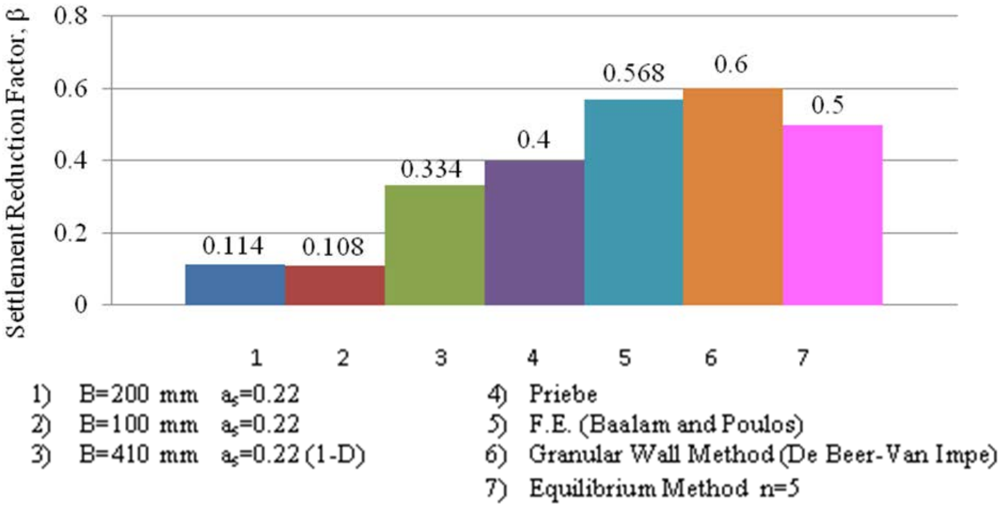

Figure 17: Comparison of the settlement ratios measured under groups with diameters of 100, 200 or 410 mm, with the design charts for the unit cell models used by different authors (Source: Fig. 2, Tekin and Ergun).

This paper details the comparison of the SRF values obtained by groups with different aspect ratios, L/B or L/d. The following points are presented: the minimum column length under a footing with diameter B should have L = B to obtain a significant settlement improvement; the settlement improvement ratio decreases approximately linearly with L/d when L/d is greater than 5; and the use of columns longer than L/B = 1.2 does not significantly contribute to settlement reduction.
The deep settlement gauge measurements also shed light on the column behaviour (Figure 18): for short columns (L/B = 0.6), significant strains are observed down to 2 L below the base of the columns. In addition, longer columns are not uniformly strained, and most of the load is transferred to the soil in their upper sections.

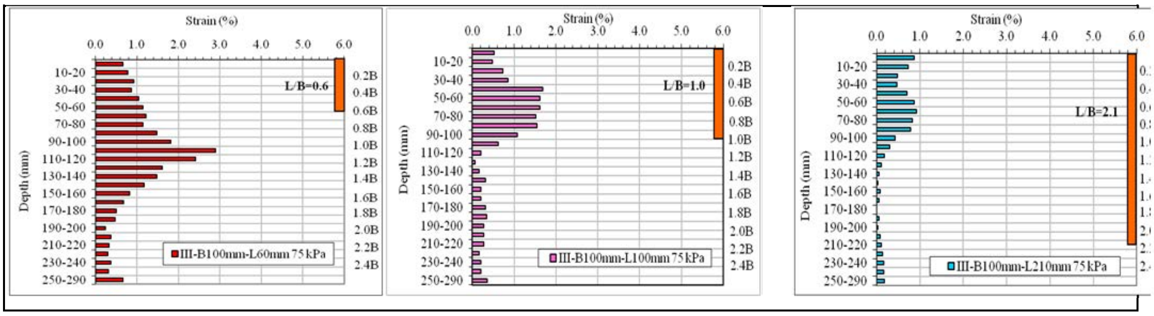

Figure 18: Velocity vector fields, displacement contours in the x and y directions (mm) and total shear strains (%) at a 20 mm footing displacement for columns with L/d ratios of 4, 6 and 8 (Source: Figs. 5, 6 and 7 from Kelly and Black).

El Mahallawy reports small-scale 1 g model tests of unreinforced and geogrid-reinforced sand beds resting on a group of 3 stone columns installed in reconstituted clay. The columns have 50 mm diameters and are installed with 75 mm spacing between them. No information is provided about their precise layout (linear or triangular). This column group is loaded through a steel plate acting as a rigid footing on top of a sand layer of varying thickness that covers the column group. No information is given about the undrained shear strength, compressibility or related state of consolidation of the clay (although the consistency index value, which is equal to 0.8, appears to represent a stiff clay). The tests performed investigate the influences of the thickness of the sand distribution layer, of the one or more geogrid layers

in the sand and of the anchoring length of the reinforcement on each side of the loading plate. Load-displacement curves are compared to those of the plate that is positioned on the unreinforced clay.
The geogrid contribution is likely to be underestimated in the 1-g small scale tests that are not capable of reproducing realistic stress fields in the sand distribution layer at the surface. The results may nevertheless bear qualitative interest: a significant improvement in the soft-soil load-bearing capacity is observed because of the placement of the sand bed over the stone columns. A geogrid layer within the sand bed also increases the load-bearing capacity and decreases the settlement of the soil. A multilayer reinforcement system is more effective and transfers a greater load onto the stone columns. A single-layer reinforcement system in the sand bed offers a similar settlement performance as that obtained with a thicker unreinforced sand layer.

5.2.4. Field projects

Kirstein et al. describe a project in which stone columns have been used to build an embankment that is 15 m high over a coal dump area in Eastern Germany. The way in which this dump was developed explains the material inhomogeneity as well as the large variations in the fine content, which are found particularly in the upper part of the dump: mixed sand, silt, boulder clay and hard clay were found up to a depth of 60 m. The grain size curves fell into a relatively broad range, as shown in Figure 19. The groundwater level has currently been lowered to at least 35 – 40 m below ground level but should be 20 m higher by the end of this century. Field investigations included cone penetration tests (CPT) and Menard pressuremeter tests as well as laboratory tests. The cone resistance up to ca. a 20 m depth varies mainly in the range of q_c = 1 MPa to 3.5 MPa.
Without ground improvement, the new road would have settled differentially with an approximately 1 m variation due to the different ages and thicknesses of the dump, the large embankment load of up to 15 m and the rise in the ground water level within the next hundred years.

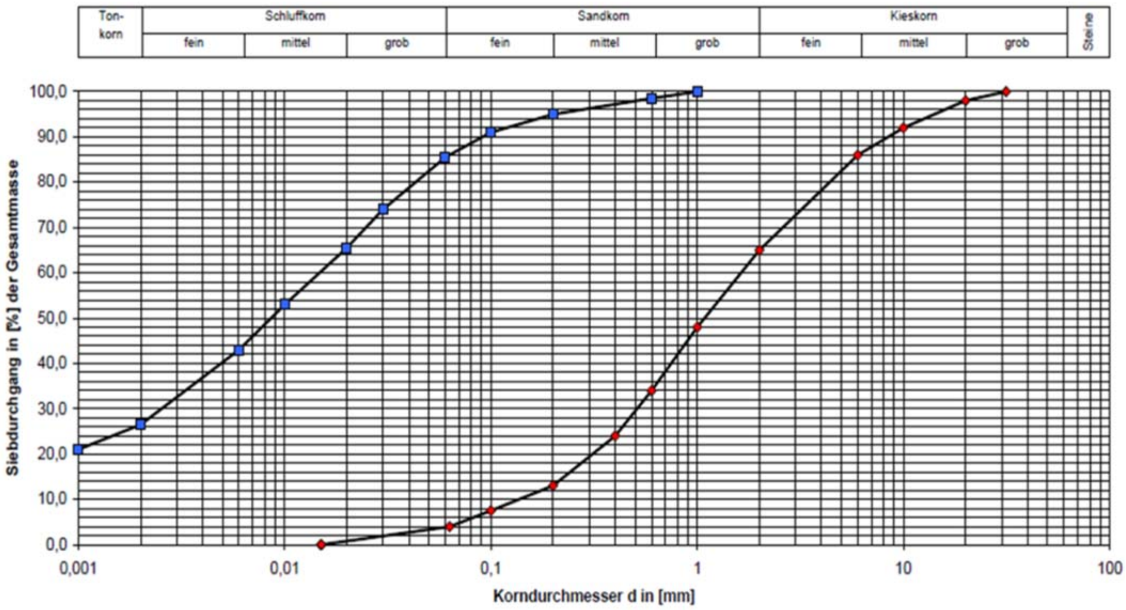

Figure 19: Range of the grain size curves of the dump material (Source: Fig. 2 Kirstein et al.).

Because of the significant stability problems under the embankment, floating stone columns that are 15 m deep to be installed in the dump of 60 m depth were submitted as an alternative bid. The design could be optimised by employing complementary Menard pressuremeter tests conducted before and after the installation of the columns. The tests demonstrated that the soil modulus between the columns was improved relative to its initial value by a factor of 2. A similar improvement could be verified with pre- and post-installation CPTs. This finding was in-line with the water content value, which remained close to the optimal Proctor value.
The friction angle of the gravel was also verified using large-scale shear tests.
Detailed numerical modelling with 2-D plane strain models was used to estimate the settlements. An averaging method was adopted in which the improved ground volume was modelled as a homogeneous material with an equivalent modulus of E = 30 MPa (the unimproved ground modulus was E = 5.5 MPa).

It is worth noting that in this case, the Mohr Coulomb elasto-plastic constitutive model resulted in twice the amount of settlements being calculated using the Plaxis Hardening soil model (50 cm). However, no further details are provided to interpret this discrepancy.
One may question the choice of the value of E = 30 MPa on the basis of either the Menard pressuremeter modulus values, which are reported in the soil (E_M = 5.5 MPa before treatment and 11 MPa after treatment) and in the columns (E_M = 100 MPa), or the cone penetration resistance values in the soil (q_c = 2 MPa before treatment and 4 MPa to 10 MPa after treatment).
The authors present the settlement results that were observed 4 months after the start of the work when the embankment reached 9 m of the final 15 m height: maximum settlements are close to 25 cm. A longer time period will clearly allow for a proper assessment of the settlement study, although the present comparison appears quite encouraging.

Yeo et al. describe the field qualification tests used to compare the soil improvement using stone columns or vibro-compaction to mitigate the risks of soil liquefaction behind a quay wall for Port Saïd Container Terminal in Egypt. The susceptibility to liquefaction was studied using CPT results according Youd et al. (2001).
Pre-CPTs and post-CPTs were conducted before and after ground improvement to verify the effectiveness of the ground improvement work. Stone columns with a diameter of 900 mm and 1.8 m spacing (coverage area ratio of 20%) were tested in one specific area where mainly hydraulically deposited material was found between 2 m and 6 m below the ground level (clayey sandy silt with high plasticity). The installation of stone columns was considered just behind the quay wall to obtain a safety factor of 2 against liquefaction susceptibility. However, the post-CPT results implemented 3 days after the completion of the work could not establish that the expected gain in the q_c values was obtained (Figure 20).

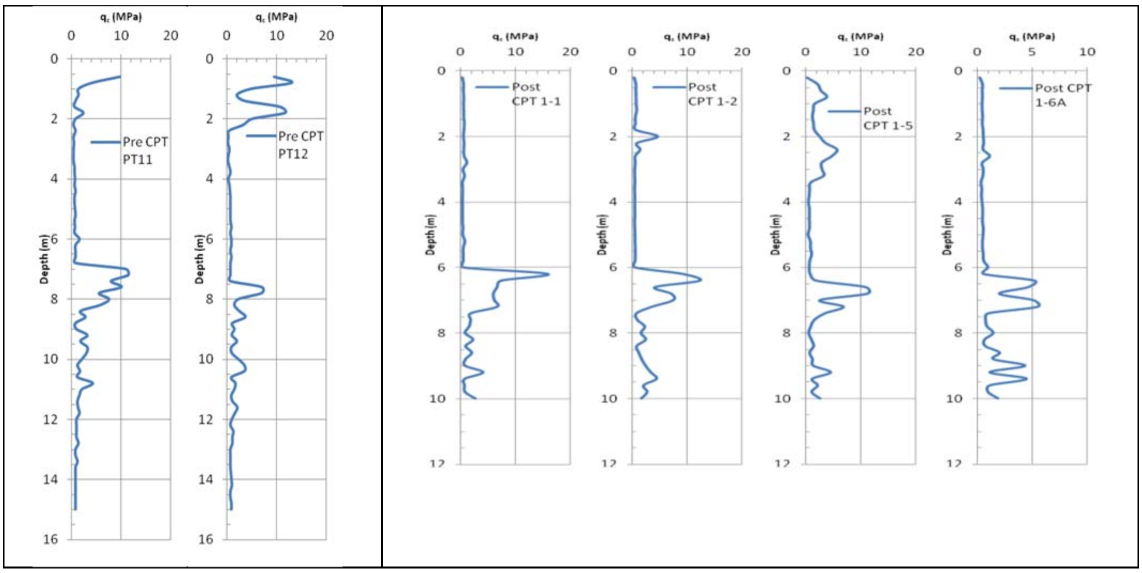

Figure 20: Comparison of pre-CPTs (left) and post-CPTs (right) in the stone column treatment area (Source: Fig. 4(a) and 4(b), Yeo et al.).

Because localised liquefiable layers remained, only the drainage through the stone columns could be relied upon to mitigate the soil liquefaction rather than the soil densification during the column installation. The prevention of the clogging of the stone column could not be guaranteed during the work life span, and it was concluded that soil improvement using stone columns was not significantly effective from these field trials. Poor draining of the installed column material could also be inferred from observing the waterlogged columns at a certain time after their installation. Plate load tests with plates that were 1.8 m in diameter were also conducted in the trial areas using up to twice the applied load. Excessive settlements in the stone column treated area were found and interpreted as the outcome of the insufficient consolidation of the surrounding soil during loading because of the lack of effective drainage through the columns.
This project illustrates several of the difficulties encountered when installing stone columns in clayey sandy silts.

Verstraelen et al. describe the use of different combinations of soil reinforcement solutions for the extension of a railway embankment. One of the solutions utilised stone columns under a mechanically stabilised embankment MSE (Figure 21). This MSE green wall comprised prefabricated cantilever walls anchored by geogrids, which were connected to permanent soil nails. On the basis of the semi-flexible-type wall, the stone columns were chosen to be cheap and quick to install, even though alluvial deposits of up to 10 m in thickness were present. The authors comment on several difficulties that arose from the connection between the geogrid and the concrete slabs. Although they provide no indication of the displacements, one may argue that the lateral loading of the wall could have generated excessive lateral displacements of the stone columns with respect to the permanent soil nails.

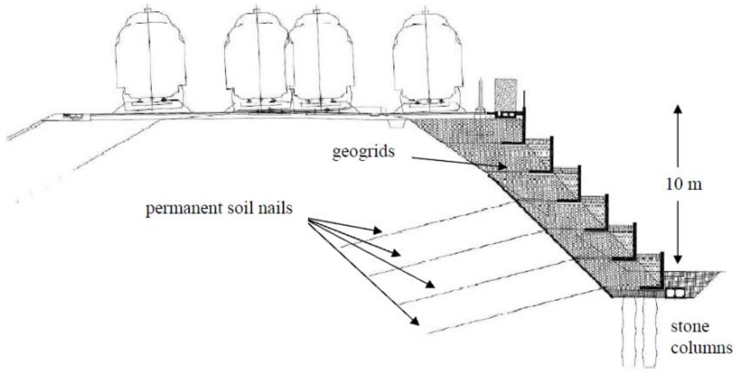

Figure 21: Green terrace with geogrids and permanent soil nails found on stone columns (Source: Fig. 2 Verstraelen et al.)

5.2.5. Miscellaneous

Reliability study of stone columns

Alonso and Jimenez present an interesting case of applying reliability methods to the assessment of the settlement (amount and rate) and bearing capacity (due to bulging only) of stone columns. Their study utilises the theoretical solution presented by Castro and Sagaseta (2009).

Reliability methods are used to consider the effects that uncertainty and variability have on the computed estimates of settlement and the bearing capacity and, hence, on the probability of failure under such failure modes. The uncertainties and the variability considered include those related to the column "as-built" properties (diameter, strength and stiffness) and the soil properties (permeability, strength and stiffness), as well as the model uncertainties (N_k factor linking σ_{hs}, σ_{vs} and c_u and k factor linking c_u and σ_{vs}).

Interestingly, the distribution of the “as-built” column diameter could be drawn on a stone column project with a total of approximately 9000 columns, all built by a specialised contractor in a well-controlled environment (Figure 22). This scenario leads to a coefficient of variation (COV) of approximately 8-10%. On that basis, the authors have retained a COV = 10% to represent “good” conditions and a COV = 20% to represent “bad” conditions.

In this specific case, results indicate that as expected (because the remaining settlements decrease with time), the probability of settlement failure decreases with time as consolidation proceeds. It is also found that the failure mode due to bulging has an approximately irrelevant role in the case of widespread loading.

The importance of the different factors is also weighted within this reliability study (Figure 23). In this specific case, the coefficient of consolidation has the greatest influence if settlement failure is considered (Figure 23a). Similarly, the column diameter and the soil and the column strength are the most important factors if bulging failure is considered (Figure 23b).

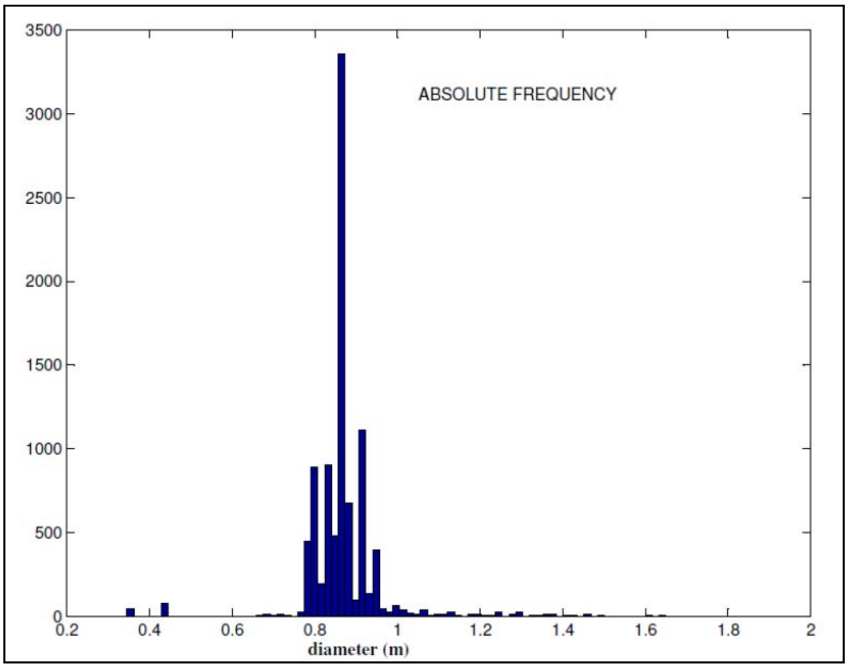

Figure 22: Frequency distribution of the measured diameter of a 9370-column work using dry bottom feed (Source: Fig. 3, Alonso and Jimenez.).

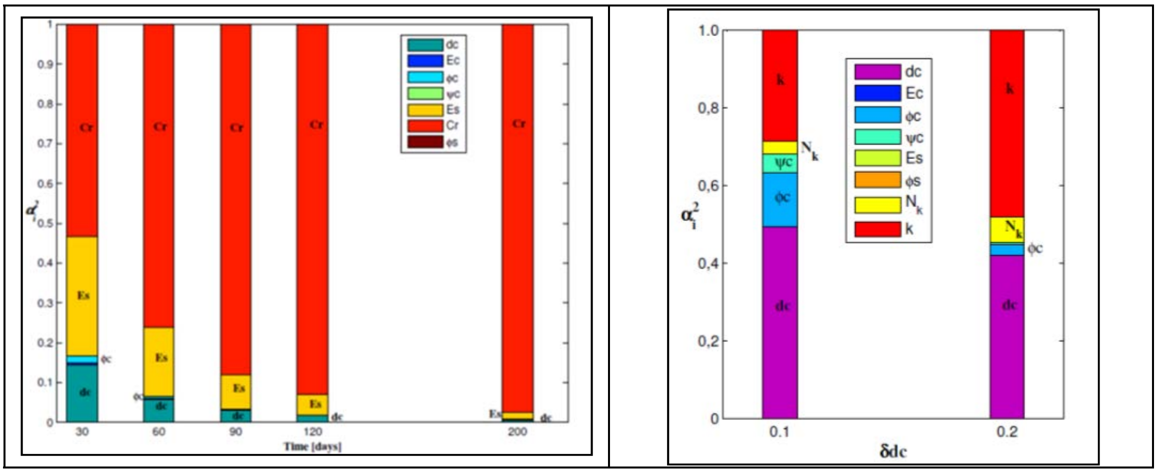

Figure 23: Relative importance of the random variables (a) left: settlement failure (b) right: bulging failure (Source: Figs. 4(b) and 5, Alonso and Jimenez.).

Repeated loading

Al-Saoudi et al. present the results of several small-scale tests on a group of ordinary and geogrid confined stone columns in reconstituted clay under repeated loading. The shear strength of undrained clay is approximately 9 kPa. Groups are composed of 8 columns, which are either ordinary or geogrid-confined stone columns and are 50 mm in diameter and 300 mm long, with 100 mm centre-to-centre spacing. A layer of geogrid was placed over the columns, and a crushed stone layer was distributed along the geogrid forming a model embankment with a height of 100 mm and a crest of 300 mm. A model footing, 200 mm wide and 400 mm long, was placed on the crest of this embankment. Repeated stress increments of 0.4, 0.6 and 0.8 of the failure stress obtained from the corresponding monotonic tests were applied, and the generated settlements versus the number of cycles to failure were recorded. All of the cases can be compared to the similar untreated case.

Under monotonic loading, the influence of the geogrid confinement of the columns becomes significant only for more than 50% of the failure load.

Up to 10000 cycles of loadings representing between 40% and 80% of the static failure load were applied on the untreated soil or on the reinforced soil. For any given percentage of the static failure load, the settlement correlates well with the logarithmic number of cycles. Extrapolation of these curves yields an estimate of the safety factor for any given number of cycles (where failure is defined as a 0.1 B settlement of the footing and the safety factor is defined as the ratio of the monotonic failure load to the monotonic load that results in the same settlement ratio s/B as the repeated load for the number of cycles under study). Figure 24 exhibits the evolution of this safety factor using the number of cycles for untreated and treated soil. Tests demonstrate that both ordinary and geogrid-confined stone columns associated with a reinforced gravel layer are effective to control settlement under repeated loading.

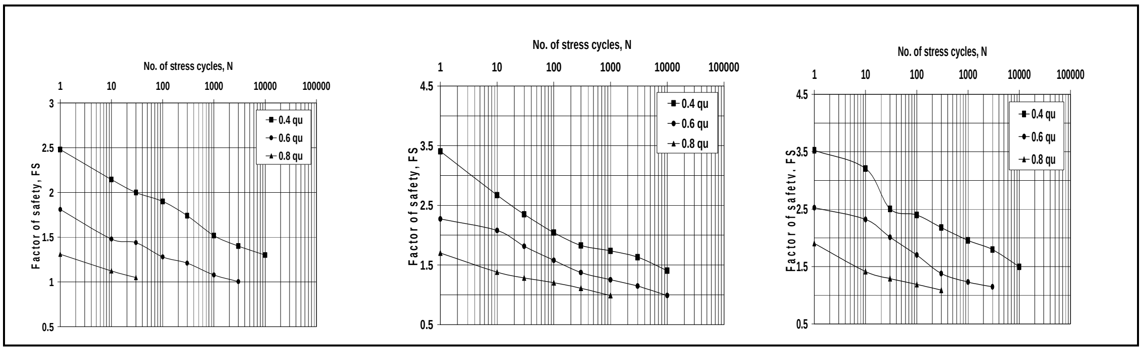

Figure 24: Safety factor versus logarithmic number of stress cycles. Left: (a) untreated soil qu/cu = 5.13; Centre: (b) ordinary stone columns and reinforced gravel layer qu/cu = 14.3; Right: (c) Encased stone columns and reinforced gravel layer qu/cu = 16.8 (Source: Figs. 3, 5 and 7, Al-Saoudi et al.)

No comparison can be made between the tests without reinforcement of the gravel layer. Because interaction between the geogrid and the gravel layer is only poorly modelled by small-scale 1-g tests, one may speculate if similar conclusions would apply without any geogrid reinforcement of the gravel layer. In addition, unfortunately, the loading frequency is not reported.

Pull-out resistance

Aljorany presents a theoretical study of the use of a Granular Pile anchor (GPA) for mitigating the problems posed by soil swelling. In a GPA system, the footing is tied to an anchor plate fixed at the bottom of a granular pile. This makes the granular pile tension resistant and enables it to absorb the tensile force caused by the footing during soil swelling.

An axisymmetric finite element model is developed. The soil swelling is simulated as a thermal expansion, which utilises the analogy between coupled temperature-displacement problems and coupled pore water pressure-displacement problems.

Different values of the GPA length/diameter (L/D) ratio have been examined both with and without swelling conditions prior to the pullout loading step. For the case without the swelling condition, the GPA behaves as a short pile for L/D ratios of up to approximately 7.5. Beyond this critical ratio, the bulging mode of failure becomes dominant.

The results indicate that the soil swelling has a significant effect on application of additional confinement that increases the pull-out resistance of the GPA, especially for L/D ratios less than 10. The value of L/D at which the mode of GPA failure changes from short pile to bulging action is approximately 7.5.

Swelling of the surrounding soil enhances the confinement on the GP, thereby increasing its pullout resistance. This finding is more pronounced for moderate L/D ratios and diminishes for L/D ratios > 10.

Interest in the analogy with heat transfer to investigate the interaction between the granular pile and a swelling soil may be limited because it ignores the drainage by the column (the flow of water towards the column that should have its counterpart in the heat problem). In addition, no indication is provided regarding the soil parameters that are adopted for numerical study. Experimental data and full-scale pullout test results would certainly be advisable to provide further assessments of this technique.

5.3. Paper on rigid inclusions

5.3.1. Load transfer to the inclusion heads

Van Eekelen and Bezuijen present field and small-scale studies of the role of a geosynthetic reinforcement at the base of a piled embankment in light of the latest design rules issued by the Netherlands, Germany or Great Britain. Their paper, which focuses on vertical loading, evaluates how the fill load can be divided into a part "A", which is directly transmitted to the pile heads by shear (or arching) within the fill, and a part "B+C", where part "B" can also be transferred through the geosynthetic reinforcement (GR) to the pile, while the remaining part "C" could be carried by the subsoil (Figure 25).

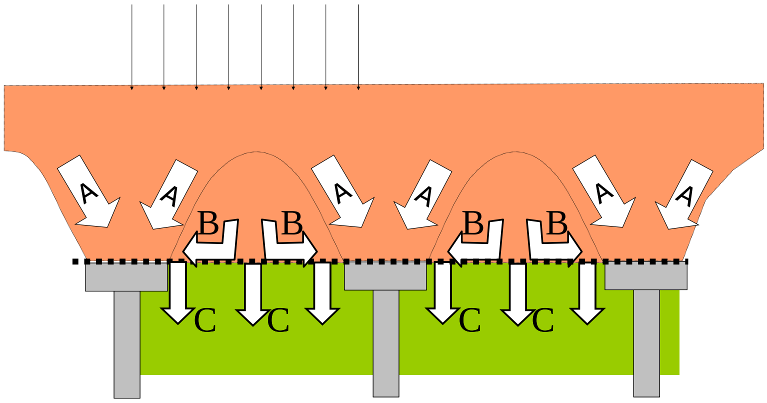

Figure 25: Load distribution in a piled embankment (Source: Fig. 2, Van Eekelen and Bezuijen).

The authors recall that the design national rules differ significantly: BS8006 assumes an equally distributed load without any allowance of soil support, and CUR and EBGEO assume a triangular distribution of load on the GR and allow for some reaction of the subsoil, which is expressed by a coefficient of subgrade reaction, to be the input in the analysis.
The paper provides valuable monitoring data on 2 piled embankments to show that the measured part "A" is higher than that predicted using EBGEO/CUR. Strains in the GR were also found to be considerably smaller than those predicted using the model of Zaeske (2001), confirming the overestimation of part "B" by the current rules.
This finding is also supported by the results of an extensive program of small-scale tests (19) that have shown that consolidation of the subsoil results in an increased part "A" in the fill, indicating that arching was not independent from the subsoil consolidation (unlike the assumption implicitly made by EBGEO/CUR or BS8006). An additional finding from these small-scale tests was that the GR strains occur mainly in the GR strips between two adjacent piles (more than in the GR strips across the diagonals of the mesh). It was also found that the load distribution on the GR agrees better with an inverted triangular shape than with the uniform distribution assumed in BS8006 (giving a parabolic GR profile) or the triangular shape adopted by EBGEO/CUR. This is a first improvement to be added to the EBGEO/CUR calculation model.
A second improvement would be to increase the supporting subsoil area to the entire available area below the GR, which is described in more detail in Lodder et al. (2012). Figure 26 shows the results of modifying EBGEO/CUR-step 2 by improving both the subsoil support and the load distribution. This leads to an improved agreement with the measurements and 19-26% less GR strain than the EBGEO/CUR assumptions. This improvement would enable the necessary GR strength.

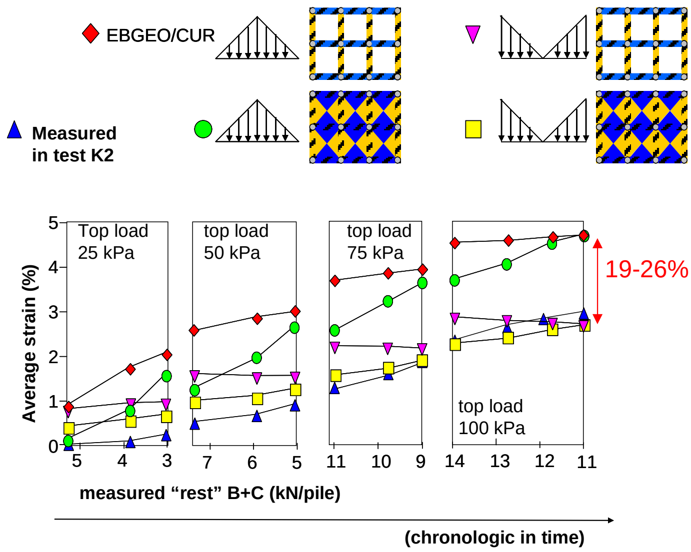

Figure 26: Comparison measurements and calculations of step 2; the effect of modifications of the CUR/EBGEO calculation model: a. modification of load distribution (from a triangular shape to inverse triangular shape) and b. modification of subsoil support (from below the GR strip only to below the entire, diamond-shaped GR area) (Source: Fig. 13, Van Eekelen and Bezuijen).

McGuire et al. report a study of the critical height based on a large set of small-scale (183) and field-scale tests (4) of column-supported embankments that they have purposely devised. The authors define the critical height as the height above which the embankment surface does not exhibit differential settlement due to the deformations that occur at the base of the embankment. The methodologies that have been adopted for their small-scale tests as well as for their field tests are original and should be of use to those interested in testing.

The bench-scale tests show that the critical height increases as the clear spacing between columns increases for a fixed column diameter, which was expected. However, when the column diameter decreases for a fixed centre-to-centre spacing of the columns, thus increasing the clear span, the bench-scale tests show that the critical height decreases rather than increases, which was predicted by the conventional approach. Mc Guire et al. interpret this outcome using the increased compliance at the top of smaller diameter columns: the settlement of the ground surface is increased directly above the column, thereby decreasing the difference between the ground surface settlement at the column location and the ground surface settlement at the location farthest from the columns within a unit cell. This is accompanied by a decrease in the critical height.

Field-scale tests investigated a column-supported embankment layout with columns that were 0.6 m diameter, had a coverage area ratio of α = 8,7% and had embankment heights between 1.2 m and 2.2 m. Monitoring confirmed that the settlements were increased in embankments below the critical height under the influence of traffic loads.

Figure 27 shows that the critical height measured from either the field-scale or bench-scale tests are consistent; both agree with the experimentally derived relationship proposed by McGuire (d is the inclusion diameter, s is the spacing of columns, and s' is the greatest distance that a location within the unit cell can be from the edge of the closest column). The dashed curve represents the conventional approach for pile caps in a square array with an average ratio, $H_{crit}/(s – a)$, equal to 1.5 (the mean value of the recommendations proposed by different authors). The conventional approach is unconservative for low values of s'/d and conservative for high values of s'/d, according to the results from the bench-scale experiments. Figure 28 shows the measurements from the bench-scale tests of the ratio of the surface settlement over the column axis to the maximum differential base settlement, S_c/dS_b, for models below the critical height. The results show that compliance over the column increases as the normalised model height increases. When the column diameter is small relative to the model height, corresponding to high values of H/d, the settlement over the column approaches the magnitude of the differential base settlement. The authors indicate that similar results were obtained from laboratory-scale multi-column tests performed by Demerdash (1996).

These interesting results show that the load transfer onto the inclusion head is controlled by the shear strength of the embankment material. For high H/d values, the inclusion head punches into the fill and the surface settlement is equal to the differential base settlement, which, in this case, is the amount of penetration of the inclusion head into the fill.

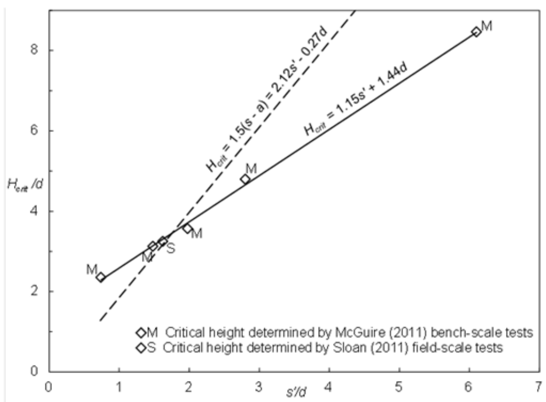

Figure 27: Critical height from tests by McGuire (2011) and Sloan (2011) (Source: Fig. 9, McGuire et al.).

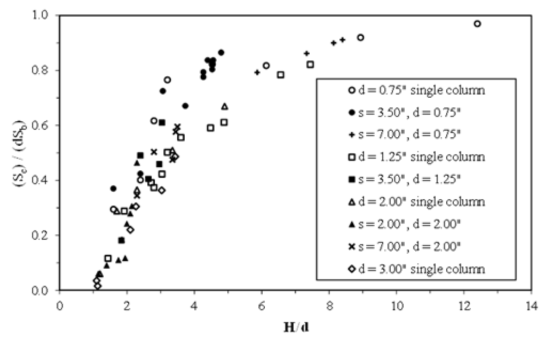

Figure 28: Measurements of the ratio of the surface settlement over the column axis to the maximum differential base settlement versus the sample height divided by the column diameter (Source: Fig. 10, McGuire et al.).

5.3.2. Behaviour of a group of rigid inclusions

Dias and Simon relate a numerical study of a single spread footing over soil reinforced by four rigid inclusions with a comprehensive range of the loading conditions, specifically load intensity or inclination. This study was performed under the funding of the ASIRI research project with the aim to generate appropriate design guidelines for such foundations. Because edge effects cannot be ignored in this small group and despite the fact that this depicts a commonly encountered situation, it proves to be a heavy modelling task to seek a proper balance between calculation practicability and solution accuracy.

A 3D finite difference model was built using the Flac 3D software. In a preliminary calibration stage, this reference model was used to simulate a few simple loading cases for which well accepted solutions exist: loading applied at the head of a single inclusion either axially or transversely, and the vertical or horizontal loading of the same footing lying on the same soil but without inclusions. Figure 29 presents the bending moment in inclusions for different loading cases; even when the loading is vertical, the inclusions are submitted to a small but non-negligible bending moment. In addition, the bending moment increases with the load inclination: the rear inclusion always bears a moment less than that of the front inclusion. For a greater inclined loading, the sliding failure of the footing is observed.

Flac 3D results are compared to those obtained with an alternate and simplified method for designing spread foundations over columnar reinforced ground (Simon, 2010). This method, which follows five successive steps, relies on tools commonly used for pile foundation design under axial or transverse loading and consists of assimilating the reinforced soil volume with the inclusions under the footing to an equivalent homogeneous monolith interacting with the exterior unreinforced soil. The calculated average displacement of the monolith serves as the input in combination with the user-defined soil-inclusion transfer curves, for the calculation of the axial force and bending moment in the inclusions.

The Flac 3D numerical results and those of the simplified method have shown to be in good agreement in all the investigated cases. An interesting point that arises from the comparison of the simplified model results with those of the 3D Flac calculation is that LTP shear strength was fully mobilised under the vertical load component, leaving no residual friction capacity in reaction to any soil-pile horizontal displacement, i.e., "the vertical axis remains a principal stress direction in the vicinity of the inclusion head during transverse loading".

Further evaluation is planned using the results of an on-going dedicated centrifuge testing program, which was also started under the funding of the ASIRI project.

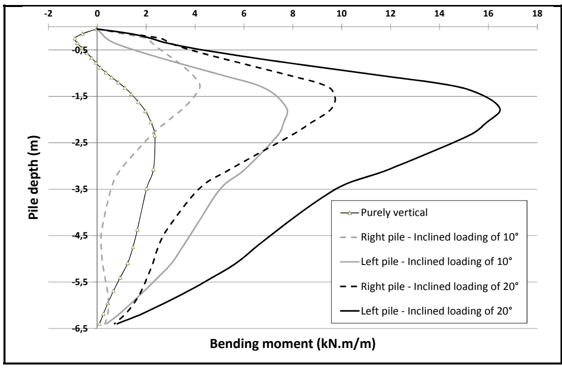

Figure 29: Bending moment for different load inclinations obtained with Flac 3D model, q =150kPa (Source: Fig. 4, Dias and Simon).

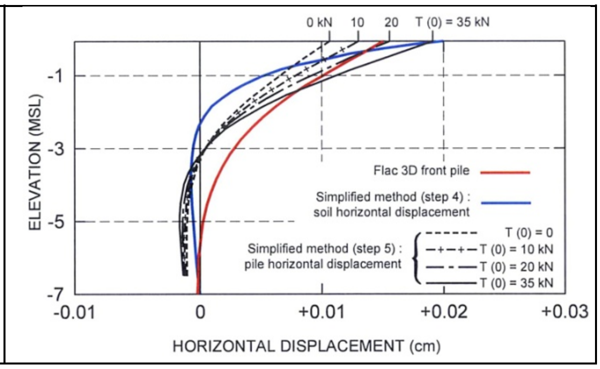

Figure 30: Comparison between the horizontal displacement profile calculated by the Flac 3D model and the simplified method for a range of shear force boundary conditions T(0) at the inclusion head – Inclined load case: q = 200 kPa θ = 10°(Source: Fig. 11, Dias and Simon).

5.3.3. Installation effects

Modoni et al. present a comparative analysis of the load settlement responses of columnar inclusions installed through different techniques (displacement piles, non-displacement piles, continuous flight auger and jet grouting). They have collected a large number of case studies, which they have classified based on the type of execution technology. They focus mainly on cases in which the axial loading tests conducted up to relatively large settlements are available along with a geotechnical investigation of the subsoil. Load settlement curves are fitted with hyperbolic curves. All fitting parameters are scaled to account for the different dimensions of the columns and are finally related to the subsoil properties to compare the trends derived for the different techniques.

As shown in Figure 31 and as expected, displacement piles (DPs) exhibit larger values of the dimensionless bearing capacity ratio $Q_{lim}/(A.q_c)$ than non-displacement piles (NDPs) and jet-grouting columns (JGCs) on a suitable representative range of L/D (20-40) (A is the shaft area + the point area). Continuous flight auger piles (CFAPs) present resistances comparable with those of DP piles, confirming that the accuracy of the installation may lead to satisfactory results. In the same range of L/D (20-40), the same conclusions result regarding the dimensionless initial stiffness $[(\Delta Q/\Delta w)_0/(q_c\ L)]$: the response of the displacement piles (DPs) is stiffer than the non-displacement piles (NDPs) and the jet-grouting columns (JGCs), with the continuous flight auger piles (CFAPs) exhibiting an intermediate behaviour (Figure 32). From the reduced scatter that is illustrated in this plot, the authors conclude that the installation technique plays a more significant role in the resistance of the reinforcing columns than in their initial stiffnesses, which they explain by the fact that the resistance depends primarily on the properties of the soil positioned near the interfaces (the shaft and base of the pile), i.e., a very thin cylinder of soil of which the properties can be significantly modified by the pile installation. On the contrary, the initial stiffness depends on the deformation of a larger mass of soil extending far from the pile axis (several or tens of metres, depending on L/D). It can be noted that no consideration is given to the interaction of the columns and the soil around them, which carries part of the total load. However, this analysis is interesting because the head behaviour in a columnar reinforcement grid reflects the behaviour of an axially loaded and isolated column (ASIRI, 2012).

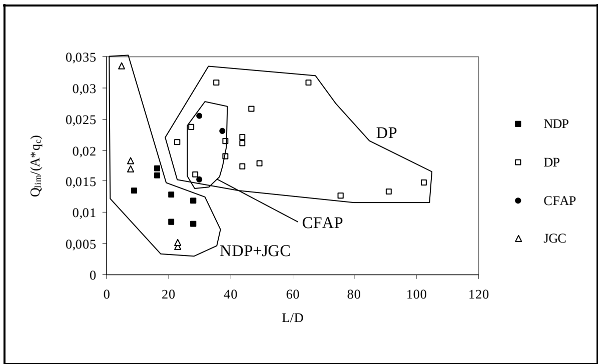

Figure 31: The bearing capacity ratio of columns installed using different techniques (Source Fig. 6, Modoni et al.).

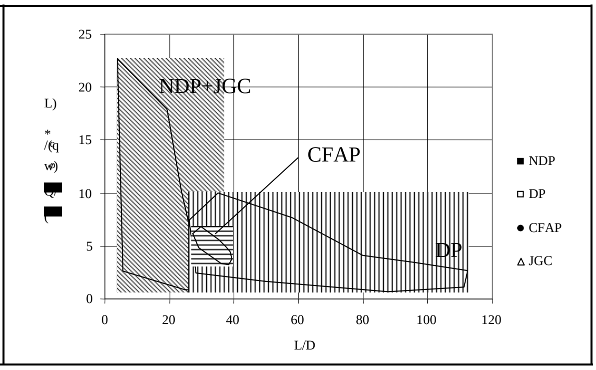

Figure 32: The dimensionless initial stiffness of the pile-soil complex (Source Fig. 7, Modoni et al.).

Reeb and Collin analyse the axial capacity of VCCs from a set of 17 case histories with load test information. VCCs are constructed in a similar way to bottom-feed stone columns but use concrete instead of stone to form the column. There currently exists no generally accepted method for estimating the bearing capacity of VCCs.

Of the total 17 collected VCC load tests, 9 were static load tests and 8 were statnamic tests. The failure load could be interpreted in only 4 of the static tests. Because the strains in the piles were not monitored in any of the static loads tests (clearly due to the difficulty of installing strain gauges in these columns), the shaft resistance and the point resistance could not be separated in those experimental failure loads.

The authors assess the accuracy of the drilled shaft and driven pile design methods for predicting VCC axial capacity. They find that drilled shaft methods generally predict a lower bound of VCC capacity, while driven pile methods generally predict an upper bound. The need for a wider database of load tests on well-instrumented VCCs is clearly stated.

5.3.4. Field projects

Buschmeier et al. describe the ground improvement studies for five large diameter tanks to be constructed along the Mississippi River at a site with up to 30 m of recent soft clay deposits covering stiff clay. A persistent thin sand layer at 21 m was found between an upper soft clay layer with high compressibility and a bottom medium-stiff to stiff, slightly overconsolidated clay layer. Tanks and their supporting platforms apply a maximum soil pressure of 150 kPa at ground level. The proposed design solution used a ground improvement scheme consisting of CMCs associated with a thick load transfer platform to support the tank.

This ground improvement solution is novel because CMCs of varying diameters were installed at two different depths, leading to different coverage area ratios that varied with depth as follows:

- 0.32 m diameter CMCs installed from GL to a depth of roughly 21 m;

- 0.47 m diameter CMCs installed from GL to the top of the very stiff clay up to a 34 m depth.

To demonstrate the validity of the design, an extensive, instrumented full-scale load test was constructed. A total of 30 CMCs were installed under a 180 m^2 area; this area was loaded by building a 6 m by 6 m rectangular box that was nearly 10 m in height, which was subsequently filled with sand (Figure 33). An impressive set of equipment was used to monitor the test for a 3 month period. The test itself was modelled using the same assumptions as the design to validate the parameters and the methodology.

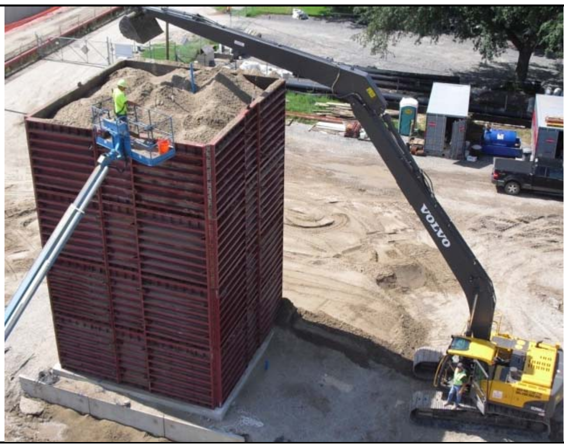

Figure 33: Picture of the construction of the Load Test Area (Form Work) (Source: Fig. 8, Buschmeier et al.).

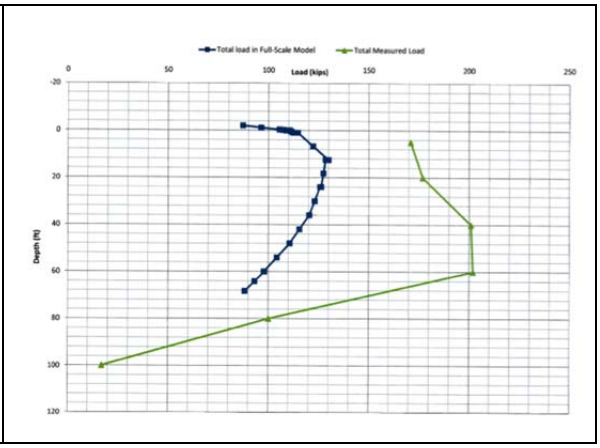

Figure 34: Load profile in CMCs – Actual vs. Model (Source: Fig. 15 Buschmeier et al.).

The monitoring data confirmed the following:

- there was a load transfer mechanism between the upper (denser) treatment zone and the lower treatment zone;
- the maximum settlement measured at the top of the load transfer platform was approximately 11 cm, a value close to the calculated value after a 3 month consolidation;
- differential settlement at the top of the LTP was less than 5 cm despite the fact that no geogrid was installed in the LTP;
- the load transfer mechanism in the LTP was more efficient than what the numerical model predicted, leading to a greater load in the CMCs than what was calculated (Figure 34);
- the profile of the column's axial load was consistent with the accepted understanding of the load transfer mechanism with a neutral point (point of maximum load in the CMC elements) located roughly at the transition between the upper and lower recent clay layers (Figure 34);
- the maximum outward displacement determined by vertical inclinometers was roughly 2.5 cm at the surface, or 25% of the maximum settlement in the test's central area. Note that this lateral displacement-settlement ratio value agrees with other similar values found in the literature (ASIRI 2012, Liu 2007).

The authors attempt to explain why the calculated settlements are in fair agreement with the observations, whereas the calculated axial loads in columns are significantly lower than those measured. This contradicts the common understanding because higher loads in the columns would normally induce smaller incremental vertical stresses in the soil; therefore, smaller settlements should occur in the field than in the model. They argue that the movement of the CMCs themselves is greater in the field than in the model because of the observed additional load in the CMCs. In the reporter's opinion, this point remains open to discussion and certainly calls for a more detailed comparison of the calculated and measured values of the settlements, both in the upper soft clay layer and in the lower soft layer.

By this approach, which combines detailed numerical modelling and full-scale field testing, the validity of the initial design could be proved.

Kirstein and Wittorf describe columnar reinforcement studies on soft plastic clay in Northern Germany. CMCs were used in the transition zone between the pile foundation of a bridge abutment and an access embankment that was 7 m high. All of the studies had to be implemented close to circulated highway lanes. A soft clay layer has a thickness between 13 m and 20 m, a water content that is approximately 100% and an undrained shear strength between 7 kPa (close to abutment) and 20 kPa (further from abutment). A staged construction of the embankment had to be followed to meet the stability conditions,

and vertical drains with spacings as small as 0.55 m were required to accelerate consolidation. Because the CMCs had to be installed partly on the preloading footprint on one side and between the previously built abutment piles on the other side, an adapted phasing of the studies had to be carefully followed. A sand layer that was 1 m thick was first dispersed onto the natural ground to serve as a working platform.
The low c_u values found in the abutment zone raised concern about the integrity of the concrete columns; integrity tests and dynamic pile tests on the first inclusions proved that the columns were not damaged and could carry more than twice their design load. Installation of a column near another recently constructed column could be facilitated through the installation of a vertical drain in the middle space. For a few hours after the CMC installation, water could be observed flowing out of the drains at the working platform surface. The authors note that compared with the other areas where CMCs were installed, both platform heave and concrete over-consumption could be reduced by the additional intermediate drains. Due to the low strength of the ground, the CMCs were designed to carry the full load, neglecting any reaction from the soil. The load transfer platform was reinforced by a steel welded wire mesh embedded in a gravel layer.
Figure 35 shows the settlements that were observed during the year following construction. The settlements are approximately 1 cm above the 6 columns found along the monitored profile and approximately 2 cm elsewhere. These settlements are much smaller than those obtained in the next unreinforced section (130 cm to 140 cm). Therefore, notwithstanding the soft soil conditions encountered at this site, a smooth transition with the piled bridge could be successfully arranged by incorporating vertical drains, CMCs and a steel-reinforced LTP.

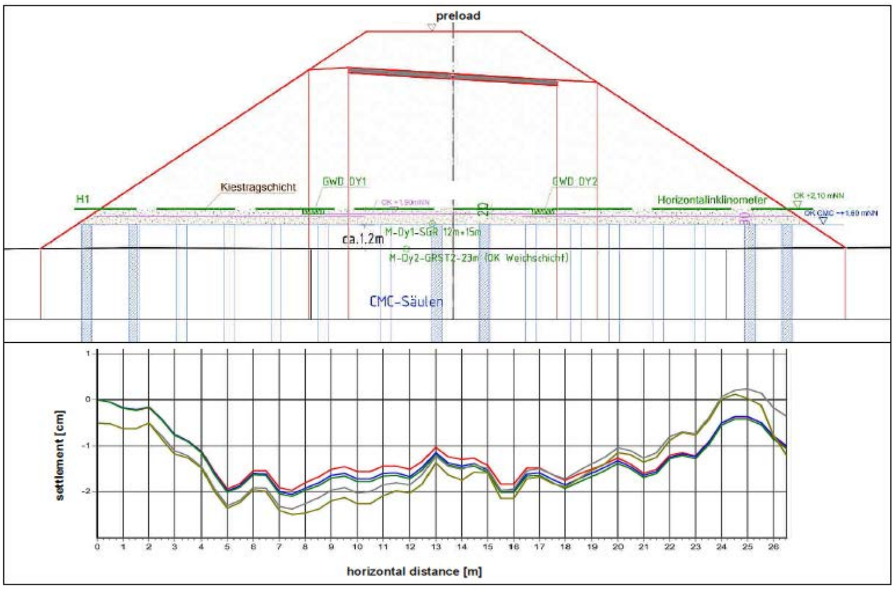

Figure 35: Horizontal inclinometer results showing approximately 1 cm of settlements above the CMCs and 2 cm of settlement elsewhere (Source: Fig. 10, Kirstein and Wittorf).

5.3.5. Loading other than vertical

Sancio et al. present a feasibility study for applying the concept of columnar reinforcement to soils other than soft soils using a different column size than that generally resorted to, involving the use of drilled shafts in very stiff clay to support a mechanically stabilised earth (MSE) wall that is 20 m high to be built in Canada. The MSE wall was to be founded over stiff, heavily overconsolidated clay shale that exhibits pre-sheared sub-horizontal planes that have been mobilised to their residual shear strength. Construction of the MSE wall could potentially lead to global instability due to the sliding surfaces that develop through the weak layers. Drilled shafts, through their shear and bending resistance, could mitigate the risk of sliding along these planes below the MSE wall.
Their numerical study is based on a 2D plane strain finite element analysis. Shear strength parameters as well as site-specific r_u values were assessed from the accumulated experience in constructing and monitoring embankments and dykes at this facility: the shear strength was as low as $\phi = 8°$ and c = 1 kPa in weak layers and $\phi = 20°$ and c = 25-50 kPa in "intact" clay shale. A parametric study was conducted to assess the effect of the following: (a) the number, depth, and thickness of the weak layers within the

shale; (b) the magnitude of the elastic modulus of the shale; and (c) the number, spacing and depth of the drilled shafts. A 1 m shaft diameter was maintained for all of the cases.

The parametric study shows that the wall can be built with a calculated factor of safety of 1.5 or greater and with displacements at the toe of 0.3 m or less. For this case, the MSE wall is to be placed over seven rows that are 1 m in diameter and drilled shafts that are 30 m long distributed in a rectangular pattern, as shown in Figure 36 (spacing in the out-of-plane direction: 3.5 m). The bending moments calculated for a case assuming four weak layers that are 0.5 m in thickness are shown in Figure 37. The drilled shafts act as dowels connecting the “intact” layers and would require between 1% and 2% steel reinforcement.

The parametric study makes a point that may be of interest to the designer: the use of structural elements (“beam elements”) with equivalent moments of inertia and axial stiffnesses instead of volume elements to characterise the columns causes the wall to exhibit deformations that are 32% larger. This finding can be clearly explained if the opposite directions of the forces that are caused by the soil-shaft friction on opposite sides when the shaft rotates are considered: these forces result in a resisting moment, which is ignored if beam elements (with an assumed nil thickness) are used instead of volume elements to represent the shaft’s real thickness.

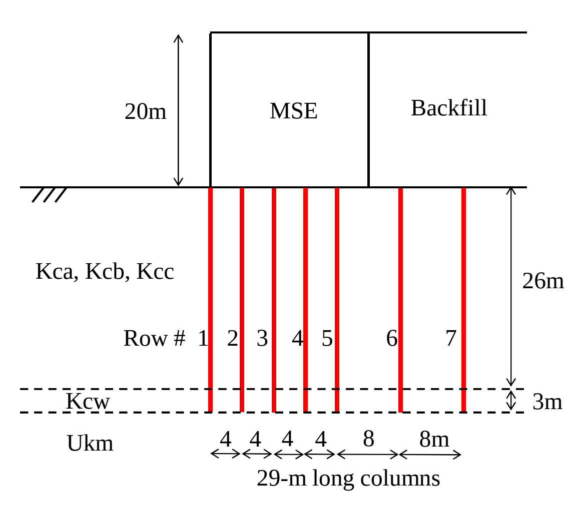

Figure 36: Schematic cross-section layout of the columnar reinforcement (Source: Fig. 3, Sancio et al.).

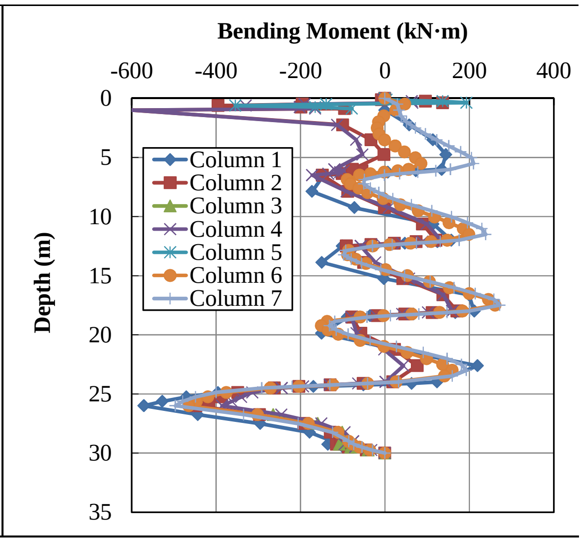

Figure 37: Bending moment diagram of the seven rows of drilled shafts (Source: Fig. 8, Sancio et al.).

Santruckova et al. present results from an experimental study of a group of 4 columns in clay supporting a footing under static and repeated loading. They use 1-g small-scale (1/10) physical tests to compare the behaviour of a group of mixed-modulus inclusion MMCs (rigid inclusions that are extended by stone columns at their tops, bearing the footing) and a group of rigid inclusions with a gravel mattress under the footing. The inclusions are 0.5 m long and have diameters of 16 mm. One of the rigid inclusions is instrumented with 20 level strain gauges to measure the flexural strain to calculate the bending moment along the pile as well as the pile’s displacement or the soil reaction. The clay used is a reconstituted clay with an undrained shear strength of c_u = 18 kPa. A combined vertical V and horizontal H loading is applied to the footing model either statically or dynamically.

A special loading procedure (“swipe test”) is first followed to establish the failure envelope in the V-H domain under static loading. It can be observed in Figure 38 that the failure envelope of the 4-MMC reinforced footing has the same shape as that of the unreinforced case, but it has a size ratio of approximately four.

Similitude requirements are not fulfilled by these 1-g models. One may also question if the reflection on the tank’s sides (2 x 2 m^2) of the waves generated by the dynamic loading of the footing (0.24 x 0.24 m^2) with a frequency of 2.7 Hz may have influenced the footing response. Figure 39 presents the results for a stone column part with a height of 5 cm: the inclusion head reveals reversible displacements during the first few cycles, but irreversible displacements accumulate in one direction after more cycles have occurred, but with some stabilization.

The parametric experimental study shows that MMCs, with shorter stone columns, allow less foundation settlement under dynamic loading. It is also found that by decreasing the stone column height, the bending moment and, therefore, the deflection of the pile head increase.

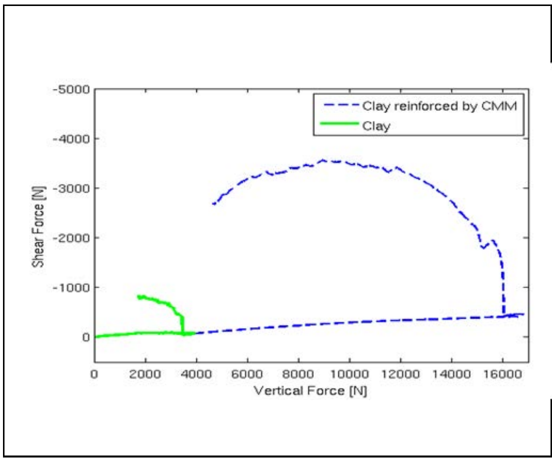

Figure 38: Comparison of the failure envelopes in the V-H domain for CMM reinforced and unreinforced footing (Source: Fig. 3, Santruckova et al.).

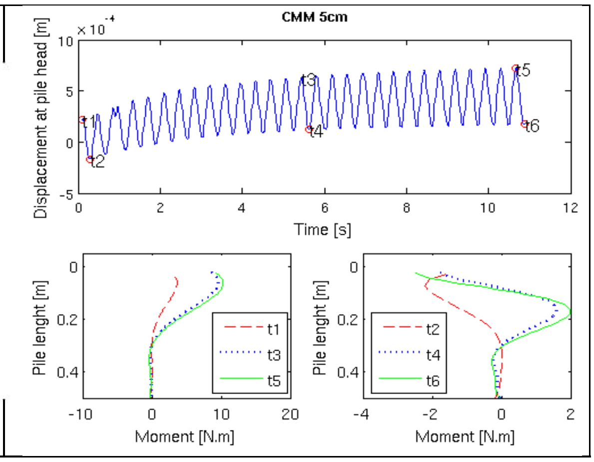

Figure 39: Bending moment along the instrumented inclusion at times t1 to t6 (Source: Fig. 6, Santruckova et al.).

The authors argue that the MMCs tend to dissipate more energy than the rigid inclusion technique. This should be considered with great care in the reporter's opinion: the stone column's behaviour strongly depends on the undrained shear strength of the clay, and while it appears that a constant undrained strength profile was prepared in the tank, it is poorly representative of normally consolidated clays, especially at the surface of the model.

5.3.6. Numerical modelling

Dias et al. present a numerical study of the enlargement of inclusion heads. This study parallels the development of a new installation technique to build a rigid circular concrete column with a reversed cone-shaped head in a single operation. This technique offers an advantage over the commonly installed cylindrical concrete columns that need to be connected to a reinforced concrete cap to obtain the required coverage area ratio. It is thus possible to substitute two separate interventions (completion of the inclusion and installation of the precast concrete cap) for a single operation. A 2D axisymmetric model of a unit cell is used to study the application of this technique to RI ground improvement under an industrial concrete slab.

Frictional interfaces are used between the column and the soil; they are given specific material properties to impose a limiting shear stress value in the interface equal to the limiting shaft friction value that is expected, considering both the soil type and the inclusion installation effects (Bustamante and Frank, 1999).

As a reference case, a 0.35 m column is extended with a reversed conical head with a maximum diameter of 0.8 m and a height of 0.6 m (the square mesh size is 2.5 m). As observed on the plot of the principal stress directions in Figure 40, the load transfer is mainly operated in the LTP volume located between the inclusion head and the corresponding part of the concrete slab. No significant rotation of the principal stress directions is found in this volume (arching effects are thus very limited). The bending resistance of the concrete slab plays a pre-eminent role in this mechanism.

The shape of the reversed conical head impedes the full development of the negative skin friction at the top of the inclusion. The conical headed column results in less settlement reduction than the cylindrical column. Figure 41 presents the maximum values of the slab settlement and the slab bending moment obtained when the conical head diameter is increased from 0.35 m (cylindrical column giving a coverage area ratio of α = 1.5%) to 2 m, representing an area ratio of α = 50%. As expected, the settlement decreases when the head diameter increases. However, the bending moment reaches a maximum value at some intermediate diameter (0.7 m). It is the reporter's opinion that this peak could be accurately explained by considering that at the inclusion head level, the load is shared between the soil (average vertical stress σ_s) and the inclusion (average vertical stress σ_p), and for any assumed angle of shearing resistance of the LTP, the maximum value of the ratio σ_p/σ_s of the material is equal to Prandtl's coefficient N_q (ASIRI, 2012). If both conditions are combined, the bending moment in an equivalent circular plate model with distributed loads equivalent to q, σ_s and σ_p shows a peak value for an intermediate value of the inclusion top diameter.

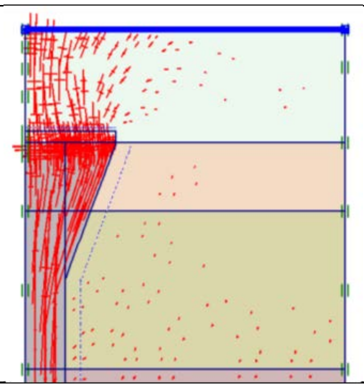

Figure 40: The principal stress distribution between the head of the column and the concrete slab (Source: Fig. 7, Dias et al.).

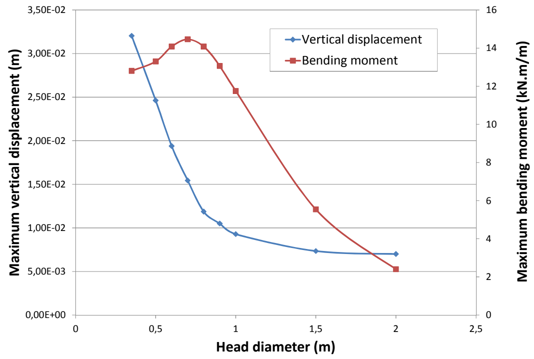

Figure 41: The maximum vertical displacement on the soil and the bending moment on the slab versus the upper head diameter (Source: Fig. 11, Dias et al.).

The comparison of the reversed conical-headed columns with the cylindrical columns shows that the two types of columns have similar behaviours when considering the bending moments in the slab, the stress efficacy or the settlement reduction ratio for a given head diameter. In fact, the cylindrical columns lead to a slightly enhanced stress or settlement efficacy. However, the substantially larger volume of concrete in the cylindrical column significantly counteracts this slight advantage.

Brinkgreve et al. analyse the capacity of embedded pile elements to be used in FE models involving lateral loading conditions. The embedded pile element, which is based on an original study by Sadek and Shahrour (2004), was further developed in the PLAXIS finite element software for the axial loading of foundation piles. The main finding of this study is that piles can be introduced into the FE model through embedded pile elements without altering the global mesh.
Although the embedded pile formulation was not intended to be used under lateral loading conditions, it was assumed that it could have good capabilities under these loading conditions. This theory has been tested by evaluating the stress and displacement patterns around a laterally loaded pile in 3D models and by comparing the results with conventional volume pile models. As an example, Figure 42 shows the results from a study of a pile section that is laterally displaced. The major principal stresses around the pile at failure for the volume pile model are shown on the left, and for the embedded pile model, they are shown on the right. The pattern along the pile’s circumference is very similar. The embedded pile almost behaves as a volume pile. However, the failure load obtained with the embedded pile element was found to be over-estimated. A refined mesh around the pile element enhances the solution. Similar results are observed when obtaining calculations from a pile loaded at its head or from the lateral soil displacement caused by an embankment.

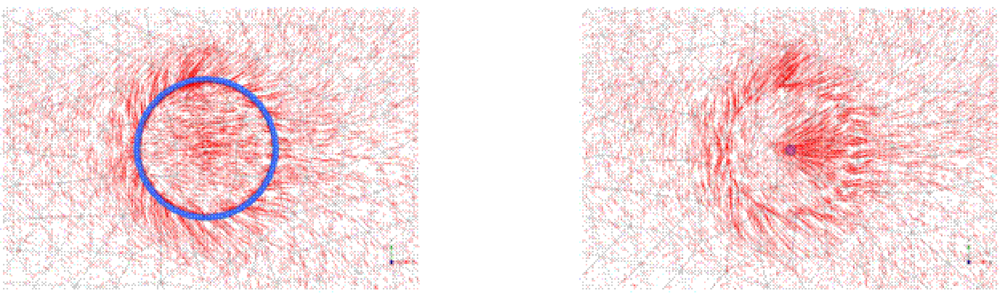

Figure 42: The major principal stresses around the pile at failure. Left: Volume pile; Right: Embedded pile (Source: Fig. 4, Brinkgreve et al.).

Regarding serviceability state calculations (small differential displacements between the pile and the soil), Brinkgreve et al. conclude that the embedded pile behaves quite realistically and similar to a “classical” finite element model in which the pile is modelled using volume elements with or without surrounding interfaces.

In considering ultimate limit state calculations (large differential displacements and failure), the authors conclude that the embedded pile generally over-estimates the lateral loading capacity, at least when it is used in a ‘normal’ way, i.e., without defining a cylinder equal to the elastic zone surrounding the embedded beam. To improve the behaviour of the embedded pile for ultimate limit states, a local refinement surrounding the embedded pile could be applied.
Despite the positive outcome of their research, the authors advise caution when using embedded piles in lateral loading situations.

Because all of the reinforcement solutions that are considered by this session involve placing either a granular layer on top of the columns (LTP) or an embankment fill, they all share the common feature that there is no connection between the columns to any other structural element. The use of the embedded pile element to simulate columnar reinforcement, even under vertical loading, requires an additional specific study in the reporter’s opinion because a point-to-volume interface can currently be included only at the pile tip, and they are also required at the pile head.

Bouassida et al. compare results obtained using dedicated software for the design of foundations on column-reinforced soil (Columns) with those of a 2D plane strain model using the Finite Element Plaxis software. The case under study appears to be virtual and based on a description of studies and soil conditions found in another paper. A road embankment that is 2 m high is to be constructed on a soft clay layer that is 15 m thick with an undrained strength of c_u = 12 kPa. Three treatment solutions are compared: the cement stabilization of soft clay down to a 5-m depth, the substitution of natural ground by compacted sand at the same depth and, last, reinforcement with columns (sand or stabilised soil) with lengths of 7.5 or 8 m. The FE results used for comparison are those presented in the paper used as a reference and concern only solutions in which the soil is replaced at a full 5 m depth. The authors claim that there is a fair agreement between the FE and Columns results. In the researcher’s opinion, this should be further documented because the behaviour of the clay was modelled with the HSM constitutive law for untreated soil case in the FE calculation, while the linear elasticity is used in the dedicated software. In addition, no indication is given about the preconsolidation profile of the soft clay layer and how it was introduced into both calculations.
The authors conclude that columnar reinforcement is a more cost-effective solution than any of the two other solutions because the volume of material in the columns is far smaller than that needed for complete soil replacement at a 5 m depth. More details about the column diameters and the associated material properties would be helpful.

5.3.7. Assessing design risks

Wehr et al. discuss the risks involved in the different ground improvement methods: soil mixing, vibro compaction and vibro stone columns, as well as rigid inclusions. The authors propose to classify these techniques into three categories with increasing risk by considering for each method whether the design is controlled mostly by the serviceability limit states (SLS) (settlement) or by the ultimate limit states (ULS) (failure of the soil or failure of the material).
In Category A, the risks would be limited to larger settlements, indicating that the design is always controlled by the SLS requirements. Wehr et al. consider that all stone columns are included in this category. Because they need to be supported by the surrounding soil, stone columns have no individual failure load. Therefore, they offer great ductility and lead to robust solutions (ability to maintain their function over a wider range of variation in soil parameters and load conditions). This opinion may appear to be schematic because it neglects the fact that stone columns can also fail by bulging.
In Category B, the risks would be extended to the internal failure of the columns and the overall bearing capacity in addition to larger settlements. Wehr et al. consider that lime/cement columns installed with the dry method or by deep soil mixing with the wet method, vibro mortar columns, vibro-concrete columns, and mixed modulus columns would be included in this category. These columns would have the fact that they exhibit plastic deformations when loaded in common, and this is accounted for by the introduction of an increased safety factor against internal failure in their design.
In Category C, the risks would be extended to failure under transverse loading and buckling. Wehr et al. consider that rigid inclusions would be included in this category when their diameters are less than 30 cm. They expose different arguments to validate their point: the bearing capacity of the column or the soil could be suddenly lost, inclusions are most often made out of non-reinforced concrete, and the embedment of an inclusion into the bearing layer is generally small. They add that non-reinforced concrete inclusions may also become damaged over the course of work (for instance, by heavy vehicle traffic after column completion). In their opinion, all of these factors would result in a lack of ductility in the foundation system using rigid inclusions.

Not all of their findings appear to be relevant in the reporter's opinion; in particular, the finding stating that the design load would be close to the failure load due to the development of negative and positive friction along the inclusion and due to a punching failure mechanism of the inclusion head into the load distribution layer (Figure 42). Experimental studies as well as numerical studies that have been conducted by the ASIRI project have shown that the load-displacement curve obtained at top of the load distribution layer smoothly increases with load (the foundation behaviour is ductile). This occurs because at any loading stage, the load is necessarily shared between the inclusion and the soil. The load shared by the soil (at the inclusion head or along the inclusion shaft) enhances the bearing capacity at the head (the punching failure mechanism is self-equilibrating) or at the neutral point (the bearing capacity of bottom part of the inclusion increases with the inclusion's axial load at the same point).

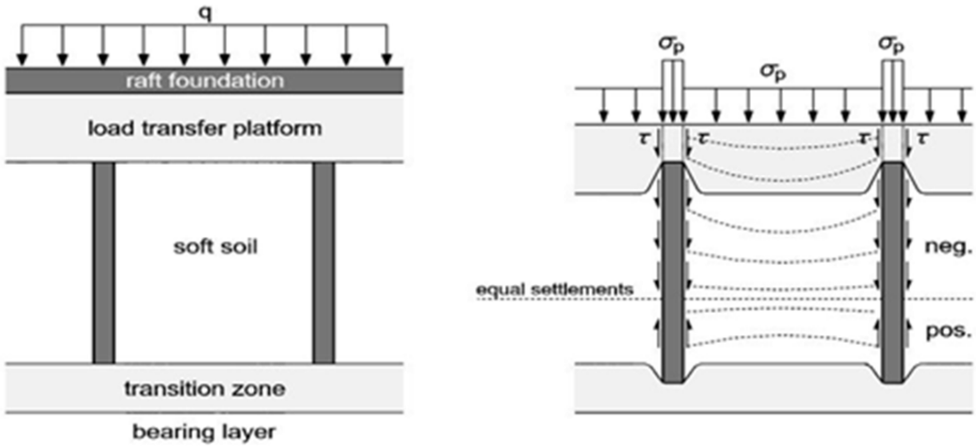

Figure 43: Functioning of the system of Category C (Source: Fig. 2, Wehr et al.).

Wehr et al. present an additional finding related to the column to soil stiffness ratio. According to the German recommendations pertaining to the use of a geosynthetic reinforcement layer in a piled embankment (EBGEO, 2011), the design of a horizontal geosynthetic reinforcement is not necessary if the column/soil stiffness ratio is less than 50, but this design is necessary if this ratio is greater than 75. The authors interpret this ratio value as optimal, stating that any further increase in the column stiffness would be ineffective and would not contribute to the increase in the settlement reduction factor. They recommend decreasing the columns' stiffness in soft soils to obtain a column/soil stiffness ratio that is less than this value. While the reporter agrees with the authors that high stiffness ratio values do not have a greater influence on the settlement efficacy, he underlines that this is true because the system efficacy becomes governed by the load transfer platform (the thickness and shear strength of its material). Limiting the column/soil stiffness ratio is, therefore, not a proper requirement, whereas imposing a suitable quality transfer layer is an appropriate requirement.
Finally Wehr et al. express their approval of the design philosophy adopted by ASIRI Recommendations (2012) to comply with the general framework of the Eurocodes.

6. CONCLUSION

A total of 26 papers (totalling 250 pages) have been collected in Session 6 regarding ground improvement using columns: half of them address the subject of stone columns and the other half relate to rigid inclusions. They present an up-to-date picture of the flourishing development of these techniques and also of the efforts that have been made in the meantime to obtain a better understanding of the complex interactions between the columns and the ground. These efforts include full-scale testing and small-scale testing as well as numerical modelling. This general report has attempted to place all of these actions into one general view of the main points that require further investigation for both of these techniques. Several papers propose interesting data, especially relating to full-scale tests that can be of great use to calibrate present calculation models, to elaborate new design guidelines or simply to update existing ones. Several other papers may also contribute to consolidating our global comprehension of the behaviour of a column-reinforced ground under wide spread loads as well as under small groups.

7. ACKNOWLEDGEMENT

The comments made by my colleagues, A. Guilloux and V. Bernhardt from Terrasol and L. Briançon from CNAM Paris, are gratefully appreciated. All the drawings used here which were not taken in the reviewed papers are original drawings by M. Anic-Antic.

REFERENCES

Papers in the Proceedings of Session 5: IS- GI Brussels, 2012

Aljorany,A.N., 2012, Modelling and analysis of the pullout behaviour of granular pile anchor in expansive soils.

Alonso, J.A., Jimenez, R., 2012, Reliability-based design of stone columns for ground improvement considering settlement and bulging as failure modes.

Al-Saoudi, N.K.S., Mahmoud, M.R., Rahil, F.H., Abbawi, Z.W.S., 2012, Ordinary and encased stone columns under repeated loading.

Bouassida, M., Hazzar, L., Mejri, A., 2012, Assessment of software for the design of columnar reinforced soil.

Brinkgreve, R.B.J., Engin, E., Dao, T., 2012, Possibilities and limitations of embedded pile elements for lateral loading.

Buschmeier, B., Masse, F., Swift, S., Walker, M., 2012, Full scale instrumented load test for support of oil tanks on deep soft clay deposits in Louisiana using Controlled Modulus Columns.

Cañizal, J., Castro, J., Cimentada, A., Da Costa, A., Miranda, M., Sagaseta, C., 2012, Theoretical analyses of laboratory tests of kaolin clay improved with stone columns.

Castro, J., Kamrat-Pietraszewska, D., Karstunen, M., 2012, Numerical modelling of stone column installation in Bothkennar clay.

Dias, D., Grippon, J., Nunez, M., 2012, Behaviour of a Pile-Supported Embankment using rigid inclusions with variable inertia.

Dias, D., Simon, B., 2012, Spread foundations on rigid inclusions subjected to complex loading: Comparison of 3D numerical and simplified analytical modelling.

Eekelen, S.J.M. van, Bezuijen, A., 2012, Basal reinforced piled embankments in the Netherlands, field studies and laboratory tests.

El Mahallawy N.A.H., 2012, Improvement of soft soils using reinforced sand over stone columns.

Gautray, J.N.F., Springman, S.M., 2012, Determination of pore size distribution to identify plastic zones around stone columns.

Kelly, P., Black, J.A., 2012, Optimisation of stone column design using transparent soil and particle image velocimetry (PIV).

Kirstein, J.F., Ahner, C., Uhlemann, S., Uhlich, P., 2012, Ground improvement methods for establishment of the federal road B 176 on a new elevated dump in the brown coal area of MIBRAG.

Kirstein, J., Wittorf, N., 2012, Rigid inclusions in combination with fast wick drain consolidation as soil improvement method in very soft and fat northern German clay.

McGuire, M., Sloan, J., Collin, J., Filz, G., 2012, Critical height of column-supported embankments from bench-scale and field-scale tests.

Modoni, G., Bzowka, J., Juzwa, A., Mandolini, A., Valentino, F., 2012, Load-settlement responses of columnar foundation reinforcements.

Özkeskin, ç, Erol, O., Çekinmez, Z., 2012, Settlement reduction and stress concentration factors in rammed aggregate piers determined from full- scale group load tests.

Reeb, A.B., Collin, J.G.,2012, Axial Capacity of Vibro-Concrete Columns.

Sancio, R., Safaqah, O., Wong, P., Li, C., Sabatini, P., Villet, B., 2012, A study on the use of drilled shafts to reinforce stiff clay with very weak sliding planes.

Santruckova, H., Foray, P., Grange, S., Cofone, A., Lambert, S., Gotteland, P., Wehr, J., 2012, Behaviour of a shallow foundation on soil reinforced by Mixed Module Columns® – Experimental study.

Tekin, M., Ergun, M.U., 2012, A model study on settlement behaviour of granular columns in clay under compression loading.

Verstraelen, J., Lejeune, C., De Clercq, E., 2012, Realisation of integrated steep landscape slopes within existing railway embankments.

Wehr, J., Topolnicki, M., Sondermann, W., 2012, Design risks of ground improvement methods including rigid inclusions.

Yeo, K.C., Yung, S.H., Liu, S.J., 2012, Stone column and vibro-compaction of soil improvement for liquefaction.

Additional references

ASIRI, 2012, Amélioration des sols par inclusions rigides, (with English translation on CD: Rigid Inclusions Ground Improvement) /Presses des Ponts/ISBN 978-2-85978-462-1.

Auvinet, G. & Rodriguez, J.F., 2006, Rigid inclusions in Mexico City soft soils: history and perspectives, Symposium Rigid inclusions in difficult subsoil conditions /ISSMGE TC36 /UNAM.

Briançon, L. 2002, Renforcement des sols par inclusions rigides – Etat de l'Art en France et à l'Etranger, (in french) / Paris/ IREX.

Briançon L. & Simon B., 2010, Full-scale experiments of pile-supported earth platform under a concrete floor slab and an embankment. Symposium: New techniques for Design and Construction on soft Clays, Garuja, Brasil .

Briançon, L. & Simon, B., 2012, Performance of a pile-supported embankment over soft soil: Full scale experiment, accepted for publication, Journal of Geotechnical and Geoenvironmental Engineering/ASCE.

BS8006 ,2010, Code of Practice for Strengthened/reinforced soils and other fills, Section 8, Design of embankments with reinforced soil foundations on poor ground.

Bustamante, M. Frank, R., 1999, Current French design practice for axially loaded piles /Ground Engineering /March, pp. 38 – 44.

Castro, J. (2008). "Análisis teórico de la consolidación y deformación alrededor de columnas de grava". Doctoral Thesis. University of Cantabria, Spain (in Spanish).

Castro, J. & Sagaseta, C., 2009, Consolidation around stone columns. Influence of column deformation. Int. Journal for Numerical and Analytical Methods in Geomechanics, 33 pp. 851-877.

Chen, R.P. Chen, Y.M. Han, J. & Xu, Z.Z. 2008. A theoretical solution for pile-supported embankments on soft soils under one-dimensional compression, Canadian Geotechnical Journal 45 pp. 611-623.

Chevalier, B., Villard, P.& Combe, G. ,2011, Investigation of load transfer mechanisms in geotechnical earth structures with thin fill platforms reinforced by rigid inclusions. International Journal of Geomechanics, Vol. 11, N° 3, June, pp. 239-250.

Chu, J., Varaksin, S., Klotz, U. & Mengé, P., 2009, State of the Art Report, Construction Processes, TC17, 17th ICSMGE, Alexandria.

Combarieu, O., 1974, Effet d'accrochage et méthode d'évaluation du frottement négatif. Bulletin de Liaison des Laboratoires des Ponts et Chaussées n°71 (mai-juin), pp. 93 à 107.

Combarieu, O., 1988 , Amélioration des sols par inclusions rigides verticales. Application à l'édification des remblais sur sols médiocres. Revue française de Géotechnique n°44, pp. 57 à 79.

Cuira, F. & Simon, B. , 2009, Two simple tools for evaluating the complex interactions in a soil reinforced by rigid inclusions.(in French). 17th ICSMGE, Alexandria, pp. 1163-1166.

CUR 226, 2010, Ontwerprichtlijn paalmatrassystemen (Design guideline piled embankments). ISBN 978-90-376-0518-1 (in Dutch).

De Buhan, P. & Sudret, B., 2000, Micropolar multiphase model for materials reinforced by linear inclusions. European Journal of Mechanics. A/Solids, Vol. 19, 669-687.

Demerdash, M. A. 1996, An experimental study of piled embankments incorporating geosynthetic basal reinforcement. Doctoral Dissertation /University of Newcastle-Upon-Tyne /Department of Civil Engineering.

DGGT, 2002, Deutsche Gesellschaft für Geotechnik e.V., Merkblatt für die Herstellung, Bemessung und Qualitätssicherung von Stabilisierungssäulen zur Untergrundverbesserung, Teil 1- CSV-Verfahren.

EBGEO, 2010, Reinforced earth Structures over Point or Linear Bearing Elements. In Recommendations for Design and analysis of Earth Structures using Geosynthetic Reinforcements (Translation of the 2nd German edition)/Ernst and Sohn/ DGGT.

Eekelen, S.J.M. van, Bezuijen, A. Duijnen, P. van & Jansen, H. L. 2009, Piled embankments using geosynthetic reinforcement in the Netherlands: design, monitoring & evaluation. 17th ICSMGE, Alexandria, pp. 1690-1693.

EN 1997-1, 2004, Eurocode 7: Geotechnical design – Part 1: general rules. European committee for Standardization.

Fioravante, V., 2011, Load transfer from a raft to a pile with an interposed layer, Geotechnique 61, N°2 pp. 121-132.

Garnier J. & Pecker A., 1999,. Use of centrifuge tests for the validation of innovative concepts in foundation engineering, 2nd Int. Conference on Earthquake geotechnical Engineering, Lisbon, 7p.

Garnier J., Gaudin C., Springman S.M., Culligan P.J., Goodings D., Konig D., Kutter B., Phillips R., Randolph M. F. & Thorel L., XXXX Catalogue of scaling laws and similitude questions in geotechnical centrifuge modelling, INT. J. Physical Modelling in Geotechnics, ISSN 1346-213X, Vol 17, n° 3, pp 1-24.

Hassen, G., 2006, Modélisation multiphasique pour le calcul des ouvrages renforcés par inclusions rigides, Thèse de l'Ecole Nationale des Ponts et Chaussées, Paris (in french).

Hassen, G. & De Buhan, P., 2005, A two-phase model and related numerical tool for the design of soil-structures reinforced by stiff linear inclusions. European Journal of Mechanics A/Solids, 24 987-1001.

Hausler, E.A. & Koeling, M., 2004, Performance of improved ground during the 2001 Nisqually earthquake, 5th Int. Conf. on Case Histories in Geot. Engineering, New York.

Hewlett, W.J. & Randolph, M.A.,1988, Analysis of piled embankments. Ground Engineering, April pp. 12-18.

Jamiolkowski, M. Ricceri & G. Simonini, P., 2009, Safeguarding Venice from high tides: site characterization and geotechnical problems, 17th ICSMGE, Alexandria, pp. 3209-3227.

Lodder, H.J., Van Eekelen, S.J.M. and Bezuijen, A., 2012, The influence of subsoil reaction on the geosynthetic reinforcement in piled embankments., to be published in the Proceedings of EuroGeo 2012, Valencia in Spain.

Liu, H.L., Ng, C.W.W, Fei, K., 2007, Performance of a Geogrid-Reinforced and Pile Supported highway embankment over soft clay: case study, J. Geotech. Geoenviron. Eng. 133, n° 12, pp. 1483-1493.

Magnan J. P., Droniuc N., Canepa Y. & Dhouib, A., 2009, Réflexions sur la conception des colonnes ballastées, 17th ICSMGE, Alexandria , pp. 1377- 1380.

Martin J. R. Olgun C. G., Mitchell J. K. Durgunoglu H. T. & Emrem, C., 2004, Preliminary findings from an Investigation of improved Ground performance during The 1999 Turkey Earthquakes, XXXX.

Mitchell, J. K., 1981, Soil improvement: State of the Art report, 10th ICSMGE, pp. 509-565.

Mitchell, J. K. & Wentz, J. R., 1991, Performance of improved ground during Loma Prieta earthquake, Report N° UCB/EERC-91-12, Earthquake Engineering Research Center, University of California, Berkeley.

Nordic Handbook, 2005, Guidelines for reinforced soils and fills, Nordic geosynthetic group, rev. B.

Okyay, U. S., Dias, D. , Thorel, L. & Rault, G., 2012, Centrifuge modeling of a pile-supported granular earth-platform over soft soils, submitted for publication in ASCE, Journal of Geotechnical and Geoenvironmental Engineering.

O'Riordan N. J. & Seaman J. W., 1994, Highway embankments over soft compressible alluvial deposits : guidelines for design and construction, Transport Research Laboratory, Contractor report 341.

Pecker, A., 2004, Design and construction of the Rion Antirion bridge. Proc. ASCE Geo-Trans 2004 on Geotechnical Aspects of Transportation Engineering.

Priebe, H., 1995, The design of vibro replacement, Ground engineering, Dec.

Priebe, H., 1998, Vibro replacement to prevent earthquake induced liquefaction, Ground engineering, Sept.

Raithel M., Kirchner A., Schade C.& Leusink E., 2005. Foundations of constructions on very soft soils with geotextile encased columns. State of the Art, ASCE Conference Geo-Frontiers, Austin, USA, pp. 923-946.

Rao, A.S., Phanikumar, B.R., Babu, R.D. and Suresh, K., 2007, Pullout Behavior of Granular Pile-Anchors in Expansive Clay Beds In Situ, J. Geotech. Geoenviron. Eng. 133, 133:5(531).

Rathmeyer, H.,1975, Piled embankment supported by single pile caps. ISSMFE Conference, Istanbul, Vol. 1, 283-290.

Sadek, M., Shahrour, I. , 2004, A three-dimensional embedded beam element for reinforced geomaterials. Int. J. Num. Anal. Meth. Geomech. 28, 931-946.

Sagaseta, C. (2006). "Avances en el diseño de las técnicas de mejora del terreno". Technical Seminars SEMSIG-AETESS 6ª. Técnicas de Meroja del Terreno.(in Spanish).

Seed, H.B. & Booker, J.R. 1977 Stabilisation of potentially liquefiable sand deposits using gravel drains. ASCE GT Journal n° 7, pp. 201-255 .

Simon B. & Schlosser F., 2006, Soil reinforcement by vertical stiff inclusions in France. Symposium Rigid inclusions in difficult subsoil conditions /ISSMGE TC36/UNAM.

Slocombe B. C., Bell A. L &, Baez J. I., 2000, The densification of granular soils using vibro methods, Geotechnique 50 , n° 6, pp 715-725.

Sondermann W. & Wehr J., 2004, Deep vibro techniques, in Ground Improvement, 2nd edition /Edit. Mosley M. P. and Kirsch K /Spon Press pp. 57-92.

Sudret, B.& De Buhan, P., 2001. Multiphase model for inclusion-reinforced geostructures. Application to rock-bolted tunnels and piled raft foundations. International Journal for Numerical and analytical Methods in Geomechanics, Vol. 25, 155-182.

Schweiger, H. F., 2008, Overview of Design Concepts of Ground Improvement Techniques in TC17 Website: www.bbri.be/go/tc17.

Vogler U. & Karstunen M., 2007, Numerical modelling of deep mixed columns with volume averaging technique, NUMOG X.

Youd et al., 2001, Liquefaction resistance of soils: Summary report from the 1996 NCEER and 1998 NCEER/NSF workshops, Journal of Geotechnical and Geoenvironmental Engineering, 127, 817-833.

Zaekse, D. & Kempfert, H. –G., 2002, Berechnung und Wirkungsweise von unbewehrten und bewehrten mineralschen Tragschichten über punkt- und linienförmingen Traggliedern. Bauingenieur, vol. 77, 80-86.

SESSION 6 – SOIL REINFORCEMENT IN FILL AND IN CUT

General Report
SESSION 6 – SOIL REINFORCEMENT IN FILL AND IN CUT

John Sankey, *The Reinforced Earth Company, USA*
H. Turan Durgunoglu, *Zetas Zemin Teknolojisi*

1 INTRODUCTION

For the technical session on Soil Reinforcement, there were 15 papers submitted. The papers cover a wide variety of topics dealing with soil additives, reinforcements of foundations and reinforced slopes and retaining walls. For the purposes of this overview, the papers were divided into the following categories:
- Additive Soil Strengthening
- Foundation Reinforcement
- Reinforced Slopes and Walls

2 OVERVIEW OF THE PAPERS

2.1 Additive Soil Strengthening

The following papers address the addition of gel or fibers to strengthen and reinforce soils:

A paper prepared by N.K. Vasiliev et al. discusses the introduction of cryotropic gels, primarily those based on polyvinyl alcohol (PVA), to provide soil strengthening. The application has practical implications in frozen soils and thawing soils to enhance strength, durability, elasticity, heat insulation and reduce permeability. Proven soil applications have been developed for quays, docks, dams and cells to control wastes in frozen areas. The method is relatively recent and requires further research to develop procedures for use in practice.

Two papers address fiber-reinforced soils. In the paper by Flora and Lirer, considerations are reported on the shear strength gain of fiber reinforced soils. The relevance of 'scale effects' on the shear strength is addressed with a simple expression of the failure envelope and an additional expression to account for the effects of non-linear anisotropy due to the placement and compaction of soil with fibers. A separate paper by Ekinci and Ferraeira addresses procedures related to compaction of fiber-reinforced clay samples prepared and tested in the laboratory by undrained triaxial and oedometer methods. The undrained shearing behavior of fiber-reinforced soils is compared to non-reinforced soils. Conclusions are drawn on fiber alignment caused by compaction method in preparing samples for testing

2.2 Foundation Reinforcement

Reinforcement applications are presented for both shallow footings and deep foundations in four papers. The single paper addressing reinforcement of soils supporting rectangular footings is authored by C. Gel et al. Cohesionless soils reinforced by geogrids are examined for footings with results showing the efficiency of the reinforcement increases with larger foundation length to width ratios. Numerical and experimental results are presented with positive correlation based on number of reinforcement layers and relative density as a function of footing shape.

The paper prepared by D. Alexiew et al. describes a 15 year overview of geotextile encased columns (GEC). The application of GEC can be performed even in extremely soft soils with long-term behavior that can now be accurately predicted subject to usual tolerances. The advantages of GEC are demonstrated by both computational and direct measurement in the paper.

Micropile reinforcement for reinforcement of existing foundations is addressed in a study presented by Bazaz and Jalilan. Their paper discusses a load test study that was performed on 6 mm and 200 mm diameter micropiles. The micropile testing resulted in development of an R Index, which accounts for a term addressed in the paper as a "Network Effect Index". An increase in the R Index and corresponding capacity was found with both increasing number of micropiles and decrease in inclination.

Drilled shaft stabilization of slopes in expansive soils is evaluated in the paper prepared by R. Kannan. Failures along long slopes, such as levees in Texas and other portions of the USA, appear to occur when fully-softened shear strength is reached rather than at residual strength. Drilled shafts placed unintentionally in repaired slopes appear to be a viable option to prevent such failures. Further research measures are recommended to evaluate drilled shaft performance and its use as a stabilization basis in designing new slopes.

2.3 Reinforced Slopes and Walls

The remaining papers in this session describe either reinforced slopes or anchored wall systems. In the paper prepared by L.F. Lopez-Tello et al., the effect of vegetation on reinforcement of slopes is evaluated by comparing climate information, soil conditions and geometric configuration. Shear strength assignments and resulting slide analyses show positive correlation between the soil and its moisture condition for promoting stability with the magnitude of vegetation development. A separate slope-related paper by Verstraelen et al. combines soil reinforcement techniques intended to enlarge and "green" embankments while maintaining active railway service. The reinforcement technologies cited in the paper incorporate different combinations of cemented backfill, high tenacity geogrids, grouted anchors, soil nails and shaft foundations. Advantages and disadvantages of the embankment combinations are described.

For the six papers associated with reinforced wall systems, there are two papers that discuss shored (steel) reinforced earth wall systems in the USA. The first of the papers prepared by J. Sankey and S. Rafalko addresses the technology as a means to use Mechanically Stabilized Earth (MSE) in locations where terrain limits the width to height aspect ratio to less than 0.7. Typically, the limited width MSE section is directly anchored to either an existing wall face or to a soil nail anchor system; however, overlapping of steel reinforcements between the front and back faces is a recent update to the technology that provides better construction flexibility. The paper presents case studies on three projects that represent the range of the technology. The second paper prepared by K. Truong et al. further explains the shored MSE wall system and its expected performance in high seismic areas. Numerical modeling is provided with positive outcome to compare the type of connection, backfill and foundation quality and the intensity and duration of earthquake for limited width to height aspect ratios of 0.3 to 0.4.

The interaction of geosynthetics and backfill are examined in two other papers that address mechanically stabilized wall (MSE) systems. In the first paper by D.M. Carlos et al., numerical modeling is used to show the build up and dissipation of pore pressures during construction of the MSE wall when using fine grained and poorly draining silts in combination with geosynthetics. The use of numerical modeling is shown as an effective tool for both analysis and planning construction in such applications. L. Ruiz-Tagle and F. Villalobos present a paper that is based on a laboratory and numerical study of a geogrid-reinforced MSE wall. The laboratory portion of the paper presents information obtained from use of Particle Image Velocimetry to show particle displacement and rotation for soil in both non-reinforced and geogrid-reinforced applications. Lab results indicate that geogrids reduce twice the volume of yielded soil and follow up numerical analyses further examine this relationship within the context of horizontal displacement in a MSE wall application.

The last two papers in the category on reinforced walls examine directly anchored soil reinforcement systems. Y. Miyata et al. presents an experimental study performed on three multi-anchored walls of 6 m height. The walls were flooded and drained with anchor pullout testing performed. Results showed that the porous nature of the wall fascia with geotextiles covering the joints prevented problems with hydrostatic pressures. In addition, pullout capacity as expected decreased with a corresponding decrease in backfill quality. The other paper by Maekelberg et al. provided a case study on a rail enlargement project in Belgium. The bases of slopes prone to landslides were evaluated for stability by use of soil nailing, tieback anchors and secant walls. A comprehensive field and laboratory study was used to accompany numerical analyses in design of the complex system of proposed reinforcements. The analytic model will be calibrated in the future on the basis of a planned instrumentation study to accompany the construction.

REFERENCE

Alexiew, D., Raithel, M., Bau-Aktiengesellschaft, J.M., Detert, O. (2012). "15 years of experience with geotextile encased granular columns as foundation system." *Proceedings of IS-GI Brussels 2012, Brussels, Belgium.*

Bazaz , J.B., Jalilan, H. (2012). "Capacity of foundations reinforced with micropiles." *Proceedings of IS-GI Brussels 2012, Brussels, Belgium.*

Carlos, D. M., Pinho-Lopes, M., Lopes, M. L. (2012). "Numerical analysis of walls constituted by fine soil reinforced with geosynthetics." *Proceedings of IS-GI Brussels 2012, Brussels, Belgium.*

Ekinci, A., Ferreira, P.M.V. (2012). "The undrained mechanical behaviour of a fibre-reinforced heavily over-consolidated clay." *Proceedings of IS-GI Brussels 2012, Brussels, Belgium.*
Flora, A., Lirer, S. (2012). "A simple expression of the shear strength of anisotropic fibre-reinforced soils." *Proceedings of IS-GI Brussels 2012, Brussels, Belgium.*

Gel, C., Akbas, S.O., Anil, O. (2012). "Comparison of the performance of rectangular footings on cohesionless soils reinforced with geogrid and geotextile." *Proceedings of IS-GI Brussels 2012, Brussels, Belgium.*

Kannan, R.C. (2012). "Drilled shafts for slope stabilization in expansive soils." *Proceedings of IS-GI Brussels 2012, Brussels, Belgium.*

López-Tello, L.F., Santa-María, C.F. (2012). "Soil reinforcement vegetation effect - an analysis applied to the earth moving volume of California high speed railway system." *Proceedings of IS-GI Brussels 2012, Brussels, Belgium.*

Maekelberg, W., Verstraelen, J., De Clercq, E. (2012). "Realization of a railway enlargement in unstable excavations alongside the existing line at Dilbeek (Belgium)." *Proceedings of IS-GI Brussels 2012, Brussels, Belgium.*

Miyata, Y., Bathurst, R. J., Konami, T., Dobashi, K. (2012). "Performance of multi-anchor walls under cyclic transient flooding." *Proceedings of IS-GI Brussels 2012, Brussels, Belgium.*

Ruiz-Tagle, L., Villalobos, F. (2012). "Laboratory study of displacements in a geogrid reinforced soil model under lateral earth pressures." *Proceedings of IS-GI Brussels 2012, Brussels, Belgium.*

Sankey, J.E., Rafalko, S. (2012) "Case studies on application of sandwich connection design for shored reinforced earth walls." *Proceedings of IS-GI Brussels 2012, Brussels, Belgium.*

Truong, K., Sankey, J., Sullivan, J. (2012). "Study of Shored MSE walls (SMSE) in high earthquake." *Proceedings of IS-GI Brussels 2012, Brussels, Belgium.*

Vasiliev N. K., Ivanov A.A., Sokurov V.V., Shatalina I.N. (2012). "Ice-Soil Composites Created by Method of Cryotropic Gel Formation: A preliminary report of direct shear and permeability tests." *Proceedings of IS-GI Brussels 2012, Brussels, Belgium.*

Verstraelen, J., De Clercq, E. (2012). "Realisation of integrated steep landscape slopes within existing railway embankments." *Proceedings of IS-GI Brussels 2012, Brussels, Belgium.*

SESSION 7 – BIOGROUT & OTHER GROUTING METHODS

General report
SESSION 7 – BIOGROUT & OTHER GROUTING METHODS

Jian Chu, Nanyang Technological University, Singapore, and presently Iowa State University, USA, jchu@iastate.edu.sg

ABSTRACT

In this report, the classification of ground improvement methods with grouting type of admixtures proposed by Chu et al. (2009a) is introduced. Modification to this classification is also made to include biogrouting as a new subcategory. A summary of the main points of the papers submitted to Session 7 of this conference on grouting methods is presented. An overview of the new subcategory, the biogouting method, is made. The advantages of biogrouting, the recent developments in the study of biogrouting and its potential engineering applications are also discussed.

1. INTRODUCTION

This general report is organized into 3 sections. A general introduction to the classification of ground improvement with grouting type of admixtures is given in Section 1. A review and summary of the papers submitted to this session is made in Section 2. An overview on the recent developments in a new type of grouting, the biogrouting, is presented in Section 3.

According to the classification adopted by TC211, ground improvement can be classified into five categories: A. Ground improvement without admixtures in non-cohesive soils or fill materials; B. Ground improvement without admixtures in cohesive soils; C. Ground improvement with admixtures or inclusions; D. Ground improvement with grouting type admixtures; and E. Earth reinforcement. The topics of this session fall into Category D. Within this category, a further classification of Category D into 6 sub-categories was proposed by Chu et al. (2009a) as shown in Table 1.

Table 1: Classification of ground improvement methods with grouting type of admixtures

Method	Principle
D1. Particulate grouting	Grout granular soil or cavities or fissures in soil or rock by injecting cement or other particulate grouts to either increase the strength or reduce the permeability of soil or ground.
D2. Chemical grouting	Solutions of two or more chemicals react in soil pores to form a gel or a solid precipitate to either increase the strength or reduce the permeability of soil or ground.
D3. Mixing methods (including premixing or deep mixing)	Treat the weak soil by mixing it with cement, lime, or other binders in-situ using a mixing machine or before placement
D4. Jet grouting	High speed jets at depth erode the soil and inject grout to form columns or panels
D5. Compaction grouting	Very stiff, mortar-like grout is injected into discrete soil zones and remains in a homogenous mass so as to densify loose soil or lift settled ground.
D6. Compensation grouting	Medium to high viscosity particulate suspensions is injected into the ground between a subsurface excavation and a structure in order to negate or reduce settlement of the structure due to ongoing excavation.
D7. Biogrouting	Use of microbial activities or products to reduce the permeability and/or increase the shear strength of soil.

In the past several years, some major progresses have been made in the development of a new technology, the so-called biogrouting. This technology is based on the use of microbial activities or products to grout soil so as to reduce the permeability and increase the shear strength of soil. Although the research has been focused on the use of this method for sandy soil so far, studies to apply it to clayey soil have also been made. This new approach possesses many advantages over the existing methods as discussed later.

Biogrouting may be one of the major developments in ground improvement in this decade. It is anticipated that this approach will eventually becomes a viable method for various engineering applications. As such, it is suggested to include a new subcategory, D7 Biogrouting, into the classification system shown in Table 1. More discussion on biogrouting will be made in Section 3.

2. REVIEW OF PAPERS SUBMITTED TO THIS SESSION

There are 16 papers submitted to this session. A list of the papers is given in Table 2. The grouting methods covered and the main topics and approaches of the papers are summarized in Table 3. Among the 16 papers, there are 10 on jet grouting, 2 on compensation grouting, 2 on cement grouting, 1 on grouting using chemical modified bentonite, and 1 on compaction grouting. In terms of approaches, there are 7 papers dealing with case histories, 6 numerical, 4 laboratory and 1 monitoring. The following review will be presented in terms of grouting methods.

2.1 Jet Grouting

It is not surprising that jet grouting is the most discussed method in this session because the jet grouting method has been increasingly used for very difficult ground conditions. Jet grouting is a method involving drilling down with a small diameter rod system, typically 90-130 mm in diameter and then injecting a high pressure fluid while rotating and withdrawing the rod to erode soil and replace or mix it with cement grout under a high pressure (~ 200 bars) to form a circular cement column of typically 1 to 1.6 m. The Jet grouting installation methods include single, double and triple methods with the triple tube being the most effective technique. As a semi- or complete replacement method, jet grouting in theory is applicable to all types of soil. Another advantage of jet grouting is that it can be used for any specific areas in the form columns or slabs or any other shapes or at any depths. This explains why the applications of jet grouting have been so diversified. There is reflected by the number of case histories papers on the use of jet grouting. Among the 10 papers on jet grouting in this session, 8 are on case histories. Jet grouting is also the method that has undergone a number of modifications and expansions as described by Chu et al. (2009a). These include superjet grouting (Burke et al., 2000), X-jet grouting (Welsh and Burke, 2000), Rasjet methods (Osborne and Ng, 2008). Some of those methods can be used to create large diameter columns. It is claimed that the superjet method can create 5 m diameter columns with strength of 6 times stronger that those of normal jet grouting columns (Hashimoto and Liu, 2011). Standards for jet grouting including BS EN12716 (2001) - Execution of Special Geotechnical Work –Jet Grouting have been established.

An interesting case history of using jet grouting for a residential project on Jaude maar, an ancient volcanic sediment in France, was presented in Paper #2 by Berthelot et al. (see Table 2). Secant jet grouting columns for excavation and load-transfer jet grouting columns for the support of a raft were used. An interesting feature of this application is the variation of the diameter (from 1.2 to 1.9 m) of the jet grouting columns to suit the ground conditions. A number of methods including a feed of pantograph type, the release of the columns head, and a geophysical method with an electric cylinder to measure the diameter of the jet grouting columns was reviewed. This is important for quality control particularly when different diameters were used. The static penetration test (CPT, I guess?) in the column before setting was identified to be a better method. It would be better if more detail could be given on how the penetration test was used for this purpose.

A good case history for using jet grouting to create large diameter columns (3.5 m) for arrival of shield tunneling machine was presented in Paper #3 by Cheng et al. The challenging parts of this project were that the jet grouting layer needed to be installed into a silty clay layer below a drainage culvert and the construction had to be carried out along a congested street. Large diameter jet grouting columns were used to reduce the number of grouting holes. A double-tube grouting system with two nozzles on the opposite side of the monitor was used. Air and jet stream was also used to cut and mix the in-situ soil with grout. A larger nozzle diameter of 3~4.2 mm was used to allow for a larger grouting rate. The grouting parameters used here were: grouting pressure = 33~37 MPa, grouting rate = 180 or 360 L/min, and rod rotation and withdrawal rate = 2~5 rpm and 10~18 min/m. Using this method, columns with diameters of 2.5 to 4.5 m can be formed to a depth of 50 m. A quality assurance program was also adopted.

An offshore jet grouting case was presented in Paper #4 by Durgunoglu et al. Jet grouting columns of 800 mm in diameter were installed into marine sediments from a spud-barge or a cantilevered platform carried by a crane. The jet grouting columns were used to strengthen the foundation soil and reduce the settlement of a museum building constructed offshore.

Table 2: List of papers submitted

#	Authors	Country	Title
1	Anthogalidis et al.	GERMANY	Numerical Studies on the Design of Compaction Grouting
2	Berthelot et al.	FRANCE	Le Grand Carré de Jaude in Clermont-Ferrand : an exceptional building site of soil treatment by Jet-Grouting in the middle of a volcano.
3	Cheng et al.	TAIWAN	A Large Diameter Jet Grouting Method for Arrival of Shield Tunnelling Machine
4	Paolo et al.	ITALY	Prediction of jet grouting efficiency and columns average diameter
5	Durgunoglu et al.	TURKEY	Offshore Jet Grouting - A Case Study
6	Essler and Rossi	UNITED KINGDOM	Construction of the Bellinzona Portal Ceneri Base Tunnel, AlpTransit Gottard Tunnel
7	Kaalberg et al.	UNITED KINGDOM	The design and execution of Compensation Grouting for Bridge 404, North South Metro Project, Amsterdam
8	Gesto et al.	SPAIN	Modelling of Jet Grouting and its interactions with surrounding soils
9	Gharouni et al.	IRAN	Laboratory investigations on groutability of type C alluvial used in ground improvement for construction metro tunnels
10	Markou et al.	GREECE	Injections of microfine cement grouts into sand columns for penetrability evaluation (GR)
11	Pinto et al.	PORTUGAL	Ground Improvement Solutions using Jet Grouting and Microplies for the new Cruise Terminal in Lisbon
12	Ponomaryov et al.	RUSSIA	Analysis of soil stabilization with the help of “jet grouting” method when constructing a municipal collector
13	Tinoco et al.	PORTUGAL	Application of a sensitivity analysis procedure to interpret uniaxial compressive strength prediction of jet grouting laboratory formulations performed by SVM model
14	Van Alboom et al.	BELGIUM	Innovative monitoring tools for on line monitoring of building excavations. A monitoring test site
15	Van der Stoel & de Koning	THE NETHERLANDS	Preservation of Panorama Mesdag, The Hague
16	Yoon & Mohtar	USA	Groutability of clean sand with sodium pyrophosphate modified bentonite suspensions

Table 3: Summary of papers submitted

#	**Grouting Methods**				**Approaches**			
	Jet grout	Compensation grout	Particulate grout	Compaction grout	Case histories	Lab studies	Analysis/ numerical	Monitoring
1				X			X	
2	X				X			
3	X				X			
4	X						X	
5	X				X			
6	X				X			
7		X			X		X	
8	X						X	
9			X			X		
10			X			X		
11	X				X			
12	X						X	
13	X					X	X	
14	X				X			X
15		X						
16			X			X		

A similar case history was reported in Paper #11 by Pinto et al. in which 1.5 m in diameter jet grouting columns were installed in muddy alluvium to support a load transfer platform for the construction of a 4.2 m high embankment for a cruise terminal. Inclined jet grouting segments of 0.6 m in diameter were also used for the anchoring of self drilling micropiles. These were used together with 1.2 m in diaster jet grouting columns of 1.0 m spacing for the refurbishment of existing quay walls in this project. As it has never been easy to predict the settlement of columns sepported platform, 3D finite element analysis using Plaxis were carried out. Good monitoring and quality control schemes were also adopted.

Another case history on the application of jet grouting was presented in Paper #5 by Essler et al. The project was to construct a railway tunnel in soft ground below a highway. Jet grouting was used at different phases during the tunnel excavation. A jet grouting umbrella consisted of jet grouting columns reinforced with steel piles for the front face stability and the installation of a reinforced sprayed concrete liner was used for the two side tunnel excavation. After this, inclined vertical jet grouting columns were installed from the bottom of the tunnels as shown in Fig. 1(a). For the top cavern excavation shown in Fig. 1(b), horizontal grouting was carried out as shown in Fig. 1(b).

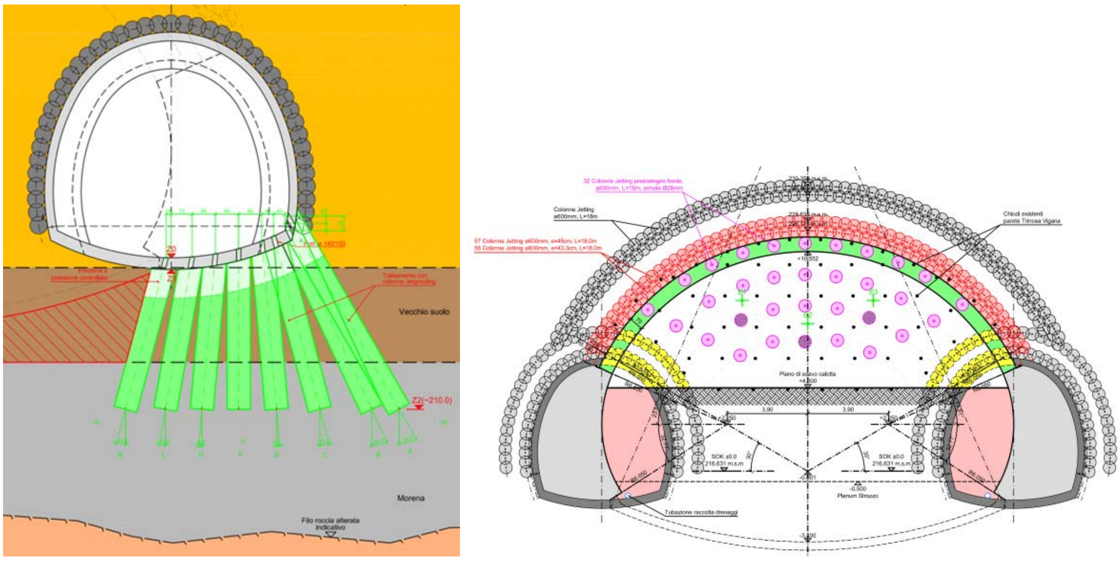

(a) (b)

Figure 1 (a) Jet grouting installed from the base of the tunnel; (b) Use of horizontal grouting for the top cavern excavation (From Paper #5 by Essler et al.)

There is only one paper on field monitoring by Alboom et al. (Paper #14) in which some innovative monitoring tools including optical fiber technology, microelectromechanical systems (MEMS) sensors, vibrating wire anchor load cells and electrical beam sensors were adopted. These techniques were used to monitor a 10 m deep excavation supported by tangent jet grouting columns wall with HEB profiles and 5 rows of nails. The deformation of the wall (x, y, z), the bending moment in the wall, the deformation of the soil (z) behind the wall and the anchorage forces for soil nails were monitored and transmitted digitally. The paper concluded that all the proposed monitoring techniques including the conventional inclinometers proved to be applicable within a construction site environment. However, the authors advised to incorporate a (limited) traditional set of monitoring tools parallel to the innovative monitoring tools. This paper did not give details on the soil conditions at the site.

There are 3 other papers on jet grouting. In Paper #4, Paolo et al. proposed a method to predict the efficiency of jet grouting and the average diameter of the columns formed. The efficiency of jet grouting was evaluated both in terms of the energy used and the volume of grout used to install a unit volume of jet grout column. The average diameter of the columns was correlated with the energy efficiency and the volume of injected grout per unit length of column. The study presented in this paper is useful for improving the reliability of design for projects using jet grouting. In Paper #8, Gesto et al. described a plastic model that could be used to model the jet-grouting treated soil. The importance of considering the thermo-hydro-chemo-mechanical (THMC) interactions was highlighted. In Paper #13 by Tinoco et al., a rational model was proposed to predict the uniaxial compressive strength of jet grouting over time using the data mining techniques.

2.2 Compensation Grouting

The term “compensation grouting” refers to a special grout injection that is designated to protect structures from potential damage as a result of adjacent or underground excavation. The principle is to inject a sufficient volume of grout into the ground to compensate for the soil movement caused by excavation so that the ground or building settlement is minimized. Two case histories of use of this method were given in this session. In Paper #7 by Kaalberg et al., a project involving tunneling below a 12 m thick very soft soil and historical buildings founded on wooden piled foundations was presented. In order to protect the bridge from unacceptable movements a combination of compensation grouting and ground improvement was carried out. Compensation grouting was installed in sand and Alleröd layer to protect the bridge during the passage of the deep tunnel. Advanced 3D numerical simulations were also used to support the design of the mitigating measures. Paper #15 by van der Stoel and de Koning described a case history of using compensation grouting in sand layer to control the ground movement for the preservation of the foundation of a monument.

2.3 Particulate Grouting

There are two papers dealing with cement grouting. Both were on laboratory study. In Paper #9 by Nik et al., the groutability of the Tehran C alluvial soil in Iran by cement grout was studied. The relative grain size of the soil and the grout has often been used to evaluate the groutability of particulate suspensions. This study showed that the groutability of soils increased with increasing grout pressure and increasing water-to-cement ratio. A relationship between groutability and soil and grout particle sizes, water-to-cement ratio, and grout pressure was presented. In Paper #10 by Markou et al., the use of microfine cement grouts in sand was studied in the laboratory. The test results showed that the use of microfine cements improved the penetrability of cement suspensions and thus was effective for grouting of medium to fine sands. Suspension penetrability was also improved by increasing water-to-cement ratio, decreasing viscosity, reducing sand relative density or saturating the sand prior to grouting.

The groutability of clean sand by sodium pyrophosphate modified bentonite suspensions was studied in Paper #16 by Yoon and Mohtar. A number of factors affecting the groutability of clean sand were studied. An empirical relationship between the groutability of bentonite grout and injection pressure, relative viscosity, relative density was given. A correlation between groutability and the injected pore volumes was also established. Using this relationship, a criterion to class a soil as “groutable” or not was proposed.

2.4 Compaction Grouting

The method involves controlled injection of very stiff, mortar-like grout (with less than 25 mm slump), at high pressure, into discrete soil zones. The grout generally does not enter soil pores but remains in a homogenous mass that gives controlled displacement to compact loose soils, lift structures, or both. This method was discussed by Paper #1 by Anthogalidis et al. in which a numerical study on the design of compaction grouting was presented. Finite element model with a hypoplasticity model was adopted. There has been an increasing use of compaction grouting in recent years (Chu et al., 2009a). Therefore, the paper is timely in addressing some of the design issues of compaction grouting.

2.5 Concluding Remarks

Overall, the papers submitted to this session are good quality. Almost all the papers addressed issues that help us to enhance our knowledge on either design or appliation. There are still a lot of research and development work to be carried out before more reliable design methods and proven construction procedures are put in place. This process can be accelerated if practicing engineers and researchers can work more closely together. For example, some of the case histories presented in this session would offer excellent research topics and opportunities for researchers to verify their theories and check the capacity of their prediction. For this purpose, I would like to propose some industry-acadmic match making sessions to be set up in the future conferences. For practicing engineers presenting case histories, more attention should be paid on site conditions, properties of soils, grouting materials and the soil improved. For researchers presenting numerical and laboratory findings, a section to highlight the engineering problems addressed and potential applications will be useful.

3. BIOGROUTING

3.1 Introduction

At the present, cement or chemicals are commonly used for grouting for civil and environmental engineering applications. However, the production of cement is energy intensive and environmentally unfriendly. The use of cement for soil improvement is also expensive and time consuming. Using the latest microbial biotechnology, a new type of construction material, biocement, can be developed as an alternative to cement (Whiffin, 2004; Ivanov and Chu, 2008). Biocement is made of naturally occurring microorganisms at ambient temperature and thus requires much less energy to produce. It is sustainable as microorganisms are abundant in nature and can be reproduced easily at low cost. The microorganisms that are suitable for making biocement are non-pathogenic and environmentally friendly. Furthermore, unlike the use of cement, soils can even be treated or improved without disturbing the ground or environment as microorganisms can penetrate and reproduce themselves in soil. Harnessing this natural, unexhausted resource may result in an entirely new approach to geotechnical or environmental engineering problems and bring in enormous economic benefit to construction industries. The application of microbial biotechnology to construction will also simplify some of the existing construction processes. For example, the biocement is much smaller in size. It can be in either solid or liquid form. In liquid form, the biogrout has much lower viscosity and can flow like water. Thus, the groutability of biocement and delivery will be much better than that for cement or chemicals.

The principle of microbial treatment is to use the microbially-induced calcium carbonate precipitation or other approaches to produce bonding and cementation in soil so as to increase the shear strength and reduce the permeability of soil or rock. To describe the two effects, biocementation and bioclogging have been used in the literature. A number of studies have been carried out in recent years (Whiffin, 2004; Mitchell and Santamarina, 2005; DeJong et al., 2006; Ivanov and Chu, 2008; Van der Ruyt and van der Zon, 2009; Van Paassen et al., 2010). Much of the work still stays at the experimental stage. However, the scale of treatment has increased rapidly with time, see Fig. 2 as an example. A few practical applications have also been reported as discussed later.

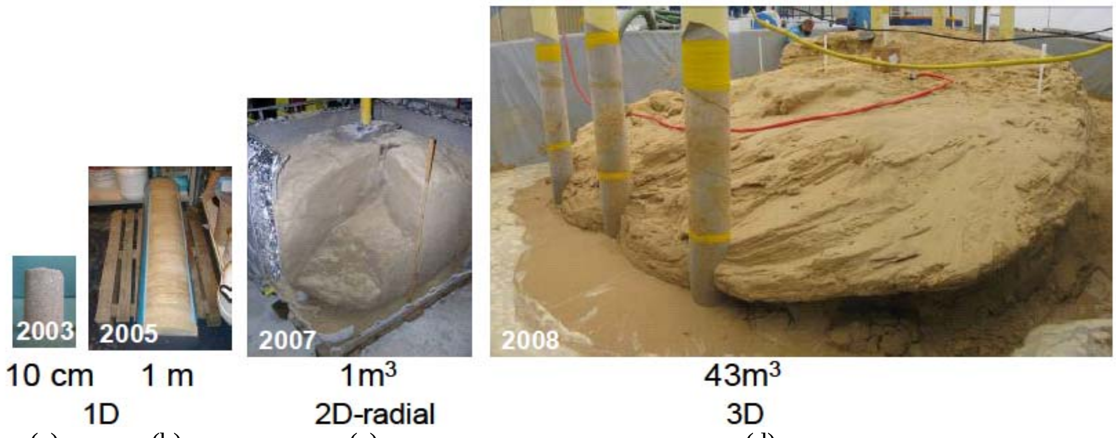

Figure 2: Increase in scale of biogrouted soil: (a) triaxial specimen, (b) 1 m column, (c) 1 m^3, (d) 50 m^3 (after van Paassen, 2011)

Biogrouting refers to a process in which microbial activities or products are adopted to reduce the permeability and/or increase the shear strength of soil. The microbiological process induces precipitation of calcium carbonate crystals or other minerals or slimes, as shown in Fig. 3. Those minerals or slimes act as cementing agencies between sand grains to increase the shear strength of soil and/or to fill in the pores in soil to reduce the permeability. It can be used to achieve either or both of the biocementation and bioclogging effects to strengthen weak ground or to control seepage or erosion. The biogrouting process is similar to that of cement or chemical grouting. As the viscosity of biogrout is low, for sandy soil, it is possible to pump in the biogrout into the ground without mixing. For clayey soil, mixing may still be required. In the laboratory, the unconfined compressive strength achieved by the calcite-precipitated sand has reached the order of 10 MPa. The permeability of clean sand can be reduced from 10^{-4} to 10^{-7} m/s.

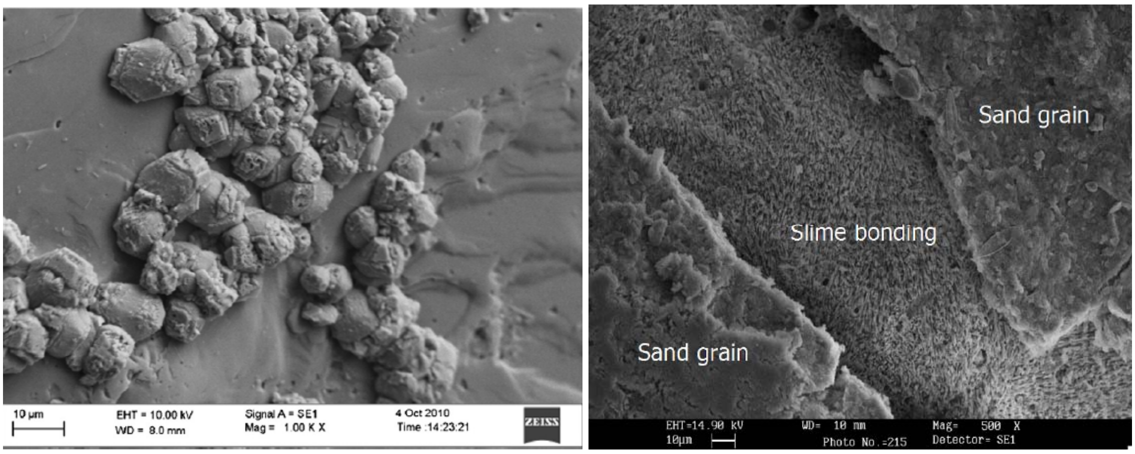

(a) (b)

Figure 3: Formation of (a) minerals on sand surface and (b) slime in between sand grains

3.2 Potential Applications of Biogrout

3.2.1 Enhancing Shear Strength of Sand

By using the microbially-induced calcium carbonate precipitation method, the shear strength of soil can be increased as shown by a number of researchers (Whiffin, 2004; DeJong et al., 2006; Chu et al., 2009b; Van der Ruyt and van der Zon, 2009; Van Paassen et al., 2010). We know that dry sand will not even stand as a column. However, when dry sand is treated by biogrout, its unconfined compressive strength (UCS) can increase to 27 MPa as shown in Fig. 4 as an example. Fig. 4 also shows the dependent of UCS on the calcium carbonate content. To increase the calcium carbonate content, more repeated round of pumping or injections are required. The delivering method to achieve a desired amount of calcium carbonate content is a research topic that still needs further study.

The above method can be used in lieu of dynamic compaction for the treatment of sand to reduce settlement or liquefaction potential of sand. Another method to mitigate liquefaction is to use biogas method as introduced below.

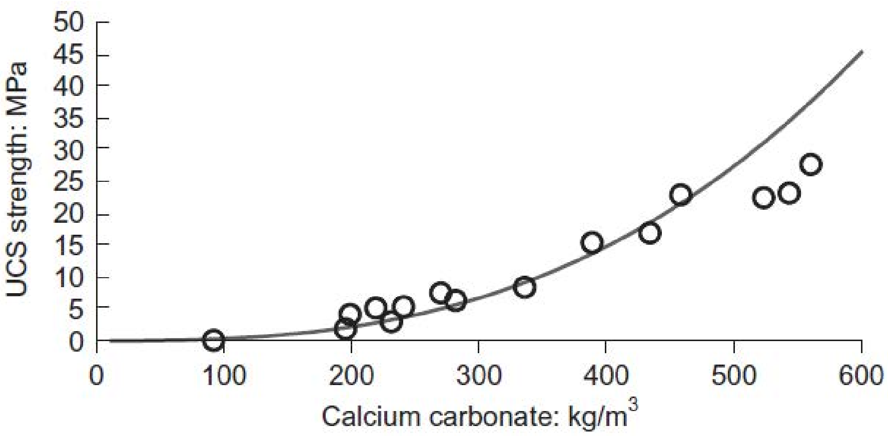

Figure 4: The unconfined compression strength (UCS) versus calcium carbonate content relationship for biogrout treated sand (after Van der Ruyt and van der Zon, 2009)

3.2.2 Mitigation of Liquefaction by Biogas

Liquefaction is one of the major factors that lead to earthquake induced disasters. The common methods that can be adopted for mitigation of liquefaction include: (1) Replacement or physical modification; (2) Densification; (3) Pore water pressure relief; and (4) Foundation reinforcement, as summarized by Chu et al. (2009a). A new approach for the mitigation of liquefaction potential of sand is to introduce tinny gas bubbles in saturated sand at where liquefaction may occur. Several studies (e.g., Yegian et al., 2007) have shown that when saturated sand is made slightly unsaturated (with a degree of saturation between 80 to 95%) by introducing gas bubbles, the amount of reduction in the excess pore water pressure of soil generated under a dynamic load will be greatly reduced. One way to introduce tinny gas bubbles is to use microorganisms. This method is promising as it has the following three advantages: (1) It may be the method that consumes the least energy; (2) The gas generated by bacteria can be distributed more evenly than other means; (3) The gas bubbles generated by bacteria can be tinnier so the gas bubbles are less prone to escaping from the ground. Such a microbial method is being developed by the author and his co-workers. Some of the results are presented in Fig. 5, where the effective stress paths of a series of consolidated undrained triaxial tests for samples with different B values are shown. The B value is the Skempton's pore water pressure parameter. The degree of saturation for a B value in the range of 0.967 to 0.351 is from 100 to 93% (He, 2012). It can be seen from Fig. 5 that with a merely small change in the degree of saturation, the resistance to liquefaction potential can be greatly increased. The samples with degree of saturation less than 100% in these tests were created using denitrifying bacteria. Shake table model tests with laminar boxes were also carried out. The results show that the pore water pressure ratio (defined by excess pore water pressure to effective overburden stress) can be reduced by half if the degree of saturation, S_r, can be reduced from 100% to 95% as shown in Fig. 6.

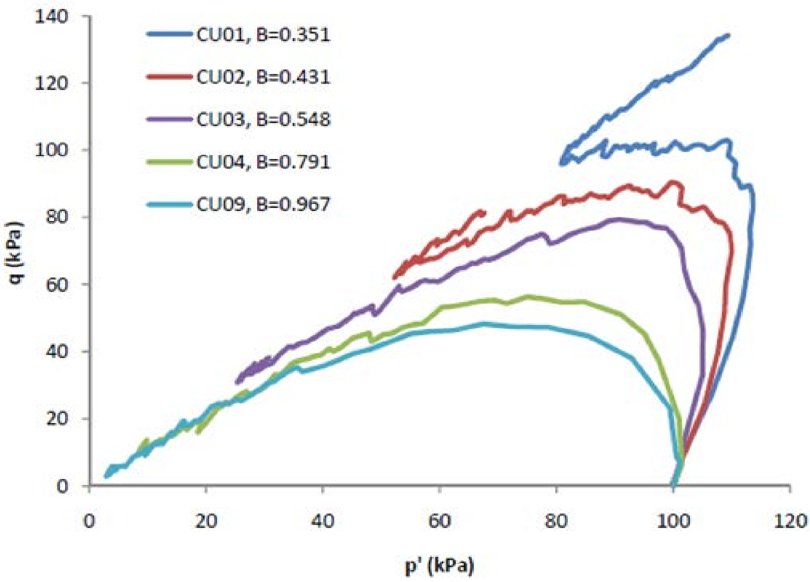

Figure 5: Increase in liquefaction resistance with B value or degree of saturation (after He, 2012)

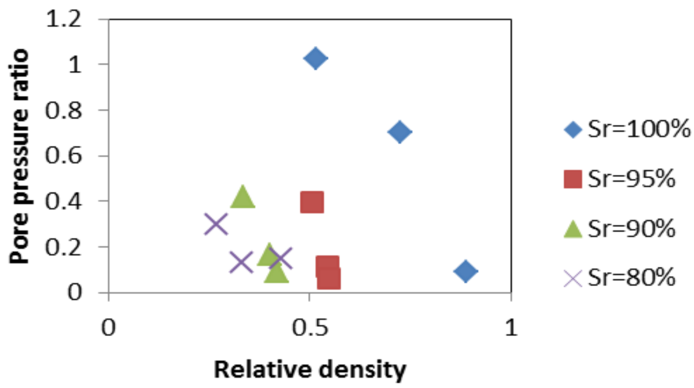

Figure 6: Pore water pressure ratios from shake table tests on bacteria desaturated sand (after He, 2012)

3.2.3 Seepage and Erosion Control

Biogrouting can also be used to reduce the permeability of sand through the so-called bioclogging mechanisms. One of the methods that has been developed by our research group is to use urea reducing bacteria to precipitate a layer of calcium carbonate on top of sand as shown in Fig. 7. This hard layer of crust has a permeability of less than 10^{-7} m/s and thus can be used as an impervious layer for water storage or for erosion control of beach or riverbank. As the layer of treatment is rather thin, the amout of biogrout used is small. Thus the method can be more economical than convertional methods. This method involing pouring and recycling of nutrent flud. Another method of forming a relatively homogeneous layer of 20 to 30 mm with reduced permeability by spray as shown in Fig. 8 was also developed. Some of the details of these methods are discussed in Stabnikov et al. (2011) and Chu et al. (2012).

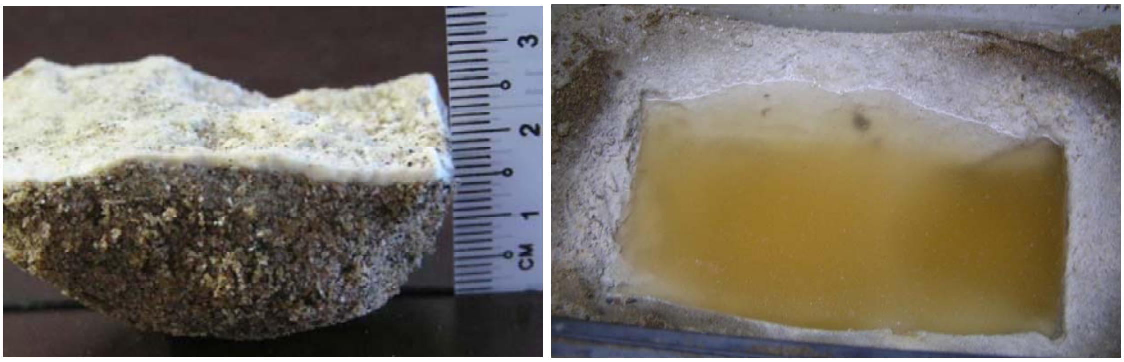

(a) *(b)*

Figure 7: Formation of (a) a thin impervious layer on top of sand using a biogrouting method and (b) a water pond model in sand using this method

(a) *(b)*

Figure 8: Formation of (a) an impervious layer in sand using a biogrouting method and (b) a water pond model in sand using this method method

3.2.4 Field Trials

Attempts to apply some of the biogrouting methods in practice have already been made. It was reported that the BioSealing technique, a type of biogrouting method developed by Deltares, was used for the first time for the Aquaduct Ringvaart Haarlemmermeer as part of the high-speed rail link project (http://www.smartsoils.nl//EN/page24.asp). Another application of biogrout for strengthening gravel for borehole stability for a gas pipeline installation project in The Netherlands was also presented by van Passen (2011). Six injection wells surrounded by 14 extraction wells were installed in a regular plot of 24 by 4 m. The electrical resistivity measurements were made before, during and after treatment together with other field testing. The amount of ammonium in the liquid extracted from the field were also measured as part of the monitoring of the flow and transport of the brine solutions as the injected bacterial suspension and substrate solutions had a large contrast with the surrounding groundwater. A comparison of the soil resistivity measured before and during the treatment was compared in Fig. 9. The high salinity of the flushed with the substrate (or brine) solutions reduced the apparent resistivity of the soil from 120 (dark blue) to 2 (purple) Ωm. Thus the change from blue to red or purple reflected the degree of treatment. However, Fig. 9 also highlights a challenge to the biogrouting method, that is, how to ensure the uniformity of the treatment which will be one of the key research topics in the future.

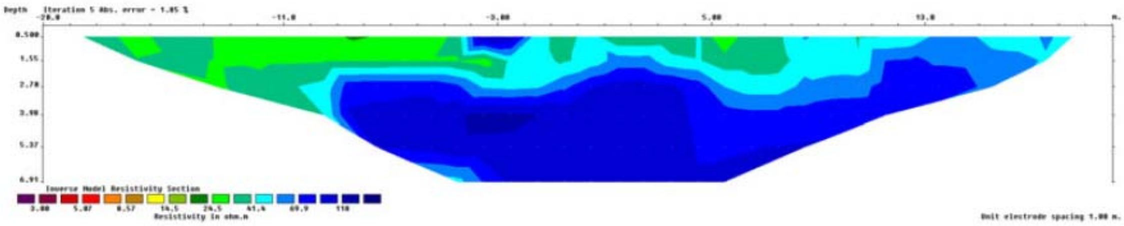

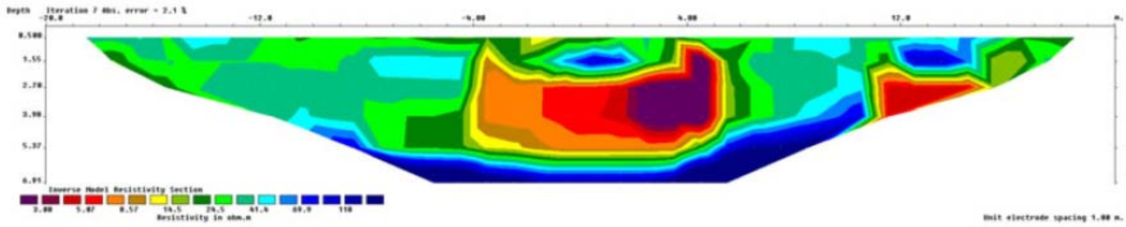

Figure 9: The geoelectrical resistivity measurements before (top) and during (bottom) biogrouting treatment. The apparent resistivity changed from the original 120 (dark blue) to 2 Ωm in the purple areas (after van Passen, 2011)

3.3 Concluding Remarks

The recent development in the biogrouting technology was reviewed. As discussed, the biogrouting method has a number of advantages over the conventional grouting methods. Several potential applications including field trials were discussed. The biogrouting method paves a more cost-effctive, sustainable and environmentally friendly solution to ground improvement. However, there are also a lot of more research work to be carried out to address the many challenges in bringing this new approach to be closer to a common practice.

4. ACKNOLEDGEMENTS

The team for the biocement research consists of Dr Volodymr Ivanov, Dr Viktor Stanikov, Jia He, Maryam Naeimi and Bing Li. Their contributions to some of the results presented in this report are gratefully acknoledged.

REFERENCES

Burke, G.K., Cacoilo, D.M. and Chadwick, K.R. (2000) Super jet grouting: new technology for In situ soil improvement. Transportation Research Record: Journal of the Transportation Research Board, No. 1721: 45-53.

Chu, J., Stabnikov, V. and Ivanov, V. (2012) "Microbially induced calcium carbonate precipitation on surface or in the bulk of soil", Geomicrobiology Journal (in press).

Chu, J., Varaksin, S., Klotz, U. and Mengé, P. (2009a) "Construction processes." State-of-the-Art-Lecture, Proc. 17th International Conf on Soil Mechanics and Geotechnical Engineering, Alexandria, Egypt, 5-9 Oct, 4: 3006-3135.

Chu, J., Ivanov, V., Lee, M.F., Oh, X.M. and He, J. (2009b) "Soil and waste treatment using biocement", Proc. International Symposium on Ground Improvement Technologies and Case Histories (ISGI09), Singapore, 165-170.

DeJong, J.T., Fritzges, M.B. and Nusslein, K. (2006) "Microbially Induced Cementation to Control Sand Response to Undrained Shear." Journal of Geotechnical and Geoenvironmental Engineering, ASCE, 132(11): 1381-1392.

Hashimoto, T. and Liu, Y.J. (2011) "New Technologies for Underground Construction in Soft Ground of Urban Area", TUNNELweb http://english.stec.net/english/english_detail.asp?id=884

He, J. (2012) "Mitigation of liquefaction of sand using microbial methods." PhD Thesis, Nanyang Technological University, Singapore.

Ivanov, V. and Chu, J. (2008) "Applications of microorganisms to geotechnical engineering for bioclogging and biocementation of soil in situ." Reviews in Environmental Science and Biotechnology 7(2): 139-153.

Mitchell, J.K. and Santamarina, J.C. (2005) "Biological Considerations in Geotechnical Engineering." ASCE Journal of Geotechnical and Geoenvironmental Engineering, 131(19): 1222-1233.

Osborne, N.H. and& Ng, C.C. (2008) "Strut Omission by Observational Approach for Deep Excavation in Singapore using Hybrid Ground treatment." Proc Int Conf on Deep Excavations. Singapore.

van Paassen, L.A., Ghose, R., van der Linden, T.J.M. van der Star, W.R.L. and van Loosdrecht, M.C.M. (2010) "Quantifying biomediated ground improvement by ureolysis: Large-scale biogrout experiment" ASCE Journal of Geotechnical & Geoenvironmental Engineering, 136(12): 1721-1728.

Van Paassen, L.A. (2011) "Bio-mediated ground improvement: From laboratory experiment to pilot applications", GeoFrontiers (2011) Advances in Geotechnical Engineering, ASCE Geotechnical Special Publication 211, 4099-4108.

Van der Ruyt, M., & Van der Zon, W. (2009) "Biological in situ reinforcement of sand in near-shore areas." Geotechnical Engineering, 162(1): 81-83.

Stabnikov, V., Naeimi, M., Ivanov, V. and Chu, J. (2011) "Formation of water-impermeable crust on sand surface using biocement." Cement and Concrete Research, 41: 1143–1149

Weaver, T., Burbank, M., Lewis, R., Lewis, A., Crawford, R. and Williams, B. (2011) "Bio-induced Calcite, Iron, and Manganese Precipitation for Geotechnical Engineering Applications." Geo-Frontiers 2011, ACSE Geotechnical Special Publication No. 211, 3975-3983.

Welsh, J.P. and Burke, G.K. (2000) "Advances in grouting technology." Proceedings of GeoEng 2000. Melbourne.

Whiffin, V.S. (2004) "Microbial CaCO3 Precipitation for the production of Biocement." Ph.D thesis, Murdoch University, Australia, 154 pp.

Yegian, M.K., Eseller-Bayat, E., Alshawabkeh, A. and Ali, S. (2007) "Induced-partial saturation for liquefaction mitigation: experimental investigation." ASCE Journal of Geotechnical and Geoenvironmental Engineering, 133(4): 372–380.

LOUIS MENARD LECTURE

Louis Ménard lecture
Recent Advances and Execution Aspects in Ground Improvement in Dredging and Environmental Marine Engineering

Patrick Mengé, DEME – Dredging International, Belgium, menge.patrick@deme.be

ABSTRACT

In this first Menard Lecture in the framework of the TC211 Symposium on Ground Improvement, the emphasis will be laid on different techniques within dredging and environmental projects. This will be mainly discussed from a 'main' contractors approach within the larger framework of land reclamation projects or brownfield restoration/remediation projects. Where relevant, elements defining the selection of a technique and executional aspects will be discussed.
In this lecture QA/QC aspects and specifications for ground improvement works, preferably being drafted from a performance driven approach, will be addressed as well.
Finally the latest developments in large land reclamation projects will be highlighted with focus on how to cope with different environmental and mineralogical conditions.

1. INTRODUCTION

As a practitioner, I was surprised to be invited to give this first TC 211 Ménard Lecture since brilliant academic researchers can be thought of to give this lecture. At earlier Ménard Lectures the honour was given to B. Ladanyi (1995) and C. Baker (2005). Both former lectures were focussed to the pressuremeter at the occasion of ISP conferences (International Symposium on Pressuremeter testing) while the actual symposium is focussed on soil improvement techniques.
I have not had the honour to know Louis Ménard as he passed away in 1978 while I still was still at secondary school. An interesting and personal bibliography of Louis Menard was written by a friend and contemporary of him, Henri Gonin (2005). This bibliography is my source of information to this celebrated scientist and practitioner, although during my almost 25 year career as geotechnical engineer I came across the Menard pressuremeter and the Dynamic Compaction method which can also be attributed to L. Ménard. Professionally, as contractor in dredging and land reclamation projects and environmental sanitation projects, I obviously also came across the company MENARD, which was founded by L. Ménard. But that is how far my acquaintance about L. Ménard reaches.
Probably the reason why the organising committee has chosen for a speaker which is rather a practitioner than a scientist is that L. Ménard combined both worlds. As far as I understand, this was one of the great gifts of L. Ménard and this was his key to a successful but too short geotechnical engineering career.
In this lecture I will not try to discuss all existing ground improvement techniques; this is available from many different conferences and authors on the numerous international conferences and symposia that have discussed this topic. My focus will be to give a survey of the techniques which are most often used in land reclamation and environmental remediation projects. Such techniques that I came and come across as a contractor will be discussed together with their practical application and problems related to design, execution, quality assurance and quality control (QA/QC).

2. CLASSIFICATION OF GROUND IMPROVEMENT TECHNIQUES

For classification techniques about soil improvement reference can be made to different authors who wrote state-of-the-art reports of books about Ground Improvement, each with their own classification systems (Mitchell , 1981; Van Impe, 1989). Also TC211 (formerly TC17) has proposed its classification system and they are working out descriptions of the different techniques in 7 working groups (Chu et al, 2009). Table 1 is taken from this reference as an example with overview of all considered techniques.
CUR and CIRIA, are preparing a Hydraulic Fills Manual (van 't Hoff and Nooy van der Kolff, 2012) in which ground improvement as used for land reclamation techniques is discussed. Table 2 is taken from this Manual and focusses on the techniques mainly used in land reclamation, together with their applicability, approximate depth of influence and main advantages. This table is containing all techniques used in land reclamation; however in the business of marine and environmental engineering even more techniques such as soil stabilisation and the use of geotextile reinforced soil are important as well.

Table 1: Classification of ground improvement techniques adopted by TC17 (Chu et al, 2009).

Category	Method	Principle
A. Ground improvement without admixtures in non-cohesive soils or fill materials	A1. Dynamic compaction	Densification of granular soil by dropping a heavy weight from air onto ground.
	A2. Vibrocompaction	Densification of granular soil using a vibratory probe inserted into ground.
	A3. Explosive compaction	Shock waves and vibrations are generated by blasting to cause granular soil ground to settle through liquefaction or compaction.
	A4. Electric pulse compaction	Densification of granular soil using the shock waves and energy generated by electric pulse under ultra-high voltage.
	A5. Surface compaction (including rapid impact compaction).	Compaction of fill or ground at the surface or shallow depth using a variety of compaction machines.
B. Ground improvement without admixtures in cohesive soils (also see Table 4)	B1. Replacement/displacement (including load reduction using light weight materials)	Remove bad soil by excavation or displacement and replace it by good soil or rocks. Some light weight materials may be used as backfill to reduce the load or earth pressure.
	B2. Preloading using fill (including the use of vertical drains)	Fill is applied and removed to pre-consolidate compressible soil so that its compressibility will be much reduced when future loads are applied.
	B3. Preloading using vacuum (including combined fill and vacuum)	Vacuum pressure of up to 90 kPa is used to pre-consolidate compressible soil so that its compressibility will be much reduced when future loads are applied.
	B4. Dynamic consolidation with enhanced drainage (including the use of vacuum)	Similar to dynamic compaction except vertical or horizontal drains (or together with vacuum) are used to dissipate pore pressures generated in soil during compaction.
	B5. Electro-osmosis or electro-kinetic consolidation	DC current causes water in soil or solutions to flow from anodes to cathodes which are installed in soil.
	B6. Thermal stabilisation using heating or freezing	Change the physical or mechanical properties of soil permanently or temporarily by heating or freezing the soil.
	B7. Hydro-blasting compaction	Collapsible soil (loess) is compacted by a combined wetting and deep explosion action along a borehole.
C. Ground improvement with admixtures or inclusions	C1. Vibro replacement or stone columns	Hole jetted into soft, fine-grained soil and back filled with densely compacted gravel or sand to form columns.
	C2. Dynamic replacement	Aggregates are driven into soil by high energy dynamic impact to form columns. The backfill can be either sand, gravel, stones or demolition debris.
	C3. Sand compaction piles	Sand is fed into ground through a casing pipe and compacted by either vibration, dynamic impact, or static excitation to form columns.
	C4. Geotextile confined columns	Sand is fed into a closed bottom geotextile lined cylindrical hole to form a column.
	C5. Rigid inclusions (or composite foundation, also see Table 5)	Use of piles, rigid or semi-rigid bodies or columns which are either premade or formed in-situ to strengthen soft ground.
	C6. Geosynthetic reinforced column or pile supported embankment	Use of piles, rigid or semi-rigid columns/inclusions and geosynthetic girds to enhance the stability and reduce the settlement of embankments.
	C7. Microbial methods	Use of microbial materials to modify soil to increase its strength or reduce its permeability.
	C8 Other methods	Unconventional methods, such as formation of sand piles using blasting and the use of bamboo, timber and other natural products.
D. Ground improvement with grouting type admixtures	D1. Particulate grouting	Grout granular soil or cavities or fissures in soil or rock by injecting cement or other particulate grouts to either increase the strength or reduce the permeability of soil or ground.
	D2. Chemical grouting	Solutions of two or more chemicals react in soil pores to form a gel or a solid precipitate to either increase the strength or reduce the permeability of soil or ground.
	D3. Mixing methods (including premixing or deep mixing)	Treat the weak soil by mixing it with cement, lime, or other binders in-situ using a mixing machine or before placement
	D4. Jet grouting	High speed jets at depth erode the soil and inject grout to form columns or panels
	D5. Compaction grouting	Very stiff, mortar-like grout is injected into discrete soil zones and remains in a homogenous mass so as to densify loose soil or lift settled ground.
	D6. Compensation grouting	Medium to high viscosity particulate suspensions is injected into the ground between a subsurface excavation and a structure in order to negate or reduce settlement of the structure due to ongoing excavation.
E. Earth reinforcement	E1. Geosynthetics or mechanically stabilised earth (MSE)	Use of the tensile strength of various steel or geosynthetic materials to enhance the shear strength of soil and stability of roads, foundations, embankments, slopes, or retaining walls.
	E2. Ground anchors or soil nails	Use of the tensile strength of embedded nails or anchors to enhance the stability of slopes or retaining walls.
	E3. Biological methods using vegetation	Use of the roots of vegetation for stability of slopes.

Table 2: Overview of ground improvement techniques relevant for land reclamation projects (van 't Hoff and Nooy van der Kolff, 2012).

					Suitable for		Improvement			
Method	Techniques	Soil types	Application depth	Treatment depth	Subsoil	Fill	Settlement behaviour	Strength / stability	Liquefaction	Drainage capacity
Consolidation	pre-loading with or without vertical drains	clay, peat, silt, but also compressible materials such as carbonate sands	drains at depth, surcharge at the surface (sand) or at depth (atmospheric pressure)	up to 30-60 m	●	●	●	●		● PVD
Compaction	Vibratory compaction: vibratory roller	granular material	at the surface	up to 0.5-1.0 m		●	●	●	●	
	polygonal drum compactor	granular and cohesive	at the surface	up to 1.5-3.0 m		●	●	●	●	
	vibroflotation	granular material (< 15% fines)	at depth	> 30 m	●	●	●	●	●	●
	vibratory probes	granular material	at depth	10 – 15 m	●	●	●	●	●	
	Dynamic compaction techniques:									
	Dynamic Compaction	granular material	from the surface	up to 8 – 12 m	●	●	●	●	●	
	Rapid Impact Compaction	granular material	from the surface	up to 6 - 7 m	●	●	●	●	●	
	High Energy Impact Compaction	granular material	from the surface	up to 2 - 4 m		●	●	●	●	
Soil replacement	Soil removal and replacement	(Very) soft cohesive soil	From seabed/surface	0 – 30 m	●		●	●		●
	stone columns	gravel, sand, silt and clay	at depth	20 – 30 m	●	●	●	●	●	●
	sand compaction piles	gravel, sand, silt and clay	at depth	20 – 30 m	●	●	●	●	●	●
	geotextile encased sand columns	clay, peat	at depth	typically 10 - 15 m	●	●	●	●		●
	dynamic replacement	gravel, sand, silt and clay	at depth	up to 6 - 7 m	●	●	●	●	●	●
	soil removal and replacement	all, mainly very soft soils	at the surface	n/a	●	●	●	●	●	●
Soil mixing	Admixtures (e.g. cement and lime stabilization), in-situ soil mixing									
	Shallow Soil Mixing	sand, soft clay, silt and organic	both at depth and at the surface	≤ 12 m (SSM)	●	●	●	●	●	
	Deep Soil Mixing	sand, soft clay, silt and organic	both at depth and at the surface	3–50 m (DSM)	●	●	●	●	●	

3. GROUND IMPROVEMENT IN DREDGING AND LAND RECLAMATION

3.1. Selection of Ground Improvement technique

Land reclamation along coastlines is one of the most significant activities of the dredging industry. In most countries coastal properties are already densely populated and yet areas nearby water continue to attract people for recreation and residence but also for industrial development (harbors and industry). Consequently, with the growth in the worldwide population, land along the coasts has become scarce.
Typically the land chosen as potential reclamation sites are shallow coastal areas or marshy lowlands. The soil in these areas often consists of thick layers of soft clay or silts. Reclamation works increase the load on these soft layers, causing (sometimes important) deformations. Acceleration, minimizing or even avoiding such settlements can be the solution for specific projects. In addition to coping with the natural subsoil, the newly reclaimed soil is often in a loose state and needs to be compacted. Typical densities obtained with hydraulic fill are given in table 3.

Table 3: Typical relative densities realized by (hydraulic fill works (from van't Hoff and van der Kolff, 2012)

Placement Method	Relative density
Discharge under water (spraying)	20 - 40 %
Discharge under water (dumping)	30 – 50 %
Discharge under water (overflow)	20 – 40 %
Discharge under water (rainbowing)	40 – 60 %
Discharge above water (free flow through pipe)	60 - 70 %
Discharge above water (rainbowing)	60 – 80 %

In the dredging industry soil improvement is typically implemented (IADC, 2008):
- To prevent excessive settlement of reclaimed land when it is being utilized for construction purposes (roads, airports, bridge and other foundations);
- To enhance the soil stiffness in order to prevent liquefaction and subsequent damage to structures in seismic-sensitive regions;
- To enhance the shear strength of the soil to prevent slip failure;
- To enhance the bearing capacity of the soil;
- To immobilize or stabilize contaminants in dredged soil in order to eliminate environmental impacts.

Soil improvement techniques vary depending on the characteristics of the soil. Some techniques are applied to improve existing loose or soft subsoil and some are specifically used for compaction of newly reclaimed soil. A distinction should be made between compaction techniques for new granular fill or loose granular subsoil and consolidation techniques for soft fine grained subsoil. This subdivision is not as clear as it seems and a good classification of the soils to be improved is necessary to select the most appropriate technique. Especially the degree of saturation and amount of silt and clay fraction or 'fines' (< 63 micron) will be a parameter that is used to select the best technique.
As for every geotechnical project, sufficient soil investigation results should be available allowing classifying and prediction of its behavior during and after the ground improvement. A problem related to this is that in land reclamation at the time of studying the project (and preparing a quotation), the fill soil as it will be realized in the reclamation is not exactly known. This depends on the available soil in the borrow/dredging area and on the effect of dredging and hydraulic transport and placement. When predicting what will be the final result in the reclamation, attention has to be paid to loss of fines, segregation and degradation of the granular material. With regard to the possibility of degradation, it is important to know the mineralogy of the material to be dredged as well.
Fine grained material normally is not used in reclamations, but is some special cases this is the case. This may lead to specific execution methods and ground improvement methods after placement as, due to hydraulic dredging, large volume increase can occur due to the addition of process water during dredging and hydraulic transport. This issue will not be discussed here in detail. Some aspects will be mentioned where relevant, but for further elaboration on this, reference can be made to van 't Hoff and van der Kolff (2012).
In the selection of the optimum ground improvement method the project planning defined by the milestones set by the client are of high importance. Following considerations have to be made:

1. Ground improvement techniques for the natural soil: to be executed before filling, during filling or after filling;

2. Point 1 can include working over water or working on land; can the considered technique be executed over water and what is the cost impact?
3. Point 1 can include the decision that a certain technique needs to be realized during the filling works (e.g. the installation of vertical drains as soon as the reclamation is above water); this requires a working pace that fits within the hydraulic fill works as the dredging plant cannot go idle or different mob/demob's are costly.
4. Hydraulic fill can be realized according to different techniques: dumping, rainbowing, spraying, land pipe lines; when the fill is above water level the layer thickness has preferably a thickness of a few meter; does one select a technique that can compact each hydraulic fill layer individually (again coinciding with the hydraulic fill works) or does one select a technique that can compact the fill after full reclamation over the full height at once?
5. Sometimes no alternative Ground Improvement methods are possible and dredging and transport technique has to be adapted to the technique used (e.g. pre-mixing method).
6. Which technique is locally available; which technique can be performed by the main contractor; for which technique a sub-contractor has to be involved; does this sub-contractor has the experience and capacity to perform within a dredging and land reclamation project?

Many more of such considerations can be made and not only limiting the cost is of importance. One also has to take into account project and method related uncertainties and try to predict/estimate the influence this can have on the whole project, including dredging operation. When during landfill operations something goes wrong and one or more dredging plants have to go idle for some time, the loss can be considerable, even not taking into account the liquidated damages that will be charged when the project milestones are not reached.

Another consideration will be whether or not the project requirements are realistic and can be met within the project milestones. When unrealistic settlement criteria are given (e.g. allowable long term settlement lower than the natural creep settlement; 100% consolidation criterion under high service loads; too high relative density under water), this has to be recognized from the tender phase and cleared out with the client and his consultant.

The design of ground Improvement in land reclamation projects is not straight forward. Generally, for the fill material well-defined relative densities under and above the water table and allowable long time residual settlements (sum of consolidation settlements and secondary compression) are specified. Additionally also a requirement can be set that the fill may not liquefy under a given earthquake defined by its peak acceleration and Magnitude. Finally the fill needs to have a certain bearing capacity and the side slopes must remain stable. In order to fulfill these requirements, the contractor needs to perform design calculations and different levels of compaction or different spacing of vertical drains might be needed depending on the requirement considered, but also depending on the area within the fill.

The issue of liquefaction is not only related to earthquake induced liquefaction, but also gravitational liquefaction of natural subsoil in the area to be filled or in the area to be dredged and steeper slopes realized, this might be an issue. This issue is seldom studied by the client and his consultant, however it may become critical and lead to considerable losses when such gravitational liquefaction occurs and needs repair before the project can continue. In some cased ground improvement by stone columns was realized under water and preliminary to the dredging operations in order to avoid such failures during dredging and/or filling operations.

3.2. Discussion of Ground Improvement techniques used in land reclamation

3.2.1. Soil replacement

Replacement of low quality soil (compressible; low shear strength, organic material) is the most straight forward and reliable technique. However, very often a too high cost is related to this technique when performed on large scale. Alternatively, in land reclamation projects, the soil replacement technique is often used at the edge of the reclamation, under breakwaters or under gravity quay wall structures in order to realize a safe foundation for the structure. This technique is commonly called the 'sand key method'. In Figure 1 the principle is shown. The layout as shown here requires different dredging and filling operations to get realized. It is understood that the soil replacement is realized in the zone where larger shear stresses are generated.

Sometimes alternative solutions would be possible with much more gentle slopes of the reclamation fill, however the need for protection on the slopes against wave and current attack dictates more steep slopes in function of revetment material selection and limitation of volume of such materials needed.

On top of the soil replacement, underwater compaction of the replaced sand will be needed in order to guarantee the required shear strength, deformation behavior and liquefaction resistance. This generally will be realized by means of vibroflotation.

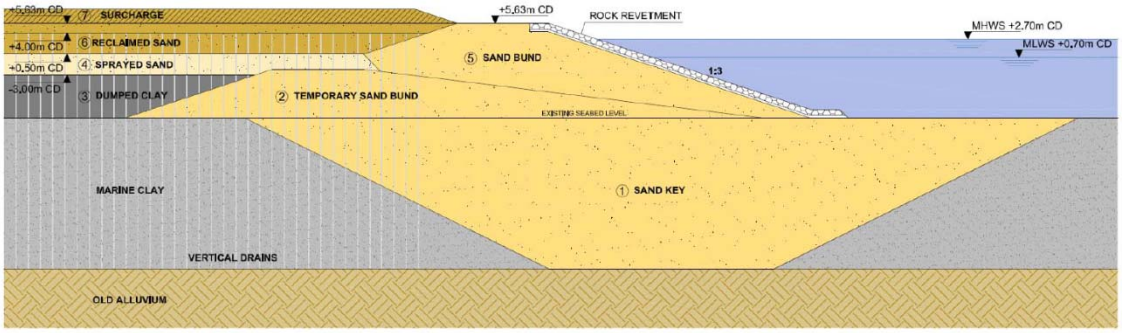

Figure 1: Principle sketch of sand key method under reclamation edge (van 't Hoff and van der Kolff, 2012).

3.2.2. Surcharge with or without vertical drains

Preloading or surcharging of fine grained subsoil and maybe also fine grained fill material is a much applied technique as it is often the most economical technique to cope with thick soft soil layers. Sometimes very large settlements can be expected (up to several m) and then the prediction of settlements is not only a geotechnical challenge, but it may define to an important extend the cost of the work as a few m over the full reclamation area easily can represent 20% to 40% of the total required fill volume. Good quality soil investigation is needed to be able to predict deformations as reliable as possible.

Surcharging is also necessary when the project requirements specify limited residual settlements under the weight of fill and future service loads. A schematic drawing demonstrating the effect of surcharge is given in Figure 2.

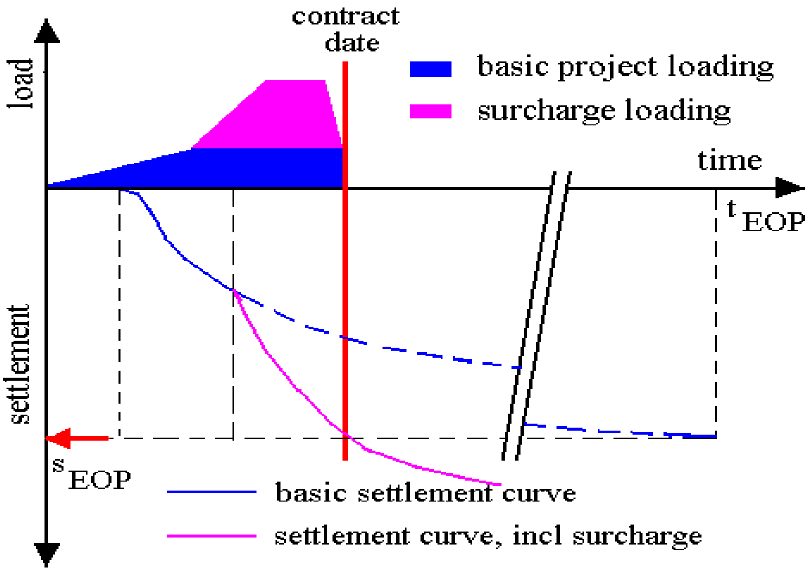

Figure 2: Sketch showing effect on surcharge on settlement behavior.

Within the available construction time and economic reality, settlements will have to occur much faster than expected from the natural consolidation process. The technique of vertical drains is a good and reliable technique, but the dimensioning requires consolidation parameters of the soil that are generally not well known. When available, laboratory consolidation tests give rather low c_v values while in situ dissipation tests give rather high c_h values and the difference between these two is not always to be attributed to the ratio of c_h/c_v which, can vary considerably (commonly between 1 and 10). As such, the design of PVD's can become tricky while again important risks can be related to too slow consolidation and thus not meeting the project milestones.

In order to allow for optimal design of deformation and consolidation behavior, a well instrumented trial embankment is required. However, seldom time is available after project award. Such testing should be realized in tender phase, again in combination with reliable and detailed soil testing.

Surcharging can be realized in different ways, but the most common is the use of excess fill material (Figure 3) which is displaced several times (provided the consolidation rate allows for multiple consolidation period within the project organization and planning) and finally used in an area where lower requirements apply. The stricter the project milestones, the more critical the predictions and the more cost is increased: more drains needed, shorter installation time, more drain installation equipment required and more surcharge material needed. One could sometimes question whether client and/or consultant are aware of this link between project requirements, executional challenges and cost.

Figure 3: Installation of PVD's and surcharge fill (in front).

The installation of the PVD’s will preferably be realized as soon as possible within the project for several reasons: minimizing length of drains and thus cost, but also to start the consolidation process as soon as possible within the project. This will allow for longer consolidation times and/or for larger drain spacing. However, for practical reasons it is required that a limited thickness of 1 m to 1.5m of sand is in place: as drainage layer (0.5 m would be sufficient), but also as stable layer to allow for the installation of the drains. On the other hand, a too thick layer of sand might require too much force to penetrate with the PVD machine and thus lead to a loss of production as well.

When realizing a fill over soft soil, the stability of (boundary) slopes need to be verified. This even becomes much more important when surcharge has to be realized with excess fill material. When drains are installed after the first fill layer, the consolidation will start before the final level is realized and thus the soil strength will increase as the rise in shear strength is proportional to the increase in effective stress. Such a working method is called staged construction and is often used/needed in filling works over soft soil (Figure 4). When applying this technique, it will to an important extend influence the whole land reclamation working method (e.g. use of spraying pontoon, use of a smaller hopper, multiple mob/demob’s).

Other means of surcharging or preloading can be the use of vacuum consolidations (Figure 5) or the use of dewatering (Figure 6). Certainly this last method is often not thought about and can be quite effective. Even more, when using PVD’s, the water table in the reclamation area itself is often not considered as a design item to be controlled. As a consequence of hydraulic fill and depending on boundary conditions such as hydraulic permeability of the natural top layers and of hydraulic fill bunds around the area, the water table in the fill may increase. This influences the drainage capacity of the PVD’s and thus influences the effectiveness of the surcharge/PVD combination.

The vacuum consolidation technique is already used for a long time (e.g. Van Impe, 1989; Smet Boring, 1992) and is discussed in lots of papers at many conferences. An advantages of this technique is the immediate increase of effective stress and thus of shear strength (Figure 7) and less or no need for surcharge material, however in general it is a more expensive technique compared to surcharging. The real driver to choose for this technique is when the area under consideration is hardly accessible at all and even hydraulic fill with its typically very gentle slopes is not possible.

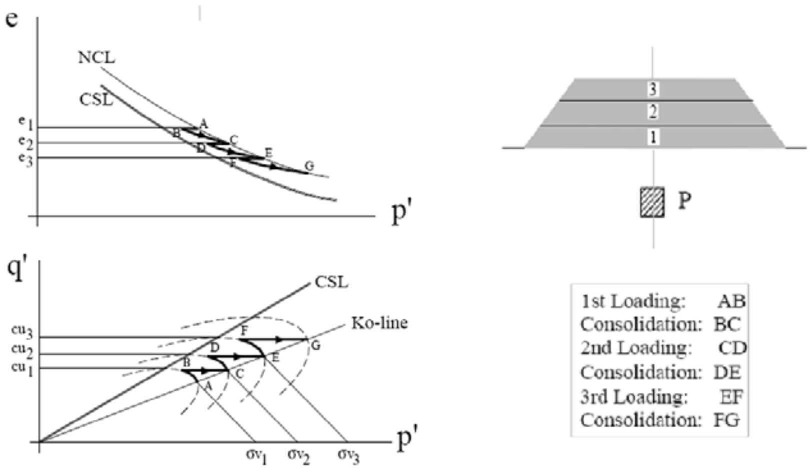

Figure 4: Staged construction and effect on soil behaviour (Van Impe and Verástegui, 2007).

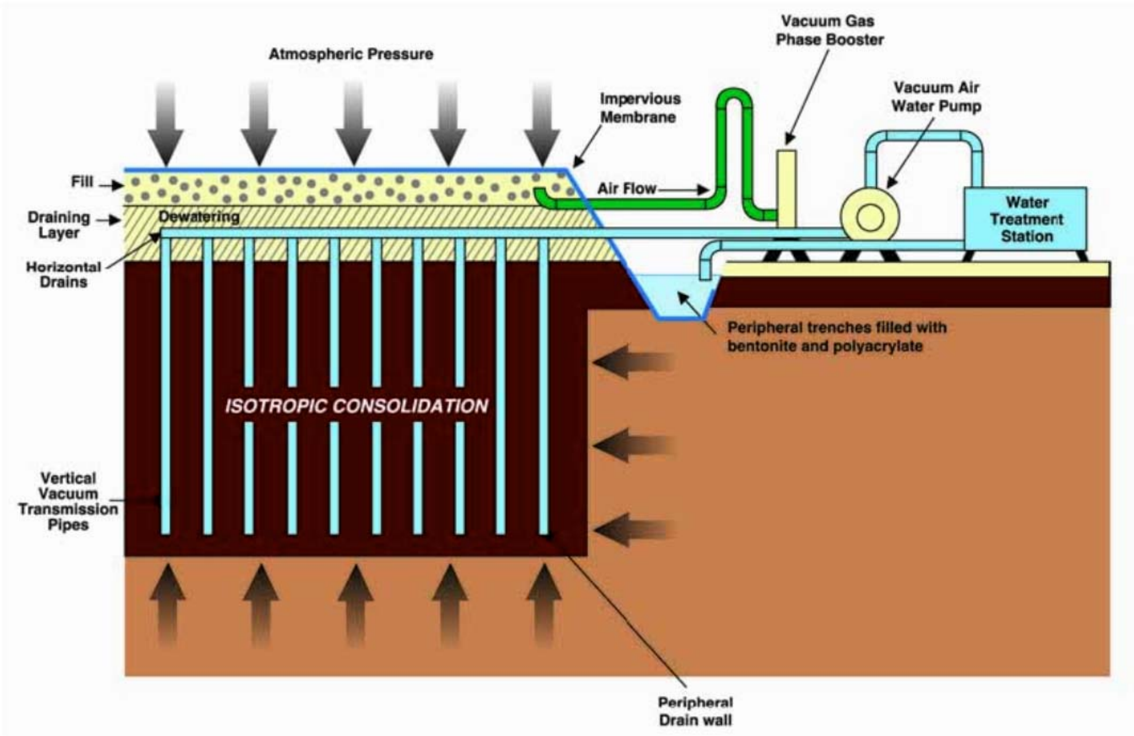

Figure 5: Principle of Vacuum consolidation (Masse et al, 2001).

In Figure 5 the general vacuum consolidation technique is depicted, also sometimes described as the ‘Ménard Vacuum consolidation’. Alternative techniques have been developed with vertical drains individually connected to a vacuum system, or connected via horizontal drains to a vacuum system. Also techniques with permeable trenches with horizontal drains or simply horizontal drains have been developed. Lots of literature exists on these items and they report the good operation of such techniques. However all are different from the basic technique (Figure 5) in which a clear situation is created with respect to effective stress and pore water stress increase in the entire soil mass (Figure 7).

A final observation with regard to surcharging is related to the effect this has on the creep behavior. Based on Bjerrum’s (1967) theory on delayed compression (Figure 8) one can derive that surcharging will cause compression which is similar to the ‘delayed compression’ that would occur under a lower stress on long term. Consequently, one can expect that after sufficient preload, the creep settlement will be very limited and can often be neglected taking into account a practical construction life-time.

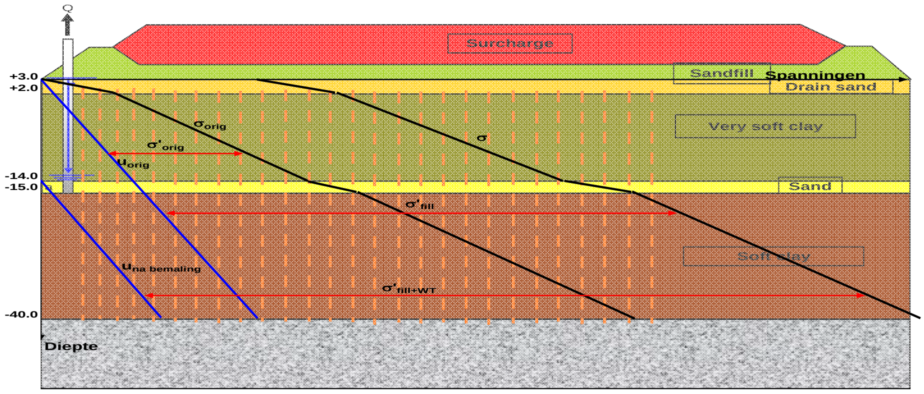

Figure 6: Schematic presentation of a project where combined effect of surcharge and water drawdown was realized.

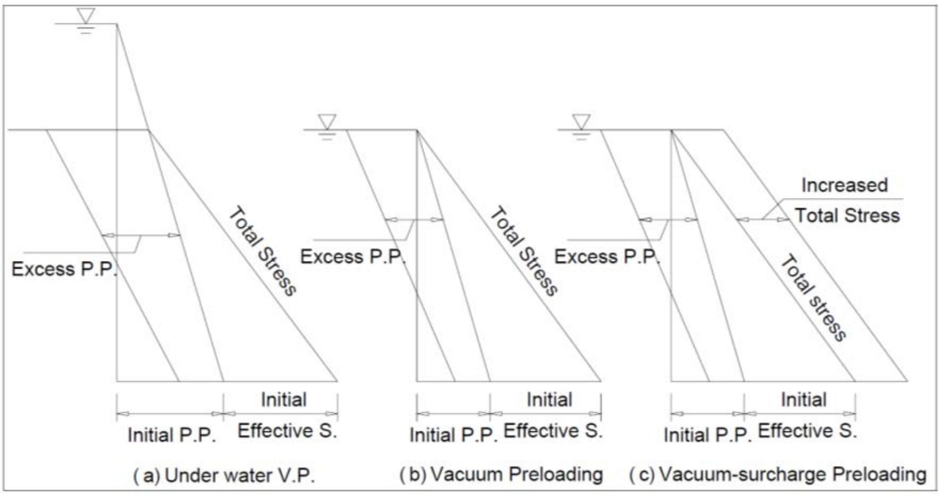

Figure 7: Stress effects during vaccuum preloading, under water, over land and combined over land with surcharge (Kwong et al, 2008).

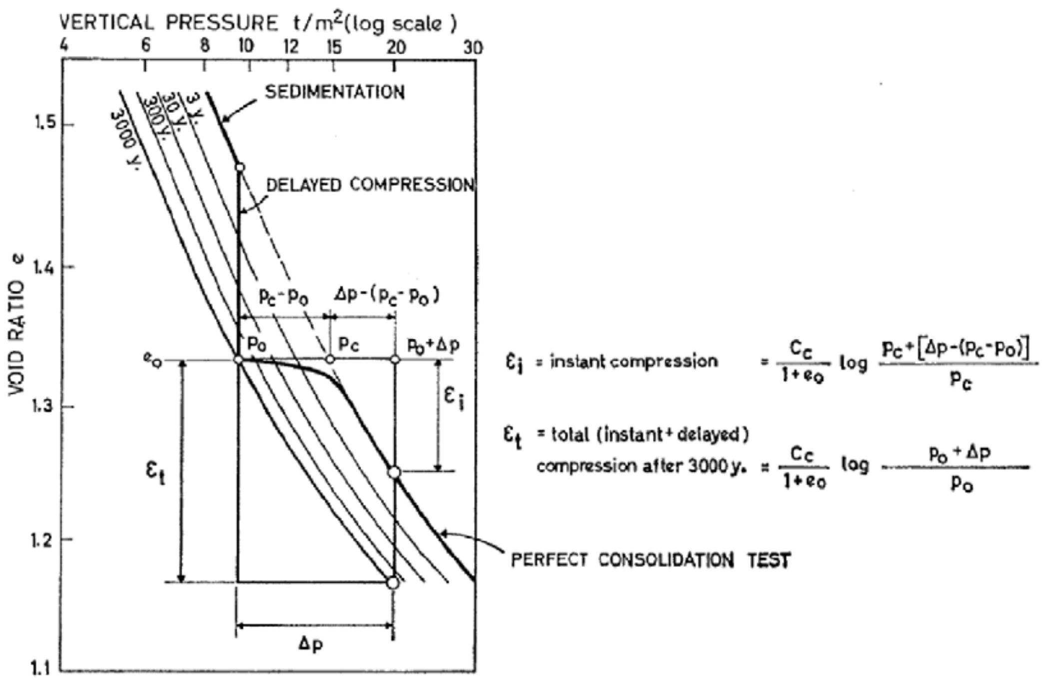

Figure 8: Deformation of soil under loading instantly and taking into account creep effects (Bjerrum, 1967).

3.2.3. Surface compaction

With ‘surface compaction’ techniques that are executed from the surface with a limited depth of influence are meant, not the deep compaction techniques, although they too are executed from the surface.

Surface compaction by means of vibratory rollers is well known in earthworks and road construction and will not be discussed here. However such techniques in general are based on the application of thin layers at the optimum water content with multiple passes of traditional vibratory rollers. Layer thickness of the layer to be compacted is linked to soil type and quality and roller weight and limited to 0.25m to 0.75m in general.

In hydraulic fill works practical working methods dictate that much thicker layers are realized in one lift. When reclaiming land in those situations where the original soil is at shallow depth or above water level, the full thickness of the reclaimed material can be limited (e.g. between 2m and 6m). In such cases the choice for the most efficient compaction technique is not always obvious.

The last decade different techniques such as vibratory rollers with polygonal drum, High Energy Impact Compaction (HEIC) and Rapid Impact Compaction (RIC) have been used so as to comply with compaction requirements while layers of minimally 2 m thickness were applied by means of hydraulic fill. Each of these techniques has its limit to depth of influence which is also varying with the type, grain size distribution and mineralogy of the fill soil to be compacted.

Both roller compaction techniques, polygonal drum (Figure 9 and Figure 10) and HEIC (Figure 11 and Figure 12), have the advantage that one must cover the full area to realize the compaction and thus the compaction energy is spread evenly all over the area to be compacted. This results in a more homogeneous top layer and in less crushing when the fill material is degradable such as carbonate sand.

The depth to which the compaction reaches is influenced by many factors such as saturation degree of the fill, the particle size and mineralogy of the material to be compacted, the amount of fines, the shape and weight of the compaction equipment and the number of passes. The result one needs to obtain and the way it is defined and tested is off course also important. Based on overall experience and with a reasonable compaction degree of 95% maximum dry density as goal, it is assumed that a 25 ton polygonal drum can compact non saturated material to a depth of approximately 1.5 m to 2 m with a relatively high number of passes (10 to 20 passes at 2 km/h). For a 12 ton HEIC compactor, a depth of 1.5 m to 2.5 m is reached with, at average, 30 passes at 12 km/h.

Rapid Impact Compaction is a also type of dynamic compaction, by which compaction energy is generated by a hydraulic hammer. A weight of 5 to 9 ton is dropped 1,2m onto a special foot assembly 40-60 times a minute (Figure 11). The foot remains in contact with the ground at all time. It is obvious that an impact crater is formed (Figure 12), which is backfilled after treatment.

The compaction unit is mounted on a hydraulic excavator, 45 T range. This method is effective up to 6m depths.

Figure 9: Polygonal drum compaction.

Tension measurements in the soil reveal the interaction of wedge (= pushing forces) and the plate (= pressure forces) directed into the depth.

Figure 10: Stress distribution with polygonal drum compaction (info BOMAG).

Figure 11: HEIC Compaction.

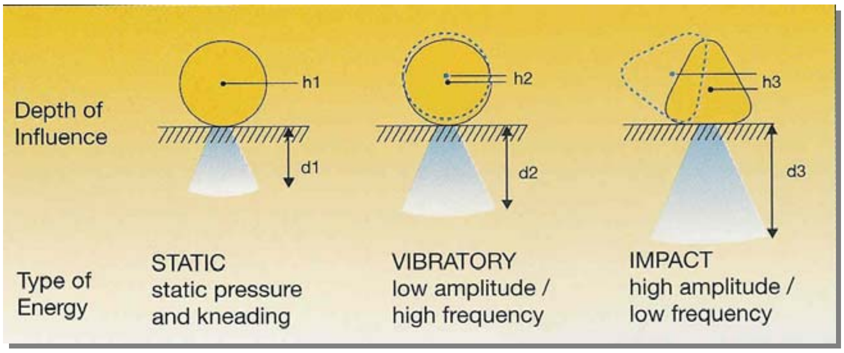

Figure 12: HEIC compaction versus static and vibratory compaction (info LANDPAC).

Figure 13: RIC compaction equipment.

Figure 14: Impact crater after RIC compaction.

As the compaction equipment is mounted on an excavator, it can shift from compaction point to compaction point swiftly. Different compaction pattern can be used as shown in Figure 15. Optimization of compaction grid and number of blows per compaction point within the selected grid has to be defined by means of a trial area.

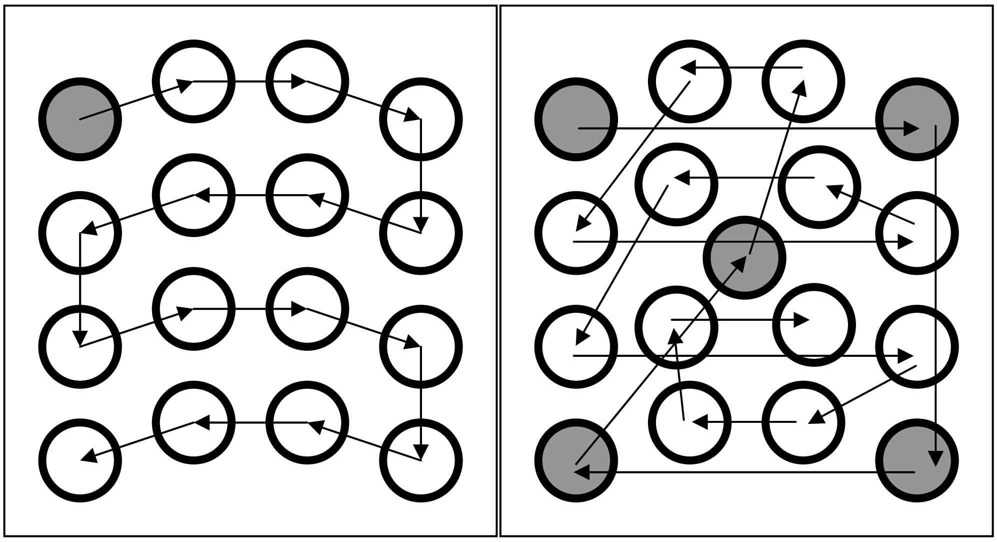

Figure 15: RIC compaction grids.

As final remark on surface compaction it should be understood that it is impossible to compact hydraulic fill layers of several meters thickness at its optimum water content, although this is sometimes required by the specifications. Watering at the surface is often used and can help, but nothing more can be done.
Whatever surface (or other) compaction technique is used to compact thick layers, the top layer will always still have to be graded and compacted by traditional vibratory roller compaction.

3.2.4. Deep compaction techniques

As deep compaction techniques two techniques are always considered: vibratory compaction by means of the Vibroflotation technique and Dynamic Compaction, also known as Ménard compaction.
Drivers behind the choice for one or another technique are:

- depth up to which compaction is required;
- soil characteristics / fines in the soil;
- degree of compaction to be reached and the way the compaction requirement is set;
- compaction above or under the water table;
- environmental boundary conditions such as vibration levels.

The necessary compaction depth is defined by the depth of the fill to be compacted and possibly also part of the natural soil that needs compaction, where applicable, after soil replacement operations. When comparing both techniques the absolute depth that can be reached is different: Vibroflotation is reported to be able to reach depths of 50m (Kirsch and Kirsch, 2010); with 25m rather as a practical application depth. Dynamic compaction will in practice be limited to 10 m to 12 m, depending on equipment mobilized and soil type to be compacted.
As always, the soil type is a very important factor. Figure 16 illustrates in which soil types which vibratory techniques can be used. Very often this is the reason why in land reclamation specifications, a maximum fines content for ‘suitable’ fill material is set. While the fines can be controlled in the fill material by selecting appropriate fill material or by the hydraulic fill execution technique, this is not the case for the natural subsoil. Also the friction ratio (R_f) derived from the CPT can be used to assess the compactability by means of vibratory compaction: R_f should be limited to 0.8 % à 1.0 %. Dynamic compaction can be effective in a wider range of soil. Good experience was obtained in a land reclamation project with compaction depth of 10 m and fines content 20% to 30%. Even clayey soils can be compacted with the dynamic compaction method. Reference can be made to the ‘standard’ publication of Louis Ménard (1975) from which Figure 17 is copied as an illustration. The figure explains the process of ‘dynamic consolidation’ in fine grained soil in different passes covering the area to be treated.
The compaction level to be reached is another issue and the practical maximum levels that can be reached again depend on soil type and equipment used. In general one can expect that Vibroflotation will lead to a more uniform compaction level, resulting in an increasing compaction level from top to bottom. With Dynamic Compaction this is differently and the compaction level will be much higher at the top compared to the bottom. This is illustrated in Figure 18, after Yee (2011).

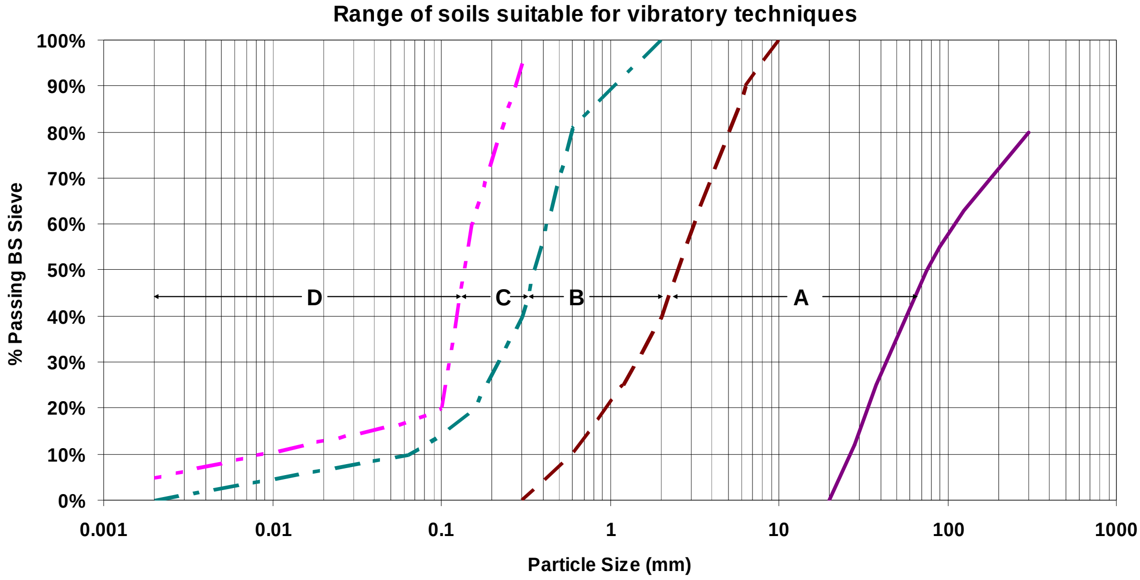

Zone A: The soils of this zone are well compactable. The right borderline is an empirically determined limit beyond which the amount and size of cobbles and boulders prevents penetration of the vibroprobe.

Zone B: The soils in this zone are ideally suited for Vibro Compaction. They have a fines content (<63µm) of less than 10 %, and mean grain size (D50) approximately in the range 0.20mm to 1.2mm.

Zone C: Compaction is only possible by adding backfill from the surface, since the in situ soil does not flow of its own accord towards the vibroprobe.

Zone D: Soils in this zone are not compactable by vibration alone. Stone columns would provide a foundation solution in these soils.

Figure 16: Range of application of deep vibrocompaction in function of soil grading (from KELLER).

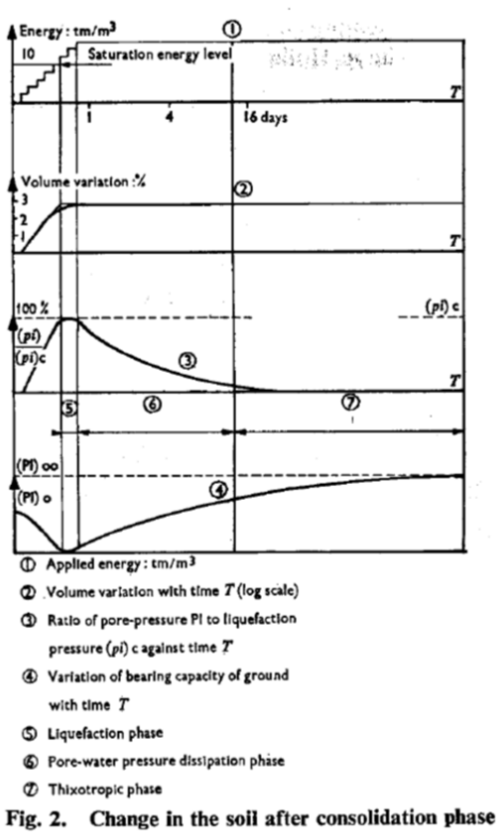

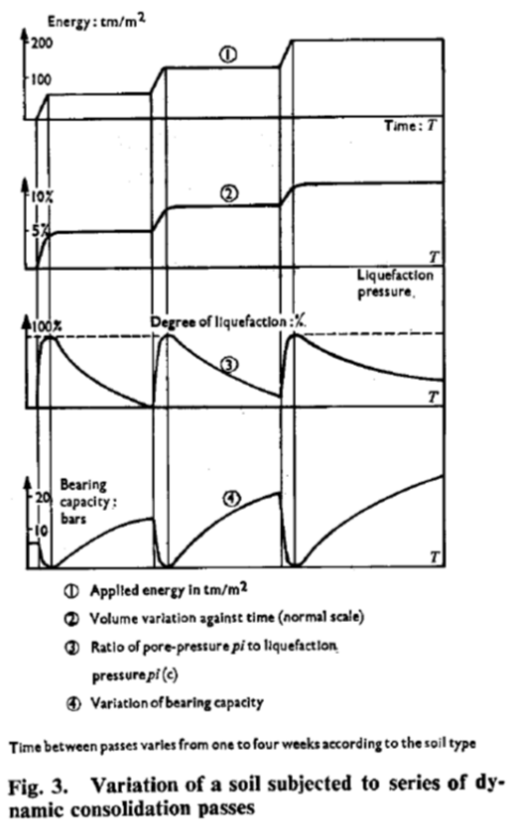

Figure 17: Extract (fig. 1 and 2) from Ménard and Broise (1975) explaining the mechanism of Dynamic Compaction.

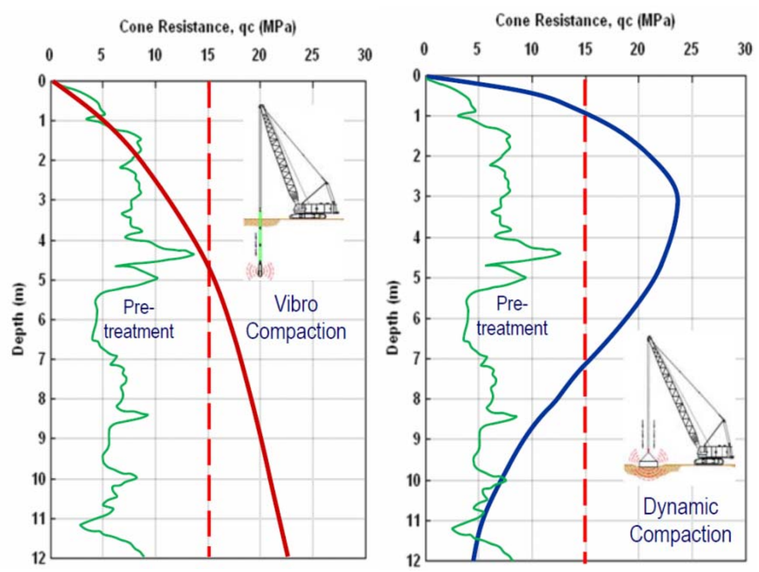

Figure 18: Depth-effect of Vibroflotation and Dynamic Compaction (Yee, 2011).

Furthermore, when underwater compaction is required, the absolute level of compaction that can be reached has a maximum, even at very high energy input. A requirement of 80% relative density under the water table is a very high requirement that hardly can be met and will require lengthy and expensive compaction work. And even in this case, at tender stage it is a risk that needs to be covered by one of the tendering parties.
As Figure 19 an example is given after Yee (2011) in which the compaction requirement was q_c = 15MPa over the full depth to be compacted. In order to be able to reach this requirement, even the two techniques were combined: Vibroflotation in the first phase to compact the deeper layers and Dynamic Compaction to compact the top layer. While this is a technical perfect example of the different techniques and their possibilities, one could question – knowing the principle of increase of q_c-value with depth for a uniform compacted layer - whether the compaction requirement is not excessive with regard to the top layers.

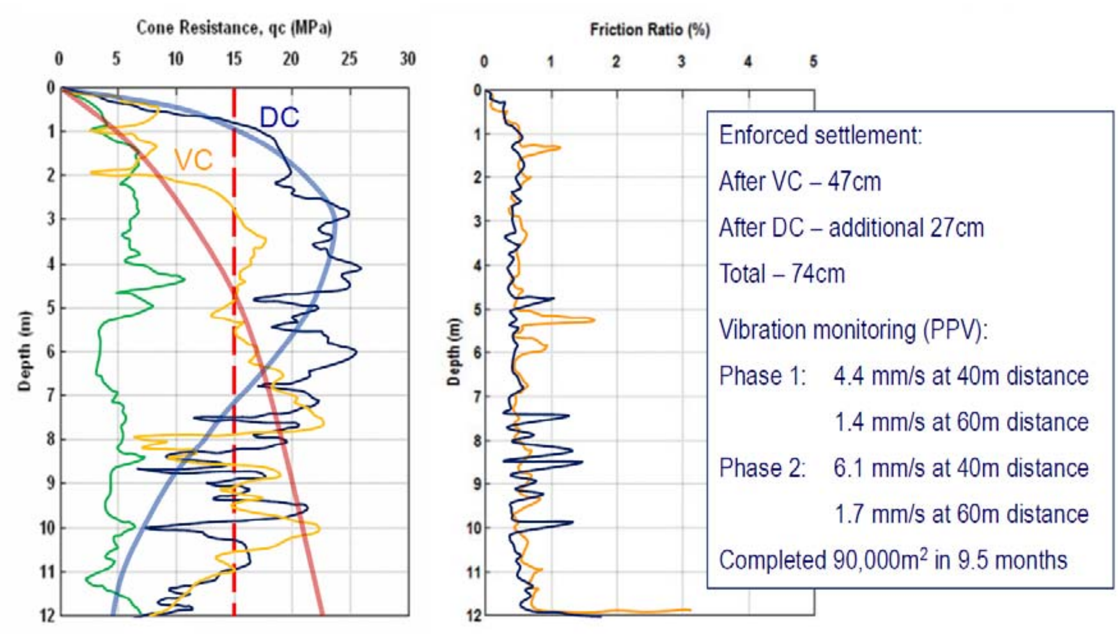

Figure 19: Combined compaction techniques used to achieve the compaction requirement (Yee, 2011).

Underwater dynamic compaction is less appropriate, although it is possible as reported by Yee (2011). Figure 20 shows a picture of the pounder used for underwater Dynamic Compaction or Dynamic Replacement. In underwater compaction generally Vibroflotation will be used unless the depth to be compacted is limited or specific situations occur.

Figure 20: Pounder for underwater Dynamic Compaction (Yee, 2011).

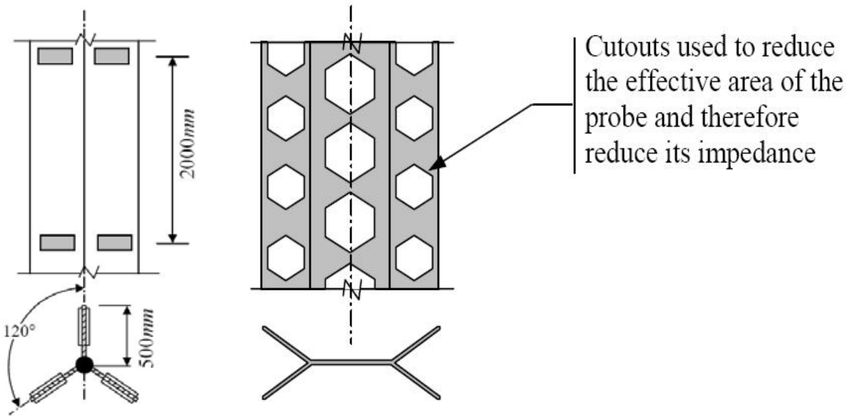

Figure 21: Left: Star profile (Van Impe, 1989); Right: double Y-probe (Van Impe et al, 1994).

Figure 22: Vibratory probe compaction with the MRC technique (Massarch, 2002).

Although vibrocompaction is often used as synonym for Vibroflotation, it needs to be mentioned that Vibratory Probe Compaction still can be an alternative for compaction work. The star-probe and double Y-probe (Figure 21) and the MRC technique (Figure 22) certainly have their merits (Massarch, 1991; Van Impe et al, 1994; Van Impe et al, 1997; Massarch, 2002). Sometimes in remote areas where limited compaction work needs to be realized and no specialized equipment and/or subcontractor is available, this technique can be a practical solution.

As a last item of this section, the effect of the mineralogy needs to be mentioned. The last decade crushability of the soil to be compacted has been a major issue in many projects in the Middle East and several authors have discussed the effect of calcareous sand (Figure 23) on compaction, but only related to the interpretation of the cone penetration test in such material (e.g. Wehr, 2005; Al-Homoud and Wehr, 2006). The influence on the crushability on the effectiveness of the compaction technique or on the required energy-input or loss of production is never described at all. Although one can expect that due to the crushing, energy is lost in the crushing work, and thus more compaction points or longer hold periods will be required, no feed-back data is available in literature.

During Vibroflotation, due to crushing, the particle distribution changes (locally) and might influence the soil permeability and the stability of the hole around the probe. This will require more jetting and feeding of sand from the top in order to obtain the required compaction result. This is a research topic that deserves more attention from the academic world.

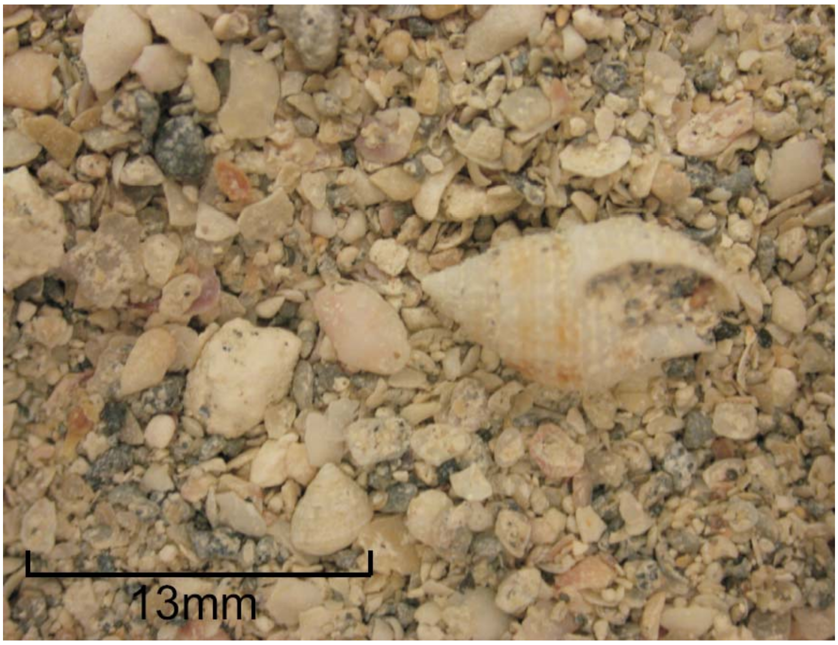

Figure 23: Example of calcareous sand.

3.2.5. Dynamic replacement

A technique that is less known, but can be used above and under water on limited layer thickness of loose to soft soil is the Dynamic Replacement technique as illustrated in Figure 24. In this figure Dynamic Replacement is compared to Dynamic Compaction (Yee, 2011); while Dynamic Compaction realizes ground improvement by compaction, Dynamic Replacement realizes ground improvement by reinforcement (similar to stone columns). Typically the diameter of such columns ranges from 2.5 m to 5 m. Depths up to 8 m can be reached.

The author has no experience with this technique, but according to literature (Gaben et al; Varaksin et al, 2009; Chu et al, 2009) it has its merits in specific situation with very low strength soil varying from loose sand to very soft fine grained material (Sabkha) and can easily be combined with Dynamic Compaction at those locations where soil quality is better.

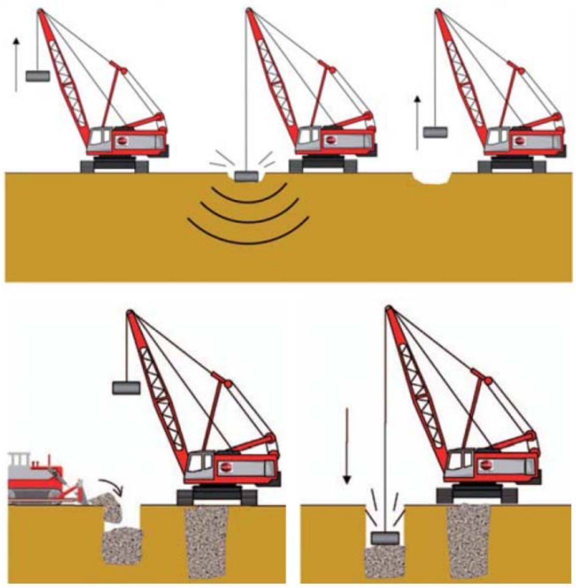

Figure 24: Dynamic Compaction (top) versus Dynamic Replacement (bottom) (MENARD).

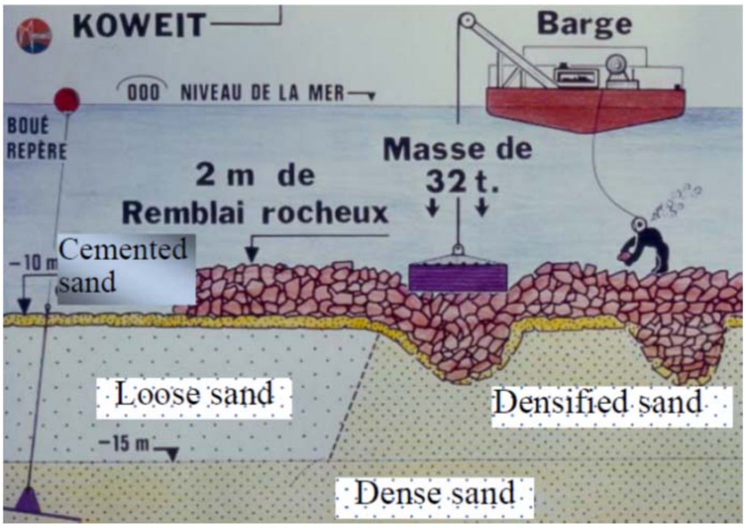

Figure 25: Example of Dynamic Replacement under water (MENARD).

A practical disadvantage of this technique and also of the techniques discussed in next section is that specific high quality aggregate is needed to realize a working platform and to be driven into the soil with the Dynamic Compaction pounder.

3.2.6. Stone columns, Sand Compaction Piles and Geotextile Encased Columns

Column type reinforcement is much less used in land reclamation projects since these techniques are only financially interesting in specific situations. The main driver for using stone columns of sand compaction piles is when the soil contains too much fines (< 63 micron) to be compacted by vibrocompaction or Dynamic Compaction, or is found at too large depth to perform Dynamic Compaction.

Again the need for special aggregates for stone columns is an important cost, certainly when large reclamation volumes are realized by means of hydraulic fill. When not locally available, this can be a major obstruction for this technique.

When stone columns have to be executed over water, the best technique: bottom feed or top feed, needs to be considered (Figure 26). Top feed (blanket method) is mostly considered and closely linked to traditional Vibroflotation and easy to perform over water. Bottom feed (hopper method) over water requires additional equipment for feeding the gravel into the compaction probe. The 'gravel jet' method as depicted in Figure 26 is an alternative bottom feed method in which a special system (Alpha-S) is used for pressurized feed of the graven to the compaction probe. Each of these techniques also has its optimum depth reach as depicted schematically in Figure 26.

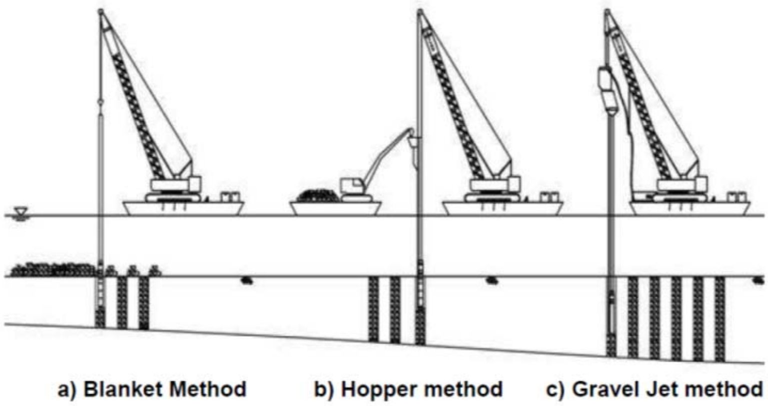

Figure 26: Execution of stone columns over water (info KELLER).

Sand Compaction Piles (SCP) are large diameter sand piles made into the soil by means of a casing pipe and compacted by vibration, dynamic impact or static pressure. A detailed description of this technique is given in Kitazume (2005). SCP's overcome the problem of the need for special granulates.
This technique has many applications in land reclamation works in Asia, where also large floating barges have been constructed for offshore installation of SCP's (Figure 27). Sand Compaction Piles can be installed in Sandy soil as well as in clayey soil and can for example be considered as alternative for a sand key solution (Figure 1). However in such case very high soil replacement ratios are used (> 50%), making this technique less interesting from an economic point of view.

Figure 27: Offshore installation of Sand Compaction Piles.

Geotextile Encased Columns have received a lot of attention the last two decades. It was used at the Airbus construction plant land reclamation works in Hamburg (Raithel et al, 2004) and it was also studied as a solution in the Netherlands for construction of rail/roads over very soft soil (RWS, 2004).
The principle of this type of sand columns is given in Figure 28. The columns are realized within a high strength (e.g. 200 kN/m to 400 kN/m) geotextile which is produced seamless so as to guarantee the optimum strength performance. This type of columns can be used in very soft soil (c_u < 15 kPa) in which normal sand or stone columns would not find sufficient lateral constraint. Design guidance is given by Van Impe (1989) and Raithel et al (2005). From this last paper Figure 29 is taken to illustrate the improvement effect of the geotextile encasing. In Figure 30, an illustration is given of the execution of GEC's over very soft soil while the machine is standing on the earlier realized columns.

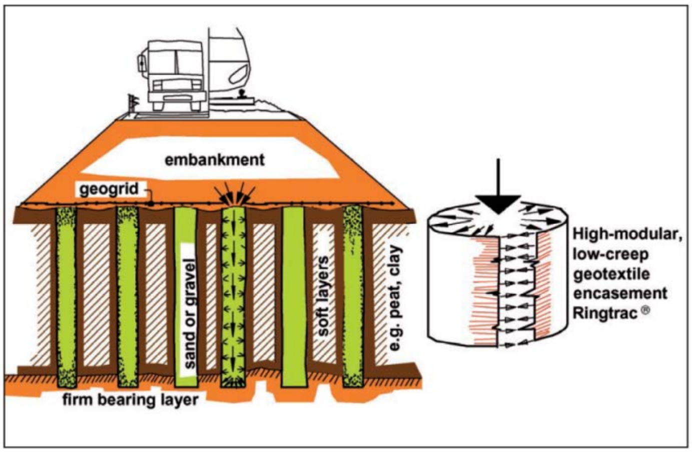

Figure 28: Principle of Geotextile Encased sand Columns (from Huesker - Ringtrac product sheet).

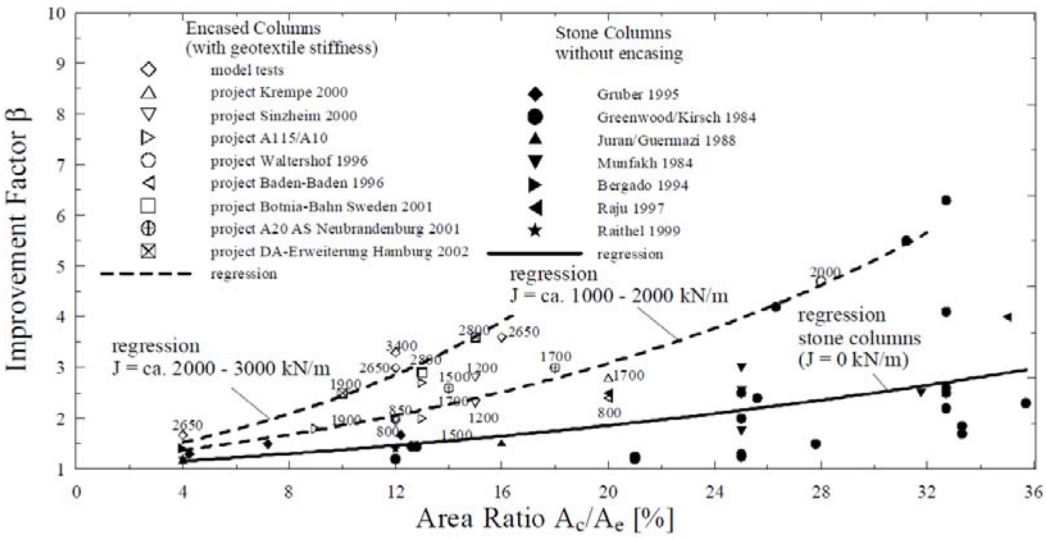

Figure 29: Improvement factor with and without geotextile encasing (Raithel, 2005).

Figure 30: Execution of Geotextile Encased sand Columns at a project site in Hamburg (from Huesker - Ringtrac product sheet).

3.2.7. (Deep) Soil Mixing Techniques

In land reclamation the use of soil mixing is limited because of the high cost related to this technique. Only where no sand can be obtained economically (e.g. Singapore) or where for environmental reasons soft soil needs to remain in place, this option is considered. For more information on this technique reference can be made to CDIT (2003). In dredging and land reclamation, the soil mixing technique is most often realized ex situ (premixing) and the mixed material is placed (back) where it is needed. Systems have been developed for pneumatic transport (no water added to the soft soil as necessary for hydraulic transport) and in line mixing of binders (Sakamoto, 1998).

The amount of binder needed depends on many factors such as type and water content of the soil material to stabilize, the final strength and stiffness to be obtained and the mixing technique. As soil premixing is a mass stabilization technique the amount of binder per m³ in general remains limited to 100 kg/m³ to 150 kg/m³.

Deep soil mixing consists of the realization of columns or panels of stabilized material. In literature the dry and wet techniques are discussed, however in offshore construction mainly the wet technique is used to stabilize the subsoil before the fill material is brought in place or before a structure is realized. Again reference can be made to Japanese literature (CDIT, 2002), however this technique is more widespread and also performed by many other companies.

DEME has patented a deep soil mixing method called Soft Soil Mixing (SSI) which is a technique for stabilizing very soft to soft sediments (c_u from 0 to 50 kPa) by means of very light (drilling) equipment on which a mixing tool with high pressure jets is installed (Figure 31). For the execution of SSI columns at a water depth of about 20 m, two masts for SSI installation were installed on a jack-up rig with large moon pool that could be covered completely with the two masts (Figure 32). This technique was used for the foundation of the closing dam in the Doeldock at Antwerp Harbor (Van Impe and Verástegui, 2007).

The 20 m high dam had to be constructed over 8 m of recently dredged very soft soil that could not be removed because of environmental reasons. The permanent (water side) slope is 10_H over 4_V and the temporary inside slope where the filling will be realized is 16_H over 4V (Figure 33). In order to stabilize the slopes of the dam, a grid of 2 m diameter SSI columns (of which some were merging into panels) was realized (Figure 34). This project is discussed in detail in De Preter and Vandycke, 2004; Van Impe and Verastegui, 2006; Van Impe et al, 2006; Van Mieghem et al, 2006.

Figure 31: DEME SSI mixing tool.

The undrained shear strength of the columns needed to be 370 kPa. The dam structure was to be constructed in stages to allow the soil in between the columns and also in between the zones with columns (Figure 33) to consolidate. As such, the ultimate strength of the columns was not needed immediately, while the quality control strength requirement was set at 28 days. Lots of preliminary lab tests were performed in order to select the optimal binder and the optimal binder content, see Figure 35. The selection was made for blast furnace cement and a binder content of 375kg/m³.

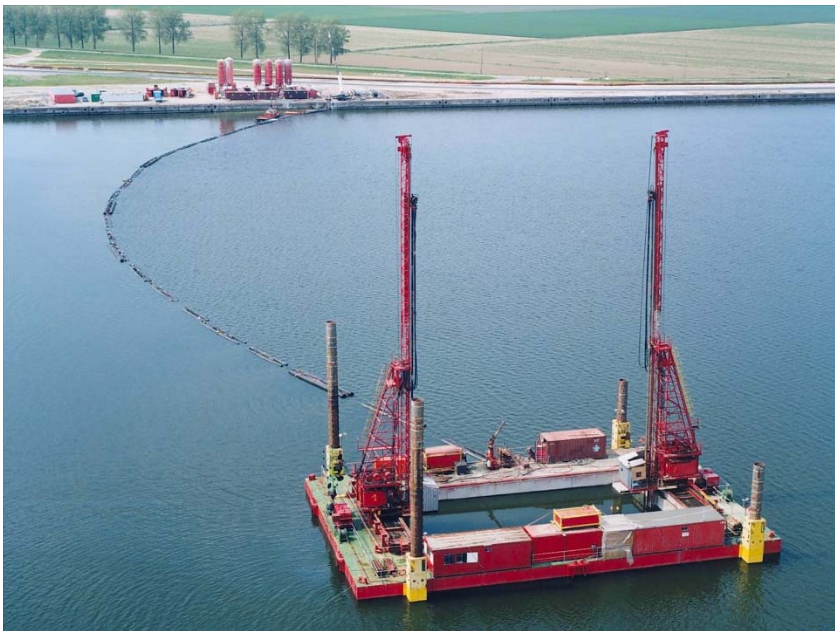

Figure 32: Execution of SSI ground improvement project at Doeldock, Antwerp, Belgium.

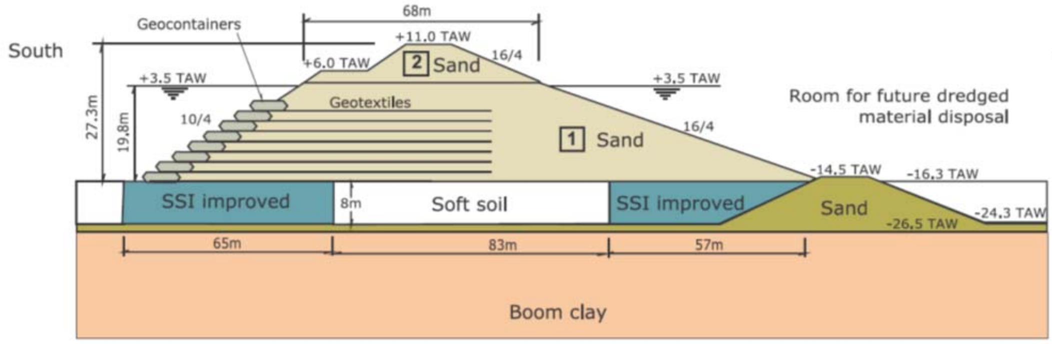

Figure 33: Typical section of the Doeldock dam structure with SSI improved zones under the slopes.

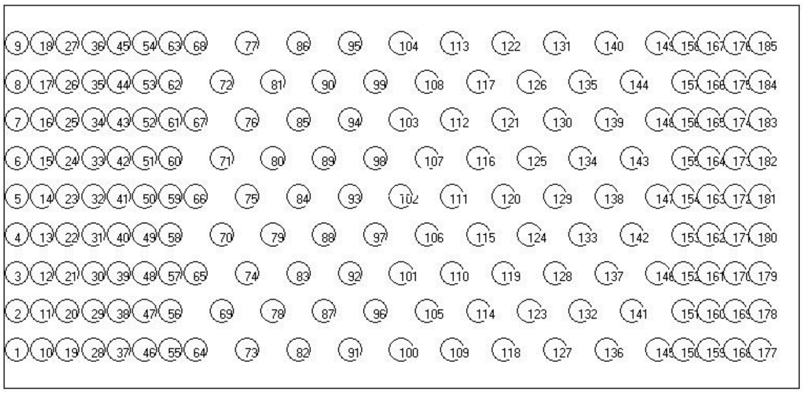

Figure 34: SSI column pattern under the permanent slope.

During quality control after execution much higher strength values were obtained, which is contrary to normal experience. After detailed investigation which included SEM photography, it was demonstrated that the testing on lab scale where the mixing was realized mechanically resulted in lower quality mixing compared to the field where the mixing was realized under the combined effect of high pressure jetting (300 bar to 400 bar) and mechanical mixing (Van Impe et al, 2005).

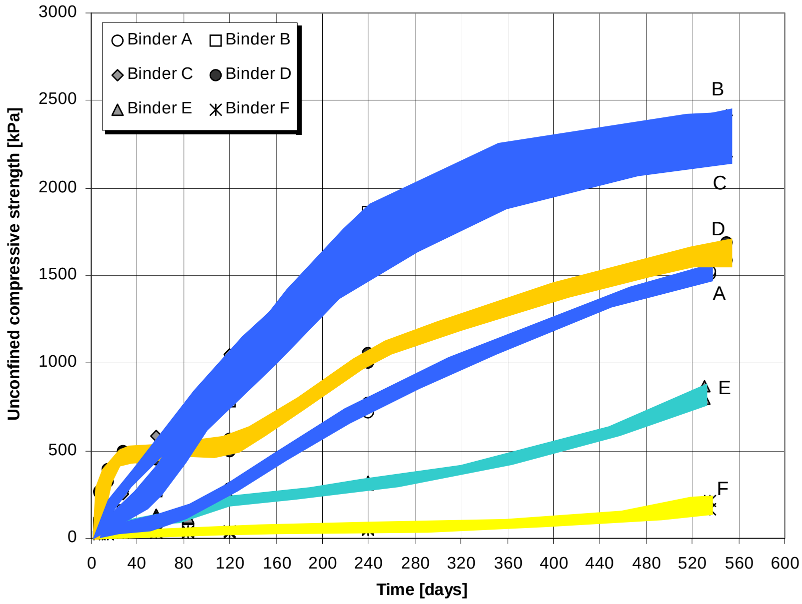

Figure 35: Strength of the soil-cement mixture in laboratory conditions for different binders in function of time.

SSI was also used for the foundation of a bund at a reclamation project in Brazil. The natural soil consists of over 30 m of very soft to soft clayey soil with some limited sandy horizons. In order to be able to construct the reclamation bund over a mangrove area which was hardly accessible, the SSI mixing system was mounted on a swamp excavator (Figure 36) which allowed constructing the columns without any preliminary soil improvement or access road. In fact the access road (base of the bund) was constructed on top of the already performed columns (after 3 days curing), as such the construction sequence allowed to progress on the recently realized work. A mixing ration of 275 kg cement/m³ was used.

Figure 36: SSI mixing tool on a swamp excavator.

3.2.8. Use of geotextiles as soil reinforcement

The use of geotextiles as ground improvement/soil reinforcing technique is a very wide topic that cannot fully be discussed here. In marine engineering the use of geotextile bags, containers and tubes has obtained wide attention as construction method for marine structures with the use of locally available sand or low quality fill material. This should to replace more expensive gravel, quarry run or rock material that need to be imported to allow construction in the harsh marine environment. In Figure 37 some typical examples of such applications are given. The correct dimensioning of such structures has been and still is a topic of research (Pilarczyk K., 2000; Klein Breteler et al, 2003; van Steeg and Klein Breteler, 2008; Oumerachi and Recio, 2009). While this is a valuable solution it is often not an economic solution for large projects. Even more, geotextile structures will need protection against damage and UV-radiation in order to be able to guarantee an engineering life-time.

An example of a temporary (5 year) structure with geotextile containers is given in Figure 38 and Figure 39. It has proven to be a very interesting and fast technique to construct a temporary sea defense without the need to import revetment material. While design formulas have been put forward, the behavior of the sand in the geotextile units and the long term geotextile strength and influences from seams are not well known and deserve further attention.

Two more examples of the use of geotextiles in marine construction can be illustrated here. The second example is the already discussed dam in the Doeldock in Antwerp harbor where geotextile containers and high strength geotextile reinforcement was used to improve the dam stability (Figure 33). Several publications are available on this topic, but the most challenging was the execution technique in order to be able to install the geotextile containers (Figure 40), enroll the geotextile, keep it on the bottom and spray sand on top of it in a well-controlled way, guaranteeing a maximum layer thickness per spraying operation of less than 0.5 m (De Preter and Vandycke, 2004).

As a third example, the construction of the new breakwater at Ostend harbor can be mentioned. In the footprint of this construction, a zone with lower bearing capacity was found. In order to guarantee stability a 'super' geotextile with nominal tension strength of 1600 kN/m was used (De Rouck et al, 2010). In Figure 41 a typical cross section of this structure is given and in Figure 42 the means of installation of the geotextile under water in open sea by means of willow mattresses is illustrated.

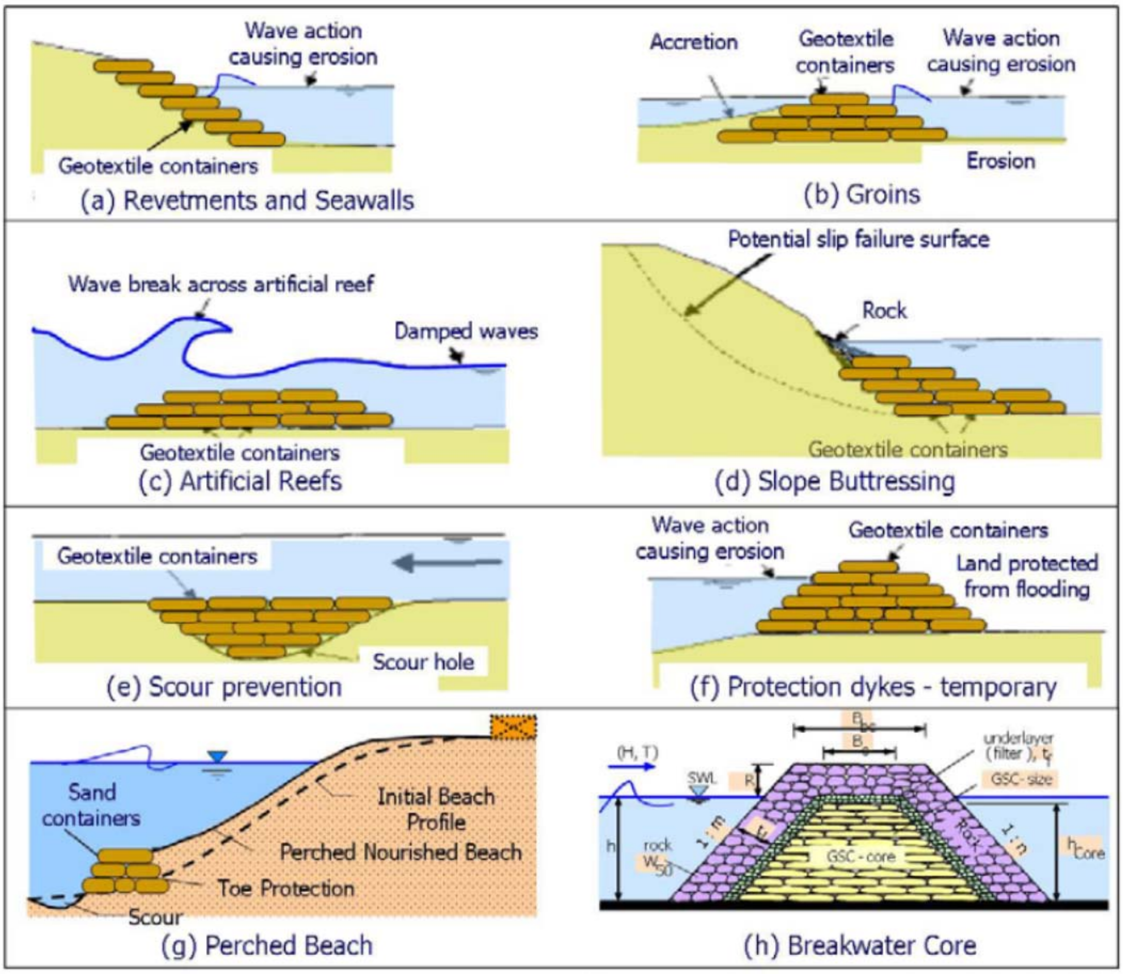

Figure 37: Examples of the use of geotextile containment units (Oumerachi and Recio, 2009).

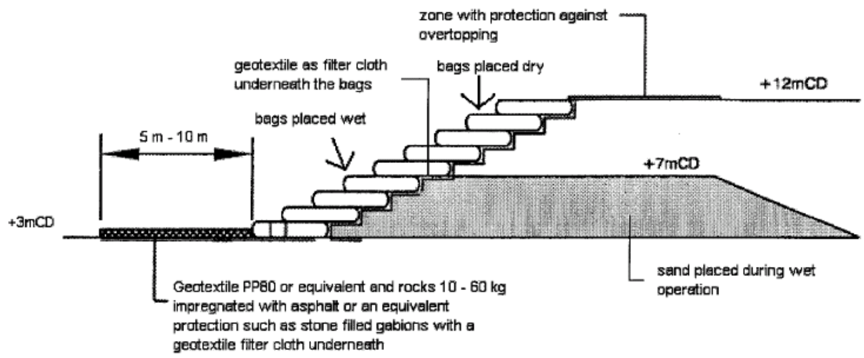

Figure 38: Principle cross section of a temporary sea defence with geotextile containers.

Figure 39: Picture of a geotextile container sea defence - inspection at low water level.

Figure 40: Installation of geotextile containers in Doeldock for an underwater geotextile reinforced dam construction.

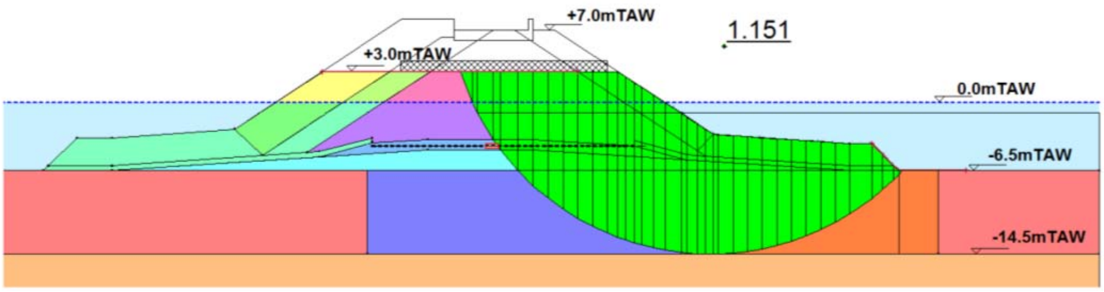

Figure 41: Ostend Breakwater; critical slip surface during construction phase (De Rouck et al, 2010).

Figure 42: Preparation of willow mattress to be towed to open sea for installation on the seabottom as improvement of the foundation for the breakwater.

4. QUALITY ASSURANCE / QUALITY CONTROL IN LAND RECLAMATION

4.1. Specifications

In land reclamation projects, the requirements for compaction/soil improvement can be very diverse. In some cases stringent requirement are set for each and every m³ of the fill while large areas might be used as green areas. Also with regard to testing sometimes excessive testing requirements are specified leading to important time and cost related to such testing. In order to try to give more guidance in defining optimum project specifications, CUR and CIRIA will publish a 'Hydraulic Fill Manual' (van 't Hoff and van der Kolff, 2012) in which the set-up of hydraulic fill project specifications is discussed starting from functional requirements following a Systems Engineering approach.

The driver for specifying compaction of ground improvement requirements should always be the expected performance of the fill in final loading situation. The later use leads to performance requirements which are defined by the use of the fill and environmental boundary conditions such as the possible occurrence of earthquakes (liquefaction). From functional requirements of the land reclamation, performance requirements should follow and these will lead to the detailed technical specification or requirement.

In specifications very often indirect parameters are defined for the real performance that is envisaged. For example a cone resistance is specified where stiffness or shear strength are of relevance. This may lead to specifications that are not correct (e.g. when literature correlation formulas are used for material outside of the validity of the correlation). Together with testing regimes that might be unrealistic for the volumes and areas of land reclamation costs, this may lead to high cost levels because of necessary testing equipment and manpower.

From engineering point of view it often would be better to rely more on Quality Assurance backed by monitoring during execution and to define performance criteria (deformation behavior and bearing capacity) which should be measured as directly as possible.

Setting the criteria to guarantee stability against liquefaction is even more difficult as all practical approaches are based on empirical correlations between the CSR and SPT or CPT values (Youd et al, 2001). The validity of these methods for the project and its sand mineralogy is often uncertain. The full theoretical approach by means of cyclic triaxial testing and cyclic simple shear testing is not often performed, but it is the only theoretical correct way out of discussions when needed. However such tests may take a long time, require qualitative geotechnical laboratories and specialized interpretation. Again calcareous sand, but also low plastic silty soils are the most critical soil types with regard to this issue.

The topic of QA/QC will not extensively be treated here. Main attention will be paid to some points of attention which may lead to confusion.

4.2. Quality assurance

Measuring all possible parameters during execution of Ground Improvement techniques has become standard (e.g. execution report of Vibrocompaction per compaction point (Figure 43) or installation report of PVD per drain). Standard monitoring and registration equipment exists and should be promoted as means for QA. At the same time, good QA should also allow for some relaxation in QC as the second comes with the first.

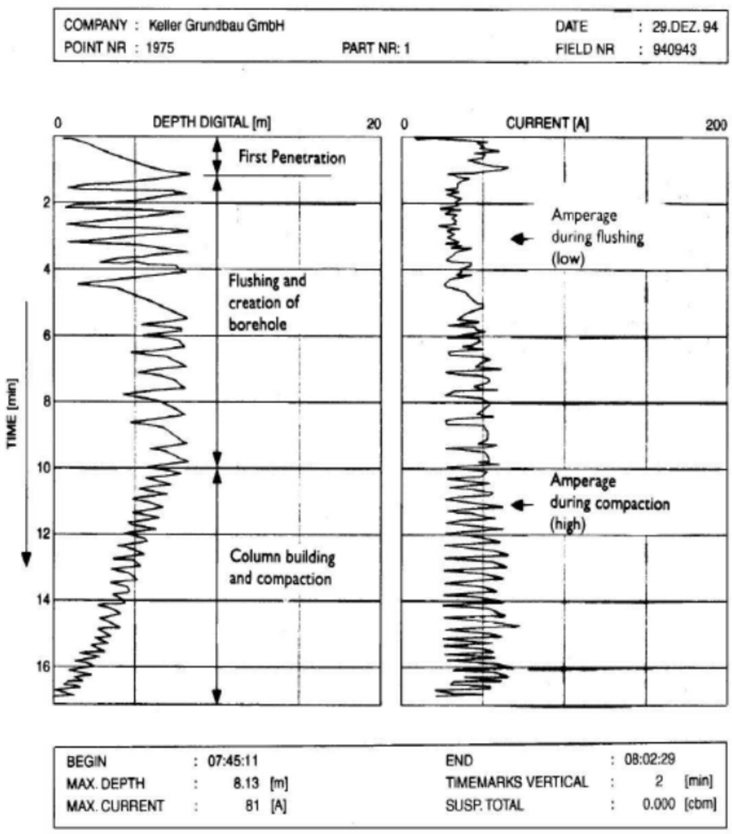

Figure 43: Monitoring during execution of stone column (from KELLER).

4.3. Quality control

4.3.1. Typical working methods

In 2011 a TC211 workshop was held in Hong Kong at the 14th Asian Regional Conference on Soil Mechanics and Geotechnical Engineering on the topic ‘QC-Methods for Ground Improvement Works’. This indicates that this topic is important and needs due attention. The presentations given at this workshop can be found on the TC211 website (www.bbri.be/go/tc211).

Quality control of ground Improvement for land reclamation fill mainly focusses on:

- Settlement monitoring during Ground Improvement; degree of consolidation;
- Soil characterization: particle size distribution (including fines content), plasticity, organic content and carbonate content;

- Compaction control: minimum relative density of relative compaction (= percentage of the maximum dry density to be reached); to be performed different techniques (e.g. in situ density measurement, CPT, SPT, DPT);
- CBR tests (in laboratory and in situ);
- Plate or Zone Load Tests;
- Check of shear strength by laboratory testing;
- Hydraulic permeability (exceptional).

Not all of these items will be discussed here, but sometimes the specification is unclear on the testing method to be used when fill is realized under water and when thick layers are compacted in one operation. A practical solution is: daily sampling at the hydraulic fill pipe; CPT testing for full height material and compaction control and in situ density testing for the top 1 m. This can then be completed by a real in situ performance test: the Zone Load Test which is a large plate load test that allows to test the (long term) deformations of the reclamation under service load (Figure 44).

Figure 44: Set-up for a Zone Load Test.

In Hong Kong, an interesting presentation if given by Hamidi (2011) about the '(In)Validity of Relative Density for Quality Control of Cohesionless Soils'. This is exactly one of the main difficulties in QC of Ground Improvement works: which formulas are to be used; which test method is to be used; many correlation formulas exist between relative density and cone resistance, between relative density and shear strength, between cone resistance and stiffness: which formulas to use; are the correlation formulas valid for the type of sand and mineralogy that occurs on site?

Especially the discussion on calcareous sand is very important in this respect as pointed out by Wehr (2005): an important difference can occur between the cone resistance in silica sand and in calcareous sand compacted at the same density (Figure 45). In practice a 'shell' correction factor is suggested to be used, however the means to define such a factor is difficult and requires calibration chamber testing as the mineralogy of the calcareous sand can change a lot from project to project. In some projects such tests have been realized on the site or together with laboratories with calibration chamber equipment. One should also realized that a specific 'shell factor' is also linked to the correlation q_c versus relative density that is used as basis to derive this shell factor.

In situ density testing at larger depth might lead to errors related to the excavation and difficult execution (Figure 46). At larger depth than about 1 m this test should not be realized or a large excavation for easy access and gentle local excavation in function of the test should be possible. Related to the verification of relative density or relative compaction is the definition of maximum and minimum density. The required tests methods should be well described and take into account the fill material's mineralogy (e.g. with crushable material the vibratory plate test is preferred over the proctor test). Finally, should one define the minimum and maximum density on the material retrieved at each in situ density test? Depending on the homogeneity of the material this might be necessary (e.g. when the sand contains larger gravel size particles from shells or caprock). This again leads to more testing without the possibility for averaging/statistical approach.

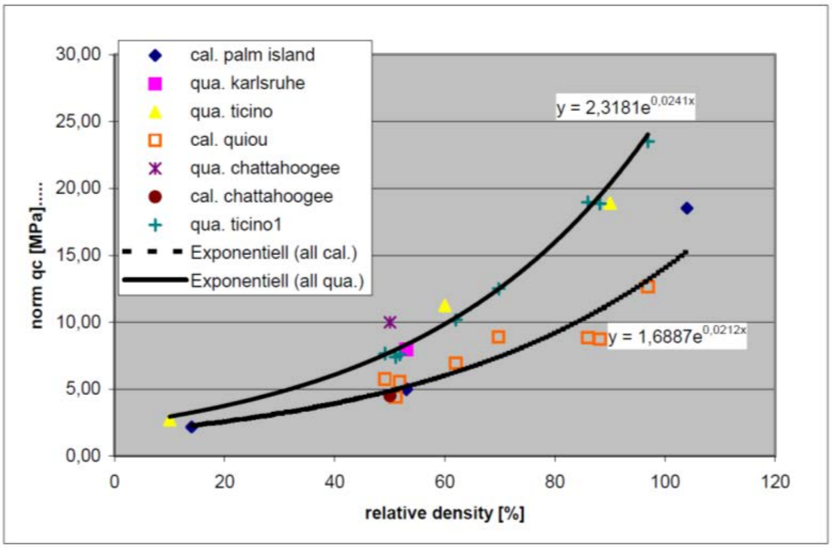

Figure 45: Normalised cone resistance for silica sand and for calcareous sand depending on relative density (Wehr, 2005).

Figure 46: Technician performing an in situ density test (Sand Cone method) in an excavation at 1 m depth.

A typical specification is a required degree of consolidation of the soft subsoil; e.g. 95% consolidation to be reached before hand over of the area. First of all it should be defined whether or not this is under the weight of the fill alone or also under the service load which might be defined. At tender stage theoretical predictions can be made, but settlement always should be based on in situ monitoring because calculations can be erroneous because of the many uncertainties. When surcharge is used, the settlement and degree of consolidation derived from measurements is not necessarily occurring under the same load as required. In that case, one has to predict the final settlement from the monitoring results (e.g. with the Asaoka method, Asaoka 1978) and then, through back calculation, define the final settlement under the required load. Only when this exercise is made, the degree of consolidation can be defined. Such specification, which clearly is a performance specification, requires analysis by geotechnical engineers, both at the side of the contractor as at the side of the client.

When performing CPT testing as QC for Ground Improvement by Vibrofolation of other local impact techniques, the soil will not be fully homogeneous and a specific testing procedure is required. In Figure 47 a sketch is given with compaction points (triangular pattern) and possible locations for testing.

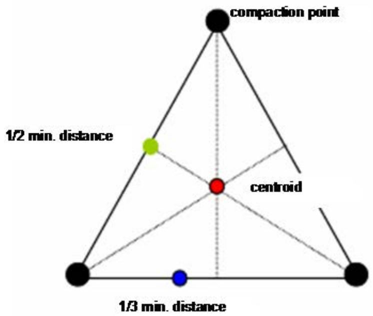

Figure 47: CPT testing within a compaction grid (van 't Hoff and van der Kolff, 1012).

In practice two points are used (e.g. centroid and 1/3 distance) and at each depth interval the average of both tests is used (average in horizontal direction). Subsequently, in order to remove local effects which are not relevant, a moving average is calculated over a height of 0.5 m or 1.0 m (averaging in vertical direction). This last result is used to compare with the compaction CPT-criterion.

4.3.2. Alternative testing methods

Alternative testing methods should focus on the performance of the reclamation that is realized. In this respect the ZLT which is used the last decade now also in land reclamation projects is an interesting development; only, at present this comes on top of all the other more usual tests …

Small Plate Load Tests are not much used in land reclamation projects, although in some countries this test is well established as compaction control test. The PLT requires more use as a replacement for the in situ density test.

More direct testing of stiffness could be realized with the seismic cone or SASW/MASW testing methods. From a theoretical point of view, this is certainly a correct approach, but in practice such specialized testing is not often used as limited qualified testing companies are available. This might, however, be a future development.

4.3.3. Menard Pressuremeter Test

In the former sections, different testing techniques for QC of Ground Improvement works are discussed. In most specifications and in most international literature on this issue the Ménard Pressuremeter Test (PMT) is not included as a reference test while French companies like MENARD do suggest and use this technique. In the framework of this Ménard Lecture it would be wrong not to mention this test as a QC test for Ground Improvement works. However, it certainly is not meant to open the discussion here about the 'most optimal' testing procedure when comparing PMT with CPT.

Somehow the PMT test fits in the above discussion as the PMT is also a test that is directly influenced by soil stiffness and thus more directly measures the real deformation performance of the soil. Disadvantage is that it is a less common type of test that requires a specialist drilling and testing company.

Some references can be given to literature where the PMT as QC test is used and/or compared to CPT: Varaksin et al (2009), Hamidi et al (2010) and Farhat et al (2005). From these references it is also clear that mostly both tests are used and complement each other.

PMT seems to be more suitable in mixed soil types where gravel, stones and boulders occur or in applications where the test is performed inside a stone column to test the design parameters of the Ground Improvement system. Qualitative installation of the PMT in such conditions is made possible with self-bored slotted tube (STAF) technique (Arsonnet et al, 2005).

5. GROUND IMPROVEMENT IN ENVIRONMENTAL ENGINEERING

5.1. Application of Ground Improvement Techniques in Environmental Engineering

In Dredging and Environmental engineering, two main applications of soil improvement can be distinguished:

- In dredging when (slightly) contaminated dredged slurry is reused in land reclamation works or needs to be disposed in a confined landfill;
- On land when contaminated (old industrial) areas or 'Brownfields' need to be remediated to give the area a new destination for industrial or public use.

Although not always named or understood in this way, Ground Improvement techniques are used in these applications as well. Different techniques to improve the sediments or contaminated soil will be discussed shortly in following sections, however in general they are similar to the already discussed techniques in the preceding sections.

5.2. Re-use or controlled disposal of contaminated dredged slurry

Dredged sludge is to be classified as very soft to soft sandy, silty clay. The contaminants will mainly stick to the clay minerals and pre-treatment such as de-sanding by means of hydrocyclones can be one of the pre-treatments to minimize the 'problematic' fraction of the contamination.

Depending on in situ water content, dredging technique (hydraulic versus mechanic) or pre-treatment steps (such as de-sanding), the water content of the sludge can be very high and needs to be lowered for two reasons: to increase the material's strength so that it can be brought into a disposal in a geotechnical safe way and to limit the volume of the sludge to be disposed. Different techniques are possible such as lagooning or mechanical dewatering by means of filter presses and multiple steps have may occur from initial sediment to final storage (Figure 48).

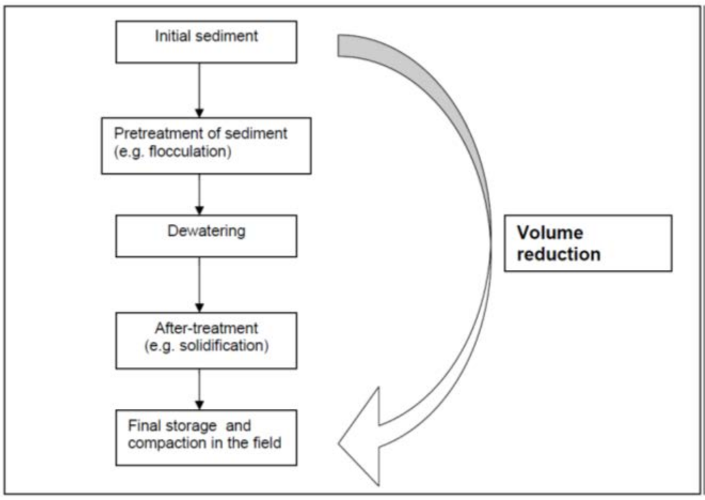

Figure 48: Volume reduction of initial sediment to final stored sediment is a function of all process steps in between.

Lagooning or landfarming (Figure 49) is often used in Belgium and is a technique to allow the sediments to dry out naturally in optimized circumstances: a well-draining bottom layer and, as soon as possible, berms are realized so as to increase the contact surface with air and wind. This process of improvement of dredged sludge is also called 'ripening'. After lagooning the water content of the material will have changed from 100% to 300% to about 25% to 40% (Dry Matter content of about 70% to 80%). Depending on the level of contamination, this material can subsequently be stored in a confined landfill or be used for specific applications. In final situation, such landfills can get different functions such as recreation park area or light industrial area. Some tests have been realized to use the lagooned material in light road foundation (Figure 50) or as cover for industrial waste disposals. In Di Emidio and Van Impe (2006) this application is studied and a practical approach is given with regard to guarantee the required hydraulic permeability of 1 10^{-9} m/s or less. Figure 51 illustrates that the achieved permeability is function of the material's plasticity, water content and the applied compaction energy.

Figure 49: Lagooning (or landfarming) at FASIVER site, Zwijnaarde, Belgium).

Figure 50: Use of 'ripened' clay in a road foundation (Van der Meer and Halter, 2005).

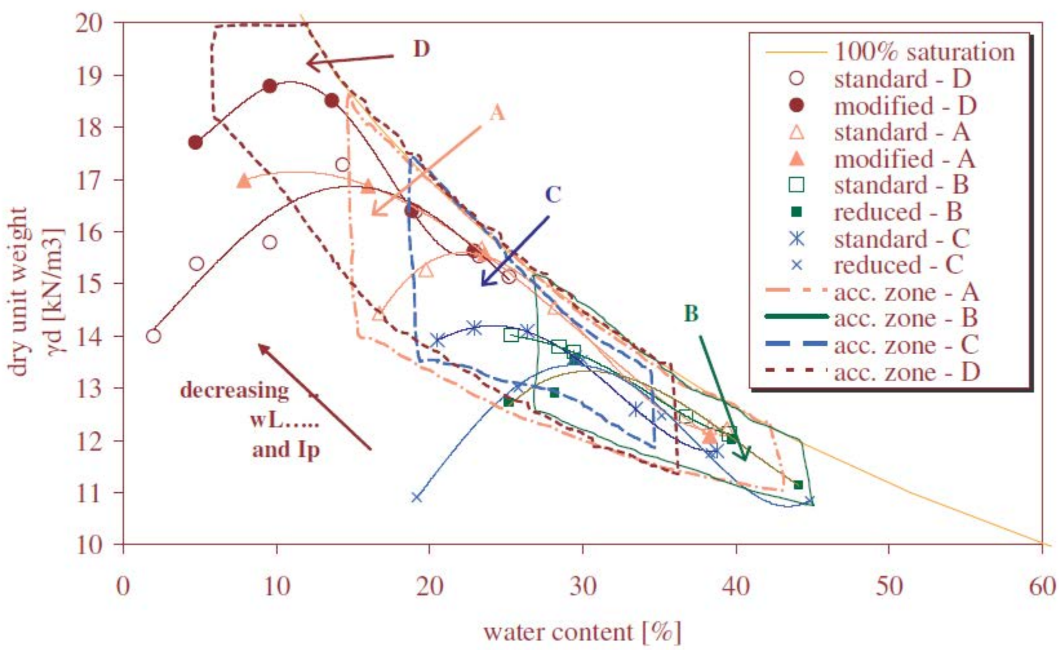

Figure 51: Relationship water content, compaction energy, compaction degree and hydraulic permeability for 4 different dredged sediments (Di Emidio and Van Impe, 2006).

Dewatering by means of filter presses (Figure 52) is less often used as it requires more effort, but for reasonable amounts, the dewatering can be realized in a faster way. The resulting 'filter cake' can (with or without solidification or immobilization treatment) be stored in a confined landfill. More information can be found in Pensaert and Van de Velde (2009) where a case is described where industrial waste products (gypsum precipitate residue from neutralization of spent hydrosulphuric acid from zinc leaching and goethite, which is extremely corrosive), hydraulically pumped into tailing ponds, are dewatered for volume minimization.

Figure 52: Filter presses in operation at an industrial site (Pensaert and Van de Velde, 2009).

As environmental attention and regulations have become more and more important over the last 2 decades, the re-use of slightly contaminated dredged sediments is often required. When studying such cases a distinct selection needs to be made between dredging technique (mechanical or hydraulic) and subsequent treatment operations, mainly aimed to (further) dewater the dredged sediments and to immobilize the contaminants. Typically treatment is to bring the dredged slurry into the reclamation/disposal area, stabilize the top layer to allow access (e.g. by mixing techniques), install prefabricated vertical drains and realize surcharge loading to consolidate/improve the sediments. The critical aspect in this approach is to make the recently dredged sludge accessible. A correct choice in dredging technique is important as well as a good selection of the sand top layer installation technique (e.g. hydraulic application of a sand layer with limited thickness by spraying or by using the very gentle slopes that can be realized hydraulically). Mostly, when only limited construction time is available, the hydraulic dredging techniques should not be used in favor of mechanically dredging such as bucket dredging, backhoe dredging or grab dredging.

Recently, a more and more popular option seems to be the use of geotextile tubes in which sediments are pumped (after treatment with flocculants and possibly other admixtures) for fast dewatering and consolidation. Multiple layers of geotextile tubes can be staggered on top of each other, causing further loading on the lower tubes (Figure 53). The final storage of the dredged and treated sludge is realized after excavation of the tubes, in a landfill where the tubes are integrated or in a useful application as dyke (Figure 54 and Figure 55).

In applications where dredged sludge is stored in geotextile tubes, it has to be considered, looking at the in situ consistency state of the sludge to be dredged, which is the best solution:

- hydraulic dredging whereby an important amount of water will be added, thus causing an important volume increase and subsequent dewatering by means of flocculants in the geotextile tubes;
- mechanical dredging and, if necessary, the application of other techniques of dewatering such as lagooning.

The volume change that occurs in the geotextile tubes after dewatering with flocculants is still very large, even when multiple filling operations are realized. As a consequence, in final situation, the effective use of geotextile is very poor. Often the afore mentioned two alternatives are not well considered or even understood.

Figure 53: Geotextile tubes to store dredged contaminated organic sediments in Hultsfreds, Svartsö, Sweden (Pensaert, 2011).

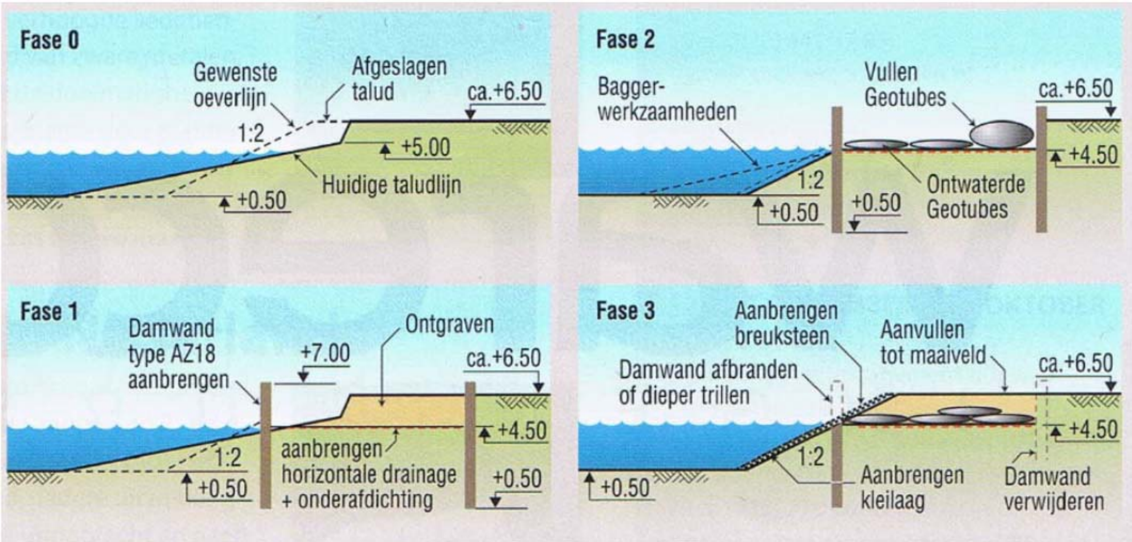

Figure 54: The use of geotextile tubes filled with dredged sludge for dyke construction or repair.

Figure 55: The use of geotextile tubes for dyke strengthening or repair in Zupthen, The Netherlands.

5.3. Contaminated sites remediation

Old industrial sites, whether or not still in use, can be heavily polluted and cause serious damage to the environment. The types of pollution that occur can be very diverse: heavy metals (Zn, Pb, Cu, Ni, Cd, Cr), Cyanides, Arsenic, Acid Tar, etc. Each of those pollutions requires a tailor-made approach to manipulate the contaminated material safely and come to a satisfying stabilization/immobilization. The Ground Improvement treatment here mainly consists of Stabilization/Solidification, leading to immobilization of the contaminants but also to a material that allows long term safe and stable (compaction, shear strength) storage. The storage often requires a confined disposal, but sometimes this will be on site and future operations must be allowable on top of such disposals (Pensaert and Maene, 2008).

The selection of the admixtures to achieve the goal of chemical treatment, immobilize contaminants, fulfilling lixiviation requirements and achieving the required soil mechanical parameters is highly specialized work where an interdisciplinary approach is needed. A few case studies of this type of Ground Improvement are discussed in Pensaert and Maene (2008), Pensaert et al (2008) and De Puydt et al (2008). A further discussion of such Soil Mixing techniques is considered outside the scope of this lecture.

As an illustration, some pictures of an Acid Tar treatment project (Pensaert et al, 2008; De Puydt et al, 2008) are given in Figure 56, Figure 57 and Figure 58. Also in situ deep soil mixing techniques can be used as well for in situ stabilization of contaminated soil (SILT, 1998).

Figure 56: Different types of Acid Tar material to be treated.

Figure 57: The Acid Tar treatment plant on site in its underpressured hall to prevent harmfull emissions to the environment.

Figure 58: Finalising the cover on top of the stabilised Acid Tar landfill at Rieme, Belgium.

6. CONCLUSIONS ON GROUND IMPROVEMENT

In this Menard Lecture about Ground Improvement in Dredging and Environmental Marine Engineering different ground improvement techniques are discussed from an executional point of view in the framework of large land reclamation projects. The selection of the most appropriate technique will be influenced by many factors and an attempt has been made to discuss the different influencing factors.
Some remarks about typical Ground Improvement Specifications are given because incorrect specifications or over-specification can lead to unnecessary high Ground Improvement efforts and related QA/QC costs.
In the last sections the use of Ground Improvement techniques in Environmental (Marine) Engineering is discussed, mainly by means of some examples and references.

REFERENCES

Aelvoet R., Van den Broeck M., Mengé P., Van Mieghem J. and De Preter H., 2005, De toepassing van geotextielen als bouwstenen bij dijkconstructies: Bouwen van een scheidingsdam in het Doeldok, Innovatieforum KVIV (in Dutch).

Al-Homoud A.S. and Wehr J., 2006, Experience of vibrocompaction in calcareous sand of UAE, Geotechnical and Geological Engineering, 24, pp. 757-774.

Arsonnet G., Baud J-P. and Gambin M., 2005, Pressuremeter inside a self-bored slotted tube (STAF), ISP 5 - PRESSIO 2005, 50 Ans de pressiomètres, Gambin, Magnan and Mestat (ed.), ENPC/LCPC press, Paris.

Asaoka A., 1978, Observational procedure of settlement prediction, Soils and Foundations, Vol 18, N° 4, December.

Baker C.N., 2005, The use of the Menard Pressuremeter in innovative foundation design from Chicago to Kuala Lumpur, ISP 5 - PRESSIO 2005, 50 Ans de pressiomètres, Gambin, Magnan and Mestat (ed.), ENPC/LCPC press, Paris.

Bjerrum L., 1967, Engineering geology of Norwegian normally consolidated clays as related to settlements of buildings, Seventh Rankine Lecture, Géotechnique, 17, pp. 81-118.

Bo M.W. and Choa V., 2004, Reclamation and Ground Improvement, Thomson, pp. 411.

Bo M.W., Chu J., Low B.K. and Choa V., 2003, Soil Improvement: Prefabricated Vertical Drain Techniques, Thomson.

CDIT, 2002, The Deep Mixing Method, Principle, Design and Construction, Coastal Development Institute of Technology, Tokyo, Japan, A.A. Balkema Publishers, Swets and Zeitlinger.

CDIT, 2003, The Premixing Method, Principle, Design and Construction, Coastal Development Institute of Technology, Tokyo, Japan, A.A. Balkema Publishers, Swets and Zeitlinger.

Chu J., Varaksin S., Klotz U. and Mengé P., 2009, State of the Art Report: Construction Processes, 17th International Conference on Soil Mechanics and Geotechnical Engineering, M. Hamza et al. (Eds.), IOS Press, pp. 3006-3135.

De Preter H and Vandycke S., 2004, Design and construction of an underwater bund built on dredged material in the Doeldock, WODCON, September.

De Puydt S., Pensaert S. and Mengé P., 2008, De verwerking van sterk verontreinigde grond en teer tot een geotechnisch stabiel materiaal. Case study: Total Ertvelde, Studiedag KVIV Intelligent gebruik van niet geschikte gronden, 10 December, Antwerpen (in Dutch).

De Rouck J., Van Doorslaer K., Goemaere J. and Verhaeghe H., 2010, Geotechnical design of breakwaters in Ostend on very soft soil, 32nd International Conference on Coastal Engineering, Shanghai, China, June 30-July 5.

Di Emidio G. and Van Impe P., 2006, Geoenvironmental characterisation of dredged sediments as alternative material for covers, Proceedings 5th ICGE Environmental Geotechnics, Cardiff, UK, June 26-30th.

Farhat H., Robert J. and Berthelot P., 2005, Extension du port de la Condamine à Monaco. Confortement des sols en place et des remblais sous-marins, Revue Française de Géotechnique, N° 112, 3th trimester.

Gaben J., Gonin H. an Liausu P., Traitement des terrains d'assise de l'extension du depot pétrolier sara a la Guadeloupe, Sols et Foundations (in French).

Gonin H., 2005, Louis Ménard, Mon camarade d'école, ISP 5 - PRESSIO 2005, 50 Ans de pressiomètres, Vol. 2, Gambin, Magnan and Mestat (ed.), ENPC/LCPC press, Paris, pp. 41-50.

Hamidi B., 2011, (In)Validity of relative density for quality control of cohesionless soils, TC211 workshop 26/5/2001, 14the Asian Regional Conference on Soil Mechanics and Geotechnical Engineering, Hong Kong (available on TC211 website).

Hamidi B., Nikraz H. and Varaksin S., 2010, Correlations between CPT and PMT at a Dynamic Compaction project, 2nd International Symposium on Cone Penetration Testing (CPT'10), Huntington Beach, California, USA, May 9.

IADC, 2008, Facts About Soil Improvement, An information update from IADC, number 5, 4 pages.

Kirsch K. and Kirsch F., 2010, Ground Improvement by Deep Vibrotary methods, Spon Press, pp. 198.

Kitazume M., 2005, The Sand Compaction Pile Method, A.A. Balkema Publushers, Taylor and Francis, London.

Klein Breteler M., Stolker C. and de Groot M.B., 2003, Afrondende studies geocontaineronderzoek, Delft Cluster, Intermediate study report DC1-321-12, June (in Dutch).

Kwong A.K.L., Han X.F., Tham L.G., Lee P.K.K. and Zhao W.B., 2008, A field test study on underwater vacuum preloading method, 6th International Conference on Case Histories in Geotechnical Engineering, Arlington, VA, August 11-16.

Ladanyi B., 1995, A brief History of Pressuremeter, The Pressuremeter and its new Avenues, Proceedings of the 4th International Symposium, Sherbrooke, Canada, May 17-19, G. Ballivy (Ed), AA. Balkema, Rotterdam.

Massarch K.R. , 1991, Deep Soil Compaction using Vibratory probes, In ASTM symposium on design, construction and testing of deep foundation improvement: stone columns and related techniques, ASTM STP, R.C. Bachus Edt, pp. 297-319.

Massarch K.R., 2002, Effects of vibratory compaction, Vibratory Pile Driving and Deep Soil Compaction, TRANSVIB2002, Holeyman, Vanden Berghe and Charue Edts., Swets and Zeitlinger, pp 33-42.

Masse F., Spaulding C.A., Wong I.C. and Varaksin S, 2001, Vacuum Consolidation: a Review of 12 years of successful development, Geo-Odyssey, ASCE/Virginia Tech, Blackburg, USA, June 9-13.

Ménard L. and Broise Y., 1975, Theoretical and Practical Aspects of Dynamic Consolidation, Géotechnique, ICE, March.

Mitchell J.K., 1981, Soil Improvement – State-of-the-Art Report, Proceedings of the 11th ICSMFE, Stockholm, Vol. 4, pp. 509-565.

Mosely M.P. and Kirsch K., 2004, Ground Improvement, Second Edition, Spon Press.

Oumeraci H. and Recio J., 2009, Geotextile sand containers for shore protection, Kim Y.C. (ed), Handbook of Ocean and Coastal Engineering, USA, World Scientific.

Pensaert S. 2011, The Svartjö Project: Application of Geotubes for Dewatering and Storage of Contaminated Paper Pulp Sludge, PRISMA, Current and novel sustainable dredging and treatment technologies in inland waterways, Rotterdam, November 17th (PPT presentation).

Pensaert S. and Maene T., 2005, La Floridienne: The first large scale immobilization project in Belgium, CONSOIL 2005, Proceedings of the 9th International FZK/TNO Conference on Soil/Water Systems, October 3-7, Bordeaux, France.

Pensaert S. and Van de Velde K., 2009, Storage Capacity optimization of Tailing Ponds by means of Mechanical Dewatering, CEDA Dredging Days, Rotterdam, The Netherlands, November.

Pensaert S., De Puydt S., Janssens T., Vanpée N., Vander Velpen B., De Cock C and Goorden G., 2008, The remediation of the acid tar lagoons at Rieme, Belgium, CONSOIL 2008, Milano, Italy, June 3-6.

Pensaert S., Zwaenepoel J., Vanhove B., Dewilde J. and De Naeyer F., 2008, Case-Study of the first remediation in Flanders by means of on-site immobilization on a heavy metal impacted site, CONSOIL 2008, Milano, Italy, June 3-6.

Pilarczyk K., 2000, Geosynthetics and geosystems in Hydraulic and Coastal Engineering, Balkema, Rotterdam.

Raithel M., Kirchner A., Schade C. and Leusink E., 2005, Foundation of Constructions on Very Soft Soils with Geotextile Encased Columns – State of the Art, Proceedings of the Geo-Frontiers 2005 congress, ASCE, Rathje E.M. (Ed.), Austin, Texas, January 24-26.

Raithel M., Küster V. and Lindmark A., 2004, Geotextile encased Columns – a foundation system for earth structures, illustrated by a dyke project for a works extension in Hamburg, Nordic Geotechnical Meeting NGM 2004, Ystad, Sweden.

RWS, 2004, Zandophoging op geokunststof omhulde zandpalen, Directoraat-Generaal Rijkswaterstaat, Product-methodeblad nummer 14, oktober (in Dutch).

Sakamoto A., 1998, Cement and Soft Mud Mixing Technique using Compresses Air-Mixture Pipeline: Efficient Solidification At a Disposal Site, Terra et Aqua, N° 73, December.

SILT, 1998, In-situ sanitation of contaminated sediments, soils and sludges, Soft Soil Improvement (SSI), Project Sheet Cargovil Project, SILT (Presently DEC), Belgium.

Smet-Boring, 1992, Bouwrijp maken van terreinen d.m.v. vacuümconsolidatie, Innovatieforum Grondmechanica en Funderingstechniek, KVIV (in Dutch).

van 't Hoff J and Nooy van der Kolff A., 2012, Hydraulic Fill Manual, CUR and CIRIA, to be published fall 2012.

Van der Meer M.T., Halter W.R., 2005, Richtlijn Ophogen met Klei uit Baggerspecie, Ministerie Verkeer en Waterstaat, Dienst Weg- en Waterbouwkunde, Publicatiereeks Grondstoffen 2005/07, DWW-2005-072, Oktober (in Dutch).

Van Impe W. and Verástegui F.D., 2007, Underwater embankments on soft soil: a case history, Taylor and Francis.

Van Impe W., 1989, Soil Improvement Techniques and their Evolution, A.A. Balkema, Rotterdam.

Van Impe W., De Cock F., Massarch K.R. and Mengé P., 1994, Recent experiences and developments of the resonance vibrocompaction technique, Proceedings of the 13th Int. Conf. on Soil Mechanics and Foundation Engineering, pp. 1151-1156.

Van Impe W.F., 1989, Soil Improvement Techniques and their Evolution, A.A. Balkema, pp 125.

Van Impe W.F., De Cock F., Van Der Cruyssen J.P., Maertens J., 1997, Soil Improvement experiences in Belgium: part II. Vibrocompaction and stone columns, Ground Improvement, 1, pp 157-168.

Van Impe W.F., Verástegui F.R.D., Mengé P. and Van den Broeck M., 2005, Considerations on Laboratory test results of cement stabilized sludge, Proceedings Deep Mixing 2005, Int. Conf. on Deep Mixing Best Practice and Advances, Swedish Deep Stabilization Research Centre, Stockholm Sweden, pp. 163-168.

Van Impe W.F., Verástegui F.R.D., Van Mieghem J, Baertsoen A. and Mengé P., 2006, Monitoring the staged construction of a submerged embankment on soft soil, Symposium on soft Soil, Vancouver, Canada.

Van Mieghem J, Van Impe W., Boone C., Mengé P. and Baertsoen A., 2006, Detailed design, validation of the design and monitoring of an underwater embankment built on dredged material in the Doeldock, PIANC.

van Steeg P. and Klein Breteler M., 2008, Large scale physical model tests on the stability of geocontainers, Delft Cluster, Study report H4595, May.

Varaksin S., Yee K. and Toh W.L., 2009, Formulation of a concept and realistic soil parameters for the foundation of randomly located structures on a mega scaled project, Ground Improvement Technologies and Case Histories, Leung C.F., Chu J. and Shen R.F. (eds), Geotechnical Society of Singapore.

Wehr J., 2005, Influence of the carbonate content of sand on vibro compaction, 6th International Conference on Ground Improvement Techniques, Coimbra, Portugal.

Yee K., 2011, On-shore and off-shore compaction for a reclamation projects, TC211 workshop 26/5/2001, 14the Asian Regional Conference on Soil Mechanics and Geotechnical Engineering, Hong Kong (available on TC211 website),

Youd T.L., Idriss I.M., Andrus R.D., Arango I., Castro G. Christian J.T., Dobry R., Finn W.D.L., Harder L.F., Hynes M.E., Ishihara K., Koester J.P., Liao S.S.C., Marcuson W.F., Martin G.R., Mitchell J.K., Moriwaki Y., Power M.S., Robertson P.K., Seed R.B. and Stokoe K.H., 2001, Liquefaction resistance of soils: summary report from the 1996 NCEER and 1998 NCEER/NSF workshops on evaluation of liquefaction resistance of soils, ASCE, JGTGE, Vol. 127, N° 10, October.

SPECIALTY LECTURE

Specialty Lecture – Design Guidelines and Full Scale Verification for MSE Walls with Traffic Barriers Impacted by Vehicles

BRIAUD J.-L., Zachry Department of Civil Engineering, Texas A&M University, College Station, Texas, 77843-3136, USA, briaud@tamu.edu
SAEZ, D., Zachry Department of Civil Engineering, Texas A&M University, College Station, Texas, 77843-3136, USA, dsaez01@neo.tamu.edu

ABSTRACT

Current design practices of Mechanically Stabilized Earth (MSE) retaining walls for highway application required the use of an L shaped barrier-foundation systems on top of the wall to contain the impact of an errant vehicle. These design procedures are moving from an Allowable Stress Design (ASD) method to a Load and Resistance Factor Design (LRDF) method. This change includes consideration of new design parameters that has not been properly defined for the LFRD design approach. Therefore, the bases of this paper is to help understand the dynamic behavior of the system under impact loads, to develop a design guideline procedure based on the LRFD design approach and to verify the propose design guideline.
In a first part, an analytical and experimental approach used to better understand the behavior of the barrier-moment slab system is described. The results of a static load test on a full scale barrier and two impact tests on the same full scale barrier are also presented. Guidelines for the dimensions of the barrier-moment slab system are presented and justified on the basis of the work described.
In a second part, the results of 4 full scale impact tests against barriers of different shape placed on top of an instrumented MSE wall are presented. The wall reinforcement consisted of 2.44 m (8 ft) long bar mats and 2.44 m (8 ft) and 4.88 m (16 ft) long strips. The impact was created by a head-on collision of a 2268 kg (5000 lbs) bogie vehicle. The results of these tests were used to develop the design guidelines of MSE wall with traffic barriers impacted by vehicles.
In a third part, a full-scale crash test on an instrumented 2.79 m (9.15 ft) high MSE wall is described and analyzed. The wall and barrier behaved very satisfactorily and represented a verification of the proposed guidelines.
Conclusions are drawn on the basis of the evidence presented and recommendations are made for future approach.

1. INTRODUCTION

Pavements are often built on top of MSE walls. The most common case is the case of an MSE wall supporting the access embankment for an overpass. Because cars and trucks travel on top of the MSE wall, traffic barriers are required. In the case of a concrete pavement, these barriers are rigidly tied to the pavement to provide the resistance needed when an impact load is generated by an errant car or truck. In the case of an asphalt pavement, that resistance is not available and the barrier must resist the impact load on its own. In this case an L shaped barrier-moment slab system is used (Briaud et al. 2008) and the resistance is generated by the inertia force required to lift the moment slab (bottom part of the L). The impact load also generates forces in the MSE wall reinforcement and wall panels in addition to the static loads due to gravity.

This paper describes the results of a project sponsored by the National Cooperative Research Highway Program (NCHRP) titled: *"Design of Roadside Barrier Systems Placed on MSE Retaining Walls"*. In the first part, the barrier stability was studied through load testing and numerical simulation and recommendations were made (Briaud et al. 2008 and Bligh et al. 2009). In the second part, a 1.89 m (6.2 ft) high wall was constructed and instrumented, and the barrier was impacted by a 2,268 kg (5000 lbs) bogie at approximately 35.41 km/h (22 mph) head on (Bligh et al. 2009 and Kim et al. 2010). The results of these crash tests along with the readings on the instruments and the numerical simulations helped draft preliminary guidelines. The third phase of the project consisted of the proposed guidelines and a full-scale test to evaluate the guidelines. This full-scale test is a pick-up truck crash test on a barrier built atop a 2.79 m (9.15 ft) high instrumented MSE wall. This section also describes the guidelines including the geotechnical design of the MSE wall to contain the truck impact, then the full-scale crash test with the pick-up truck with the results, and then how the result confirm the guidelines. Note that numerical simulations of the impact were also carried out to help in finalizing the guidelines presented here and are described elsewhere (Bligh et al. 2009).

2. DESIGN IMPACT LOADS

The design loads for evaluation of barriers placed on top of MSE retaining wall are based on the current design loads presented in AASHTO LRFD Table A13.2-1 “Design Forces for Traffic Railings” (AASHTO LRFD 2007). These design forces correspond to test levels defined in NCHRP Report 350, "*Recommended Procedures for the Safety Performance Evaluation of Highway Features*" (Ross et al. 1993). This report contains six test levels for evaluation of longitudinal barriers. Test levels 1 through 3 (TL-1 to TL-3) relate to passenger vehicles (820C to 2000P) and vary by impact speed and impact angle. Test levels 4 through 6 retain consideration of passenger cars, but also incorporate consideration of heavy trucks. The research presented in this paper covers TL-3(11) impacts, which, according to the definition of NCHRP Report 350, refers to a pick-up truck weighting 2000 kg (4400 lb.) impacting the barrier at speed of 100 km/hr. (62 mph) at an angle of 25 degrees.

The AASHTO LRFD design loads for TL-3 is 240 kN (54 kips). This load was derived using data from the instrumented wall testing program conducted at TTI during the 1980’s (Beason and Hirsch 1989). The barrier is evaluated using the ultimate strength design procedure (yield line analyses) described in AASHTO LRFD.

However, the AASHTO Manual for Assessing Safety Hardware (MASH) was published in 2009 (MASH 2009). This report is an update to NCHRP Report 350 as an assessment procedure for the performance evaluation of traffic barriers. MASH was developed under NCHRP Project 22-14(2), ‘*Improvement Procedures for Safety-Performance Evaluation of Roadside Feature*” by researchers at Midwest Roadside Safety Facility (MwRSF) at the University of Nebraska. Changes included new design test vehicles, revised test matrices, and revised impact conditions (vehicle mass, impact velocity and impact angle). A comparison between the NCHRP Report 350 and the MASH specification is shown in Table 1.

Table 1: Comparison of test matrices between NCHRP Report 350 and MASH (Ross et al. 1993; MASH 2009)

NCHRP Report 350		*MASH*	
Test Vehicle Designation and Type	Vehicle Weight, kg/ Imp. Velocity, km/h/ Imp. Angle, degrees	Test Vehicle Designation (Vehicle Type)	Vehicle Weight, kg/ Imp. Velocity, km/h/ Imp. Angle, degrees
700C (Small Car)	700 50 20	1100C (Passenger Car)	1100 50 25
820C (Small Car)	820 70 20	1500A (Passenger Car)	1500 70 25
2000C (Pickup Truck)	2000 100 25	2270P (Pickup Truck)	2270 100 25
8000S (Single-Unit Van Truck)	8000 80 15	10000S (Single-Unit Truck)	10000 90 15
36000V (Tractor-Van Trailer)	36000 80 15	36000V (Tractor-Van Trailer)	36000 80 15
36000T (Tractor-Tank Trailer)	36000 80 15	36000T (Tractor-Tank Trailer)	36000 80 15

The new changes introduced by MASH have led to a need of revising the existing design loads recommended in the AASHTO LRFD specification. Under an ongoing research project, sponsored by NCHRP, researchers at the Texas Transportation Institute (TTI) at Texas A&M University conducted an extensive study using existing full-scale crash testing and finite element analyses (FEA) to help update the design loads to be in accordance with MASH. This study has been focused on heavy vehicle impact

(TL-4 and TL-5) since the changes incorporated in MASH for passenger cars and pick-up trucks did not substantially increased the design impact load. The preliminary results of this investigation are presented in Tale 2.

Table 2: Recommended design loads for TL-4 and TL-5 impact (Bligh et al. 2011)

Design Forces and Designations	TL-3(1)	TL-4	TL-5	
Rail Height, H (m)	0.81	≥0.91	1.07	>1.07
F_t Transverse (kN)	240	356	712	1157
F_L Longitudinal (kN)	80	120	334	334
F_v Vertical (kN)	20	169	712	356
Longitudinal Distribution, L_L (m)	1.22	1.22	3.05	3.05
Vertical Distribution, L_v (m)	5.5	5.5	12.2	12.2
Application Point, $H_{e\text{-min}}$ (m) 2	0.6	0.76	0.86	1.1(3)

(1) As currently defined in AASHTO LRFD
(2) Vertical height of the resultant load.
(3) If barriers taller than 1.37 m are used, use $H_{e\text{-min}}$= 1.32 m.

3. CURRENT PRACTICE

AASHTO is in the process of changing from Allowable Stress Design (ASD) to Load and Resistance Factor Design (LRFD) (AASHTO LRFD 2007). The 2004 AASHTO ASD makes use of a 44.5 kN (10 kips) equivalent static design load for the design of the traffic barrier and of the MSE wall below (in the form of added load for the reinforcement). The 2007 AASHTO LRFD makes use of a 240 kN (54 kips) design load corresponding to TL-3 for the design of the traffic barrier and a 44.5 kN (10 kips) design load for the design of the MSE wall. Therefore, there has been a significant increase in the design load for the barrier. The increase from 44.5 kN (10 kips) equivalent static load to 240 kN (54 kips) dynamic load for the structural design of the barrier (design criterion 1: breaking the barrier) does not increase the size of the barrier significantly because 44.5 kN (10 kips) is used with an elastic design analysis while 240 kN (54 kips) is used with an ultimate strength analysis. However when it comes to the moment slab design, the change from 44.5 kN (10 kips) equivalent static to 240 kN (54 kips) dynamic requires a proportional increase in the width of the moment slab if the 54 kips is taken as an equivalent static load. This is where the controversy is. Indeed one would calculate a 1.37 m (4.5 ft) wide moment slab with AASHTO ASD and a 1.37 m (4.5 ft) x 54/10 = 7.4 m (24.3 ft) wide moment slab with AASHTO LRFD. This comes from the fact that 240 kN (54 kips) is taken as a static load when in fact it is a dynamic load. From experience, practitioners think that a 7.4 m (24.3 ft) wide moment slab would be unreasonably conservative. The question is to find out how to take into consideration the 240 kN (54 kips) for overturning and sliding of the barrier.

The design of the barrier against overturning consists of applying the load to the barrier at the prescribed height and then using moment equilibrium to find out how wide the moment slab has to be while satisfying a factor of safety against overturning equal to 2. This factor of safety of 2 is consistent with the requirement for overturning of an MSE wall but is not written in the AASHTO ASD for overturning of barriers. The point of rotation for the analysis is taken to be at the bearing point between the barrier and the soil.

The design of the barrier against sliding consists of applying the load to the barrier and then using horizontal equilibrium to find out how wide the moment slab has to be while satisfying a factor of safety of 1.5. This factor of safety of 1.5 is consistent with the requirement for sliding of an MSE wall but is not written in the AASHTO ASD for sliding of barriers.
In LRFD, the recommendations are not as detailed. The load factor γ is taken as 1.0 for load combination of Service I and the resistance factor for sliding as 0.8 for cast in place concrete on soil. There are no recommendations for the resistance factor against overturning.

4. STATIC AND DYNAMIC STUDY

A static and dynamic study was conducted on a barrier-moment slab system to help evaluate the kinematic behavior of the system when subjected to a static and dynamic load. The maximum static and dynamic forces resisted by a barrier in a sliding failure mode and in an overturning failure mode were determined and compared to quantify the dynamic amplification factor (DAF). These analyses were performed by conducting full-scale tests and FEA using the commercially available finite element program LS-DYNA (*LS-DYNA* 2007). Figure 1 shows the section of the barrier-moment slab system used to conduct the static and the dynamic study.

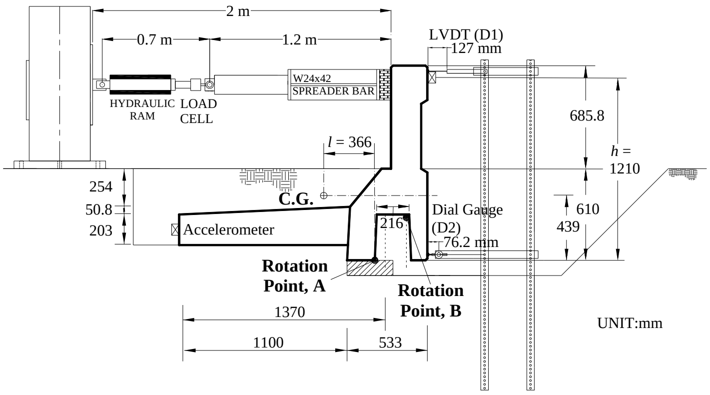

(a)

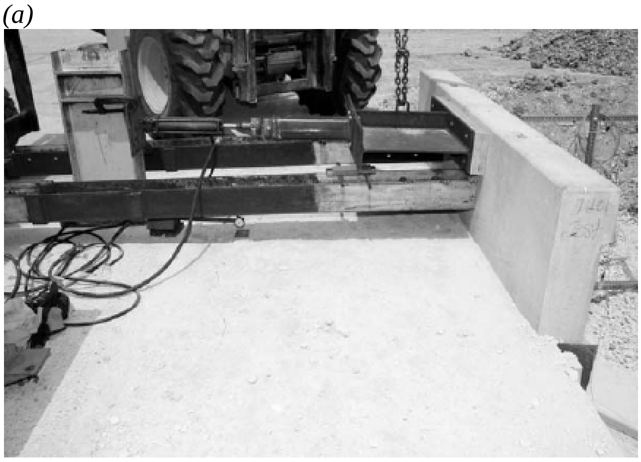

(b)

Figure 1: (a) Details of the barrier-moment slab system and (b) static test. (1 mm = 0.0394 in.)(Briaud et al. 2008)

The first part of these studies was to estimate the force required to generate sliding (F_s) and overturning (F_o) of the barrier-moment slab system using equilibrium equations. These forces were computed using eq. (1) for sliding and eq. (2) for overturning:

$$F_s = W \tan\phi \tag{1}$$

$$F_o = W\, l / h \tag{2}$$

where W is the weight of the barrier- moment slab-soil system (69.6 kN or 15.7 kips), $\tan\phi$ is the moment slab-soil frictional coefficient, ϕ is the friction angle of the soil, *l* is the moment arm of the weight of the system (0.369 m or 1.3 ft), and *h* is the moment arm of the force applied to the system (1.21 m or 3.97 ft).

The results of these analyses are shown on Figure 2 as a function of the length of the barrier-moment slab system. For the 3.05 m (10 ft) length barrier system, the required static force is 46.96 kN (10.6 kips) for sliding and 22.8 kN (5.1 kips) for overturning. Based on these results, overturning controls the stability of the system.

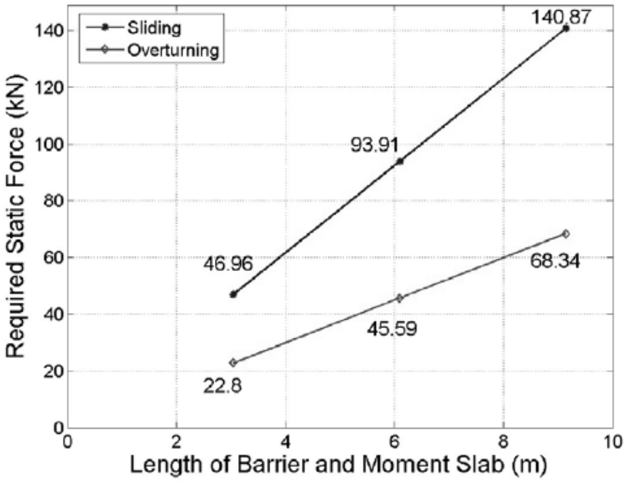

Figure 2: Required Static Force to Induce Sliding or Overturning. (1 kN = 0.22481 kips, 1 mm = 0.0394 in.)(Briaud et al. 2008)

The second part of these studies was to develop a Finite Element (FE) model of the barrier-moment slab system using LS-DYNA (LS-DYNA 2007). The objectives were to simulate both static and dynamic behavior system. The results of the FEA were used to help plan the full-scale static and dynamic test conducted on the barrier-moment slab system. The vertical parapet, moment slab, and overburden soil were described using solid elements. The vertical parapet and moment slab were rigid materials. The soil was an elastic-plastic soil using a two invariant geologic cap model *(*LS-DYNA 2007*)*. The FEA showed that the system failed by overturning, not by sliding. The result of the simulation for the static test is presented in Figure 3 as a load displacement curve. The maximum load in the simulation is 35 kN (7.9 kips) while the static hand calculations gives 22.8 kN (5.1 kips). The difference is that the soil resistance at the edges surrounding the moment slab is included in the simulation but not in the hand calculations.

The third part of these studies was to conduct a full-scale static and dynamic test. The static load test was conducted prior to the dynamic bogie impact tests. The purpose of the static test was to quantify the magnitude of force required to initiate movement of the barrier-coping-moment slab system. The setup for the static load test of the barrier system is illustrated in Figure 1. The load was measured with a load cell and distributed over a longitudinal barrier length of 1 m (3 ft) through the use of a spreader beam. The load test was stopped at a load of 40 kN (9 kips). The force-displacement curves generated from the test data are shown in Figure 3. The load-deflection response of the barrier-coping-moment slab system was linear up to a load of 22.3 kN (5 kips). This load corresponds quite well with the load capacity of this 3 m (10 ft) barrier system based on the rigid body, static equilibrium analysis shown previously (Figure 2). Figure 3(a) shows the load test results compared to the numerical simulation and the hand calculation. This comparison indicates that the static resistance is made of two components: the component due to the weight of the moment slab and overburden soil, and the component due to the friction between the moment slab-overburden soil and the surrounding soil. Back-calculations indicate that the average shear strength of the concrete soil interface at that shallow depth was 6.3 kPa or 126 psf. The results confirm that overturning is the likely mode of failure since sliding develops more resistance. This comparison also gives credibility to the numerical simulation.

Upon completion of the static load test, the soil on and around the moment slab was recompacted for the dynamic bogie impact. Two head-on impact tests were conducted using a 2,268 kg (5000lb) bogie vehicle, shown in Figure 4. The impact velocity of the first and second bogie impact tests was 21 km/h (13 mph) and 29 km/h (18 mph), respectively. These velocities were determined using FEA. The targets affixed to the end of the vertical barrier section were used as reference points to determine angular and translational displacement of the barrier from a high-speed video tape. Figure 5 shows the results of the maximum dynamic displacement of the barrier in the horizontal direction from the two dynamic tests. From film analyses, the dynamic displacement of the barrier for the first test was 125 mm (4.9 in.) at the top (D1) and 69 mm (2.7 in.) at the ground level (D2). For the second test, the dynamic displacement of the barrier for the first test was 200 mm (7.8 in.) at the top (D1) and 104 mm (4.1 in.) at the ground level (D2).

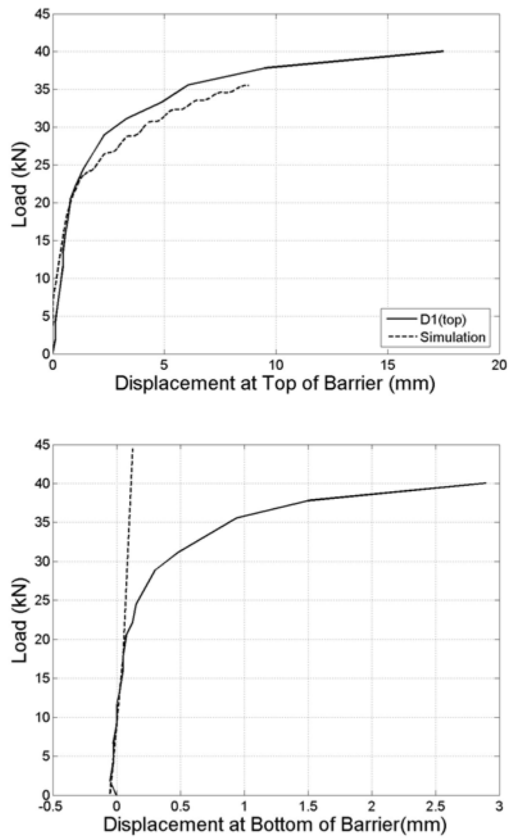

(a) *(b)*

Figure 3: (a) Comparison of static test and FE static model at D1 and (b) static test at D2. (1 kN = 0.22481 kips, 1 mm = 0.0394 in.)(Briaud et al. 2008)

Figure 4: Bogie test with bogie. (Briaud et al. 2008)

Figure 6 shows the comparison of the load displacement curves for the full-scale static test and the dynamic tests. As can be seen the ratio between peak dynamic force and the peak static force is 4.5 for the 21km/h (13 mph) impact test and 5.4 for the 29 km/h (18 mph) impact test.

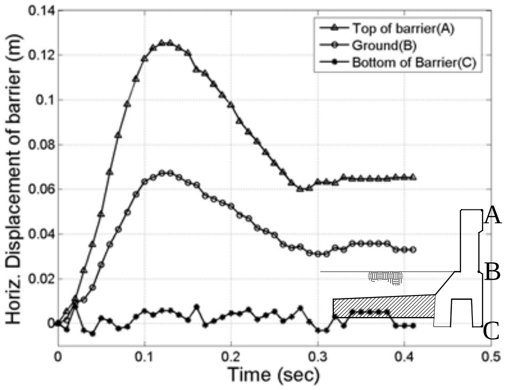

a)

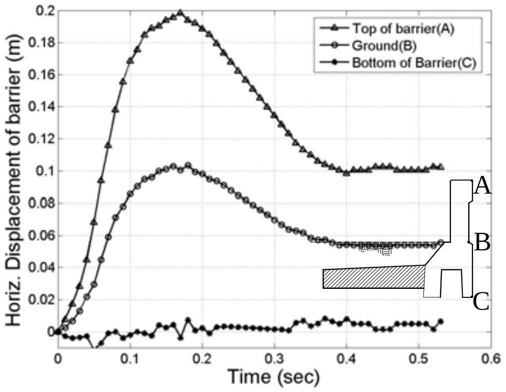

b)

Figure 5: Horizontal displacement of barrier measured from the film of the (a) 21km/h, and (b) 29 km/h impact test (1 mm = 0.0394 in.).(Briaud et al. 2008)

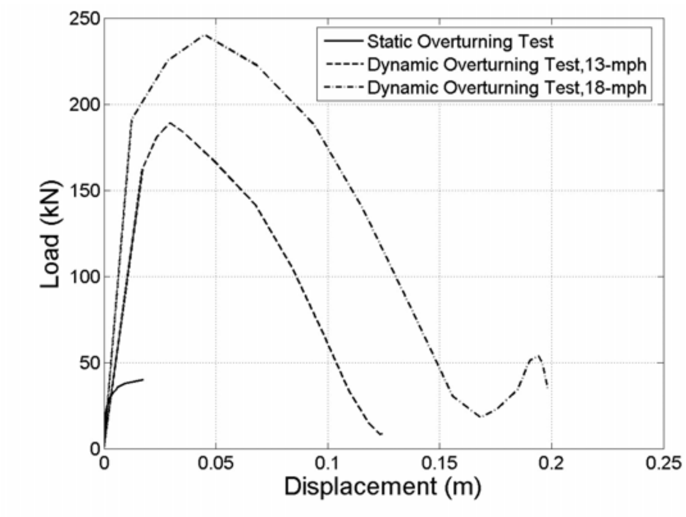

Figure 6: Comparison of static and dynamic overturning tests (1 kN = 0.22481 kips, 1 mm = 0.0394 in.)(Briaud et al. 2008)

5. FULL-SCALE TEST WALL TO DEVELOP THE GUIDELINES

A test wall of 18.3 m (60 ft) long and 1.52 m (5 ft) high was constructed and instrumented. Four impact tests were conducted using a bogie vehicle of 2268 kg (5000 lbs). The objectives of the tests were to quantify the movement of the barrier, the moment slab, and the wall panels during impact, and to measure the barrier impact force and the forces in the reinforcement during impact. An elevation of the test installation is shown in Figure 7.

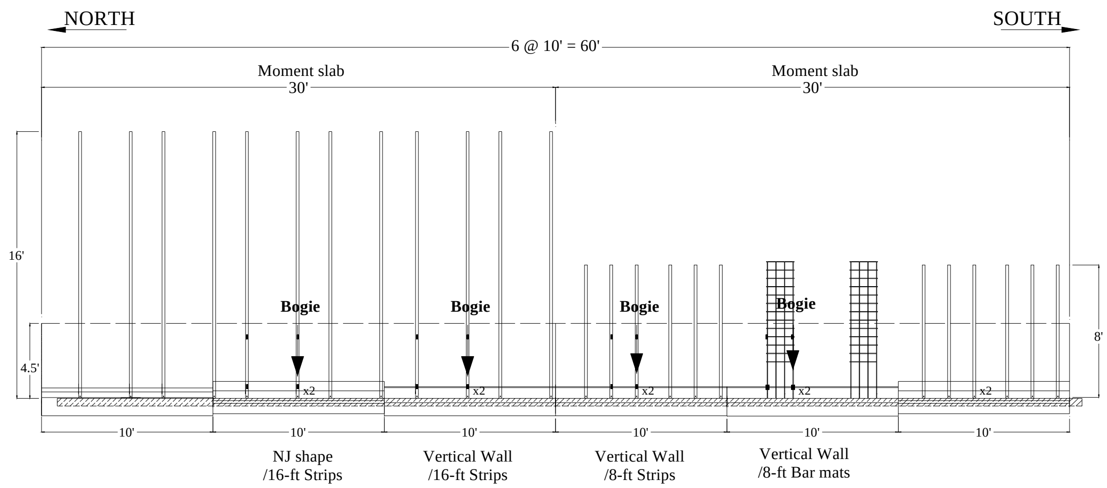

(a)

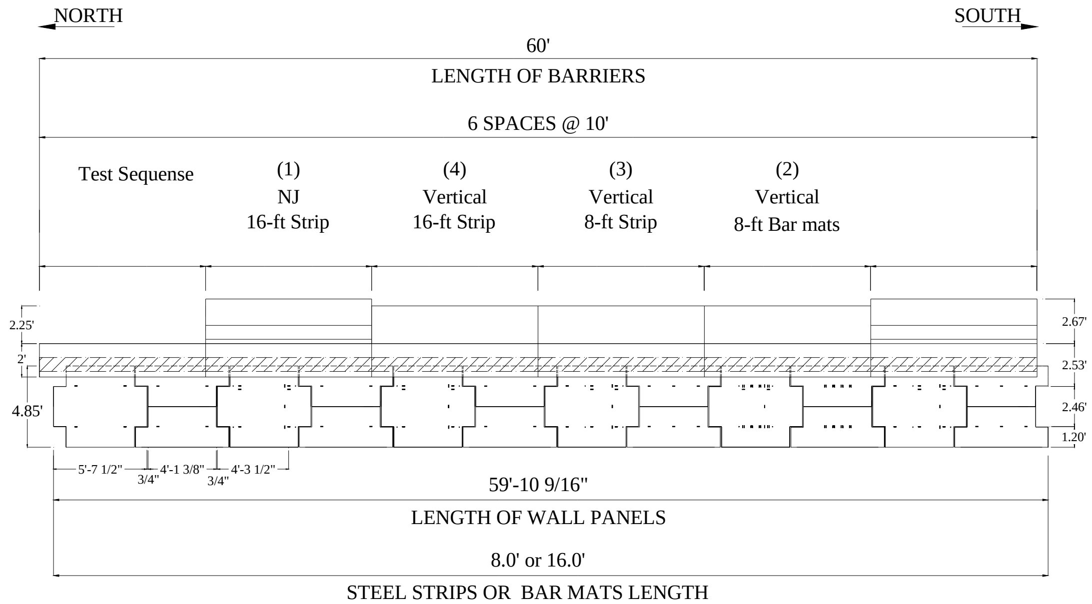

(b)

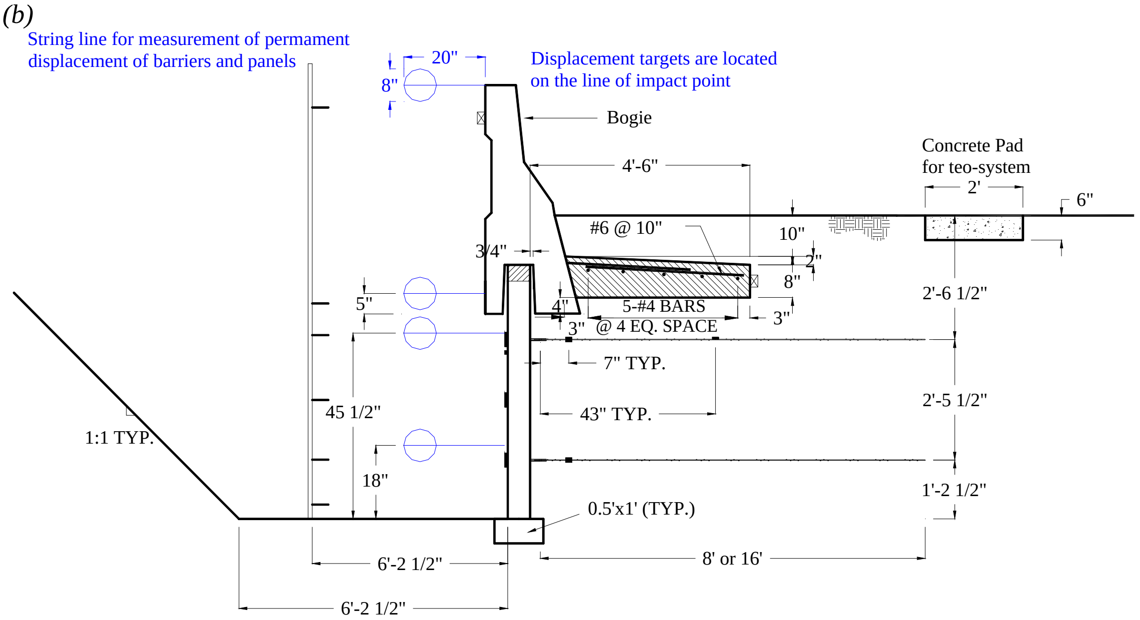

(c)

*Figure 7 **:** Instrumented test wall – plan (a), elevation (b) and side (c) views of test plan (Kim et al. 2010)*

5.1 Design, construction and instrumentation of the test wall

The test wall was designed based on the Load and Resistance Factor Design (LRFD) procedure outlined in the AASHTO Standard Specifications for Highway Bridges (AASHTO 2004). The expected forces on the soil reinforcement due to the design impact load were calculated and compared to those measured in the dynamic impact experiments.

To calculate the force T expected in each strip due to the soil weight and the impact load, the following equation in AASHTO-LRFD was used:

$$T = A_t \times \left(\sigma_h + \Delta\sigma_{h,\max}\right) \tag{3}$$

where A_t is the panel tributary area of one strip, σ_h is horizontal stress due to the soil weight ($\sigma_h = K_r \times \sigma_v$), K_r is the horizontal earth pressure coefficient given by 1.7 K_a, $\Delta\sigma_{h,max} = 2P_{hl} / l_1$ is the horizontal stress due to the impact load P_{h1} on the barrier, and l_1 is the depth of influence of the impact load down the wall face.

To calculate the factored pullout resistance of the soil reinforcement the following equation in AASHTO-LRFD was used:

$$P = F^* \times \alpha \times \sigma_v \times C \times L_e \tag{4}$$

where P is the ultimate pullout resistance (AASHTO LRFD Eq. 11.10.6.3.2-1), F^* is the pullout friction factor (AASHTO LRFD Figure 11.10.6.3.2-1), α is the scale effect correction factor (AASHTO LRFD Table 11.10.6.3.2-1), σ_v is the vertical stress at the depth of the soil reinforcement, C is the overall reinforcement surface area geometry factor based on the gross perimeter of the reinforcement and is equal to 2 for strip, grid and sheet-type reinforcements, and L_e is the length of reinforcement in the resisting zone (effective length). Table 3 shows the results of the estimated design load and the calculated factored pullout resistance based on AASHTO-LRFD design procedure.

Table 3: Calculated design and ultimate resistant load in the soil reinforcement

	Test 1 (New Jersey) (4.88 m Long strips) (4 per panel)	Test 2 (Vertical Wall) (2.44 m Long Bar mat) (Ave. load per bar)	Test 3 (Vertical Wall) (2.44 m Long strips) (6 per panel)	Test 4 (Vertical Wall) (4.88 m Long strips) (4 per panel)
Total Design Tensile Load (kN)	6.5 (upper) 8.9 (lower)	4.3 (upper) 6.1 (lower)	4.3 (upper) 6.1 (lower)	6.5 (upper) 8.9 (lower)
AASHTO Pullout Resistance (kN)	13.4 (upper) 23.6 (lower)	6.2 (upper) 11.1 (lower)	6.7 (upper) 12 (lower)	13.4 (upper) 23.6 (lower)

The MSE test wall shown in Figure 7 was 18.29 m (60 ft) long and 1.52 m (5 ft) high (one panel height).The wall-barrier system was planned on the premise that multiple impacts could be conducted on barrier segments connected to the same moment slab. Half of the wall was constructed using two types of 2.44 m (8 ft) long reinforcement (strips and bar mats) while the other half was constructed with 4.88 m (16 ft) long reinforcement strips, as presented in Table 3. The strips were 50 mm (2 in.) wide and 5 mm (0.2 in.) thick. Each layer of bar mats consisted of two sections of 6 × 6 - W 10 × W 10 bar attached to the wall panel using clevis loops. The 2.44 m (8 ft) long reinforcement represents the minimum length allowed in current practice. Such lengths are commonly used in low height wall segments such as at the beginning or ending of an elevated overpass structure.

The backfill for the wall was crushed rock that met TxDOT specification Type B backfill (TXDOT 2004). The estimated friction angle for the crushed rock was 35 degrees and the unit weight was 20 kN/m^3 (125 pcf). The backfill was compacted in 0.15 m (6 in.) layers with 10 passes of a 1.32 ton (2905 lbs) and 89 cm (35 in.) width drum roller. Also, the surface layer of soil was re-compacted after each test.

The panels of the wall were arranged in a succession of one 1.52 m (5 ft) high full panel followed by two 0.76 m (2.5 ft) high half-panels. All panels were 1.52 m (5 ft) wide. The wall panels were placed on a 0.31 m (1 ft) wide × 0.15 m (6 in.) thick concrete leveling pad.

Six precast barrier and coping sections were placed on top of the wall panels. The panels were recessed inside the coping sections a distance of 0.23m (9 in.) comprised of 0.1 m (4 in) of leveling concrete pad plus 0.13 m (5 in.) of engaged panel. The moment slab connecting the precast barrier-coping sections was cast in two 30-ft lengths connected to one another using two 0.91 m (3 ft) long No. 9 shear dowels. The moment slabs were 1.37 m (4.5 ft) wide from the back face of the wall panel to the end of the moment slab.

The reinforcement was instrumented with strain gages to capture the tensile forces transmitted into the reinforcement during each bogie vehicle impact. A total of 8 strain gages were used for each test. The placement of these strain gages was selected to measure the maximum tensile load in each layer of reinforcement as well as give an indication of the distribution of forces in lateral, longitudinal, and vertical directions. Five strain gages were used on the upper reinforcement layer, and three strain gages were placed on the lower reinforcement layer. Two strain gages were used on both layers of reinforcement adjacent to the wall panel at the point of impact to provide some redundancy at the location expected to experience maximum tensile loading.

A contact switch was placed on the inside face (traffic side) of the concrete leveling pad cast on top of the wall panels to indicate the time at which the barrier came in contact with the wall panel.

The wall panel below the point of impact on each barrier was instrumented with five concrete strain gages to capture normal strains in the panel at impact. Two of the five strain gages were placed in a horizontal direction just below the anchor point of the upper layer of reinforcement (region of maximum negative moment). The other three strain gages were placed in the vertical direction: two were adjacent to the anchorage locations for the upper and lower layer of reinforcement at the point of impact, and one was placed between in the middle of the panel between the two layers of reinforcement (region of maximum positive moment).

An accelerometer was mounted behind each barrier section at the height of impact to help analyze its dynamic response. Another accelerometer was placed at the end of each of the two 9.14 m (30 ft) long moment slabs at their midpoints to measure any acceleration imparted to the moment slab during impact. Additionally, the bogie vehicle was instrumented with an accelerometer.

Rotation as well as vertical and horizontal displacements of the barrier and wall panels were determined from high-speed video operating at 1000 frames/second. Displacement gages were placed at the top and bottom of the precast barrier-coping section and at the upper and lower strip locations on the wall panel to assist with the displacement analysis.

Independently secured string lines were placed 1.22 m (4 ft) behind the barrier and wall to measure the permanent deflection of the barrier and wall after impact. The permanent movement of the four corners of the back of the barrier and the permanent movement of five points on each panel were measured after each test.

The test sequence was selected such that the first two tests involved impacting the barrier segments in the middle of each moment slab (one N.J. barrier and one vertical wall). The other two tests were conducted on vertical concrete barrier located at the end of each moment slab with different strip length and density.

A 2268 kg (5000 lbs) bogie vehicle impacted each test section at a speed of approximately 35.4 km/h (22 mph) for the N.J. barrier and 32.19 km/h (20 mph) for the vertical concrete barriers. Loading each barrier near the ultimate load of the barrier ensured that the maximum impact load was transferred into the MSE wall.

5.2 Impact Test Results

Each time the 2268 kg (5000 lbs) bogie vehicle, shown in Figure 8(b), impacted the barrier head-on at a speed ranging from 32.5 km/h (20.19 mph) to 35 km/h (21.8 mph) (the results are summarized in Table 4).

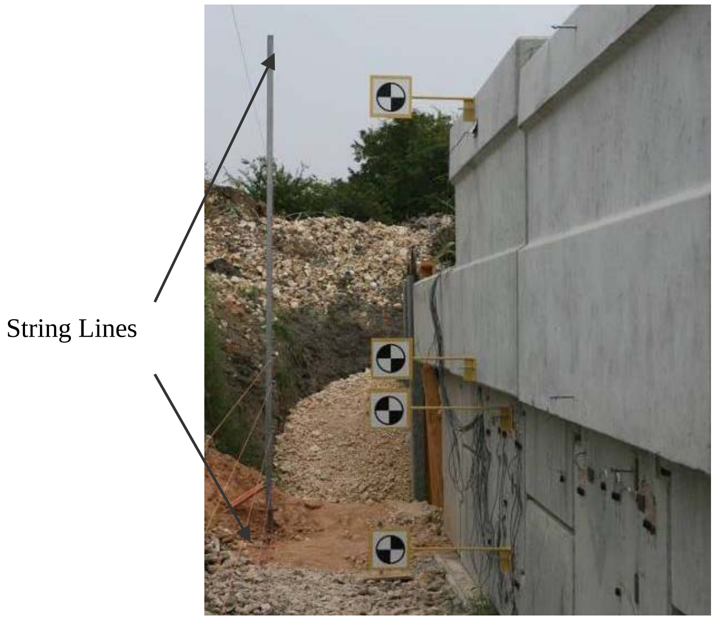

(a) Location of displacement targets and sting line.

(b) Test installation after test.

Figure 8: MSE wall installation before and after tests (Kim et al. 2010)

The impact point for each test is shown on Figure 7. The impact point was positioned above the reinforcement that was instrumented to record the maximum impact forces. The test results include accelerometer data and associated forces and displacements (bogie, barrier, moment slab), high speed film analysis, string line measurements and associated displacements (barrier, wall panel), strain gages and associated forces in the reinforcement (strips, bar mats), and accumulated damage of the barrier, soil, and wall panels.

5.2.1 Dynamic impact load and displacement results

Data obtained from the bogie-mounted accelerometer were analyzed and a 50 millisecond (msec.) moving average was generated. The peak accelerations are shown in Table 4. Based on the acceleration and the mass of the bogie, the maximum impact force was calculated as shown in Table 4. Note that the peak impact forces vary from 286.55 kN (64.42 kips) to 324.72 kN (73.4 kips) and are all higher than the 240 kN (54 kips) dynamic force associated with the design of barriers for test level 3.

Targets were affixed to the top of the barrier, the bottom of the barrier, and the wall panel at a location corresponding to the top and the bottom layers of reinforcement (Figure 7). The maximum dynamic horizontal displacement at the top of the barrier varied from 131 mm (5.17 in.) to 156 mm (6.14 in.). The maximum dynamic horizontal displacement at the bottom of the barrier varied from 18 mm (0.69 in.) to 30 mm (1.16 in.).

Table 4: Test Matrix and Results (1 kN = 0.225 kips, 1 m/sec = 2.237 mi/h, 1 mm = 0.039 in.) (Kim et al. 010)

	Test 1	Test 2	Test 3	Test 4
Barrier Type	New Jersey	Vertical Wall	Vertical Wall	Vertical Wall
Reinforcement	4.88 m long Strip (4 per panel)	2.44 m long Bar Mat	2.44 m long Strip (6 per panel)	4.88 m long Strip (4 per panel)
Speed of Bogie Vehicle	35.08 km/h	32.67 km/h	32.49 km/h	32.49 km/h
Peak Bogie Acceleration	14.45 g	13 g	13.82g	12.69 g
Impact Force	326.5 kN	294 kN	312.1 kN	286.55 kN
Peak Barrier Acceleration	7.36 g	10.71 g	10.16 g	13.04 g
Peak Moment Slab Acceleration	1.84 g	-	1 g	-
Displacement Top of Barrier (mm)	156 (dynamic) 76.2 (permanent)	153.4 (dynamic) 101.6 (permanent)	131.3 (dynamic) 63.5 (permanent)	152.9 (dynamic) 76.2 (permanent)
Displacement Bottom of Coping (mm)	28.5 (dynamic) 14 (permanent)	24 (dynamic) 12.7 (permanent)	29.5 (dynamic) 15.2 (permanent)	17.5 (dynamic) 5.6 (permanent)
Displacement of Panel (mm) (upper layer)	16 (dynamic) 6.1 (permanent)	9.4 (dynamic) 5.1 (permanent)	23.4 (dynamic) 14 (permanent)	7.6 (dynamic) 1.8 (permanent)
Displacement of Panel (mm) (bottom layer)	No movement	2.5 (dynamic) 0.5 (permanent)	4.8 (dynamic) 4.6 (permanent)	1.8 (dynamic) 0.0 (permanent)
Max, 50 msec Avg. Loads In Strips At Top Layer	31.98 kN* (35.36 kN-T, 28.6 kN-B) **	6.85 kN* (6.41 kN-T, 7.25 kN-B) **	9.47 kN* (-1.33 kN-T, 20.28 kN-B) **	33.18 kN* (33.49 kN-T, 32.92 kN-B) **
Estimated Design Load At Top Layer	23.53 kN	5.03 KN	1.98 kN	24.42 kN
Max, 50 msec Avg. Loads In Strips At Bottom Layer	-5.34 kN* (-2.14 kN-T, -8.54 kN-B) **	0.36 kN* (-0.71 kN-T, 1.38 kN-B) **	5.29 kN* (4.36 kN-T, 6.23 kN-B) **	0.67 kN* (-10.85 kN-T, 12.19 kN-B) **
Estimated Design Load At Bottom Layer	-3.91 kN	0.27 kN	3.91 kN	0.49 kN

The maximum dynamic horizontal displacement of the panel at the top layer of reinforcement varied from 8 mm (0.3 in.) to 23 mm (0.92 in.). The maximum dynamic horizontal displacement of the panel at the bottom layer of reinforcement varied from 0 mm to 5 mm (0.19 in.).

The permanent movements of the target locations were obtained in two ways: high speed film analysis and distances from the reference string line stretched in front of the wall (Figure 7). The string line permanent measurements consisted of measuring the distance with a tape measure from the target to the string before and after each test. The permanent horizontal displacement at the top of the barrier varied from 6.3 mm (0.25 in.) to 99 mm (3.9 in.). The permanent horizontal displacement at the bottom of the barrier varied from 8 mm (0.31 in.) to 20 mm (0.79 in.). The permanent horizontal displacement of the panel at the level of the top row of reinforcement varied from 1 mm (0.04 in.) to 16 mm (0.63 in.). The permanent horizontal displacement of the panel at the level of the bottom row of reinforcement varied from 0 mm to 4.1 mm (0.16 in.).

Even though the wall systems were subjected to higher than design conditions, all movements were considered acceptable from a performance point of view. The wall system comprised of the 2.44 m (8 ft) strip reinforcement (Test 3) lead to the highest panel movements, while the lowest movements were recorded for the configuration that incorporated 4.88 m (16 ft) strips and the vertical wall parapet (Test 4). However, the Test 4 configuration also had the most extensive panel damage. In this test, the top panel exhibited a horizontal flexure crack along a line corresponding to the location of the top layer of reinforcement.

5.2.2 Load on the wall reinforcement

The wall reinforcement was instrumented with a total of 32 strain gages (8 for each test) to capture the tensile forces transmitted to the reinforcement during the bogie impacts. The 8 strain gages were placed on 6 strips in two locations: 0.18 m (7 in.) and 1.09 m (43 in.) behind the connection to the panel. Two strips receiving a pair of gages (top and bottom) and the other 4 strips received only one strain gage (top only). Because a fair amount of bending unexpectedly took place in the strips during the impact, the positions which had only one gage did not lead to reliable data. The positions which had two gages permitted cancellation of the bending stresses so that the true tensile load in the strip could be obtained. As a result there are only two strip loads reported for each test in Figure 9. For the bar mats, the strain gages were placed on the bars in similar fashion. The load vs. time history in the reinforcement is a 50 msec. average. Note that the strain gages were zeroed after the MSE wall was built and, therefore, the loads shown do not include the static load necessary to retain the soil mass.

The maximum dynamic load in the strips (50 msec. average) varied from 6.85 kN (1.54 kips) (Test 2) to 33.18 kN (7.46 kips) (Test 4). The higher loads were associated with the 4.88 m (16 ft) long strips while the lower loads were associated with the 2.44 m (8 ft) long reinforcement.

The back-calculated f* values (friction coefficient between the strips and the soil) ranged from 2.58 to 4.51. These measured instantaneous values are much higher than the design recommendation for this case which is 1.79. This is not unusual since the recommended values represent a lower bound of the values measured by many researchers. Note that these friction values are much higher than might seem appropriate at first glance. The reason they are higher than unity is that the strips have ribs which engage the bearing capacity of the surrounding soil in addition to the friction. So, the pull out of strips is not a pure friction phenomenon. The bearing capacity effect is also lumped into the recommended friction factor.

Note also that the sum of the strip forces does not have to add to the impact force because other forces contribute to the resistance including the barrier inertia force and the barrier-soil friction force.

A tape switch was adhered to the back face of the leveling pad extension on top of the wall panels. The idea was to identify whether or not the barrier coping contact and engage the panel during an impact event. The contact duration is indicated in Figure 9 by an arrow labeled “tape switch.” Note that sometimes there are two time periods over which the contact took place indicating that a bouncing phenomenon developed.

As previously noted, the peak dynamic loads against the barriers were higher than 240 kN (54 kips) which is the design load prescribed by AASHTO. To obtain the load on the strips for an impact force equal to 240 kN (54 kips), the loads were reduced by the ratio between the peak dynamic load actually measured and the 240 kN (54 kips) load. So, for Test 1 for example, the strip load corresponding to a 240 kN (54 kips) barrier impact load would be obtained as follows:

$$\text{Estimated strip load for 240 kN (54 kips):} = \frac{54}{73.4} \times \text{Maximum Measured Strip} \quad (5)$$

The estimated strip loads associated with a 240 kN (54 kips) design impact load are shown in Table 4. Note that the peak dynamic impact load on the barrier (Figure 9) occurred before the maximum load in the strips. This seems to indicate that there is a lag time between the barrier movement and the soil deformation which engages the strip loads.

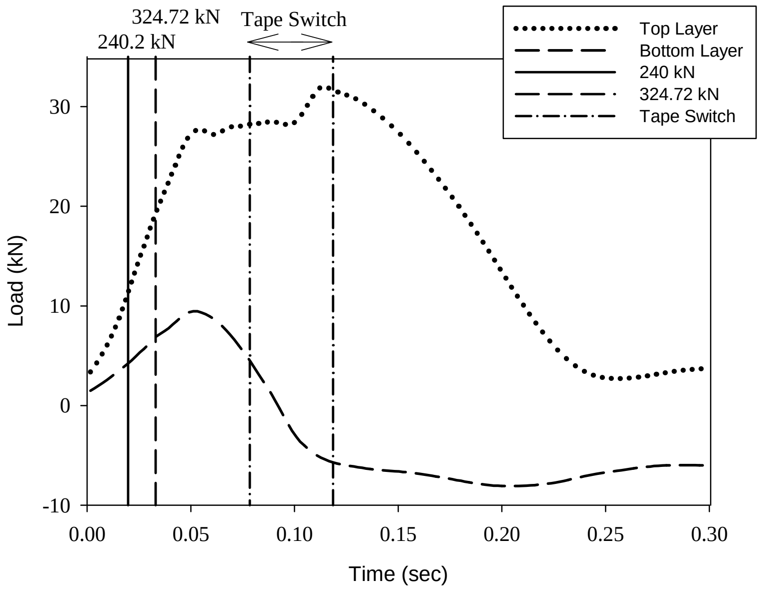

(a) Test 1: 4.88 m long strips on the N.J. barrier.

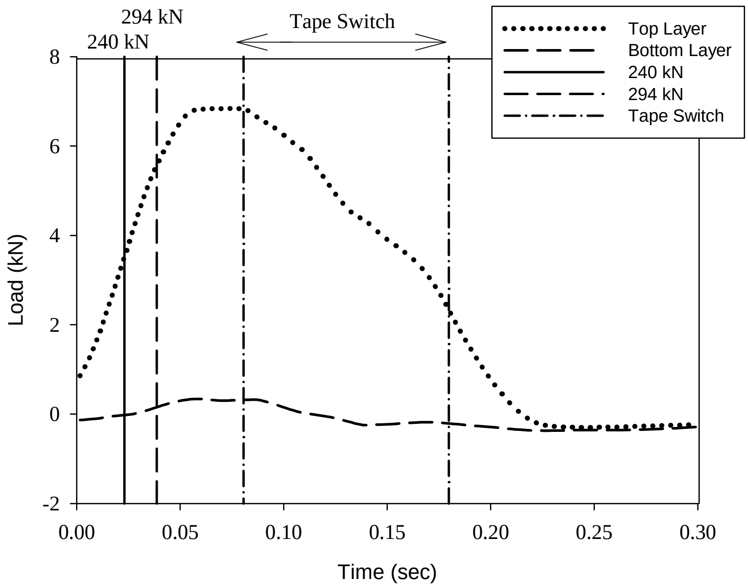

(b) Test 2: 2.44 m long bar mats on the vertical wall barrier.

Figure 9: 50 msec. average load of on the reinforcement (Kim et al. 2010).

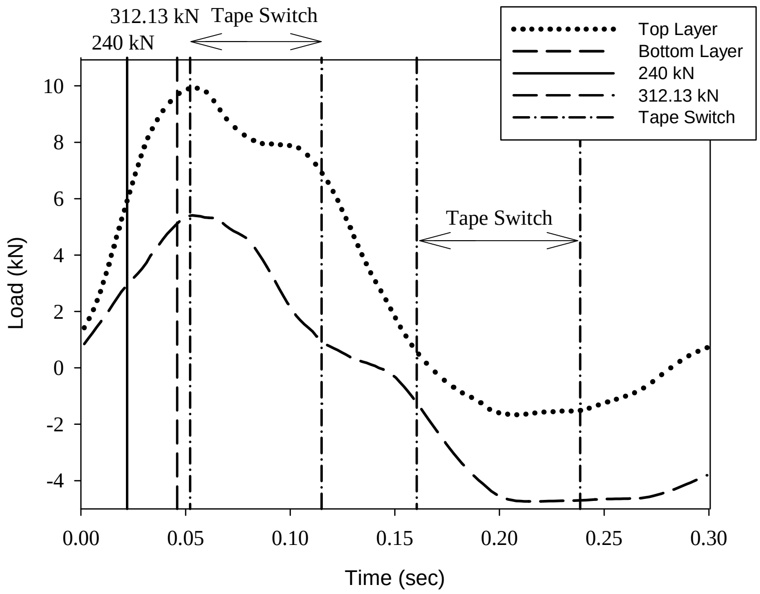

(c) Test 3: 2.44 m long strips on the vertical wall barrier

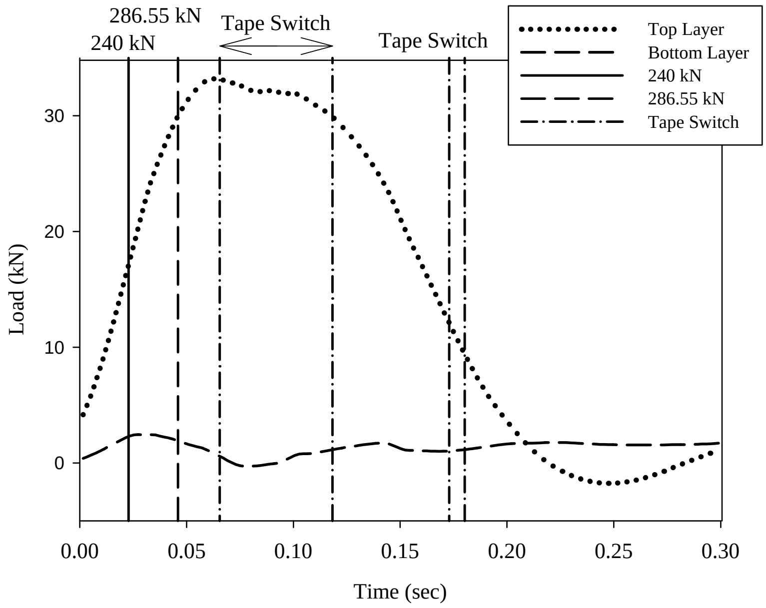

(d) Test 4: 4.88 m long strips on the vertical wall barrier.

Figure 9: 50 msec. average load of on the reinforcements (continued) (Kim et al. 2010).

The second row of reinforcement experienced much lower loads including compression loads in some cases. The reason for this is attributed to rotation of the panel around the first anchor point provided by the top row of reinforcement. This rotation creates a possible inward movement of the bottom of the panel. This compression can be resisted by a combination of strip load and by pressure against the soil mass.

5.2.3 Damage to the barrier and the panels

In all tests, the most severe damage occurred in the barriers. In a real situation, these barriers would have to be replaced. However, it should be noted that the impact load was designed to fail the barrier and exceeded the 240 kN (54 kips) design load. The N.J. barrier in Test 1 failed along a horizontal line located at the change in thickness of the cross section with some evidence of V-shaped cracks. The vertical wall barrier in Test 2 failed along a combination of half V half horizontal line; the reason is that the point of impact was closer to one edge of the 3.05 m (10 ft) long barrier to position the point of impact over one of the bar mats. The vertical wall barrier in Test 3 failed in a V shape pattern with a horizontal line at its base and so did the vertical wall barrier in Test 4. None of the barriers failed in the assumed V shape associated with a traditional yield line failure but rather in a V shape combined with a horizontal flexure mode.

The damage to the MSE wall panels consisted of spalling around the connection between the top of the panel and the bottom of the barrier. This is attributed to the shearing process that broke the bond between concrete leveling pad and the wall panels. This spalling took place in all four tests. In addition, in Test 4 (vertical wall with 4.88 m (16 ft) long strips), a flexural crack developed horizontally across the wall panel at the level of the first row of reinforcement. There was no external evidence of failure of the moment slab, front face of the coping and wall reinforcement. The high speed films did indicate that the edge of the moment slab lifted during impact. A small gap could be seen after the tests at the interface between the moment slab and the soil behind it. Furthermore for the tests near the connection between the two 9.14 m (30 ft) long moment slabs (Tests 3 and 4), the film showed that the edge of the moment slab lifted over the entire 18.29 m (60 ft) indicating that the dowels engaged both 9.14 m (30 ft) length lengths.

6. RECOMMENDED DESIGN GUIDELINES

These guidelines include the barrier-moment slab stability and the geotechnical design of the MSE wall. While the barrier-moment slab stability is not a geotechnical problem it is included here for the sake of completeness and because it helps to understand the geotechnical design of the wall (Kim et al. 2012).

6.1 Stability of the barrier-moment slab system

The guideline for evaluation of stability of the barrier-moment slab system is based on the sliding and the overturning failure mode. For the system to be stable against sliding, the factored static resistance (ϕP) to sliding along its base must be greater than or equal to the factored equivalent static load (γL_s) due to the dynamic impact force (Figure 10).

$$\phi\, P \geq \gamma\, L_s \tag{6}$$

$$P = W \tan \varphi_r \tag{7}$$

where ϕP is the factored static resistance of the system, L_s is the equivalent static load (for load level TL-3, L_s is 44.5 kN according to the results of the aforementioned static and dynamic test), W is the weight of the monolithic section of barrier and moment slab plus any material laying on top of the moment slab and φ_r is the friction angle of the soil-moment slab interface.. The value of ϕ, the resistance factor, is equal to 0.8, and the value of γ, the load factor, is equal to 1.0 because this event is considered to be an extreme event. If the soil-moment slab interface is rough (cast in place), φ_r is equal to the friction angle of the soil φ_s. If the soil - moment slab interface is smooth (precast), φ_r would be reduced accordingly (ϕ_r=2/3tanϕ_s). (Kim et al. 2012).

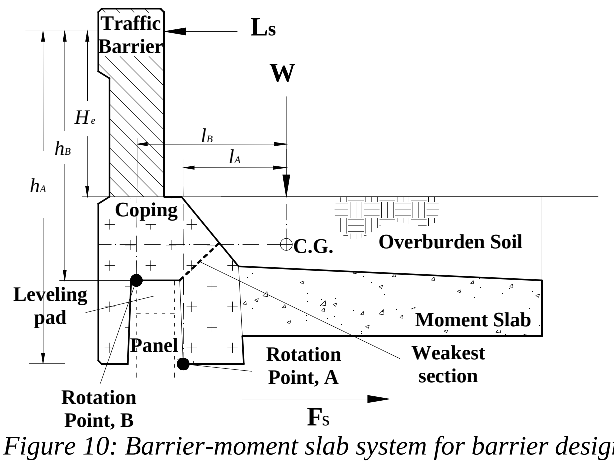

Figure 10: Barrier-moment slab system for barrier design guideline (Kim et al. 2012)

If the barrier-moment slab system rotates during the impact, the point of rotation influences the response. Depending on the design, two points of rotation of the barrier-moment slab system are possible as shown in Figure 10. The point of rotation is determined based on the interaction between the barrier coping and the top of the wall panel. With reference to Figure 10, the point of rotation is taken as Point A if the top of the wall panel is isolated from contact with the coping by presence of an air gap or sufficiently compressible material. The point of rotation is taken as Point B if there is direct bearing between the bottom of the coping and the top of the wall panel or level up concrete. In the full-scale crash test, the point of rotation was Point B.

For the system to be stable against rotation, the factored static moment resistance (ϕ M) to overturning must be greater than or equal to the factored static load (γ L_s) due to the impact force times the moment arm h_A or h_B taken as the vertical distance from the point of impact due to the dynamic force to the point of rotation A or B (Figure 10).

$$\phi M \geq \gamma L_s (h_A \text{ or } h_B) \tag{8}$$

$$M = W (l_A \text{ or } l_B) \tag{9}$$

where ϕ M is the factored static moment resistance (for load level TL-3, L_s is 44.5 kN as mentioned previously, ϕ is the resistance factor equal to 0.9 and γ is the load factor equal to 1.0), W is the weight of the monolithic section of barrier and moment slab plus any material laying on top of the moment slab, and l_A or l_B is the horizontal distance from the center of gravity of the weight W to the point of rotation A or B. The moment contribution due to any coupling between adjacent moment slabs, shear strength of the overburden soil, or friction which may exist between the backside of the moment slab and the surrounding soil is neglected (Kim et al. 2012).

During the impact, the section of the barrier which is most likely the critical section is the narrow part of the coping (Figure 10). This section must be designed to resist the applicable impact load conditions for the appropriate test level as defined in AASHTO LRFD.

6.2 Pullout of the wall reinforcement

The factored static resistance (ϕ P) to pullout of the reinforcement must be greater than or equal to the sum of the factored static load (γ_s F_s) due to the earth pressure and the factored dynamic load (γ_d F_d) due to the impact. The static load F_s is obtained from the static earth pressure p_s times the tributary area A_t of the reinforcement unit. The dynamic load F_d is obtained either from a pressure distribution p_d (Figure 11 (a) for load level TL-3) times the tributary area A_t of the reinforcement unit or the line load Q_d (Figure 11 (b) for load level TL-3) times the longitudinal spacing (S_L) of the reinforcement. The two approaches are equivalent and are presented for convenience as some prefer to use pressures and others prefer to use line loads. The pressure distribution and the line loads are based on measurements made during the impact tests in the instrumented test wall presented before (kim et al. 2012).

$$\phi P \geq \gamma_s F_s + \gamma_d F_d \tag{10}$$

$$\phi P \geq \gamma_s p_s A_t + \gamma_d p_d A_t \tag{11}$$

$$\phi P \geq \gamma_s p_s A_t + \gamma_d Q_d S_L \tag{12}$$

where ϕ is the resistance factor equal to 1.0, γ_s is the static load factor equal to 1.0, and γ_d is the dynamic load factor equal to 1.0. The reinforcement resistance P for strips and bar mats is calculated according to AASHTO LRFD guidelines (eq. (4)). Note that eq. (11) with load and resistance factors equal to 1, as recommended, means that the strips can be designed to be at pull out failure during the impact. This is permitted as the pull out failure condition only exists for a very short time (milliseconds) and did not lead to excessive deflections in the experiments (Kim et al. 2012).

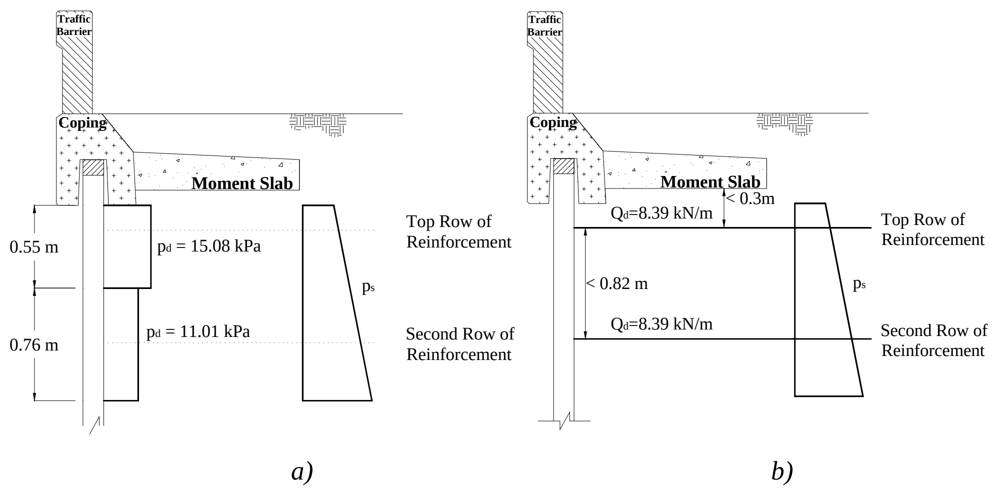

Figure 11: Design load for reinforcement pullout: (a) Pressure distribution p_d , (b) Line load Q_d (Kim et al. 2012)

6.3 Yielding of the wall reinforcement

The factored resistance (ϕ R) to yielding of the reinforcement must be greater than or equal to the sum of factored static load (γ_s F_s) due to the earth pressure and the factored dynamic load (γ_d F_d) due to the impact. The static load F_s is obtained from the static earth pressure p_s times the tributary area A_t of the reinforcement unit. The dynamic load F_d is obtained either from the pressure distribution p_d (Figure 12(a) for load level TL-3) times the tributary area A_t of the reinforcement unit or line load Q_d (Figure 12(b) for load level TL-3) times the longitudinal spacing (S_L) of the reinforcement. The two approaches are equivalent and are presented for convenience as some prefer to use pressures and others prefer to use line loads. The pressure distribution and the line loads are based on measurements made during the impact tests in the instrumented test wall presented before (Kim et al. 2012).

$$\phi R \geq \gamma_s F_s + \gamma_d F_d \quad (13)$$

$$\phi R \geq \gamma_s p_s A_t + \gamma_d p_d A_t \quad (14)$$

$$\phi R \geq \gamma_s p_s A_t + \gamma_d Q_d S_L \quad (15)$$

where ϕ is the resistance factor equal to 1.0, γ_s is the static load factor equal to 1.0, and γ_d is the dynamic load factor equal to 1.0. The reinforcement resistance R for strips and bar mats is calculated by AASHTO LRFD guidelines. Note that eq. (14) with load and resistance factors equal to 1, as recommended, means that the strips can be designed to be at yielding during the impact. This is permitted as the yielding condition would only exist for a very short time (milliseconds) (Kim et al. 2012).

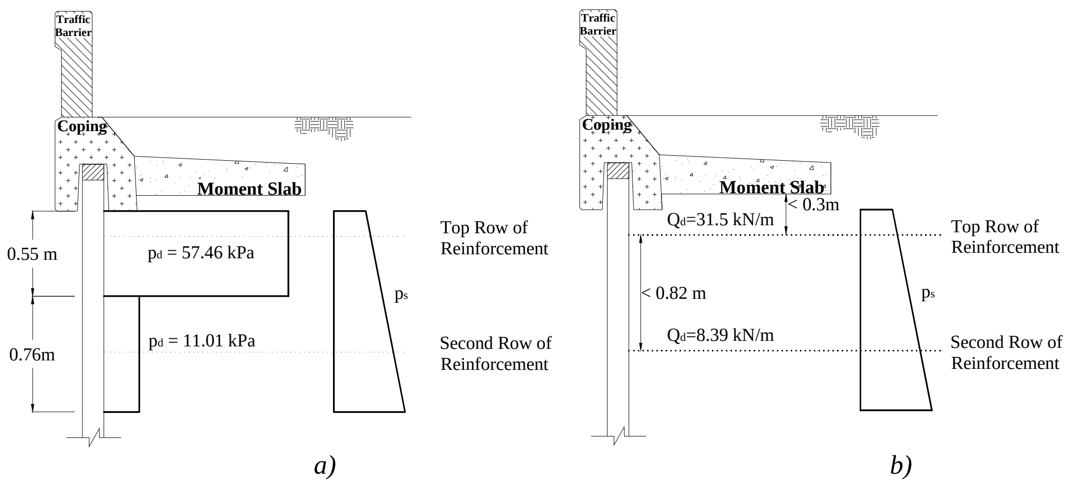

Figure 12: Design load for reinforcement rupture: (a) Pressure distribution p_d , (b) Line load Q_d (Kim et al. 2012).

Note that Figure 11 and Figure 12 are different for the following reason. Figure 12 corresponds to the dynamic loads Q_m actually measured in the strips during impact. The strips do experience the load Q_m and must be safe against yielding under these conditions. The loads Q_m measured in the strips were about 4 times higher than the maximum pull out resistance Q_c of the strips calculated according to AASHTO LRFD. Therefore it was decided that the recommended design values for pull out (Figure 11) should be 4 times less than the recommended design values for yielding (Figure 12). This comment applies to the first row of strips but not the second one. For the second row of strips, the measured loads Q_m were not larger than the calculated loads Q_c, therefore the recommended values for the second layer of reinforcement is the same for pull out and yielding (Kim et al. 2012).

7. FULL-SCALE CRASH TEST TO VERIFY THE GUIDELINES

7.1 MSE Wall Design, Construction, and Instrumentation

The MSE wall and the barrier-moment slab system were designed according to the above guidelines. An overall layout of the MSE wall that was used for the full-scale crash test verification is shown in Figure 13. The instrumented MSE wall was 27.53 m (90.3 ft) long and 2.79 m (9.2 ft) high and the panels were 1.52 m (5 ft) by 1.52 m (5 ft). The MSE wall had three layers of reinforcement. The steel reinforcement strips were 3.05 m (10 ft) long and the reinforcement had a density of three strips per layer per panel.

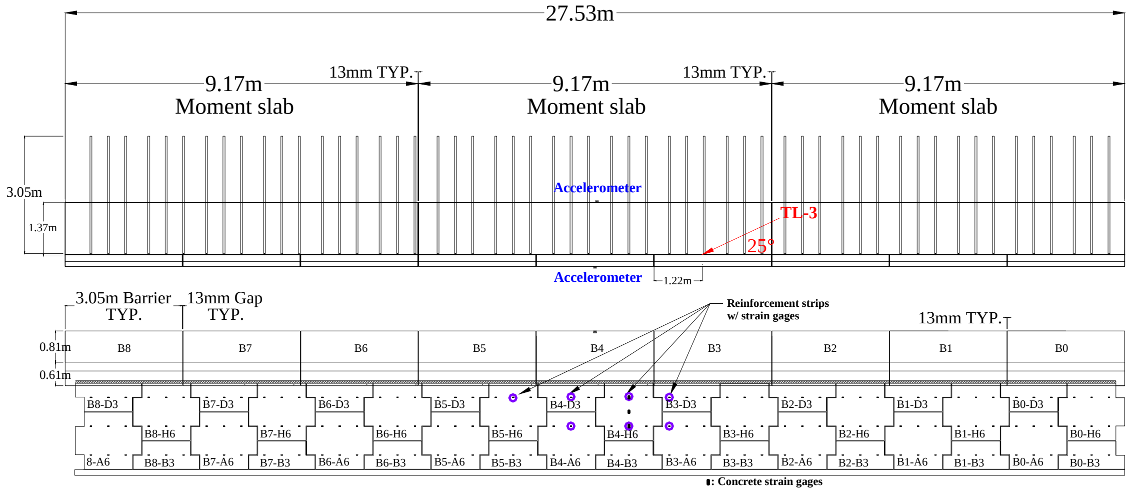

a)

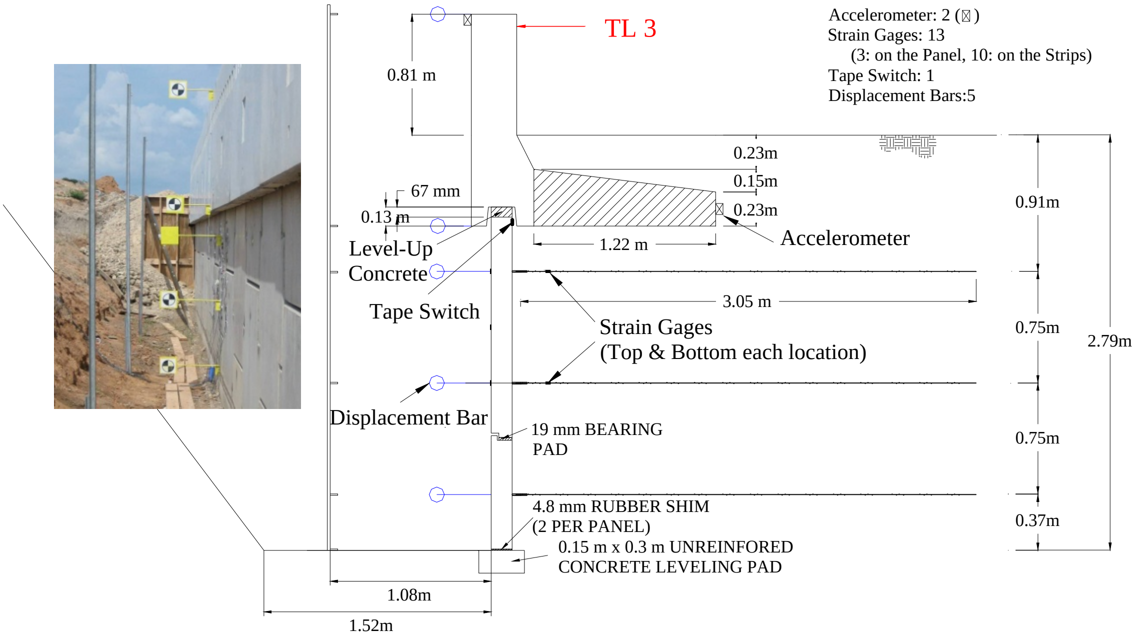

b)

Figure 13: Drawing of barriers on MSE wall: (a) top and plan view and (b) side view (Kim et al. 2012)

The barrier-coping sections rested on a 67 mm (2.6 in.) thick layer of a level-up concrete placed on top of the wall panels. The moment slabs connecting the 3.05 m (10 ft) long precast barrier-coping sections were cast-in-place in three 9.17 m (30 ft) lengths. Three 1.37 m (4.5 ft) wide × 9.17 m (30 ft) long moment slabs were connected to one another using two 0.9 m (3 ft) long No.9 shear dowels across each joint. To enable comparison of forces and displacements, barriers were assigned alphanumeric designators as shown in Figure 13(a).

The barrier portion of the precast barrier-coping sections consisted of a vertical concrete barrier that conforms to the Texas Type T221 traffic rail. Figure 13(b) shows a cross section of the barrier-coping section and MSE wall.

The MSE wall backfill was made of two layers: poorly graded clean sand from the bottom of the wall to the bottom of the moment slab (2.18 m (7.15 ft)) and a limestone rock fill usually used as road base from the bottom of the moment slab to the riding surface (0.61 m (2 ft)). Both the sand and the road base layers were properly compacted.

Seven reinforcement strips in the MSE wall were instrumented with strain gages to capture the tensile forces experienced by the reinforcement during the full-scale crash test as shown in Figure 13(a). These strips were selected because numerical simulation results had indicated that they developed the maximum tensile loads during impact. Two strain gages were used at each selected location (one on the top of the strip and one on the bottom of the strip) to compensate for any bending in the strip.

A contact switch was placed on the top edge of the traffic face (inside face) of the wall panels inside the coping recess. The switch was installed to indicate the time of contact in case the barrier would move sufficiently for the coping to contact the wall panel (Figure 13 (b)).

Two accelerometers were mounted: one behind and at the top of the barrier section immediately downstream of the impact which was shown in the simulation to experience the maximum load and displacement, and one on the end of the 1.22m (4 ft) wide moment slab to monitor the behavior of the moment slab (Figure 13(b)).

Displacement and rotation of the barrier and wall panels were determined from high-speed camera operating at 1000 frames/second. Displacement gages were placed at the top and bottom of the precast barrier-coping section and on the wall panels at heights corresponding to the three layers of soil reinforcement.

7.3 Test Description and Impact Test Results

The TL-3 crash test guidelines described in the Manual for Assessing Safety Hardware (MASH 2009) were followed. This MASH test calls for a 2270P vehicle weighing 2270 kg (5000 lb) hitting the barrier at a speed of 100 km/h (62 mph) at an angle of 25 degrees.

The 2004 Dodge Ram 1500 quad-cab pickup truck (Figure 14) used in the test weighed 2246 kg (4950 lb) and was instrumented with three solid-state angular rate transducers to measure roll, pitch, and yaw rates; a triaxial accelerometer near the vehicle center of gravity (C.G.) to measure longitudinal, lateral, and vertical deceleration levels; and a backup biaxial accelerometer in the rear of the vehicle to measure longitudinal and lateral deceleration levels.


0.000 sec


0.086 sec


0.171 sec


0.340 sec

Figure 14: Sequential photos of MASH test 3-11 **(***Kim et al. 2012)*

7.3.1 Dynamic impact load and displacement results

The 2270P vehicle impacted the MSE wall at a velocity of 101.7 km/h (63.2 mph) and 25.6 degrees. The location of the impact point was 1.22 m (4 ft) upstream of the fourth barrier joint (Figure 13). Figure 14 shows the sequential photos for crash test.

The maximum 50 msec. average longitudinal and lateral accelerations were -6.5 g and 15.67 g, respectively. Data obtained from the truck-mounted accelerometer were analyzed to estimate the impact force using eq. (15).

$$F_i(t) = F_x(t)\sin\beta(t) - F_y(t)\cos\beta(t) = m\left(\vec{a}_x(t)\sin\beta(t) - \vec{a}_y(t)\cos\beta(t)\right) \quad (15)$$

where $F_i(t)$ is the impact force; $\beta(t)$ is the vehicular impact angle as a function of time (yaw angle); $F_x(t) = m\vec{a}_x(t)$ is the longitudinal component of the inertia force; $F_y(t) = m\vec{a}_y(t)$ is the lateral component of the inertia force; and m is the mass of the truck.

The maximum 50 msec. average resultant impact force was 371.3 kN at a time of 0.062 sec. as shown in Figure 15(a). Eq. (15) assumes that the vehicle is a rigid body. In fact, crushing of the front end takes place during the impact. This crushing process absorbs energy and therefore the force obtained from eq. (15), 371.3 kN will be higher than the real force. The numerical simulations of this full scale tests indicated that the real force was 248 kN. According to those numbers the impact force is 67% of the force calculated by eq. (15) (Kim et al. 2012).

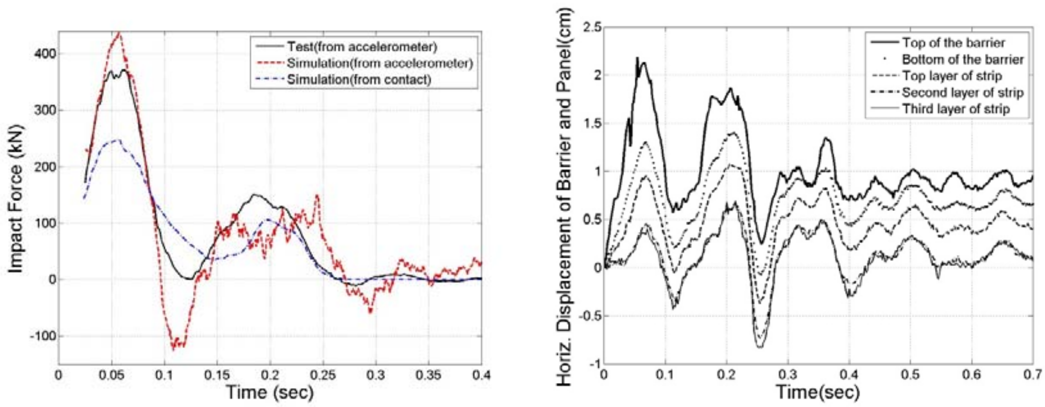

a) *b)*

Figure 15: a) Impact load, b) displacement results (Kim et al. 2012)

The displacement was measured in two ways: videotaping of targets affixed to the wall and barrier, and measurements of permanent displacement after the impact with respect to a benchmark away from the test area. Ten millimeter diameter 0.3 m (1 ft) long steel bars were secured to the top and bottom of the barrier as well as to the top and bottom of the first panel at the level of the strip locations. Targets were attached to the steel bars and were monitored during the impact by a high-speed camera (Figure 13(b)). Note that the location of the targets corresponds to the centerline of panel (B5-H6). The initial position on the movie before impact provided the initial position of the targets and the displacements were recorded with reference to that initial position. Two distinct impacts are evident in the displacement data corresponding to the front end and rear end of the vehicle during the impact. The dynamic displacement associated with the initial impact of the barrier was 21.3 mm (0.84 in.) at the top of the barrier and 13 mm (0.51 in.) at the bottom of the barrier (coping) as shown in Figure 15(b). After the first impact, the barrier began to rebound. The subsequent rear end impact (back slap) resulted in dynamic displacements at the top of the barrier and bottom of the coping of 18.8 mm (0.74 in.) and 14 mm (0.55 in.), respectively. Therefore the first impact was more severe than the back slap impact. The permanent displacement of the barrier was 9.4 mm (0.37 in.) at the top of the barrier and 6.4 mm (0.25 in.) at the bottom of the coping. The maximum dynamic displacement of the panel was 10.7 mm (0.42 in.) at the level of the upper most layer of reinforcement while the permanent displacement was 6.1 mm (0.24 in.) at the same location. No movement was measured at the level of the second reinforcement layer.

After the impact and when the vehicle had come to rest, the permanent deflection measured with respect to the benchmark ranged from 13 mm (0.51 in.) at the top of the joint between barrier segment “B4” and “B5” to 1 mm (0.04 in.) at the bottom of the coping on barrier segment “B5” (Figure 13(a)). The permanent deflection obtained from the film analysis, which tracked the targets placed at the end of the displacement bars affixed to the barrier-coping section, was 9.4 mm (0.37 in.) at top of the barrier and 6.4 mm (0.25 in.) at the bottom of the coping.

All the displacement measurements indicated that the wall and barrier movement are within the tolerance of 25 mm (1in.); therefore the wall and the barrier were satisfactorily designed.

7.3.2 Loads in the wall reinforcement

To enable comparison of forces and displacements, barriers and selected strip locations were assigned alphanumeric designators that describe their horizontal position and vertical reinforcement layer. For example, strip “B4-B-1st” is the strip on barrier B4 at position B and in the first (i.e., upper) layer of reinforcement as shown in Figure 16(a).

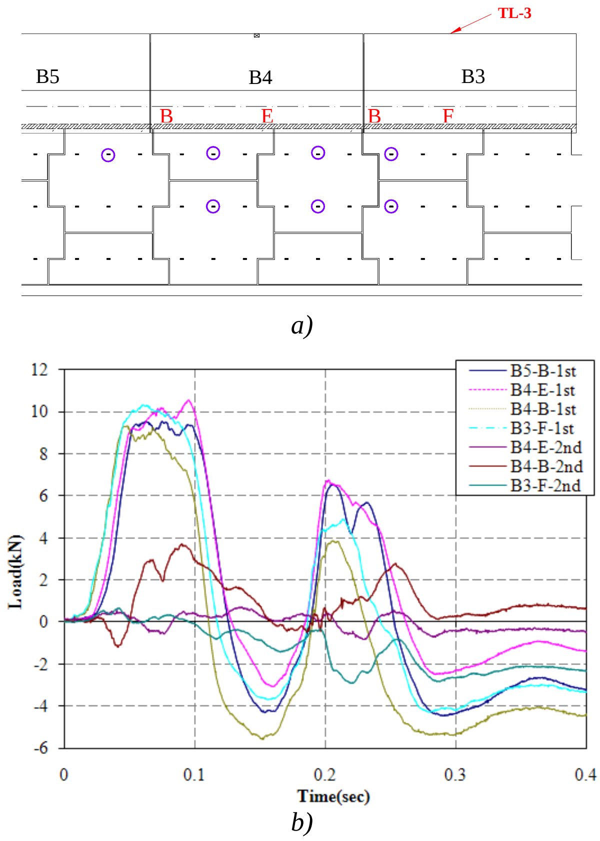

Figure 16: Location indicators and dynamic strip load. (Kim et al. 2012)

The static pull out resistance of the strips was calculated according to AASHTO LRFD and is shown in Table 5.

Table 5: Measured loads and calculated resistances for the wall reinforcement (Kim et al. 2012).

	Static Load (measured) (kN)	Dynamic Load * (measured) (kN)	Measured Total Loads (kN)	Calculated Unfactored Ultimate Resistance** (kN)
Top Layer	3.34	9.79	13.12	6.41
Second Layer	8.23	2.94	11.16	12.01

*: this dynamic load is the maximum of the max. 50-msec average loads in Table 2.
**: AASHTO LRFD Eq. 11.10.6.3.2-1

The static load in the strips due to the earth pressures behind the wall was measured during the construction of the wall. The strain gages on the strips were re-zeroed before the impact test. The dynamic loads generated during the impact test were measured and are shown in Figure 16(b) as 50 msec. averages as a function of time. The maximum value of the raw data and 50 msec. averages are shown in Table 6. Note that all those measured values correspond to a maximum load of 371.3 kN obtained as the truck mass times the maximum truck deceleration. This load is larger than the maximum impact force at the truck-barrier point of impact because it ignores the strain energy absorbed by the crushing of the truck body. The true impact force was estimated from the numerical simulation as 248 kN which is reasonably close to the barrier dynamic design load of 240 kN prescribed by AASHTO LRFD.

Table 6: Measured dynamic loads in excess of the static loads in the wall reinforcement during impact (Kim et al. 2012)

	Top layer (kN)			
	B5-B-1st	B4-E-1st	B4-B-1st	B3-F-1st
Maximum Load from Raw Data	9.56	10.54	9.34	10.32
Maximum 50-msec avg. Load	9.25	9.83	8.63	9.79
	Second Layer (kips)			
		B4-E-2nd	B4-B-2nd	B3-F-2nd
Maximum Load from Raw Data		0.71	3.69	0.67
Maximum 50-msec avg. Load		0.40	2.94	0.27

As can be seen from Table 5 and Table 6, the total load measured in the first level of reinforcement exceeds the calculated pull out resistance by AASHTO significantly. Since the measured load was about two times larger than the AASHTO calculated load, and since the panel pulled out about 10 mm (0.39 in.) during impact, it is possible that the strips were at pull out failure during the impact. Indeed a pull out movement of 10 mm (0.39in.) is typically sufficient to generate the full friction of a soil steel interface for a relatively rigid member such as a strip. It is also possible that the calculated pull out resistance was underestimated by the use of lower bound values of F^* for the friction between the strips and the soil as recommended by AASHTO LRFD. It is also possible that the dynamic resistance is higher than the static resistance; however this possibility was dispelled by tests performed at different rates in an earlier part of the study (Kim et al. 2012). In any case, even if the strips were at pull out failure during the impact as allowed in the proposed guidelines, the wall behaved very satisfactorily and it would be fine to have the strips at pull out failure for this extreme and very short duration event. A more proper design would consider a deflection based design as is done in earthquake engineering (Wartman et al. 2006); this approach is more complicated but more fundamentally acceptable and work is progressing in that direction.

7.3.3 Damage to the barrier and wall panels

The panels did not crack during the impact. This was later confirmed by observation. The contact switch placed on the top edge of the level-up concrete on top of the wall panel inside the coping recess indicated that the coping did not contact the wall panel. Damage to the barrier was mostly cosmetic. There was a crack in the soil along the edge of the moment slab. This crack was about 2 mm (0.08 in.) wide and existed over two moment slabs, from B0 to B5, for a length of 18 m (59 ft) (Figure 13(a)). Overall the test was deemed successful because the vehicle did not go over the barrier, did not roll over, and was safely redirected on the road way.

8. SUMMARY AND CONCLUSIONS

Guidelines for traffic barriers on top of MSE walls were developed on the basis of full scale bogie and pickup truck tests (Bligh et al. 2009; Briaud et al. 2009; Kim et al. 2012) and are presented in an LRFD format. They address pullout and rupture of the MSE wall reinforcement, structural adequacy of the MSE wall panels, sliding and overturning of the barrier-moment slab system, and structural adequacy of the coping. The dynamic design loads for the reinforcement are specified using a pressure distribution approach or a line load approach.

A full-scale pickup truck (TL-3) crash test into a vertical wall barrier mounted on the edge of a 2.78 m (9.1 ft) tall MSE wall was performed. Damage and displacement of the MSE wall panels and the barrier system were minimal and within tolerance. The load in the top level of reinforcement was much higher than the maximum load calculated by AASHTO-LRFD Bridge Specifications. This is due to the fact that these specifications are quite conservative. These high loads also mean that the reinforcement could have been at pull out failure during most of the impact. This situation is deemed acceptable and allowed in the guidelines because it occurs over a very short period of time (about 20 ms) and because the observed wall displacement during that very short time is within tolerance (less than 25 mm). A more proper design would consider a deflection based design; this approach is more complicated but more fundamentally acceptable and work is progressing in that direction.

The barrier was made of 3.05 m (10 ft) long precast barrier-coping sections connected to a 1.37 m (4.5 ft) wide and 9.17 m (30 ft) long moment slabs and performed as well as the wall. This wall barrier system was designed according to the guidelines presented at the beginning of the paper. It behaved very well and no repairs would be necessary. Since it performed very well, this full scale crash tests represents a verification of the proposed guidelines.

9. ACKNOWLEDGMENTS

The content of this paper presents a summary of the final result of a project sponsored by the National Cooperative Highway Research Program (NCHRP). The opinions expressed in the paper are those of the authors and not necessarily those of NCHRP. The authors wish to thank the research team involve in that project, Dr. Roger Bligh, Dr. Akram Abu-Odeh and Dr. Kang-mi Kim, and the NCHRP panel members for their input and help in particular Mark McClelland, chair of the panel. The authors also wish to sincerely thank the Reinforced Earth Company (Pete Anderson, John Sankey) for providing the barrier, sharing data, and answering many questions. Finally, the authors wish to thank Foster Geotechnical (William Neely) for sharing their experience on MSE walls.

REFERENCES

AASHTO. (2004). AASHTO LRFD bridge design specifications, 3rd Ed. AASHTO, Washington, D.C.

AASHTO. (2007). AASHTO LRFD bridge design specifications, 4rth Ed. AASHTO, Washington, D.C.

AASHTO. (2009). Manual for Assessing Safety Hardware, AASHTO, Washington, D.C.

Beason, W.L. and T.J. Hirsch (1989). Measurement of heavy vehicle impact forces and inertia properties. Research Report, Texas Transportation Institute, College Station, TX, 1989.

Bligh, R. P., Briaud, J.-L., Abu-Odeh, A. Kim, K.-M and Saez, D.-O. (2011). "Interim Report: Design Guidelines for TL-3 through TL-5 roadside barrier systems placed on mechanically stabilized earth (mse) retaining walls", Interim report prepared for National Cooperative Highway Research Program project 22-20(2), Transportation Research Board, National Research Council, performed by Texas Transportation Institute, College Station, Tex.

Bligh, R. P., Briaud, J.-L., Kim, K.-M. and Abu-Odeh, A. (2009). "Design of roadside barrier systems placed on mse retaining walls", Final report prepared for National Cooperative Highway Research Program project 22-20, Transportation Research Board, National Research Council, performed by Texas Transportation Institute, College Station, Tex.

Briaud, J.-L., Bligh, R. P., Abu-Odeh, A., and Kim, K. (2008). "Stability analysis and full scale test of a traffic barrier-moment slab system", Transportation Research Record: Journal of the Transportation Research Board, Volume 2050, 26-38.

Kim, K-M. Briaud, J.-L., Bligh, R. P., Abu-Odeh, A., and Saez D. O. (2012). "Design Guidelines and full scale verification for MSE wall with traffic barriers", Journal of Geotechnical and Geoenvironmental Engineering, Vol. 137, No.6, ASCE.

Kim, K-M. Briaud, J.-L., Bligh, R. P., and Abu-Odeh, A. (2010). "Full scale impact testing of four traffic barriers on top of an instrumented MSE wall", Journal of Geotechnical and Geoenvironmental Engineering, Vol. 136, No.3., ASCE.

LS-DYNA: Keyword User's Manual, Version 971, Livermore Software Technology Corporation, Livermore, California, 2007.

Ross, H.E., Jr., D. L. Sicking, R. A. Zimmer, and J. D. Michie (1993). NCHRP Report 350: Recommended Procedures for the Safety Performance Evaluation of Highway Features. Transportation Research Board of the National Academies, Washington, D.C., 1993

Texas Department of Transportation (2004). Standard specification for construction and maintenance of highways, streets, and bridges. TxDOT, June 2004.

Wartman, J., Rondinel-Oviedo, E. A., Rodriguez-Marek, A. M. (2006). "Performance and Analysis of Mechanically Stabilized Earth (MSE) Walls in the Tecomán, Mexico Earthquake," Journal of Performance of Constructed Facilities, Vol. 20, No. 3, pp. 287-299.

VARIOUS CONTRIBUTIONS

Study on pore water pressure dissipation phenomena of soft clays through consolidation using vertical drains

Manish V. Shah, The Maharaja Sayajirao University of Baroda, India, mvs2212@yahoo.co.in
Arvind V. Shroff, The Maharaja Sayajirao University of Baroda, India, dravshroff@yahoo.co.in

ABSTRACT

Paper represents the most critical part of the one dimensional consolidation process through radial flow using vertical geodrains that is development and dissipation of hydrostatic pore water pressure at constant magnitude of stresses. Complete consolidation test was carried out on modified hydraulically pressurized Oedometer with three vertical drains viz. sand drains, coir-jute fiber drain and polypropylene fiber drain of 'n'(ratio of drain diameter to diameter of soil sample) values 11.04, 16.93 and 21.71. Various consequences associated with consolidation of soft clays like non-homogeneity, time effects intrinsic to the soil skeleton along with physico-chemical changes and compressibility of the pore fluid and solids along with variation of compressibility and permeability are attributed to be mainly influenced by drain material, drain size, and drain shape. Theory of consolidation proposed by authors to obtained degree of consolidation based on pore pressure measurements(isochrones) introduces lump parameter 'λ' which reflects efficacy of vertical drain for particular soil conditions. Comparative results of all three vertical drains matched well with author's theory of consolidation through radial flow.

1. INTRODUCTION

India is a country having long coastal line of nearly 5000km length having deposits of soft, weak and highly compressible soft soil mass. Due to rapid infrastructure activity on these coastal planes, ground improvement by vertical geodrains is one better solution for large areas and that also by using local available filler materials will be most preferred by an engineer. Vertical drain design is a function of permeability (discharge) which is function of compressibility of soil skeleton and which is further dependant on dissipation of pore water pressure under constant magnitude of stresses. So through this study an attempt is made to propose a theoretical philosophy of role of clay particle structure on pore water particle between soil and at drain interface. Kaolin clays are produced by chemical weathering of alumino-silicates and are generally grouped as colloidal particles. Clay particles are plate shaped or tubular because the layer-lattice structure results in strong bonding along two axes but weak bonding between layers. The variation in specific surface area is primarily due to different thicknesses of the tubular particles. Variation in other two dimensions of clay particles is related to degree of crystallinity of the clay minerals. Generally water adsorption and formation of gels at low concentrations are properties of colloidal particles depending on specific surface area. The main force bonding water to the surface is due to hydrogen bond and as we are dealing with consolidation of saturated clays role of such bonds on particle orientation and its possibility to diffuse at various stress levels should be properly determined. Overall this paper divides the study and analysis in two stages; one is author's theory of one dimensional consolidation through radial flow and determination of average degree of consolidation using isochrones and second is to study effect on soil-structure during different stages of consolidation using micrographs based on scanning electron microscopy (SEM) of consolidated clay samples with central vertical drain. Objective of this study to present experimental model of vertical drains viz. sand drain, coir-jute fiber drain, polypropylene fiber drain reinforced soft soil mass of three different diameters to expedite the rate of consolidation due to radial drainage. The effects of vertical drains of different 'n' values (ratio of drain diameter to sample diameter) on consolidation characteristics (coefficient of consolidation 'Cr' due to radial drainage) of Kaolinite clay are undertaken to investigate the settlement characteristics and pore water pressure dissipation phenomena under different magnitude of loadings. Comparison of theoretical isochrones and experimental isochrones obtained from pore pressure measurements at various radial distances using Author's solution for the case of equal vertical strain condition. Also an brief discussion is made on some new defined parameters affecting soil-structure behavior like viscosity of fluid (turbid clay water), viscosity of clay gel(paste at plastic state) and transformation of liquid clay to semi-solid state and its impact on particle orientation, dissipation of air bubbles and its diffusion creating clog inside pore, reaction of pore space on dissipation and creation of pore tublet into layers of soil mass and intra-tubular pore creation under different magnitude of loadings, rotation of clay fiber due to velocity of fluid (turbulent flow) and creation of passage of pore water through inter channels of drain, inter-relation of strain generated due to diffusion of pore water and displacement of clay particle both radially and vertically. At last of this paper summarizes some of the important aspects of author’s consolidation theory and its practical applications.

2. LABORATORY INVESTIGATIONS

The large size oedometer of diameter 254mm were used for testing the remolded samples. A uniform pressure is applied by means of conventional hydraulic pressure system on the convoluted rubber jack which transfers uniform pressure on the soil sample placed in the cell. Pore pressure measuring points at the three radial distances located at 120^o each with r/re distances as r/4, r/2 and 3r/4 respectively using both conventional dial gauge and bishop system along with displacement transducers & pore pressure transducers connected to data logger system interfaced with PC. For all the tests diameter to height ratio of soil sample was kept constant (see fig. 1).

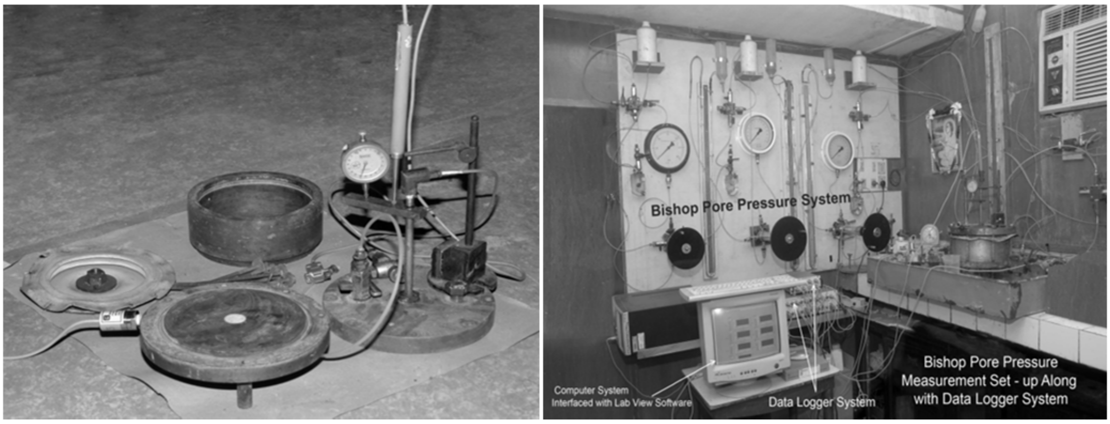

Figure 1: Components of Oedometer and complete set-up of advanced consolidation laboratory

2.1. Modified Oedometer

The two different diameters of oedometer i.e. 254mm and 152mm were used for testing the remolded samples. The cell body is machined from aluminum bronze sating which is resistant to corrosion. The base plate and top plate are bolted to the flanges while at the base ‘o’ ring is provided to make it water seal. A uniform pressure is applied by means of conventional hydraulic pressure system on the convoluted rubber jack which transfers uniform pressure on the soil sample placed in the cell. To achieve equal strain condition a rigid top platen is inserted between the jack and the sample.

2.1.1. Drainage and Pore pressure measurement

Inward radial drainage was provided in our case. The drainage outlet is via the centre of the settlement hollow rod and a short length of flexible tube leading to valve at the edge of the cell cover. No vertical drainage is allowed and so the top of the sample is sealed with the jack alone or with a rigid impervious top platen between the sample and the jack. The important factor in all the above set-up is full control over drainage and uniform settlement measurement of the sample. For both the oedometer test diameter to height ratio was kept constant. The side friction was reduced by means of application of silicon grease on the walls of the cell.

2.2.2. Preparation of clay samples

The sample is made from soft kaolin clay obtained commercially in the form of powder from the vadodara city. The clay powder was tested by doing dehydration test. The specific gravity of clay powder G = 2.592, liquid limit (L_L) = 67%, plasticity Index (PI) = 33.43 and belonging to CH (clay of high plasticity) group according to I.S. Classification system. To ensure full maturation of the sample the clay was mixed to form slurry with twice the liquid limit using a de-aired distilled water. After 24 hours of placing the slurry into the cell a static load of 10kPa is applied gradually for the period up to 25days. The clay is then scribed level and a filter paper followed by saturated flexible bronze drain is placed on the top. Free water is poured onto the drain and the rubber jack is lowered into the position through the water to exclude all air. Before that initial moisture content and void ratio are determined. Also the shear strength is measured with the help of laboratory vane shear apparatus.

2.2.3. Preparation and Installation of vertical drains

Three types of vertical geodrains were fabricated indigenously viz. sand drain (sand as filler material using mandrel), coir-jute drain (coir-jute fibers of maximum 120mm length placed radially wrapped by filter paper) & polypropylene drain (polypropylene fiber as filler wrapped by filter paper thus prepared in accordance with 'n' value equal to 11.04, 16.93 and 21.71 is inserted (placed) in the predrilled hole, formed by thin mandrel at centre of the soil sample in the oedometer. Also the shear strength is measured with the help of laboratory vane shear apparatus.

2.2.4. Testing Program

After installation of sample and fixing top platen along with dial gauge, displacement transducers, pore pressure transducers, bishop's apparatus are connected to their respective locations. Load increment is applied from constant pressure system to sample through water filed jacket, with closed position of the drainage valve at the top plate. Pressures are applied in the range of 20 kPa, 40 kPa, 80kPa, 160kPa and 320kPa with $\Delta p/p = 1.0$.Each load increment is kept constant for about 96 hrs and secondary compression is also recorded. After completion of the test, the sample is taken for final moisture content measurement.

3. THEORETICAL REVIEW, PLOTS & ANALYSIS

3.1. Author's Theory of One-Dimensional Consolidation through Radial Flow

Shroff & Shah (2006) proposed a new mathematical theory which incorporates non-homogeneity, time effects intrinsic to the soil skeleton along with physico-chemical changes, compressibility of pore fluid and solid, variation of compressibility and permeability during consolidation, type of the drain material, tortousity effect, k_h/k_v ratio under load variation, effect of 'n' value (drain diameter) and drainage path. The lump parameter'λ' incorporates above all factors. Isochrones for various positive and negative values of parameter λ are obtained from which average degree of consolidation is computed using Simpson's rule as explained in Taylor (1948) and Lambe-Whitman (1969).Author also proposes a generalized solution for computing average degree of consolidation (U_r) for different values of λ as shown here:

$$U_r = \frac{e - e_o}{e_1 - e_o} =$$

$$\exp\left\{\left(\lambda/2\right)\right\}\left[\frac{\mathrm{Sinh}\,\lambda/2\,R}{\mathrm{Sinh}\,\lambda/2} + 2\pi\sum_{n=1}^{\infty}\frac{(-1)^n .n\,\mathrm{Sin}(n\pi R)}{\lambda^2/4 + n^2\pi^2}\exp -\left\{\left(\lambda^2/4 + n^2\pi^2\right)\,T_r\right\}\right] +$$

$$\exp\left\{-\left(\lambda/2\right)\right\}\left[\frac{\mathrm{Sinh}\,\lambda/2\,(1-R)}{\mathrm{Sinh}\,\left(\lambda/2\right)} - 2\pi\sum_{n=1}^{\infty}\frac{n\,\mathrm{Sin}(n\pi R)}{\lambda^2/4 + n^2\pi^2}\exp\left\{-\left(\lambda^2/4 + n^2\pi^2\right)\right\}T_r\right]$$

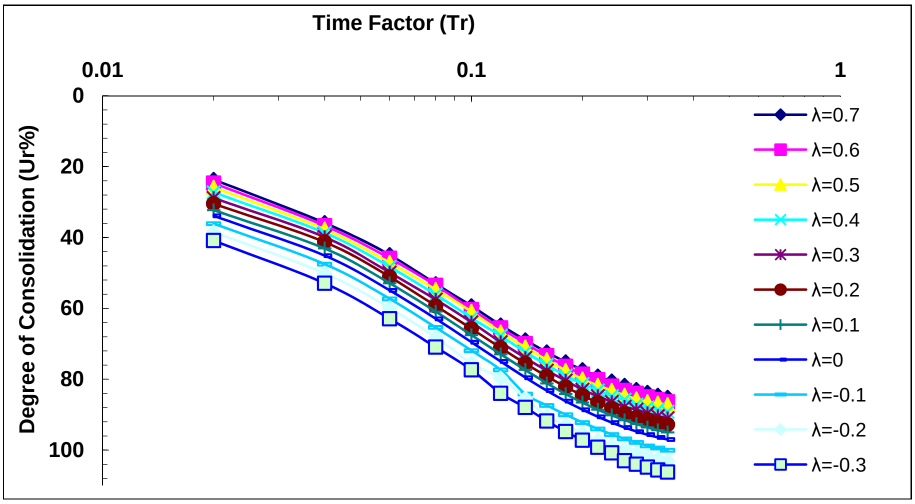

Figure 2: Degree of consolidation vs. time factor for various ranges of lump parameter 'λ'

In the theoretical derivation of above theory it is reflected that the rate of outflow of fluid, that is rate of change of fluid in the element is dependent on excess fluid pressure gradient which will be function of the type of drain material used in fabricating vertical geodrain being ‘k’ will be function of both porosity and void ratio ’e’ which ultimately reflects in coefficient of consolidation (C_r) in the derivation. Further lumped parameter (λ) is the ratio of (C_e/ C_r) $r_{e,}$ where C_r is coefficient of consolidation due to radial drainage and C_e is coefficient due to permeability and porosity which is to some extent due to small magnitude of radial strain which helps in redistributing loads to the surface at interface of drain giving same settlement supporting ‘equal strain’ condition. In turn C_r will vary with the drain material reflecting in the values of (λ). In the present case, the optimum lump parameter (λ) is deduced for all the drains on the basis of average degree of consolidation (U_r).

3.2. Comparison of Plots

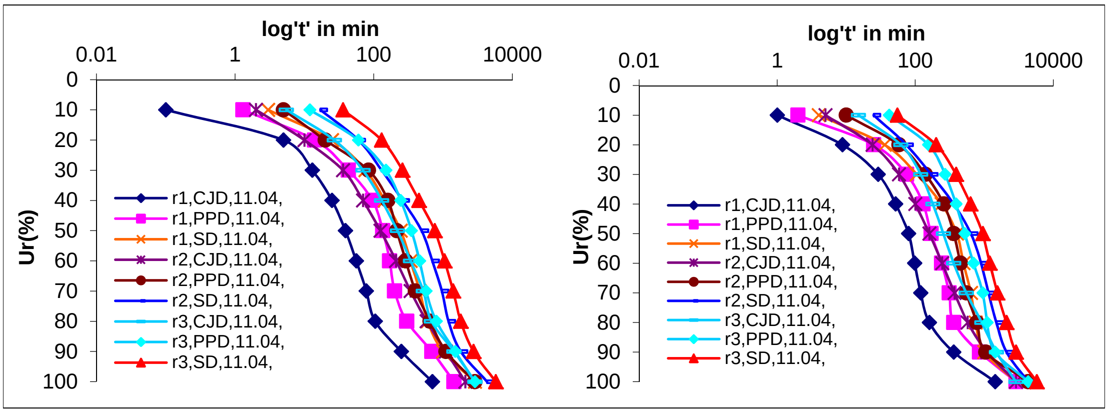

Figure 3: Comparison of excess pore water pressure dissipation at 40kPa and 160kPa for ‘n’11.04

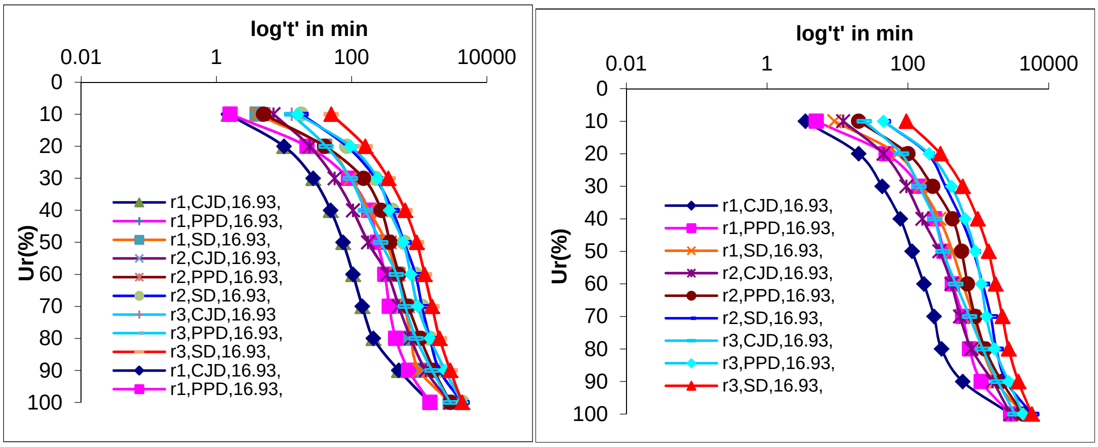

Figure 4: Comparison of excess pore water pressure dissipation at 40kPa and 160kPa for ‘n’16.93

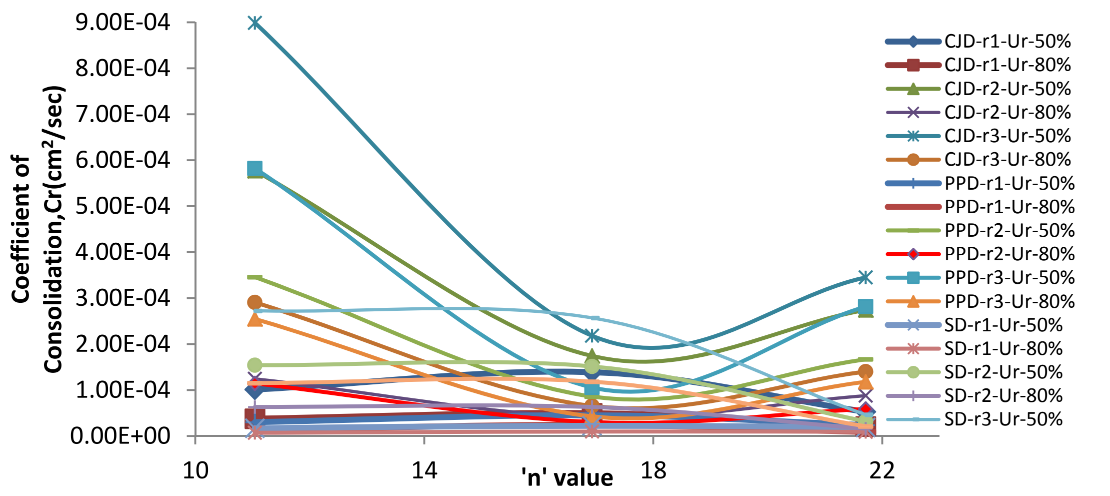

Figure 5: Comparison of coefficient of consolidation (Cr) vs. 'n' value at 40kPa applied pressure

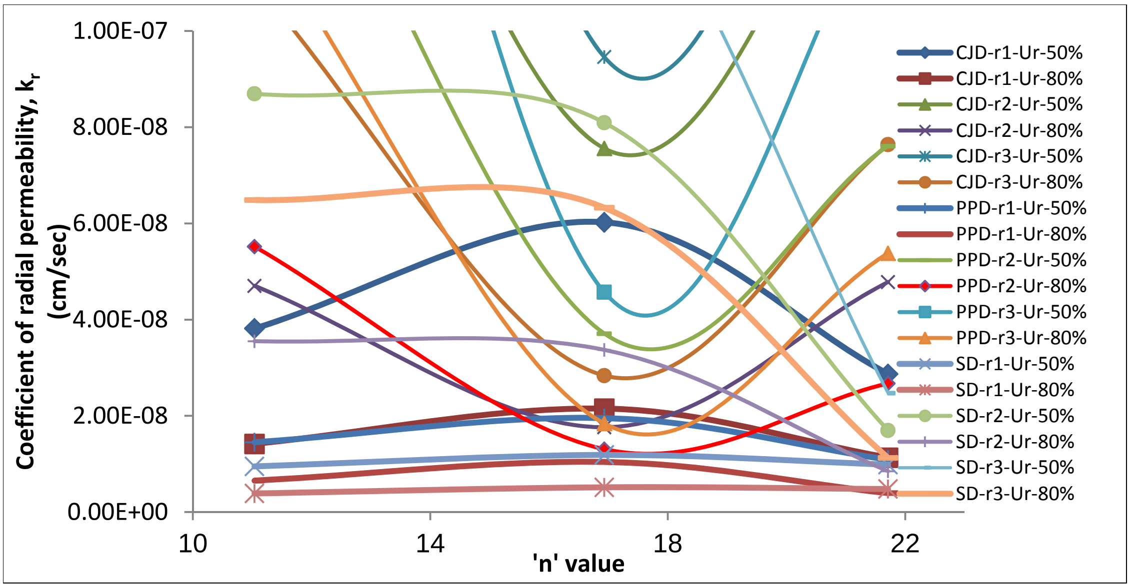

Figure 6: Comparison of coefficient of radial permeability (k_r) vs. 'n' value at 40kPa applied pressure

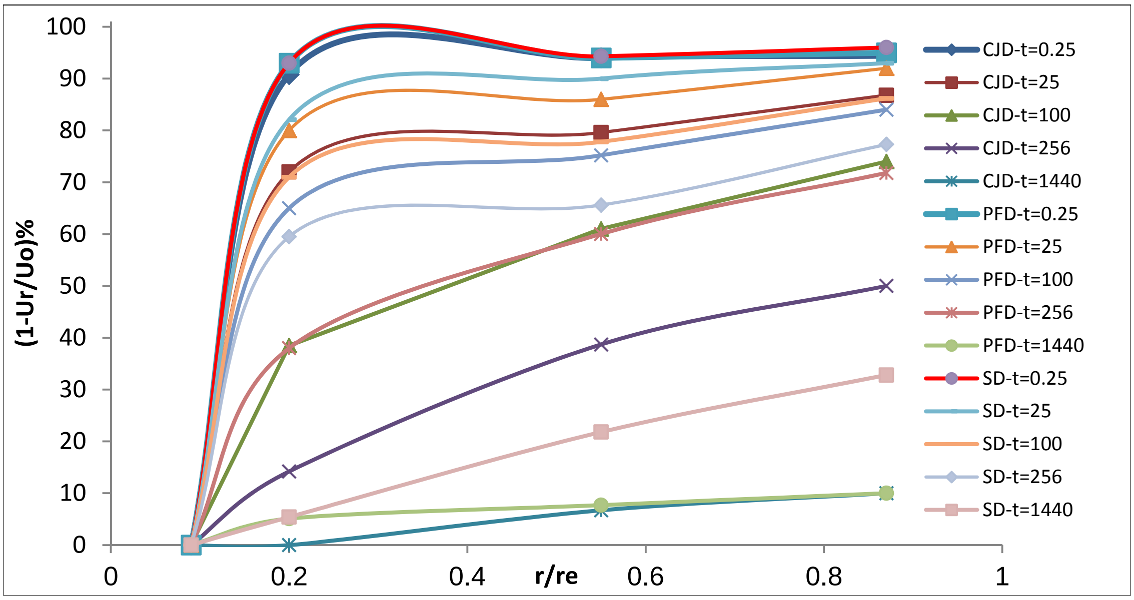

Figure 7: Comparison of experimental isochrones w.r.t. time for n'11.04 at 160kPa applied pressure

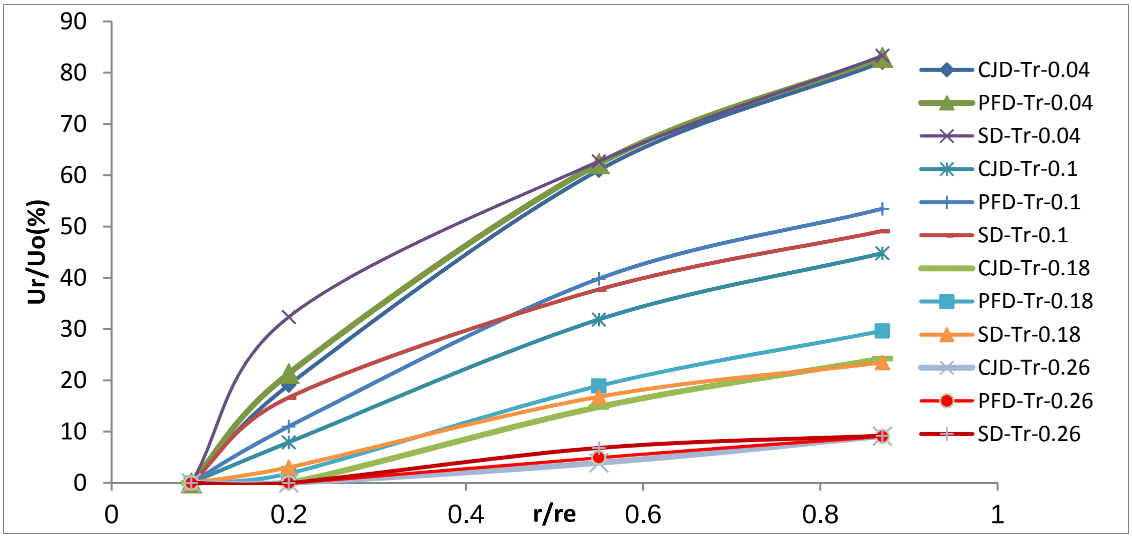

Figure 8: Comparison of experimental isochrones for selected time factors (T_r) at 160kPa pressure

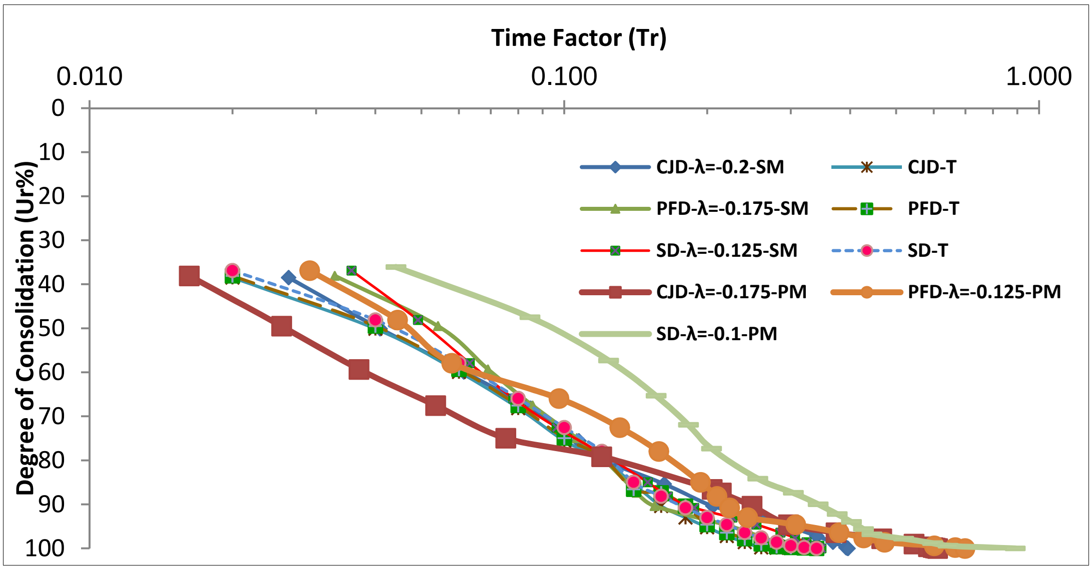

Figure 9: Comparison of degree of consolidation based on settlement measurements (SM) and pore pressure measurements (PM) at 160kPa pressure

3.3 Results of Scanning Electron Microscopy (SEM)

The following table illustrates the detail of SEM analysis carried out on consolidated clay samples of with central vertical drain viz. sand drain and coir-jute fiber drain at various locations (refer figure 10 to13) The further analysis of microscopy results was carried out using analysis was carried out using Quanti-image analyzer with system of micro structure characterization (MIC) software based on ASTM method.

Table 1: Schedule of SEM

Type of Drain	SD	SD	SD	SD	CJD	CJD	CJD	CJD
‘n’ value	11.04	11.04	11.04	11.04	11.04	11.04	11.04	11.04
Location	h_{tr2}	h_{cr2}	h_{br2}	I_{crd}	h_{tr2}	h_{cr2}	h_{br2}	I_{crd}
Magnification factor	X2700	X2700	X2700	X2700	X2700	X2700	X2700	X2700

Where, r_d = radius of drain, r_1 = first radial point for measurement of pore pressure at a distance of r/4

r_2 = second radial point for measurement of pore pressure at a distance of r/2, r_3 = third radial point for measurement of pore pressure at a distance of 3r/4, h = thickness of final consolidated clay sample, h_{tr2}= Top of final consolidated clay sample at first radial point r_2, h_{cr2}= Centre of final consolidated clay sample at first radial point r_2
h_{br2}= Bottom of final consolidated clay sample at first radial point r_2, I_{trd} = Clay-Drain interface at top of final consolidated clay sample at location r_d, I_{crd} = Clay-Drain interface at centre of final consolidated clay sample at location r_d, I_{brd} = Clay-Drain interface at bottom of final consolidated clay sample at location r_d.

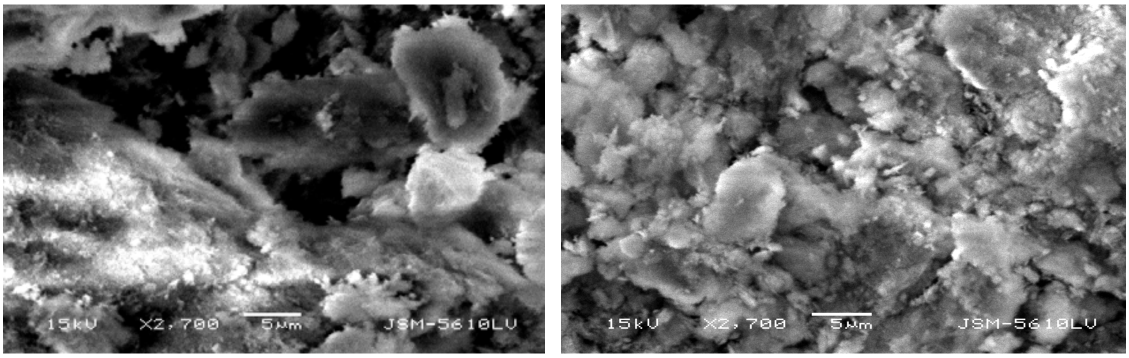

Figure 10: Microscopy of SD at location h_{tr2} & h_{cr2} at X2700

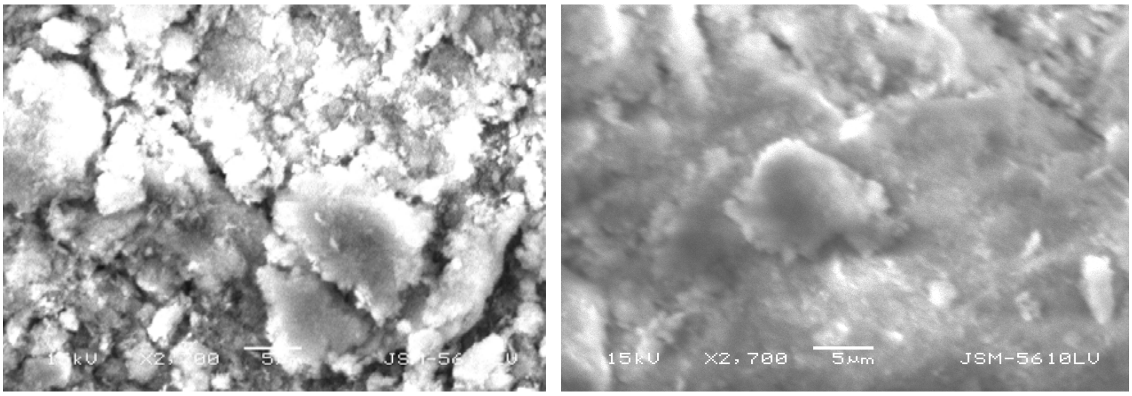

Figure 11: Microscopy of SD at location hbr2 & Icrd at X2700

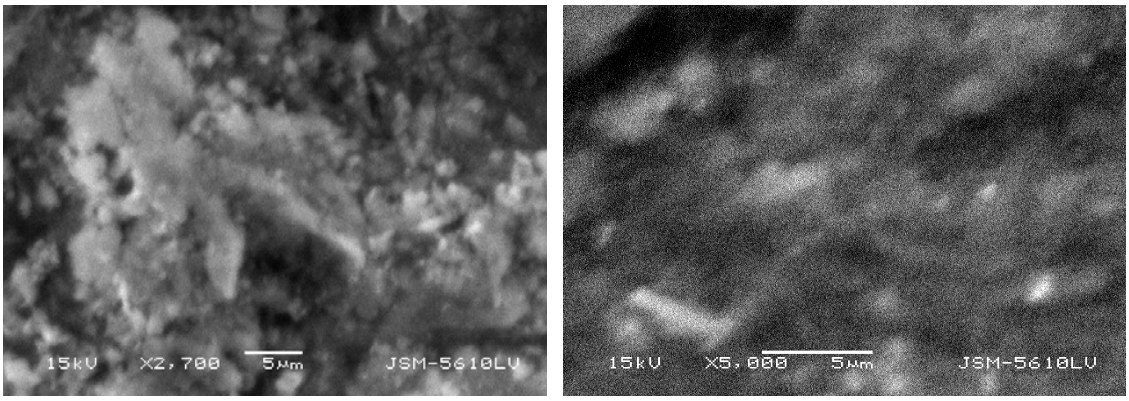

Figure 12: Microscopy of CJD at location htr2 & hcr2 at X2700

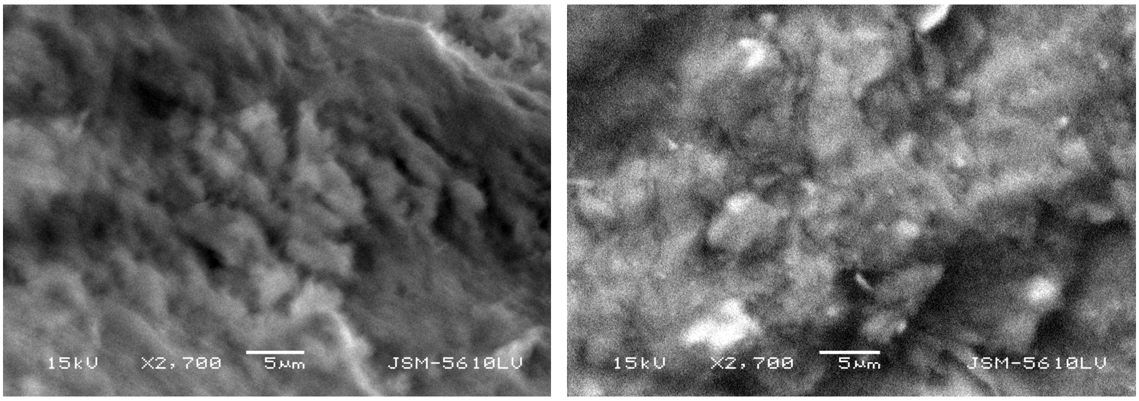

Figure 13: Microscopy of CJD at location hbr2 & Icrd at X2700

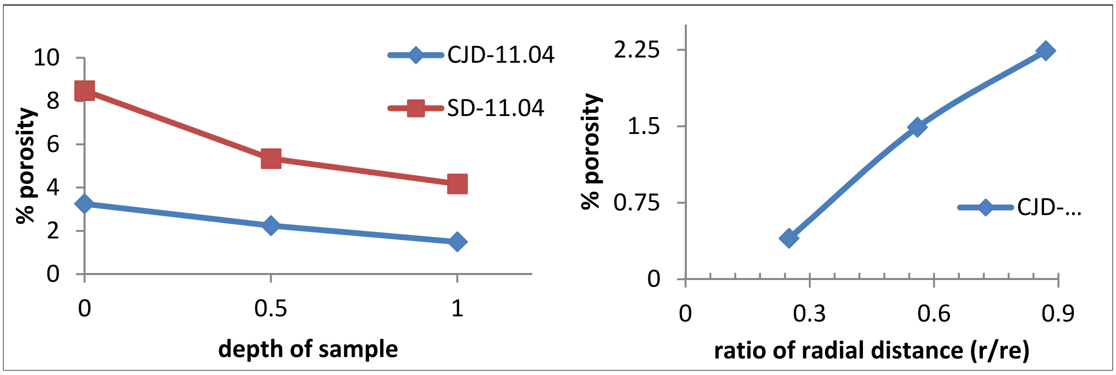

Figure 14: (a) Comparison of micro porosity vs. depth of sample at end of 320kPa pressure

(b) Comparison of micro porosity vs. ratio of radial distance at end of 320kPa pressure

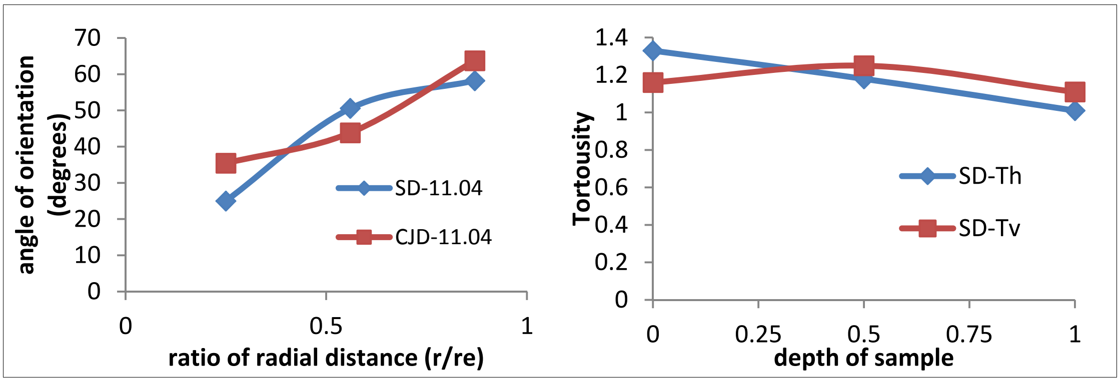

Figure 15: (a) Comparison of angle of orientation Vs. ratio of radial distance using micrograph

(b) Comparison of horizontal tortousity (T_h) and vertical tortousity (T_v) vs. depth of sample

4. CONCLUSIONS

- From pore pressure measurements, (figure 3&4) it infers that for 50% consolidation and mid plane radial point r_2, n=11.04 takes 59% and 76% less time compared to n=16.93 and 21.71 for any drain material under light loading and 65%, 77%, under constructional loading. Similarly for 80% consolidation, n=11.04 takes 42% and 61% less time compared to n=16.93 and 21.71 for any drain material under light loading and 51%, 67% under constructional loading.

- From settlement and pore pressure measurement considerations it infers that CJD under light loading takes 49% less time in compare to PPD, 56% in compare to SD,while for 80% consolidation CJD takes 35% less time in compare to PPD and 44% in compare to SD and under constructional loading CJD takes 58% less time in compare to PPD, 58% in compare to SD, while for 80% consolidation CJD takes,41% less time in compare to PPD and 47% in compare to SD. (averagely)

- Rate of drainage of a radial points nearer to drainage being faster the time taken for particular % of consolidation is less in compare to radial points farther away, it also reflects this observation in settlement measurements to some extent showing more compressibility gradient towards central drain. It seems from the micrograph of several drains the pore space in terms of nanomeasurement is larger compare to other drains. This reflects the efficiency of CJD with respect to micro structure opening even under light and heavy constructional loading.

- Cr for CJD from mid plane pore pressure measurements for 50% consolidation work out to be averagely 229% & 279% more compare to other drain materials under light and heavy construction loading. Similarly for 80% consolidation it is averagely 97% & 137% more (refer fig.5). Effectiveness of PPD seems too remote from realty compare to functioning of other drains. While effectiveness of PPD is less than CJD but higher then SD. Under any strain condition because of the flexibility CJD drain shows higher horizontal permeability compare to others.

- Lesser variation in Cr value is observed for radial point's r2 and r3 for all drain materials and for all applied pressures. Though CJD shows more inter-rate of dissipation of excess hydrostatic pore water pressure even at successive pressures in compare to other drain materials. n=16.93 shows averagely 92% higher C_r value under light loading while 60% higher under constructional loading compare to n=21.71 but 61% lower compare to n=11.04 under light loading and 56% lower under constructional loading. In pore pressure measurement under lighter loading there is variation in Cr value, but constancy is maintained after 50KPa for any 'n' value.

- Comparing three drain materials (refer fig. 6) it indicates that coefficient of radial permeability (Kr) value of drain increases the efficacy of rate of drainage through soil thereby it reflects coefficient of transmisvity of water through soil. For any pressure the Kr value of CJD remains efficient compare to others. From above analysis for middle radial point r_2 it concludes that n=11.04 for 50% consolidation shows 72% and 55% higher Kr value compare to n=16.93 and 21.71 for any drain material under light loading and 86% and 84% under constructional loading. Similarly for 80% consolidation shows 57% and 32% higher Kr value compare to n=16.93 and 21.71 for any drain material under light loading and 80% and 78% under constructional loading.(pore pressure)

- Average Cr value for n=16.93 remain in between n=11.04 and n=21.71.The lowest average value of n=21.71 signifies inefficiency of the drains of any material compare to drains of other 'n' value. With the same drain Cc value shows increasing trend with higher 'n' value. It signifies that because of low rate of dissipation in higher 'n' values the magnitude of compressibility increases at particular period of interval. This behavior is similar for all drains. Cc value for CJD, , PPD, SD for n=11.04 are 0.272, 0.292, and 0.312 respectively.

- With reference to isochrones (refer fig.7 &8) for various T_r values reveals that sequence of consolidation for CJ of n=11.04 at any radius of influence seems to be efficient compare to all other drains. Comparing isochrones of all three 'n' values it is concluded that n=11.04 is more effective compare to n=16.93 and n=21.71, while n=16.93 is more superior compare to n=21.71 for all drain materials. Trajectory of isochrones for n=11.04 lies above the n=16.93 and n=21.71 for both light and constructional loading. Also trajectory of isochrones for n=16.93 lies above n=21.71 for all drain materials and loadings.

- Considerable gain in shear strength of soft soil mass was observed at the end of consolidation for any drain material of same 'n' value. Maximum shear strength was in the range of 100 - 140 kPa compared to 6-18 kPa of initial shear strength. CJD has exhibited highest strength of 150kPa compared to other drains.

- As 'λ' value increases, drain diameter ('n' value) decreases. Theoretical solution of author's non-linear equal strain theory of consolidation by radial flow fits very well with experimental results for various soil conditions. Various factors affecting rate of consolidation like drain material, drain size, drain shape, ratio of horizontal permeability to vertical permeability, physico-chemical factors are well considered in authors theory and its effect are reflected because of typicality of pore pressure dissipation phenomena. At this stage author proposes some new defined factors based on soil structure study done using scanning electron microscopy of consolidated samples. This factors are viscosity of fluid (turbid clay water), viscosity of clay gel(paste at plastic state) and transformation of liquid clay to semi-solid state and its impact on particle orientation, dissipation of air bubbles and its diffusion creating clog inside pore, reaction of pore space on dissipation and creation of pore tublet into layers of soil mass and intra-tubular pore creation under different magnitude of loadings, rotation of clay fiber due to velocity of fluid (turbulent flow) and creation of passage of pore water through inter channels of drain, inter-relation of strain generated due to diffusion of pore water and displacement of clay particle both radially and vertically.

- The orientation of clay particle depends on rate of loading and dissipation of pore water which ultimate depends on discharge capacity of vertical drain. Author assumes that structural viscosity of turbid clay water is very high in compare to viscosity of surface clay water thus allowing easy slippage of clay particle into more random orientation. This phenomenon takes sufficient time to come at equilibrium stage where viscosity of turbid clay water now starts creating fluid friction and particles do not get fast displaced due to transformation of clay gel into more plastic state itself into pore spaces. The diffusion of this pore spaces is very much necessary for pore water to create new paths for dissipation from drain. For this drains should have high suction capacity along with good discharge capacity and this was well determined by doing SEM (refer fig. 10 to 13 and table 1) on clay-drain interfaces. It was observed that sand particles just not flow away with fine clay boundary but they due to high plasticity of clay turbid water they create clogging and at higher loads they itself get displaced to accommodate strain. This fact can be seen by comparing % porosity depth wise as well as radial distance wise, indicating that % pores reduces towards bottom of sample and near the drain (refer fig. 15). Between nearest radial point r_1 and clay-drain interface the percentage decrease of micro pore is more compared to mid plane radial point r_2 and outward radial point r_3.Because of faster rate of dissipation the achieved void ratio or porosity which is worked out is less in case of coir-jute fiber drain compare to sand drain. This is true for same vertical drain material of other ‘n’ values also.Also while studying orientation of particle with reference to face-to-face contact and face –to-edge contact it was found that inter-tubular pores and their diffusions creates displacements of clay particle along with rotation of clay particle leading into more random orientation at lighter loads (refer fig.15). Under heavy loads this inter-tubular pores get break or diffused and clay particle orients into more parallel arrangement. Use of hydraulically pressurized Oedometer for consolidation through radial flow proves to be powerful tool to study nano mechanics of pore water dissipation at various time intervals.But still how this transformation of pore channels takes place and at what rate it undergoes deformation needs nano studies on pore water diffusion.

- Experimental results almost match with theoretical results with λ=-0.2 particularly for CJD for n=11.04, λ = -0.19 for n=16.93 and λ = -0.18 for n=21.71 proves to be efficient amongst other drains. From theoretical considerations n=11.04 proves to be efficient amongst other ‘n’ values. Comparing degree of consolidation based on settlement analysis and pore pressure analysis it is found that pore pressure results are more reliable, accurate and gives clear picture of behavior of compressibility of clay water system using various vertical drains (refer fig. 10).

So overall it is concluded that coir-jute fiber drain of ‘n’ equal 11.04 is most efficacious in dissipating pore water pressure at shortest time along with higher gain in shear strength of consolidated mass. Author’s theory of consolidation based on pore water dissipation (isochrones) yields better comparative results more easily applicable to fields by design engineers. Also trajectory of curves for various degrees of consolidation acts as a readymade tool for selection of optimum drain w.r.t material, shape and size. The appropriate value of lumped parameter (λ) will directly give the clue to design engineer regarding the selection of prefabricated vertical geodrain with respect to field conditions.

5. ACKNOWKEDGEMENTS

The authors are highly thankful to the Prof.(Dr) Ambika Misra, Dean, Faculty of Technology & Engineering, Prof. (Dr) I.I. Pandya Head, AMD, Prof. (Dr) D.L.Shah, P.G.Incharge, AMD, The Maharaja Sayajirao University of Baroda, Vadodara and Prof. M.N.Patel, Dean, L.D.College of Engineering and Prof.(Dr) R.K.Gajjar,Head, AMD,LDCE, Ahmedabad, India for providing all necessary research facilities.

REFERENCES

Barron, R. 1948, Consolidation of fine grained soils by drain wells, Trans A.S.C.E., Vol.113, pp. 718-754

Hansbo, S. 1960, Consolidation of clay, with special reference to influence of vertical sand drains, Proc.Swedish Geo-tech Instt. No.18, pp.160

Hansbo, S. 1981, Consolidation of Fine-grained soils by prefabricated drains, Proc. of 10^{th} Int. Conf. on Soil Mechanics and Foundations Engineering, Stockholm, Vol-3, pp-677-682

Rowe P.W and Barden.L.(1966),”A new consolidation cell”, Geotechnique, 16:2:162

Shroff, A.V. and Shah, M.V. 2006, Effect of ratio of influence zone and type of vertical drain on consolidation of soft clay due to radial flow, Proc. Fourth International conference on Soft- soil Engineering, Canadian Geotechnical Society, University of Alberta, Canada,Vol-I,pp-765-773

Shah, M.V. and Shroff, A.V. (2010),” Soil-Structure interaction of soft clay using prefabricated Vertical geodrains under seismic stresses”, Proc. Fifth International conference on Recent Advances in Geotechnical Earthquake Engineering and Soil Dynamics, Missouri University of Science and Technology, International Society of Soil Mechanics and Geotechnical Engineering, San Diego, CA, USA, Vol-II, paper no.5.53a

Shah, M.V. and Shroff, A.V. (2010),”Modeling of Vertical geodrains using modified hydraulically pressurized oedometer”, Proc. Sixth International congress on Environmental Geotechnics, Indian Geotechnical Society & International Society of Soil Mechanics and Geotechnical Engineering, New Delhi, Vol-I.

Shah, M.V. and Shroff, A.V. (2011),”Influence of vertical geodrains on consolidation characteristics of soft clays using Oedometer”, Proc. of 5th International Symposium on Deformation characteristics of Geomaterials (IS-Seoul 2011), Korean geotechnical society & International Society of Soil Mechanics and Geotechnical Engineering, Seoul, Korea, Vol-II, pp-1095-1102

Walker, R, Indraratna, B.et.al, (2009),” Vertical and Radial consolidation analysis of multilayered soil using the spectral method”, *Journal of Geotechnical and Geoenvironmental Engg.*, 135(5), pp-657-663

Wang, X.-S., and Jiao, J. J, (2004), “Analysis of soil consolidation by vertical drains with double porosity model,” *Int. J. Numer. Analyt. Meth. Geomech.*, 28, 1385–1400.

Monitoring HEIC using Landpac CIR and CIS Technologies

Dermot Kelly, Landpac, United Kingdom, DKelly@landpac.co.uk
José Gil, Landpac, South Africa, jose@landpac.co.za

ABSTRACT

Poor or unstable ground conditions can make traditional and conventional forms of construction expensive and unviable. In such instances, it may be economically viable to improve the engineering properties of poor ground before continuing with any construction process. Ground improvement, unlike ground treatment, is the process of modifying the ground underlain by suspect or uncontrolled fills, as well as sites with soft or loose soils, through the use of mechanical means. The twin drum high energy impact compaction (HEIC) process of ground improvement is a well known technique used on highly voided mixed fills for Brownfield site development or on dredged marine sands for marine construction projects. It offers a unique, technically and economically viable solution for ground improvement and for general earthworks operations, supported by the control and certification thereof using the Continuous Impact Response (CIR) and Continuous Induced Settlement (CIS) monitoring systems that are fully integrated with GPS. These technologies and their applications are documented in this paper, with references made to projects using the technologies in conjunction with other deeper ground improvement processes on marine related projects.

1. INTRODUCTION

Quality control, in any industry, is a methodology employed that, if properly implemented, ensures that a performed service adheres to the requirements of the project design specification. Quality control is thus a process that is employed by a provider which includes actions deemed necessary to ensure that control and verification of certain characteristics are provided for, with the basic process goal being that the result meets specifications and/or expectations and that the quality of the works is assured.

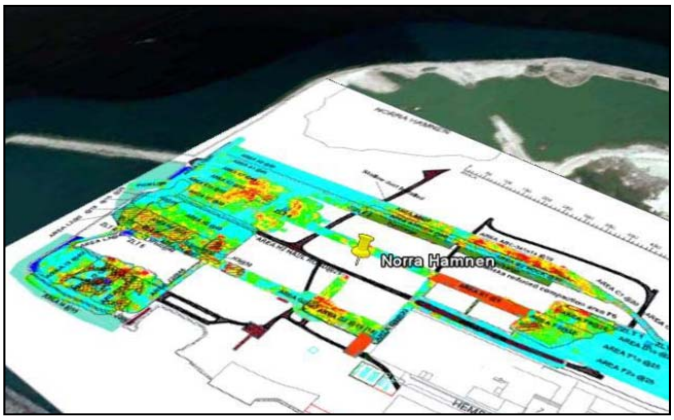

Figure 1a: Typical CIR overlay for 23 Hectare HEIC treatment area - Copenhagen Malmo Port (CMP) Container Terminal, Malmo, Sweden

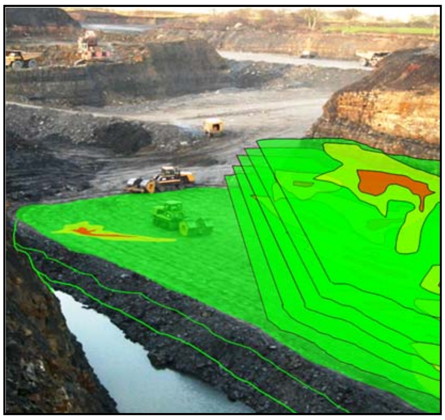

Figure 1b: Schematic of typical CIR overlay for HEIC 1m thick layerworks - Polkemmet Colliery Rehabilitation, Scotland

The well known twin drum HEIC application has proven viable in offering robust solutions to the ground and civil engineering industries, with unique ground improvement alternatives applicable to the global marine sector industry. The need for a reliable control and verification tool that supports the application of the technology led to the development of the Landpac Continuous Impact Response (CIR) and Continuous Induced Settlement (CIS) measurement systems which are fully integrated into the quality control process The process captures the specification requirements as established by the design/consulting engineers, develops correlations between measured data and the specific engineering properties being measured and requiring control, establishes control limits, captures data and plots the results for verification. Sections that fail to meet the specification requirements are clearly highlighted and emphasis can be placed on developing a corrective action process that remediates such sections.

The CIR is a specialised technique for monitoring the soil's response to the loads delivered by the twin drum HEIC process, with fully integrated GPS for accurate positioning, effectively producing an accurate indication of the soil's strength/stiffness across an entire site during the twin drum HEIC process. The CIS, employing a differential GPS, allows for levels to be accurately recorded during the same process. The CIR and CIS measurement systems thus offer the industry an opportunity to reliably and easily control the improvement and vastly improve the quality assurance of the engineered works.

2. THE TECHNOLOGY OF HIGH ENERGY IMPACT COMPACTION (HEIC)

Twin drum High Energy Impact Compaction (HEIC) involves the transfer of compaction energy into the soil by means of the lifting and falling motion of non-circular rotating masses. The rotation of such masses to their highest point results in an effective potential energy build-up. Further rotation of these masses results in the conversion of this potential energy into a falling kinetic energy, which is transferred to the soil upon the impact of the lowest point of the masses with the surface of the soil. The amount of energy transferred, in the form of compactive effort, is closely related to the amount of potential energy generated in the lifting process.

Figure 2a: 3-Sided 25kJ Landpac HEIC working on dredged marine sands in Morocco

The main features of this high energy impact compaction (HEIC) process include the following:

- Compaction Loads: the high energy and dynamic compaction action of the HEIC equipment leads to typical compaction loads of between 1200kN and 2500kN being generated depending upon the type and condition of the material being compacted.
- Material Moisture Condition: The high energy of the HEIC equipment leads to the ability to compact material to a higher maximum dry density than is achievable with conventional roller type of compaction equipment. This high energy also allows for the compaction of material over a wider range of moisture conditions particularly dry of optimum moisture content.
- Depth of Influence: The high compaction loads that are generated by the HEIC equipment lead to high surface contact pressure on the soil. This, coupled to the relatively large contact area over which the compaction energy transfer takes place, leads to a vastly increased depth of influence of the compaction. Ground improvement is typically measured to effective depths of 2m-3m with depths of up to 5m being recorded in some applications.
- Soil Compressibility: The shape of the non-circular masses allows for the high energy parcels to be transferred in the form of a "rolling impact". This means that the load duration of the HEIC process is relatively long [typically 0.12s]. This extended load transfer duration in turn leads to a softer soil response to the load and hence enhanced soil compressibility is achievable.
- Compaction Productivity: The relatively high operating speed and depth of influence of the HEIC process leads to very high productivity of compaction. The HEIC process can typically cover 15,000m² per hour per surface coverage. The productivity of the HEIC process can be between 2 and 5 times higher than that of conventional shallow compaction equipment when performing fills work and many times more productive than that when it comes to the improvement of in-situ materials.

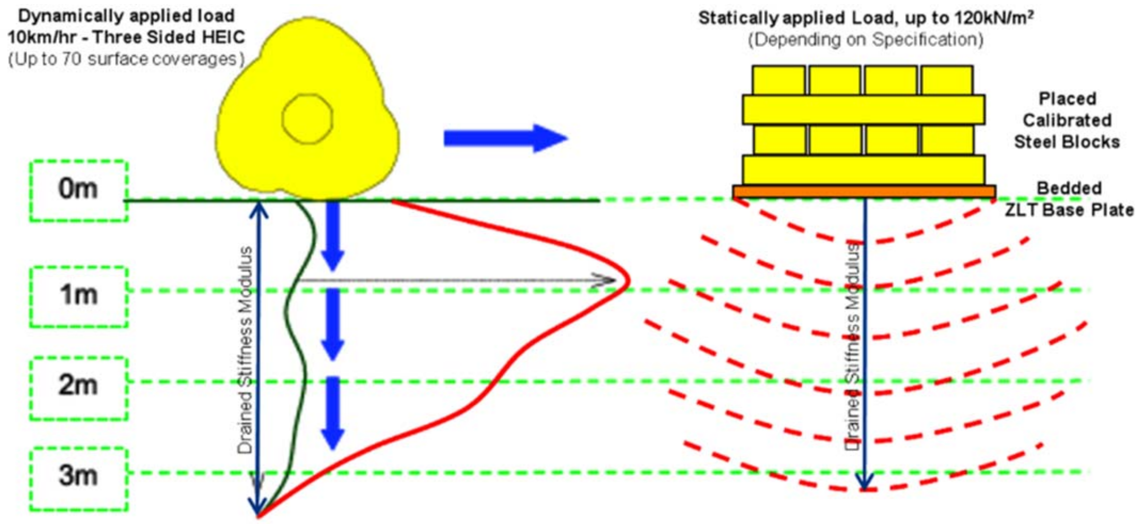

Figure 2b: Schematic of typical Drained Stiffness Modulus after HEIC for 30 surface coverages as demonstrated by 2m x 2m steel plate Zone Load Testing (ZLT) of 10 to 30MPa

HEIC provides a process that allows for a wide range of applications from fill works compaction through to deep in-situ ground improvement. In all of the appropriate applications, it is possible to ensure project cost savings whilst at the same time enhancing the quality assurance of the works relative to the "in service" performance of the materials that have been treated.

The deep ground improvement capabilities of the equipment and technologies allow for innovative alternative solutions to be considered on many earthworks projects. Such innovation requires "out of the box thinking" although some of the more common alternative solutions include the following:

- Improvement of in-situ sub-grade materials providing benefits such as:
  - Improved sub-grade strength.
  - Potential elimination of some costly imported layer-works.
  - Reduced sub-grade settlement / differential settlement.
- Ironing of Vibro-compacted and dynamically compacted material.
- Fast and cost effective alternative to "remove and replace" improvement of in-situ materials.
- Thick Lift fills work.
- Reduced water requirements compaction works.
- Pavement rehabilitation from existing pavement surface eliminating large removal and rework costs.
- Proof rolling for settlement and differential settlement removal.
- Permeability reduction/Accelerated consolidation of saturated materials.

3. QUALITY CONTROL

3.1 Traditional Approaches to Compaction Control

The traditional approaches to compaction specification and control are limited in that there is typically an extremely small ratio between the volume of the material tested and that compacted (typically up to 1:100,000). Other limitations that traditional compaction testing and control approaches have include the following:

- The lack of correlation between laboratory and field compaction test results;
- The poor reproducibility of results;
- The long duration of certain testing methods; and
- The difficulty in testing heterogeneous materials.

3.2 Counteracting the Traditional Testing Approach Limitations

In view of the limitations associated with the use of traditional testing methods, new methods of compaction specification and control have been developed in order to exploit the capabilities of twin drum HEIC. The new approach for testing and certification of ground improvement using twin drum HEICequipment revolves around the direct measurement of engineering properties of the material. In order to achieve this, the Continuous Impact Response (CIR) System, was developed by Landpac. This system is capable of measuring the soil response to every impact of the impact compactor, resulting in a direct measurement of the material stiffness.

The Continuous Impact Response measurement system employs the Landpac Impactometer to measure peak decelerations of the compaction masses with each impact. Each of these points is recorded relative to its position on site as determined by an integrated global positioning system. These accurately measured and recorded decelerations are then correlated back to a measurement of engineering properties using traditional testing method, such as density, Cone Penetration Testing (CPT), Dynamic Cone Penetration (DCP), Plate Load Testing (PLT), Zone Load Testing (ZLT), and California Bearing Ratio (CBR). The CIR system generates colour coded maps indicating the relative measure of the appropriate engineering property.

The maps generated by the CIR system can be used in conjunction with conventional testing techniques to provide a quality assurance system capable of certifying the entire site at a reduced cost and an increased level of certainty. The system is currently widely used and has proven to be a very useful tool in controlling the ground improvement process.

By using the CIR technology to identify the relative strength and stiffness of the material being treated, it is possible to focus the conventional tests in the relatively weaker areas. By ensuring that the relatively weaker areas conform to specification, it is then possible to use the CIR results to extrapolate the conventional test results over the entire site thereby increasing the certainty of the overall future performance of the compaction works. This process can actually allow for a reduced level of conventional testing thereby reducing the cost of testing whilst increasing the level of certainty of the test programme.

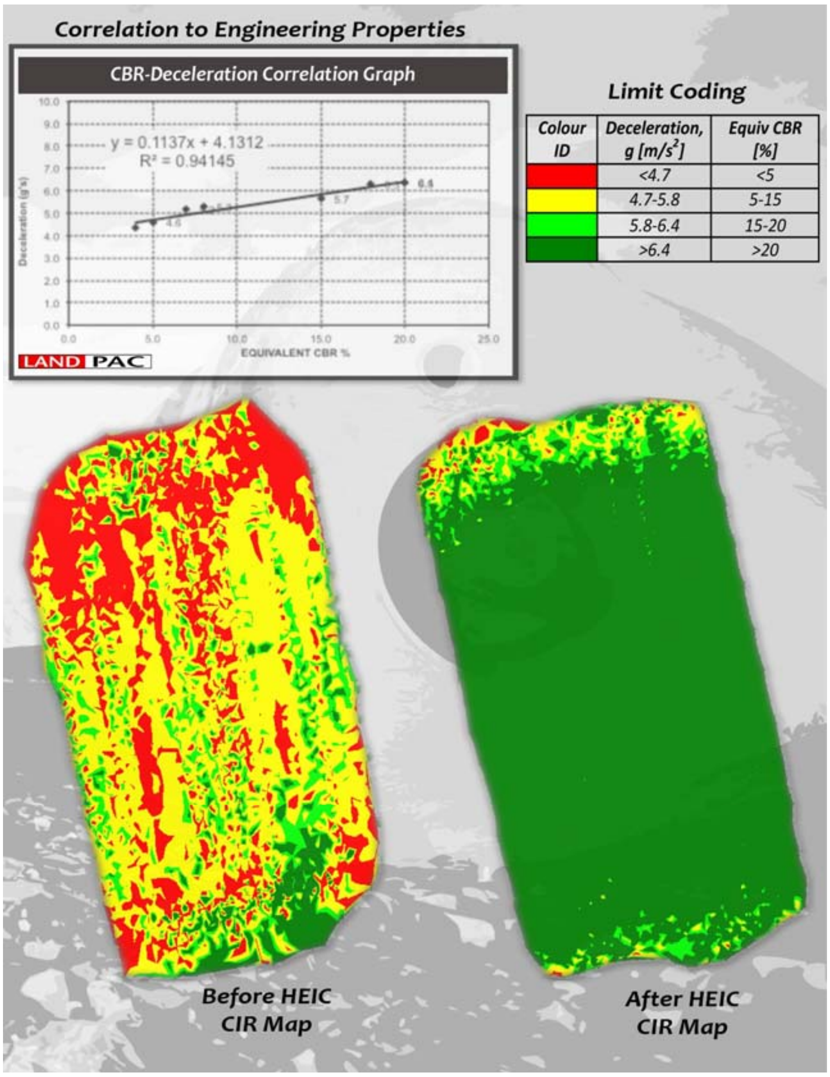

Figure 3a: Developing CIR Maps from Correlations between Decelerations and Engineering Properties

The CIR provides a quality control system that quantifies the ground strength and stiffness during the compaction process whilst also monitoring the number of coverages and actual area compacted. These ground improvement maps can be used in the following ways:
- To indicate relative strength of the material during the varying stages of the ground improvement process and monitor improvement;
- To pin point focused areas for conventional testing;
- To identify weak areas requiring additional testing and remedial action; and
- To spread the conventional test results over the entire site thereby enhancing the quality assurance of the ground improvement.

In addition to Continuous Impact Response (CIR) measurement, it is also possible to simultaneously measure the relative settlement that is induced by the impact compaction ground improvement process.

The measurement of such settlement can be continuously monitored and colour coded maps of such Continuous Induced Settlement (CIS) can be generated. Such CIS maps can be used in the following ways:
- To indicate continuous settlement throughout the process;
- To indicate relative differential settlement,
- To monitor areas and volumes; and
- To monitor the absolute level of the ground improvement operation.

The combination of CIR and CIS maps provide a detailed record of ground improvement works that can be used to greatly enhance the quality assurance of the works performed with high energy impact compaction.

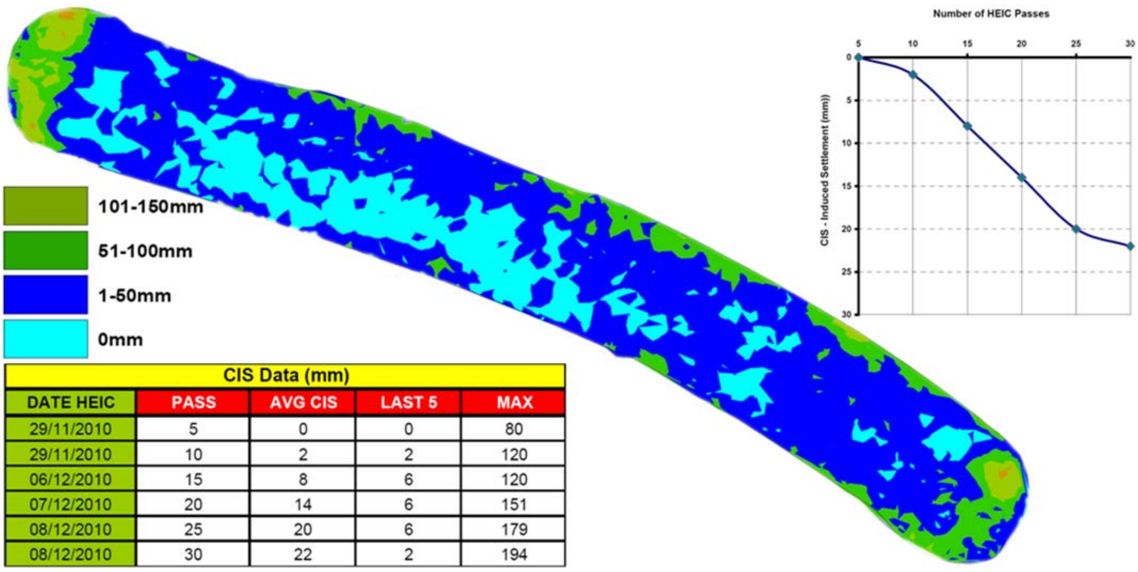

CIS Data (mm)				
DATE HEIC	PASS	AVG CIS	LAST 5	MAX
29/11/2010	5	0	0	80
29/11/2010	10	2	2	120
06/12/2010	15	8	6	120
07/12/2010	20	14	6	151
08/12/2010	25	20	6	179
08/12/2010	30	22	2	194

Figure 3b: Typical CIS data for each batch of 5 HEIC surface coverages (to a max of 30) London Gateway Container Terminal, UK

4. PROJECT STUDIES

In order to demonstrate the capabilities of high energy impact compaction, not only as a standalone ground improvement alternative but also as a complimentary tool to other deeper ground improvement mechanisms, and the value of using CIR and CIS as a quality control and assurance tools, several project studies have been summarised below. These include:
- Jebel Ali Port, Dubai
- HEIC after Vibro Compaction;
- Tanger Med II, Morocco
- HEIC after Vibro Compaction;
- Copenhagen Malmo Port (CMP), Sweden
- HEIC on mixed fills over reclaimed sea
- Port Botany, Sydney, Australia
- HEIC after Dynamic Compaction

Figure 5: HEIC on dredged Sand materials at the London Gateway Container Terminal, UK

4.1 Project Study: Jebel Ali Port, Dubai

4.1.1 Project Statement

In July and August 2004, reclamation was done behind the new Quay 4 and Berth 21 of the Jebel Ali Port, Dubai (Middle East). Dredged marine sands were backfilled to a total depth of approximately 16m. Messrs. Belhasa Six Construct LLC was instructed by the client to commence with soil improvement works to induce settlement of the reclaimed marine sands. A specialised subcontractor was appointed to execute the improvement works that consisted of Vibro compaction and soil replacement, wherever Vibro compaction was not recommended (i.e. on silty soils). On completion of Vibro compaction works, the specified Cone Penetration Test (CPT) cone resistance of 6 MPa was not achieved in the top 2.0m. HEIC was contracted to improve the bearing characteristics of the dredged marine sands in the top 2.0m of the soil profile.

4.1.2 Material Classification

Laboratory testing indicated that the material could be classified as poorly graded sand with silt. The quality of material for subgrade is good and the material is of A-1-b (0) quality according to the AASHTO classification system.

4.1.3 Site Treatment and Results

The extended Berth 21 was created by deposition of dredged sand between a new quay wall and the existing container terminal platform. The material below sea level was initially improved by means of Vibro compaction. Cone penetration testing (CPT) results obtained after Vibro compaction, showed that compaction was generally poor down to approximately 2.0m depth (weighted average CPT cone resistance was 4.8MPa). Normally, excavation and re-compaction by means of conventional vibratory rollers is required in order to decrease the variability in the load bearing characteristics of the sand, to reduce differential settlement, to increase the bearing strength of the material by densification, and to increase aging, thereby reducing the rate of secondary creep settlement. The alternative method employed was the surface ironing using a 3 sided 25 kJ high energy impact compactor, resulting in significant increases in material consistency to depth, with improvement recorded up to 5.0m deep and that the largest improvement recorded between 0.5m and 2.0m. The weighted average cone resistance recorded in the top 2.0m improved from 4.7 MPa to 11.6 MPa after completion of 40 passes of the impact compactor (measured from compacted surface downwards), with the weighted average cone resistance over 4.8m depth improving from 8.9 MPa to 13.6 MPa after impact compactor.

Initial average decelerations were improved from 5.3g to up to a maximum of 11.4g after the completion of 40 passes of the impact compactor. A CPT-CIR relationship was derived by correlating the average CPT value in the top 2.0m of the soil profile to an average deceleration value obtained in the CPT test point area. With the correlations established, limits were set and a CIR map was plotted, as depicted in Figure 6b. Sections failing to meet specification were clearly identified, as highlighted by the colour red, and were remediated with additional impact compactor passes.

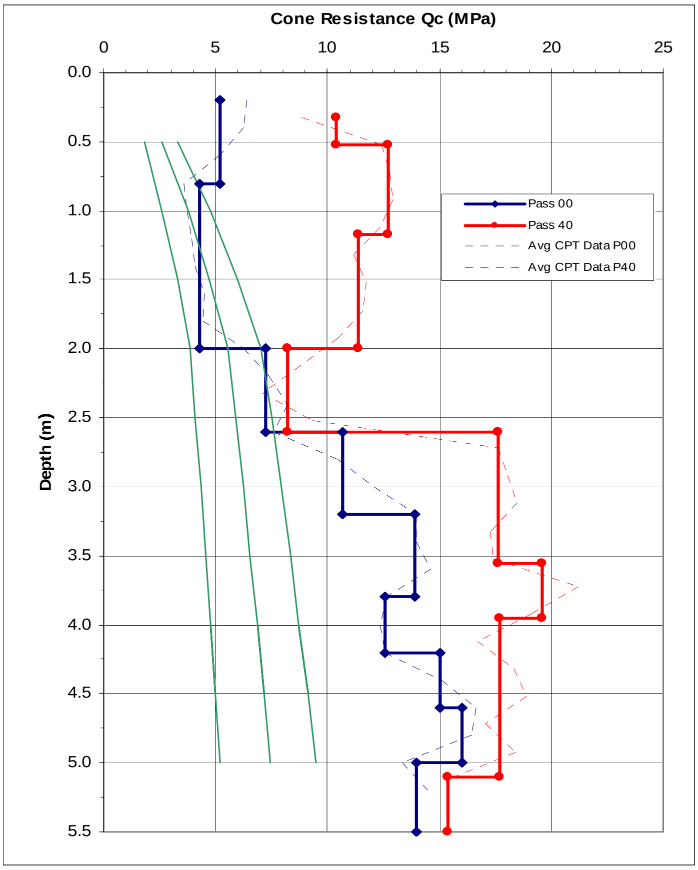

Figure 6a: CPT Results before and after HEIC

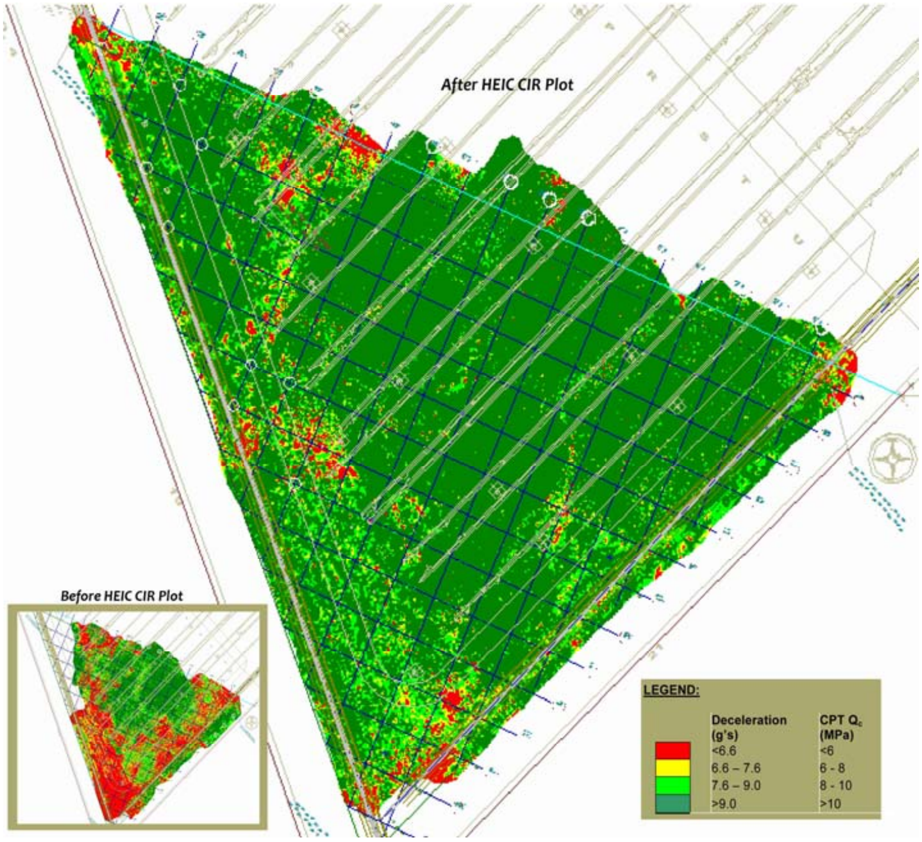

Figure 6b: CIR Map after HEIC

4.2 Project Study: Tanger Med II Container Terminal, Morocco

4.2.1 Project Statement

The Tanger MED II project is a continuation of the Tanger Med I project, which was completed several years ago, requiring up to a 140 hectare platform area to be constructed through a combination of a dredging/backfilling operation combined with deep and surface ground improvement, prior to pavement construction for a future container terminal. Up to five million cubic metres of material will be dredged, sourced offshore, and backfilled onto an area behind quay walls (currently being constructed). The backfilled dredged material will then be strengthened using deep Vibro compaction, with the final compaction planned for HEIC as a method of improving the top disturbed 2 to 3 meters created by the process of Vibro compaction.

4.2.2 Material Classification

Figure 7a shows typical particle size distribution of the dredged marine sands encountered at the site, basically a course grained marine sand.

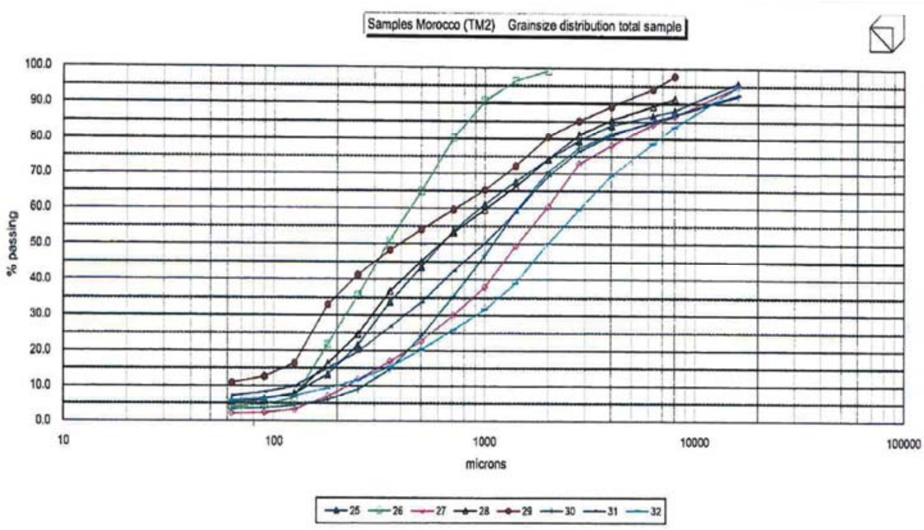

Figure 7a: Typical material grading analysis

4.2.3 Improvement Specification

Although of a poor quality, the material can be improved through the process of Vibro compaction and, although density and CBR requirements have been identified, the following controlling specification requirements have been set as the minimum:
- Cone Resistance (CPTU)$\geq$ 10MPa at surface through to -2m below the surface;
- Ev2 $\geq$ 100MPaat the surface; and
- k (Ev2/Ev1) $\leq$ 2 at the surface.

4.2.4 Site Treatment and Results

At the time of writing this paper, the final pavement design had yet to be finalised. There was, however, a 500mm layer of rock fill specified as part of the subgrade, which was to be introduced after improving the dredged material, prior to the 1m pavement structure. The section was treated with several methodologies in combination withHEIC and specification was achieved involving the following processes:
- Vibro compaction, to achieve CPTU$\geq$10MPa to -2m below ground level, followed by;
- Placement of a 250mm layer of Rockfill, then;
- Treated with a Landpac 3 sided 25kJ HEIC, to achieve CPTU $\geq$ 10MPa 0m to -2m below ground level, and finally;
- 8 passes of a smooth drum roller with moisture conditioning, to achieve Ev2 $\geq$ 100MPa & k $\leq$ 2.

The results are summarised as follows:
- CPTU results indicated Qc values $\geq$ 10MPa to the required depth of -2m below ground level, with similar improvement experienced between 3 and 5m in some sections.

- Plate load tests indicated Ev2 values ranging from 107 to 145 MPa, exceeding the specification requirements of 100 MPa at the surface.
- Ev2/Ev1 ratios (k) ranged between 1.72 and 2.0, also within the required specification.
- Average induced settlement (CIS) of 218mm was experienced, with a maximum settlement of 287mm recorded; confirming differential settlements have been reduced by the HEIC process.
- 80 Passes with recorded CIR decelerations ranging between 14 and 15 m/s^2 (18.16 m/s^2max), resulting in a correlation with CPTU data that would require a g > 12 m/s^2 to achieve a Cone Resistance > 10 MPa, as specified.

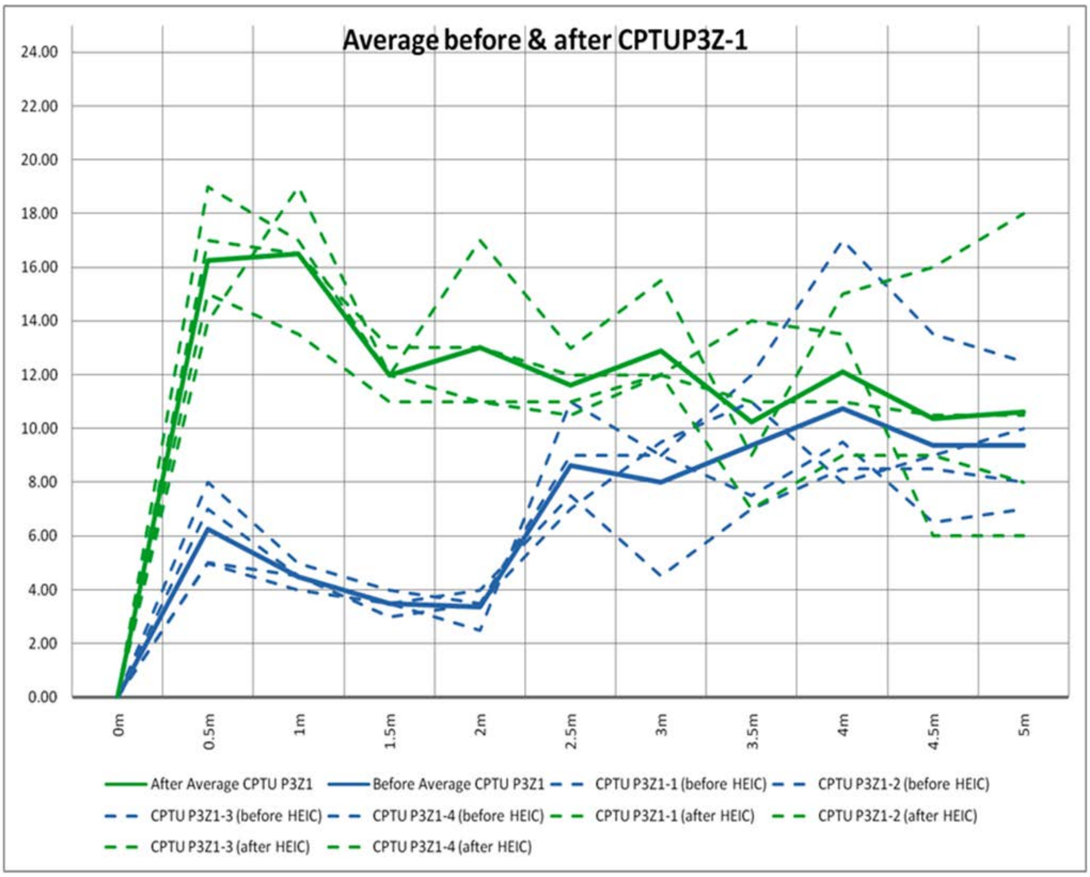

Figure 7b: CPT Results before and after 80 HEIC passes

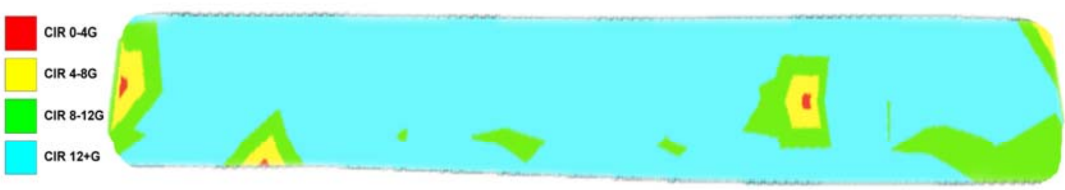

Figure 7c: Typical CIR plot after 60 HEIC passeson a test strip with specification adherence shown in blue, Qc>10MPa

4.3 Project Study: Copenhagen Malmo Port (CMP), Sweden

4.3.1 Project Statement

LANDPAC were appointed by Skanska, to undertake ground improvement HEIC works as part of the "site preparatory works" on behalf of the client – Copenhagen Malmo Port (CMP) and the client's consultant – Ramböll to characterise the site and permit the development to support proposed container terminal pavements, externals and rail corridor. City of Malmö signed an agreement with Skanska to build a major new port facility for CMP in Norra Hamnen on 23 Hectares within the overall 150 Hectare site. The development included three new terminals and associated pavement & rail-line construction. The joint project involved the City of Malmö, who owns the land in Norra Hamnen, and CMP, which operates the port. The area earmarked is the result of landfilling over sea, thus land reclamation, including earth from the then City Tunnel project in Malmö.

4.3.2 Material Classification

The site comprises reclaimed land with approximately 3m to 6m thickness of 'end-tipped' soil from the nearby Malmo City Rail tunnelling project and sea dredged materials from past harbour maintenance. No compaction had taken place prior to HEIC. Some locations, the existing materials contained soil to be a mixture of concrete and demolition debris from gravel to boulder size in a matrix of silty sand and sandy gravelly clay. Other locations, the existing materials varied from a mixture of granular / cohesive / Silt fills. Groundwater was at about 2m to 3m depth.

4.3.3 Improvement Specification

Although of a poor and varied quality, the majority of the mixed fill materials were to be improved through the process of HEIC, investigative CIR & CIS and soft spot identification / removal / replacement with the following controlling specification requirement having been set as the minimum:
- Ev2 $\geq$ 30MPa; and
- kvalue (Ev2/Ev1) $\leq$ 2.5

4.3.4 Site Treatment and Results

CIR stiffness profile monitoring was used during the HEIC application to characterise and verify Ev2 specification, after correlation with CIR, of the site existing fill material. The CIR data was to be correlated with numerous Dynamic Plate Test (DPT) results, which allowed a site wide characterisation and also determined the soil replacement areas for the client, which resulted in minimising costly excavations.

The site was treated with HEIC and specification was achieved involving the following methodology:
- Treat with a Landpac 5 sided 22kJ HEIC, to induce maximum settlement possible& Ev2$\geq$ 30MPa,
- Dynamic Plate Testing (DPT) at surface and at varying depths
- Correlate CIR and DPT data
- CIR characterisation of the treated area/s to identify soft spots needing removal & replacement.
- Soft sections, highlighted and precisely marked using the CIR, were removed, replaced and recompacted to specification

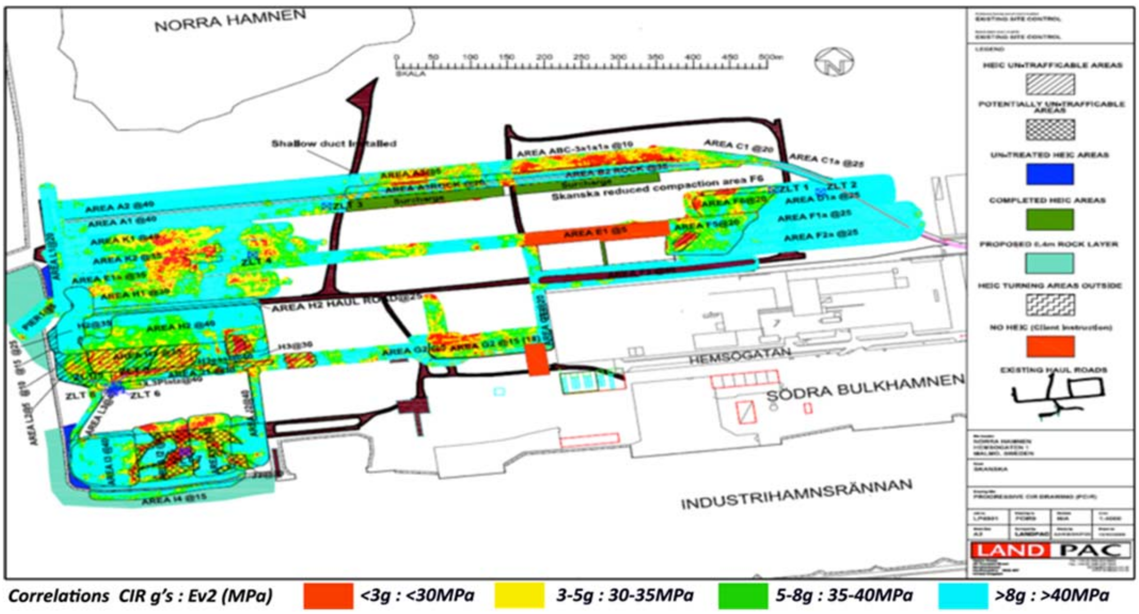

Figure 8: CIR correlated with Dynamic Plate Tests (Ev2) and site characterized for soft spots

4.4 Project Study: Port Botany, Sydney, Australia

4.4.1 Project Statement

The project involved the reclamation of 63Ha with 8 million m^3 of dredged sand, making it one of the largest port projects ever undertaken in Australia in the last 30 years. The project infrastructure included a new container terminal and almost 2km of extra berth length. The new berth structures required the construction of blockwork and counterfort walls up to 21m high. Also included in the project was the reclamation of a 2Ha area for a public boat ramp and a car parking area.

Figure 9a: HEIC process post Dynamic Compaction improvement at Port Botany.

4.4.2 Material Classification

The borrow area consists of fine to medium grained marine sands with lenses containing organic and clay. The specification for the dredged sand used for the reclamation requires less than 10% fines passing through the 75μm sieve.

4.4.3 Site Treatment and Results

The Impaction Compaction process in the early work areas were carried out on a nominal 300mm Sandstone constraining layer that was placed over the sand fill that had been subject to Dynamic Compaction. The 300mm layer formed part of a working layer for the construction access and hardstand areas. Cone Penetrometer testing was carried out on these areas to verify the compaction results. The average Cone Resistance (Qc) improved from an average of less than 8MPa post dynamic compaction to an average exceeding 15MPa post HEIC in the top 2m. Cone resistances exceeding 20MPa were recorded between 2 and 4m, post HEIC treatment.

The Impact Compaction in the New Terminal area was carried out on the sand fill surface that had been subject to either Vibro Compaction or dynamic compaction. Density tests were carried out in test pits to verify the compaction results. The average density recorded in the depth range from 100-1800mm below the compacted surface, at an average field moisture content of 6.9%, was 106.9%.

The final area treated was the Public Boat Ramp area and although pre-compaction CPTs were not done, post compaction results indicated an average Cone Resistance (Qc) of 15MPa in the top 1m, greater than 20MPa from 1-2m below the surface, tapering down to approximately 10MPa from 2 to 3m below the surface.

With the specification set to achieving a density index of 75% in the top 2m and a Cone Resistance (Qc) exceeding 5 MPa in the full depth of the reclamation area, HEIC was successfully used to improve the top 4m that would not have met specification post treatment by the deep ground improvement techniques that had been employed. Results beyond 4m were within the requirements of the specification. The combination of the two technologies certainly offered a cost effective solution to the project.

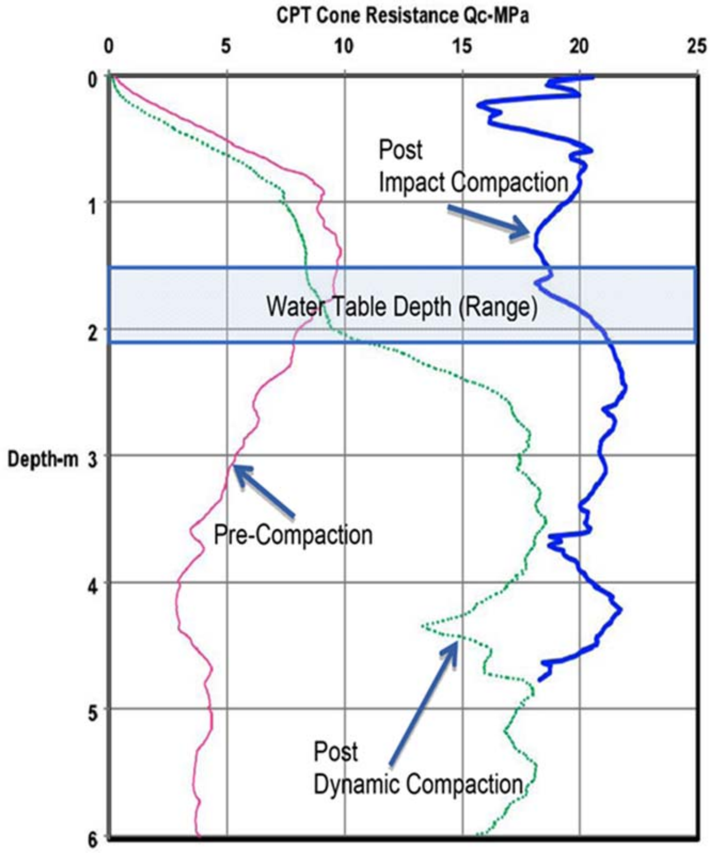

Figure 9b: CPT results showing the improvement of Cone Resistance post HEIC

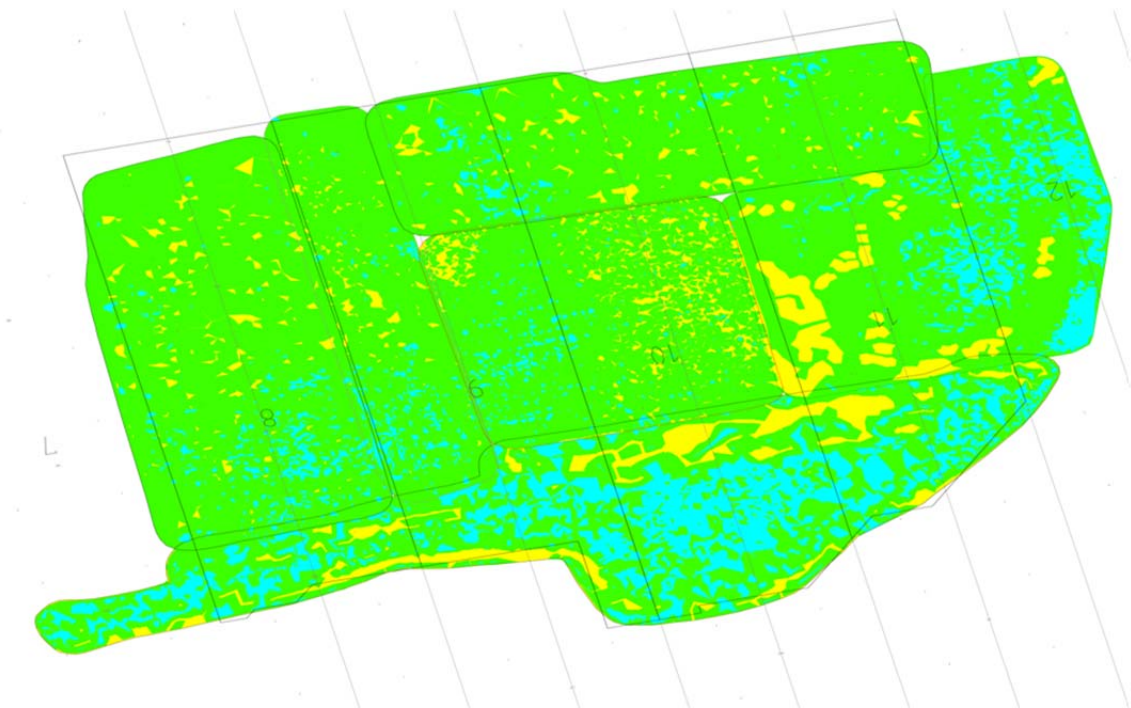

Figure 9c: Typical CIR plot post HEIC treatment where sections not meeting specification would have been highlighted in red.

5. CONCLUSION

Rapid industrial growth has increased demand for further land development through land reclamation and utilisation of unsuitable and environmentally affected materials. The conversion of such requirements into usable land has been made possible through the adoption of one or more ground improvement techniques, making this a rapidly expanding field of applications.

Ground improvement techniques are used extensively to solve a broad spectrum of geotechnical problems, with the techniques enabling innovative solutions to be considered and applied. The utilisation of the twin drum HEIC has proven to be innovative in not only solving some of the geotechnical concerns with ground improvement, but also offering it cost effectively with improved production possibilities. Although the technology has been very successful in offering stand alone solutions to some problems, it has been equally successful in offering solutions in conjunction with deeper ground improvement technologies, like vibro and dynamic compaction, in mixed and contaminated fills and, specifically, on dredged marine sands.

Problematic material improvement places an increased importance on quality control measures. The Landpac developed CIR and CIS technologies, with fully integrated GPS, used in conjunction with the twin drum HEIC, involves the direct measurement of engineering properties of the material with real time continuous measurement, offering high levels of quality control and improvement certification.

The increase in the scope and complexity of current global ground improvement projects places a great deal of emphasis on innovative solutions with improved quality control techniques. The advantages associated with HEIC and the CIR and CIS quality control systems have been documented in this paper, with references made to actual case projects.

REFERENCES

McCann K. & Schofield N., 2007, "Innovative Methods in the In-situ Determination of Design Parameters on Heterogeneous Sites Subject To Ground Treatment Using Deep Impact Compaction", ANZGEO2007 - 10th Australia New Zealand Conference on Geomechanics, Brisbane, Australia.

Jumo I. and Geldenhuys J., 2004,"Impact Compaction of Subgrades – Experience on the trans-Kalahari highway including Continuous Impact response (CIR) as a method of Quality Control", Proceedings of the 8th Conference on Asphalt Pavements for Southern Africa (CAPSA 04).

Wilken P.J., 2001, "The development of the Continuous Impact Response (CIR) system", Seminar on Ground Improvement through the Geotechnical Division of the South African Institution of Civil Engineering, Pretoria, South Africa.

Kelly D., 2000, "Deep In-situ Ground Improvement using High Energy Impact Compaction (HEIC) Technology", GeoEng 2000 – International Conference on Geotechnical and Geological Engineering, Melbourne, Australia.

Controlled Modulus Columns (CMC): A New Trend in Ground Improvement and Potential Applications to Indonesian Soils

Kenny Yee, BUT Menard Geosystems, Jakarta, Indonesia, kenny@menard-asia.com
Ryan Ade Setiawan, BUT Menard Geosystems, Jakarta, Indonesia, ryan@menard-asia.com
Olivier Bechet, BUT Menard Geosystems, Jakarta, Indonesia, olivier.bechet@menard-asia.com

ABSTRACT

Controlled Modulus Columns (CMC) was a result of many years of research and development carried out at Menard France to meet the increasingly demanding requirements for ground improvement technology to take higher imposed loads and more stringent settlement criteria. Besides, the call for wider use of green technology and environmental friendly solutions has led to the development of CMC in the late 1990s with improved construction method and refined design methodology. CMCs are vertical semi-rigid inclusions (columns) designed to obtain a composite soil-CMC mass when they are installed in the ground. These inclusions are low-strength cement grout injected under low pressure through a hollow stem equipped with an auger unit which causes lateral soil displacement during installation. CMCs are installed without surface vibration and minimum spoil. Hence, CMCs are most suitable for sensitive environment applications as in the case of urban areas. This paper will present details on the installation method, design philosophy and a case study in Indonesia. The potential of CMC applications in Indonesia will also be discussed.

1. INTRODUCTION

In the rapid expansion in housing, infrastructure and utilities developments, engineers have to deal with less favorable sites such as non-engineered fill ground, coastal lowlands and swamps, reclaimed land, etc. All these developments on marginal ground would have been economically non-viable and/or technically non-feasible if they had been constructed using conventional methods meant for good ground. For mega-size projects, it was necessary to explore the innovations of using non-conventional methods when poor soil conditions may impair the integrity and serviceability of the structures. In such situations, the natural condition of poor soil needs to be improved to meet the intended purposes of construction. Ground improvement is used to (i) control deformation and accelerate consolidation; (ii) increase bearing capacity and provide lateral stability; and (iii) increase resistance to liquefaction.

When the imposed loads are moderate and the settlement criteria are not too stringent (e.g. road embankment), ground improvement techniques such as vertical drains and/or stone columns usually provide a good solution in terms of cost and performance. However, when the ground is very poor and the imposed load is high coupled with strict settlement criteria, ground improvement may be considered inadequate especially in the case of a tight construction schedule. Very often, structural solution using piled foundation is adopted. CMC was specifically developed to fill in the gap between conventional ground improvement methods such as vertical drains or stone columns (non-rigid inclusion) and that of RC piles (rigid inclusion). Semi-rigid inclusions of CMC prove to be of higher performance than non-rigid inclusions in very poor ground and less costly than rigid inclusions of RC piles. The term "controlled modulus column" is meant to provide the necessary composite effect of poor soil with stiffer CMC inclusions designed to achieve the required composite stiffness for the intended purpose of the construction. The semi-rigid CMC inclusion does not suffer column bulging as in the case of non-rigid stone column when it is loaded in very soft soil. For rigid RC pile, imposed load is transferred by the pile cap or RC slab through the rigid pile shaft to load bearing layer deep below ground as in most cases. For the composite soil-CMC mass, the load is uniformly distributed by the upper layer of compacted sand blanket and hence, the CMC inclusions are not necessarily end-bearing as shown in Fig. 1. Without the pile cap and/or RC slab and shorter length of inclusions, CMC has proven to be the cheaper option compared with piled foundation.

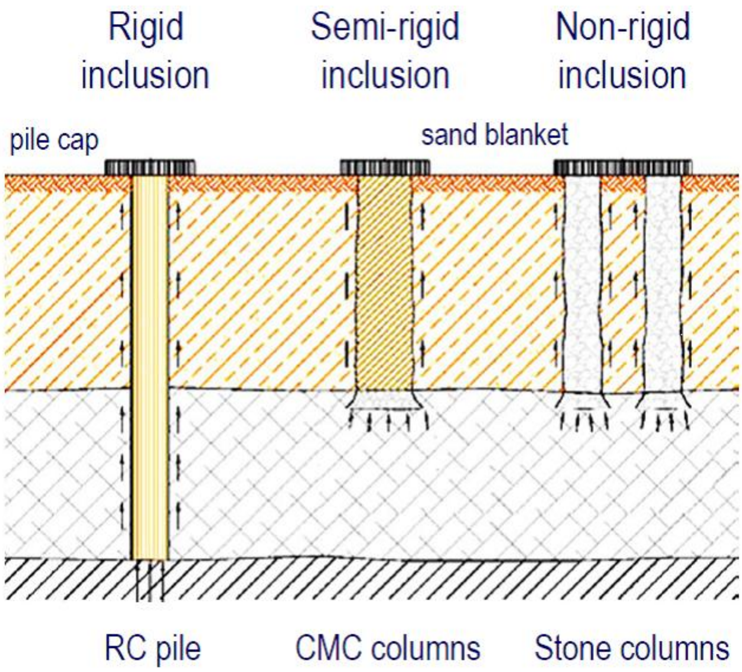

Figure 1: Different types of inclusions

2. CONTROLLED MODULUS COLUMNS

2.1. Construction

CMCs are installed using a hollow stem equipped with a displacement auger coupled with a high torque coming from a high capacity pull-down CMC installation rig. The displacement auger consists of three components:

- The bottom part of the auger with its constant flight volume will evacuate the spoil upward during penetration.
- The middle part of the auger is the displacement part which has the same diameter as the auger and the hole. It prevents the spoil from reaching to the surface. It displaces it laterally, thus providing compaction to the soil.
- The upper part of the auger has flight in the opposite direction compared to the lower part. As a result, it brings any spoil caused by potential collapse of the hole downward to the displacement section. Hence, it improves the efficiency and the overall quality and continuity of the CMC inclusion.

The CMC rig has a high torque and strong downward thrust. The auger is advanced into the ground while rotating. No grout is injected at this stage. When the required depth is reached, the grout is pumped through the hollow stem with low pressure sufficient to prevent “caving-in” due to lateral pressure of the surrounding soil. The auger is extracted while the rotation is maintained in the same direction as during the penetration stage in order to prevent loss of grout along the shaft of the hole and along the Kelly bar. Fig.2 shows the installation of CMC.

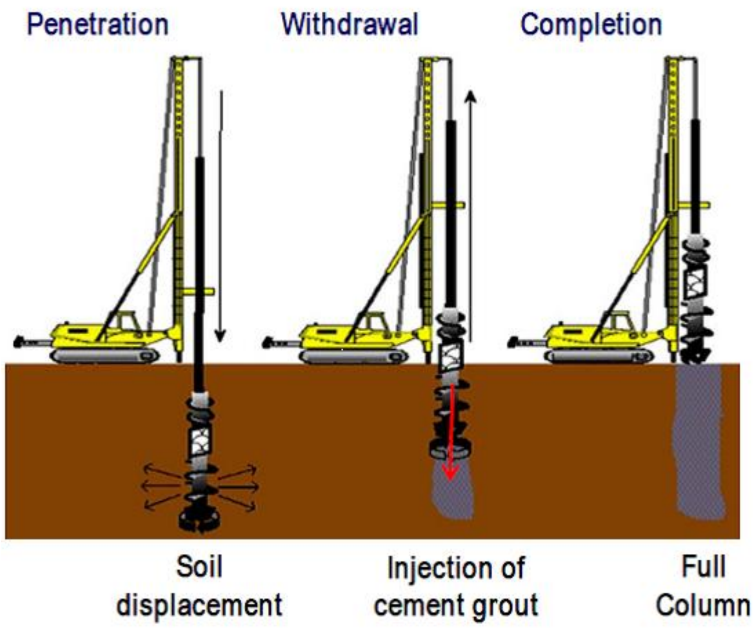

Figure 2: Installation of CMC

The cement grout used for CMC inclusion has a compressive strength of 10 – 20 MPa and a slump of 20cm for pumpability. During the installation process, the following information is monitored and recorded by the on-board computer system (Fig. 3):

- Speed of rotation and advancement of auger.
- Torque, downward-thrust and augering energy during penetration.
- Pressure and volume of injected grout.

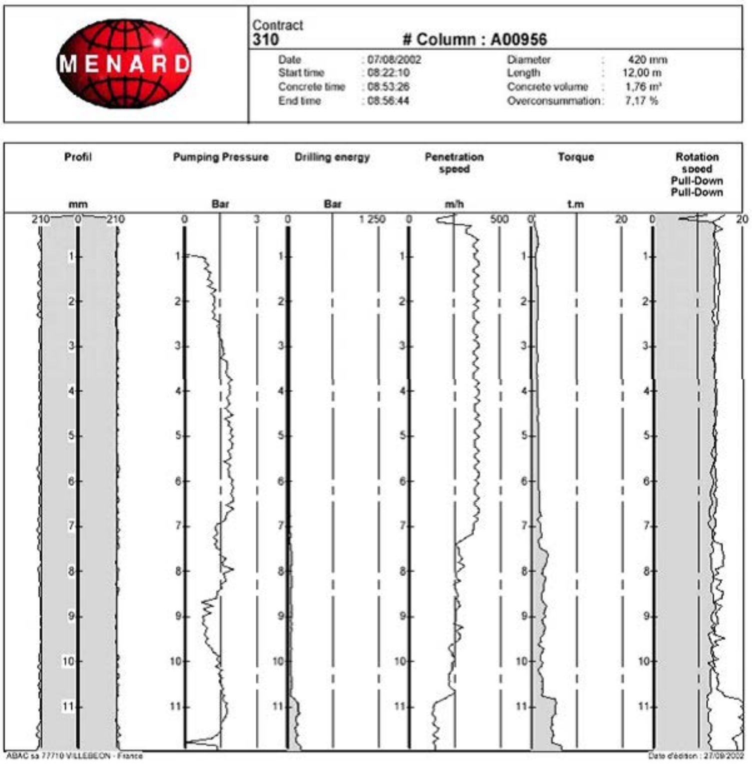

Figure 3: Installation record for CMC

With the above information, the computer computes the diameter of CMC inclusion against the length as it is being installed.

The displacement method used has no spoil during installation and no surface vibration. It does not require any water jetting or compressed air injection for penetration as in the case of installing stone columns. Hence, this method is environmental friendly and it is most appropriate for urban environment type of construction.

2.2. Design

The design of CMC considers both serviceability and stability. For structures on CMC, the governing factor is usually deformation (settlement). For embankments on CMC, beside serviceability the global stability is also checked especially during construction.

2.2.1 Deformation Analysis

The deformation analysis is based on the optimum load sharing between the CMCs and the surrounding soil. This is aided by a layer of compacted sand blanket on top of the CMC acting as load distribution layer as opposed to the 100% of load transferred to the piles with no load in the soil (Fig. 4).

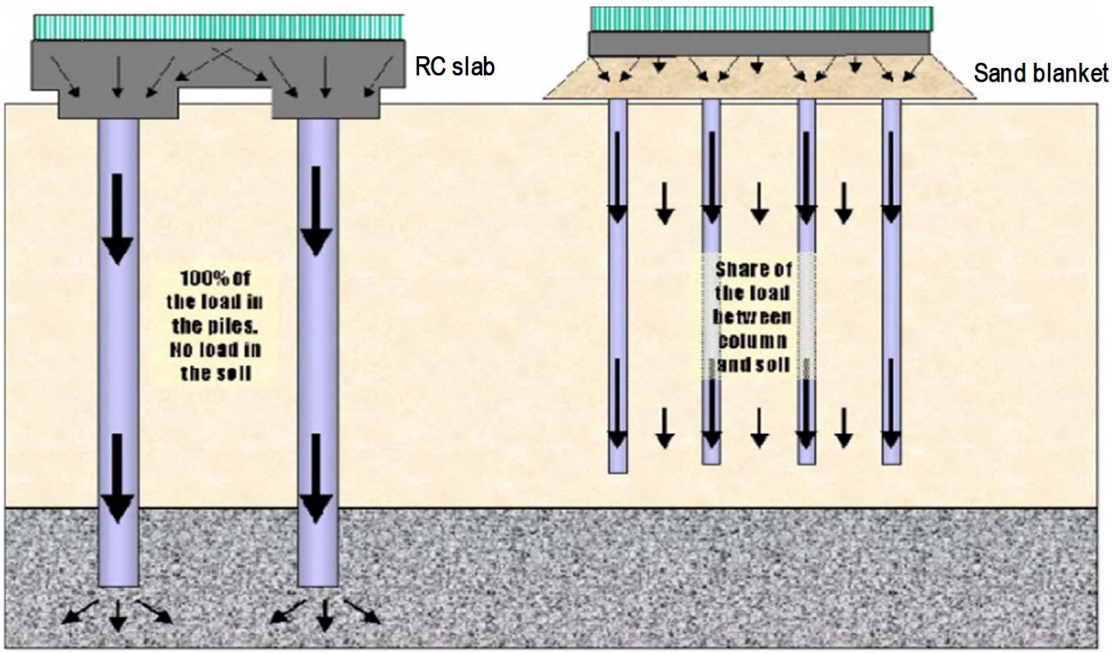

Figure 4: Concept of load sharing in CMC and piled system

The process of load sharing mechanism in CMC is illustrated in Fig. 5. Since the ratio of stiffness between CMC and the soil is between 1:1,000 to 1:10,000 it is necessary to consider the vertical deformation separately for the CMC and the soil. The deformation of a point inside the CMC at a given initial depth is different from an adjacent point at the same depth in the soil. In other words, there exists a different field of deformation between the CMC and the surrounding soil as explained below:

- Stage 1: Due to the transfer of imposed stress to the soil (σ_{soil}) through the load distribution layer (sand blanket), vertical deformation (settlement) of the soil (δ_{soil}) occurs due to consolidation.
- Stage 2: As a result of consolidation settlement, stress is transferred from the surrounding soil to the CMC. The deformation at the same given depth (except at neutral plane) in the soil (δ_{soil}) is different from the CMC (δ_{CMC}) due to different stiffness ($E_{CMC} > E_{soil}$) and that $\delta_{soil} > \delta_{CMC}$, negative skin friction is developed in the CMC.
- Stage 3: At greater depth, the point deformation $\delta_{CMC} > \delta_{soil}$ resulting in a stress transfer from the CMC back to the competent soil. This induces positive skin friction and base resistance.
- Stage 4: Overall, an equilibrium state of load distribution is achieved where the tip resistance, friction resistance and soil resistance is equals to the total load.

Fig. 6 shows the locations of the neutral plane where point deformation of CMC and soil is the same. At this location, the CMC column carries the maximum stress.

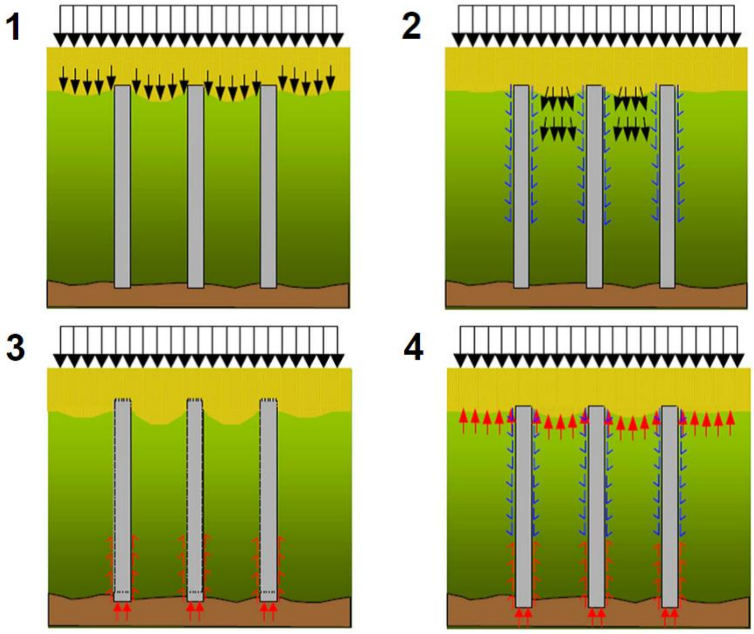

Figure 5: Load sharing mechanism in CMC

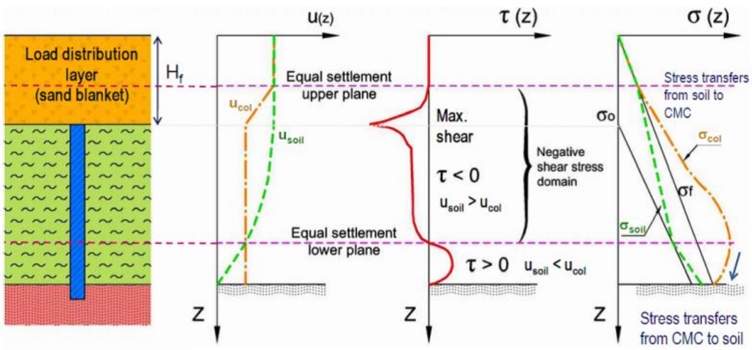

Figure 6: Stress distribution in soil-CMC mass

Finite element method (FEM) is used for the deformation analysis. It considers the "punching" effect of the CMC into the sand blanket at the top and anchoring at the bottom into competent soil layer. It also considers the stress-strain behavior of the CMC grout and the surrounding soil as well as the load transfer between CMC and the surrounding soil.

The analysis is carried out in two phases. An axisymmetry model with a single CMC inclusion (Fig. 7) is first analyzed based on the imposed load on the selected CMC design grid spacing, diameter and length of CMC, mechanical properties of cement grout and sand blanket with or without reinforcement. Stresses and deformation are analyzed. If results are unsatisfactory, refinement can be carried out on the design parameters.

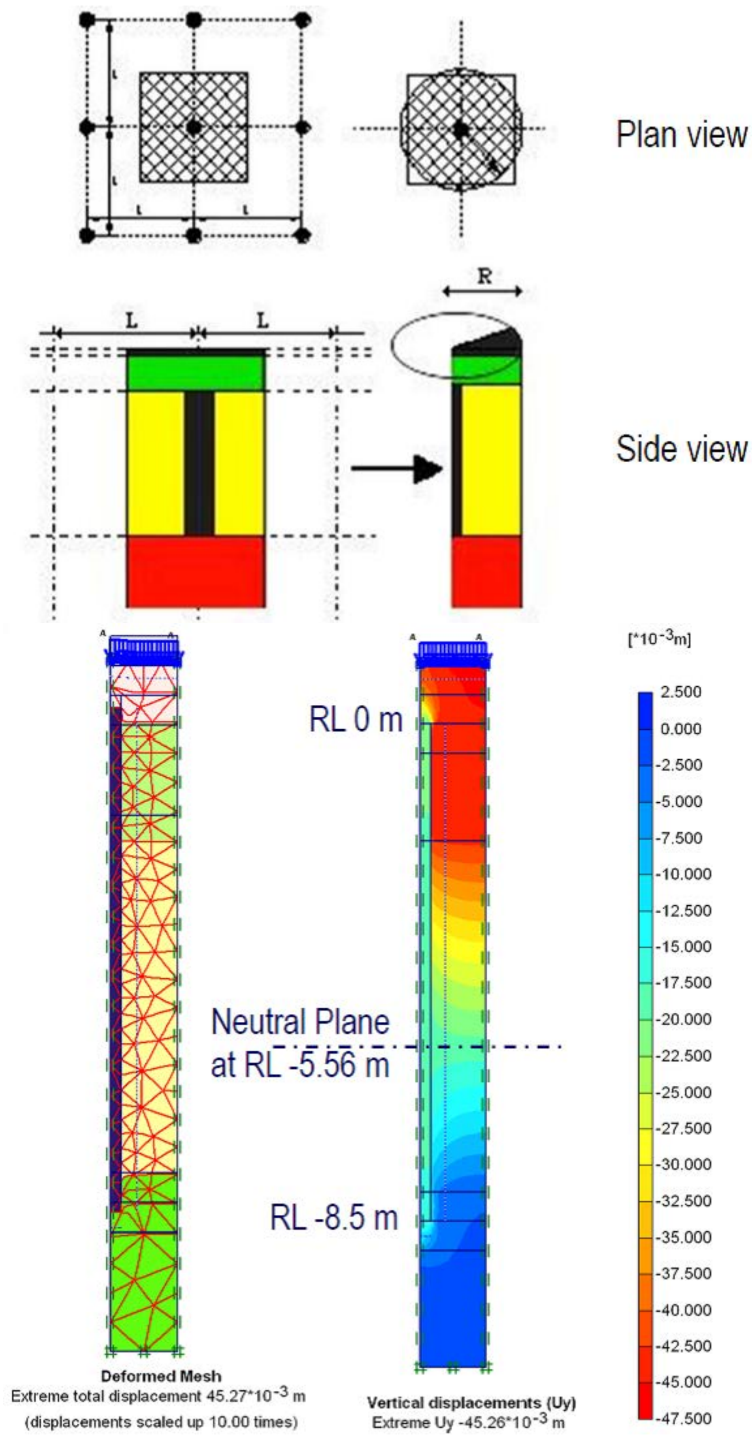

Figure 7: Axisymmetry model of CMC

Once the design parameters have been validated to be acceptable at the "microscopic" level with the axisymmetry model, a "global macroscopic" elasto-plastic model can be performed taking into account the "true" geometrical representation and specific boundary conditions such as:

- Variable fill height or non-symmetry loading condition.
- Different construction stages with time.
- Variation in ground conditions.
- Variation in CMC spacing and length.

The second phase analysis provides confirmation of compliance with the deformation criteria and stability requirement. It also confirms the allowable stresses in the CMC and the surrounding soil. Depending on the complexity of the problem, the second phase analysis is carried out using a 2-dimensional (Fig. 8) or a 3-dimensional model (Fig. 9).

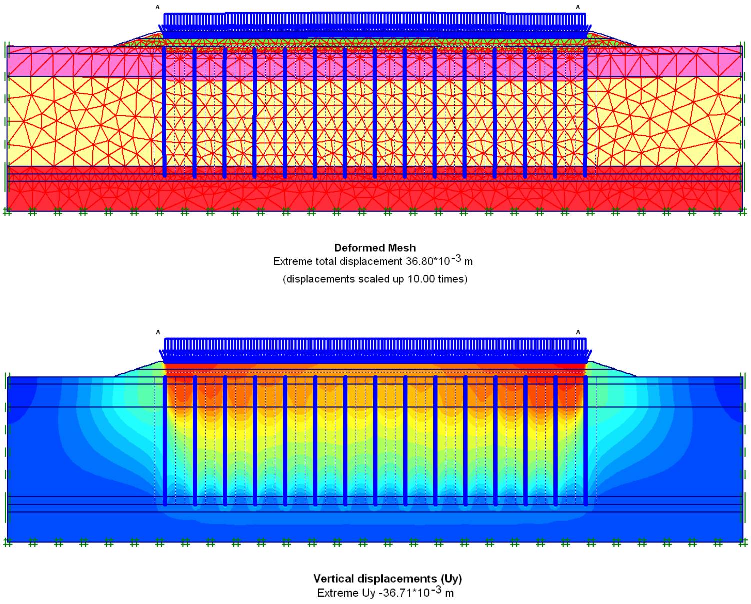

Figure 8: 2-D plane strain model of an embankment on CMC

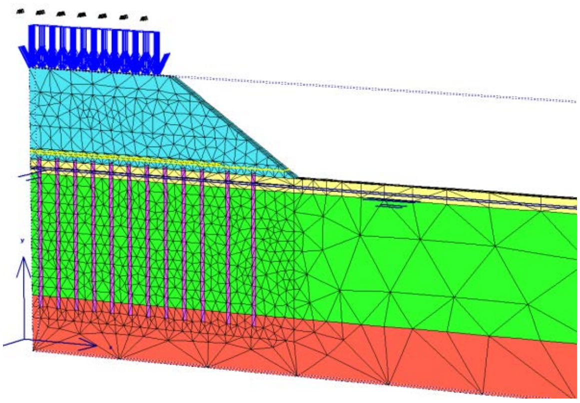

Figure 9: 3-D plane strain model of an embankment on CMC

2.2.2 Stability Analysis

When CMCs are installed in soft soil to support an embankment, stability analysis is carried out using slope stability programs capable of incorporating the beneficial effects of the CMC inclusions as shown in Fig. 10.

Fig. 11 shows the vertical reaction force Ri and the sub-horizontal force Ti. The vertical reaction Ri from the CMC supports a significant portion of the embankment load which may accounts for about 70% to 90% of the total imposed load depending on the CMC grid spacing, embankment thickness and type of soil. The remaining (lesser) load goes to the weaker soil and hence, increases the stability.

The sub-horizontal reaction Ti develops a resisting shear force directly opposing the potential shear failure surface. The resisting shear force is developed due to a differential field of deformation between the CMC and the soil on each side of the potential failure surface as explained earlier. The differential deformation of the soil above and below the potential failure surface induces shear force against the CMC inclusion.

For stability analysis, the following steps are carried out:

Evaluation of the vertical reaction Ri in the CMC which depends on the embankment height, CMC spacing and diameter.

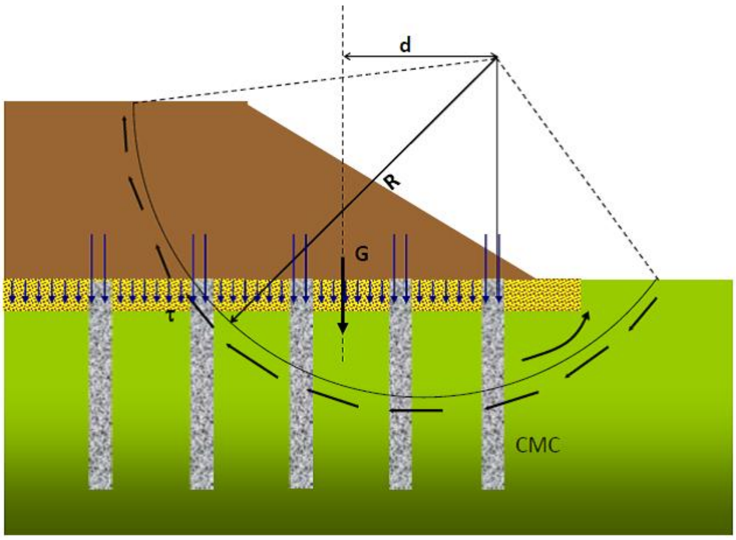

Figure 10: Stabilizing effects of CMC against global instability

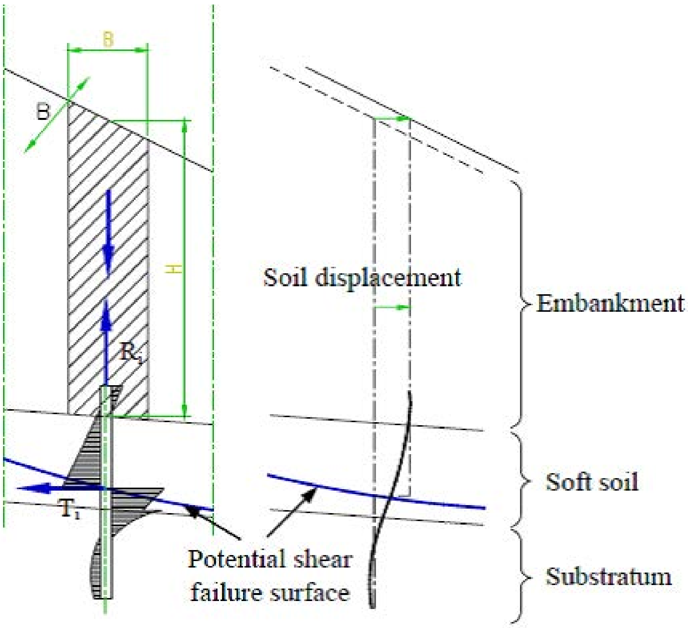

Figure 11: Resisting forces to shear failure

- Calculation of the maximum allowable bending moment Mi in the CMC which is limited by the acceptable stresses (σ_{CMC}) of the CMC grout material given by:

$$\sigma_{CMC} = \frac{Ri}{\pi.D^2/4} \pm \frac{Mi}{\pi D^3/32} \tag{1}$$

where D is the CMC diameter.
- Calculation of the shear stress capacity Ti of the CMC in the deformation field which is determined by the maximum allowable bending moment in the CMC. The shear stress is calculated using:

$$\delta\sigma.B = Ks * B * \delta y \tag{2}$$

where
$\delta\sigma$ = differential pressure of the soil between each side of the CMC with $\delta\sigma$ limited to the pressuremeter creep pressure P_f.
δy = differential displacement between soil and CMC
Ks.B = reaction modulus of the soil applied over the width B of the CMC.

Knowing the axial vertical stress Ri, the maximum allowable bending moment on the CMC is then calculated from the acceptable maximum compression and tensile stresses of the CMC grout material which is controlled by the following criteria:
- Compressive stress (σ_{CMC}) $\leq$ 5 MPa.
- Maximum M/N $\leq$ D/8 with D being the diameter of CMC; M is the bending moment and N is the axial force.
- No tensile stress in the CMC.

Under the combined axial force N and bending moment M, maximum compressive stress in the CMC is given by equation (1). Further details are found in Plomteux & Lacazedieu (2007).

Allowable shear stress in the CMC during potential slope failure will corresponds to the shear stress obtained for the soil deformation field that creates the maximum allowable bending moment in the CMC column.

3. CASE HISTORY

3.1. Brief Description

The project consists of constructing an airport apron measuring about 65,000m^2. The apron is constructed as part of an extension to an existing international airport in Indonesia. The apron extension is to accommodate aircraft to the size of Boeing 747. The pavement is 105cm thick reinforced concrete slab with 45cm thick crushed rock sub-base. The total design load of the aircraft, the pavement and fill material is 70 kN/m^2. The design load of the aircraft at rest is 50 kN/m^2. The design load of the apron is considered critical with low aircraft speed and/or aircraft at rest. The required CBR is 6% for the pavement design.

3.2. Ground Conditions

Geotechnical investigation was carried out including 3 nos. of exploratory boreholes, 10 nos. of cone penetration tests (CPT), 4 nos. of plate bearing tests and 4 nos. of CBR tests. The locations of these tests are shown in Fig. 12. The ground water table is about 3m below existing surface grade which is also the final finished level of the pavement. From the investigation results, the ground condition is deemed highly heterogeneous (Fig. 13) with competent layers found at varying depths of 3m to 12m below grade. Generally, there is an upper layer of soft to medium stiff silty clay ($N_{SPT} \sim 3 – 8$) overlying dense sand or stiff clay layer ($N_{SPT} > 10$). In some areas, there are two layers of soft to medium stiff silty clay in-between dense sand or stiff clay. Organic matter is found intermittently in the upper silty clay layer.

Results of plate bearing tests and CBR tests confirmed the inadequacy of the CBR values to achieve the required serviceability of the airport apron. Hence, ground improvement was considered to improve the existing ground conditions to meet the specification requirement of CBR = 6%.

3.3. Ground Improvement

Since the apron extension is located within an operating airport facility, environmental constraints such as minimum noise and surface vibration during construction; minimum quantity of spoil from installation works (which alleviate problems of sludge disposal within and off-site); and minimise adverse environmental impacts from the use of water jetting or high pressure compressed air (as in the case of stone columns installation works) or any form of mechanical soil mixing (as in the case of deep soil mixing method) which may remould the existing soft soil; all of these determine the choice of ground improvement method to be adopted.
Due to the environmental friendliness of CMC, this method was selected. Furthermore, CMC provides the flexibility to adapt on site by varying the length of the inclusions, the grid spacing and the strength of CMC grout according to the prevailing ground conditions to achieve the required performance.

3.4. Design & Implementation

Due to the heterogeneous ground conditions and the requirement of CBR = 6%, the design for the CMC system follows a dual-grid system as shown in Fig. 14.

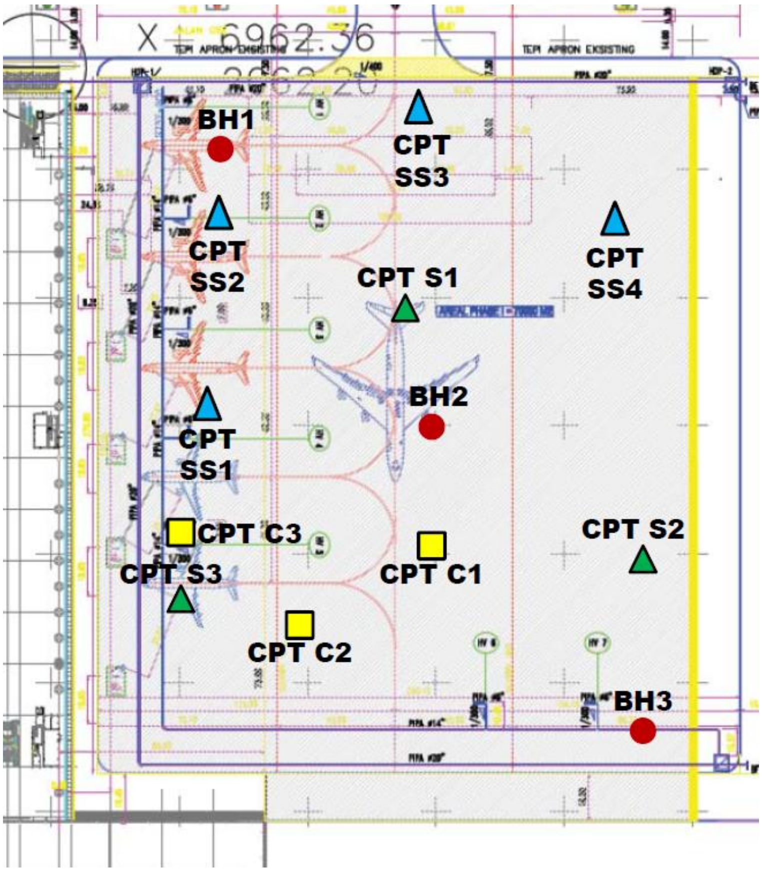

Figure 12: Locations of boreholes (BH) and cone penetration tests (CPT)

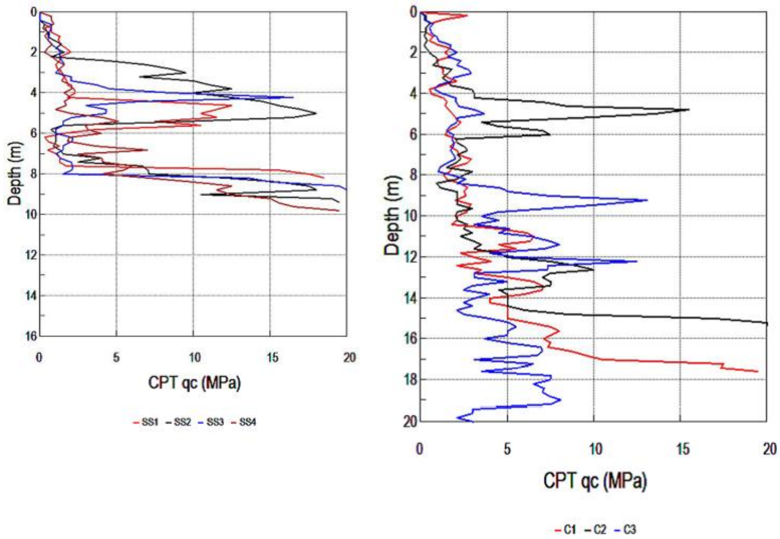

Figure 13: CPT results indicating the heterogeneous ground conditions

The CMC inclusions are 32cm in diameter with a compressive strength of 10 MPa for the cement grout. The upper layer consists of both the primary CMC and the secondary CMC. The grid spacing is 2 columns per 3m square. The objective is to increase the CBR values and to reduce post construction settlement. The lower layer consists of the primary CMC. The grid spacing is 1 column per 3m square. The objective is to reduce post construction settlement. The length of the primary CMC varies from 6.5m to 12m while the length of the secondary CMC is from 1m to 9m.
Due to the heterogeneous ground conditions and to maintain its cost effectiveness, the apron area is divided into 8 different zones of treatment. Each zone has different column length for both the primary and secondary CMC but with the same grid spacing as shown in Fig. 14. The eight zones of treatment are shown in Fig. 15.

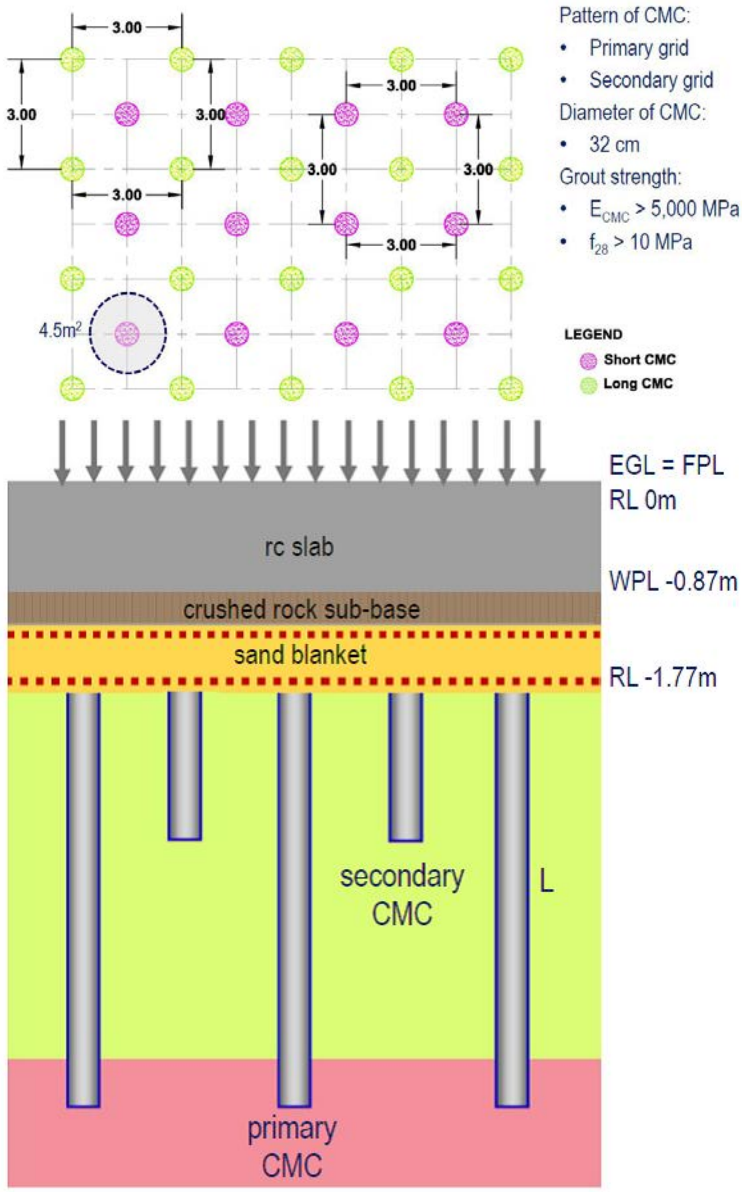

Figure 14: Dual grid CMC design: plan view (top) and elevation view (bottom)

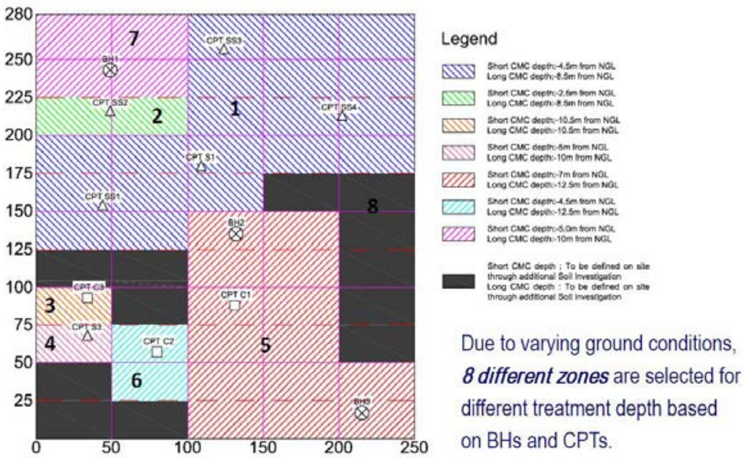

Figure 15: Eight different zones of treatment

Due to the complexity of the dual grid CMC system, a 3-D analysis was carried out to determine the settlement and the CBR values. Fig. 16 shows a 3-D analysis and the results of the analysis is given in Fig. 17.

Zone	Termination Short CMC	Termination Long CMC	Settlement δ	Stiffness Modulus E_Y	Westergaard Modulus K_W	CBR
1	EL -4.5m	EL -8.5m	35 mm	26 MPa	64 MPa	9.4
2	EL -2.5m	EL -8.5m	32 mm	30 MPa	74 MPa	11.2
3	EL -10.5m	EL -10.5m	58 mm	23 MPa	56 MPa	8.2
4	EL -5m	EL -10m	41 mm	21 MPa	51 MPa	7.1
5	EL -7m	EL -12.5m	53 mm	20 MPa	48 MPa	6.7
6	EL -5.5m	EL -12.5m	52 mm	18 MPa	44 MPa	6.0
7	EL -5m	EL -10m	45 mm	19 MPa	46 MPa	6.4
8	EL -4.8m	EL -11.7m	51 mm	21 MPa	51 MPa	7.2

Figure 16: 3-D FEM analysis for the dual grid CMC

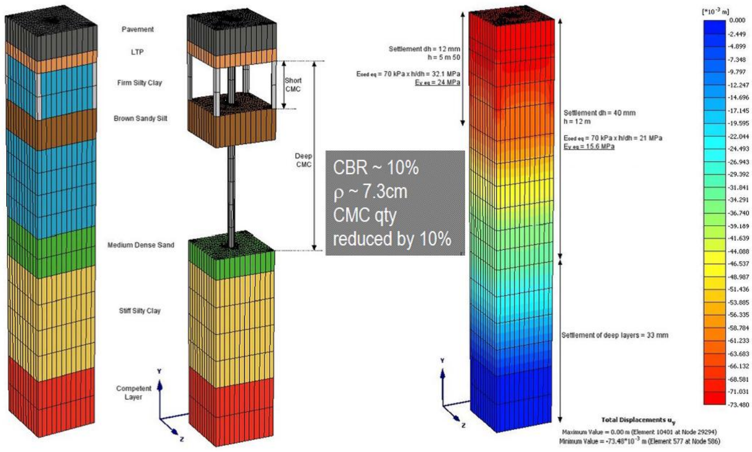

Figure 17: Results of FEM analysis

The computed settlement varies from 3cm to 6cm with an average of 4.5cm. Differential settlement is about 1.3cm to 1.5cm. The CBR value varies from 6% to 11%. The maximum compressive stress in the CMC is about 2.2 MPa. Fig. 18 shows the installation of CMC.

Figure 18: Installation of CMC columns

3.5. Plate Load Tests (PLT)

Six numbers of plate load tests (PLT) were carried out after 28 days on selected CMC. The tests were carried out to 150% of the working load to reach a compressive stress of 3.3 MPa in the CMC. Fig. 19 shows a selected CMC to be tested.

Fig. 19: Selected CMC column for PLT

The PLT test results registered settlement of 9mm to 18mm under 100% of working load (σ_{CMC} = 2.2 MPa) and 13mm to 28mm under 150% of working load (σ_{CMC} = 3.3 MPa). These values were checked against a simulated PLT model using FEM and the results of the analysis indicated an average settlement of 44mm under 100% of working load. Hence, the measured settlement being less than the calculated settlement using the same analytical model used for the design suggest that the design and analysis is satisfactory.

4. CONCLUSION

CMC has been successfully used in Europe and North America for more than a decade. Through continued research and development and with successful field experiences, the method is now recognised and accepted as an established ground improvement method.

In Vietnam and Malaysia, CMC has been used to support embankments, foundations of industrial buildings and container terminals. The potential applications of CMC in Indonesia are similar to these countries with potential applications to replace conventional RC piles (rigid inclusions) and stone columns (non-rigid inclusions). The role of CMC being a semi-rigid inclusion is to fill the gap between rigid inclusions and non-rigid inclusions. CMC has proven to be cost effective compared with RC piles and has lesser settlement under higher imposed load compared with stone columns.

In this aspects, potential applications of CMC in Indonesia should include columns supported embankments for highways and railways; foundation support for large area of container terminal, airport apron and large platform; foundation for buildings, warehouses and other structures. The range of soils deemed suitable for CMC is by far the widest among all the ground improvement methods; from non-engineered fill to loose sand, from compressible soil to organic soil. Together with its great adaptability to ground conditions and the imposed load, CMC will be next to piled foundation in every sense of its applications.

REFERENCES

BUT Menard Geosystems, 2010 Technical Design Report for Apron Terminal III Pier I (45 pages).

Plomteux, C. & Lacazedieu, M 2007 Embankment Construction on Extremely Soft Soils using Controlled Modulus Columns for Highway 2000 Project in Jamaica 16th Southeast Asian Geotechnical Conference, 8 – 11 May 2007, Kuala Lumpur.

SPONSORS

PLATINUM SPONSORS

On 26 October 2000, 7 foundation companies decided to represent the interests of the foundation sector through the creation of a non-profit association under the name ABEF. Meanwhile, the association already consists of 17 members.

The association aims to create healthy relationships in the foundation sector and to represent and defend the economical and moral interests of its members, as long as it concerns matters that are related to the foundation business.

It seeks to achieve this aim with all legal resources by:

- promoting a constructive relation between the members, associations, companies and institutions who come into contact with the sector;
- adopting positions regarding the preparation of rules, regulations, documents, etc. which are applicable on foundation works,
- attracting employees and promoting professional competence;
- organizing training in deep foundation techniques for workers and site-managers;
- the pursuit of a high quality label in all aspects of the foundation sector;
- delivering opinions to the members in possible conflicts;
- the connection to and the participation in the European Federation EFFC (European Federation of Foundation Contractors;
- the participation in working groups and committees in the framework of National and European standards, directives, documents and research programs;
- undertaking all other legal interventions that are in line with the objectives of the association.

ABEF
Lombardstraat 34-42 – B-1000 BRUSSEL
T: 00 32 (0)2 545 57 58 - F: 00 32 (0)2 513 24 16
info@abef.be
www.abef.be

The non-profit association ABEF is since 2012 part of FEDECOM, - the federation of complementary companies of the construction sector, that is on its turn part of the federation of Belgian building contractors.

The members of ABEF are:

OLIVIER SOLID FOUNDATIONS
FONDEDILE
EURODRILL
Smet-Boring
de waal PALEN - PIEUX
VOTQUENNE FOUNDATIONS
CVR
SOILTECH SOIL & PILING CONTRACTORS
PROFFUND N.V.
SOLETANCHE BACHY
Franki Foundations Belgium
FONTEC
LAMEIRE future foundation technics
HEVI BVBA
FUNDEX
VOTQUENNE
WIG PALEN

ABEF
Lombardstraat 34-42 – B-1000 BRUSSEL
T: 00 32 (0)2 545 57 58 - F: 00 32 (0)2 513 24 16
info@abef.be
www.abef.be

BESIX

Beyond Challenges

Port and marine projects have been one of BESIX's spearheads since the company was first established. BESIX focuses on the design and implementation of on-shore and offshore projects: locks, breakwaters, seawalls, seawater intakes, quay walls, gas or ore terminals, and LNG (liquefied natural gas) jetties.

Investors are attracted by BESIX's international experience, know-how, its technical skills and the innovatory solutions it offers, as well as by the marine equipment at its disposal, enabling work to get started quickly.


www.besix.com

Cofra

CDC compaction

Applications of the CDC technique include:
> Improvement of land reclamation projects
> Preparation for tank terminals
> Preparation for major infrastructure projects in granular soils
> Densification of embankments

Advantages of CDC:
> Cost-effective
> Compaction impact down to depths of up to 9 metres
> Real-time GPS monitoring
> Flexibility

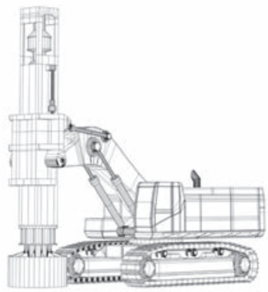

MebraDrain vertical drainage

Applications of vertical drainage include:
> Accelerated preparation of construction sites
> Site preparation for different types of infrastructure projects
> Construction of embankments
> Soil improvement for land reclamation projects

Advantages of MebraDrain vertical drainage:
> Sophisticated equipment - light to heavy duty
> Short consolidation periods
> Quick installation
> Installation to a drain depth of 65 m

BeauDrain(-S) vacuum consolidation

Applications of BeauDrain include:
> Accelerated preparation of construction sites
> Site preparation for different types of infrastructure projects
> Soil improvement for land reclamation projects
> Expedited construction of embankments

Advantages of BeauDrain:
> Short installation period
> Clean work area after installation (BeauDrain)
> Very large working depths possible (BeauDrain-S)
> Suitable for installation through thick sand layers (BeauDrain-S)

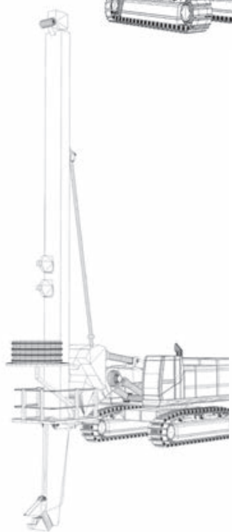

AuGeo embankment

Applications of AuGeo include:
> Construction and widening of embankments
> Construction and widening of various types of infrastructure
> Foundation of roads in urban development areas
> Foundation of industrial flooring systems

Advantages of AuGeo:
> Quick, vibration-free and low-noise installation
> No settlement period and no risk of instability
> No impact on the surrounding area
> Guaranteed pile diameter in peat soil

Building worldwide on our strength

A multidisciplinary approach for new horizons




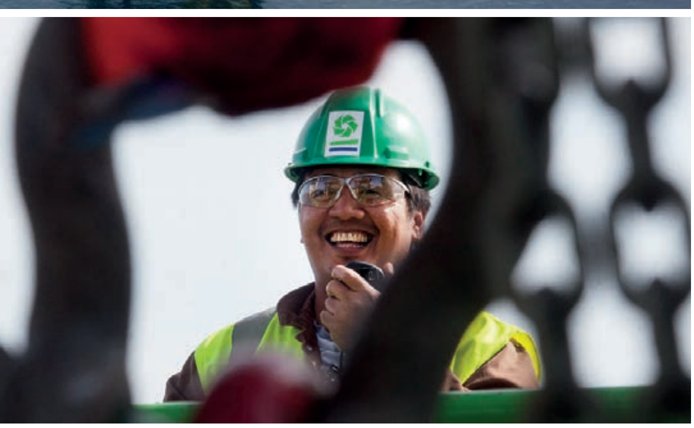


GROUND IMPROVEMENT SPECIALIST

Dynamic Compaction - Dynamic Replacement - Stone Columns
Bi Modulus Columns - CMC - Vibro Compaction
Menard Vacuum - Vertical Drains - Jet Grouting
Slurry Wall - Soil Mixing - Compaction Grouting

Central Processing Facility
Yoloten - TURKMENISTAN

Ronald Reagan Airport
Washington DC - USA

Wind Power to Lauzitsring
GERMANY

Gdansk Ringway
POLAND

A89
FRANCE

Jakarta Airport
INDONESIA

Warehouse in Oise Department
FRANCE

Sport Complex - La Baie
QUEBEC

MENARD
2, rue Gutenberg - BP 28 - 91620 NOZAY (FRANCE)
Tél :0169013738 - Fax : 0169017505
courrier@menard-mail.com
www.menard-web.com

As a specialist geotechnical contractor, Menard delivers complete design-build foundation systems using ground improvement techniques. Our solutions are creative and cost-saving alternatives to the deep foundations traditionally used to support buildings and structures.

A Comprehensive Service

As a result of the geotechnical know-how accumulated through the completion of thousands of projects, MENARD consistently provides the essentials for success: a good price, a reliable schedule, well managed construction techniques and a commitment to excellence in safety and environmental protection.

A Complete Solution

Often involved from the project conception onwards, Menard works closely with clients in analyzing their objectives. Based on the geotechnical investigation report and the description of the structures to be built, MENARD will recommend the most appropriate soil improvement technique, depending on the analysis of the soil, the structure and the environmental constraints. MENARD engineers will then produce a detailed design, and the subsequent construction will be carried out by dedicated teams based in more than 50 locations worldwide. Finally, our quality control procedures will allow us to complement our design and construct package with a long-term guarantee.

State of the Art Technology

Over the last 50 years, MENARD has improved and developed a complete range of innovative and sustainable soil improvement techniques. A fundamental objective of the company has always been to remain at the forefront of technological advances in this field and to offer more efficient, reliable and economical solutions. Our leading expertise is built on our field experience, our numerical modelling capabilities and the development and optimization of specialised construction equipment.

Siège Social :
2 rue gutenberg
91620 NOZAY
Tel : 01 69 01 37 38
Fax : 01 69 01 75 05

www.menard-web.com

First application of the Geomix® process as ground improvement in a seismic area

Fort de France prefectural headquarters/Martinique

The major earthquake suffered by Martinique in 2007 showed once more the urgency, for the prefectural authorities, to construct two new administrative buildings as a replacement for one older building. The call for tenders issued for the construction of the foundations sought two technical solutions: one, very traditional solution, using piles and barrettes; and the other, on the face of it less expensive, using ballasted columns and rigid inclusions. The objective, in both cases, was to transfer the load from the buildings onto "good" ground through the layer of alluvial sands, at a depth of 12 to 19m on the site.

"Although, obviously, there were no feasibility problems with the technique of piles and barrettes," explains Emmanuel Ollier, the head of Bachy Fondaco Caraïbes, "the envisaged ground improvement solution did not seem to us to be suitable, bearing in mind the great thickness and the high potential for liquefaction of the ground in Fort de France. In the event of an earthquake, at the final stage of deterioration, the ground actually 'flows', depending on the angle of inclination of the upper surface of the substrate."

A grid of Geomix® retaining walls will provide earthquake protection for the new buildings

In this case, the difference in level of the top of the good ground is substantial, as it is up to 7m over a length of only 40m. Rigid inclusions and/or ballasted columns would not therefore be strong enough to withstand the intensity of the forces created by an earthquake.

Not wishing to waste the opportunity of putting forward a cost-effective alternative to the basic solution, Bachy Fondaco Caraïbes proposed a grid of Geomix®* walls 0.50m thick under the whole building, on a layout of approximately 4.30m by 4m. This unusual alternative has a number of advantages: it blocks liquefaction of the ground in the event of an earthquake and, during the works phase, it causes less disturbance (vibrations) for neighbours. It also reduces to a minimum the need to use machinery on the site, as the process generates very little spoil and only requires a limited supply of cement and water.

Although it was not the least expensive bid submitted, Bachy Fondaco Caraïbes' tender was accepted as being the best for the construction of the foundations for the two buildings. One is a four-storey and the other a five-storey, with a total ground area of approximately 600m² each (i.e. a total of 1,115m²).

"This new technique, implemented over a very short period of time between mid-October 2010 and mid-January 2011, represents a big step forward in the approach to foundations in a seismic zone," considers Emmanuel Ollier. "If generalised, it could create a revolution for us, encouraging us to obtain the appropriate plant and develop this new expertise."

** Geomix®: a retaining wall and foundation process combining Hydrofraise trench cutting with deep soil mixing.*

Participants
Client: French Ministry of the Interior
Client representative: Direction Départementale de l'Équipement
Project manager: DHA joint venture (Arch'Îles Concept, CIEC Engineering)
Deep foundations: Bachy Fondaco Caraïbes

SOLETANCHE BACHY

GOLD SPONSORS

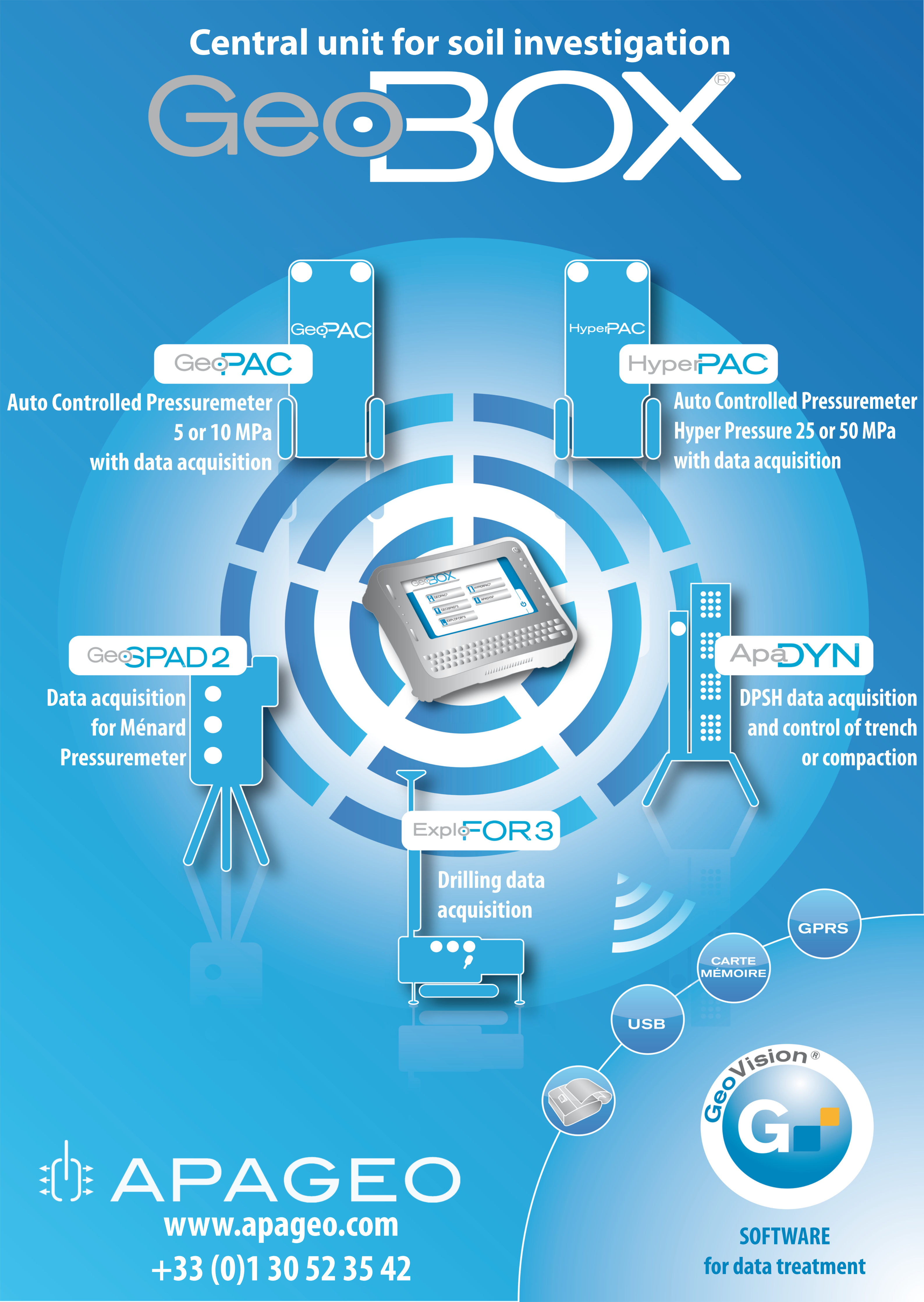
Central unit for soil investigation
GeoBOX®
GeoPAC
GeoPAC
Auto Controlled Pressuremeter
5 or 10 MPa
with data acquisition
HyperPAC
HyperPAC
Auto Controlled Pressuremeter
Hyper Pressure 25 or 50 MPa
with data acquisition
GeoSPAD 2
Data acquisition
for Ménard
Pressuremeter
ApaDYN
DPSH data acquisition
and control of trench
or compaction
ExploFOR 3
Drilling data
acquisition
GPRS
CARTE MÉMOIRE
USB
GeoVision®
SOFTWARE
for data treatment
APAGEO
www.apageo.com
+33 (0)1 30 52 35 42

Experience the progress.

Liebherr-Werk Nenzing GmbH
P.O. Box 10, A-6710 Nenzing/Austria
Tel.: +43 50809 41-473
Fax: +43 50809 41-499
crawler.crane@liebherr.com
www.liebherr.com

LIEBHERR
The Group

SILVER SPONSORS

PLATINUM SPONSORS

ABEF BESIX Cofra

DEME Dredging, Environmental & Marine Engineering menard SOLETANCHE BACHY

GOLD SPONSORS

APAGEO DENYS EIFFAGE FUGRO Holcim

LIEBHERR Tensar TERRASOL TERRE ARMEE SUSTAINABLE TECHNOLOGY CATHIE ASSOCIATES

SILVER SPONSORS

ISCHEBECK TITAN Wicks KELLER

ORGANIZING SECRETARIAT

BBRI **Belgian Building Research Institute**

With the support of TIS-SFT

TIS Speciale funderingstechnieken